PHASE II REPORT

SEISMIC SAFETY INVESTIGATION OF EIGHT SCS DAMS IN SOUTHWESTERN UTAH

Earth Sciences Associates

PHASE II REPORT

SEISMIC SAFETY INVESTIGATION OF EIGHT SCS DAMS IN SOUTHWESTERN UTAH

Prepared for

Soil Conservation Service
West Technical Service Center
511 NW Broadway, Room 510
Portland, Oregon 97209

Submitted by

Earth Sciences Associates, Inc.
701 Welch Road
Palo Alto, California 94304
(415) 321-3071

February 1983 - D118

PHASE II REPORT

SEISMIC SAFETY INVESTIGATION OF EIGHT SCS DAMS
IN SOUTHWESTERN UTAH

Table of Contents

Table of Contents (Continued)

I. INTRODUCTION

A. General

This Phase II report describes the results of engineering analyses carried out to determine the safety of eight Soil Conservation Service (SCS) flood control dams located in southwestern Utah, with respect to vibratory ground motion and surface fault rupture produced by an earthquake of Magnitude 6 occurring in the immediate vicinity of the sites. The Phase I report previously submitted to the SCS provided a detailed description of the field investigations, local and regional geology and tectonics, seismicity of the region, and general characteristics of the embankments and foundations of the eight SCS dams.

Based on our review of ESA field data and information available from the SCS, the following four dams were selected for detailed analysis:

- Green's Lake Dam No. 3
- Warner Draw Dam
- Frog Hollow Dam, and
- Ivins Diversion Dam No. 5

Criteria that were considered in making this selection were summarized in our letter to the SCS dated December 15, 1981. Subsequently, the SCS authorized additional simplified analyses to assist in evaluating the seismic stability of the following four dams:

- Green's Lake Dam No. 2
- Green's Lake Dam No. 5
- Gypsum Wash Dam, and
- Stucki Dam

The various simplified procedures to be used in the analyses of these dams were described in a letter to the SCS dated June 23, 1982 and are discussed in detail in this report.

B. Purpose and Scope

The major purpose and scope of the Phase II studies are:

- To establish the magnitude and direction of surface rupture which could occur along faults in the foundation area of the various dams during a Magnitude 6 earthquake.

- To develop an acceleration time history representative of the ground motions expected to occur at the dam sites from a Magnitude 6 earthquake occurring on a fault in close proximity to the dam sites.

- To perform dynamic response analyses and simplified analyses to determine the magnitude of earthquake-induced stresses to which the dams would be subjected to during a nearby Magnitude 6 earthquake.

- To establish the static and cyclic strength characteristics of the various materials comprising the dam embankments and their foundations by means of laboratory tests on representative samples obtained during the Phase I field investigation.

- To evaluate the static, seismic, and post-earthquake stability of the four dams selected for detailed analyses. Where appropriate, estimates of the amount of deformation which the dam embankments might undergo due to vibratory ground motion were made.

- To evaluate the effects of fault movement for those dams situated on a fault and to make recommendations regarding remedial measures which would improve the behavior of the dam from the damaging effects of fault rupture offset.

C. Performance

Work on this project was performed for the SCS West Technical Center in Portland, Oregon. C. Edward Stearns served as the Project Coordinator for the SCS, and Joan K. Johnson was the Contract Administrator. Other SCS personnel who have been directly involved with this project are Don Wallin, Bob Nelson, Bob Rasely, and Claud Scoles.

ESA personnel who have worked on the Phase II studies include: Julio E. Valera, who served as overall project manager and assisted in the fault rupture and engineering evaluations; Michael L. Traubenik, who reviewed and summarized all of the available data, supervised the laboratory testing, and performed the engineering analyses; Eugene A. Nelson, who assisted in the fault rupture and remedial measures evaluation; Bill Welter, who performed all of the laboratory testing; and Catherine J. Povejsil, who assisted in the engineering analyses. The report was written by Michael L. Traubenik, Julio E. Valera, and Eugene A. Nelson.

Richard J. Proctor of Lindvall, Richter and Associates, (LRA) which worked as a subcontractor to ESA, assisted in the studies to establish the effects of fault rupture offset on the dams and in providing recommendations for remedial measures. The assistance from LRA is greatly appreciated.

II. SUMMARY OF CONCLUSIONS AND RECOMMENDATIONS

The studies presented in this report were aimed at establishing the performance of the eight SCS dams located in Southwestern Utah during and after the occurrence of a Magnitude 6.0 earthquake in close proximity to the dam sites. Based on the results of this investigation and the previous Phase I investigation, we have arrived at the conclusions and recommendations outlined below.

Most of the conclusions have been based on data and analyses which are explained in detail in the main text and appendices of this report. While the analyses and data presented in this report tend to support the conclusions summarized below, it should be noted that they are based on a number of conservative simplifying assumptions, two of which are that the dams impound some water and significant portions of the embankments and foundations are saturated at the time of the postulated earthquake. These assumptions are conservative since the intended use of the dams is to impound rainfall runoff water for only brief periods of time. While these conditions may be conservative, they are not impossible. However, it is our judgment that as long as the impounded water is rapidly discharged from the reservoir (as is intended), these conditions would probably exist for only short periods of time. Under these conditions, the potential of the dams considered in this investigation would be greatly reduced.

A. Conclusions

Fault Offset

1. Of the eight dams studied during this investigation, four (the three Green's Lake Dams and Gypsum Wash Dam) have some potential for fault offset. There is direct evidence of 2 inches of displacement within the foundation materials underyling the Gypsum Wash Dam during about the last 1500 years and 4 or more feet during what is estimated to be the last 10,000 to 25,000 years. At the Green's Lake Dam sites, no direct evidence of fault offset in the foundation of the dams was established, but the dams are situated within the Hurricane fault zone which exhibits abundant fresh-appearing topographic features that are interpreted to be related to surface faulting.

2. For the postulated Magnitude 6.0 earthquake selected for analyses, a surface displacement of approximately 1 foot may take place on the earthquake producing fault.

3. Even though 1 foot of offset could possibly occur through the Gypsum Wash Dam during the postulated Magnitude 6.0 earthquake, a rapid failure resulting from piping or erosion along the plane of offset appears to be unlikely.

4. Both the embankment and foundation of Green's Lake Dam No. 3 could be subject to piping or erosion if 1 foot of offset was to occur at this site. Only the embankment of Green's Lake Dam No. 2 appears to be susceptible to this problem. Failure of these dams could occur within a period of a few hours to a few days. However, it should be noted that this type of failure can occur only if these dams are impounding water at the time of the postulated earthquake. Piping failure of Green's Lake Dam No. 5 is unlikely.

Ground Shaking

1. All of the dams considered in this investigation may be subjected to strong ground shaking during the postulated Magnitude 6.0 earthquake. For seven out of the eight dams, peak horizontal accelerations greater than 0.60 g may occur at the sites due to their close proximity to earthquake-generating faults.

2. Analyses indicate that if the embankments and foundation soils are allowed to become saturated, Green's Lake Dam 3 and Ivins Diversion Dam No. 5 would perform poorly during and/or after the ground shaking produced by the postulated Magnitude 6.0 earthquake.

3. The performance of Frog Hollow Dam during and after the postulated earthquake should be satisfactory provided that repairs to this structure are made in accordance with the general recommendations provided in this report.

4. Warner Draw Dam should perform satisfactorily during and after the postulated earthquake.

5. While detailed seismic stability analyses were not performed on Green's Lake Dams No. 2 and No. 5, Gypsum Wash and Stucki Dams, it is our judgment that these embankments should perform satisfactorily during and after the ground shaking produced by the postulated Magnitude 6.0 earthquake.

B. Recommendations

1. The following measures are recommended to mitigate the potential hazards posed by the possible failure of several of the dams:

   a) It is our judgment that the condition of the Green's Lake Dam No. 3 embankment and foundation soils at this site are so poor that this structure should be taken out of service. If it is decided to replace this structure, the guidelines provided in Chapter VIII should be adhered to.

   b) The reservoir level at Green's Lake Dam No. 2 should not be allowed to reach the emergency spillway elevation. This would result in only 2.5 feet of freeboard. Because of the potential for fault rupture at this site, a minimum of 4 feet of freeboard should be maintained.

   c) The cracks present in the Frog Hollow Dam embankment should be repaired in accordance with the recommendations provided in Chapter VIII.

   d) The possibility of saturated foundation conditions at Ivins Diversion Dam No. 5 should be investigated by installing piezometers along the downstream slope and toe of the embankment.

2. A number of safety procedures have been recommended to ensure that all eight dams perform satisfactorily. These are presented in Chapter VIII.

III. FAULT RUPTURE POTENTIAL

Tectonic Setting

Of the eight dams being evaluated during this investigation, four (the three Green's Lake dams and Gypsum Wash Dam) may be subjected to fault offset during their lifetime. A fault was also mapped in the Triassic foundation rock of Warner Draw Dam but trench exposures showed that it does not affect overlying soil deposits. This fault is considered to not be active and it, therefore, is not discussed in this chapter.

The Green's Lake dams are located within the complex zone of faulting that characterizes the Hurricane Fault in the Cedar City area. Although no direct evidence of faulting within the immediate foundation areas of the embankments was found by ESA in the trenches excavated during this investigation, topographic features suggestive of Quaternary surface offsets are present in adjacent areas (see Figure VIII-10, Photogeologic Map of the Cedar City area in the Phase I report). Age dating of charcoal collected from deposits in the Green's Lake Dams 2 and 3 area showed that alluvial fan deposits underlying these embankments range from 1060 $\pm$ 100 to 4100 $\pm$ 660 years old. Within the trench exposures developed during this investigation, there is no evidence of fault offset of these deposits.

At Gypsum Wash, trenches excavated during this investigation exposed offsets within soil and bedrock materials that underlie the southern portion of the dam embankment (see Figure VIII-6 of the Phase I report, map showing fault and trench locations at Gypsum Wash). Very young-appearing alluvial fan deposits (estimated to be about 1500 years old) are offset 2 inches. Older fan deposits (estimated to be 10,000 to 25,000 years old) are offset at least 4 feet.

To summarize, there is direct evidence of 2 inches of displacement within the foundation materials underlying Gypsum Wash Dam during about the last 1500 years and 4 or more feet during what is estimated to be the last 10,000 to 25,000 years. At the Green's Lake Dam sites no. 2 and 3, no direct evidence of fault offset in the foundation of the dams was established, but the dams are situated

within a complex zone of deformation that exhibits abundant fresh-appearing topographic features that are probably of Quaternary age and are interpreted to be related to surface faulting.

Geologic and tectonic conditions in the vicinity of the Green's Lake dams and Gypsum Wash Dam are discussed in detail in Chapter VIII, Sections A, B, and C (respectively) of the Phase I report. Tectonic conditions in these two areas are schematically shown in Figures VIII-5 and VIII-7 of the Phase I report. The evidence for fault rupture potential at each of the four dams is summarized in Table III-1.

Expectable Size of Displacements

The results of the Phase I investigation suggest that a Magnitude 6 earthquake would be a reasonable seismic event from which to derive the parameters necessary for the analyses of the eight dams. This was agreed to by the SCS in their letter of May 20, 1982.

Initially, it was hoped that use could be made of published estimates of slip rates together with information on recurrence intervals to arrive at estimates of the displacements associated with earthquakes of different magnitudes. However, this approach is subject to large uncertanties due to the fact that slip rates can vary significantly at different locations along a fault and estimates of recurrence intervals are also subject to wide variations. The results obtained using this approach led to very small values of displacement which, in our opinion, were unconservative.

Based on discussion with Professor Arabasz, who was a consultant to ESA on this project, it was decided that the most appropriate method for obtaining reasonable estimates of surface displacement was to rely on available data on historic faulting for similar faults (normal and normal-oblique) located in the same or similar tectonic environment. The available data were reviewed and are summarized in Table III-2. (Slemmons, 1977; 1980; Bucknam et al., 1980; Arabasz, Personal Communications, 1982).

Table III-1

Summary of Dams With Fault Rupture Potential

Dam	Fault	Total Length (mi)	Estimated Age of Last Surface Displacement (yrs)	Magnitude of Apparent Vertical Measured Offset
Green's Lake No. 2	Hurricane	160	1060 ± 100 to 4100 ± 660 (1)	No offset in soils
Green's Lake No. 3	Hurricane	160	1060 ± 100 to 4100 ± 660 (1)	No offset in soils
Green's Lake No. 5	Hurricane	160	Not established	3 ft in old fan
Gypsum Wash	Washington	40	Less than 1500 (2) 10,000-25,000 (2)	2 inches in young fan 3-4 ft in old fan

(1) Based on radio-carbon age dating of materials found in excavated trenches.

(2) Based on estimate made by Dr. Roy Shlemon by visual observation in the field.

Statistical analyses of the data presented in Table III-2 were performed to establish relationships between earthquake magnitude and maximum surface displacement. Least squares fit relationships of the entire data set, and of the data corresponding to the Basin and Range Province region only, were determined. Mean and mean plus and minus one standard deviation relationships, established on the basis of the least squares fit, are plotted in Figures III-1 and III-2, together with the individual data points.

Based on the above analysis, average values of maximum displacements corresponding to earthquakes of various magnitudes were estimated and are summarized in Table III-3. Also given in this table is the recurrence interval corresponding to each earthquake magnitude. These are the same as those presented in the Phase I report. For the postulated Magnitude 6 earthquake, an average surface displacement of about 1 foot is obtained. For a Magnitude 7 earthquake the average displacement is about 5 feet. If it is assumed that the 4 plus feet of offset measured at Gypsum Wash occurred during one single event of Magnitude 7, then the measured value agrees reasonably well with the available data (see Figures III-1 and III-2). In the next chapter of this report, the effects and consequences of the estimated surface displacement occurring at each of the dam sites listed in Table III-1, during the postulated Magnitude 6 earthquake, are addressed.

Table III-2

Summary of Historic Surface Faulting for Normal and Normal-Oblique Faults

Locality	Fault	Date	M	Length (km)	Maximum Displacement (m)
Cutch, India	Allah Bund	06-16-1819	—	128.7	9.14
New Zealand	Wairapa	01-23-1855	8.0	160.0	3.05
Corinth, Greece	—	12-26-1861	7.5	13.0	2.0
Owens, California	Several	03-26-1872	8.0	110.0	6.44
Sonora, Mexico	—	05-03-1887	7.3	50.0	4.0
Miro-Owari or Nobi, Japan	Neodani, etc.	10-28-1891	8.4	80.0	8.0
Locris, Greece	—	04-27-1894	6.9	59.0	2.0
Riku-U, Japan	Senya, Kawafume	08-31-1895	7.5	60.0	3.0
Assam, India	--	06-12-1897	8.7	--	10.67
Gurban Saikan, Mongolia	—	02-01-1903	7.8	15.0	3.0
Mongolia	Tsetserleg	07-09-1905	8.4	115.0	—
Taiwan	Meitzukeng	03-17-1906	7.1	11.0	2.71
Pleasant Valley, Nevada	Several	10-02-1915	7.75	62.0	5.6
Subukai, Kenya	Gomura	01-06-1928	7.1	32.0	3.35
Chirpan, Bulgaria	—	04-14-1928	6.8	47.0	0.5
Popovitsa, Bulgaria	—	04-18-1928	7.0	29.0	3.5
N-Izu, Japan	Tanna, etc.	11-25-1930	7.1	32.0	3.3
Cedar Mountain, Nevada	Several	12-20-1932	7.2	61.0	0.9
Excelsior Mountains, Nevada	Endowment Mine	01-30-1934	6.3	1.45	0.12
Hansel Valley, Utah	Kosmo	03-12-1934	6.6	11.5	0.52
Turkey	Anatolia	11-26-1943	7.6	265.0	1.5
Ancash, Peru	--	11-10-1946	7.25	--	3.5

Table III-2 (Continued)

Summary of Historic Surface Faulting for Normal and Normal-Oblique Faults (Continued)

Locality	Fault	Date	M	Length (km)	Maximum Displacement (m)
Fuqui, Japan	—	06-28-1948	7.3	25.0	2.30
Ft. Sage Mountain, California	—	12-14-1950	5.6	8.85	0.61
Fallon-Stillwater, Nevada	Rainbow Mtn.	07-06-1954	6.6	17.7	0.30
Fallon-Stillwater, Nevada	Rainbow Mtn.	08-23-1954	6.8	30.6	0.76
Dixie Valley, Nevada	Several	12-16-1954	6.9	61.2	3.25
Fairview Peak, Nevada	Several	12-16-1954	7.1	58.0	5.62
Baja California, Norte	San Miguel	02-09-1956	6.8	19.3	1.20
Hebgen Lake, Montana	Several	08-17-1959	7.25	29.1	6.10
Ethiopia	—	06-02-1961	6.4	40.0	1.90
Gediz, Turkey	Several	03-28-1970	7.0	31.0	2.20
Pocatello Valley, Idaho-Utah Border	—	03-1975	6.0	--	0.13
Oroville, California	Cleveland Hill	08-01-1975	5.7	10.0	0.06

After Slemmons, 1977, 1980; Bucknam, Algermissen and Anderson, 1980; Arabasz, Richins and Langer, 1981; Arabasz, Personal Communications, 1982.

Table III-3

Summary of Reccurence Interval and Estimated Maximum Displacement for Surface Faulting for Various Levels of Earthquake Magnitudes

Magnitude	Recurrence Interval (yrs)	Estimated Average Maximum Displacement, ft	
		Basin-Range	Worldwide
6.0	200-300	0.9	1.2
6.5	500-800	2.0	2.4
7.0	1,000-10,000	4.4	4.9
7.5	1,000-10,000	9.7	9.8

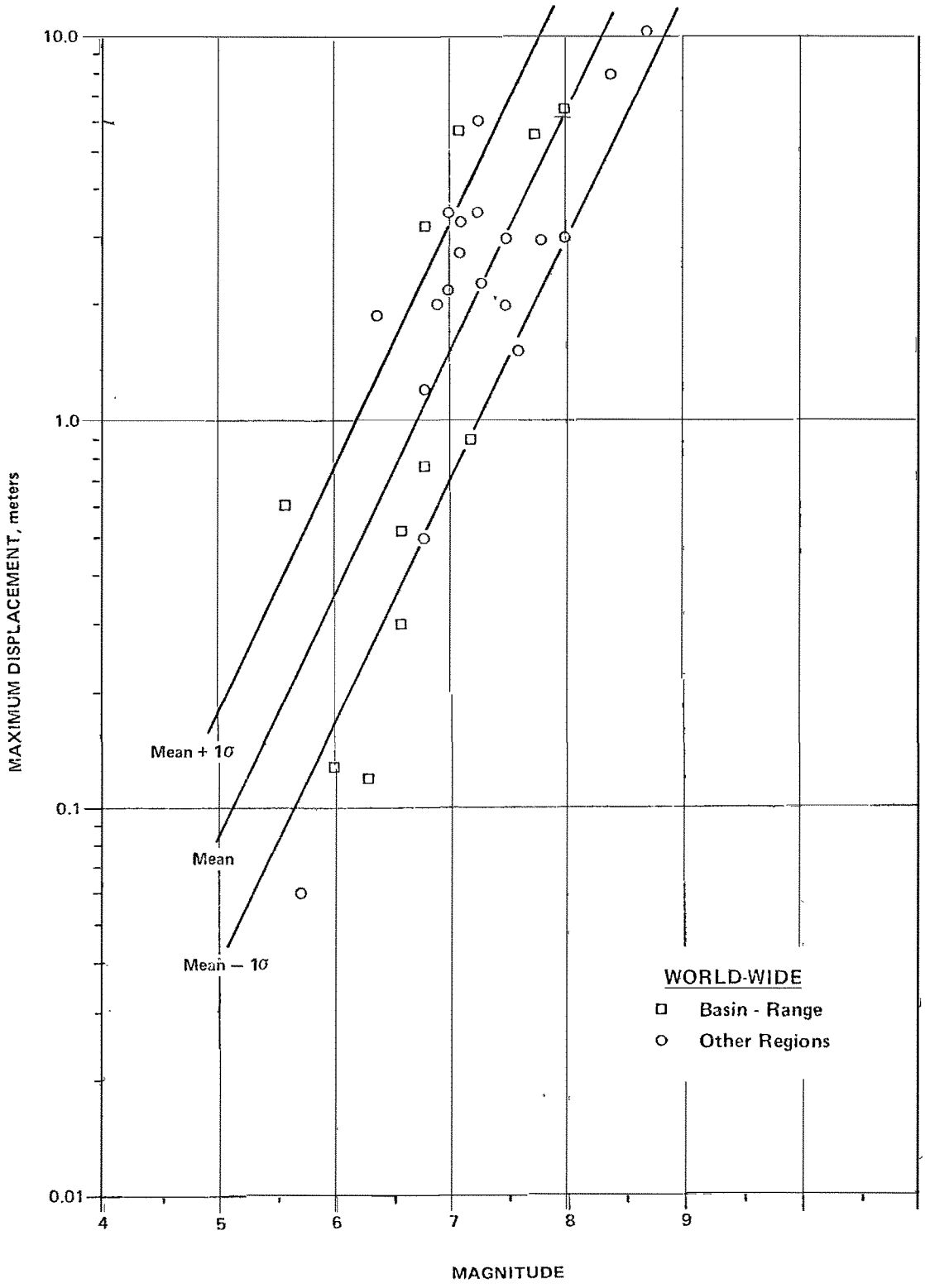

Earth Sciences Associates
Palo Alto, California

SEISMIC SAFETY INVESTIGATION OF EIGHT SCS DAMS
HISTORIC SURFACE FAULTING
WORLDWIDE
NORMAL AND NORMAL-OBLIQUE FAULTS

Checked by	Date 9/28/82	Project No.	Figure No.
Approved by Julio Valera	Date 9/29/82	D118	III-1

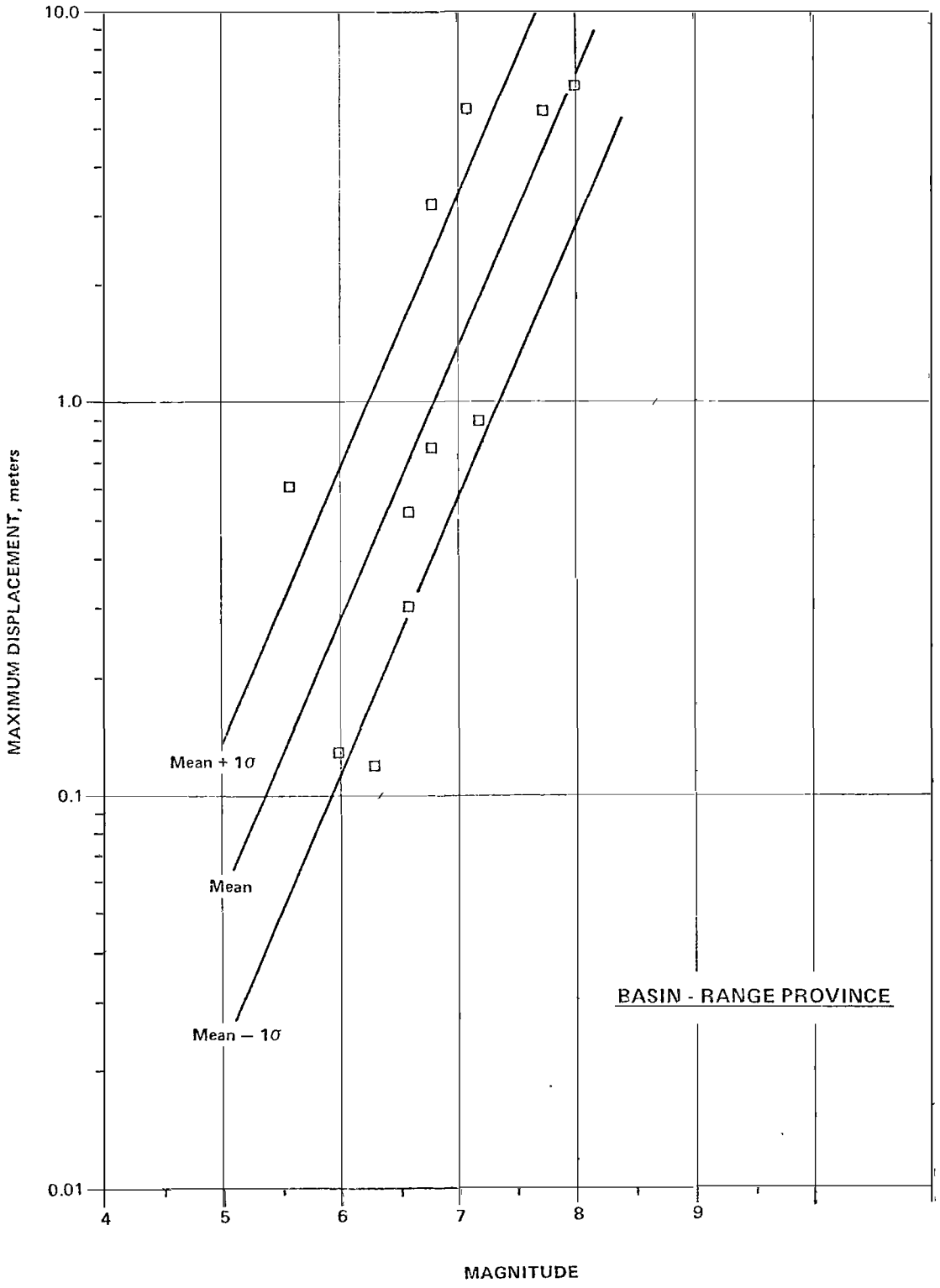

Earth Sciences Associates
Palo Alto, California

SEISMIC SAFETY INVESTIGATION OF EIGHT SCS DAMS
HISTORIC SURFACE FAULTING
BASIN AND RANGE PROVINCE
NORMAL AND NORMAL-OBLIQUE FAULTS

Checked by MLT Date 9/28/82	Project No.	Figure No.
Approved by Julio Valera Date 9/29/82	D118	III-2

IV. EFFECTS OF POTENTIAL FAULT DISPLACEMENT ON DAM EMBANKMENTS AND FOUNDATIONS

While the likelihood of fault rupture through the foundation and embankment of Gypsum Wash Dam or the three Green's Lake dams during their useful life is slight (see Chapter III), our evaluation indicates there to be some potential for up to one foot of offset at any one of these dam sites. The effect of such an offset upon the foundation and embankment of each dam is discussed below, in order of decreasing potential of occurrence.

A. Gypsum Wash Dam

At least 4 feet of offset of the soil/bedrock contact has occurred near the south end of Gypsum Wash Dam within the last 10,000 to 25,000 years. The embankment of Gypsum Wash Dam is zoned and includes a chimney drain which is 6 feet wide. The materials used for embankment construction are mainly silty and clayey sands. The foundation of the dam consists of gypsiferous shale of the Moenkopi Formation of Triassic geologic age.

Because the embankment materials are sandy, there would seem to be some potential for erosion. However, even if 1 foot of offset was to occur, the 6 foot wide chimney drain would still function and thus prevent migration of materials to the downstream face of the dam during full (or partially full) reservoir conditions. This should serve to prevent, or at least to retard, piping erosion along a shear within the embankment.

The Gypsum Wash Dam foundation rock is well consolidated and clayey, and no erosion of this material is likely to occur along the plane of a 1 foot offset.

Thus, even though a 1 foot offset could possibly occur through Gypsum Wash Dam under full (or partially full) reservoir conditions, a rapid failure (within a few hours) as a result of piping along the plane of offset appears to be unlikely.

B. Green's Lake Dams No. 2 and 3

No offsets were found in trenches excavated in the foundation materials of Green's Lake Dams No. 2 and 3 which were determined to be about 1000 to 4000 years old. However, the dams are within the complex zone of faulting that characterizes the Hurricane fault zone in this area, so there appears to be some chance of fault offset during the life of the dams. The embankments of both dams are unzoned and consist mainly of silty sand. The foundation of Green's Lake Dam No. 2 is clayey and gravelly at depth, while the foundation at Green's Lake Dam No. 3 consists of silty sand.

If 1 foot of offset were to occur through either of these dams, there appears to be some potential for piping along the fault plane because of the sandy nature of the materials involved. Both the embankment and foundation of Green's Lake Dam No. 3 could be affected, while only the embankment of Green's Lake Dam No. 2 appears to be susceptible to this problem. The time required for a failure by piping to occur along a fault shear plane cannot be accurately estimated. Even at full reservoir level, the head acting on the failure plane would be relatively low at these dams, which is fortunate considering the embankment and foundation conditions.

In the unlikely event that 1 foot of fault offset were to occur through either of these embankments under full (or partially full) reservior conditions, it is our opinion that there is some likelihood of a piping failure within a period of a few hours to a few days.

C. Green's Lake Dam No. 5

The main dam of Green's Lake Dam No. 5 is located across a side canyon draining westward from the broad north-south valley in which Cedar City is located. As shown on the diagramatic geologic cross section presented in Figure VIII-5 of the Phase I report, faults (which are part of the complex Hurricane fault zone in the Cedar City area) form a graben bounding the Green's Lake Dam No. 5 reservoir area on the west and east. Although the western fault is near the main

dam site, it trends north-south just east of the embankment. Consequently, there is little likelihood of offset of the main embankment. The two long, low subsidiary dikes could, however, be offset by fault movement.

Both the embankment and foundation materials at Green's Lake Dam No. 5 consist of clayey soils which are not highly dispersive nor erosive. Consequently, if 1 foot of offset were to occur through the embankment or foundation of the main dam, it is very unlikely that a piping failure would occur.

V. GROUND MOTION CHARACTERISTICS

The results of the Phase I investigation indicated that a Magnitude 6 earthquake could occur during the life of any of the eight SCS dams. A recurrence interval of 200 to 300 years was established for an earthquake of this size occurring on the faults located in close proximity to the dam sites. Based on these findings, the SCS requested that the effects of ground shaking (in addition to fault rupture offset) on the dams be evaluated for a Magnitude 6 earthquake.

In order to carry out the proposed dynamic response analyses on the four selected dams, it was first necessary to develop an appropriate acceleration time history corresponding to a Magnitude 6 earthquake. In Table V-1, the closest fault to each dam site, the distance from the fault to the dam site, and the corresponding value of peak horizontal acceleration which would be expected to occur at each dam site are tabulated. Values of peak horizontal acceleration were established on the basis of published acceleration attenuation relationships for rock sites (Seed, 1980). It can be seen from the information presented in this table that for seven out of the eight dams considered, peak horizontal accelerations greater than 0.60g will develop due to their close proximity to the earthquake-generating fault.

In addition to the values of peak acceleration tabulated in Table V-1, other ground motion parameters were established for the postulated Magnitude 6 earthquake. These are presented in Appendix E together with a detailed discussion on the development of a representative accelerogram corresponding a near-field Magnitude 6 event. This accelerogram was used in the dynamic response analysis performed on four of the eight dams.

Table V-1

Values of Peak Horizontal Acceleration
at Dam Sites Produced by a
Near-Field Magnitude 6 Earthquake

Dam	Closest Fault to Dam Site	Distance (mi)	Peak Acceleration (g)
Green's Lake No. 2	Hurricane	0	0.66
Green's Lake No. 3	Hurricane	0	0.66
Green's Lake No. 5	Hurricane	0	0.66
Gypsum Wash	Washington	0	0.66
Warner Draw	Washington	1	0.66
Stucki	Washington	0.5	0.66
Frog Hollow	Hurricane	2	0.66
Ivins Diversion No. 5	Grand Wash	5	0.38

VI. EVALUATION OF LIQUEFACTION POTENTIAL

Introduction

The various analyses that were performed to evaluate the liquefaction potential of the embankment and foundation soils present at the eight SCS dams located in Southwestern Utah are briefly described in this chapter. Conclusions on the liquefaction and/or cyclic mobility of the embankment and foundation soils are summarized in the last section of this chapter. A more detailed description of the analyses, results, and conclusions are presented in Appendix G of this report. The four dams that were selected for detailed stability and deformation analyses include:

1) Green's Lake Dam No. 3
2) Warner Draw Dam
3) Frog Hollow Dam
4) Ivins Diversion Dam No. 5

In addition to the analyses performed on these four selected dams, simplified analyses were carried out on the remaining embankments to help in evaluating the performance of these embankments during the postulated earthquake ground motions. The dams for which simplified analyses were performed are:

1) Green's Lake Dam No. 2
2) Green's Lake Dam No. 5
3) Gypsum Wash Dam
4) Stucki Dam

Review of Procedures Used to Evaluate Liquefaction and Cyclic Mobility

The basic cause of liquefaction or cyclic mobility in a saturated cohesionless soil during an earthquake is the result of a build up of excess pore pressure due to the application of cyclic shear stresses induced by earthquake ground motions. "Liquefaction" denotes the condition where the porewater pressure equals the effective confining stress. In this state, a soil will undergo continued deformation

at a low residual resistance. The occurrence of liquefaction will depend on the void ratio or relative density of the soil as well as other factors. It may also be caused by a hydraulic gradient during an upward flow of water in a deposit. The "cyclic mobility" of a soil denotes the condition in which a number of cyclic stress applications develop peak cyclic pore pressures equal to the applied effective confining pressure and subsequent applied cyclic and/or static stresses cause limited strains to develop.

There are basically three methods available for evaluating the liquefaction or cyclic mobility potential of a saturated cohesionless soil subjected to earthquake ground shaking (Seed, 1979a, SW-AJA, 1972). They are:

1. Methods based on observations of saturated cohesionless soil deposits in previous earthquakes,

2. Methods based on evaluation of stress conditions in the field and determinations of stress conditions causing liquefaction or cyclic mobility of soils in the laboratory, and

3. Comparisons of the gradations of soils with the gradations of materials which have liquefied during past earthquakes and which are considered most susceptible to liquefaction in laboratory tests.

The first method is based primarily on results of Standard Penetration Tests (SPT) performed in saturated cohesionless soil deposits. In this method, corrected SPT blow counts obtained from a comprehensive collection of site conditions, where evidence of liquefaction or no liquefaction was known to have taken place during past earthquakes, were used to develop empirical relationships which correlate the values of cyclic stress ratio (τ/σ_o') required to cause liquefaction or liquefaction with limited shear strain potential. Relationships of this type have been developed for earthquakes of various magnitudes and can be used for any given site (subjected to a given earthquake ground surface acceleration) to evaluate the possibility of liquefaction or the cyclic mobility potential. While this method is intended for use in the evaluation of soil liquefaction and cyclic mobility for level ground conditions, results of this method provides a useful guide in the evaluation of the liquefaction potential for other ground conditions.

The second method requires two independent determinations consisting of: 1) an evaluation of the cyclic stresses induced at different levels in the deposit by the earthquake shaking, along with 2) a laboratory investigation to determine the cyclic stresses which will cause the soil to liquefy or undergo various degrees of cyclic strain. The evaluation of liquefaction or cyclic mobility of the soil is then based on a comparison of the cyclic stresses induced in the field with the stresses required to cause liquefaction or limited straining in representative laboratory test samples.

The third method simply requires a comparison of gradations of the soils, for which the liquefaction characteristics are being assessed, with a compilation of gradations of soils which have liquefied during past earthquakes and/or considered most susceptible to liquefaction in laboratory tests. Comparisons of this type should only be used as a preliminary guide for establishing the liquefaction potential of a soil. The empirical relationships are based on observations which suggest that fine sands and silty sands (i.e., generally cohesionless soils) are most susceptible to liquefaction. Cohesive soils do not undergo liquefaction and the liquefaction potential of gravelly soils is considered as being low, due to their generally high permeability which prevents the build up of high excess pore pressures.

For those embankments for which detailed stability and deformation analyses were not performed, the liquefaction potential of the embankments and foundation soils was evaluated using Methods 1 and/or 3. Methods 1 and 3 were used in the liquefaction evaluation of Green's Lake Dam No. 2, Gypsum Wash Dam and Stucki Dam. Method 3 was used in the evaluation of Green's Lake Dam No. 5. Method 1 was not used in the case of this dam since the embankment and foundation soils are generally clayey (cohesive) in nature and since this method is only applicable to generally cohesionless soils. Since cohesive soils do not undergo liquefaction, comparisons of the gradations of the embankment and foundation soils with the gradations of soils susceptible to liquefaction are presented for completeness only. Method 2 was not used in the liquefaction evaluation of the four dams mentioned above since this method requires results of a relatively detailed laboratory testing investigation which was not included in the scope of work of this study.

All three methods were used to evaluate the liquefaction potential of the embankment and foundation soils in the cases of Green's Lake Dam No. 3, Warner Draw Dam and Ivins Diversion Dam No. 5. Method 2 was employed in the evaluation of all the above-mentioned dams for the following reasons: 1) laboratory tests were performed on representative samples of the embankment and foundation soils, and 2) the comparisons of the cyclic stress ratios induced by the postulated earthquake ground motions with those used in the laboratory tests provides an indication of the behavior of the various soils during the postulated earthquake ground motions. Method 3 was used in the case of Frog Hollow Dam. Methods 1 and 2 were not employed in this case since the embankment and foundation soils are generally clayey in nature and therefore the soils can be considered as having a low liquefaction potential.

Summary and Conclusions

Each of the analyses procedures outlined above that have been used to evaluate the liquefaction potential and/or cyclic mobility of the embankment and foundation soils are described in detail in Appendix G of this report. Results of these analyses, as well as other considerations, have been used as a guide in developing the conclusions summarized in Table VI-1 and in determining the behavior of the dams when subjected to ground motions expected during the postulated Magnitude 6.0 earthquake.

It is our judgment that, with the exception of the foundation soils at Green's Lake Dam No. 3 and Ivins Diversion Dam No. 5, the embankment and foundation soils should behave satisfactorily (i.e., should not liquefy) during the postulated Magnitude 6.0 earthquake. During the cyclic loading produced by an event of this magnitude, and under certain in situ conditions, the various field and laboratory test data suggest that some excess pore pressures may develop in the embankment and foundation soils that could produce moderate reductions in the shear strengths of these soils. It is likely that only limited cyclic straining would occur which would not impair the performance and operation of the dams. Some of the foundation soils at Green's Lake Dam No. 3 and at Ivins Diversion Dam No. 5, on the other hand, may be subject to liquefaction and/or excessive cyclic straining. After the earthquake, significant levels of pore pressure could be built up which would result in significant reductions in shear strength in these soils.

While the analyses and data presented in Appendix G tend to support the conclusions summarized in Table VI-1 and those discussed above, it should be noted that they are based on a number of conservative assumptions. These include:

1. The earthquake ground motions that have been postulated for each of the dam sites are based on the closest source-to-site distances. Based on published data, this assumption is probably conservative and should yield ground motions which possess high levels of ground acceleration (and velocity) at frequencies which are in the range of those of the dam embankments. The stresses induced in the soils by these motions are, in our judgment, conservative.

2. The results of cyclic triaxial tests performed on medium dense to dense soils produce cyclic strains and pore pressures that are usually greater than those that would be experienced by the soils in situ during an earthquake. Even though the behavior of the embankment soils during cyclic loading was, in most cases, quite good, it is our judgment that the in situ behavior of these soils, during the postulated earthquake motions, would be better than that observed in the laboratory.

3. Significant portions of the embankments and the entire soil foundations (if present) were assumed to be saturated at the time of the earthquake. This assumption is conservative since the intended use of the dams is to impound rainfall runoff water for only brief periods of time. While saturated soil conditions may be a conservative assumption, it is not an "impossible" condition. Successive rainstorms coupled with the rather pervious soils which comprise most of the embankments and foundations could produce saturated conditions. However, as long as the impounded water is discharged rapidly this condition would probably exist for only brief periods of time.

Since liquefaction can only occur if saturated conditions exist, the conclusions presented herein emphasize the need for careful maintenance of systems used to discharge rainfall runoff. Conditions similar to those which existed during 1967 at Green's Lake Dam No. 3 (see Appendix G of Phase I report - water was allowed to remain in the reservoir for up to 3 months) should not be allowed to develop in any of the dams.

Table VI-1

Summary of Liquefaction Evaluation Conclusions

Dam	Liquefaction Potential Embankment	Foundation	Remarks
Green's Lake No. 2	Low	Low	
Green's Lake No. 3	Low	High	High pore pressures may develop in foundation soils during cyclic loading which may cause liquefaction, excessive cyclic straining or severe reduction in shear strength.
Green's Lake No. 5	Low	Low	
Gypsum Wash	Low	---	
Warner Dam	Low	Low	
Stucki	Low	Low to Limited	Excess pore water pressure may develop in some of the foundation soils at depth, having little or no effect on the embankment's performance.
Frog Hollow	Low	Low	
Ivins Diversion No. 5	Low	High	High pore pressures may develop in foundation soils during cyclic loading which may cause liquefaction, excessive cyclic straining or severe reduction in shear strength.

VII. STABILITY ANALYSES

Introduction

The liquefaction potential of the various soils which comprise the embankments and foundations of the eight dams considered in this investigation has been addressed in the previous chapter of this report. Based on the results of the analyses and other considerations presented in Appendix G and summarized in Chapter VI, the foundation soils at Green's Lake Dam No. 3 and Ivins Diversion Dam No. 5 were found to be susceptible to liquefaction if saturated conditions were present at the time of the postulated Magnitude 6.0 earthquake. The high pore pressures that would be built up in these soils during the earthquake would lead to significant reductions in shear strength after the earthquake. The embankment and foundation soils at the remaining six dams were found to have low liquefaction potential, however, they could experience moderate reductions in shear strength as a result of excess pore pressures produced by the earthquake.

If liquefaction and/or significant loss of shear strength occurs in the foundation soils at Green's Lake Dam No. 3 and Ivins Diversion Dam No. 5 during the earthquake, then failure of these embankments would be likely. It is, therefore, of interest to evaluate the stability of these two embankments assuming that the following conditions might exist at these dam sites at the time of the earthquake:

1) Lower pore pressures in the foundation soils than those measured in laboratory tests;

2) A lower phreatic surface than that corresponding to the steady-state seepage condition.

A number of analyses were performed to ascertain the effects of the above two conditions on the stability of these two embankments. In addition, stability analyses were performed on representative cross sections of the Warner Draw and Frog Hollow dam embankments under static, seismic, and post-earthquake loading conditions.

The cross sections analyzed were developed from available SCS "as-built" drawings and represent the geometry of the embankments near their maximum cross sections. Water levels in the reservoir were assumed to be at the principal (or primary) spillway crest elevations. Phreatic surfaces present within the dams were first determined for steady-state seepage conditions. For Green's Lake Dam No. 3 and Ivins Diversion Dam No. 5, phreatic surfaces representing conditions other than the steady-state seepage condition were also assumed in the analyses. Both the upstream and downstream slopes of each dam cross section were analyzed.

A general purpose slope stability computer program developed at Purdue University was used to perform the analyses (Siegel, 1975; Boutrup, 1977). The program was written for the general solution of slope stability problems using a two-dimensional limit equilibrium method. Calculation of the factor of safety against instability of the slope is performed by the method of slices using either Janbu's method or the Modified Bishop method. The program is capable of analyzing circular failure surfaces, irregular failure surfaces of random shape, or sliding wedges. For purposes of this study, the circular failure surface option of the program based on the Modified Bishop method was used.

For each of the cases analyzed, 100 trial circular failure surfaces were generated and the corresponding factors of safety were calculated. The ten most critical surfaces were then considered in greater detail. Material properties and strength parameters were assigned on the basis of the laboratory test data, as well as other considerations, presented in Appendix A.

It should be noted that the material properties used in the analyses described herein are "average" properties which are based on a limited number of laboratory tests together with considerable engineering judgment. Since many of the dams considered in this investigation have very long crest lengths, it would be extremely difficult (and costly) to evaluate the subsurface conditions (and therefore the soil properties) along the entire length of each embankment.

It is common in engineering practice to drill a limited number of exploratory boreholes and/or excavate test pits to investigate the subsurface conditions at particular locations at a site and to obtain representative soil samples for

laboratory testing. This information is supplemented by a geologic evaluation of the site and, as in the case of an earth embankment, available construction records in order to establish "representative" soil profiles and embankment cross sections.

The stability analyses described in this Chapter were conducted in the following sequence:

1. Static (pre-earthquake) conditions.
2. Post-earthquake conditions.
3. Seismic stability including cumulative deformation evaluation.

Post-earthquake stability analyses were performed prior to the seismic and cumulative deformation analyses since the latter is not valid if the embankment slopes are found to be unstable under conditions following the earthquake.

The text of this chapter is organized in the following manner: The various stability analyses performed on Green's Lake Dam No. 3 and Ivins Diversion Dam No. 5 are presented first. The cross sections and strength parameters used in the analyses are also discussed. The stability analyses performed on the Warner Draw and Frog Hollow Dams are then described. The last section of this chapter summarizes the results of all the analyses and presents our conclusions regarding the overall performance and behavior of these dams during and after the ground shaking produced by the postulated Magnitude 6.0 earthquake.

Stability Evaluation - Green's Lake Dam No. 3 and Ivins Diversion Dam No. 5

The static and post-earthquake stability of the upstream and downstream slopes of Green's Lake Dam No. 3 and Ivins Diversion Dam No. 5 near their maximum cross sections was first investigated assuming steady-state seepage conditions. The phreatic surfaces corresponding to the reservoir levels at the principal (or primary) spillway crest elevations were developed using Casagrande's solution (Harr, 1962).

The effective strength parameters summarized in Table A-8 of Appendix A were used in the static stability analyses. The range of the ten most critical failure surfaces for the upstream and downstream slopes of Green's Lake Dam No. 3 and Ivins Diversion Dam No. 5 under this loading condition are summarized in Table VII-1. For comparitive purposes, the factors of safety for infinite slope type failures are also given in this table.

Table VII-1

Summary of Factors of Safety Under Steady-State Seepage Conditions - Green's Lake No. 3 and Ivins Diversion No. 5 Dams

	Range of Factors of Safety for the 10 Most Critical Failure Surfaces			
	Green's Lake No. 3		Ivins Diversion No. 5	
Type of Analysis	Upstream	Downstream	Upstream	Downstream
Static	1.9 - 2.1	1.3 - 1.6	2.3 - 2.9	1.2 - 1.4
Infinite Slope	2.1	1.4	2.3	1.6
Post-Earthquake	$\leq$ 1.0	$\ll$ 1.0	1.5 - 1.6	$\ll$ 1.0

For the upstream slopes of both embankments, the ten most critical failure surfaces vary from infinite slope type and shallow failures to deep-seated failures which involve a significant portion of the embankments' crests. Factors of safety for Green's Lake Dam No. 3 range from 1.9 to 2.1 and 2.3 to 2.9 for Ivins Diversion Dam No. 5. Plots showing failure surfaces which involve the dam crests are shown in Figures VII-1 and VII-2 for Green's Lake Dam No. 3 and Ivins Diversion Dam No. 5, respectively.

For the downstream slope of Green's Lake Dam No. 3, the ten most critical failure surfaces involve primarily the embankment soils. The failure surfaces range from shallow infinite slope failures to failures starting at the toe and ending up at the crest of the embankment. Factors of safety range from 1.3 to 1.6. The ten most critical failure surfaces for Ivins Diversion Dam No. 5 are deeper failure

surfaces involving the dam crest and are caused by the weaker foundation conditions at this site. The factors of safety range from 1.2 to 1.4. It is important to note that the factors of safety for the downstream slopes of both embankments are significantly lower than the upstream slopes under static, steady-state seepage conditions. This is due to the steeper downstream slopes which are 2(H):1(V) versus 3(H):1(V) for the upstream slopes.

The post-earthquake stability of the upstream and downstream slopes of the two embankments was also evaluated assuming the steady-state seepage conditions described above. The post-earthquake effective strength parameters summarized in Table A-14 were used in these analyses and the factors of safety are listed in Table VII-1. With the exception of the upstream slope of Ivins Diversion Dam No. 5, the factors of safety for this condition indicate that failure of the embankments would occur during or after the earthquake ground shaking postulated for these sites. The high excess pore pressures that would be built up in the foundation soils during the earthquake result in a severe reduction in the shear strengths of these soils. If steady-state seepage conditions exist at the time of the earthquake, the stability analyses indicate that either deep-seated rotational-type failures and upstream and/or downstream movement of the embankment would occur. Failures would involve the dam crest and significant portions of the foundation soils, leading to overtopping or breaching of the embankments.

While the embankments are unstable under post-earthquake loading when steady-state seepage conditions are assumed, it is of interest to investigate the stability of the dams if different conditions were to exist at the time of the earthquake.

One of the parameters which greatly affects the results of the analyses is the build-up in excess pore pressure that occurs during earthquake shaking. The results of cyclic triaxial tests performed on the foundation soils obtained from the two embankment sites indicate that very high excess pore pressures will develop during cyclic loading (see Appendix A). If the actual pore pressures that develop in the field are less than those measured in the laboratory, how much less do they have to be in order to maintain stable slope conditions? A number of stability analyses were performed to answer this question.

The analyses were again performed by assuming that steady-state seepage conditions exist at the time of the earthquake. The pore pressure parameters of the foundation soils were varied until marginally stable slope conditions were obtained. Since the upstream slope of Ivins Diversion Dam No. 5 was found to be stable in the previous post-earthquake stability analysis, this slope was not re-analyzed. Results of the analyses performed on the downsteam slope of Green's Lake Dam No. 3 indicate that the in situ pore pressures would have to be approximately 60 percent less than those used in the previous post-earthquake stability analyses in order for the slope to be nearly (or marginally) stable. Similarly, the downstream slope of Ivins Diversion Dam No. 5 becomes marginally stable if pore pressures are assumed to be approximately 70 percent less than those used in the previous analyses. These results clearly show that, if steady-state seepage conditions exist at the time of the earthquake, even relatively moderate increases in pore pressures would cause strength reductions in the foundation soils resulting in unstable slope conditions.

The stability of the slopes is also affected by the position of the phreatic surface. If a phreatic surface different than the steady-state seepage condition is assumed, do the downstream slopes of the embankments become stable under post-earthquake loading conditions? Analyses were also performed to evaluate the influence of the location of the phreatic surface on the embankment stability. The two phreatic surfaces illustrated in Figure VII-3 were assumed and the stability of the slopes under static and post-earthquake loading conditions was evaluated. The effective strength parameters summarized in Tables A-13 and A-14 were used in the static and post-earthquake analyses, respectively. Factors of safety for the Case A phreatic surface condition are summarized in Table VII-2.

Table VII-2

Summary of Factors of Safety Under Lowered Phreatic Conditions (Case A) - Green's Lake No. 3 and Ivins Diversion No. 5 Dams

	Range of Factors of Safety for the 10 Most Critical Failure Surfaces			
	Green's Lake No. 3		Ivins Diversion No. 5	
Type of Analysis	Upstream	Downstream	Upstream	Downstream
Static	1.9 - 2.4	1.3 - 1.6	---	1.7 - 1.9
Post-Earthquake	$\leq$ 1.0	$\ll$ 1.0	---	$\ll$ 1.0

The static stability of both downstream slopes is only slightly improved for the phreatic surface condition shown by Case A in Figure VII-3. The ten most critical failure surfaces for the downstream slope of Green's Lake Dam No. 3 are relatively shallow or are infinite slope type failures involving only embankment soils. The failure surfaces for Ivins Diversion Dam No. 5 are also relatively shallow, however, they involve a small amount of foundation soils. Typical failure surfaces for Case A are shown in Figures VII-1 and VII-2 for the two embankments.

The post-earthquake stability of the downstream slopes are not improved for the Case A phreatic surface shown in Figure VII-3. The stability analyses indicate that deep failures would still occur in these slopes. The upstream slope of Green's Lake Dam No. 3 is also unstable under this condition.

Finally, the static and post-earthquake stability of the upstream and downstream slopes of the embankments was evaluated for the phreatic surface shown for Case B in Figure VII-3. This phreatic surface represents unsaturated downstream foundation conditions. It is only for this condition that the downstream slopes remain stable following the postulated earthquake. The stability of the upstream slope of Green's Lake Dam No. 3, however, is unaffected by the Case B phreatic surface assumed. If the upstream foundation soils of this embankment are saturated at the time of the earthquake, failure of this slope is likely. Typical failure surfaces for this slope are deep rotational failures involving the dam crest.

Stability Evaluation - Warner Draw and Frog Hollow Dams

The stability of Warner Draw and Frog Hollow Dams was evaluated under static, seismic, and post-earthquake loading conditions. The objective of the analyses described herein was to evaluate the overall performance and behavior of these dams prior to, during, and after the occurrence of the postulated Magnitude 6.0 earthquake.

From the results of analyses presented in Appendix G and laboratory test results in Appendix A, it was determined that the soils comprising these embankments were not subject to liquefaction but could experience moderate reductions in strength as a result of cyclic loading when saturated.

Static stability analyses were performed using the effective strength parameters summarized in Table A-8 and phreatic surfaces approximating steady-state seepage conditions. Reservoir levels were assumed to be at the principal spillway crest elevations. Effective strength parameters for the Zone III soils comprising the shell of Warner Draw Dam were assumed to be equal to those obtained for the Zone I materials. The Zone II materials, old embankment fill, and downstream "waste" materials, at Frog Hollow Dam were assumed to have an effective friction angle of 40°. The soils comprising Zone II and old embankment fill of Frog Hollow Dam are medium-dense to dense coarse sands and gravels with cobbles in a silty and/or clayey matrix. The downstream waste materials consist of basalt rubble.

The range of factors of safety obtained from the static stability analyses of these two embankments are summarized in Table VII-4. The failure surfaces for the ten most critical factors of safety for both slopes of Warner Draw Dam and the downstream slope of Frog Hollow Dam range from infinite slope type failures to relatively shallow failures involving the dam crest. The failure surfaces for the upstream slope of Frog Hollow Dam range from shallow to deep-seated failures involving significant portions of the dam crest.

Table VII-4

Summary of Factors of Safety Under Steady-State Seepage Conditions - Warner Draw and Frog Hollow Dams

Type of Analysis	Range of Factors of Safety for the 10 Most Critical Failure Surfaces			
	Warner Draw		Frog Hollow	
	Upstream	Downstream	Upstream	Downstream
Static	2.2 - 2.4	1.5 - 1.9	3.6 - 3.8	2.5 - 2.8
Infinite Slope	2.3	1.5	*	*
Post-Earthquake	1.6	1.2 - 1.3	4.0 - 4.3	2.7 - 3.0

Note:

(*) Not evaluated due to geometry of the embankment.

Post-earthquake analyses of both embankments were conducted to establish their stability after having been subjected to the postulated earthquake ground motions. For this case, the post-earthquake effective strength parameters listed in Table A-14, and the average post-cyclic undrained strength parameters listed in Table A-13, were utilized for saturated portions of Warner Draw and Frog Hollow Dams, respectively. The effective strength parameters listed in Table A-8 were used for the unsaturated portions of the embankments. The phreatic surfaces corresponding to steady-state seepage conditions were used. The ranges of factors of safety for the post-earthquake stability analyses are summarized in Table VII-4. Typical failure surfaces for the upstream and downstream slopes of the two embankments are shown in Figures VII-4 and VII- 5.

The failure surfaces for the downstream slope of Warner Draw Dam are deep failures involving the entire dam crest (see Figure VII-4). Failure surfaces for the upstream slope include shallow and deep surfaces. The factors of safety for both slopes are reduced from those of the static stability analysis due to the reductions in shear strength of the soils caused by cyclic loading.

The failure surfaces and factors of safety for the downstream slope of Frog Hollow Dam are only slightly affected by cyclic loading. The factors of safety for

the upstream slope, on the other hand, are slightly greater than the static steady-state seepage condition. This is the result of the higher cohesions exhibited by the clayey Zone I soils under undrained loading conditions versus the smaller apparent cohesion in drained loading. The failure surfaces for the post-earthquake stability analyses of the upstream slope are similar to those obtained from the static analyses. An example which involves a portion of the dam crest is shown in Figure VII-5.

The results of the post-earthquake stability analyses described above indicate that the slopes of both Warner Draw and Frog Hollow Dams should remain stable following the postulated earthquake. However, during earthquake ground shaking, the embankments may undergo some permanent deformations. The following text describes the method used to estimate these deformations.

Cumulative Deformation Analyses

Pseudo-static methods of slope stability have often been used in the past to evaluate the seismic stability of earth dams. This method is a limit-equilibrium method in which the resistance along a postulated failure surface is based on the static strength of the soil, and an additional horizontal force is added to represent the inertia forces produced by the design earthquake.

With the development of sophisticated analytical techniques in recent years, the pseudo-static method of analysis has often been criticized as not truly representing the effects of earthquake loading on an embankment. The accuracy of pseudo-static methods is limited by two factors. The first is that the actual inertia forces developed during an earthquake are cyclic in nature, rather than a single force acting in one direction; and the second is that the method, as usually applied, does not consider the possible loss in strength of soils subjected to cyclic loading. This second factor is especially important for loose saturated granular soils and hydraulic fill materials which may develop large cyclic or permanent strains under undrained cyclic loading. Nonetheless, pseudo-static methods of analysis have, until quite recently, continued to be used by many engineers.

Another method of analysis which does take account of the reversing inertia forces generated during an earthquake was proposed by Newmark (1965). Since the development of Newmark's original cumulative deformation procedure, additional modifications and improvements have been made by various investigators (Sarma, 1975; Franklin and Chang, 1977; Makdisi and Seed, 1978). The various published procedures are quite similar and will generally give similar results when used properly. This type of analysis has recently received considerable attention and appears to provide a simple procedure for estimating the magnitude of earthquake-induced deformations of slopes and embankments consisting of soils which do not liquefy or undergo significant strength loss under cyclic loading (Seed, 1979b). Since it has been demonstrated in the previous section of this chapter that both the Warner Draw and Frog Hollow Dams would remain stable after earthquake shaking, this approach was used to estimate the amount of permanent deformations which the two embankments might undergo as a result of the postulated earthquake motions.

The initial step in the analysis is to establish the value of the yield acceleration, k_y, corresponding to the critical failure surface using pseudo-static methods of analysis and appropriate values of soil shear strength. Horizontal seismic coefficients ranging from 0.05 to 0.35 g were used in these analyses to establish the factor of safety for the critical failure surfaces shown in Figure VII-4 and VII-5. These surfaces were determined from the post-earthquake stability analyses. The results of the pseudo-static analysis show the variation of factor of safety with the seismic coefficient acting on the critical failures surfaces of the two embankment cross sections. The yield acceleration is defined as the seismic coefficient which produces a factor of safety of 1.0. The yield accelerations obtained for the two dam cross sections are summarized in Table VII-5.

Table VII-5

Seismic Coefficient Corresponding to a Factor of Safety of One

Dam	Yield Acceleration, k_y(g) Upstream Slope	Downstream Slope
Warner Draw	0.20	0.10
Frog Hollow	0.45	0.45

The next step in the analysis requires that the average accelerations corresponding to the critical failure surfaces be evaluated. As shown in Figures VII-4 and VII- 5, the various critical failure surfaces all extend from near the toe of the embankment to the crest. Makdisi and Seed (1978) have summarized the results of various dynamic analyses performed on a number of dams and have developed relationships which allow an estimate of the average maximum acceleration, k_{max}, for a particular location of the critical sliding surface to be made once the maximum crest acceleration, u_{max}, is known. For the postulated Magnitude 6.0 earthquake, the estimated maximum crest accelerations computed from the dynamic response analyses presented in Appendix F were found to be approximately 0.48 g and 0.45 g for the Warner Draw and Frog Hollow Dam embankments, respectively (see Table F-3). For critical surfaces which extend over the entire height of the embankment cross sections, values of about 0.17 g and 0.16 g are obtained for the average maximum accelerations.

Having established the yield acceleration and average maximum acceleration for the critical failure surfaces, an estimate of the amount of permanent deformation can be calculated. Makdisi and Seed (1978) have conducted analyses of this type using a range of yield accelerations, average maximum accelerations, and strong-motion records corresponding to various earthquake magnitudes. Their results are presented in Figure VII-6. With the exception of the downstream slope of Warner Draw Dam, the ratio of the yield acceleration to the average maximum acceleration is always greater than 1.0. Figure VII-6 indicates that for these values of acceleration ratio, the amount of permanent deformation resulting from the postulated earthquake ground motions would be insignificant.

For the downstream slope of Warner Draw Dam, an acceleration ratio, k_y/k_{max}, of 0.59 is obtained. A value for $U/k_{max} \times g \times T_o$ approximately equal to 0.01 is obtained from Figure VII-6 for a Magnitude 6.5 earthquake. To complete the calculation of the amount of permanent deformation, the fundamental period, T_o, of the embankment must be known. This value was calculated in Appendix F and is tabulated in Table F-4. A value of T_o approximately equal to 0.40 second was calculated using the average shear wave velocity obtained from the dynamic response analysis of this cross section. Using this value of the fundamental period, the amount of permanent deformation expected to occur in the downstream slope of Warner Draw Dam is estimated to be less than 1 inch. Thus, on the basis of the cumulative deformation procedure, virtually no deformation would be expected to develop in either the Warner Draw or Frog Hollow Dams during the postulated Magnitude 6.0 earthquake.

Other Considerations Related to Dam Stability

The stability analyses described above are based on representative cross sections of the dam embankments developed from a review of SCS files and results of our field investigation. Strength parameters used in the analyses were based on results of static and cyclic triaxial tests performed on soil samples obtained during the Phase I field investigation and engineering judgment. The models of the embankment slopes and foundation soils were developed assuming that uniform soil conditions exist throughout the embankment cross sections. This assumption (or approximation) is one that is commonly made in analyses of this type. In the cases of Green's Lake Dam No. 3 and Frog Hollow Dam, however, this assumption may not be reasonable and is the topic of the discussions that follow.

In the Phase I report (see Appendix G), the operational problems that have occurred at Green's Lake Dam No. 3 were summarized. The dams and foundation soils have been subject to subsidence and extensive cracking since 1963. Cracks in the embankment and foundations widened due to erosion and piping and some block rotation occurred along portions of the dam crest. Repairs to the cracks in the embankment and reservoir area were initiated in the spring of 1969. Cracks were filled with large quantities of soil-slurry mixture which was pumped into the voids. Most cracks in the dam were found to be interconnected while the cracks in the

reservoir were found to be generally shallow and not usually connected. At the time of the field investigation conducted during Phase I, cracks along the upstream face and transverse to the crest of the embankment were observed. Settlement along the dam crest was also quite noticeable.

Determination of the stability of the Green's Lake Dam No. 3 embankment is complicated by the factors described above. The factors of safety calculated for the downstream slope of this embankment under static steady-state seepage conditions indicate that it is stable (factors of safety range from 1.3 to 1.6) when uniform soil conditions are assumed. Since the strength parameters and true extent of the soil-slurry mixture present in the embankment and foundation could not be determined during the course of this investigation, the factors of safety for the "repaired" embankment could not be meaningfully evaluated. It is our judgment, however, that if stability analyses could be performed on a reasonable representation of the repaired embankment, the factors of safety for static steady-state seepage conditions would be significantly lower than those determined from the analyses presented in this report. Correspondingly, the stability of this embankment for other loading conditions would also be affected. Based on these considerations, it is our judgment that Green's Lake Dam No. 3 is probably only marginally stable under the present (unsaturated) conditions. If the embankment and foundation soils were to become saturated, unstable conditions may develop resulting in failure of the embankment.

Frog Hollow Dam has also experienced some cracking problems since the construction of the raised portion of the embankment in 1978 (see Appendix G of Phase I report). Cracks that formed were mostly transverse to the centerline of the embankment and were found to extend through the entire embankment. They ranged from 3 to 9 feet in depth. The cracking has been attributed to desiccation of the fill materials. Longitudinal cracking was also noted along the upstream face of the embankment. At the time of the writing of this report, the cracks in the embankment were not yet repaired and this problem was under a thorough investigation by the SCS.

During the drilling operations conducted as part of the Phase I field investigation, a zone of apparently low density materials was encountered. This

zone has been attributed to backfill which was poorly placed after the removal of an old 24 inch corrugated metal pipe (see Appendix G, Phase I report). While the laboratory tests conducted on these materials are somewhat weaker than the Zone I materials that were also tested, it is our judgment that it would not have a significant effect on the stability of the dam since it is confined to a relatively narrow zone.

The stability analysis of the Frog Hollow Dam embankment presented in this chapter indicates that, if the soils comprising the various zones of the embankment are more or less "uniform", then the dam should be stable under all the loading conditions considered in this investigation. As was the case for Green's Lake Dam No. 3, the cracking present within the embankment soils makes the actual stability of the dam extremely difficult to assess unless the cracks are properly repaired. If it is decided to repair the cracks in the embankment, we recommend that the materials within the zone of cracking be removed and replaced with a compacted engineered fill. The repaired embankment should then have properties which are similar to those used in this investigation and the results of the stability analyses previously described should be valid.

Summary and Conclusions

Detailed stability analyses have been performed on the following dams:

1. Green's Lake Dam No. 3
2. Warner Draw
3. Frog Hollow, and
4. Ivins Diversion Dam No. 5.

Warner Draw and Frog Hollow Dams have been analyzed under static, seismic, and post-earthquake loading conditions. Because of the poor foundation conditions present at Green's Lake Dam No. 3 and Ivins Diversion Dam No. 5, these dams were analyzed under only static and post-earthquake loading conditions. The results of the stability analyses and other considerations indicate the following:

1. Unstable slope conditions may develop, even under static loading conditions, if steady-state seepage conditions are allowed to develop at Green's Lake Dam No. 3.

2. The downstream slope of Ivins Diversion Dam No. 5 may be subject to failure under post-earthquake loading conditions if the foundation soils are allowed to become saturated.

3. Warner Draw Dam should behave satisfactorily during and after the postulated Magnitude 6.0 earthquake. Cumulative deformations consisting of downstream movement, settlement, and/or cracking should be negligible.

4. Frog Hollow Dam should behave satisfactorily during and after the postulated earthquake if the zones of cracking in the embankment are removed and repaired using a well-compacted engineered fill.

5. If the foundations and embankments are unsaturated at the time of the earthquake, all of the dams, with the exception of Green's Lake Dam No. 3, should behave satisfactorily during and after the earthquake. Under these conditions, some minor damage consisting of surficial raveling and/or cracking may occur which should not impair the performance of the dams.

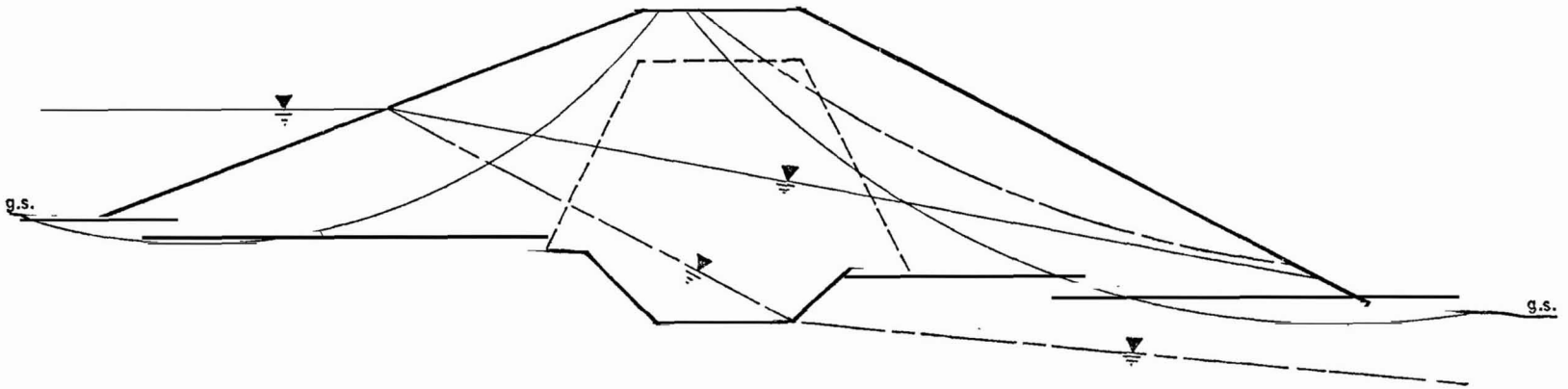

KEY

———— Phreatic surface and typical critical failure surface for steady state seepage conditon.

— — — — Phreatic surface and typical critical failure surface for assumed location of phreatic surface, Case A (Figure VII-3).

Earth Sciences Associates
Palo Alto, California

SEISMIC SAFETY INVESTIGATION OF EIGHT SCS DAMS
TYPICAL CRITICAL FAILURE SURFACES –
GREEN'S LAKE DAM NO. 3

Checked by MLT	Date 9/28/82	Project No.	Figure No.
Approved by Julio Valera	Date 9/29/82	D118	VII-1

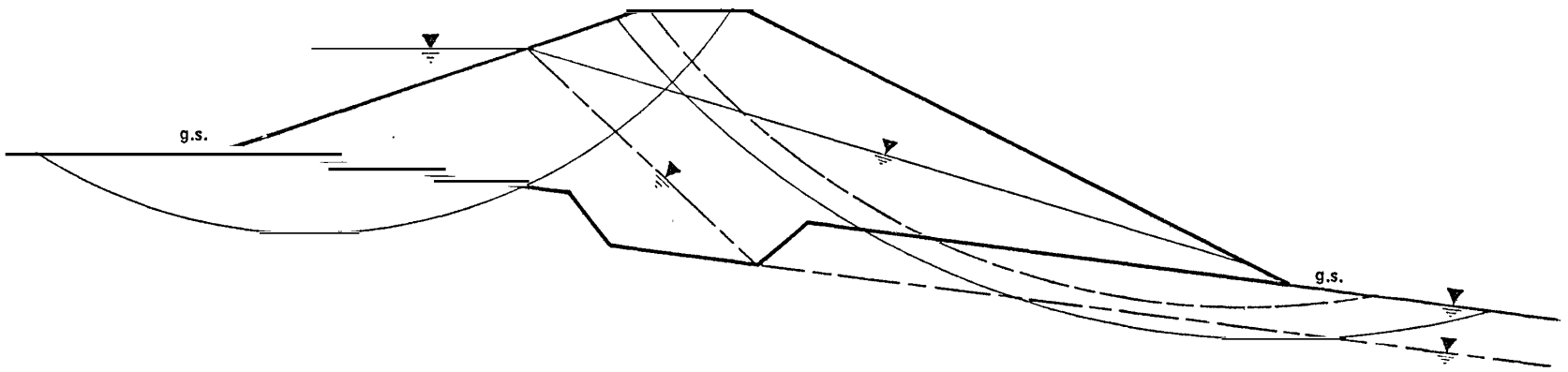

KEY

———— Phreatic surface and typical critical failure surface for steady state seepage conditon.

— — — — Phreatic surface and typical critical failure surface for assumed location of phreatic surface, Case A (Figure VII-3).

Earth Sciences Associates
Palo Alto, California

SEISMIC SAFETY INVESTIGATION OF EIGHT SCS DAMS
TYPICAL CRITICAL FAILURE SURFACES –
IVINS DIVERSION DAM NO. 5

Checked by MLT Date 9/29/82 Approved by Julio Valera Date 9/29/82	Project No. D118	Figure No. VII-2

CASE A

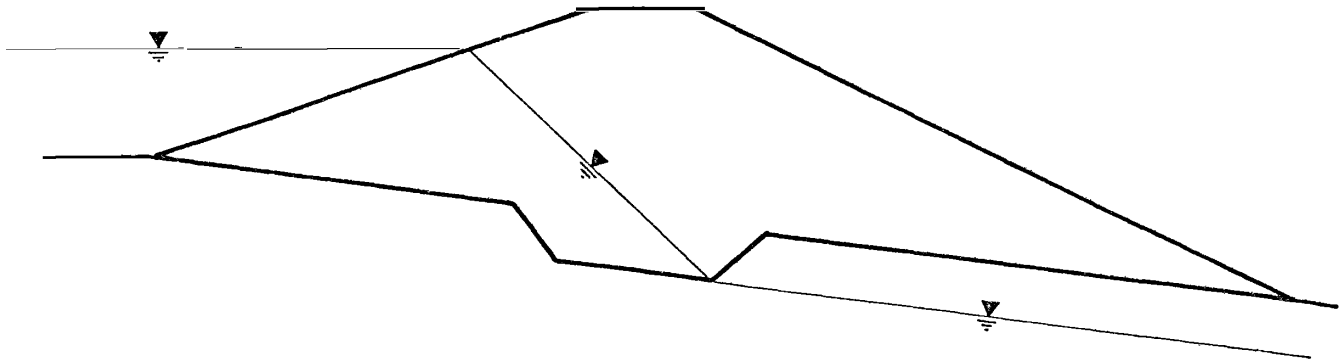

CASE B

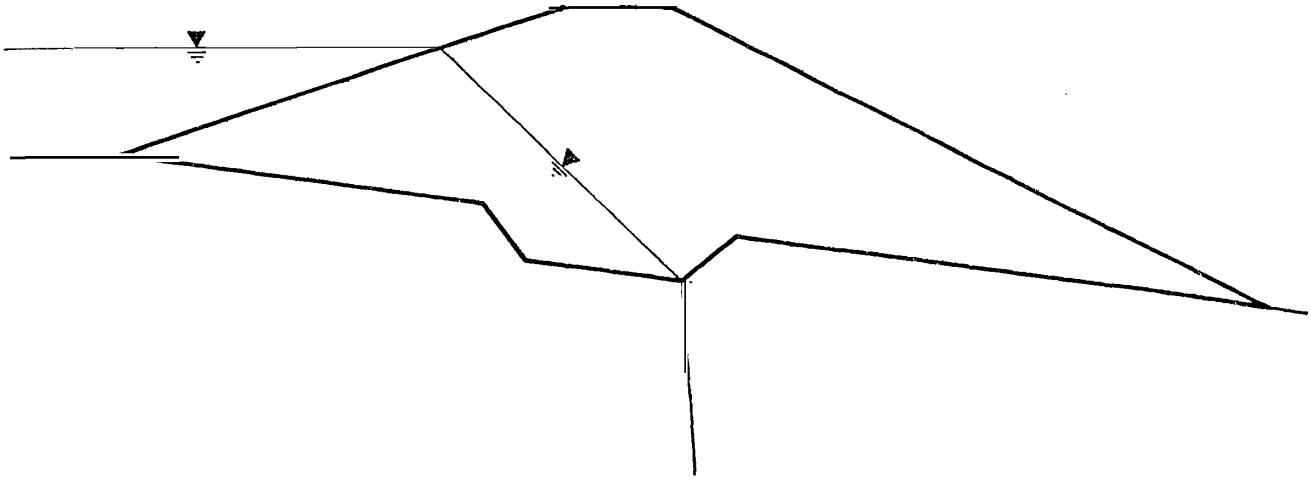

Earth Sciences Associates
Palo Alto, California

SEISMIC SAFETY INVESTIGATION OF EIGHT SCS DAMS
LOCATION OF ASSUMED PHREATIC SURFACES

Checked by MLT Date 9/28/82	Project No.	Figure No.
Approved by Julio Valera Date 9/29/82	D118	VII-3

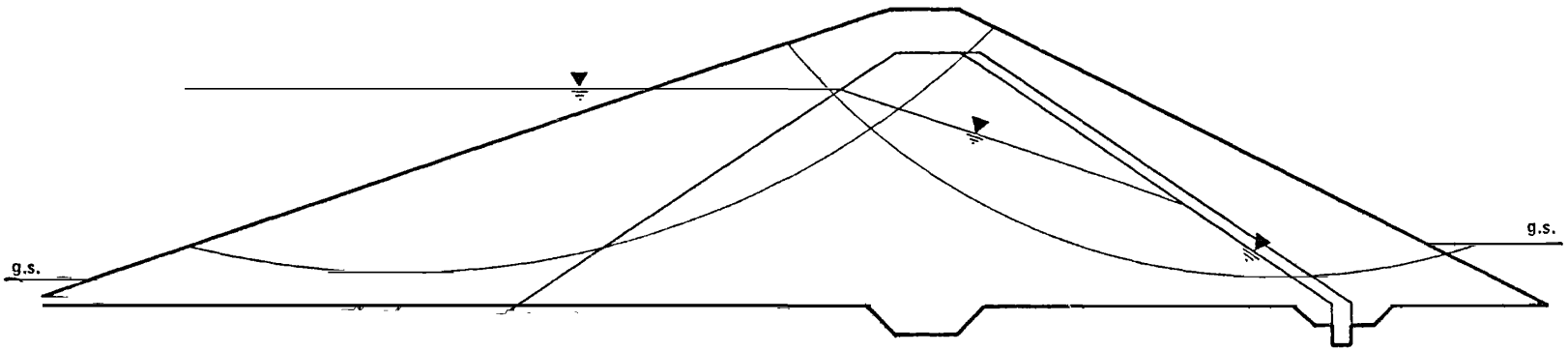

Earth Sciences Associates
Palo Alto, California

SEISMIC SAFETY INVESTIGATION OF EIGHT SCS DAMS
TYPICAL CRITICAL FAILURE SURFACES
POST-EARTHQUAKE STABILITY ANALYSES –
WARNER DRAW DAM

Checked by MLT Date 9/28/82	Project No.	Figure No.
Approved by Julio Valera Date 9/29/82	D118	VII-4

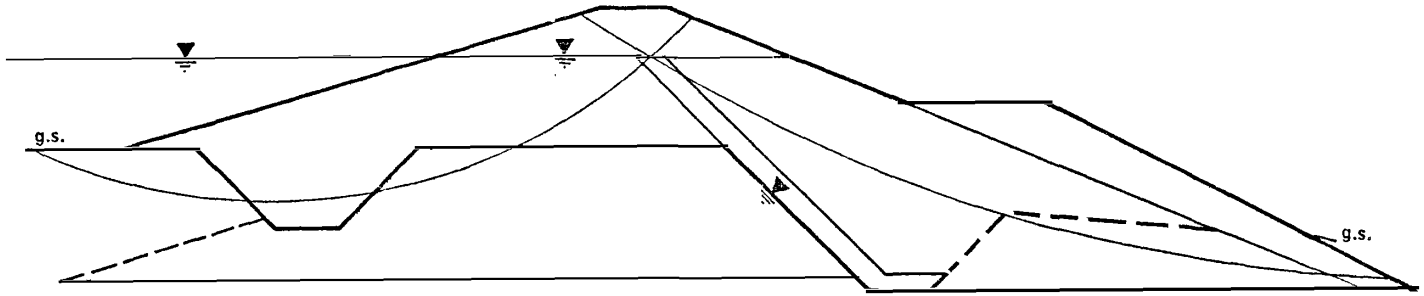

Earth Sciences Associates
Palo Alto, California

SEISMIC SAFETY INVESTIGATION OF EIGHT SCS DAMS
TYPICAL CRITICAL FAILURE SURFACES
POST-EARTHQUAKE STABILITY ANALYSES –
FROG HOLLOW DAM

Checked by MLT	Date 9/28/82	Project No.	Figure No.
Approved by Julio Valera	Date 9/29/82	D118	VII-5

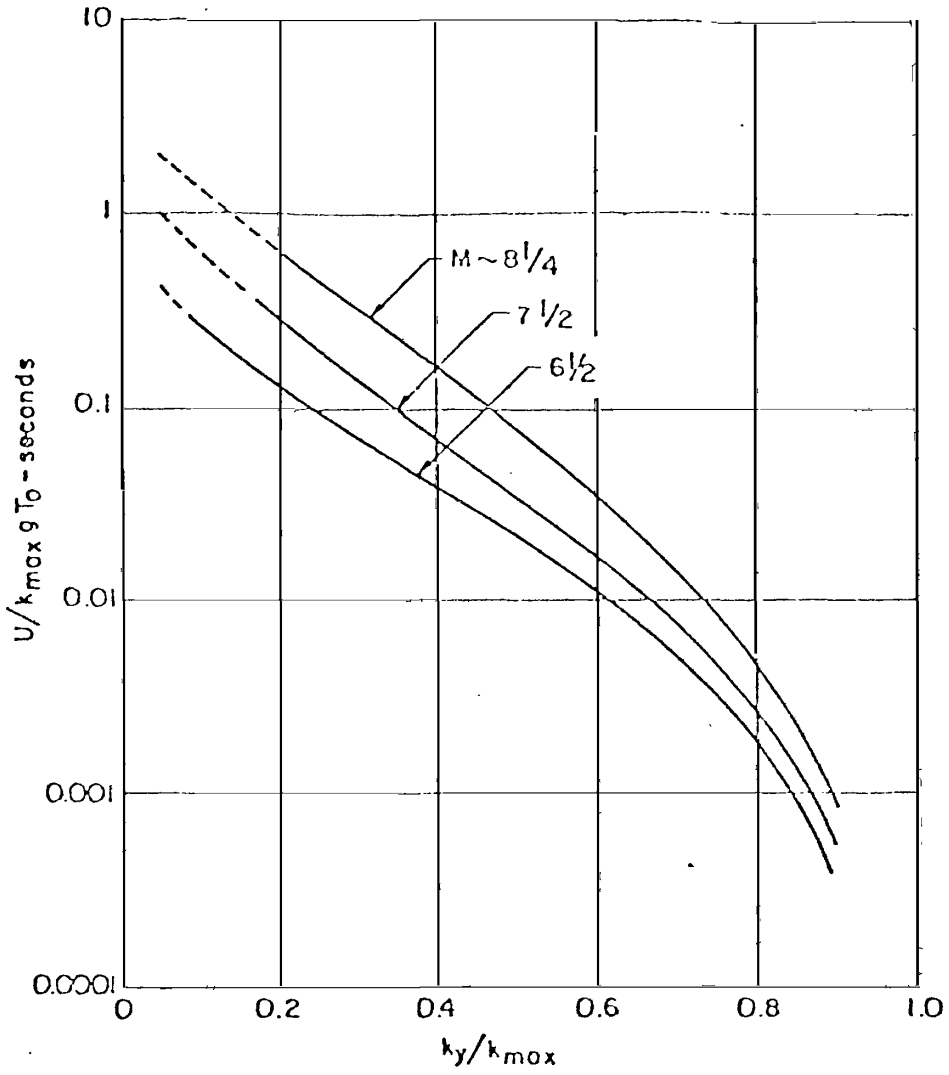

Earth Sciences Associates
Palo Alto, California

SEISMIC SAFETY INVESTIGATION OF EIGHT SCS DAMS
VARIATION OF AVERAGE NORMALIZED DISPLACEMENT WITH YIELD ACCELERATION RATIO

Checked by	Date	Project No.	Figure No.
Approved by Julio Valera	Date 9/29/82	D118	VII-6

VIII. EXPECTED PERFORMANCE AND RECOMMENDED REMEDIAL MEASURES

Potential causes of damage to the eight SCS dams located in Southwestern Utah have been addressed in detail in previous chapters of this report. The effects of fault rupture on those dams situated on, or in close proximity to, active faults are discussed in Chapter IV. The effects of strong ground shaking on the various dams associated with a near-field Magnitude 6 earthquake are addressed in Chapters VI and VII. Based on these studies it has been concluded that several of the dams could suffer considerable damage as a result of either fault offset or strong ground shaking if the dams impound a significant amount of water at the time of the earthquake. If the dams do not impound water prior to, during, or after an earthquake the hazards associated with these dams would be significantly reduced.

A summary of the major hazards associated with each dam site are tabulated in Table VIII-1, together with the expected performance of each embankment after either fault offset or ground shaking has occurred. This summary indicates that Green's Lake Dams No. 2 and 3 would have a high likelihood of a piping failure occurring within a period of a few hours to a few days after fault offset has occurred. Gypsum Wash Dam should perform fairly well if offset by fault movement. While the soils comprising this embankment may be subject to some erosion and/or piping under high heads, the "as-built" drawing of this embankment indicates that it has a six-foot wide chimney drain which would tend to prevent erosion of the embankment materials.

Table VIII-1 also indicates that Green's Lake Dam No. 3 and Ivins Diversion Dam No. 5 would perform poorly during and after the occurrence of the postulated Magnitude 6 earthquake. If the foundation soils at these two dams are allowed to become saturated, they could liquefy and/or suffer a significant loss of strength as a result of strong earthquake ground shaking. The performance of Frog Hollow Dam during and after the postulated earthquake should be good provided repairs to this structure are done in accordance with the general recommendations provided later in this chapter.

Based on the result of our studies, we recommend that the following measures be undertaken to mitigate the potential hazards posed by the possible failure of the above-mentioned dams:

Table VIII-1

Summary of Hazards and Expected Performance

Dam	Liquefaction Potential	Seismic Stability	Active Fault at Dam Site	Expected Performance	
				After Fault Offset	After Ground Shaking
Green's Lake No. 2	Low	N.A.	Yes	Poor	Good
Green's Lake No. 3	High	Poor	Yes	Poor	Poor
Green's Lake No. 5	Low	N.A.	Yes	Good	Good
Warner Draw	Low	Good	No	N.A.	Good
Gypsum Wash	Low	N.A.	Yes	Fair-Good	Good
Stucki	Low	N.A.	No	N.A.	Good
Frog Hollow	Low	Good[1]	No	N.A.	Good[1]
Ivins Diversion No. 5	High	Poor	No	N.A.	Poor

Notes: General

N.A. is indicated where detailed analyses were not performed or where hazard is not present.

Expected performance shown in table is based on results of detailed analyses presented in this report together with engineering judgment.

[1]Performance should be satisfactory provided repairs to the embankment are done in accordance with the general recommendations outlined in this report.

1. It is our judgment that the condition of the Green's Lake Dam No. 3 embankment and foundation soils at this site are so poor that this structure should be taken out of service. If it is decided to replace this structure, the following guidelines should be observed:

   a. Poor foundation soils should be identified and removed, or improved, before construction of the new embankment.

   b. The new embankment should be located, if possible, so as to avoid known active or potentially active faults.

   c. Since unmapped splays of the Hurricane fault system could exist at the site, the new embankment should be zoned to prevent erosion and/or piping failure in the event of fault rupture.

   d. The new structure should be operated in such a way as to release diverted flood waters as rapidly as possible.

2. It is our judgment that the reservoir level at Green's Lake Dam No. 2 should not be allowed to reach the emergency spillway elevation which results in only 2.5 feet of freeboard. Because of the potential for fault rupture at this site, a minimum of 4 feet of freeboard should be maintained.

3. The cracks present in the Frog Hollow Dam embankment should be repaired. Zones of cracking should be removed and replaced with a well compacted engineered fill. The fill materials should be similar to that used in the original, raised embankment. The cracks should not be repaired using a soil-slurry mixture. Measures to prevent dessication of the embankment soils may be desirable.

4. The possibility of saturated foundation conditions at Ivins Diversion Dam No. 5 should be investigated. This could be accomplished by installing piezometers along the downstream slope and toe of the embankment and measuring water level readings before, during, and

after flood stages. If it is found that the foundation soils remain unsaturated during and after floods, no remedial measures are necessary. If saturated conditions are found to exist, liquefiable (i.e., loose) foundation soils should be identified through a detailed field exploration program. Remedial measures would most likely consist of removal and/or improvement of the unsuitable soils.

To ensure that all of the eight dams perform satisfactorily at all times during their operational life we also recommend that the following safety procedures be put into effect:

1. All dams should be inspected at least once a year by trained personnel and the condition of the dams should be documented. Inspection should be conducted prior to disturbing the embankments and foundation soils. The need for any repairs or maintenance should be identified and attended to promptly. Proper maintenance of the trash racks and outlet works would ensure that the dams are operated as temporary flood control structures.

2. When any of the reservoirs contain a significant volume of water, the embankment should be carefully examined, as necessary, to make sure that there are no signs of distress.

3. If an earthquake producing strong ground shaking in the St. George or Cedar City areas occurs when the reservoirs contain water, the embankments should be examined as soon as possible after the earthquake, with priority given to Green's Lake Dam Nos. 2 and 3 and Ivins Diversion Dam No. 5. If any dam shows significant signs of distress, steps should be taken to evacuate areas that could be flooded by a dam failure or repairs (and/or other actions) to mitigate a failure should be made as quickly as possible.

4. If the reservoirs do not contain water at the time of the earthquake, the dams should be inspected for any damage that might render them ineffective as flood control structures.

5. An inundation map should be prepared for areas downstream from all the dams (if this has not been done) and copies should be made available to the local sheriff's departments with jurisdiction over areas subject to flooding.

6. An evacuation plan should be developed for the areas subject to severe flooding and the implementation of this plan worked out with the local sheriffs' offices in advance of a need to evacuate people from downstream areas.

APPENDICES

Table of Contents

Table of Contents (Continued)

Table of Contents (Continued)

Table of Contents (Continued)

APPENDIX A

LABORATORY INVESTIGATION

Appendix A

LABORATORY INVESTIGATION

Various laboratory tests were conducted on selected representative samples obtained from several of the dam embankments and their foundations. The following types of tests were performed:

- Moisture and density
- Sieve analysis (≤3/4")
- Hydrometer analysis
- Atterberg limits
- Standard Proctor compaction
- Consolidated-undrained triaxial; saturated with pore pressure measurements
- Stress-controlled cyclic triaxial and post-cyclic static testing to failure
- Pinhole dispersion
- Organic sample age dating

Moisture and density tests, sieve analysis, hydrometer analysis, and Atterberg limits tests were conducted to aid in identification and correlation of the different soil types. The grain size distribution of the various materials were also used to compare with the grain size distribution of soils which have liquified during previous earthquakes. These comparisons are presented in Appendix G. Standard Proctor compaction tests were performed to establish the optimum dry density and moisture content of representative materials and, thus, the relative compaction of the in situ soils. The results of these tests have been presented in Appendix D of the Phase I report.

"Average" static shear strengths of the embankment and foundation materials were established from the results of consolidated-undrained triaxial tests performed on saturated samples from Green's Lake No. 3, Warner Draw, Frog Hollow, and Ivins Diversion No. 5 dams and engineering judgment. Pore pressures were measured during shearing of the samples to failure. The liquefaction potential and cyclic strength characteristics of these materials under simulated earthquake loading conditions were established by performing stress-controlled cyclic triaxial tests. Where applicable, residual shear strengths were also obtained by conducting static consolidated-undrained triaxial tests on samples initially subjected to cyclic loading.

Pinhole tests were performed to establish the dispersion characteristics and piping potential of selected samples. Radiocarbon age dating determinations were made on several organic samples obtained within several of the trenches excavated as part of the Phase I field investigation.

Classification and Index Properties Tests

Atterberg limits tests consisting of determination of the liquid limit, LL, the plastic limit, PL, and the plasticity index (PI = LL - PL) were conducted on a number of fine-grained soil samples to establish the degree of plasticity of these soils. Many engineering properties can be correlated with the liquid limit and plasticity index of a soil. Results of these tests are summarized in Figures A-1, A-2, and A-3 and in Table A-2. In general, all of the soils tested have plasticity indexes less than 10 indicating that the materials have low plasticity. Liquid limits are in the range of 18 to 30 percent. Soil samples obtained from Ivins Diversion Dam No. 5 were found to be non-plastic.

The grain size distribution of a soil is established from sieve analyses and/or hydrometer tests. Gradation curves obtained from these types of tests for the embankment and foundation materials comprising the various dams are presented in Figures A-4 through A-10. The gradations for samples on which static and cyclic triaxial tests were performed are shown in Figures A-4 through A-7, whereas the gradations for samples on which pinhole dispersion tests were performed are shown in Figures A-8, A-9, and A-10.

Dispersion Characteristics

To establish the dispersibility and/or piping potential of the embankment and foundation materials at those dams where fault rupture could occur, a number of pinhole tests were conducted on selected samples. The pinhole test was performed in accordance with the procedure developed by Sherard and his associates (Sherard et al., 1976). The test is appropriate only for compacted fine-grained soils. The grain size distributions of the samples tested are shown in Figures A-8 through A-10 from which it can be seen that the samples generally range from sandy clays to clayey and silty sands.

The pinhole test result is evaluated from the appearance of the water, the rate of flow, and final size of the hole in the specimen. The test is highly reproducible and the results of each individual test can be categorized easily into one of the six categories shown in Table A-1.

Table A-1

Categories of Pinhole Test Results

Classification of Individual Test Results (1)	Classification of Soil (2)
D1 and D2	Dispersive soils: fail rapidly under 2-in. (50-mm) head.
ND4 and ND3	Intermediate soils: erode slowly under 2-in. (50-mm) or 7-in. (180-mm) head.
ND2 and ND1	Nondispersive soil: no colloidal erosion under 15-in. (380-mm) or 40-in. (1,020-mm) head.

Results of the pinhole tests are tabulated in Table A-2. All of the samples tested, except for two, classified as nondispersive soils. The remaining two classified as intermediate soils. None of the soils tested were found to be highly dispersive on the basis of the pinhole test results.

Table A-2

Summary of Pinhole Dispersion Test Results

Dam	Test Pit or Boring	Sample	Depth	Material	Soil Classification	Percent Passing #200	Atterberg Limits LL	Atterberg Limits PI	Dispersion Designation
Green's Lake No. 2	GL2/TP-2	Bulk	--	shell (Zone I)	SM-SC	39.0	18.8	4.2	ND1
	GL2/TP-5	Bulk	--	foundation	SM-SC	39.9	23.4	4.6	ND1
	GL2-1	PB-2/S-1	8.0-10.5	core (Zone II)	SM-SC	38.8			ND1
Green's Lake No. 3	GL3-1	B-9	18.0-19.5	core (Zone II)	SM	38.8	non-plastic		ND4
	GL3-1	B-12	26.0-27.5	foundation	SM	32.2	non-plastic		ND1
	GL3-1	PB-5/S-4	19.5-22.0	foundation	ML	59.9	25.0	6.6	ND1
Green's Lake No. 5	GL5/TP-1	Bulk	--	embankment	CL	88.9	32.1	14.4	ND2
	GL5/TP-2	Bulk	--	foundation	SM-SC	41.4	21.9	4.7	ND1
	GL5-1	PB-2/S-2	8.0-10.5	embankment	CL	89.2	29.5	13.5	ND3
Gypsum Wash	GW-TP3	Bulk	--	shell (Zone III)	SM	36.7	22.3	3.1	ND1
	GW-1	PB-6/S-6	25.0-27.5	core (Zone I)	ML	54.1	19.0	4.4	ND1
	GW-1	PB-2/S-2	8.5-11.0	core (Zone I)	CL-ML	57.5	20.3	4.9	ND1
Warner Draw	WD-1	B-16	57.8-59.5	core (Zone I)	SM-SC	29.9	20.6	5.8	ND1
	WD-1	B-8	31.5-33.0	core (Zone I)	SM-SC	34.7	20.1	7.1	ND1
Frog Hollow	FH-1	B-10	36.5-38.0	core (Zone I)	CL	87.7	30.7	9.6	ND1
	FH-2	B-14	29.5-31.0	core (Zone I)	CL-ML	52.6	21.6	6.6	ND1
	FH-4	B-2	51.5-53.0	core (Zone I)	CL	53.8	26.6	13.3	ND1

Radioactive Age-Dating Determinations

Charcoal samples obtained from certain exploratory trenches in the Cedar City area were submitted for C_{14} analysis in order to age-date the enveloping sedimentary deposits. These samples were collected from selected horizons in the trench walls by Mr. Dwight Hunt, Senior Geologist of Earth Sciences Associates, during the Phase I field investigation.

The samples were air-dried and thoroughly examined under a binocular microscope to remove all root hairs and other young organic material. Considerable time was required per sample to remove the visible organic contaminants. Because the charcoal grains were small and crumbly, no attempt was made to separate them from the matrix.

The results of the age dating determinations are summarized in Table A-3.

Strength Characteristics

A number of static and cyclic triaxial tests were conducted on representative, relatively undisturbed Pitcher samples (3 inches in diameter) of embankment and foundation soils, obtained during the Phase I field investigation, to evaluate their behavior under static, earthquake, and post-earthquake loading conditions. Tests were performed on samples obtained from the following dams:

- Green's Lake Dam No. 3
- Warner Draw
- Frog Hollow
- Ivins Diversion Dam No. 5

Where possible, samples were selected in pairs from the same Pitcher tube. One of the samples was failed statically, and the other sample was first subjected to a prescribed cyclic loading and, then, subsequently failed by application of a static load. In some cases, the sample liquefied dramatically during the cyclic loading portion of the test and it was not possible to perform the post-cyclic static test.

Table A-3

Summary of Age-Dating Determinations

Sample #	Sample Location and Relationship to Fault(s)	Testing Laboratory	Results
GL-5a	Green's Lake Dam No. 5, north dike; offset alluvium, east side of Cross Hollow Hills; western margin of Hurricane fault zone.	Teledyne Isotopes, N. J.	Sample of insufficient volume; resubmitted to University of Arizona for testing by mass accelerator technique. Results anticipated in late 1982.
GL-3b-02 (1 of 2)	Green's Lake Dam No. 3, right abutment; unbroken alluvial fan deposits overlying ruptured bedrock; main lineament and mapped trace of Hurricane fault.	Teledyne Isotopes, N. J.	Sample of insufficient volume; resubmitted to University of Arizona. Sample age: 3470 years B. P., ± 260.
(2 of 2)	"	Geochron Laboratories, Mass.	Sample age: 4100 years B. P. ± 660.
GL-3b-87	"	Geochron Laboratories, Mass.	Sample of insufficient volume.
GL-2d-87	Green's Lake Dam No. 2; unbroken alluvial fan deposits along projection of suspected rupture, Hurricane fault zone.	Geochron Laboratories, Mass.	Sample of insufficient volume.
GL-3a	Green's Lake Dam No. 3; unbroken alluvial fan deposits along projection of major lineament and mapped trace of Hurricane fault.	Teledyne Isotopes, N. J.	Sample age: 1060 years B. P., ± 100.

Prior to testing, the majority of the samples were initially saturated and consolidated isotropically (K_c = 1) to a range of effective stress conditions representative of those existing in the field. In order to ensure complete saturation of the samples, a backpressure was applied to all samples tested.

Summaries of the static and cyclic triaxial tests performed on the soils obtained from the four dams are tabulated in Tables A-4 through A-7.

Static Triaxial Tests

A series of consolidated-undrained triaxial tests with pore pressure measurements were conducted to establish average effective and undrained strength parameters of the different soil types present at the four dam sites under consideration. Test results including stress-strain relationships for each test are included in Appendix B. These results generally indicate an increase in deviator stress with increasing axial strain and a tendency for the pore pressures to initially increase for axial strains in the range of 1 to 3 percent and then to decrease for higher strain levels. Based on these results, an axial strain of 5 percent was conservatively selected as an appropriate strain value at which to evaluate strength characteristics for stability analyses of the downstream and upstream slopes of the selected dam embankments.

In Figures A-11 through A-14, the static test results corresponding to an axial strain of 5 percent have been plotted in terms of effective stress parameters. On these figures, the value of $\bar{p}$ (i.e., $\bar{\sigma}_1 + \bar{\sigma}_3/2$) has been plotted against the shear strength, q (i.e., $\bar{\sigma}_1 - \bar{\sigma}_3/2$). The straight line drawn through the data points represents the "average" effective strength failure line (K_f line). Values of effective strength parameters established on the basis of these results are tabulated in Table A-8.

TABLE A-4
SUMMARY OF TRIAXIAL TESTS
GREEN'S LAKE DAM NO. 3

	TEST NUMBER	BORING/ SAMPLE NUMBER	DEPTH (ft.)	LOCATION	SOIL CLASSIFI-CATION	SOIL TYPE	RELATIVE* COMPACTION BEFORE CONSOL. (%)	K_c	σ_{3c} (psf)	σ_{1c} (psf)	BEFORE CONSOLIDATION			AFTER CONSOLIDATION			% PASSING NO. 200 SIEVE
											H (in.)	W/C (%)	γ dry (psf)	H (in.)	W/C (%)	γ dry (pcf)	
SUMMARY OF STATIC TRIAXIAL TESTS	S-1A	GL3-1/PB2-S2	8.0-10.5	embankment	SM	silty sand	93	1.0	1109	1109	6.00	13.8	114.3	5.97	–	–	40.6
	S-1B	"	"	"	"	"	–	1.0	2218	2218	–	–	–	5.42	15.0	117.6	–
	S-2	GL2-1/PB6-S5	24.0-26.5	foundation	SC	clayey sand with gravel	N.A.	1.0	2174	2174	5.98	12.2	116.8	5.92	13.0	117.4	35.9
	S-3	GL3-1/PB9-S8	35.5-38.0	foundation	ML-CL	clayey silt / silty clay	N.A.	1.0	3053	3053	5.94	13.5	105.1	5.85	19.2	105.6	62.3
	S-4A	GL3-1/PB6-S5	23.5-26.0	foundation	SM	silty sand	90	1.0	2174	2174	5.77	13.2	110.8	5.72	–	–	34.6
	S-4B	"	"	"	"	"	–	1.0	4349	4349	–	–	–	5.48	16.5	112.5	–
	S-5	GL2-1/PB2-S1	8.0-10.5	embankment	SM	silty sand	96	1.0	1354	1354	5.89	8.5	118.4	5.84	13.9	118.7	38.8
	S-6	GL3-2/PB6-S4	25.5-28.0	foundation	SM	silty sand with gravel	N.A.	1.0	2016	2016	5 98	12.4	119.9	5.95	13.9	120.1	16.4
	S-7A	GL3-2/PB7-S5	29.5-32.0	foundation	SM	silty sand	N.A.	1.0	3024	3024	5.98	22.8	99.7	5.97	–	–	36.5
	S-7B	"		"	"	"	—	1.0	6048	6048	–	–	–	5.91	19.8	100.0	–
SUMMARY OF CYCLIC TRIAXIAL TESTS	C-1	GL3-1/PB2-S2	8.0-10.5	embankment	SM	silty sand	94	1.0	1109	1109	6.00	12.3	116.2	5.97	15.2	116.4	43.5
	C-2	GL3-2/PB6-S4	25.5-28.0	foundation	SM	silty sand with gravel	N.A.	1.0	2016	2016	5.94	13.3	113.5	5.89	14.9	113.8	16.2
	C-3	GL3-2/PB7-S5	29.5-32.0	foundation	SM	silty sand	N.A.	1.0	3024	3024	6.00	13.5	108.6	5.97	21.8	108.8	10.9
	C-4	GL2-1/PB2-S1	8.0-10.5	embankment	SM	silty sand	N.A.	1.0	1354	1354	5.81	9.6	114.7	5.80	23.5	114.8	66.3

*Relative compaction determined from compaction tests performed during Phase I on similar material types. "N.A" applies to those samples for which compaction test data are not available.

TABLE A-5
SUMMARY OF TRIAXIAL TESTS
WARNER DRAW DAM

	TEST NUMBER	BORING/ SAMPLE NUMBER	DEPTH (ft.)	LOCATION	SOIL CLASSIFI-CATION	SOIL TYPE	RELATIVE* COMPACTION BEFORE CONSOL. (%)	K_c	σ_{3c} (psf)	σ_{1c} (psf)	BEFORE CONSOLIDATION			AFTER CONSOLIDATION			% PASSING NO. 200 SIEVE
											H (in.)	W/C (%)	γ dry (psf)	H (in.)	W/C (%)	γ dry (pcf)	
SUMMARY OF STATIC TRIAXIAL TESTS	S-1	WD-1/PB2-S2	8.5-11.0	embankment	SM	silty sand	105	1.0	1440	1440	6.00	8.5	124.5	6.00	13.6	124.5	20.1
	S-2	WD-1/PB6-S6	25.0-27.5	embankment	SC-SM	clayey sand/silty sand	111	1.0	2678	2678	5.97	12.7	122.1	5.91	11.8	122.5	28.1
	S-3	WD-1/PB10-S10	41.0-43.5	embankment	SC-SM	clayey sand/silty sand	108	1.0	3902	3902	6.00	11.0	127.0	5.98	11.1	127.2	20.5
	S-4	WD-1/PB13-S13	53.0-55.5	embankment	SC-SM	clayey sand/silty sand	N.A.	1.0	4810	4810	6.00	11.7	124.8	5.92	10.8	125.3	29.2
	S-5	WD-2/PB6-S6	24.5-27.0	embankment	SC-SM	clayey sand/silty sand	N.A.	1.0	2678	2678	6.00	9.4	130.6	5.97	10.5	130.8	24.7
	S-6A	WD-2/PB2-S2	8.5-11.0	embankment	SC-SM	clayey sand/silty sand	108	1.0	1440	1440	5.98	9.8	129.3	5.94	–	–	23.0
	S-6B	"	"	"	"	"	–	1.0	2880	2880	–	–	–	5.68	11.1	131.6	23.0
	S-7A	WD-2/PB13-S13	52.5-55.0	embankment	SC	clayey sand	114	1.0	5198	5198	6.07	10.5	125.6	5.98	–	–	34.2
	S-7B	"	"	"	"	"	–	1.0	7790	7790	–	–	–	5.70	9.2	127.9	–
SUMMARY OF CYCLIC TRIAXIAL TESTS	C-1	WD-1/PB2-S2	8.5-11.0	embankment	SM	silty sand	103	1.0	1440	1440	6.00	9.9	122.8	6.00	12.0	122.8	19.5
	C-2	WD-2/PB6-S6	24.5-27.0	embankment	SC-SM	clayey sand/silty sand	N.A.	1.0	2678	2678	5.97	11.1	121.2	5.90	11.3	121.7	24.3
	C-3	WD-1/PB10-S10	41.0-43.5	embankment	SC-SM	clayey sand/silty sand	N.A.	1.0	3902	3902	5.98	10.5	127.4	5.93	9.8	127.7	23.9
	C-4	WD-1/PB13-S13	53.0-55.5	embankment	SC-SM	clayey sand/silty sand	N.A.	1.0	4810	4810	5.97	11.3	124.7	5.88	10.1	125.3	24.4
	C-5	WD-2/PB6-S6	24.5-27.0	embankment	SC-SM	clayey sand/silty sand	N.A.	1.5	2448	3672	5.99	10.4	123.6	5.89	11.0	124.4	27.1

*Relative compaction determined from compaction tests performed during Phase I on similar material types. "N.A" applies to those samples for which compaction test data are not available.

TABLE A-6
SUMMARY OF TRIAXIAL TESTS
FROG HOLLOW DAM

	TEST NUMBER	BORING/ SAMPLE NUMBER	DEPTH (ft.)	LOCATION	SOIL CLASSIFI-CATION	SOIL TYPE	RELATIVE* COMPACTION BEFORE CONSOL. (%)	K_c	σ_{3c} (psf)	σ_{1c} (psf)	BEFORE CONSOLIDATION			AFTER CONSOLIDATION			% PASSING NO. 200 SIEVE
											H (in.)	W/C (%)	γ_{dry} (psf)	H (in.)	W/C (%)	γ_{dry} (pcf)	
SUMMARY OF STATIC TRIAXIAL TESTS	S-1A	FH-2/PB6-S4	23.0-25.5	foundation	CL	sandy clay	91	1.0	1800	1800	5.91	19.8	107.1	5.83	—	—	60.2
	S-1B	"	"	"	"	"	—	1.0	2707	2707	—	—	—	5.60	18.1	108.7	—
	S-2	FH-1/PB6-S5	22.5-25.0	embankment	CL	sandy clay	97	1.0	2707	2707	6.00	16.5	113.7	5.97	19.3	113.7	63.7
	S-3	FH-1/PB10-S9	38.0-40.5	embankment	CL	silty clay	100	1.0	3499	3499	6.00	17.9	113.0	5.93	18.3	113.4	91.7
	S-4	FH-1/PB14-S12	55.0-56.8	embankment	CL	sandy clay	104	1.0	4507	4507	5.98	11.7	122.5	5.90	13.0	123.0	61.6
	S-5	FH-4/PB3-S3	53.0-55.0	embankment	CL	sandy clay	N.A.	1.0	4507	4507	5.98	14.1	116.6	5.88	14.1	117.1	51.0
	S-6	FH-2/PB7-S5	27.0-29.5	foundation	CL	sandy clay	N.A.	1.0	2189	2189	5.96	17.9	111.5	5.92	16.5	111.8	52.6
	S-7A	FH-1/PB4-S3	14.5-17.5	embankment	CL	silty clay	97	1.0	2045	2045	5.00	19.8	109.0	5.96	—	—	79.1
	S-7B	"	"	"	"	"	—	1.0	4090	4090	—	—	—	5.76	19.8	110.3	—
	S-8	FH-1/PB12-S11	46.0-48.5	embankment	CL	sandy clay	N.A.	1.0	4896	4896	5.98	13.8	122.2	5.90	11.6	122.7	51.0
SUMMARY OF CYCLIC TRIAXIAL TESTS	C-1	FH-1/PB4-S3	14.5-17.5	embankment	CL	silty clay	97	1.0	2045	2045	5.98	18.6	108.8	5.96	18.9	108.9	78.4
	C-2	FH-1/PB6-S5	22.5-25.0	embankment	CL	silty clay	100	1.0	2707	2707	5.98	19.1	111.7	5.91	19.0	112.1	88.0
	C-3	FH-1/PB10-S9	38.0-40.5	embankment	CL	silty clay	102	1.0	3499	3499	5.99	16.0	113.8	5.90	18.6	114.3	94.1
	C-4	FH-1/PB14-S12	55.0-56.8	embankment	CL	sandy clay	94	1.0	4507	4507	5.99	17.9	110.1	5.87	15.6	110.7	58.6
	C-5	FH-1/PB10-S9	38.0-40.5	embankment	CL	silty clay	100	1.5	3197	4795	6.00	17.5	111.9	5.91	17.5	112.7	85.1
	C-6	FH-1/PB4-S3	14.5-17.5	embankment	CL	silty clay	100	1.5	1872	2808	5.95	17.0	112.5	5.89	19.6	112.8	86.5

*Relative compaction determined from compaction tests performed during Phase I on similar material types. "N.A" applies to those samples for which compaction test data are not available.

TABLE A-7
SUMMARY OF TRIAXIAL TESTS
IVINS DIVERSION DAM NO. 5

	TEST NUMBER	BORING/ SAMPLE NUMBER	DEPTH (ft.)	LOCATION	SOIL CLASSIFI-CATION	SOIL TYPE	RELATIVE* COMPACTION BEFORE CONSOL. (%)	K_c	σ_{3c} (psf)	σ_{1c} (psf)	BEFORE CONSOLIDATION			AFTER CONSOLIDATION			% PASSING NO. 200 SIEVE
											H (in.)	W/C (%)	γ_{dry} (psf)	H (in.)	W/C (%)	γ_{dry} (pcf)	
SUMMARY OF STATIC TRIAXIAL TESTS	S-1	IV-3/PB1-S1	4.0-6.5	embankment	SM	silty sand	99.4	1.0	1181	1181	6.00	15.5	109.9	5.98	17.9	109.9	43.9
	S-2	IV-2/PB3-S2	12.0-14.5	embankment	SM	silty sand	87.9	1.0	1253	1253	5.99	14.0	104.2	5.92	19.4	104.6	34.4
	S-3A	IV-1/PB1-S1	4.0-6.5	embankment	SM	silty sand	95.6	1.0	720	720	6.08	12.5	116.1	6.06	–	–	27.8
	S-3B	"	"	"	"	"	–	1.0	1440	1440	–	–	–	6.05	13.7	116.3	–
	S-4A	IV-5/PB4-S2	19.0-21.0	foundation	SM	silty sand	87.2	1.0	576	576	5.93	18.0	105.9	5.93	–	–	17.5
	S-4B	"	"	"	"	"	–	1.0	1728	1728	–	–	–	5.83	19.3	106.4	–
	S-5A	IV-4/P2-S1	8.0-10.5	foundation	SM	silty sand	87.5	1.0	763	763	6.00	19.5	103.8	5.97	–	–	38.5
	S-5B	"	"	"	"	"	–	1.0	1526	1526	–	–	–	5.83	18.7	104.7	–
	S-6	IV-2/PB4-S3	16.0-18.5	foundation	SM	silty sand	82.6	1.0	1584	1584	5.80	21.0	100.4	5.77	22.9	100.5	28.4
SUMMARY OF CYCLIC TRIAXIAL TESTS	C-1	IV-1/PB1-S1	4.0-6.5	embankment	SM	silty sand	98.7	1.0	720	720	5.99	11.5	117.0	5.99	14.4	117.0	24.4
	C-2	IV-3/PB1-S1	4.0-6.5	embankment	SM	silty sand	100.7	1.0	1181	1181	6.06	13.3	111.4	6.00	17.8	111.7	43.1
	C-3	IV-2/PB4-S3	16.0-18.5	foundation	SM	silty sand	82.1	1.0	1584	1584	5.93	14.3	97.4	5.87	23.2	97.7	25.3
	C-4	IV-4/PB2-S1	8.0-10.5	foundation	SM	silty sand	N.A.	1.0	763	763	5.98	16.6	106.1	5.94	17.9	106.3	27.2

*Relative compaction determined from compaction tests performed during Phase I on similar material types. "N.A" applies to those samples for which compaction test data are not available.

Table A-8

Summary of Static Effective Strength Parameters

Dam	Friction Angle ϕ' (degrees) Embankment	Foundation	Apparent Cohesion c' (psf) Embankment	Foundation
Green's Lake No.3	35	35	—	—
Warner Draw	37 (core)	—	—	—
Frog Hollow	35	35	250	250
Ivins Diversion No. 5	38	34	—	—

Undrained strength parameters were established for the Frog Hollow Dam materials from the results of the static tests. Plots of the shear stress on the failure plane at failure, τ_{ff}, versus the effective consolidation stress acting on the failure plane σ_{fc}, are presented in Figure A-15. From this plot, average undrained strength parameters were developed and are listed in Table A-9. (This is further explained on page A-16.)

Table A-9

Average Static Undrained Strength Parameters

Frog Hollow Dam

	Friction Angle ϕ (degrees)	Cohesion c (psf)
Embankment	20	1375
Foundation	20	575

Cyclic Strength Characteristics of Soils

"Liquefaction" and "Cyclic Mobility"

The prediction of the behavior of saturated cohesionless soils during earthquakes has been the subject of considerable research in the past 10 to 15 years. Two different phenomena can be observed when a saturated cohesionless soil is subjected to cyclic loading, namely, liquefaction and cyclic mobility.

Casagrande (1971, 1975) proposed the use of the term "cyclic mobility" for the cyclically-induced strains observed in laboratory tests performed on medium-dense to dense sands. Cyclic mobility consists of gradually increasing cyclic strains along with accompanying increases in pore pressure but does not entail a significant loss in shear strength.

"Liquefaction", on the other hand, corresponds to a condition in which a loose saturated sand, under undrained loading conditions (either static or cyclic), develops excess pore pressures equal to the effective confining stress. As the material begins to strain, the resistance to deformation is quite small and does not change with the strain level. Both liquefaction and cyclic mobility have in common the development of high pore pressures at constant volume. Liquefaction consists of a significant loss in shear strength. In this respect, liquefaction is similar to the behavior of a sand in a flow slide in which the sand suffers such a substantial reduction of its shear strength that the mass of soil seems to flow like a liquid. The fact that such failures resemble the flow of a heavy liquid is due to the fact that the large loss in shear strength affects a major portion of the mass rather than only the soil along a sliding surface.

Field experience and laboratory tests results indicated that liquefaction can develop only in loose sand deposits, whereas, cyclic mobility can be induced in the laboratory even in the densest sand. Cyclic mobility of a sand would cause limited but, perhaps, damaging deformations of slopes or foundations. In the case of a horizontal ground surface with no structures resting on it, the only evidence of cyclic mobility would be the effects of the dissipation of the pore pressure which could result in settlement of the ground surface and sometimes sand boils which are the result of the upward flow of water.

Discussion of Cyclic Triaxial Test

The cyclic triaxial test has been the most widely used laboratory test for evaluating the liquefaction potential, cyclic mobility, and cyclic strength characteristics of soils under simulated earthquake loading conditions. However, its use requires the application of various correction factors to the test data and considerable engineering judgment in order to allow for its limitations and shortcomings. In a cyclic triaxial test, in situ loading conditions are only roughly approximated. A correction to account for differences in stress and deformation conditions between the cyclic triaxial test and those believed to exist in the field during an earthquake are usually made.

Two types of cyclic triaxial tests may be performed. In order to represent field conditions where there are no initial shear stresses acting on horizontal planes (such as those existing below a level ground surface), isotropically consolidated tests are performed (see Figure A-16). Under these conditions, cyclic loading may cause increased pore pressures and cyclic strains but no permanent deformations are developed. In order to represent field conditions where there are initial shear stresses acting in the horizontal direction (such as in the case of sloping ground conditions), anisotropically consolidated tests are performed. The principal effect of cyclic loading under these conditions is that permanent deformations will usually develop in the direction of the initial shear stress and these may be accompanied by increasing pore pressures and cyclic strains (see Figure A-17).

The behavior of saturated cohesionless soils under simulated earthquake loading conditions is most often investigated in the laboratory by performing cyclic triaxial tests on samples which have been initially consolidated under an all-around confining pressure. The sample is subjected to a cyclic deviator stress of equal magnitude in compression and extension. Figure A-16 and the following summarizes the events observed during the test:

1. Up to a certain number of cycles, the strains that develop during each cycle are very small, however, the pore pressure shows a cumulative increase.

2. A point is reached after which the value of the pore pressure, at zero deviator stress, is momentarily equal to the confining pressure. This means that the effective stress acting on the sample momentarily drops to zero. This constitutes the onset of "initial liquefaction".

3. After "initial liquefaction", the strains during each subsequent cycle become progressively larger as more cycles of load are applied. During each cycle, the pore pressure becomes equal to the confining pressure when the deviator stress is zero but drops substantially when either the axial extension or axial compression load is applied. After "initial liquefaction", the strains increase rapidly for loose specimens, whereas they increase only slowly for dense specimens.

4. When the cyclic strains become excessively large (>15% peak-to-peak) the sand is said to have developed "complete liquefaction".

The cyclic triaxial compression test does not exactly reproduce the in situ initial stress conditions in the ground since it must be performed with an initially ambient pressure condition ($K_o = 1$) to represent level ground conditions. The cyclic stress ratio (τ cyclic/σ_{3c}) causing failure in isotropically consolidated cyclic triaxial tests are normally reduced by some factor (in the range of 0.6 to 0.7) to obtain stress ratios representative of field simple shear conditions. Less research has been done on the comparison of anisotropically consolidated ($K_c > 1$) cyclic triaxial tests and cyclic simple shear tests with initial shear stresses acting on the failure planes. A limited number of tests on silty sands obtained from Sheffield Dam indicated that for values of $K_c = 1.5$, the two tests gave similar results.

The results obtained from cyclic triaxial compression tests performed on isotropically consolidated soil samples are also influenced by a number of other factors. These may be summarized as follows:

1. The principal stress directions rotate through an angle of 90 degrees, during the two halves of the loading cycle, which is different than that in the field. The reversal of shear stresses produces a severe stress gradient condition on the sample which results in the development of high pore pressures even on dense samples.

2. The intermediate principal stress does not have the same relative value during the two halves of the loading cycle.

3. Cyclic stress ratios greater than about 0.5 usually cannot be achieved due to the tendency for the cap to lift off the sample.

4. Necking may develop and invalidate the test results. This occurs quite frequently.

5. Axial extension loads are applied to the sample which will quite often cause premature failure. This type of failure cannot occur in the field.

6. Water migration during the test causes a redistribution of the water content within the sample which affects the test results.

Castro (1969) performed a series of cyclic triaxial tests on isotropically consolidated saturated sand samples at various densities to evaluate the effects of the above factors on the test results. By freezing samples after subjecting them to cyclic loading, he was able to establish the variations in relative density and water content redistribution of different portions of the samples. The results of his study clearly demonstrated that during this type of test, a significant redistribution of water content takes place whenever the magnitude of the cyclic strains reaches a few percent and possibly even at much smaller strains. Therefore, both the recorded pore pressures and axial strains during cyclic loading cannot be attributed entirely to the behavior of a uniform sample but probably depend largely on the development of loose zones which form within the sample during cyclic loading. Thus, the results of the cyclic triaxial tests underestimate the ability of a dense cohesionless soil to withstand cyclic loading.

Sands which are medium dense or dense show, in general, a tendency to decrease in volume slightly under small shear strains and to increase in volume substantially under large shear strains. During cyclic load tests, and especially during the axial extension stage, it is likely that a slightly weaker part of the specimen would strain more and, therefore, will become looser at the expense of compaction of the other part. Because of the cyclic nature of these tests, this phenomenon repeats in every cycle. The loosening and softening of a portion

of the specimen accentuates itself progressively until it reaches the extreme condition observed during these tests. Although the sand may be strongly dilative during a static test, nevertheless, every time it is cycled through the hydrostatic state of stress, it develops a slightly contractive response over a small range of deviator stress and pore pressures will be induced. Pumping action of the vertical cyclic loads tends to move the excess water towards the top of the specimen (Casagrande, 1975). Specimens which are less uniform at the start of the test will develop cyclic mobility in fewer cycles, since the looser zones of the specimens will provide a focus for concentrations of shear strains and increase in water content.

Larger deformations are usually observed in extension than in compression in the great majority of cyclic triaxial tests in which the same deviator stress is applied in compression and extension. Since necking resulting from axial extension is peculiar to the triaxial test and does not correspond to the field conditions one intends to represent in the laboratory, the cyclic triaxial test will exaggerate the cyclic deformations that might develop in the field.

From the above considerations, it follows that the cyclic triaxial test performed on isotropically consolidated samples will tend to underestimate the resistance to cyclic loadings of sands, particularly when they are medium dense or denser. Thus, the results of cyclic triaxial tests must be carefully evaluated in light of the above factors and considerable judgment used in arriving at a decision as to how the materials will behave in situ, under the postulated earthquake ground motions.

Results of Cyclic Triaxial Tests

As part of this investigation, a series of stress-controlled cyclic triaxial tests was conducted to establish the liquefaction potential, cyclic mobility, and dynamic strength characteristics of the various materials comprising the dam embankments and their foundations, under simulated earthquake loading conditions. Cyclic stresses considered to be representative of those expected to develop in situ during the postulated Magnitude 6.0 earthquake were applied in the tests. Of major interest was the development of large cyclic strains and high excess pore pressures during and after completion of the tests. It has become common practice in this type of test to rely on the build up of excess pore pressure and the development of

cyclic strains as an indicator of the soil's liquefaction potential, cyclic mobility, or limited strain potential (Seed, 1979a; Soil Dynamics Committee, 1978). The effects of cyclic loading on the residual shear strength of the materials were also investigated.

A total of 19 samples were tested under cyclic loading conditions. These are summarized in Table A-10 together with the effective stresses to which they were consolidated and other pertinent information. Sixteen of the samples were isotropically consolidated (K_c = 1.0) and the remaining 3 were anisotropically consolidated (K_c = 1.5). Samples were subjected to 8 uniform stress cycles at a frequency of 1 Hertz, or a fewer number if the applied cyclic load decreased signficantly. Studies by various investigators have shown that 8 cycles of loading represents a conservative estimate of the number of uniform stress cycles corresponding to a Magnitude 6.0 earthquake (Seed, 1979a; Valera and Donovan, 1977).

Axial load, axial strain, and pore pressure were monitored during each test and recorded on a strip-chart recorder. After completion of the cyclic portion of the test, the sample was allowed to sit with the pore pressure lines closed until the excess pore pressure developed during cyclic loading had stabilized throughout the sample. A static consolidated-undrained triaxial test with pore pressure measurement was then conducted (if possible) to evaluate the residual shear strength characteristics of the material.

Results of the stress-controlled cyclic triaxial test performed on individual samples are presented in Table A-10. For most tests, a cyclic shear stress ratio, τ_{cy}/σ_{mc}, in the range of 0.30 to 0.50 was used for establishing the initial value of applied cyclic shear stress. Values of average applied cyclic shear stress $(\tau_{cy})_{avg}$, average cyclic shear stress ratio $(\tau_{cy}/\sigma_{mc})_{avg}$, peak pore pressure ratio $(\Delta u/\sigma_{mc})_{peak}$, peak-to-peak axial strain and peak permanent axial strain (for anisotropic tests only) are tabulated in Table A-10 for 8 stress cycles.

In Table A-11, the data presented in Table A-10 have been summarized to indicate the range of cyclic strains, cyclic pore pressures, and corresponding residual values for the samples corresponding to the various dam embankments and foundations. The overall behavior of the embankment and foundation materials has been classified as poor, fair, or good solely on the basis of the cyclic triaxial test results.

TABLE A-10
SUMMARY OF CYCLIC TRIAXIAL TESTS

DAM	TEST NUMBER	LOCATION	SOIL CLASSIFICATION	K_c	σ_{ic} (psf)	σ_{mc} (psf)	TOTAL NUMBER OF APPLIED CYCLES	N = 8 CYCLES					RESIDUAL		COMMENTS
								$(\tau_{cy})_{avg.}$ (psf)	$\left(\frac{\tau_{cy}}{\sigma_{mc}}\right)_{avg.}$	$\left(\frac{\Delta_u}{\sigma_{mc}}\right)_{peak}$	PEAK-TO-PEAK AXIAL STRAIN (%)	PEAK AXIAL STRAIN (%)	$\frac{\Delta_u}{\sigma_{mc}}$	AXIAL STRAIN AFTER DYNAMIC TEST (%)	
GREEN'S LAKE DAM NO. 3	C-1	embankment	SM	1.0	1109	1109	8	517	0.47	0.94	1.01	—	0.51	0.21	
	C-2	foundation	SM	1.0	2016	2016	8	945	0.47	1.00	6.04	—	0.93	-3.1	Sample exhibited tendency to neck
	C-3	foundation	SM	1.0	3024	3024	8	1219	0.40	1.02	12.60	—	0.95	-6.5	" "
	C-4.	embankment	SM	1.0	1354	1354	8	618	0.46	1.04	3.79	—	0.76	-2.3	" "
WARNER DRAW DAM	C-1	embankment	SM	1.0	1440	1440	8	428	0.30	0.89	0.60	—	0.77	-0.80	
	C-2	embankment	SC-SM	1.0	2678	2678	8	1029	0.38	0.93	8.95	—	0.82	-3.8	
	C-3	embankment	SC-SM	1.0	3902	3902	8	1656	0.42	1.14	2.94	—	0.80	-0.87	
	C-4	embankment	SC-SM	1.0	4810	4810	8	2016	0.42	1.38	4.90	—	0.79	-1.35	
	C-5	embankment	SC-SM	1.5	3672	2856	9	1507	0.53	1.21	2.72	2.39	0.65	2.70	
FROG HOLLOW DAM	C-1	embankment	CL	1.0	2045	2045	8	777	0.38	0.58	0.34	—	0.30	-0.15	
	C-2	embankment	CL	1.0	2707	2707	8	1082	0.40	0.70	0.47	—	0.28	-0.07	
	C-3	embankment	CL	1.0	3499	3499	8	1442	0.41	0.72	2.24	—	0.55	-0.59	
	C-4	embankment	CL	1.0	4507	4507	8	1691	0.38	1.12	10.8	—	0.87	3.2	Sample taken from weak embankment zone
	C-5	embankment	CL	1.5	4795	3730	8	2088	0.56	0.89	1.90	1.49	0.49	0.75	
	C-6	embankment	CL	1.5	2808	1872	8	1133	0.52	0.90	1.49	1.16	0.43	0.06	
IVINS DIVERSION DAM NO. 5	C-1	embankment	SM	1.0	720	720	8	351	0.49	1.08	0.40	—	0.44	-0.23	
	C-2	embankment	SM	1.0	1181	1181	8	410	0.35	0.59	~0.0	—	0.15	0.00	
	C-3*	foundation	SM	1.0	1584	1584	3 8	698 277	0.44 0.36	1.08 1.08	5.45 9.67	— —	0.95	4.97	Sample tended to compress due to large decrease in extension load
	C-4	foundation	SM	1.0	763	763	8	312	0.41	1.07	2.49	—	0.87	0.93	

*Load dropped off significantly after 3 cycles, however test carried out to 8 cycles.

Table A-11

Behavior of Embankment and Foundation Soils
Under Undrained Cyclic Loading

Dam	Location	(N=8) $\frac{\Delta u}{\sigma mc}$	(N=8) εpeak-peak (%)	(Residual) $\frac{\Delta u}{\sigma mc}$	(Residual) ε axial (%)	Behavior
Green's Lake No. 3	Embankment	0.9 to 1.0	1.0 to 4.0	0.5-0.8	+0.2 to -2.0	Good
	Foundation	1.0	6.0 to 13.0	0.9-1.0	-3.0 to -6.0	Poor to fair
Warner Draw	Embankment	0.9 to 1.0	0.6 to 9.0	0.6-0.8	-4.0 to +3.0	Fair to good
*Frog Hollow	Embankment	0.6 to 0.9	0.3 to 2.0	0.3-0.6	-0.6 to +0.8	Good
Ivins Diversion No. 5	Embankment	0.6 to 1.0	0.0 to 0.4	0.2-0.4	0.0 to -2.0	Good
	Foundation	1.0	2.0 to 10.0	0.9-1.0	+0.9 to +5.0	Poor to fair

*Test on weak embankment sample not included

It can be noted from the data presented in Table A-11 that the majority of the embankment materials exhibited reasonably good behavior (with the exception of the weak embankment sample from Frog Hollow and one sample from Warner Draw). This is true even though most of the samples reached a condition of "initial liquefaction" during cyclic loading. On the other hand, the foundation materials at Green's Lake Dam No. 3 and Ivins Diversion Dam No. 5 behaved rather poorly. These samples developed moderate to large strains during cyclic loading and had, for all practical purposes, reached a state of "complete liquefaction" at the end of cyclic loading.

The above findings are in general agreement with the results of the field investigations in that the embankment materials were found to be medium dense to dense, whereas some of the foundation soils were found to be loose to medium dense. They are also supported by the results of the static triaxial tests presented in Appendix B. The stress-strain charactertistics of most of the embankment materials exhibited dilatant behavior which is characteristic of a medium-dense to dense soil. Similar behavior was observed in the medium-dense to dense foundation soils. However, contractive behavior was noted in a number of the foundation samples tested which is characteristic of a loose material.

As previously discussed, the results of cyclic triaxial tests performed on medium-dense to dense soils would yield cyclic strains and pore pressure that are probably greater than those that would be experienced by the soils in situ during an earthquake. Even though the behavior of the embankment soils during cyclic loading was quite good, it is our judgment that the in situ behavior of these soils, during the postulated earthquake ground motions, would be better than that observed in the laboratory (see Table A-11).

The results of cyclic triaxial tests performed on the loose to medium-dense foundation soils present at Green's Lake Dam No. 3 and Ivins Diversion Dam No. 5, on the other hand, probably provide a reasonably good indication of their in situ behavior during the postulated Magnitude 6.0 earthquake. Difficulty was experienced in obtaining good quality Pitcher tube samples of the foundation soils at these sites during the Phase I field drilling investigation. Some of the foundation soils tended to fall or wash out of the Pitcher tube during sampling which suggests loose soil conditions. During the laboratory testing program, the samples of the foundation soils that were recovered were extremely fragile and difficult to

extrude. The samples were wet and tended to slump or tilt under their own weight during extrusion. Due to these difficulties, the number of cyclic triaxial tests of these soils had to be reduced since good quality samples could not be obtained from the available Pitcher tubes.

In light of these sampling and testing difficulties, it is our judgment that the "best" samples of the foundation soils present at these two dam sites were tested in the laboratory. Based on these considerations, the in situ behavior of the foundation soils during an earthquake should not be expected to be any better than that observed in the laboratory.

Comparison of Static and Post-Cyclic Static Test Results

Consolidated-undrained triaxial tests were performed on most of the samples subjected to cyclic loading to evaluate their post-cyclic stress-strain characteristics. For clayey materials, such as those present at Frog Hollow Dam, comparison of these data with those obtained from static triaxial tests provides an indication of the reduction in static undrained shear strength due to cyclic loading. For embankments and foundations consisting of sandy materials, the pore pressure characteristics observed during the post-cyclic tests permit an evaluation of the pore pressures which might exist in the field after the occurrence of the postulated earthquake.

Results of the post-cyclic triaxial tests are presented in Appendix D. These results are similar in most respects to those presented in Appendix B for the static tests, however, there are some significant differences which will be discussed subsequently.

The results of the post-cyclic tests, in terms of effective strength parameters, are plotted in Figures A-11 through A-14. The data points for the post-cyclic tests are shown as darkened symbols. It can be seen that the majority of the points fall on the same failure envelope established from the static test results. The major difference is that because of build up of pore pressure due to cyclic loading, the points corresponding to the post-cyclic static tests have been shifted down the failure (K_f) line towards the origin.

For clayey materials, such as those found at Frog Hollow Dam, it is useful to plot the post-cyclic test data in the form shown in Figure A-15 (Lowe, 1967). In this figure, the shear stress, τ_{ff}, acting on the failure plane at the peak principal stress ratio ($\bar{\sigma}_1/\bar{\sigma}_3$) is plotted versus the mean effective confining stress acting on the failure plane at the end of consolidation (σ_{fc}). The data are plotted for both the static (open symbols) and post-cyclic static tests (darkened symbols). The test data plotted in this figure indicates that low to moderate strength loss has occurred as a result of cyclic loading as shown by the shear strengths exhibited by tests S-3 and PC-5 (and PC-3).

Comparisons of the stress-strain characteristics of static and post-cyclic tests performed on paired samples initially consolidated to the same confining stress are presented in Figures A-18 through A-22. The results of these paired tests have been carefully reviewed in an attempt to determine why, in some cases, significant differences occur in both the pore pressure and deviator stress characteristics. The tests which have been compared are tabulated in Table A-12, together with additional information on the test conditions and remarks on the stress-strain characteristics. Examination of these test results leads to the following conclusions:

1. For samples with similar densities, the stress-strain characteristics are generally similar if high pore pressures or moderate to large cyclic strains did not develop during cyclic loading. Examples of this behavior are shown in Figures A-19, A-22, and A-24 for Warner Draw, Frog Hollow, and Ivins Diversion Dam No. 5, respectively.

2. If high pore pressures or moderate to large cyclic strains developed during cyclic loading, significant differences in stress-strain behavior exist. This is primarily due to the initially high value of pore pressure existing in the post-cyclic static test which results in a lower shear strength. The post-cyclic static tests exhibit less dilatency than the samples not subjected to cyclic loading. This is true even when the initial densities of the paired samples are similar. The cyclic test produces a loosening or softening of the sample during cyclic loading as was previously discussed. This type of behavior is illustrated in Figure A-20 for Warner Draw Dam and Figure A-25 for Ivins Diversion Dam No. 5.

Table A-12

Comparison of Static and Post-Cyclic Static Triaxial Tests

Dam	Test No. Static	Test No. P.C.	K_c Static	K_c P.C.	σ_{1c} (psf)	* (after cyclic loading) Δu (psf)	* (after cyclic loading) ε (%)	Dry Density (pfc) Static	Dry Density (pfc) P.C.	Difference in Density (pfc)	Remarks on Stress-Strain Characteristics of Static & Post-Cyclic Tests: Deviator Stress	Remarks on Stress-Strain Characteristics of Static & Post-Cyclic Tests: Pore Pressure
Green's Lake No. 3	S-6	PC-2	1.0	1.0	2016	1875	-3.1	120.1	113.8	6.3	P.C. test developed much lower shear strengths. Mainly a result of large excess pore water pressure built-up during cyclic loading.	P.C. test behavior different than static test. P.C. test did not exhibit same level of dilation present in static test.
Warner Draw	S-1	PC-1	1.0	1.0	1440	1109	-0.80	124.5	122.8	1.7	Similar shapes. P.C. test initially lower than static test due to excess pore pressure existing at end of cyclic loading.	Similar shapes offset initially by an amount equal to excess pore pressure developed during cyclic loading.
Warner Draw	S-3	PC-3	1.0	1.0	3902	3122	-0.87	127.2	127.7	0.5	P.C. test developed much lower shear strengths. Mainly a result of large excess pore water pressure built-up during cyclic loading.	Somewhat similar curves. However, P.C. test did not exhibit same level of dilation as developed during static test.

*Values taken or computed from Table A-10.

Table A-12 (Continued)

Comparison of Static and Post-Cyclic Static Triaxial Tests

Dam	Test No. Static	Test No. P.C.	K_c Static	K_c P.C.	σ_{1c} (psf)	* (after cyclic loading) Δu(psf)	* (after cyclic loading) ε(%)	Dry Density (pfc) Static	Dry Density (pfc) P.C.	Difference in Density (pfc)	Remarks on Stress-Strain Characteristics of Static & Post-Cyclic Tests: Deviator Stress	Remarks on Stress-Strain Characteristics of Static & Post-Cyclic Tests: Pore Pressure
Warner Draw	S-5	PC-2	1.0	1.0	2678	2196	-3.8	130.8	121.7	9.1	P.C. test developed significantly lower strengths. Mainly a result of large excess pore water pressure built-up during cyclic loading.	Very different shapes. P.C. test exhibited no dilation whereas static test exhibit significant dilation.
Warner Draw	S-5	PC-5	1.0	1.5	2678/ 2856	1856	+2.7	130.8	124.4	6.4	Similar shapes. However, P.C. test curve lower than static test.	Both curves have similar shapes and exhibit similar dilation characteristics. However, P.C. test curve offset by an amount approximately equal to excess pore water pressure built-up during loading.

*Values taken or completed from Table A-10.

Table A-12 (Continued)

Comparison of Static and Post-Cyclic Static Triaxial Tests

Dam	Test No. Static	Test No. P.C.	K_c Static	K_c P.C.	σ_{1c} (psf)	* (after cyclic loading) Δu(psf)	* (after cyclic loading) ε (%)	Dry Density (pfc) Static	Dry Density (pfc) P.C.	Difference in Density (pfc)	Remarks on Stress-Strain Characteristics of Static & Post-Cyclic Tests: Deviator Stress	Remarks on Stress-Strain Characteristics of Static & Post-Cyclic Tests: Pore Pressure
Frog Hollow	S-2	PC-2	1.0	1.0	2707	758	-0.07	113.7	112.1	1.6	Nearly identical curves.	Nearly identical curves. P.C. test curve offset initially by a small amount equal to excess pore water pressure built-up during cyclic loading.
Frog Hollow	S-4	PC-4	1.0	1.0	4507	3921	3.2	123.0	110.7	12.3	P.C. test developed much lower shear strengths due to large built-up of excess pore water pressure during cyclic loading.	Very different shapes. P.C. test exhibit no dilation, whereas static test exhibited moderate dilation for strains 2%.
Ivins	S-1	PC-2	1.0	1.0	1181	177	0.0	109.9	111.7	1.8	Nearly identical curves.	Nearly identical curves. Both showed dilatant behavior.

*Values taken or completed from Table A-10.

Table A-12 (Continued)

Comparison of Static and Post-Cyclic Static Triaxial Tests

Dam	Test No. Static	Test No. P.C.	K_c Static	K_c P.C.	σ_{1c} (psf)	(after cyclic loading) Δu(psf)	(after cyclic loading) ε(%)	Dry Density (pfc) Static	Dry Density (pfc) P.C.	Difference in Density (pfc)	Remarks on Stress-Strain Characteristics of Static & Post-Cyclic Tests: Deviator Stress	Remarks on Stress-Strain Characteristics of Static & Post-Cyclic Tests: Pore Pressure
Ivins	S-5A	PC-4	1.0	1.0	763	664	0.93	106.4	106.3	0.1	P.C. test developed lower strengths due to large built-up of pore water pressure during cyclic loading.	Similar shapes. However, P.C. test offset by an amount equal to the excess pore water pressure.

*Values taken or completed from Table A-10.

3. In some cases, the differences in stress-strain behavior existing between paired samples is probably due to differences in the density of the two samples. This occurred in the tests shown in Figures A-18 and A-23 for Green's Lake Dam No. 3 and Frog Hollow Dam, respectively.

While some of the cyclic triaxial test samples of the embankment soils developed moderate cyclic strains and high pore pressure during cyclic loading, most of the samples gained some strength rather rapidly (i.e., at small axial strains) during the post-cyclic static test due to their dilatant behavior. The post-cyclic shear strengths of most of the embankment soils were, in general, less than the original static strengths. The clayey embankment soils present at Frog Hollow Dam experienced the least amount of strength reduction after cyclic loading. The post-cyclic strength of the sandy embankment and foundation soils was dependent on the magnitude of the pore pressure that developed during cyclic loading, as well as the degree of dilation exhibited during the post-cyclic static test.

The strength parameters of the embankment and foundation soils used in the post-earthquake stability analyses described in Chapter VII of this report were developed from the results of the post-cyclic static test results described above. In performing this type of analysis, strength parameters may be specified either in terms of undrained shear strengths (Lowe, 1967) or effective strengths with estimates of the in situ pore pressures developed during the earthquake (Seed, 1979b).

For Frog Hollow Dam, the post-earthquake stability analyses was performed using the undrained strength soil parameters determined from a comparison of the static and post-cyclic static strengths measured in the laboratory, as was previously described. The test data plotted in the form shown in Figure A-15 (similar to Lowe, 1967) show that only a moderate reduction in shear strength occurs in these soils due to cyclic loading. The average post-cyclic undrained strength parameters developed from this data for Frog Hollow Dam are summarized in Table A-13.

For those embankments and foundations consisting of sandy soils, strength parameters for use in post-earthquake stability analyses were defined in terms

Table A-13

Average Post-Cyclic Undrained Strength Parameters - Frog Hollow Dam

	Friction Angle ϕ (degrees)	Cohesion c (psf)
Embankment	20	850
Foundation	20	350*

Note:

*Developed from results of post-cyclic static tests performed on embankment soils.

Table A-14

Post-Earthquake Effective Strength Parameters

Dam	Friction Angle ϕ' (degrees)		Pore Pressure Parameter, r_u	
	Embankment	Foundation	Embankment	Foundation
Green's Lake No. 3	35	35	0.30	0.90
Warner Draw	37	--	(K_c=1.0) 0.70 (K_c=1.5) 0.35	--- ---
Ivins Diversion No. 5	38	34	0.10	0.80

of effective strengths (Seed, 1979b). Post-cyclic strength parameters defined in this way require estimates for the magnitude of pore pressure that will exist in the field after the earthquakes. The pore pressures induced by cyclic loading are then superimposed on the in situ hydrostatic pressures. Since an axial strain of 5 percent was chosen as an appropriate strain value at which to evaluate the static strength of these soils, the pore pressure present at this strain level in the post-cyclic static tests was used as a guide in developing the post-earthquake effective strength parameters summarized in Table A-14. The friction angles listed on this table are the same as those listed on Table A-8. The pore pressure parameter, r_u, defined as the ratio of pore pressure at 5 percent axial strain (Δ_u) to the mean effective confining stress at the end of consolidation (σ_{mc}), ranges from 0.10 to 0.70 for the embankment soils, and 0.80 to 0.90 for the foundation soils.

The high values of the pore pressure parameter listed in Table A-14 for the foundation soils at Green's Lake Dam No. 3 and Ivins Diversion Dam No. 5 reflect the poor behavior of these soils during the cyclic and post-cyclic static tests. It is significant to note that two of the four post-cyclic static test samples of these soils had very little or no strength after cyclic loading; even after significant strains had developed in the post-cyclic static tests (see tests C-3 and PC-3 for Green's Lake Dam No. 3 and C-3 for Ivins Diversion Dam No. 5, Appendices C and D). In fact, the post-cyclic static test of cyclic test C-3 for Ivins Diversion Dam No. 5 could not be performed since the sample could not sustain any static load after cyclic loading. As was the case in the cyclic triaxial tests, it is our judgment that the behavior of these soils during the post-cyclic static tests is probably fairly representative of the behavior expected to occur in the field after the postulated earthquake. Because of the high pore pressures that develop in these soils during cyclic loading, the post-cyclic strengths of these soils will probably be low. Excessive (and probably unacceptable) amounts of deformation would have to develop in the field before the materials would gain some strength.

The somewhat lower pore pressure parameters listed in Table A-14 for the embankment soils reflect the dilatant behavior of these medium-dense to dense soils. Although, high residual pore pressures were developed during the cyclic tests, the pore pressures usually dropped to a lower value after a strain

of 5 percent had developed in the post-cyclic static test. It is our judgment that the pore pressure parameters listed in Table A-14 soils are probably conservative (i.e., high). The pore pressures that would develop in situ during the postulated earthquake would probably be less than those measured in the laboratory as was previously discussed.

Limitations

It should be noted that the various soil properties that were discussed in this Appendix are "average" properties which are based on a limited number of laboratory tests together with considerable engineering judgment. Since many of the dams considered in this investigation have very long crest lengths, it would be extremely difficult (and costly) to evaluate the subsurface conditions (and therefore the soil properties) along the entire length of each embankment considered in this investigation.

It is common in engineering practice to drill a limited number of exploratory boreholes and/or excavate test pits to investigate the subsurface conditions at particular locations at a site, and to obtain representative soil samples for laboratory testing. This information is supplemented by a geologic evaluation of the site and, as in the case of an earth embankment, available construction records in order to establish "representative" soil profiles, embankment cross sections and soil properties. "Unknowns", such as undetected weak soil strata or seams, are usually compensated for in analyses by making conservative simplifying assumptions (when assumptions are required) and by applying reasonable engineering judgment.

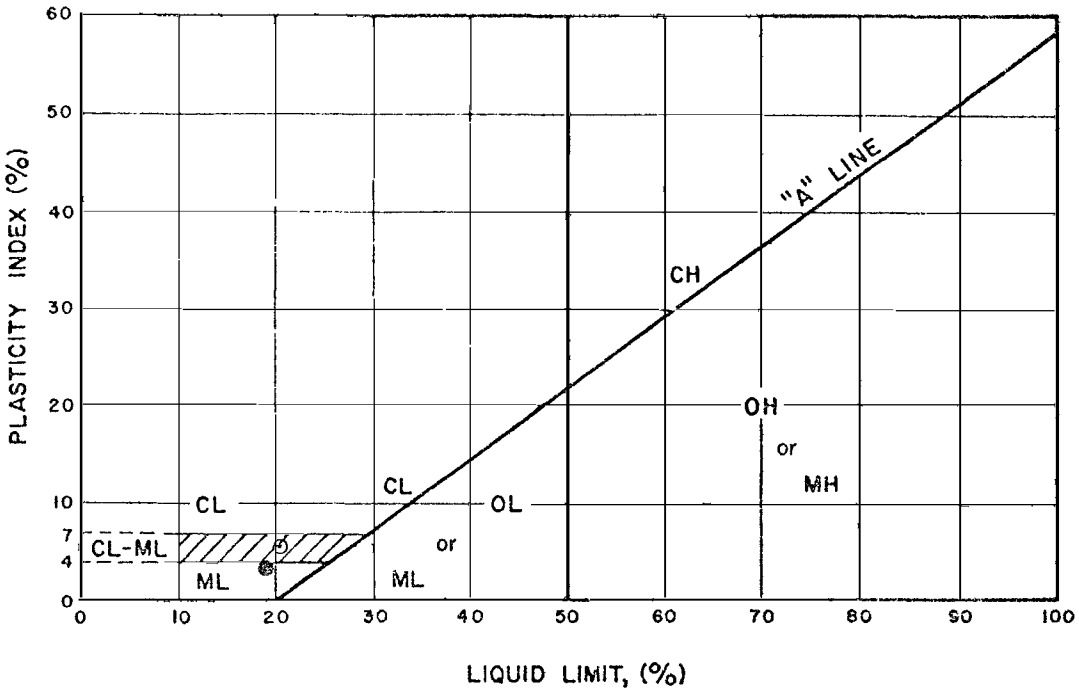

SYMBOL	BORING NO.	DEPTH, FT.	LIQUID LIMIT, %	PLASTICITY INDEX, %	USC SYMBOL
⊙ (S-3)	GL3-1/PB9-S8	35.5-38.0	21.0	5.9	CL/ML
● (S-4) ↑ Triaxial Test No.	GL3-1/PB6-S5	23.5-26.0	19.2	3.6	SM

Earth Sciences Associates
Palo Alto, California

SEISMIC SAFETY INVESTIGATION OF EIGHT SCS DAMS
SUMMARY OF ATTERBERG LIMITS
GREEN'S LAKE DAM NO. 3

Checked by M.F. Date 9/20/82
Approved by J.C. Valera Date 9/22/82
Project No. D118
Figure No. A-1

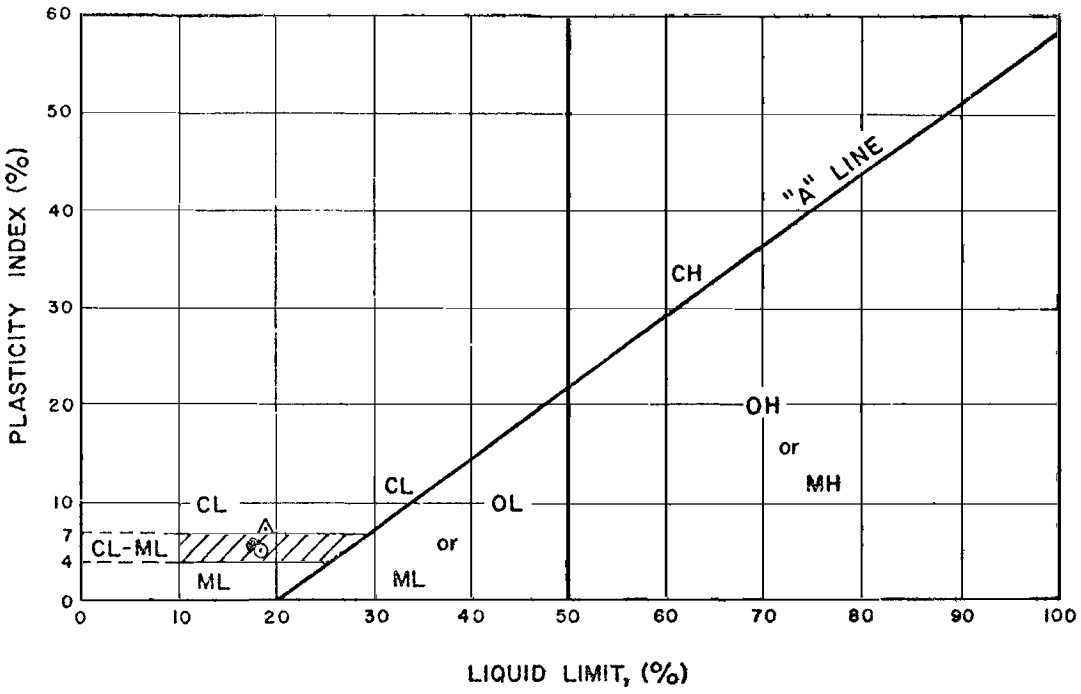

SYMBOL	BORING NO.	DEPTH, FT.	LIQUID LIMIT, %	PLASTICITY INDEX, %	USC SYMBOL
⊙ (C-2)	WD-2/PB6-S6	24.5-27.0	18.1	5.6	SC-SM
● (C-4)	WD-1/PB13-S13	53.0-55.5	17.8	6.7	SC-SM
△ (C-3)	WD-1/PB10-S10	41.0-43.5	18.5	7.3	SC-SM

↑ Triaxial Test No.

Earth Sciences Associates
Palo Alto, California

SEISMIC SAFETY INVESTIGATION OF EIGHT SCS DAMS
SUMMARY OF ATTERBERG LIMITS
WARNER DRAW DAM

Checked by M.L.T. Date 9/20/82
Approved by J.E. Valera Date 9/22/82
Project No. D118
Figure No. A-2

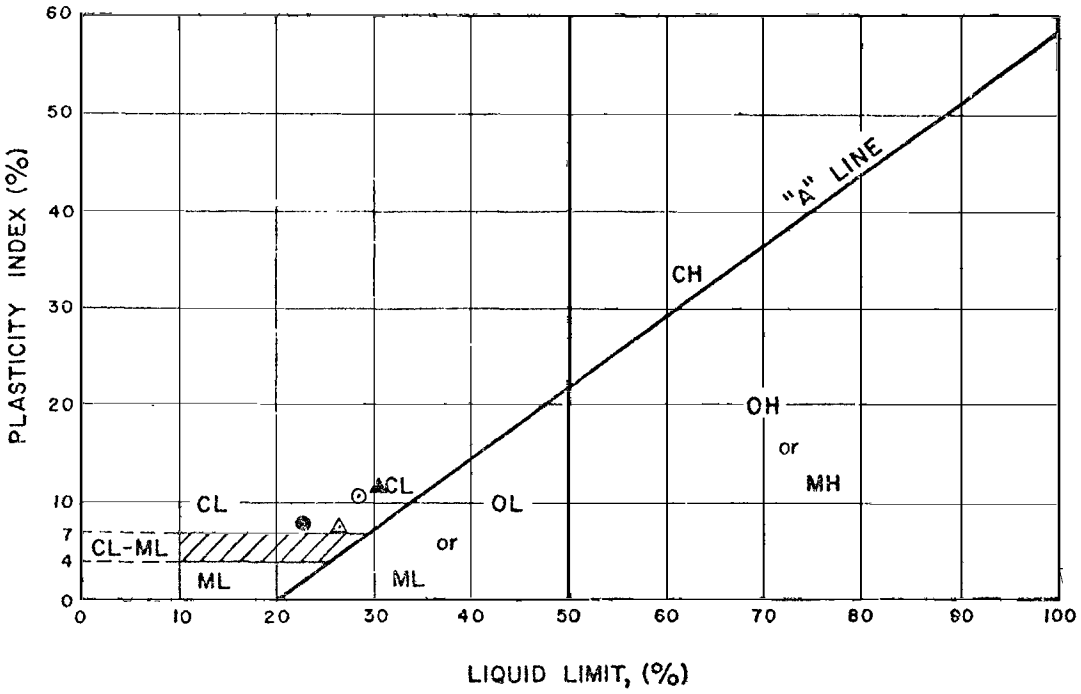

SYMBOL	BORING NO.	DEPTH, FT.	LIQUID LIMIT, %	PLASTICITY INDEX, %	USC SYMBOL
⊙ (C-2)	FH-1/PB6-S5	22.5-25.0	28.8	10.8	CL
● (C-4)	FH-1/PB14-S12	55.0-56.8	22.6	7.9	CL
△ (C-1)	FH-1/PB4-S3	14.5-17.5	26.5	7.5	CL
▲ (C-5)	FH-1/PB10-S9	38.0-40.5	30.8	11.4	CL

↑ Triaxial Test No.

Earth Sciences Associates
Palo Alto, California

SEISMIC SAFETY INVESTIGATION OF EIGHT SCS DAMS
SUMMARY OF ATTERBERG LIMITS
FROG HOLLOW DAM

Checked by MLT Date 9/20/82
Approved by J.C. Valera Date 9/22/82
Project No. D118
Figure No. A-3

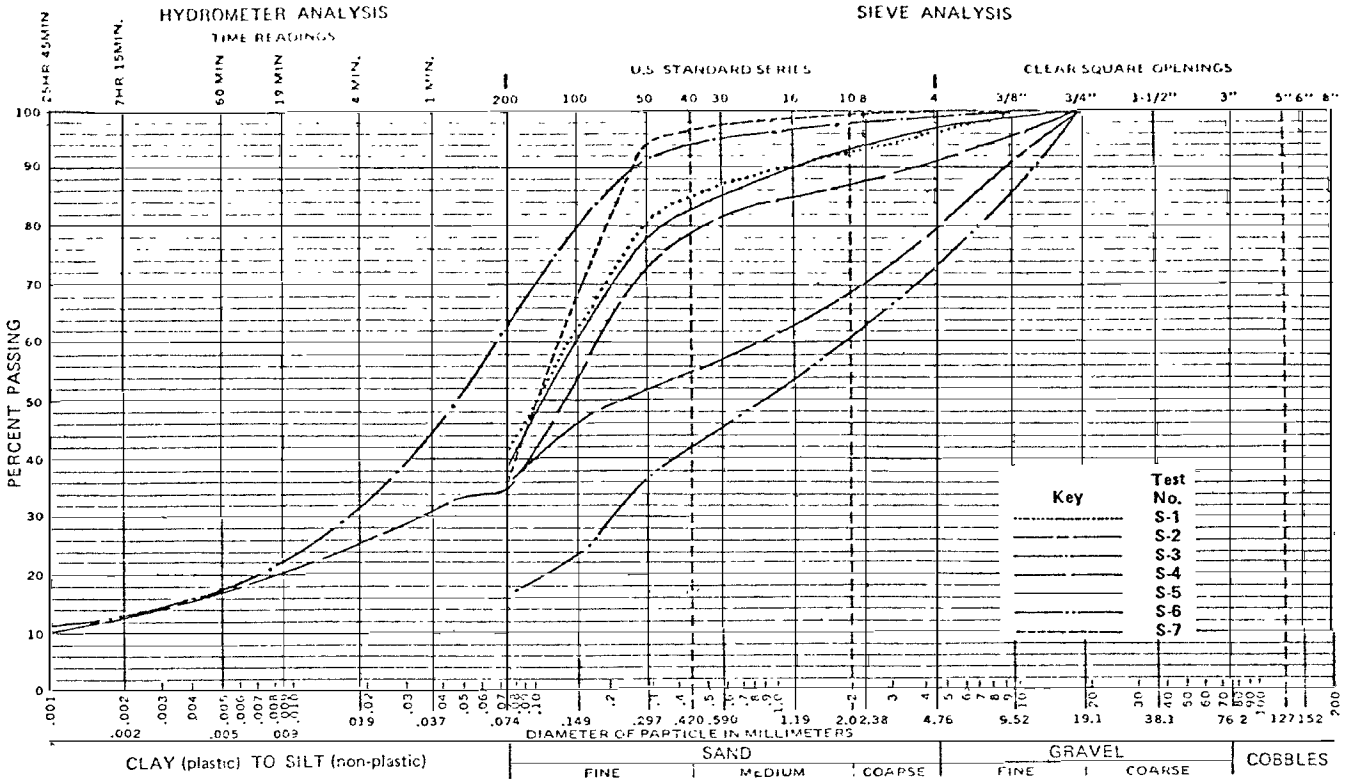

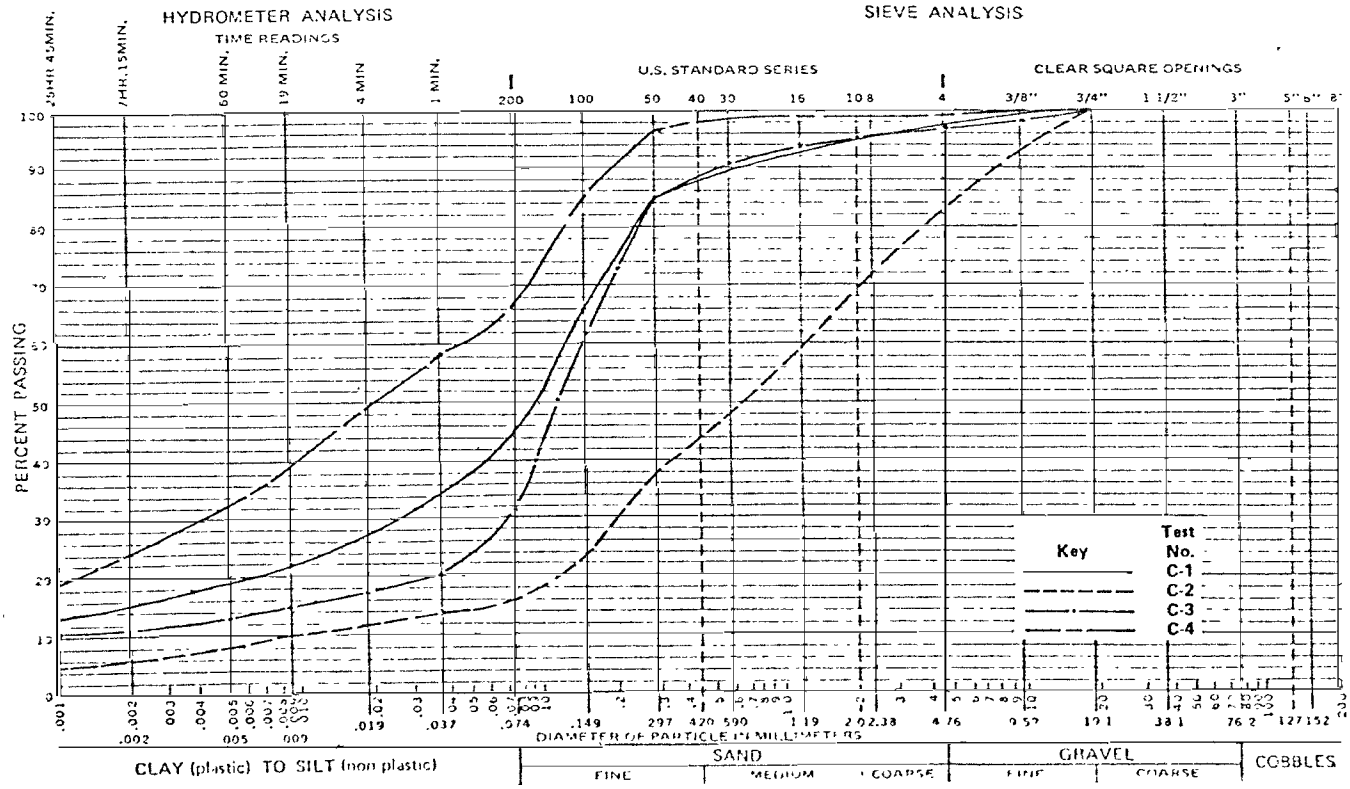

Earth Sciences Associates
Palo Alto, California

SEISMIC SAFETY INVESTIGATION OF EIGHT SCS DAMS
SUMMARY OF GRADATIONS – TRIAXIAL TESTS
GREEN'S LAKE DAM NO. 3

Checked by MLT	Date 9/20/82	Project No.	Figure No.
Approved by J.E. Valera	Date 9/22/82	D118	A-4

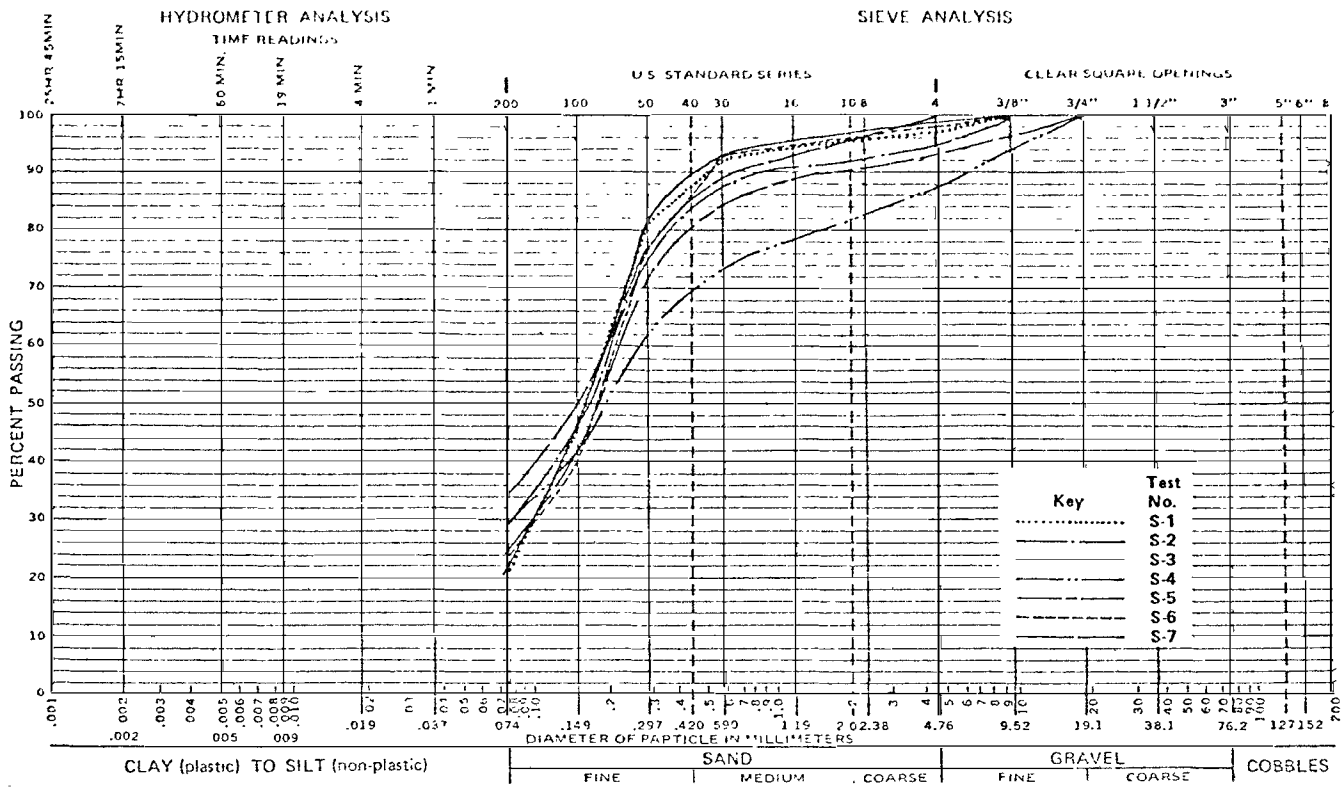

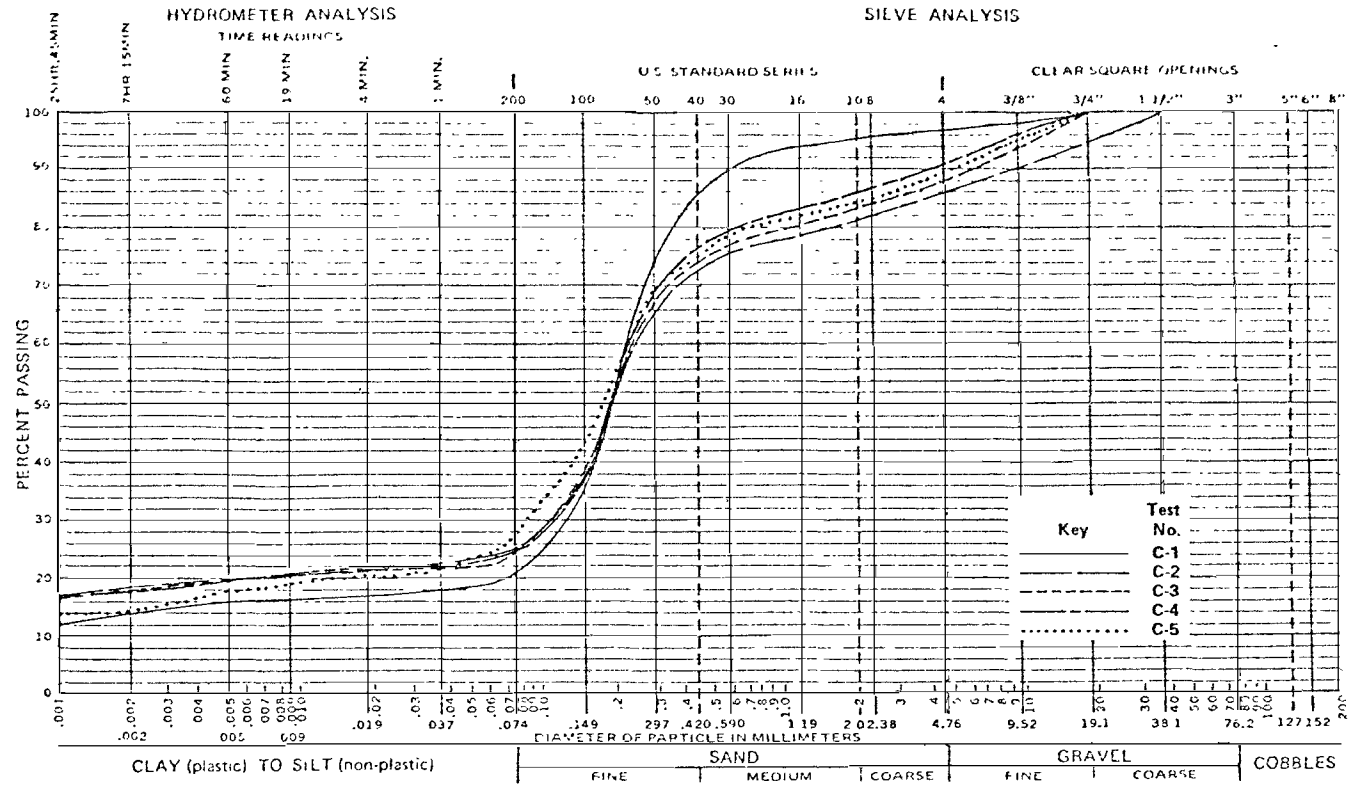

Earth Sciences Associates
Palo Alto, California

SEISMIC SAFETY INVESTIGATION OF EIGHT SCS DAMS
SUMMARY OF GRADATIONS – TRIAXIAL TESTS
WARNER DRAW DAM

Checked by MLT Date 9/20/82	Project No.	Figure No.
Approved by J.E. Valera Date 9/22/82	D118	A-5

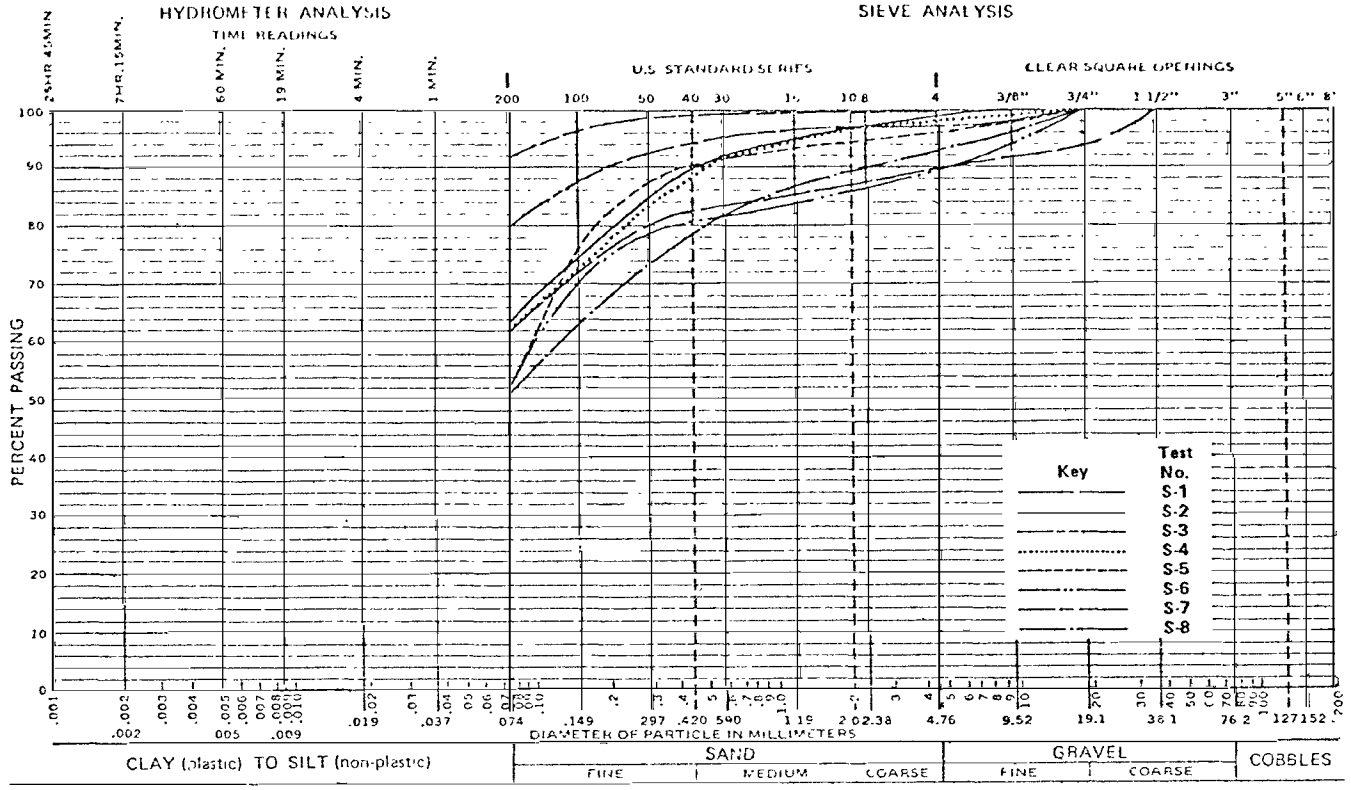

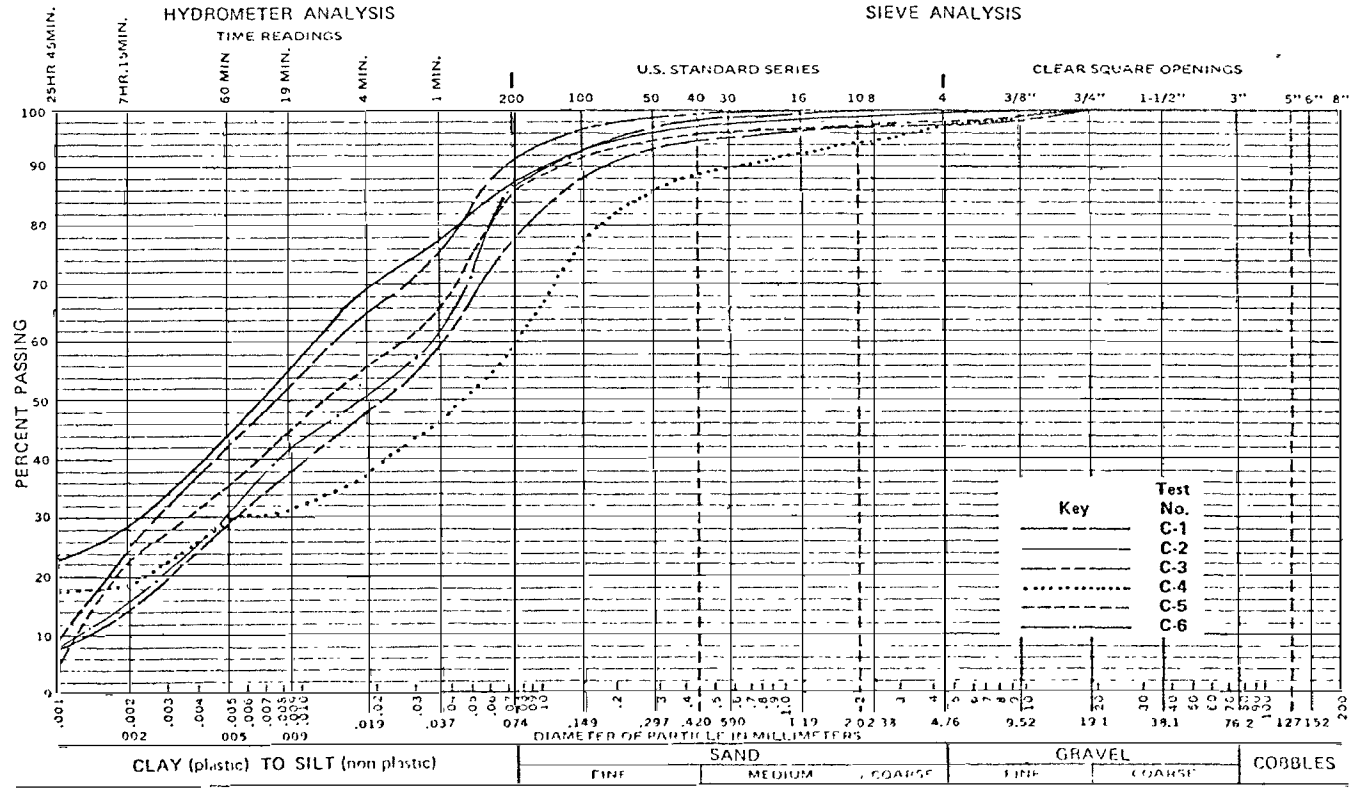

Earth Sciences Associates
Palo Alto, California

SEISMIC SAFETY INVESTIGATION OF EIGHT SCS DAMS
SUMMARY OF GRADATIONS – TRIAXIAL TESTS
FROG HOLLOW

Checked by MLT	Date 9/20/82	Project No.	Figure No.
Approved by J.E. Valera	Date 9/22/82	D118	A-6

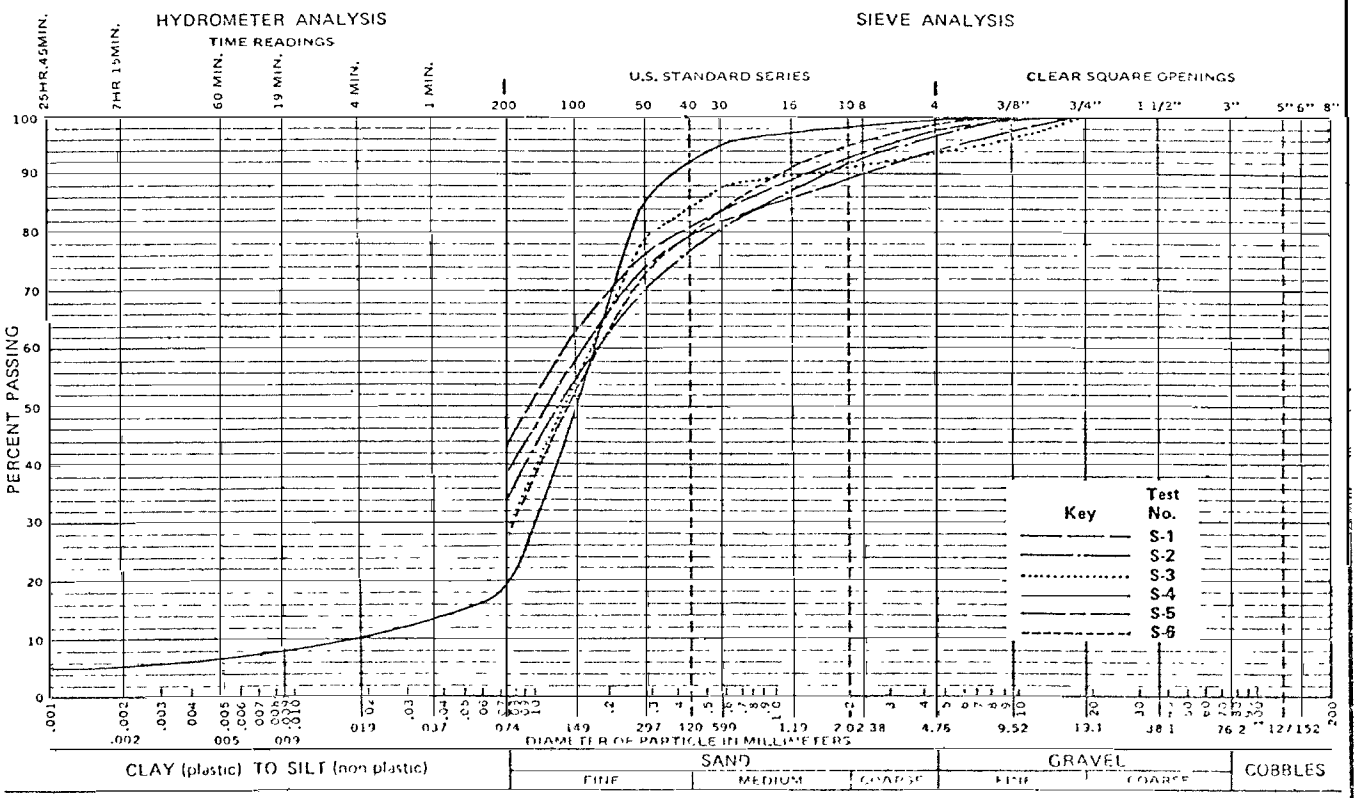

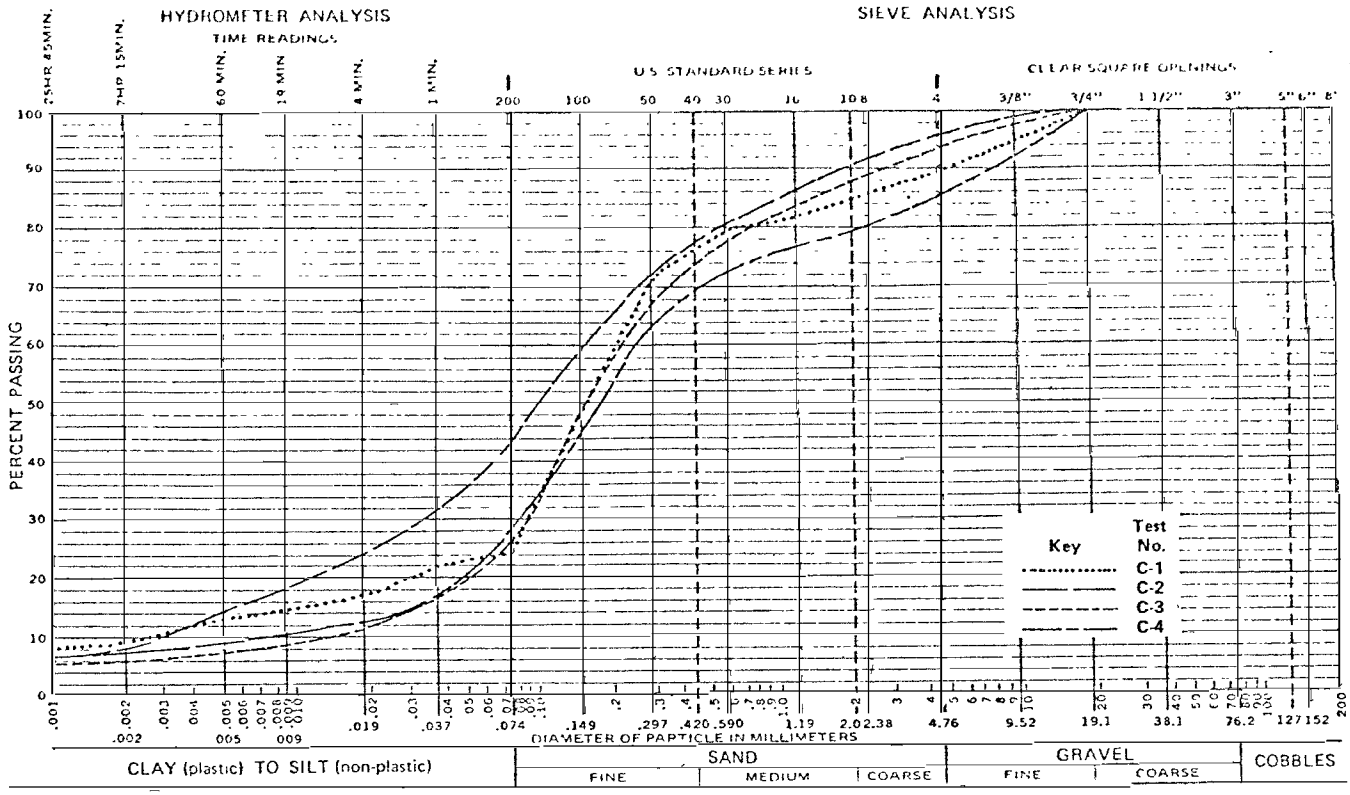

Earth Sciences Associates
Palo Alto, California

SEISMIC SAFETY INVESTIGATION OF EIGHT SCS DAMS
SUMMARY OF GRADATIONS – TRIAXIAL TESTS
IVINS DIVERSION DAM NO. 5

Checked by MLT	Date 9/20/82	Project No.	Figure No.
Approved by J.E. Valera	Date 9/22/82	D118	A-7

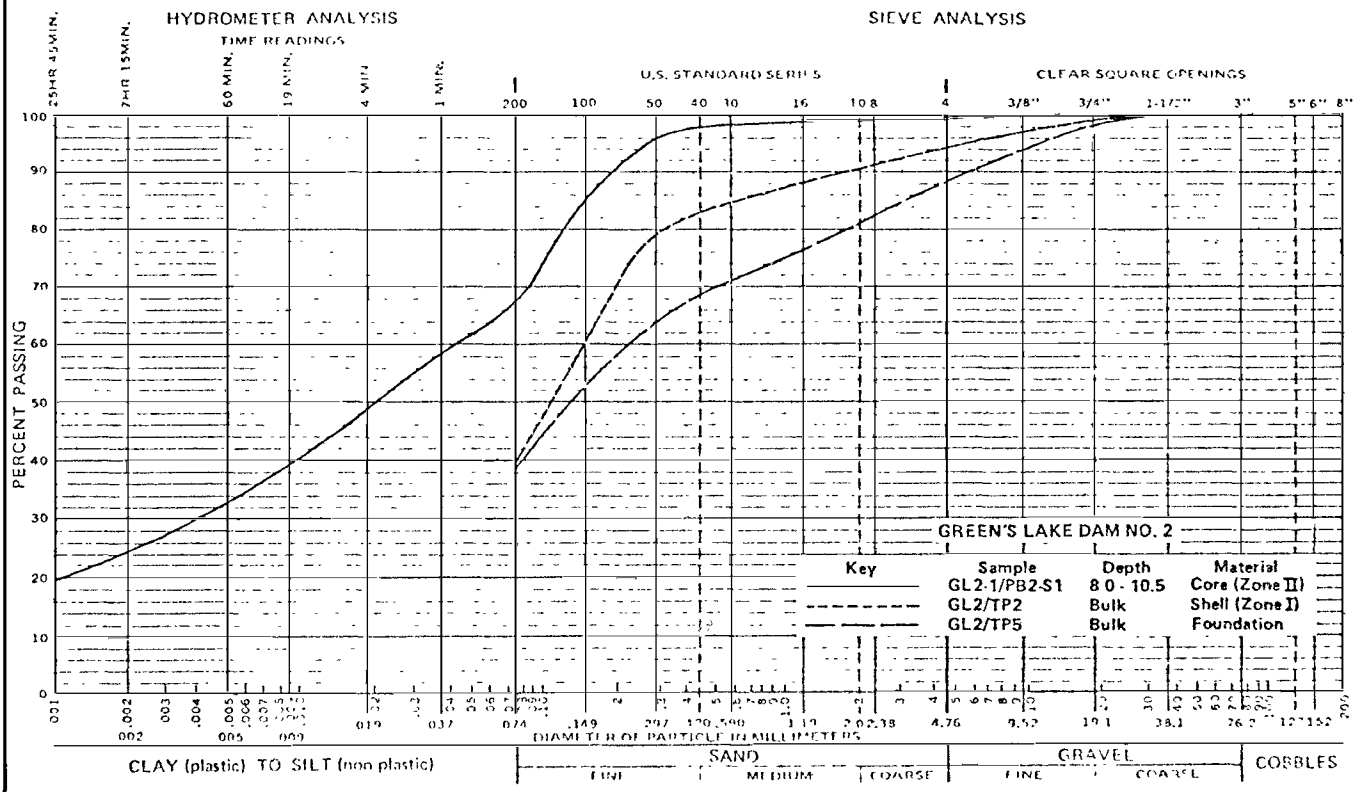

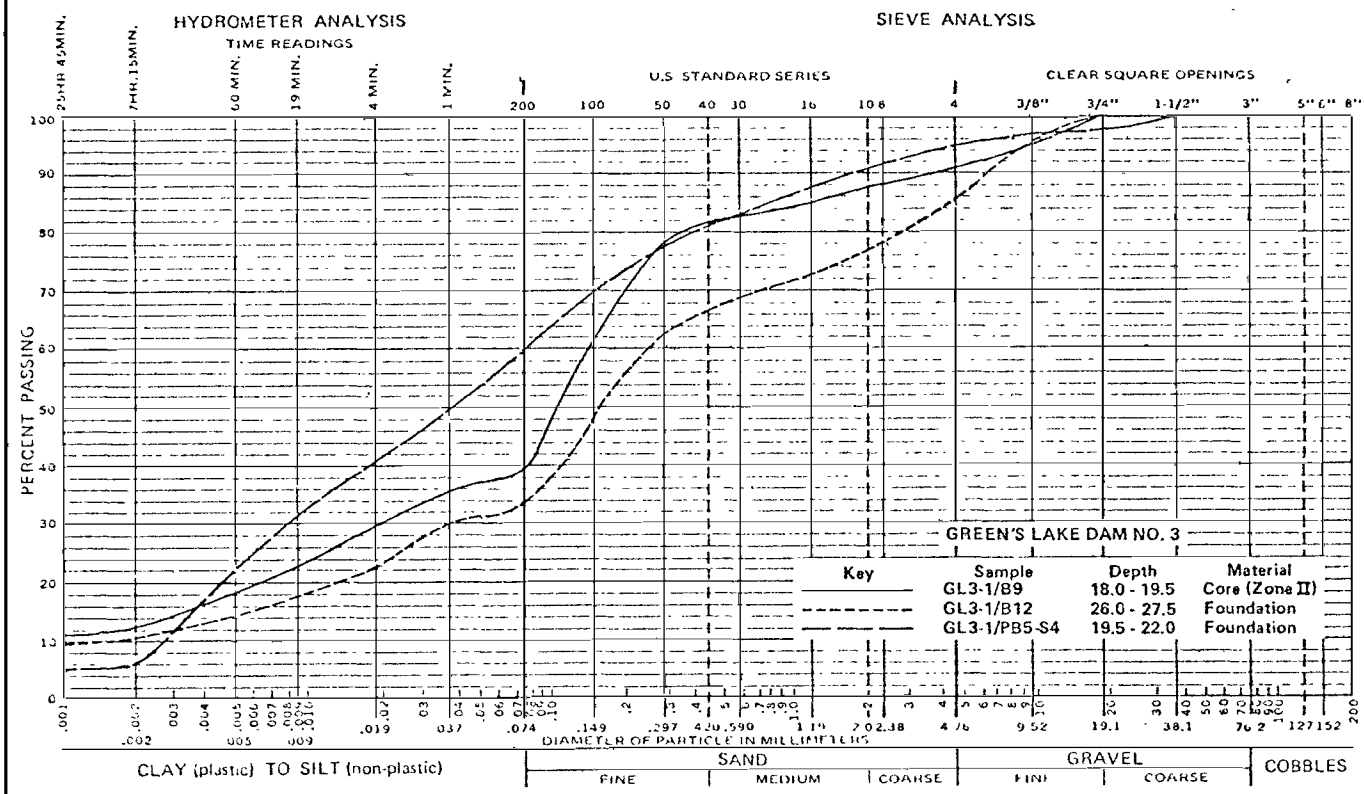

Earth Sciences Associates
Palo Alto, California

SEISMIC SAFETY INVESTIGATION OF EIGHT SCS DAMS
SUMMARY OF GRADATIONS
PINHOLE TESTS

Checked by MLT	Date 9/20/82	Project No.	Figure No.
Approved by J.E. Valera	Date 9/22/82	D118	A-8

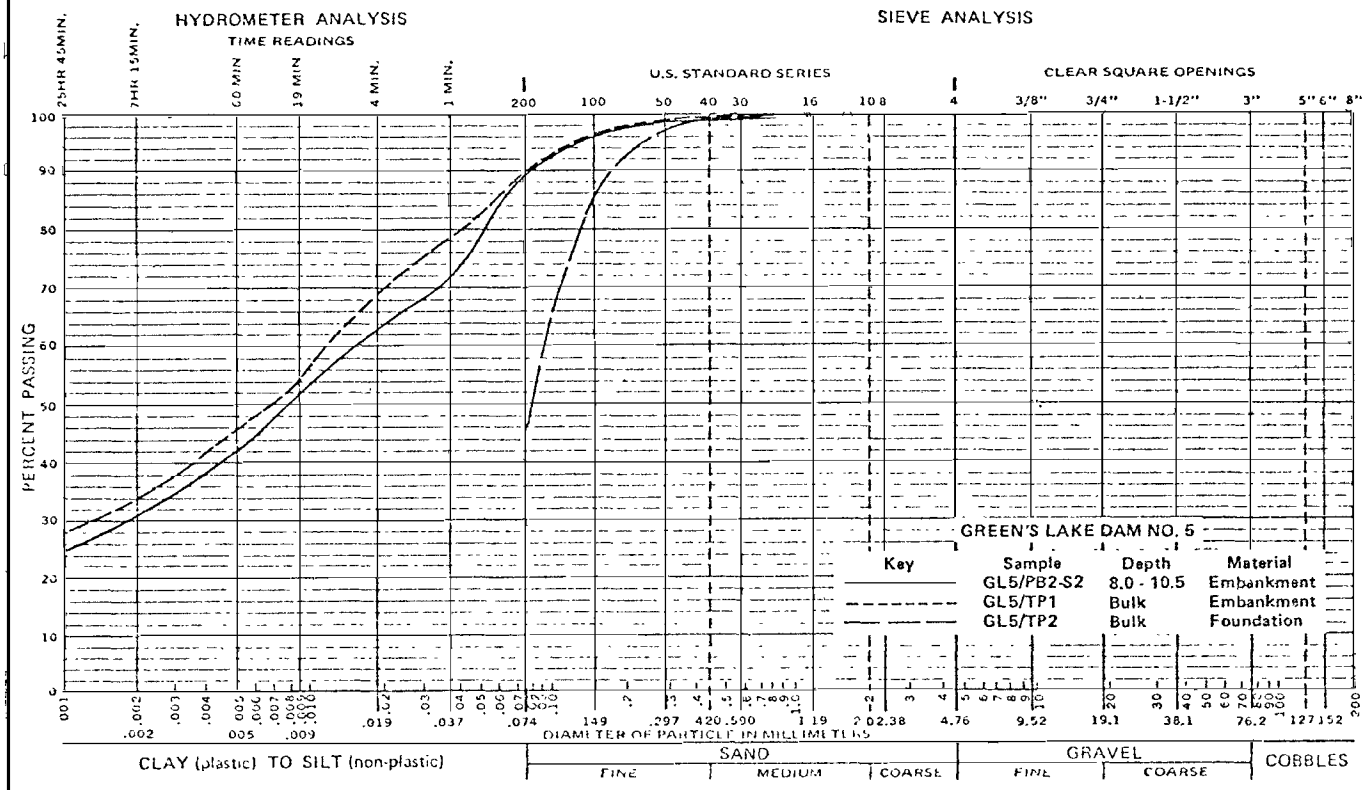

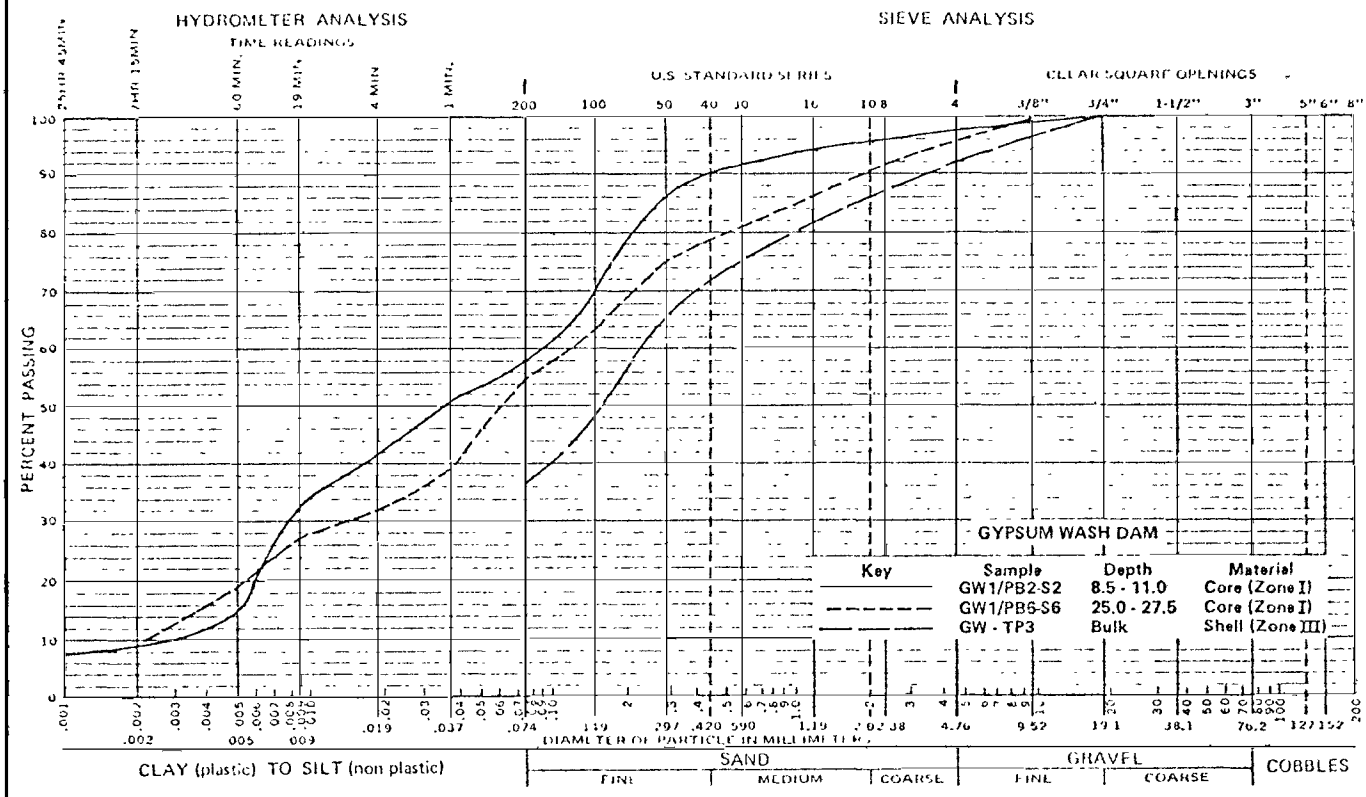

Earth Sciences Associates
Palo Alto, California

SEISMIC SAFETY INVESTIGATION OF EIGHT SCS DAMS
SUMMARY OF GRADATIONS
PINHOLE TESTS

Checked by MLT	Date 9/20/82	Project No.	Figure No
Approved by J.E. Valera	Date 9/22/82	D118	A-9

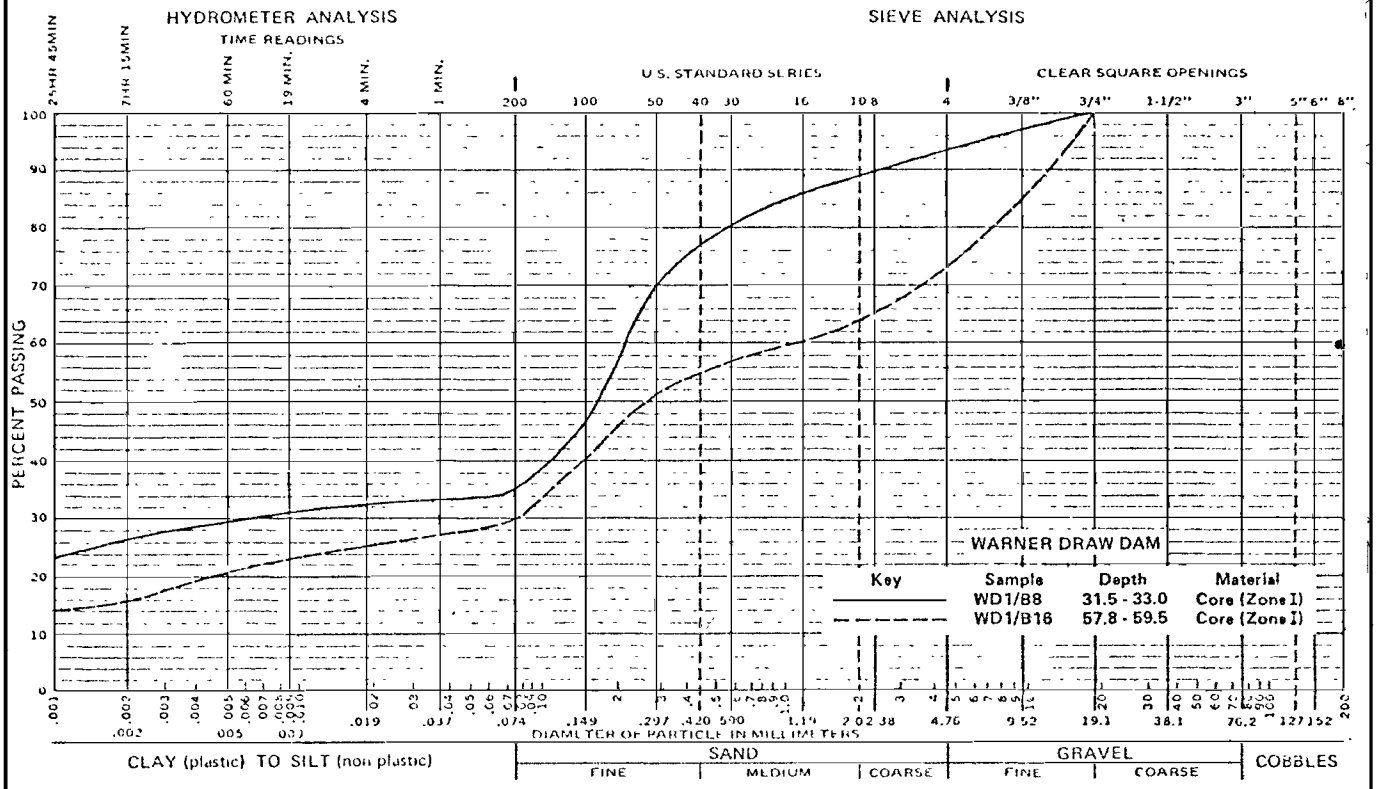

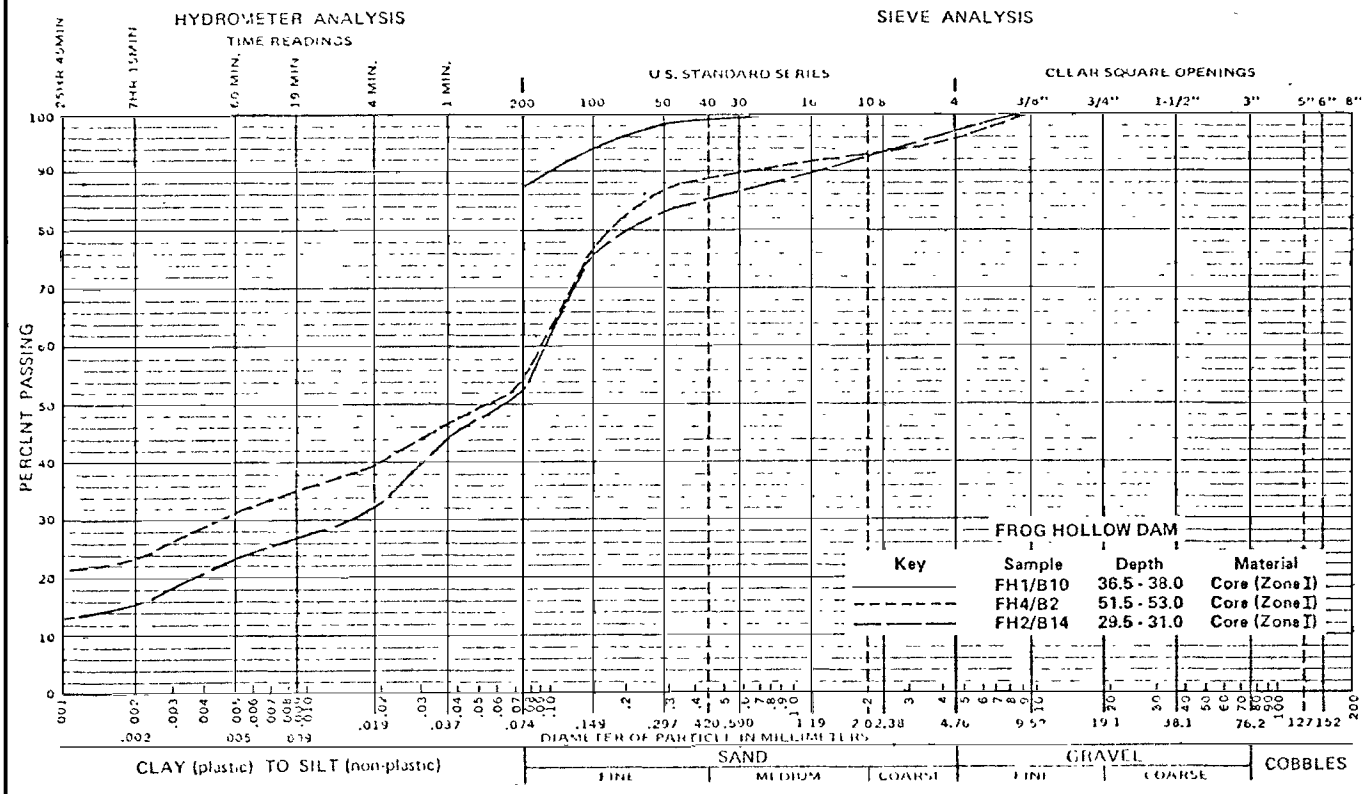

Earth Sciences Associates
Palo Alto, California

SEISMIC SAFETY INVESTIGATION OF EIGHT SCS DAMS
SUMMARY OF GRADATIONS
PINHOLE TESTS

Checked by MLT	Date 9/20/82	Project No.	Figure No.
Approved by J.E. Valera	Date 9/22/82	D118	A-10

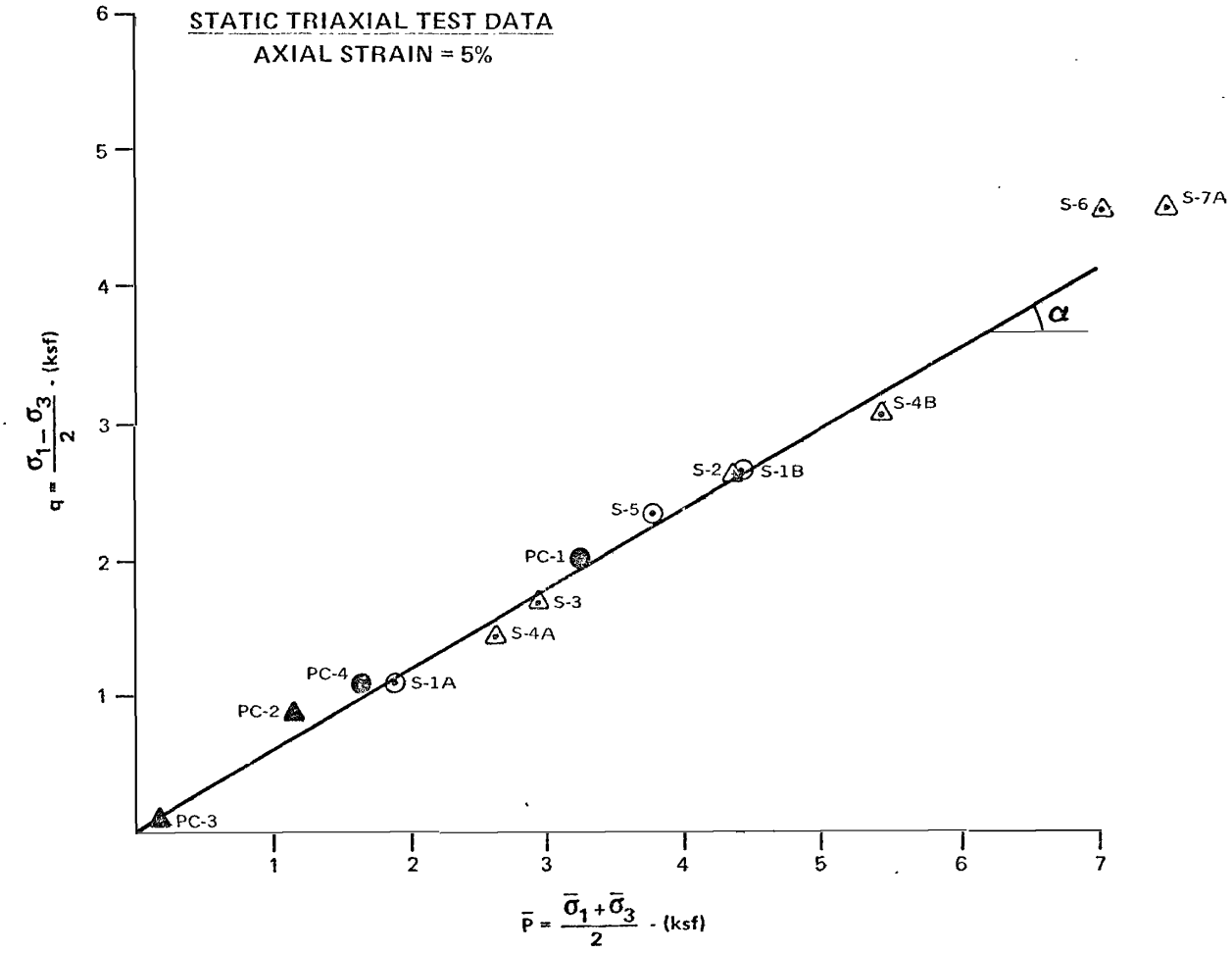

Embankment	Foundation
⊙ K_c = 1.0	△ K_c = 1.0
α = 30°	α = 30°
$\bar{\phi}$ = 35°	$\bar{\phi}$ = 35°
$\bar{c}$ = 0 psf	$\bar{c}$ = 0 psf

Solid symbols indicate post cyclic static triaxial tests.

NOTE: Data point for test S-7B not plotted since it is off the scale shown. Point does not change general interpretation of the data.

Earth Sciences Associates
Palo Alto, California

SEISMIC SAFETY INVESTIGATION OF EIGHT SCS DAMS
EFFECTIVE STRENGTH ENVELOPE
GREEN'S LAKE DAM NO. 3

Checked by M.L.T. Date 9/20/82
Approved by J. E. Valera Date 9/22/82

Project No.	Figure No.
D118	A-11

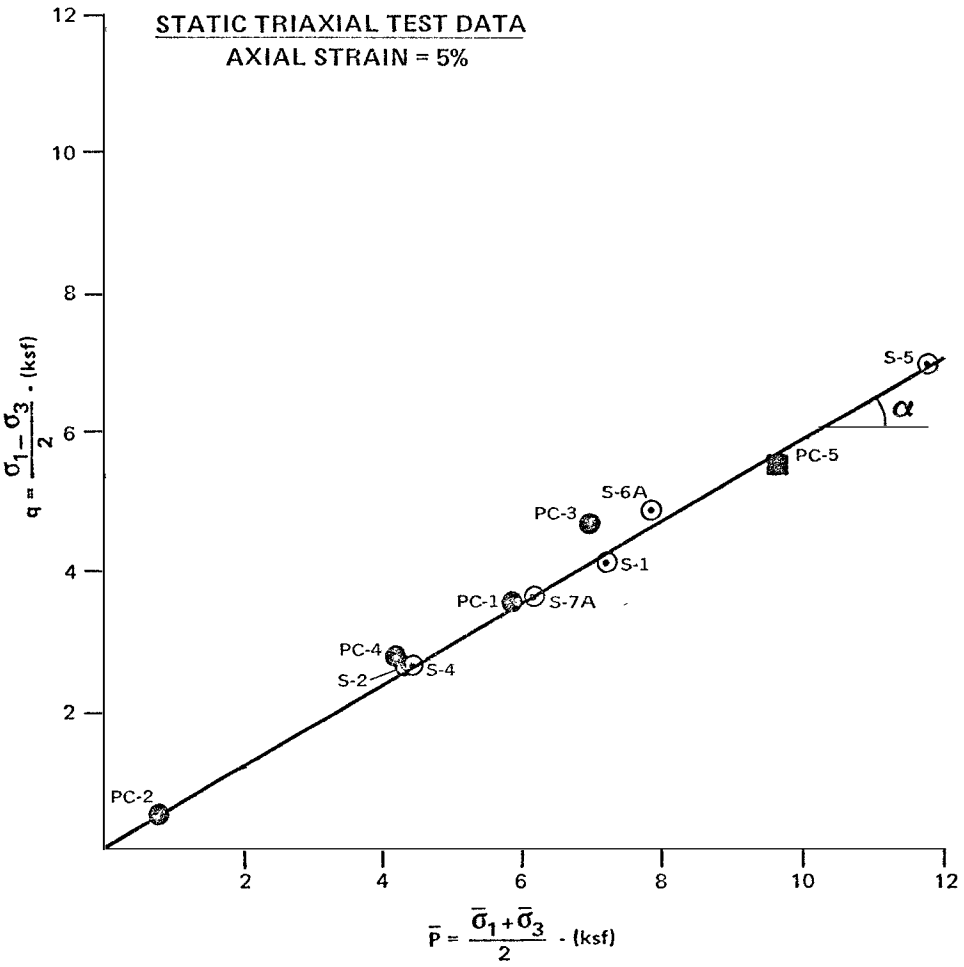

Embankment

⊙ $K_c = 1.0$

⊡ $K_c = 1.5$

$\alpha = 31°$

$\bar{\phi} = 37°$

$c = 0$ psf

Solid symbols indicate post cyclic static triaxial tests.

NOTE: Data points for tests S-3, S-6B, and S-7B not plotted since they are off the scale shown. Points do not change general interpretation of the data.

Earth Sciences Associates
Palo Alto, California

SEISMIC SAFETY INVESTIGATION OF EIGHT SCS DAMS
EFFECTIVE STRENGTH ENVELOPE
WARNER DRAW DAM

Checked by M.F. Date 9/20/82	Project No.	Figure No.
Approved by J.E. Valera Date 9/22/82	D118	A-12

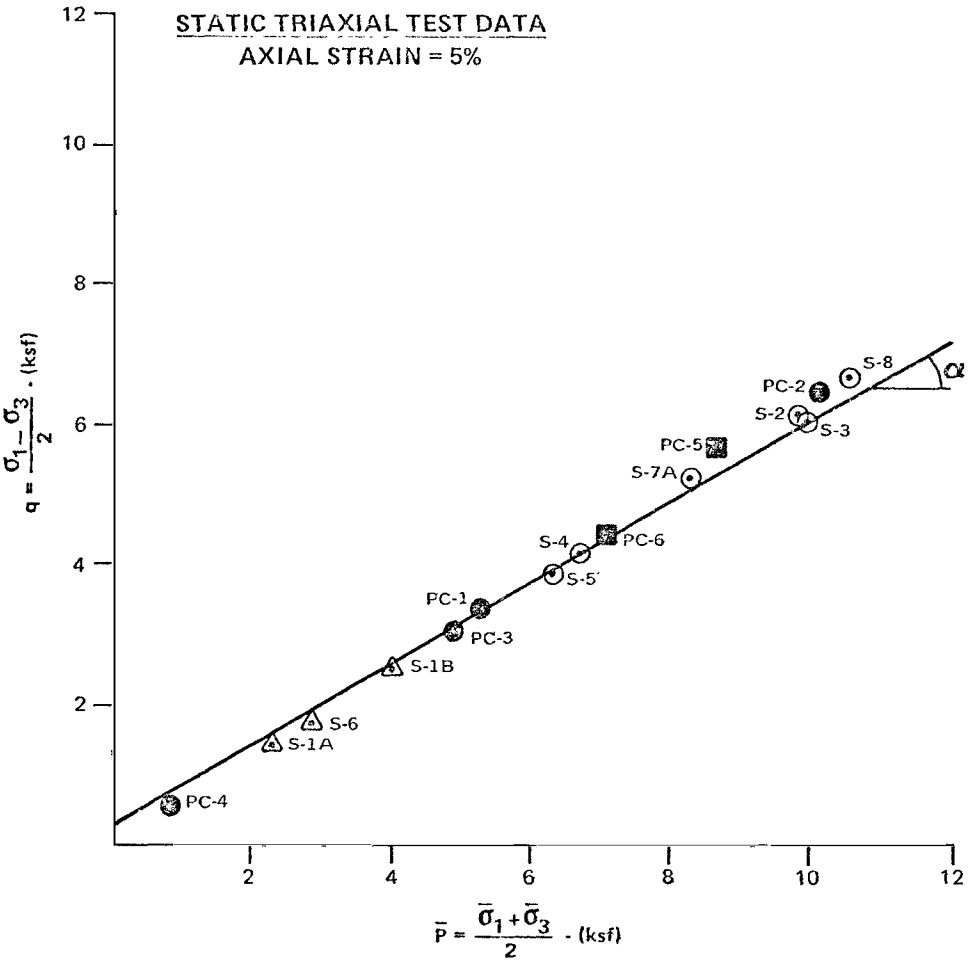

Embankment	Foundation
⊙ K_c = 1.0	△ K_c = 1.0
⊡ K_c = 1.5	
α = 30°	α = 30°
$\bar{\phi}$ = 35°	$\bar{\phi}$ = 35°
$\bar{c}$ = 250 psf	$\bar{c}$ = 250 psf

Solid symbols indicate post cyclic static triaxial tests.

NOTE: Data point for test S-7B not plotted since it is off the scale shown. Point does not change general interpretation of the data.

Earth Sciences Associates
Palo Alto, California

SEISMIC SAFETY INVESTIGATION OF EIGHT SCS DAMS
EFFECTIVE STRENGTH ENVELOPE
FROG HOLLOW DAM

Checked by MLT Date 9/20/82	Project No.	Figure No.
Approved by J.C. Valera Date 9/22/82	D118	A-13

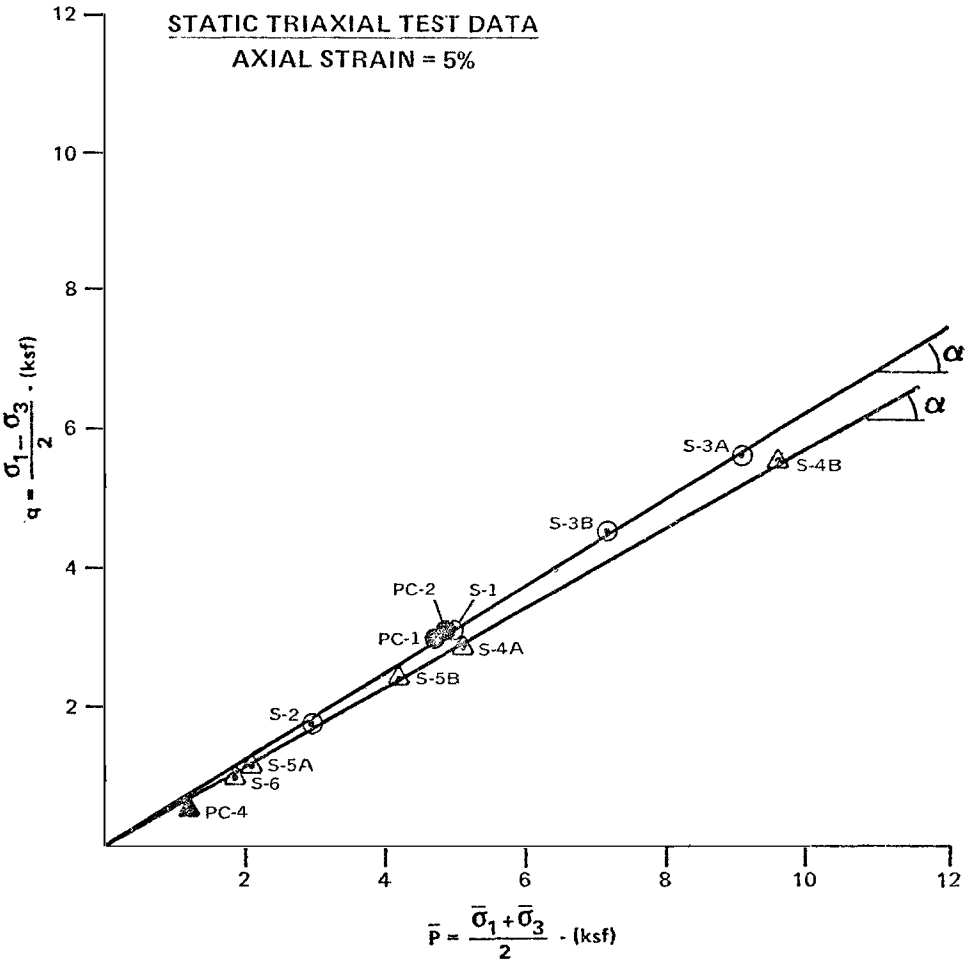

Embankment	Foundation
⊙ K_c = 1.0	△ K_c = 1.0
α = 32°	α = 29°
$\bar{\phi}$ = 38°	$\bar{\phi}$ = 34°
$\bar{c}$ = 0 psf	$\bar{c}$ = 0 psf

Solid symbols indicate post cyclic static triaxial tests.

Earth Sciences Associates
Palo Alto, California

SEISMIC SAFETY INVESTIGATION OF EIGHT SCS DAMS
EFFECTIVE STRENGTH ENVELOPE
IVINS DIVERSION DAM NO. 5

Checked by MLT Date 9/20/82	Project No.	Figure No.
Approved by J. E. Valera Date 9/22/82	D118	A-14

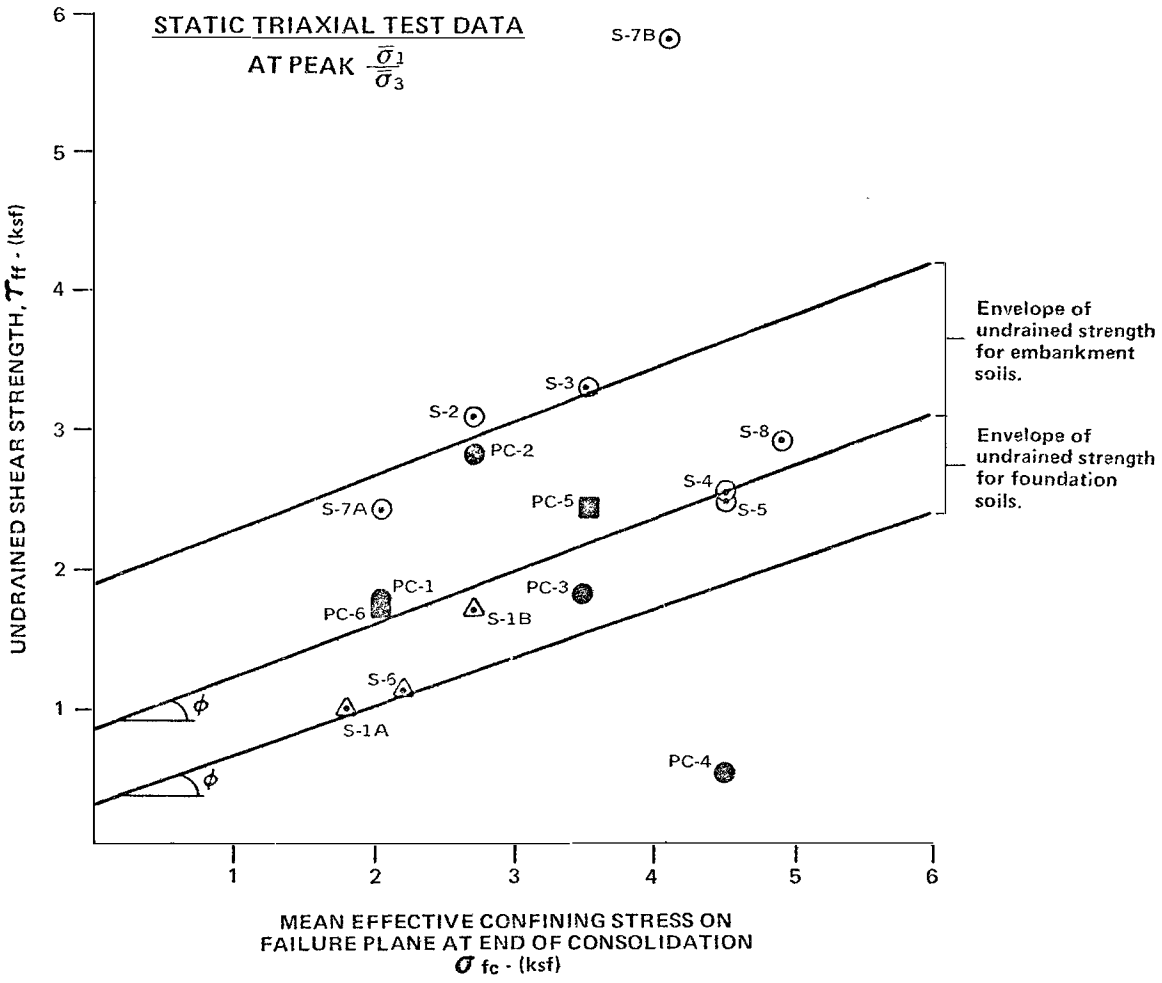

EMBANKMENT

⊙ K_c = 1.0

⊡ K_c = 1.5

FOUNDATION

△ K_c = 1.0

Solid symbols indicate post cyclic static triaxial tests.

AVERAGE UNDRAINED STRENGTH PARAMETERS

EMBANKMENT		FOUNDATION
Static	Post cyclic	Static
ϕ = 20°	ϕ = 20°	ϕ = 20°
c = 1375 psf	c = 850 psf	c = 575 psf

Earth Sciences Associates
Palo Alto, California

SEISMIC SAFETY INVESTIGATION OF EIGHT SCS DAMS
τ_{ff} VERSUS σ_{fc}
FROG HOLLOW DAM

Checked by M.L.T. Date 9/20/82	Project No.	Figure No.
Approved by J. E. Valera Date 9/22/82	D118	A-15

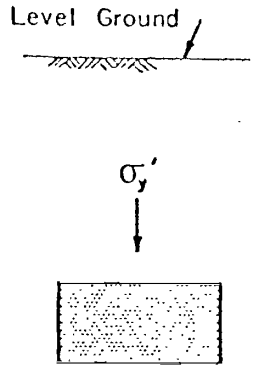

Field Condition

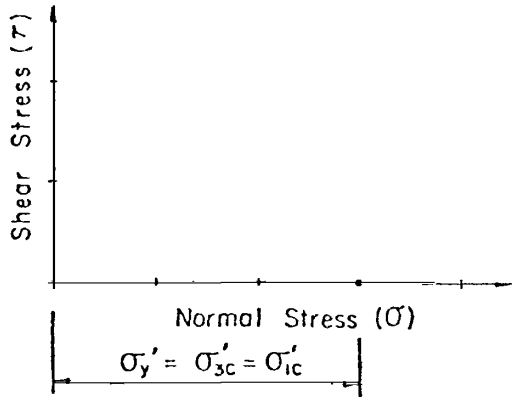

Mohr Diagram

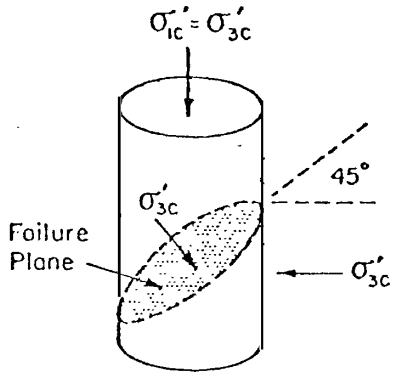

$$K_c = \frac{\sigma_{ic}'}{\sigma_{3c}'} = \frac{\sigma_{3c}'}{\sigma_{3c}'} = 1.0$$

Triaxial Sample

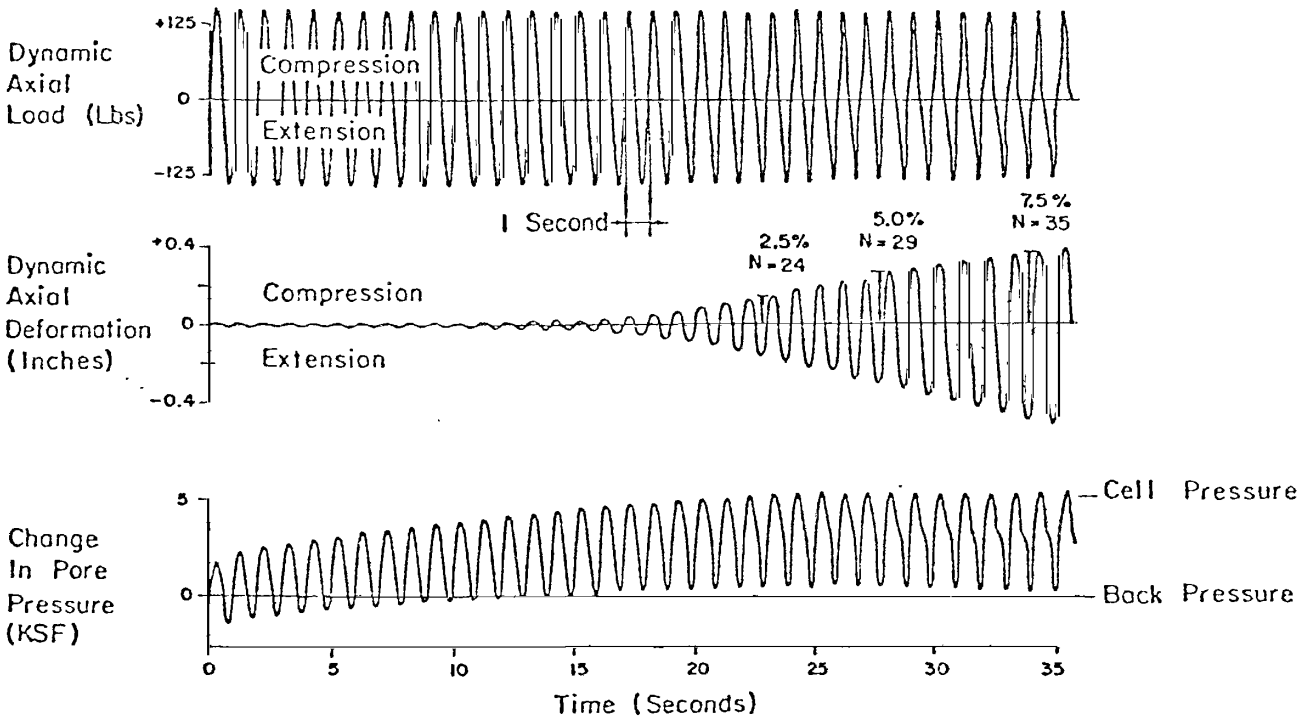

Earth Sciences Associates Palo Alto, California			
SEISMIC SAFETY INVESTIGATION OF EIGHT SCS DAMS STRESS CONDITION AND TYPICAL RESULTS OF CYCLIC TRIAXIAL TEST OF ISOTROPICALLY-CONSOLIDATED SAMPLE			
Checked by MLT Date 9/20/82 Approved by J.E. Valera Date 9/22/82	Project No. D118	Figure No. A-16	

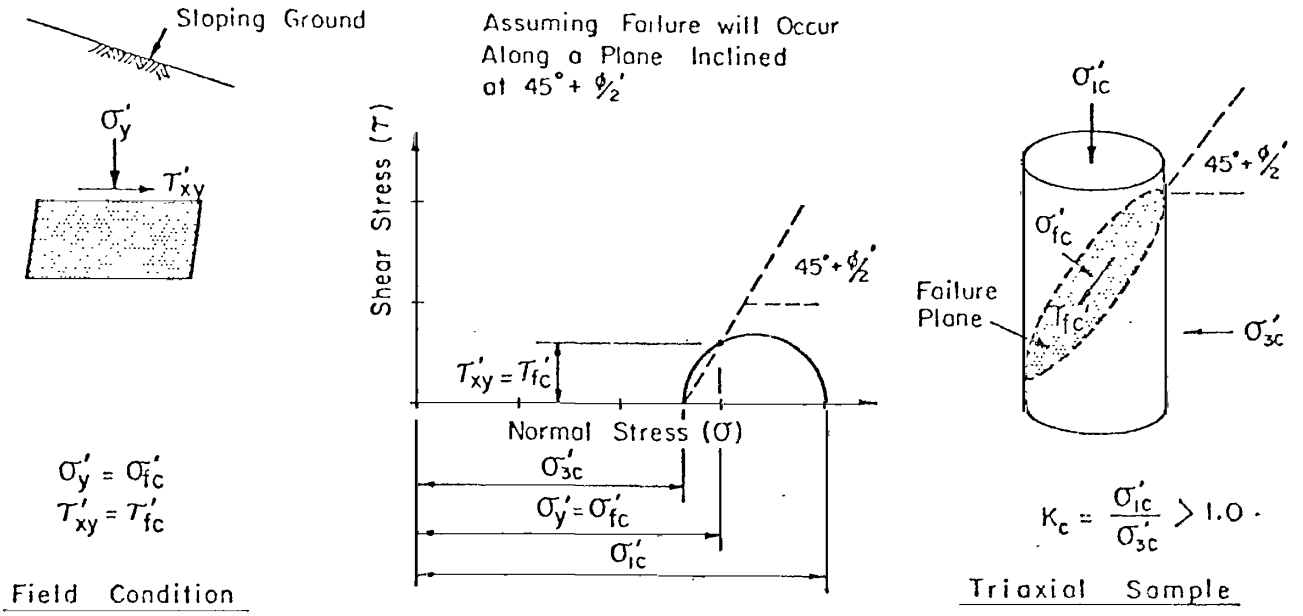

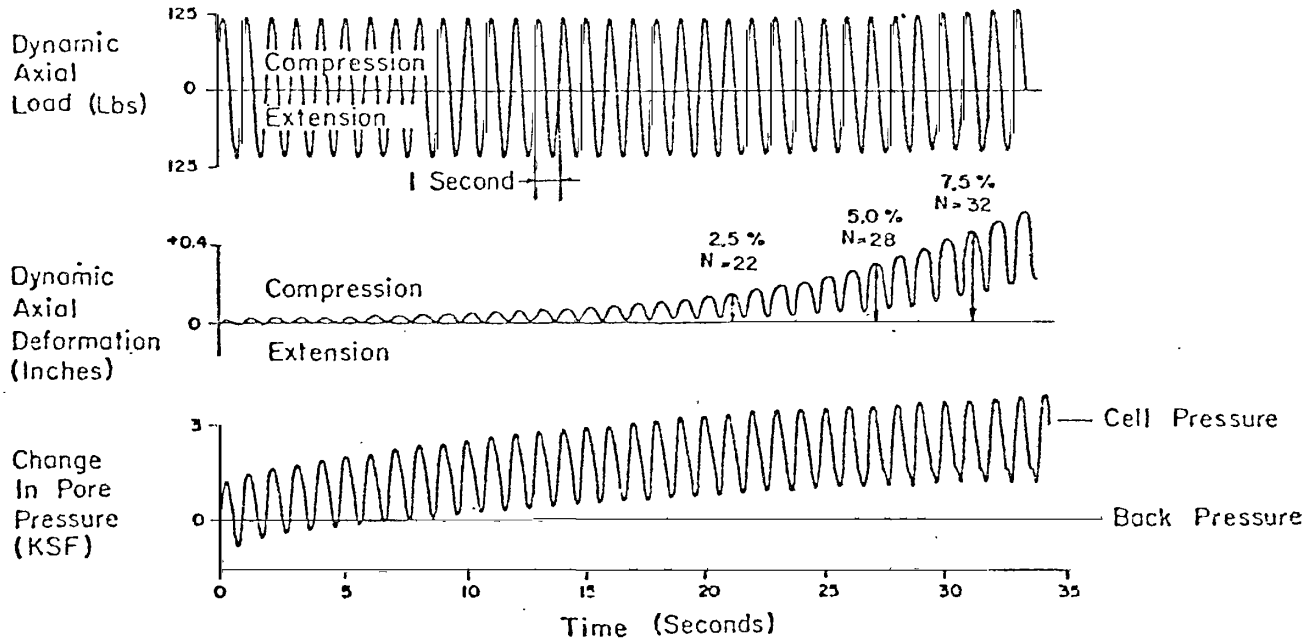

Earth Sciences Associates Palo Alto, California			
SEISMIC SAFETY INVESTIGATION OF EIGHT SCS DAMS STRESS CONDITION AND TYPICAL RESULTS OF TRIAXIAL TEST ON ANISOTROPICALLY-CONSOLIDATED SAMPLE			
Checked by MCT Date 9/20/82 Approved by J.E. Valera Date 9/22/82		Project No. D118	Figure No. A-17

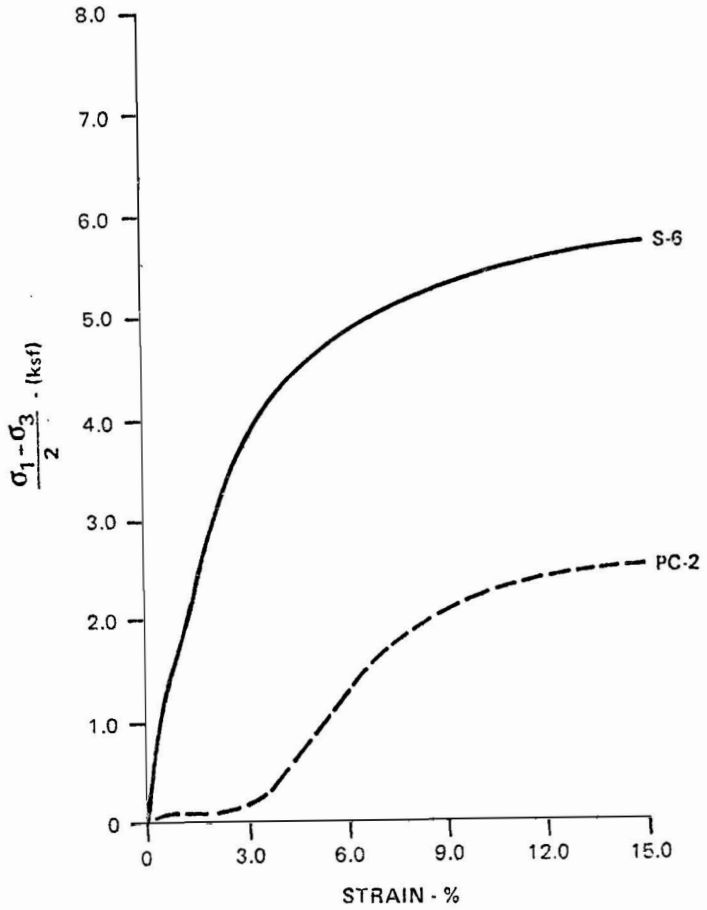

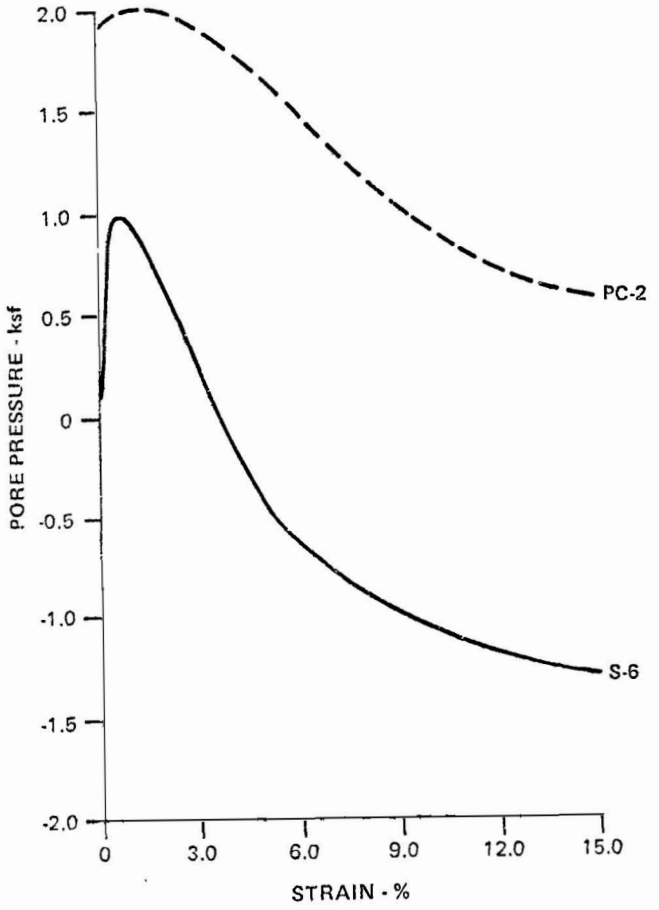

Static Test

Post Cyclic Static Test

Earth Sciences Associates
Palo Alto, California

SEISMIC SAFETY INVESTIGATION OF EIGHT SCS DAMS
COMPARISON OF STATIC
AND POST CYCLIC STATIC TESTS
GREEN'S LAKE NO. 3

Checked by MLT	Date 9/20/82	Project No.	Figure No.
Approved by J. E. Valera	Date 9/22/82	D118	A-18

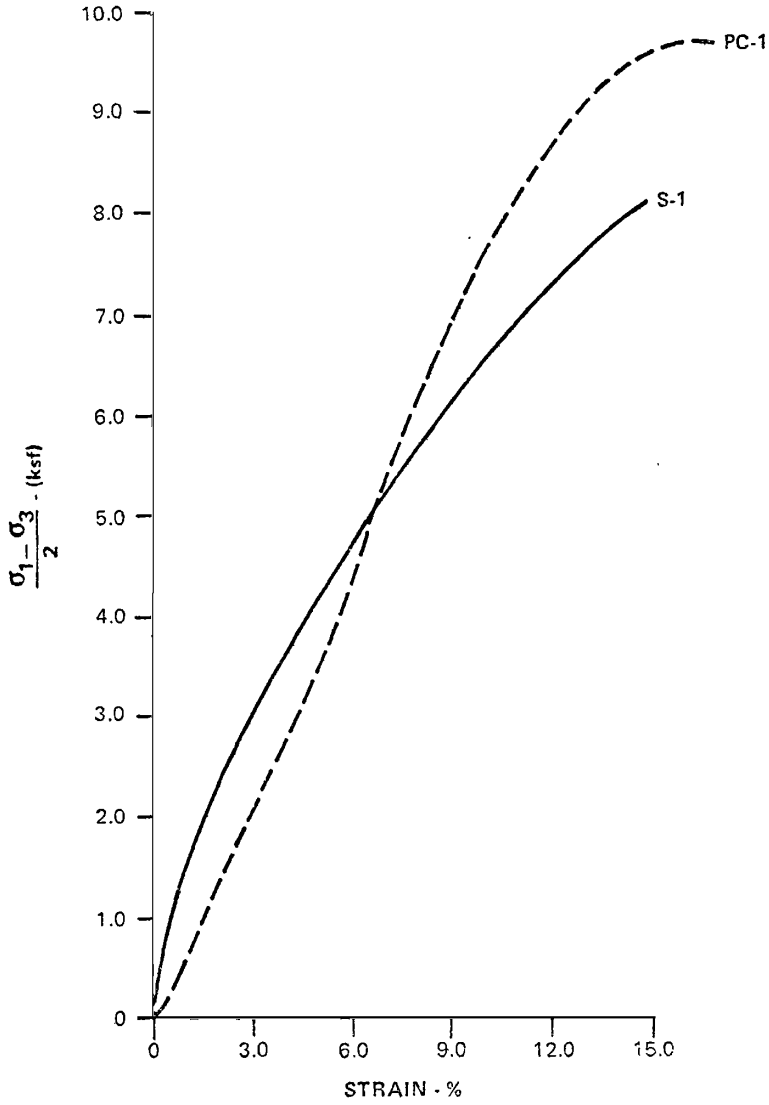

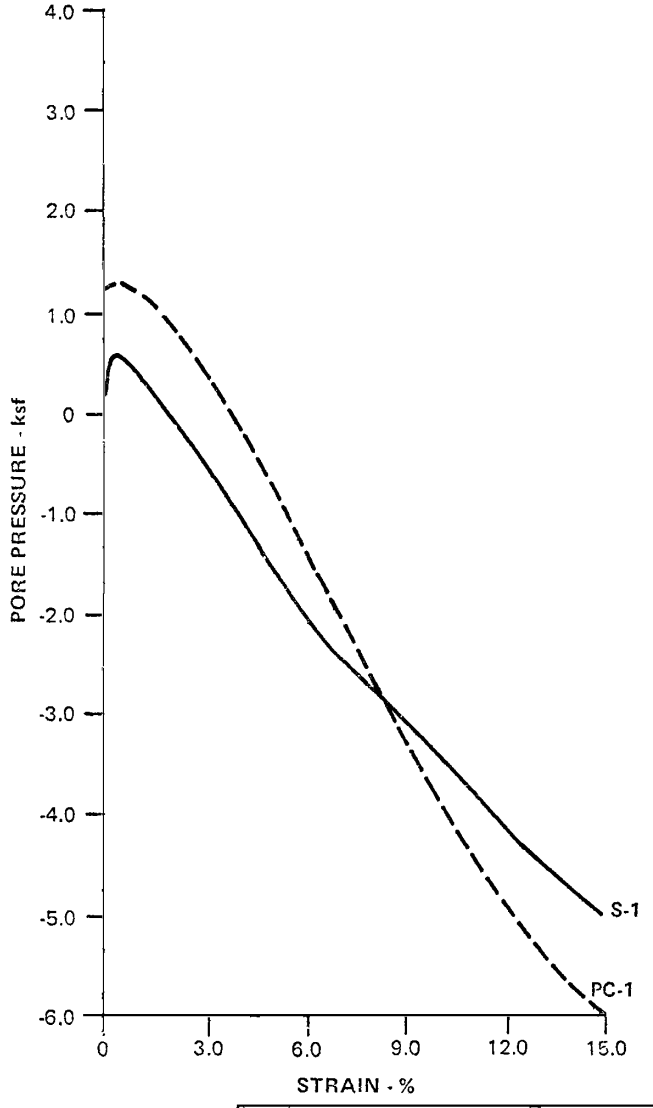

Static Test

Post Cyclic Static Test

Earth Sciences Associates
Palo Alto, California

SEISMIC SAFETY INVESTIGATION OF EIGHT SCS DAMS
COMPARISON OF STATIC
AND POST CYCLIC STATIC TESTS
WARNER DRAW DAM

Checked by MLT	Date 9/20/82	Project No.	Figure No.
Approved by J.E. Valera	Date 9/22/82	D118	A-19

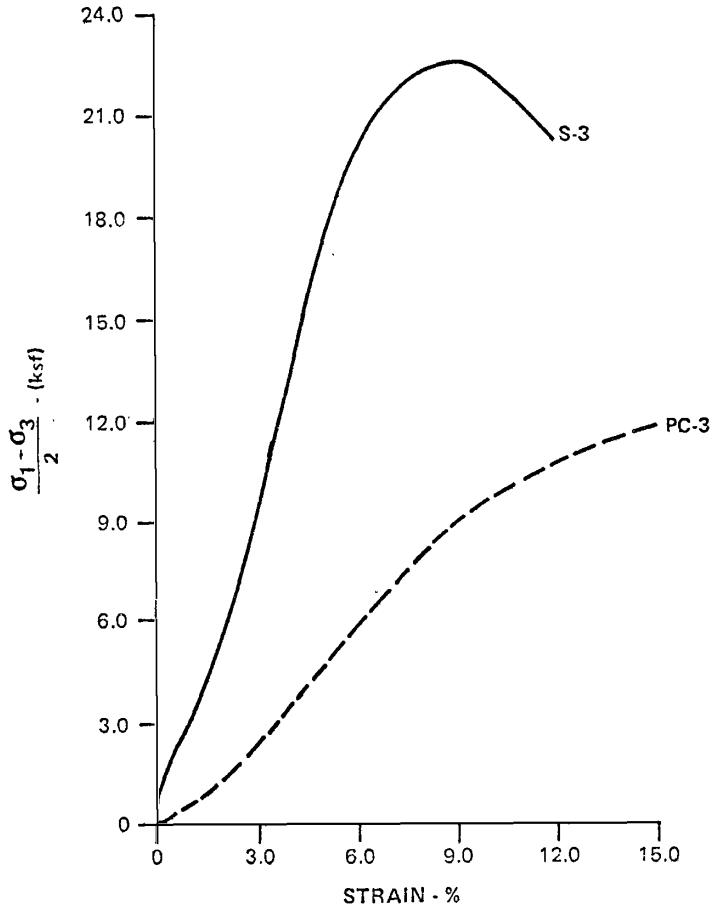

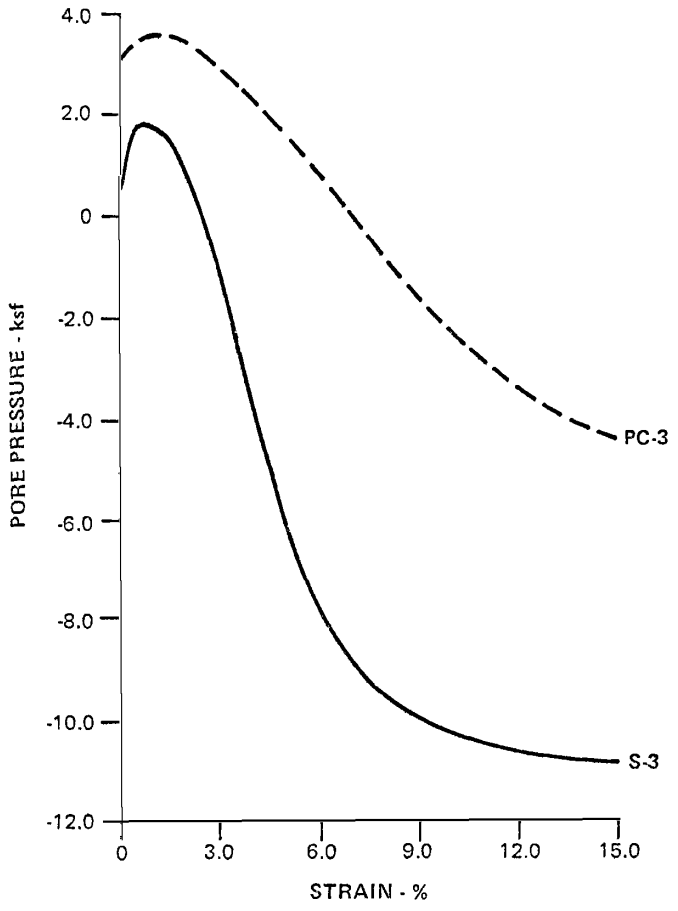

Static Test

Post Cyclic Static Test

Earth Sciences Associates
Palo Alto, California

SEISMIC SAFETY INVESTIGATION OF EIGHT SCS DAMS
COMPARISON OF STATIC
AND POST CYCLIC STATIC TESTS
WARNER DRAW DAM

Checked by MLT	Date 9/20/82	Project No.	Figure No.
Approved by J. C. Valera	Date 9/22/82	D118	A-20

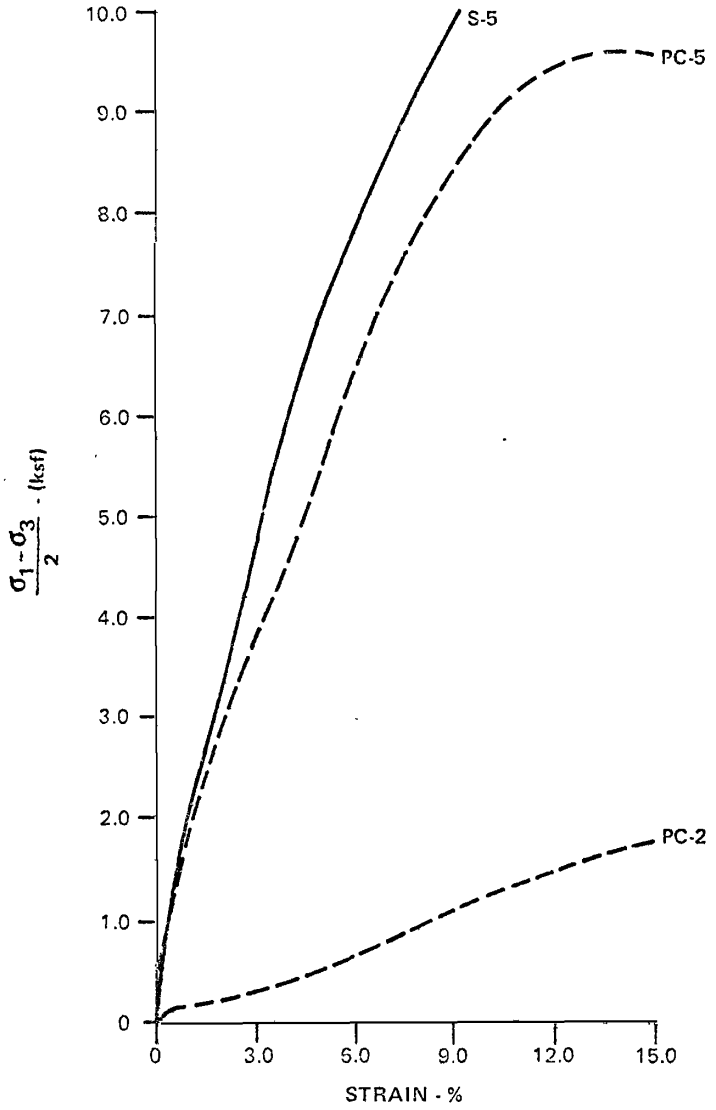

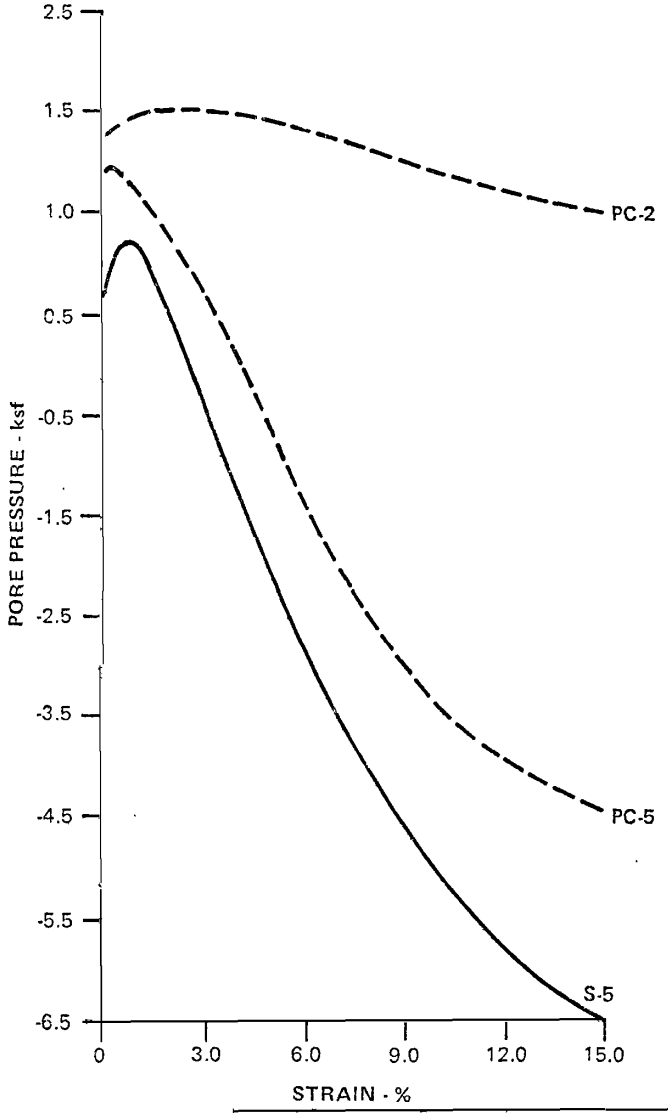

Static Test

Post Cyclic Static Test

Earth Sciences Associates
Palo Alto, California

SEISMIC SAFETY INVESTIGATION OF EIGHT SCS DAMS
COMPARISON OF STATIC
AND POST CYCLIC STATIC TESTS
WARNER DRAW DAM

Checked by MLT Date 9/20/82	Project No.	Figure No.
Approved by J.E. Valera Date 9/22/82	D118	A-21

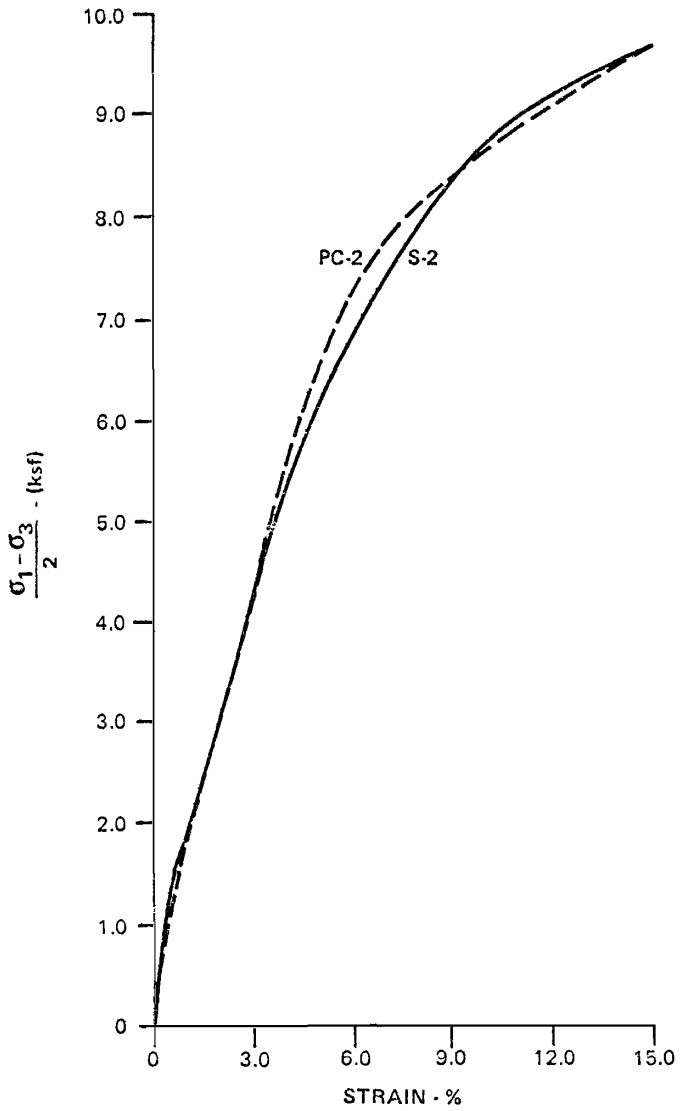

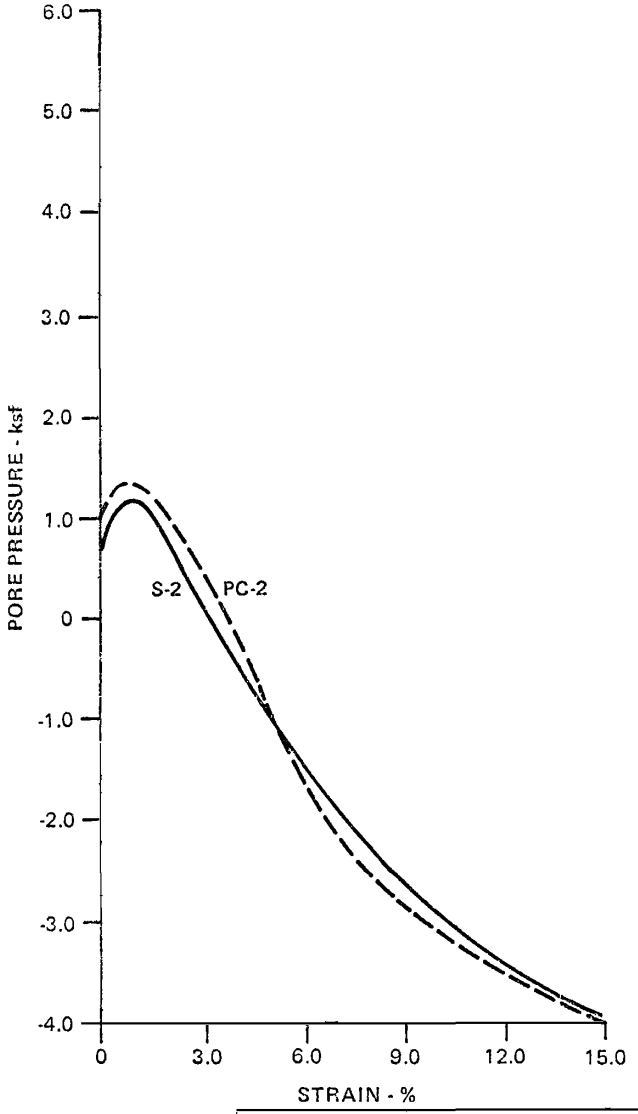

Static Test

Post Cyclic Static Test

Earth Sciences Associates
Palo Alto, California

SEISMIC SAFETY INVESTIGATION OF EIGHT SCS DAMS
COMPARISON OF STATIC
AND POST CYCLIC STATIC TESTS
FROG HOLLOW DAM

Checked by MLT	Date 9/20/82	Project No.	Figure No.
Approved by R. E. Valera	Date 9/22/82	D118	A-22

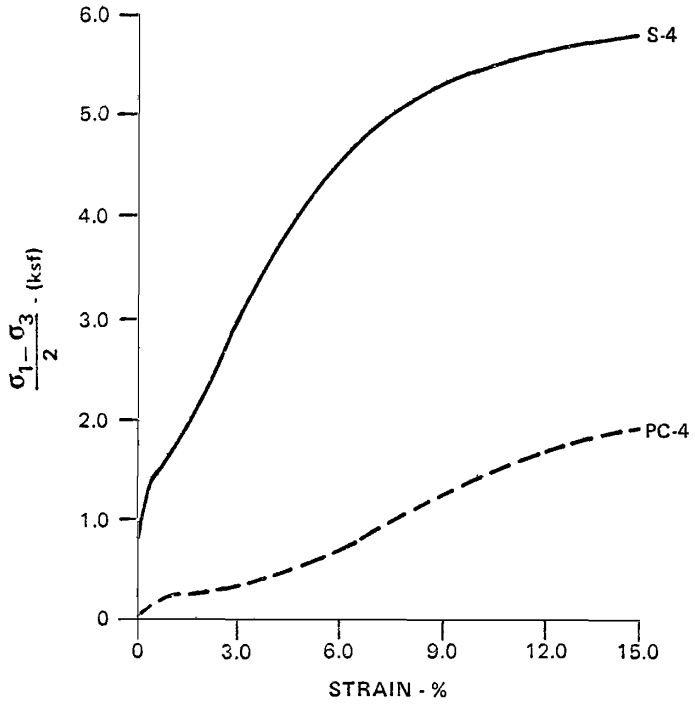

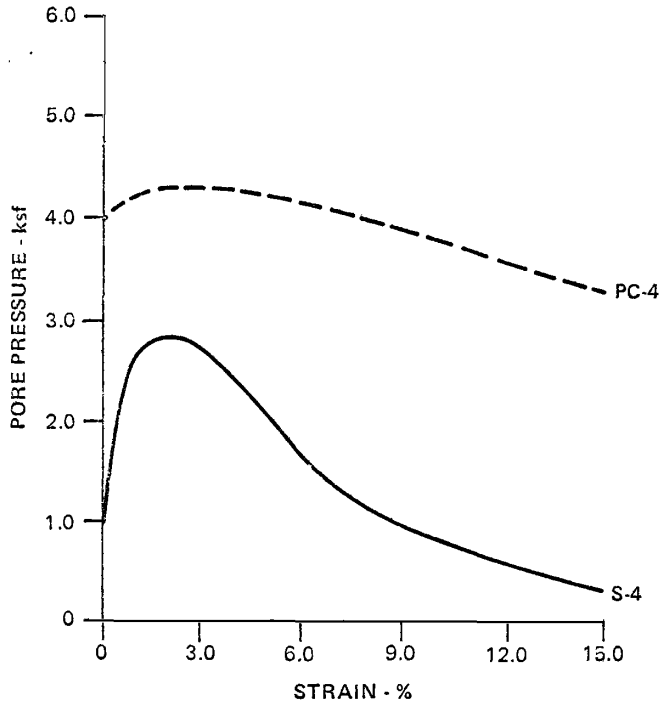

Static Test

Post Cyclic Static Test

Earth Sciences Associates
Palo Alto, California

SEISMIC SAFETY INVESTIGATION OF EIGHT SCS DAMS
COMPARISON OF STATIC
AND POST CYCLIC STATIC TESTS
FROG HOLLOW DAM

Checked by MLT	Date 9/20/82	Project No.	Figure No.
Approved by J.E. Valera	Date 9/22/82	D118	A-23

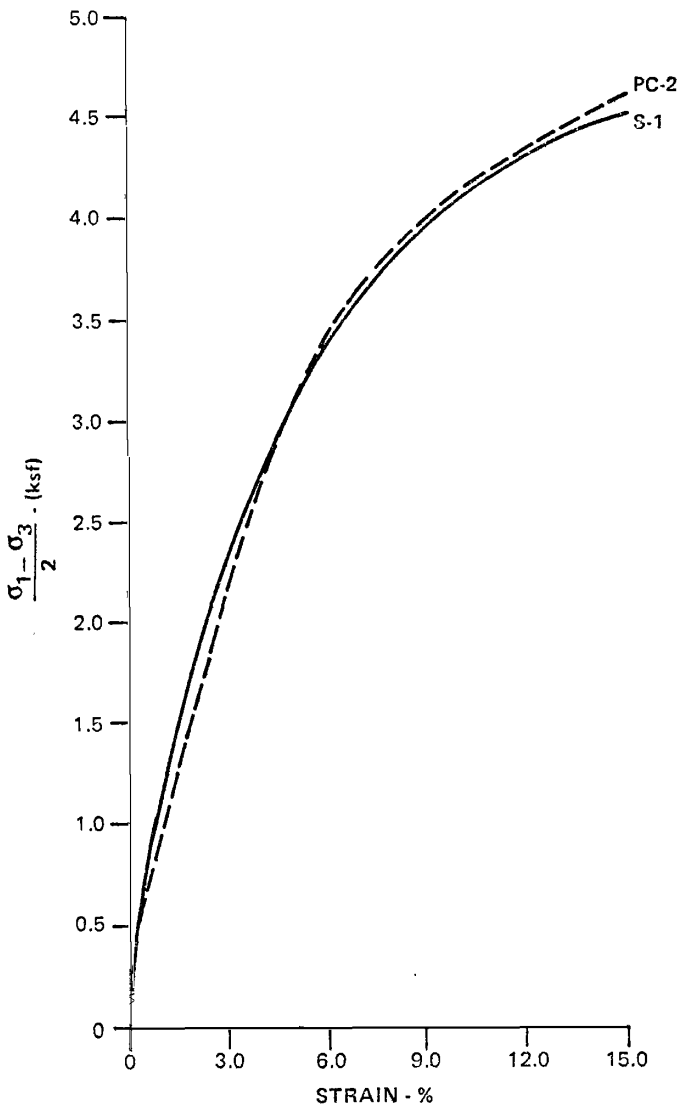

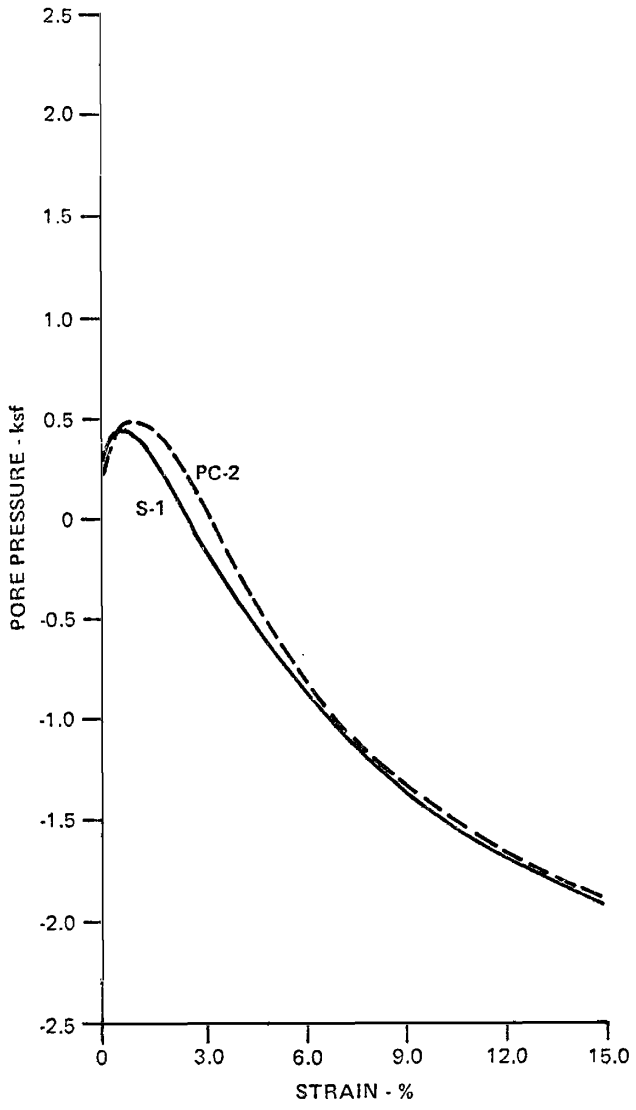

Static Test

Post Cyclic Static Test

Earth Sciences Associates
Palo Alto, California

SEISMIC SAFETY INVESTIGATION OF EIGHT SCS DAMS
COMPARISON OF STATIC
AND POST CYCLIC STATIC TESTS
IVINS DIVERSION DAM NO. 5

Checked by M.L.T. Date 9/20/82	Project No.	Figure No.
Approved by J.E. Valera Date 9/22/82	D118	A-24

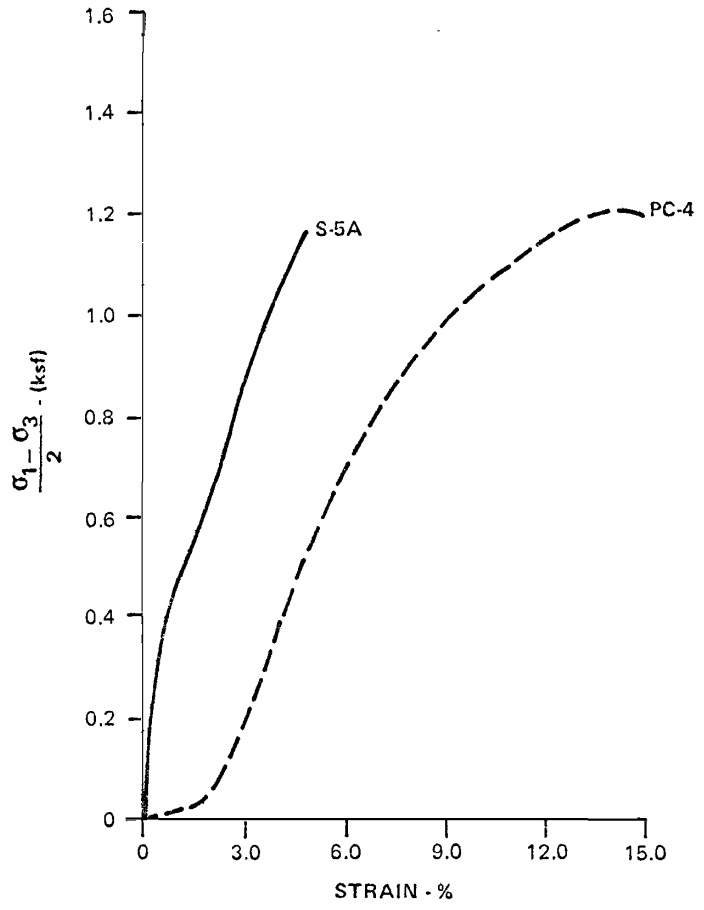

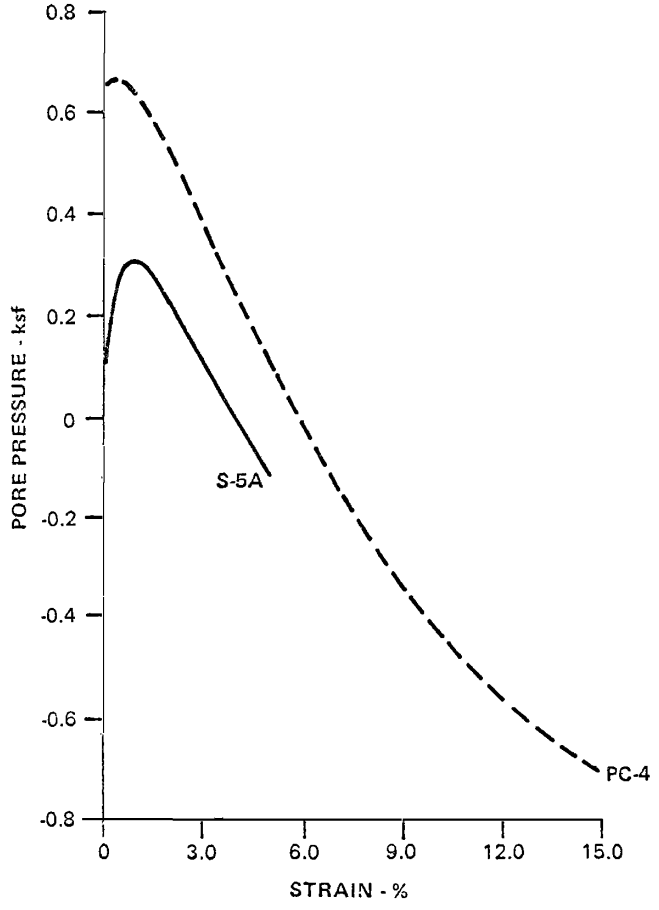

Static Test

Post Cyclic Static Test

Earth Sciences Associates
Palo Alto, California

SEISMIC SAFETY INVESTIGATION OF EIGHT SCS DAMS
COMPARISON OF STATIC
AND POST CYCLIC STATIC TESTS
IVINS DIVERSION DAM NO. 5

Checked by M.Y.T. Date 9/20/82
Approved by J.C. Valera Date 9/22/82

Project No. D118

Figure No. A-25

APPENDIX B

RESULTS OF STATIC TRIAXIAL TESTS

GREEN'S LAKE DAM NO. 3

CONSOLIDATED UNDRAINED TRIAXIAL TEST
WITH PORE PRESSURE MEASUREMENT

STATIC TX=GL1 KC-1.0
D118-23APR_82
BORING:GL3-1 SAMPLE:PB2
SILTY FINE SAND

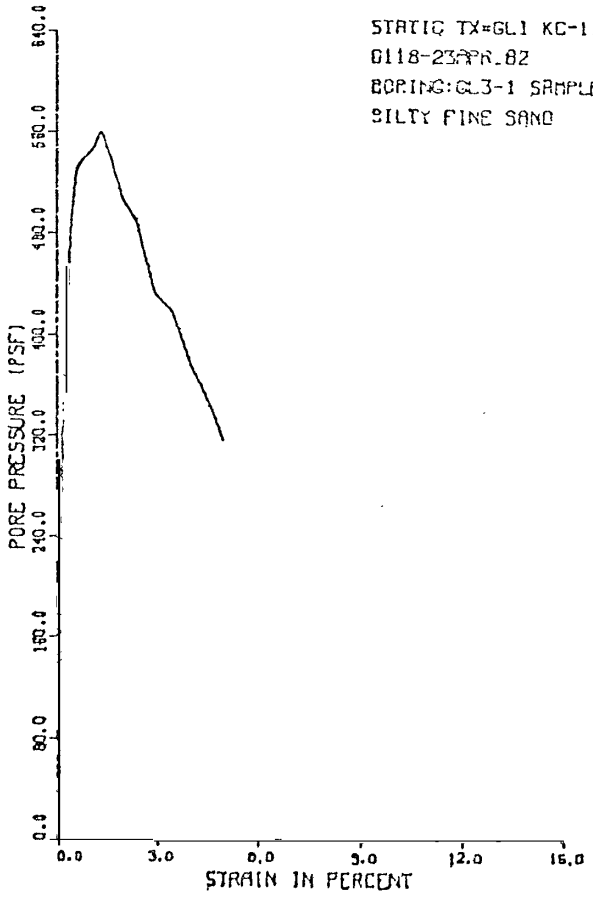

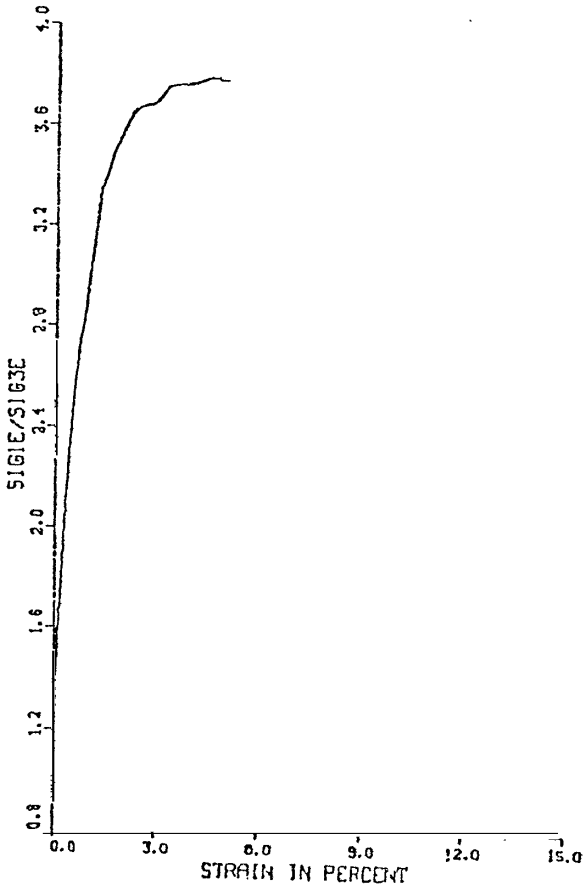

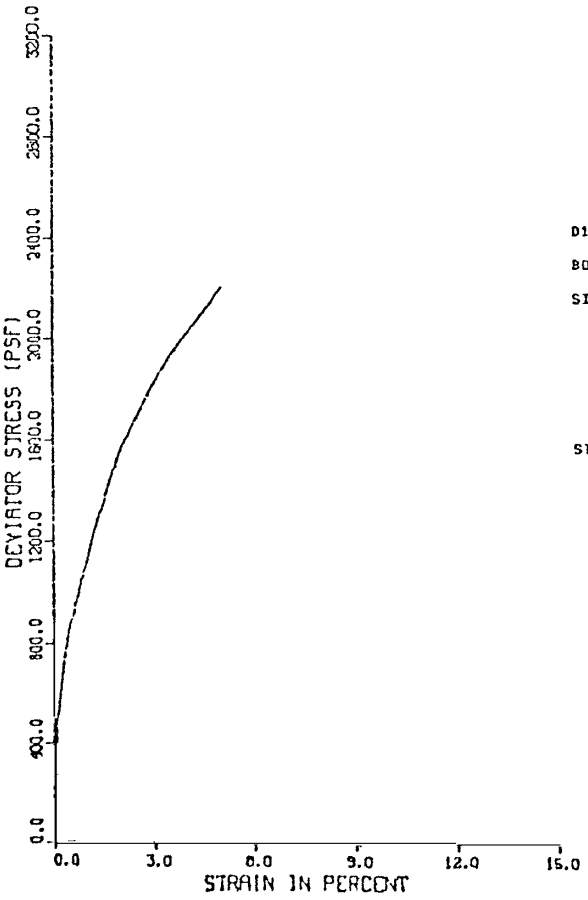

ISOTROPIC CONSOLIDATED UNDRAINED TRIAXIAL TEST
WITH PORE PRESSURE MEASUREMENTS
D118-UTAH DAMS-GREENS LAKE#3 STATIC TX#1A STAGE 1 4/23/82 RED. BY BW

BORING:GL3-1 SAMPLE:PB-2/S-2 DEPTH:8.0-10.5

SILTY FINE SAND

AT END OF CONSOLIDATION :
SAMPLE HEIGHT ..... = 5.970 INCHES
SAMPLE AREA ..... = 6.335 SQ. INCHES
EFFECTIVE CONFINING STRESS . = 1109. PSF
EFFECTIVE MAJOR PRIN. STRESS = 1109. PSF
PRINCIPAL STRESS RATIO ..... = 1.00

STRAIN PCT	SIGMA3E PSF	SIGMA1E PSF	RATIO SIG1E/SIG3E	PPRESS PSF	PBAR PSF	PTOT PSF	Q PSF
.0	1109.	1109.	1.0	0.	1109.	1109.	0.
.1	850.	1326.	1.6	259.	1088.	1347.	238.
.3	691.	1394.	2.0	418.	1043.	1460.	351.
.4	619.	1457.	2.4	490.	1038.	1527.	419.
.6	576.	1502.	2.6	533.	1039.	1572.	463.
1.1	562.	1753.	3.1	547.	1157.	1704.	596.
1.3	547.	1826.	3.3	562.	1187.	1748.	639.
1.5	562.	1905.	3.4	547.	1233.	1781.	672.
1.7	576.	2007.	3.5	533.	1291.	1824.	715.
2.0	605.	2164.	3.6	504.	1384.	1888.	780.
2.4	619.	2283.	3.7	490.	1451.	1941.	832.
2.9	677.	2486.	3.7	432.	1582.	2014.	905.
3.5	691.	2622.	3.8	418.	1657.	2074.	965.
4.0	734.	2763.	3.8	374.	1749.	2123.	1014.
4.6	763.	2889.	3.8	346.	1826.	2172.	1063.
5.0	792.	2995.	3.8	317.	1893.	2210.	1101.

STATIC TRIAXIAL TEST: S-1A
GREEN'S LAKE DAM NO. 3

CONSOLIDATED UNDRAINED TRIAXIAL TEST
WITH PORE PRESSURE MEASUREMENT

STATIC TX=GL1B KC=1.0
0118-23APR.82
BORING:GL3-1 SAMPLE:PB2
SILTY SAND

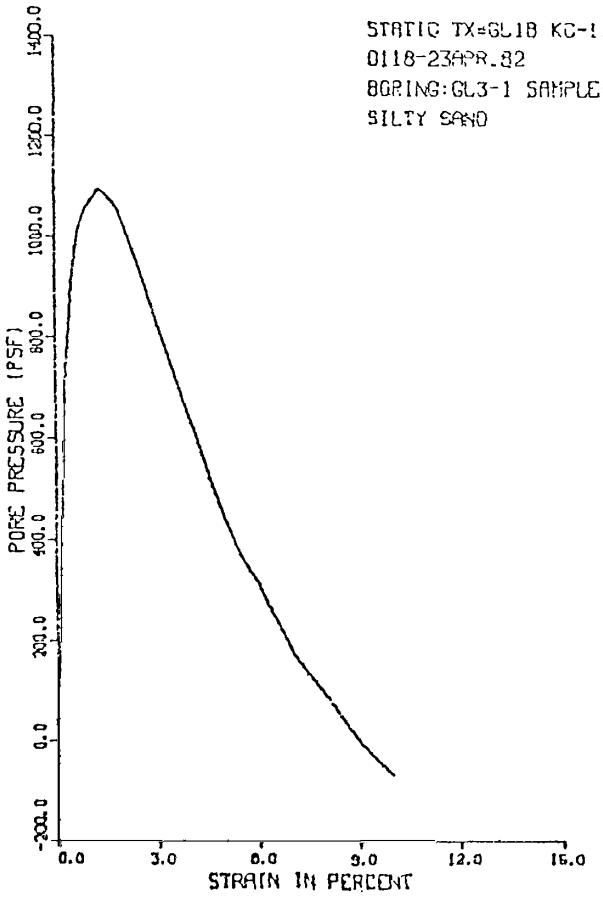

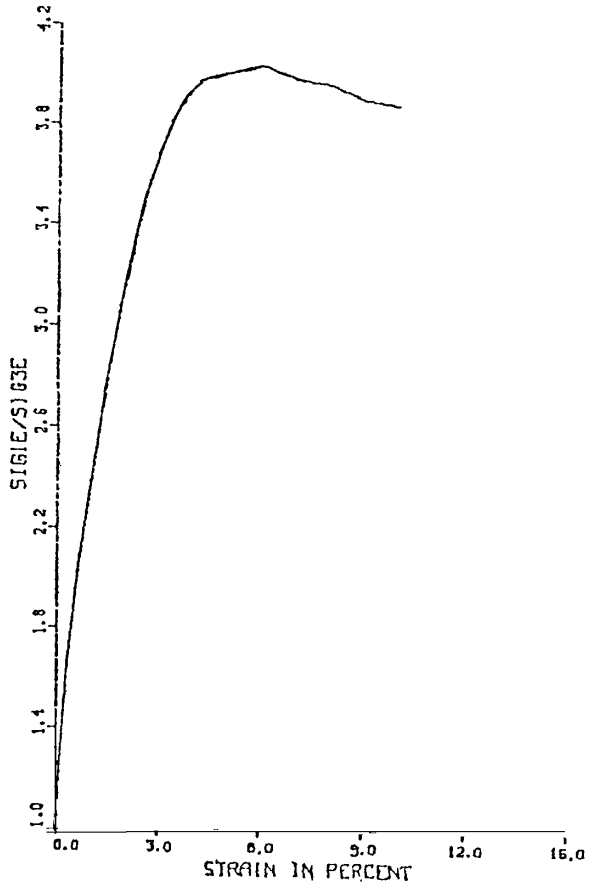

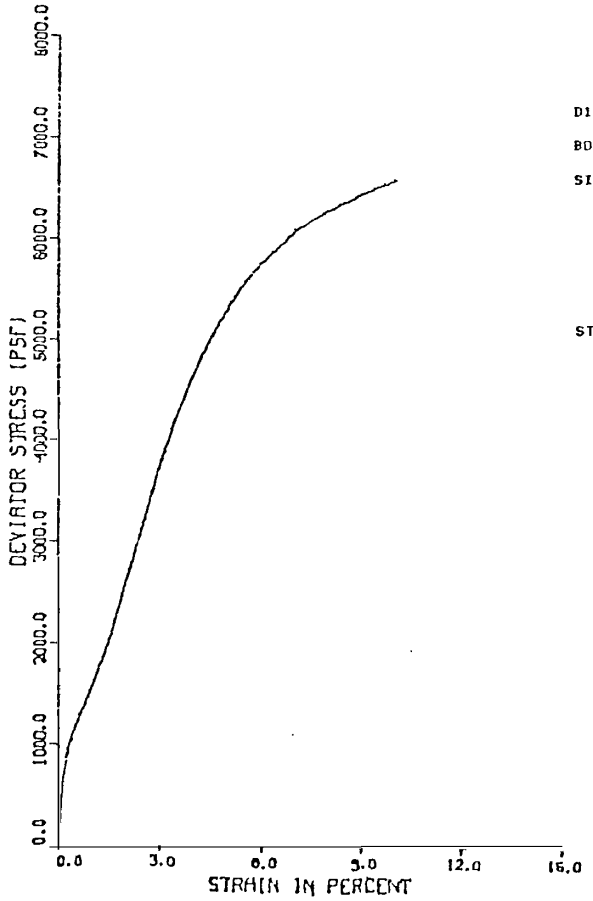

ISOTROPIC CONSOLIDATED UNDRAINED TRIAXIAL TEST
WITH PORE PRESSURE MEASUREMENTS
D118-UTAH DAMS-GREENS LAKE#3 STATIC TX#GL1B STAGE2 4/23/82 RED. BY BW

BORING:GL3-1 SAMPLE:PB-2/S-2 DEPTH:8.0-10.5

SILTY SAND

AT END OF CONSOLIDATION :
SAMPLE HEIGHT ..... = 5.423 INCHES
SAMPLE AREA ..... = 6.783 SQ. INCHES
EFFECTIVE CONFINING STRESS . = 2218. PSF
EFFECTIVE MAJOR PRIN. STRESS = 2218. PSF
PRINCIPAL STRESS RATIO ..... = 1.00

STRAIN PCT	SIGMA3E PSF	SIGMA1E PSF	RATIO SIG1E/SIG3E	PPRESS PSF	PBAR PSF	PTOT PSF	Q PSF
.0	2218.	2218.	1.0	0.	2218.	2218.	0.
.1	1886.	2459.	1.3	331.	2173.	2504.	286.
.3	1512.	2443.	1.6	706.	1978.	2683.	466.
.5	1310.	2451.	1.9	907.	1881.	2788.	570.
.7	1210.	2517.	2.1	1008.	1863.	2871.	654.
.9	1166.	2639.	2.3	1051.	1903.	2954.	736.
1.3	1123.	2967.	2.6	1094.	2045.	3140.	922.
1.5	1138.	3146.	2.8	1080.	2142.	3222.	1004.
1.9	1166.	3583.	3.1	1051.	2375.	3426.	1208.
2.2	1238.	4082.	3.3	979.	2660.	3639.	1422.
2.6	1310.	4618.	3.5	907.	2964.	3871.	1654.
3.0	1397.	5164.	3.7	821.	3281.	4101.	1884.
3.4	1469.	5631.	3.8	749.	3550.	4299.	2081.
3.8	1555.	6088.	3.9	662.	3822.	4484.	2267.
4.2	1627.	6466.	4.0	590.	4047.	4637.	2420.
4.6	1714.	6836.	4.0	504.	4275.	4779.	2561.
5.0	1771.	7096.	4.0	446.	4433.	4880.	2662.
5.4	1843.	7403.	4.0	374.	4623.	4998.	2780.
6.0	1901.	7668.	4.0	317.	4785.	5101.	2884.
7.0	2045.	8144.	4.0	173.	5094.	5267.	3050.
8.1	2131.	8435.	4.0	86.	5283.	5370.	3152.
9.1	2232.	8695.	3.9	-14.	5464.	5449.	3232.
10.0	2290.	8881.	3.9	-72.	5585.	5513.	3296.

STATIC TRIAXIAL TEST: S-1B
GREEN'S LAKE DAM NO. 3

CONSOLIDATED UNDRAINED TRIAXIAL TEST
WITH PORE PRESSURE MEASUREMENT

STATIC TX-GL2 KC-1.0
D116-22?PR.62
BORING:GL2-1 SAMPLE:PB6
GRAVELLY CLAYEY SAND

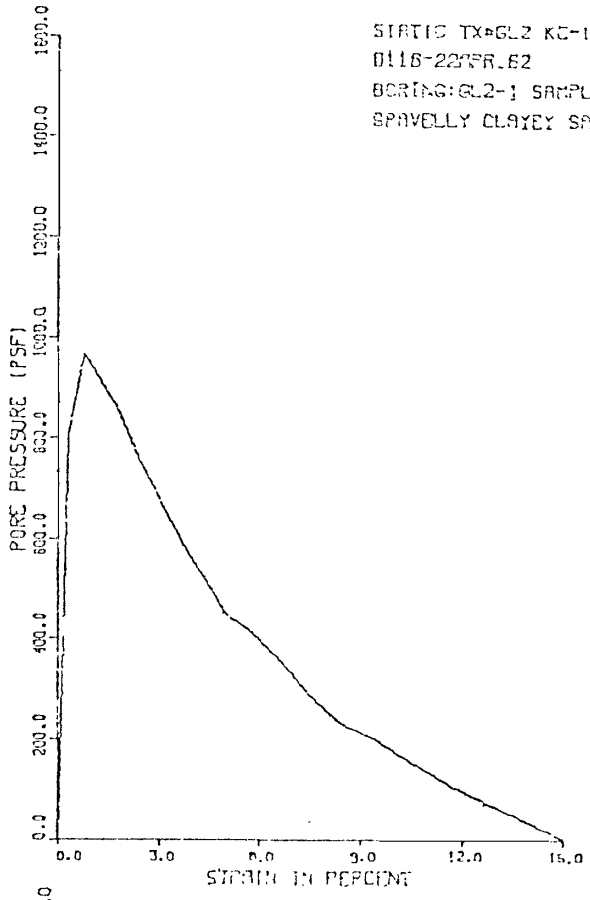

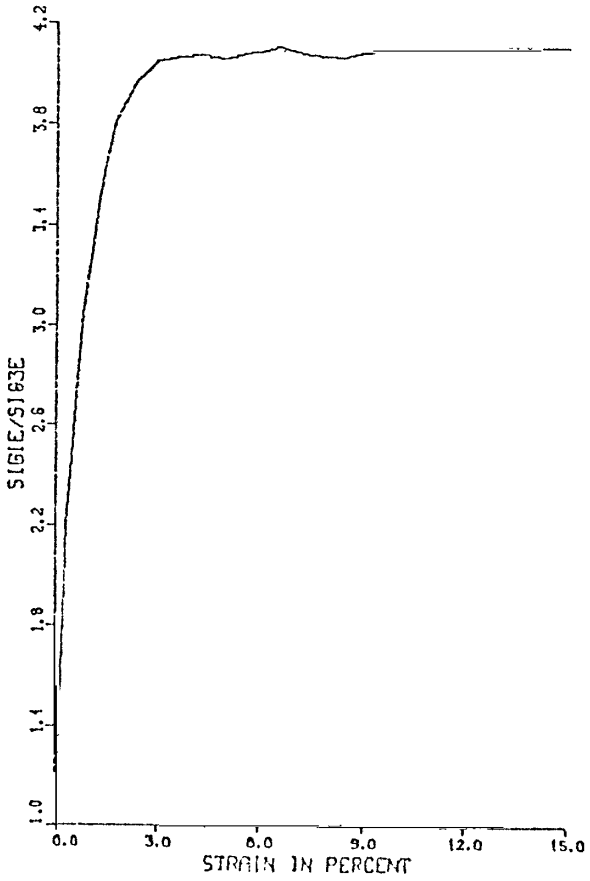

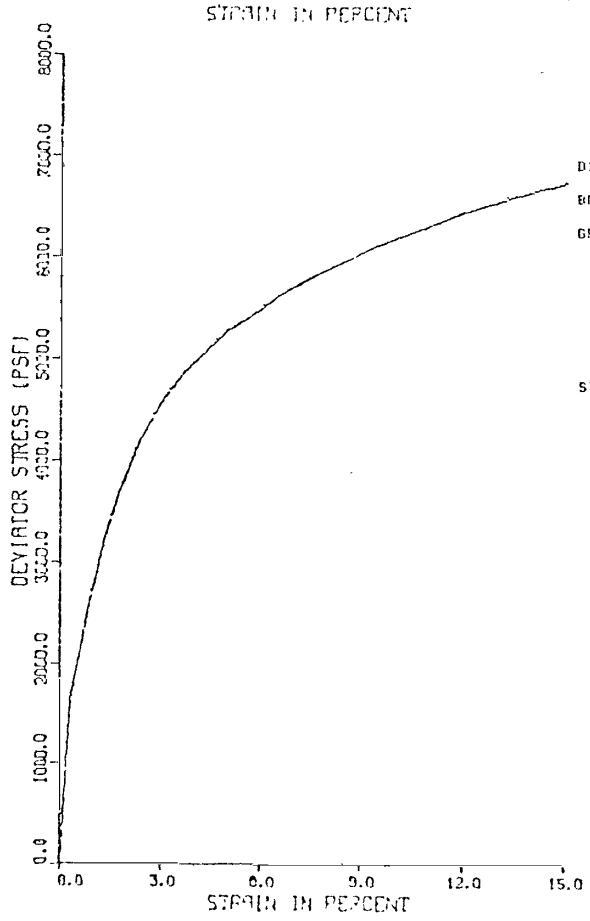

ISOTROPIC CONSOLIDATED UNDRAINED TRIAXIAL TEST
WITH PORE PRESSURE MEASUREMENTS
D116-UTAH DAMS-GREENS LAKE#3 STATIC TX(GL2 4/22/82 REDUCED BY BW

BORING:GL2-1 SAMPLE:PB-6/S-5 DEPTH:24.0-26.5

GRAVELLY CLAYEY SAND

AT END OF CONSOLIDATION :
SAMPLE HEIGHT ..... = 5.916 INCHES
SAMPLE AREA ..... = 6.806 SQ. INCHES
EFFECTIVE CONFINING STRESS . = 2174. PSF
EFFECTIVE MAJOR PRIN. STRESS = 2174. PSF
PRINCIPAL STRESS RATIO ..... = 1.00

STRAIN PCT	SIGMA3E PSF	SIGMA1E PSF	RATIO SIG1E/SIG3E	PPRESS PSF	PMAX PSF	PTOT PSF	Q PSF
.0	2174.	2174.	1.0	0.	2174.	2174.	0.
.3	1368.	3015.	2.2	806.	2191.	2998.	823.
.8	1210.	3679.	3.0	965.	2414.	3409.	1234.
1.3	1267.	4466.	3.5	907.	2867.	3774.	1600.
1.7	1310.	4969.	3.8	864.	3139.	4003.	1829.
2.4	1411.	5597.	4.0	763.	3504.	4267.	2093.
3.0	1499.	6061.	4.0	677.	3779.	4456.	2282.
3.7	1584.	6438.	4.1	590.	4011.	4601.	2427.
4.4	1656.	6736.	4.1	518.	4196.	4715.	2540.
5.0	1728.	7012.	4.1	446.	4370.	4817.	2642.
5.6	1757.	7165.	4.1	418.	4471.	4878.	2704.
6.6	1814.	7442.	4.1	360.	4628.	4988.	2814.
7.5	1886.	7690.	4.1	288.	4788.	5076.	2902.
8.4	1944.	7899.	4.1	230.	4921.	5152.	2977.
9.4	1973.	8075.	4.1	202.	5024.	5225.	3051.
10.0	2002.	8194.	4.1	173.	5098.	5270.	3096.
11.8	2074.	8495.	4.1	101.	5285.	5385.	3211.
13.7	2131.	8750.	4.1	43.	5441.	5488.	3313.
15.0	2174.	8929.	4.1	0.	5552.	5552.	3377.

STATIC TRIAXIAL TEST: S-2
GREEN'S LAKE DAM NO. 3

CONSOLIDATED UNDRAINED TRIAXIAL TEST
WITH PORE PRESSURE MEASUREMENT

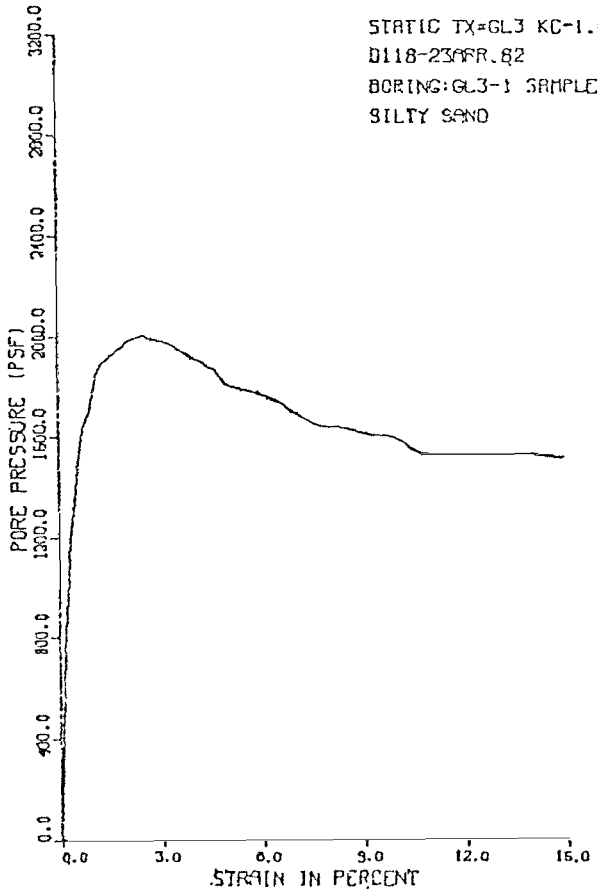

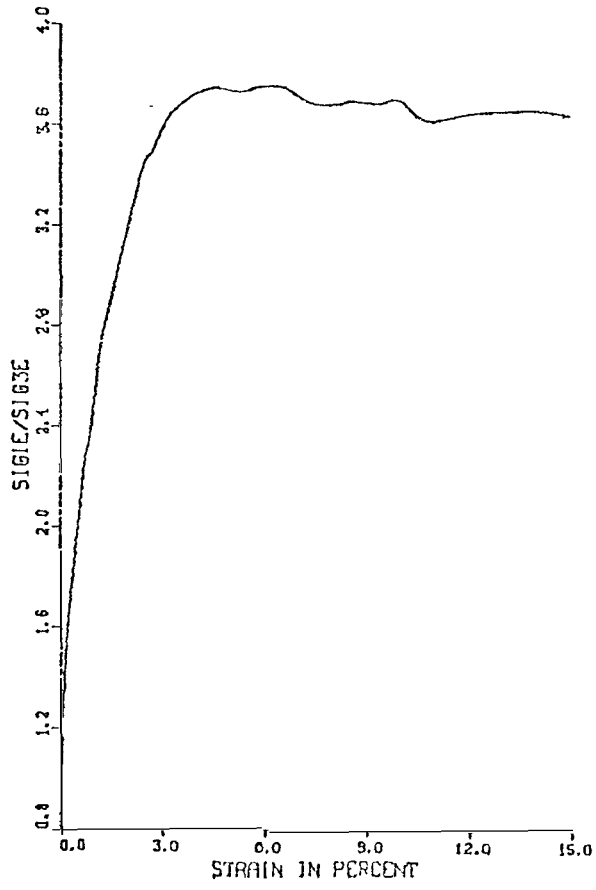

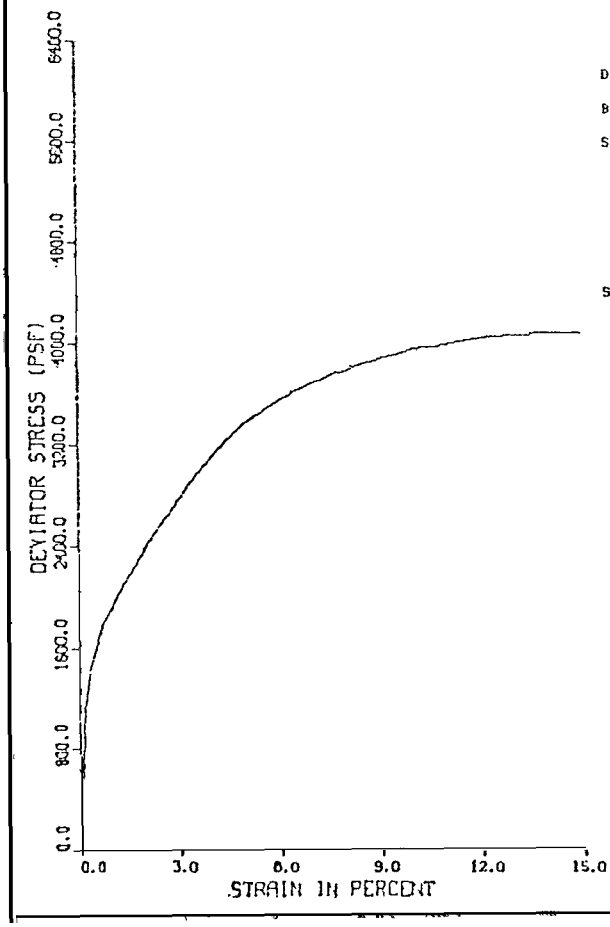

ISOTROPIC CONSOLIDATED UNDRAINED TRIAXIAL TEST
WITH PORE PRESSURE MEASUREMENTS
D118-UTAH DAMS-GREENS LAKE#3 STATIC TX#GL3 4/23/82 REDUCED BY BW

BORING:GL3-1 SAMPLE:PB-9/S-8 DEPTH:35.5-38.0

SILTY SAND

AT END OF CONSOLIDATION :
SAMPLE HEIGHT ..... = 5.849 INCHES
SAMPLE AREA ..... = 6.335 SQ. INCHES
EFFECTIVE CONFINING STRESS . = 3053. PSF
EFFECTIVE MAJOR PRIN. STRESS = 3053. PSF
PRINCIPAL STRESS RATIO ..... = 1.00

STRAIN PCT	SIGMA3E PSF	SIGMA1E PSF	RATIO SIG1E/SIG3E	PPRESS PSF	PBAR PSF	PTOT PSF	Q PSF
.0	3053.	3053.	1.0	0.	3053.	3053.	0.
.2	2318.	3430.	1.5	734.	2874.	3609.	556.
.4	1872.	3322.	1.8	1181.	2597.	3778.	725.
.5	1584.	3234.	2.0	1469.	2409.	3878.	825.
.7	1426.	3208.	2.3	1627.	2317.	3944.	891.
.9	1354.	3223.	2.4	1699.	2288.	3988.	935.
1.1	1224.	3203.	2.6	1829.	2213.	4042.	989.
1.3	1166.	3231.	2.8	1886.	2199.	4085.	1032.
2.2	1066.	3512.	3.3	1987.	2289.	4276.	1223.
2.5	1051.	3643.	3.5	2002.	2347.	4349.	1296.
2.7	1066.	3719.	3.5	1987.	2392.	4380.	1327.
3.3	1080.	3939.	3.6	1973.	2509.	4482.	1429.
4.0	1138.	4237.	3.7	1915.	2687.	4603.	1550.
4.7	1195.	4488.	3.8	1858.	2842.	4699.	1646.
5.0	1253.	4621.	3.7	1800.	2937.	4737.	1684.
5.9	1282.	4812.	3.8	1771.	3047.	4818.	1765.
6.7	1325.	4973.	3.8	1728.	3149.	4877.	1824.
7.5	1411.	5155.	3.7	1642.	3283.	4925.	1872.
8.5	1426.	5271.	3.7	1627.	3348.	4976.	1923.
9.5	1454.	5364.	3.7	1598.	3409.	5008.	1955.
10.0	1454.	5403.	3.7	1598.	3429.	5027.	1974.
10.7	1526.	5505.	3.6	1526.	3516.	5042.	1989.
12.3	1526.	5574.	3.7	1526.	3550.	5076.	2024.
13.9	1526.	5598.	3.7	1526.	3562.	5088.	2036.
15.0	1541.	5618.	3.6	1512.	3579.	5091.	2039.

STATIC TRIAXIAL TEST: S-3
GREEN'S LAKE DAM NO. 3

CONSOLIDATED UNDRAINED TRIAXIAL TEST
WITH PORE PRESSURE MEASUREMENT

STATIC TX-GL4R KC-1.0
D118-27APR.82
BORING:GL3-1 SAMPLE:PB6
CLAYEY SAND

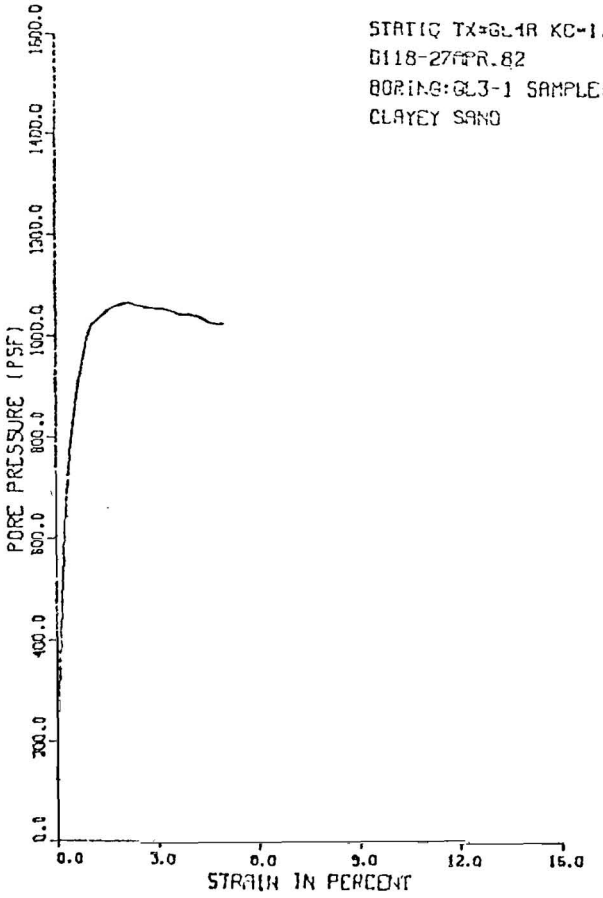

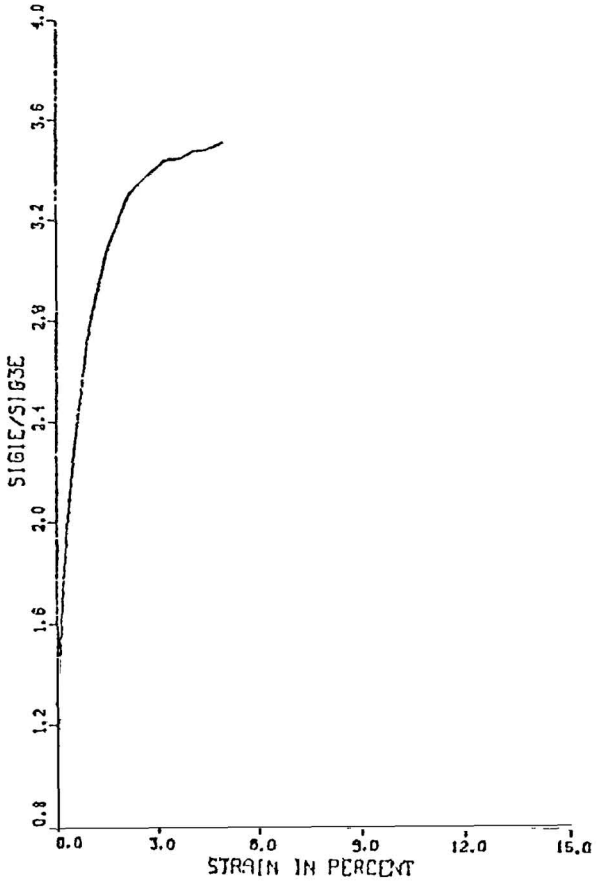

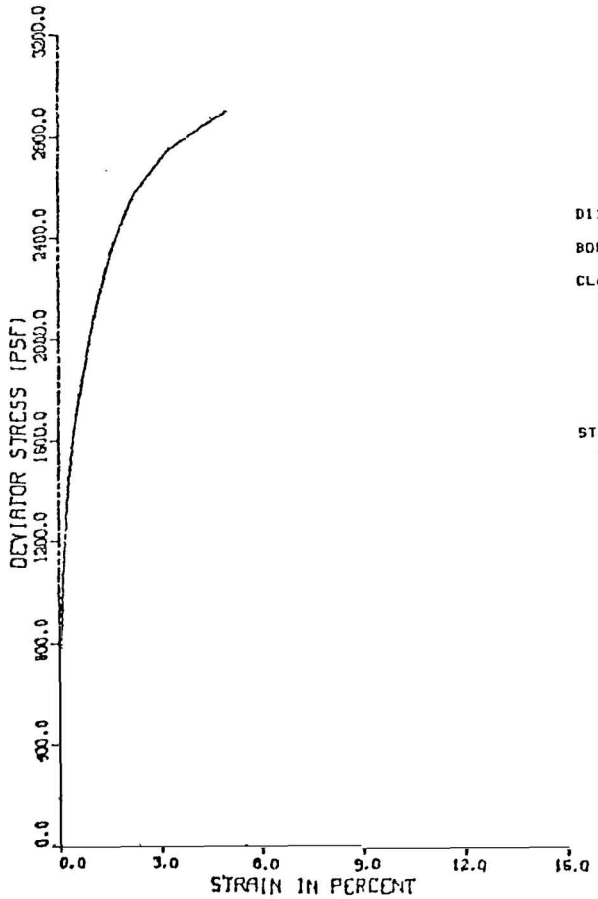

ISOTROPIC CONSOLIDATED UNDRAINED TRIAXIAL TEST
WITH PORE PRESSURE MEASUREMENTS
D118-UTAH DAMS-GREENS LAKE#3 STATIC TX#GL4A STAGE1 4/27/82 RED BY BW

BORING:GL3-1 SAMPLE:PB-6/S-5 DEPTH:23.5-26.0

CLAYEY SAND

AT END OF CONSOLIDATION :
SAMPLE HEIGHT ..... = 5.721 INCHES
SAMPLE AREA ..... = 6.554 SQ. INCHES
EFFECTIVE CONFINING STRESS . = 2174. PSF
EFFECTIVE MAJOR PRIN. STRESS = 2174. PSF
PRINCIPAL STRESS RATIO ..... = 1.00

STRAIN PCT	SIGMA3E PSF	SIGMA1E PSF	RATIO SIG1E/SIG3E	PPRESS PSF	PBAR PSF	PTOT PSF	Q PSF
.0	2174.	2174.	1.0	0.	2174.	2174.	0.
.1	1944.	2647.	1.4	230.	2295.	2526.	351.
.2	1699.	2840.	1.7	475.	2270.	2745.	570.
.3	1512.	2914.	1.9	662.	2213.	2875.	701.
.4	1382.	2979.	2.2	792.	2181.	2973.	798.
.6	1296.	3043.	2.3	878.	2170.	3048.	874.
.7	1238.	3114.	2.5	936.	2176.	3112.	938.
.9	1181.	3163.	2.7	994.	2172.	3165.	991.
1.0	1152.	3239.	2.8	1022.	2196.	3218.	1044.
1.5	1123.	3460.	3.1	1051.	2292.	3343.	1169.
2.2	1109.	3666.	3.3	1066.	2388.	3453.	1279.
2.7	1123.	3775.	3.4	1051.	2449.	3500.	1326.
3.2	1123.	3867.	3.4	1051.	2495.	3546.	1372.
3.7	1138.	3930.	3.5	1037.	2534.	3571.	1396.
4.1	1138.	3962.	3.5	1037.	2550.	3587.	1412.
4.6	1152.	4024.	3.5	1022.	2588.	3611.	1436.
5.0	1152.	4053.	3.5	1022.	2603.	3625.	1451.

STATIC TRIAXIAL TEST: S-4A
GREEN'S LAKE DAM NO. 3

CONSOLIDATED UNDRAINED TRIAXIAL TEST
WITH PORE PRESSURE MEASUREMENT

STATIC TX#GL4B KC-1.0
D118-27APR.82
BORING:GL3-1 SAMPLE:PB6
CLAYEY SAND

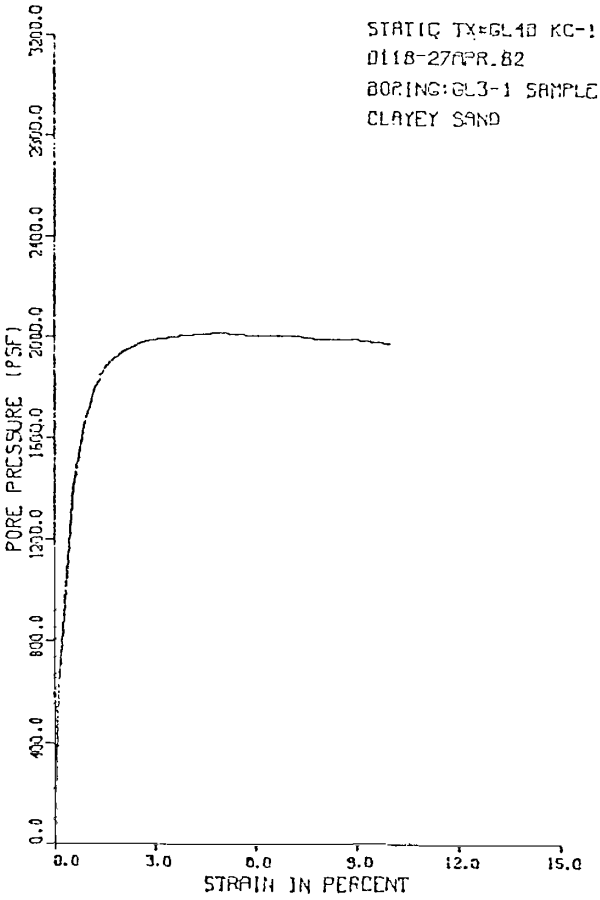

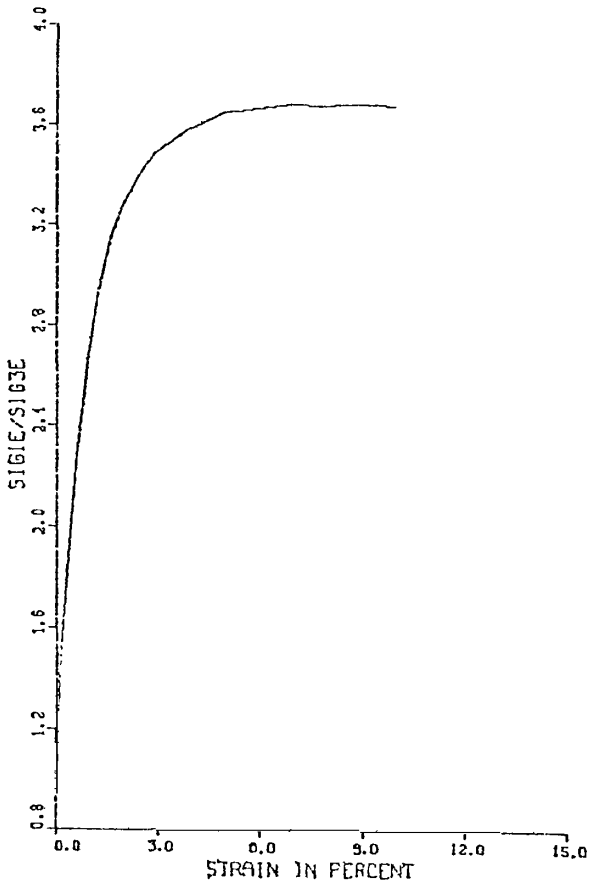

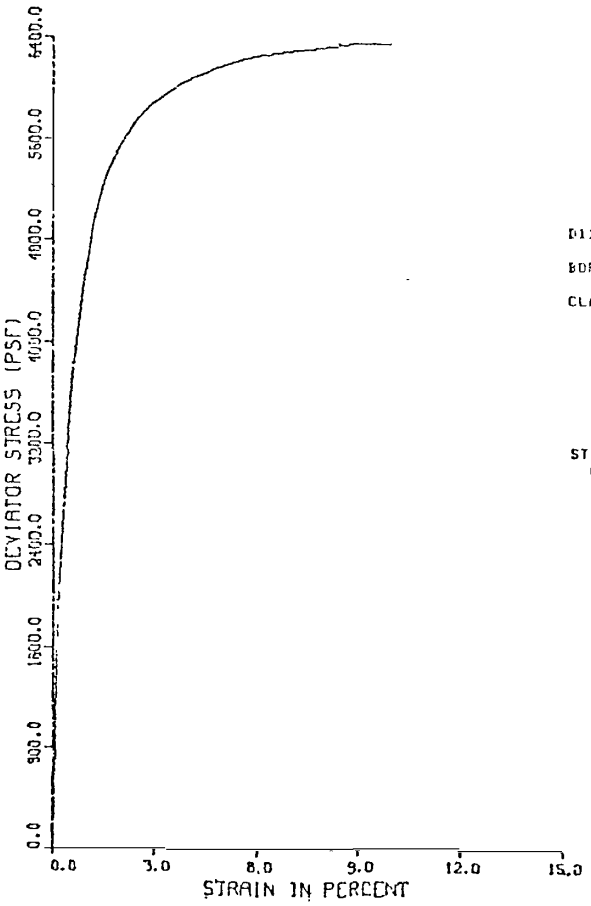

ISOTROPIC CONSOLIDATED UNDRAINED TRIAXIAL TEST
WITH PORE PRESSURE MEASUREMENTS
D118-UTAH DAMS-GREENS LAKE#3 STATIC TX#GL4B STAGE2 4/27/82 RED. BY BW

BORING:GL3-1 SAMPLE:PB-6/S-5 DEPTH:23.5-26.0

CLAYEY SAND

AT END OF CONSOLIDATION :
SAMPLE HEIGHT ..... = 5.484 INCHES
SAMPLE AREA ..... = 6.754 SQ. INCHES
EFFECTIVE CONFINING STRESS . = 4349. PSF
EFFECTIVE MAJOR PRIN. STRESS = 4349. PSF
PRINCIPAL STRESS RATIO ..... = 1.00

STRAIN PCT	SIGMA3E PSF	SIGMA1E PSF	RATIO SIG1E/SIG3E	PPRESS PSF	PBAR PSF	PTOT PSF	Q PSF
.0	4349.	4349.	1.0	0.	4349.	4349.	0.
.1	3730.	5624.	1.5	619.	4677.	5296.	947.
.5	2952.	6599.	2.2	1397.	4776.	6172.	1824.
.9	2707.	7103.	2.6	1642.	4905.	6547.	2198.
1.2	2549.	7476.	2.9	1800.	5013.	6813.	2464.
1.6	2462.	7750.	3.1	1886.	5106.	6993.	2644.
2.0	2419.	7938.	3.3	1930.	5178.	7108.	2759.
2.5	2376.	8133.	3.4	1973.	5254.	7227.	2878.
2.9	2362.	8220.	3.5	1987.	5291.	7278.	2929.
3.9	2347.	8393.	3.6	2002.	5370.	7372.	3023.
5.0	2333.	8511.	3.6	2016.	5422.	7438.	3089.
6.0	2347.	8602.	3.7	2002.	5475.	7476.	3127.
6.9	2347.	8636.	3.7	2002.	5492.	7493.	3145.
7.9	2362.	8682.	3.7	1987.	5522.	7509.	3160.
8.9	2362.	8712.	3.7	1987.	5537.	7524.	3175.
10.0	2376.	8727.	3.7	1973.	5552.	7524.	3176.

STATIC TRIAXIAL TEST: S-4B
GREEN'S LAKE DAM NO. 3

WITH PORE PRESSURE MEASUREMENT

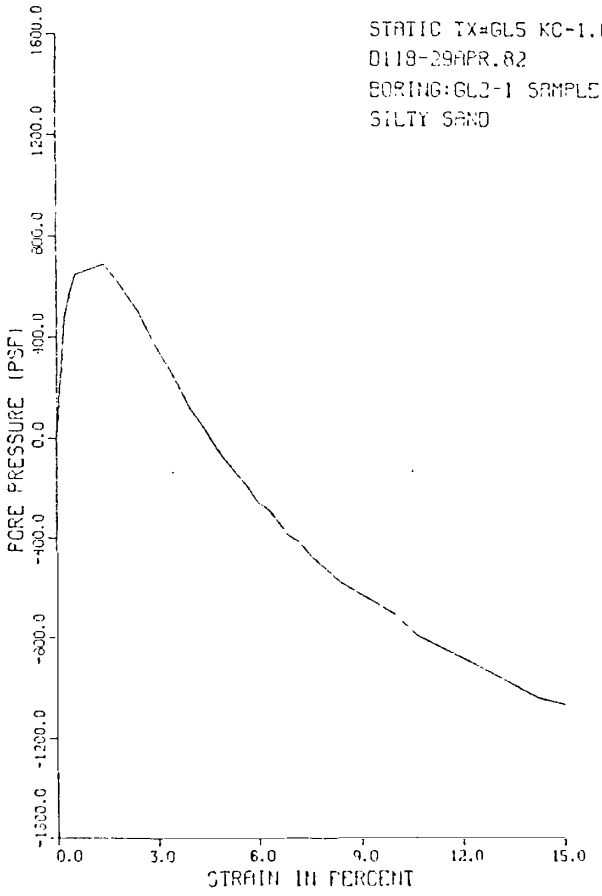

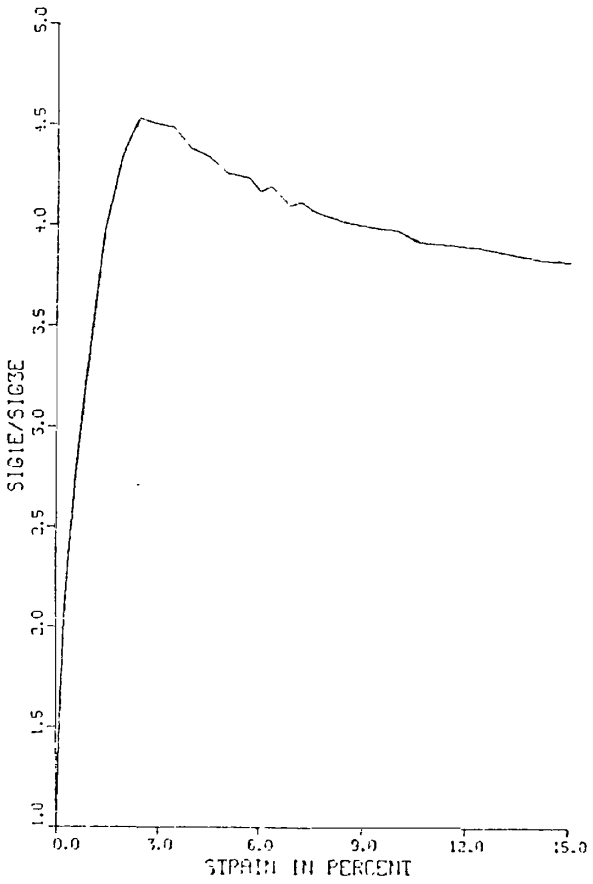

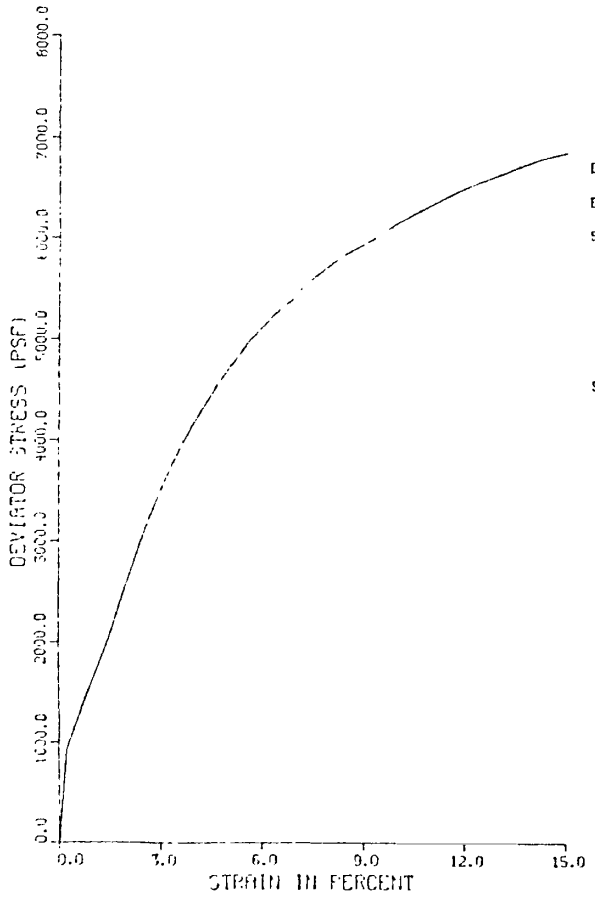

ISOTROPIC CONSOLIDATED UNDRAINED TRIAXIAL TEST
WITH PORE PRESSURE MEASUREMENTS
D118-UTAH DAMS-GREENS LAKE#3 STATIC TX#GL5 4/29/82 REDUCED BY BW

BORING:GL2-1 SAMPLE:PB-2/S-1 DEPTH:8.0-10.5

SILTY SAND

AT END OF CONSOLIDATION :

SAMPLE HEIGHT	=	5.837 INCHES
SAMPLE AREA	=	6.553 SQ. INCHES
EFFECTIVE CONFINING STRESS .	=	1354. PSF
EFFECTIVE MAJOR PRIN. STRESS	=	1354. PSF
PRINCIPAL STRESS RATIO	=	1.00

STRAIN PCT	SIGMA3E PSF	SIGMA1E PSF	RATIO SIG1E/SIG3E	PPRESS PSF	PBAR PSF	PTOT PSF	Q PSF
.0	1354.	1354.	1.0	0.	1354.	1354.	0.
.2	878.	1799.	2.0	475.	1339.	1814.	460.
.4	778.	1872.	2.4	576.	1325.	1901.	547.
.6	706.	1951.	2.8	648.	1328.	1976.	623.
1.4	662.	2634.	4.0	691.	1648.	2339.	986.
1.6	691.	2832.	4.1	662.	1762.	2424.	1071.
1.9	749.	3249.	4.3	605.	1999.	2604.	1250.
2.4	850.	3852.	4.5	504.	2351.	2855.	1501.
2.9	979.	4414.	4.5	374.	2696.	3071.	1717.
3.4	1094.	4914.	4.5	259.	3004.	3264.	1910.
3.9	1224.	5361.	4.4	130.	3293.	3422.	2069.
4.5	1325.	5755.	4.3	29.	3540.	3569.	2215.
5.0	1440.	6137.	4.3	-86.	3788.	3702.	2348.
5.7	1541.	6537.	4.2	-187.	4039.	3852.	2498.
6.0	1613.	6735.	4.2	-259.	4174.	3915.	2561.
6.3	1642.	6809.	4.2	-288.	4266.	3978.	2624.
6.9	1742.	7145.	4.1	-387.	4444.	4056.	2701.
7.2	1771.	7297.	4.1	-418.	4534.	4116.	2763.
7.6	1829.	7456.	4.1	-475.	4642.	4167.	2814.
8.4	1910.	7766.	4.0	-574.	4848.	4272.	2918.
9.3	2002.	8002.	4.0	-648.	5002.	4354.	3000.
10.0	2059.	8210.	4.0	-706.	5135.	4429.	3075.
10.7	2146.	8428.	3.9	-792.	5287.	4495.	3141.
12.4	2261.	8825.	3.9	-907.	5543.	4636.	3282.
14.2	2390.	9197.	3.8	-1037.	5793.	4757.	3403.
15.0	2419.	9292.	3.8	-1066.	5855.	4790.	3436.

STATIC TRIAXIAL TEST: S-5
GREEN'S LAKE DAM NO. 3

CONSOLIDATED UNDRAINED TRIAXIAL TEST
WITH PORE PRESSURE MEASUREMENT

STATIC TX#GL6 KC-1.0
D118-29PR-82
BORING:GL3-2 SAMPLE:PB6
CLAYEY COARSE SAND

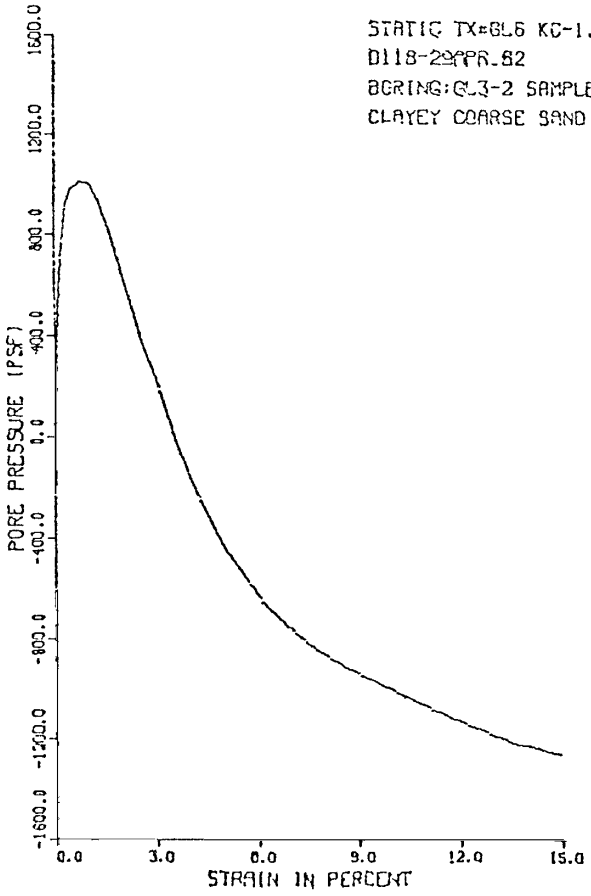

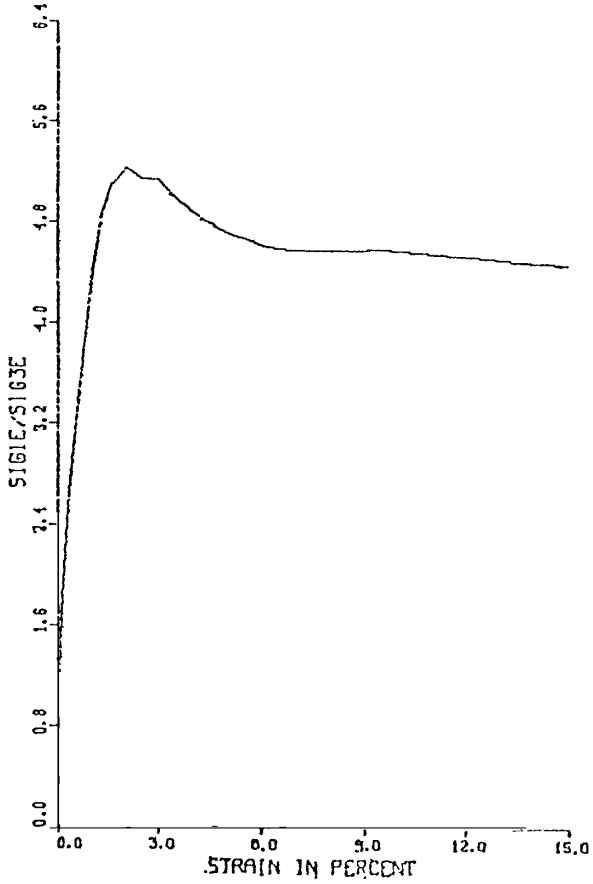

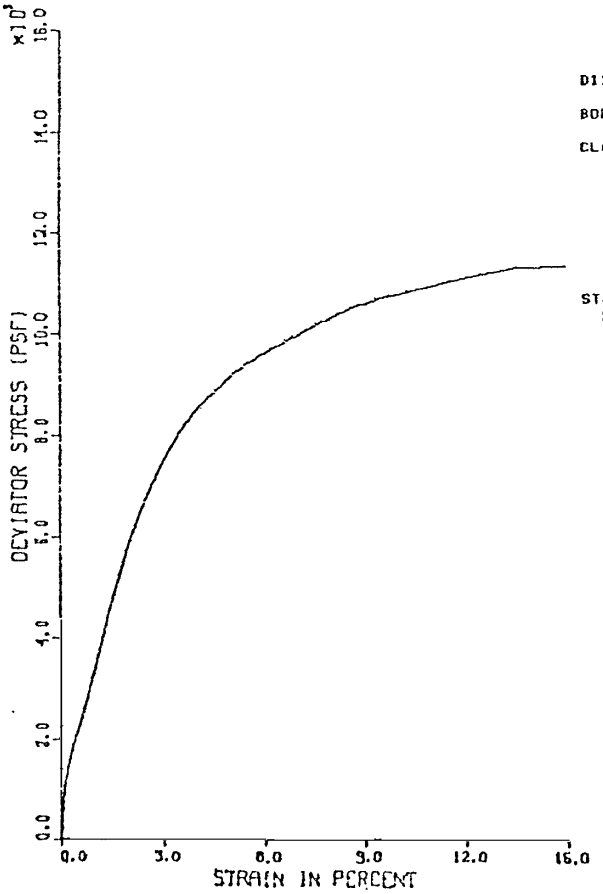

ISOTROPIC CONSOLIDATED UNDRAINED TRIAXIAL TEST
WITH PORE PRESSURE MEASUREMENTS
D118-UTAH DAMS-GREENS LAKE#3 STATIC TX#GL6 4/29/82 REDUCED BY BW

BORING:GL3-2 SAMPLE:PB-6/S-4 DEPTH:25.5-28.0

CLAYEY COARSE SAND

AT END OF CONSOLIDATION :
SAMPLE HEIGHT ..... = 5.945 INCHES
SAMPLE AREA ..... = 6.632 SQ. INCHES
EFFECTIVE CONFINING STRESS . = 2016. PSF
EFFECTIVE MAJOR PRIN. STRESS = 2016. PSF
PRINCIPAL STRESS RATIO ..... = 1.00

STRAIN PCT	SIGMA3E PSF	SIGMA1E PSF	RATIO SIG1E/SIG3E	PPRESS PSF	PBAR PSF	PTOT PSF	Q PSF
.0	2016.	2016.	1.0	0.	2016.	2016.	0.
.1	1498.	2539.	1.7	518.	2018.	2537.	521.
.2	1253.	2726.	2.2	763.	1989.	2753.	737.
.3	1094.	2912.	2.7	922.	2003.	2925.	909.
.5	1037.	3176.	3.1	979.	2106.	3086.	1070.
.7	1008.	3788.	3.8	1008.	2398.	3406.	1390.
1.0	1022.	4504.	4.4	994.	2763.	3757.	1741.
1.3	1094.	5315.	4.9	922.	3205.	4126.	2110.
1.6	1210.	6144.	5.1	806.	3677.	4483.	2467.
2.1	1411.	7365.	5.2	605.	4388.	4993.	2977.
2.5	1642.	8434.	5.1	374.	5038.	5412.	3396.
3.0	1814.	9311.	5.1	202.	5563.	5764.	3748.
3.5	2016.	10061.	5.0	0.	6039.	6039.	4023.
4.0	2189.	10671.	4.9	-173.	6430.	6257.	4241.
4.5	2333.	11165.	4.8	-317.	6749.	6432.	4416.
5.0	2462.	11600.	4.7	-446.	7031.	6585.	4569.
5.5	2563.	11957.	4.7	-547.	7260.	6713.	4697.
6.2	2693.	12386.	4.6	-677.	7539.	6862.	4846.
6.9	2779.	12724.	4.6	-763.	7752.	6989.	4973.
7.8	2866.	13099.	4.6	-850.	7982.	7133.	5117.
8.6	2938.	13451.	4.6	-922.	8195.	7273.	5257.
9.5	2995.	13722.	4.6	-979.	8358.	7379.	5363.
11.7	3139.	14254.	4.5	-1123.	8697.	7573.	5557.
13.5	3240.	14580.	4.5	-1224.	8910.	7686.	5670.
15.0	3283.	14671.	4.5	-1267.	8977.	7710.	5694.

STATIC TRIAXIAL TEST: S-6
GREEN'S LAKE DAM NO. 3

CONSOLIDATED UNDRAINED TRIAXIAL TEST
WITH PORE PRESSURE MEASUREMENT

STATIC TX#GL7A KC=1.0
D118-14MAY82
BORING:GL3-2 SAMPLE:PB7
SILTY SAND

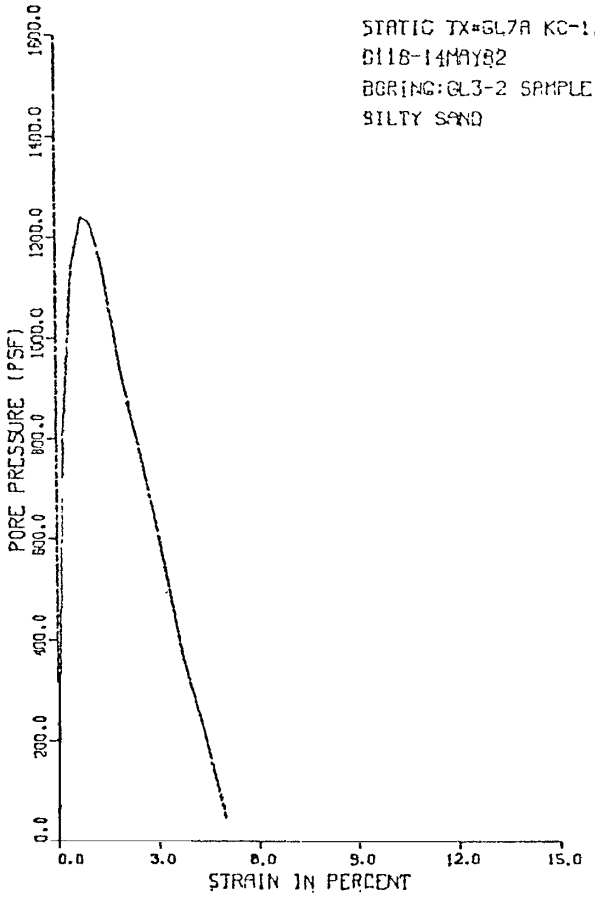

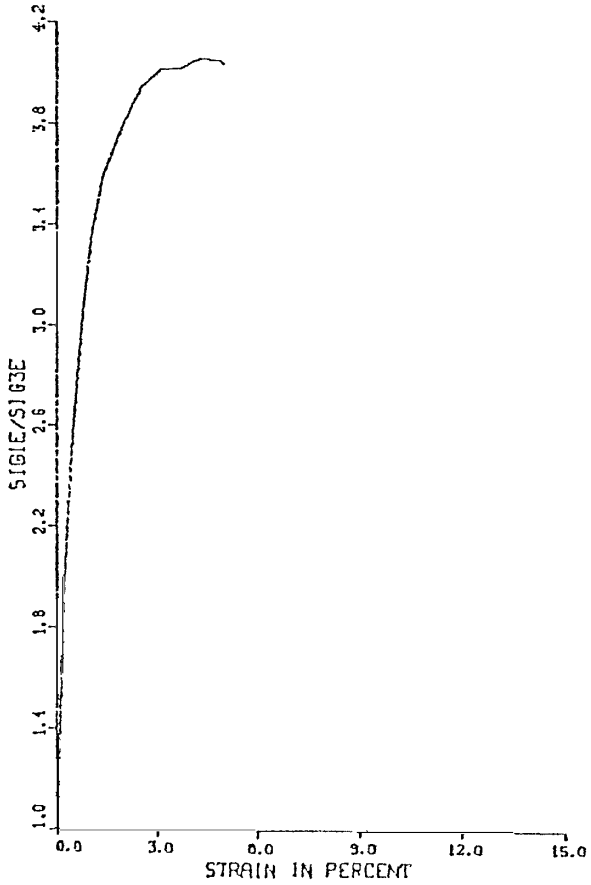

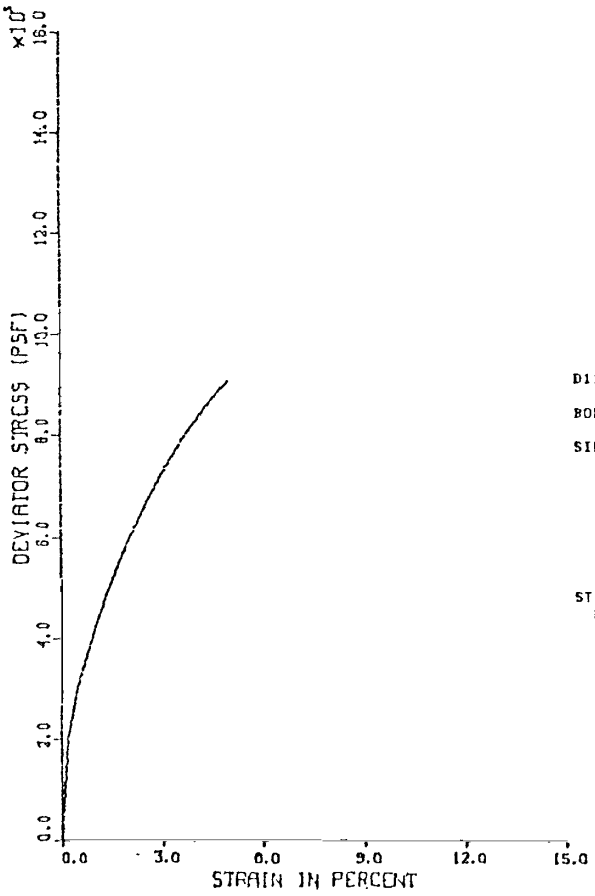

ISOTROPIC CONSOLIDATED UNDRAINED TRIAXIAL TEST
WITH PORE PRESSURE MEASUREMENTS
D118-UTAH DAMS-GREENS LAKE STATIC TX#GL7A STAGE 1 5/14/82 RED BY BW

BORING:GL3-2 SAMPLE:PB-7/S-5 DEPTH:29.5-32.0

SILTY SAND

AT END OF CONSOLIDATION :
SAMPLE HEIGHT ..... = 5.967 INCHES
SAMPLE AREA ..... = 6.501 SQ. INCHES
EFFECTIVE CONFINING STRESS . = 3024. PSF
EFFECTIVE MAJOR PRIN. STRESS = 3024. PSF
PRINCIPAL STRESS RATIO ..... = 1.00

STRAIN PCT	SIGMA3E PSF	SIGMA1E PSF	RATIO SIG1E/SIG3E	PPRESS PSF	PBAR PSF	PTOT PSF	Q PSF
.0	3024.	3024.	1.0	0.	3024.	3024.	0.
.2	2232.	4222.	1.9	792.	3227.	4019.	995.
.5	1886.	4818.	2.6	1138.	3352.	4490.	1466.
.8	1786.	5435.	3.0	1238.	3610.	4848.	1824.
1.0	1800.	6052.	3.4	1224.	3926.	5150.	2126.
1.3	1872.	6702.	3.6	1152.	4287.	5439.	2415.
1.9	2088.	7889.	3.8	936.	4988.	5924.	2900.
2.5	2261.	8912.	3.9	763.	5587.	6350.	3326.
3.1	2448.	9831.	4.0	576.	6139.	6715.	3691.
3.7	2650.	10648.	4.0	374.	6649.	7023.	3999.
4.3	2794.	11335.	4.1	230.	7064.	7295.	4271.
4.9	2952.	11966.	4.1	72.	7459.	7531.	4507.
5.0	2981.	12050.	4.0	43.	7515.	7559.	4535.

STATIC TRIAXIAL TEST: S-7A
GREEN'S LAKE DAM NO. 3

CONSOLIDATED UNDRAINED TRIAXIAL TEST
WITH PORE PRESSURE MEASUREMENT

STATIC TX#GL7B KC-1.0
D118-14MAY82
BORING:GL3-2 SAMPLE:PB7
SILTY SAND

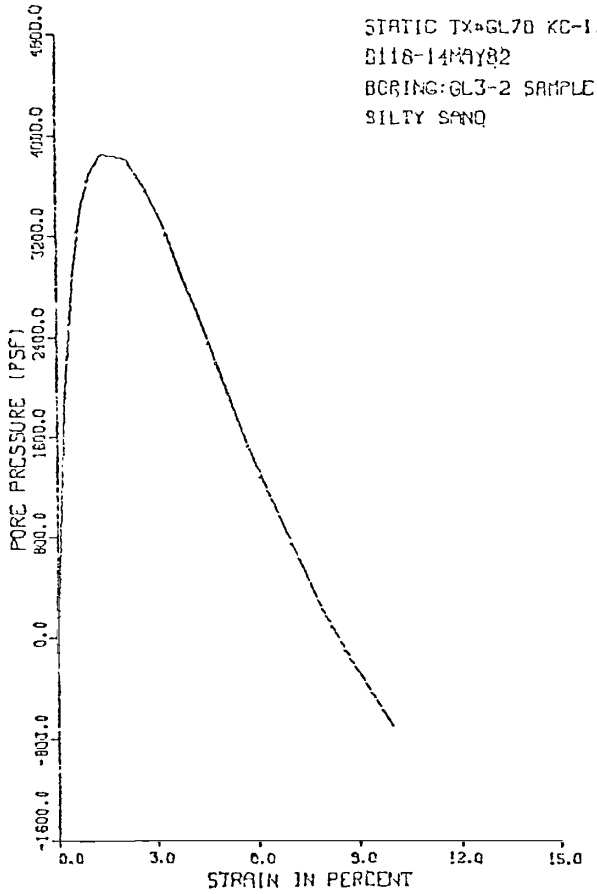

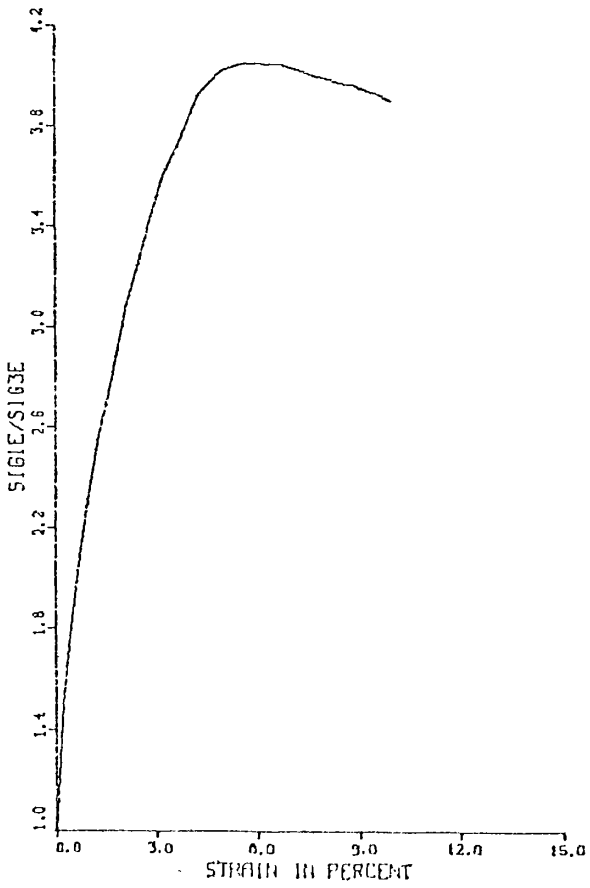

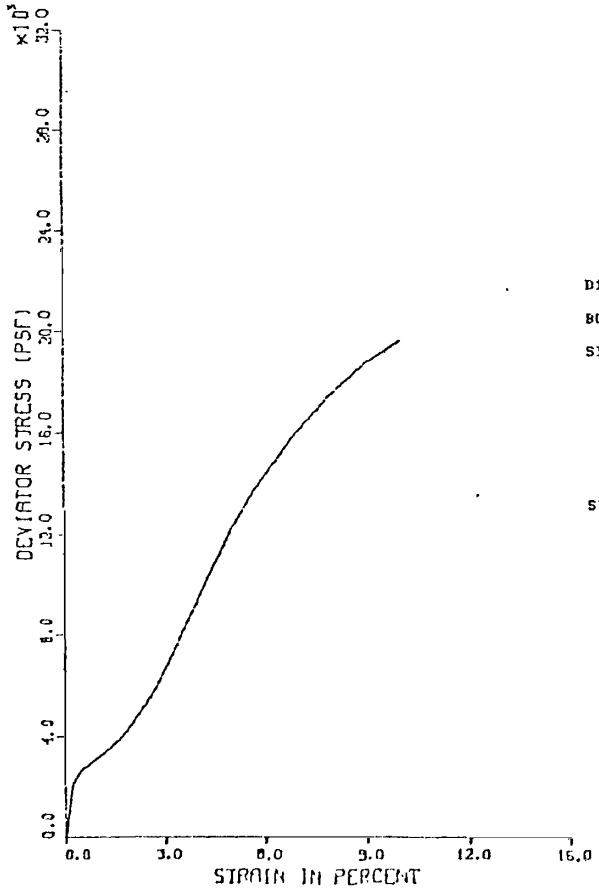

ISOTROPIC CONSOLIDATED UNDRAINED TRIAXIAL TEST
WITH PORE PRESSURE MEASUREMENTS
D118-UTAH DAMS-GREENS LAKE STATIC TX#7B STAGE 2 5/14/82 RED. BY BW

BORING:GL3-2 SAMPLE:PB-7/S-5 DEPTH:29.5-32.0

SILTY SAND

AT END OF CONSOLIDATION :

SAMPLE HEIGHT	=	5.913 INCHES
SAMPLE AREA	=	6.543 SQ. INCHES
EFFECTIVE CONFINING STRESS .	=	6048. PSF
EFFECTIVE MAJOR PRIN. STRESS	=	6048. PSF
PRINCIPAL STRESS RATIO	=	1.00

STRAIN PCT	SIGMA3E PSF	SIGMA1E PSF	RATIO SIG1E/SIG3E	PPRESS PSF	PBAR PSF	PTOT PSF	Q PSF
.0	6048.	6048.	1.0	0.	6048.	6048.	0.
.2	4205.	6291.	1.5	1843.	5248.	7091.	1043.
.5	3139.	5767.	1.8	2909.	4453.	7362.	1314.
.8	2606.	5511.	2.1	3442.	4059.	7500.	1452.
1.0	2347.	5527.	2.4	3701.	3937.	7638.	1590.
1.3	2232.	5707.	2.6	3816.	3969.	7785.	1737.
1.6	2203.	6015.	2.7	3845.	4109.	7954.	1906.
2.1	2246.	6941.	3.1	3802.	4594.	8395.	2347.
2.7	2462.	8245.	3.3	3586.	5354.	8939.	2891.
3.2	2750.	9885.	3.6	3298.	6318.	9615.	3567.
3.8	3139.	11759.	3.7	2909.	7449.	10358.	4310.
4.3	3485.	13677.	3.9	2563.	8581.	11144.	5096.
5.0	3989.	16053.	4.0	2059.	10021.	12080.	6032.
5.7	4493.	18215.	4.1	1555.	11354.	12909.	6861.
6.8	5155.	20875.	4.0	893.	13015.	13908.	7860.
7.9	5803.	23200.	4.0	245.	14501.	14746.	8698.
9.0	6336.	25081.	4.0	-288.	15708.	15420.	9372.
10.0	6768.	26436.	3.9	-720.	16602.	15882.	9834.

STATIC TRIAXIAL TEST: S-7B
GREEN'S LAKE DAM NO. 3

WARNER DRAW DAM

Earth Sciences Associates

CONSOLIDATED UNDRAINED TRIAXIAL TEST
WITH PORE PRESSURE MEASUREMENT

STATIC TX-WD-1 KC-1.0
G118-10MAR.82
BORING:WD-1 SAMPLE:PB-2
SILTY SAND

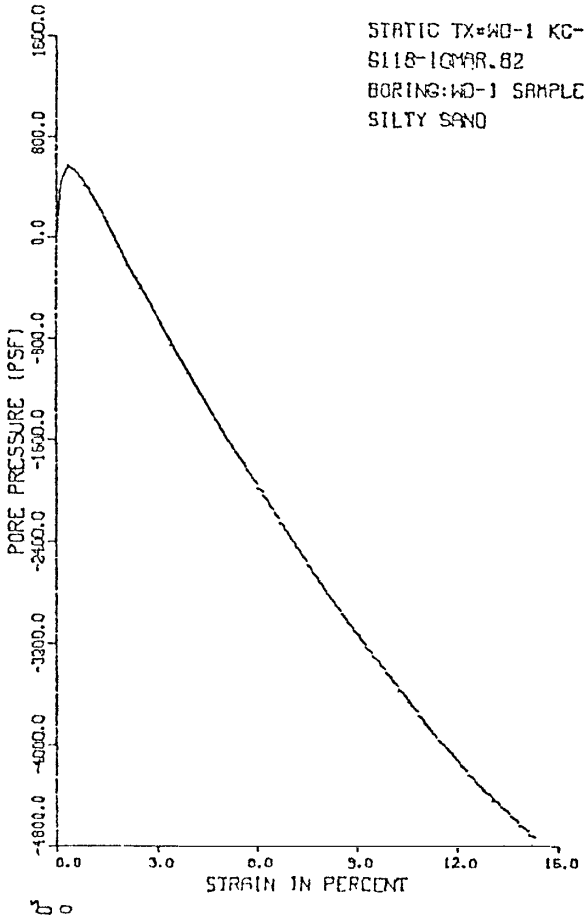

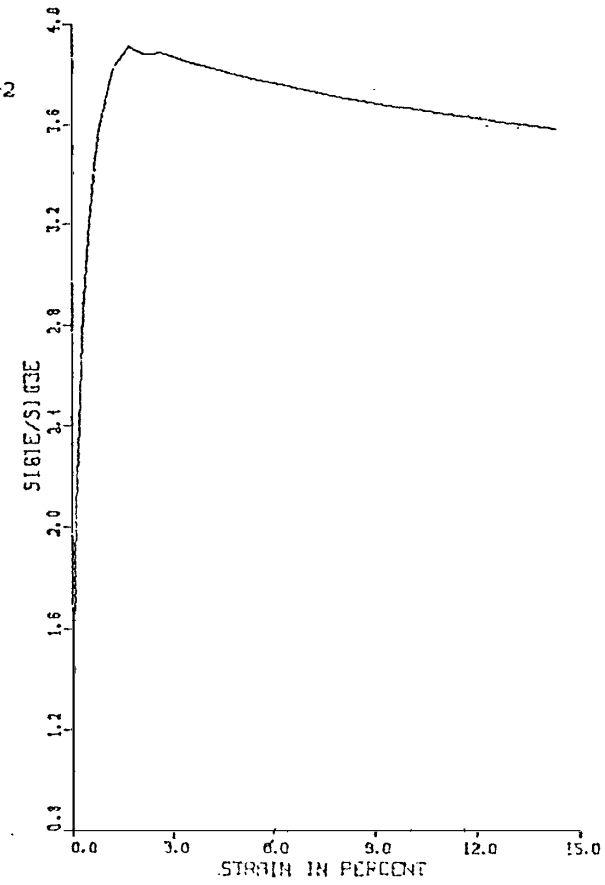

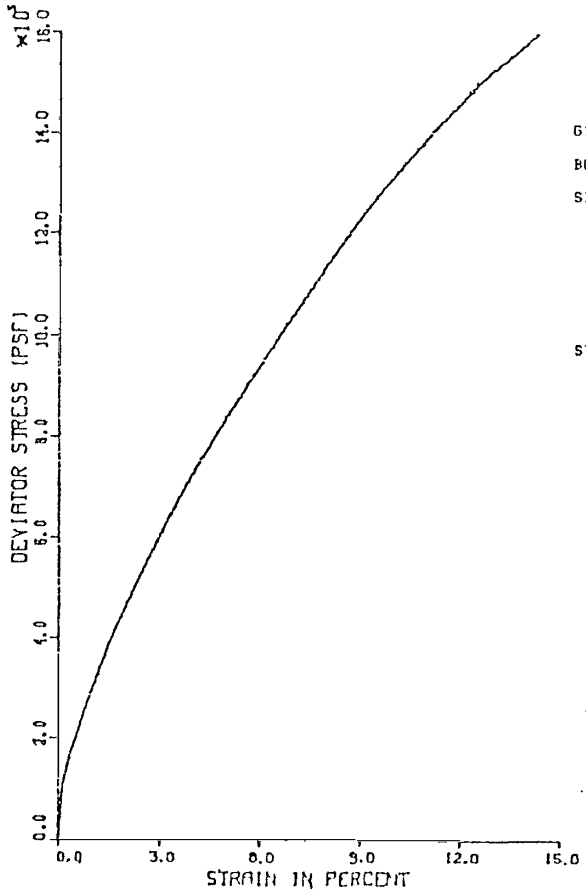

ISOTROPIC CONSOLIDATED UNDRAINED TRIAXIAL TEST
WITH PORE PRESSURE MEASUREMENTS
G118 UTAH DAMS-WARNER DRAW DAM STATIC TX-WD1 3/10/82 REDUCED BY BW

BORING:WD-1 SAMPLE:PB-2/S-2 DEPTH:8.5-11.0

SILTY SAND W/OCCASSIONAL GRAVEL

AT END OF CONSOLIDATION :

SAMPLE HEIGHT	=	5.998 INCHES
SAMPLE AREA	=	6.352 SQ. INCHES
EFFECTIVE CONFINING STRESS .	=	1440. PSF
EFFECTIVE MAJOR PRIN. STRESS	=	1440. PSF
PRINCIPAL STRESS RATIO	=	1.00

STRAIN PCT	SIGMA3E PSF	SIGMA1E PSF	RATIO SIG1E/SIG3E	PPRESS PSF	PBAR PSF	PTOT PSF	Q PSF
.0	1440.	1440.	1.0	0.	1440.	1440.	0.
.1	1008.	2095.	2.1	432.	1551.	1983.	543.
.3	878.	2505.	2.9	562.	1692.	2253.	813.
.6	907.	2959.	3.3	533.	1933.	2466.	1026.
.8	979.	3476.	3.6	461.	2228.	2689.	1249.
1.2	1181.	4518.	3.8	259.	2849.	3109.	1669.
1.7	1426.	5572.	3.9	14.	3499.	3513.	2073.
2.1	1685.	6543.	3.9	-245.	4114.	3869.	2429.
2.6	1915.	7456.	3.9	-475.	4686.	4211.	2771.
3.1	2146.	8296.	3.9	-706.	5221.	4515.	3075.
3.6	2376.	9130.	3.8	-936.	5753.	4817.	3377.
4.1	2592.	9920.	3.8	-1152.	6256.	5104.	3664.
5.0	2995.	11351.	3.8	-1555.	7173.	5618.	4178.
6.6	3658.	13710.	3.7	-2218.	8684.	6466.	5026.
8.2	4262.	15775.	3.7	-2822.	10019.	7196.	5756.
9.2	4637.	17073.	3.7	-3197.	10855.	7658.	6218.
10.0	4925.	18043.	3.7	-3485.	11484.	7999.	6559.
11.2	5328.	19399.	3.6	-3888.	12363.	8475.	7035.
12.7	5803.	20938.	3.6	-4363.	13371.	9007.	7567.
14.3	6192.	22176.	3.6	-4752.	14184.	9432.	7992.

STATIC TRIAXIAL TEST: S-1
WARNER DRAW DAM

CONSOLIDATED UNDRAINED TRIAXIAL TEST
WITH PORE PRESSURE MEASUREMENT

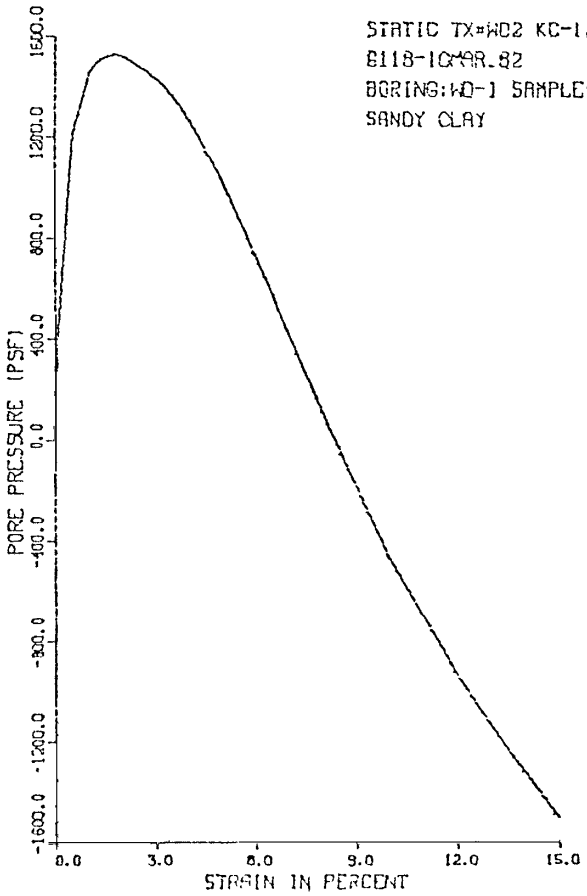

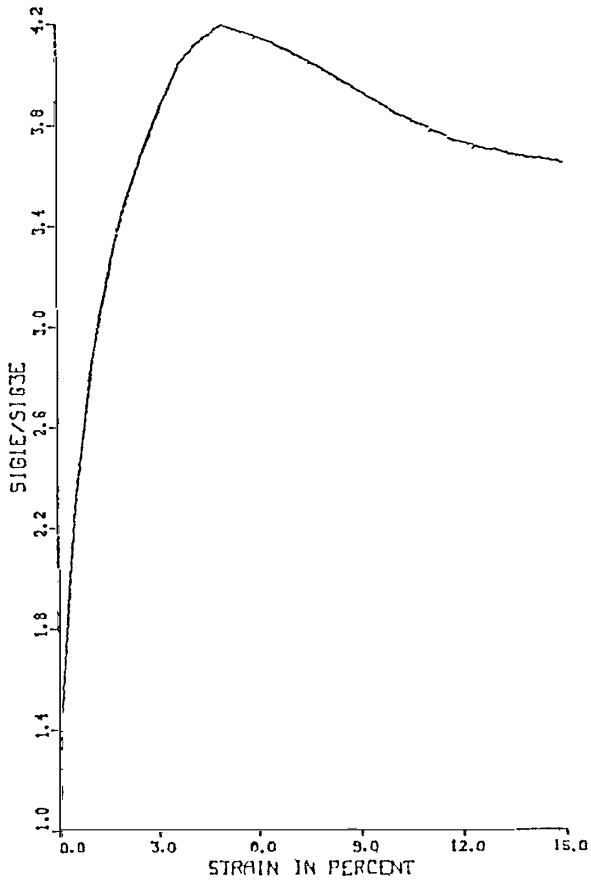

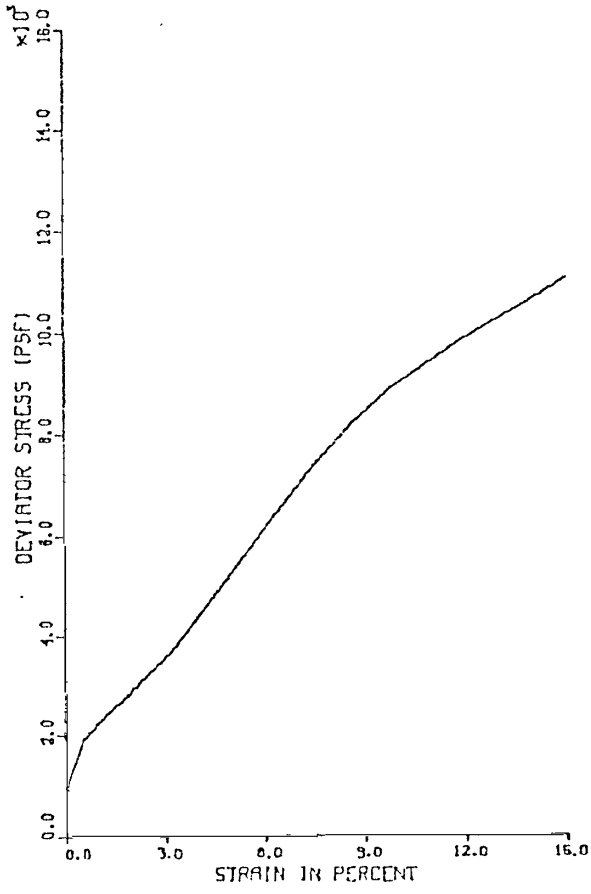

ISOTROPIC CONSOLIDATED UNDRAINED TRIAXIAL TEST
WITH PORE PRESSURE MEASUREMENTS
G118 UTAH DAMS-WARNER DRAW DAM STATIC TX#WD2 3/10/82 REDUCED BY BW

BORING:WD-1 SAMPLE:PB-6/S-6 DEPYH:25.0-27.5

SANDY CLAY

AT END OF CONSOLIDATION :

SAMPLE HEIGHT	=	5.907 INCHES
SAMPLE AREA	=	6.398 SQ. INCHES
EFFECTIVE CONFINING STRESS .	=	2678. PSF
EFFECTIVE MAJOR PRIN. STRESS	=	2678. PSF
PRINCIPAL STRESS RATIO	=	1.00

STRAIN PCT	SIGMA3E PSF	SIGMA1E PSF	RATIO SIG1E/SIG3E	PPRESS PSF	PBAR PSF	PTOT PSF	Q PSF
.0	2678.	2678.	1.0	0.	2678.	2678.	0.
.1	2304.	3316.	1.4	374.	2810.	3184.	506.
.5	1469.	3349.	2.3	1210.	2409.	3619.	940.
1.0	1224.	3474.	2.8	1454.	2349.	3803.	1125.
1.3	1181.	3602.	3.1	1498.	2392.	3889.	1211.
1.8	1152.	3870.	3.4	1526.	2511.	4037.	1359.
2.1	1166.	4075.	3.5	1512.	2621.	4133.	1454.
2.6	1210.	4475.	3.7	1469.	2842.	4311.	1633.
3.2	1267.	4928.	3.9	1411.	3098.	4509.	1830.
3.7	1354.	5470.	4.0	1325.	3412.	4737.	2058.
4.3	1469.	6057.	4.1	1210.	3763.	4973.	2294.
5.0	1642.	6880.	4.2	1037.	4261.	5298.	2619.
6.3	2030.	8401.	4.1	648.	5216.	5864.	3185.
7.5	2405.	9757.	4.1	274.	6081.	6354.	3676.
8.7	2765.	10967.	4.0	-86.	6866.	6779.	4101.
9.9	3110.	12036.	3.9	-432.	7573.	7141.	4463.
10.0	3154.	12148.	3.9	-475.	7651.	7175.	4497.
12.0	3614.	13483.	3.7	-936.	8549.	7613.	4934.
13.5	3917.	14412.	3.7	-1238.	9165.	7926.	5248.
15.0	4190.	15286.	3.6	-1512.	9738.	8226.	5548.

STATIC TRIAXIAL TEST: S-2
WARNER DRAW DAM

CONSOLIDATED UNDRAINED TRIAXIAL TEST
WITH PORE PRESSURE MEASUREMENT

STATIC TX#W03 KC=1.0
G118-12MAR_82
BORING:WD-1 SAMPLE:PB10
CLAYEY SAND

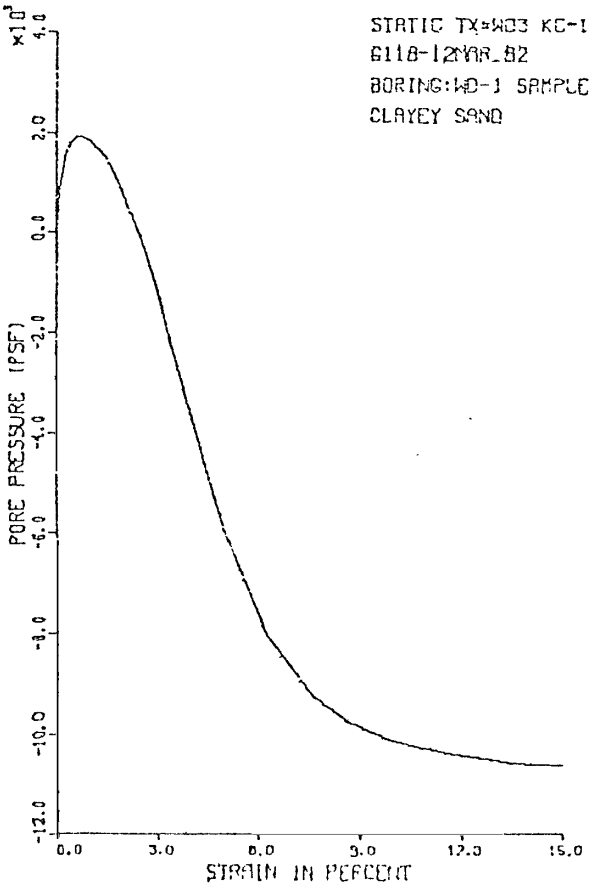

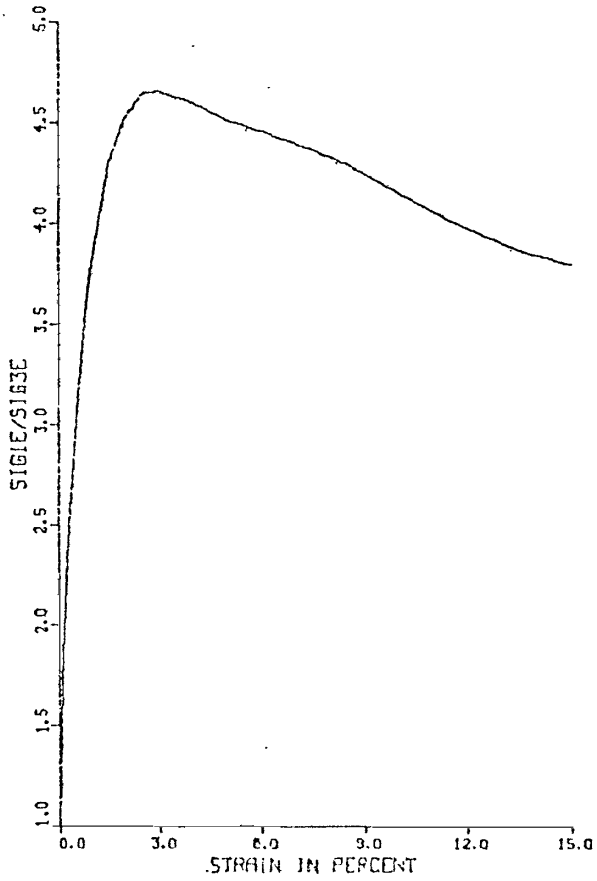

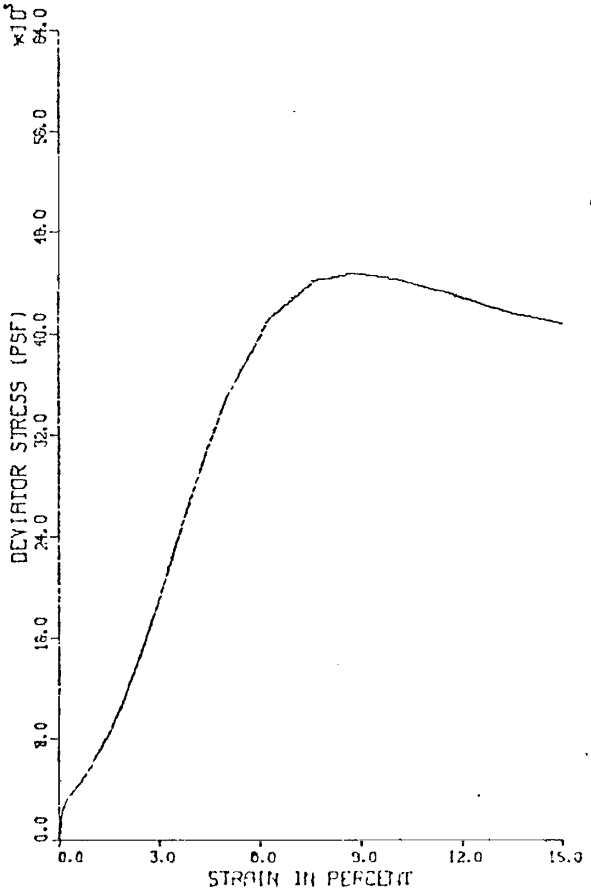

ISOTROPIC CONSOLIDATED UNDRAINED TRIAXIAL TEST
WITH PORE PRESSURE MEASUREMENTS
G118 UTAH DAMS-WARNER DRAW DAM STATIC TX#W03 3/12/82 REDUCED BY BW

BORING:WD-1 SAMPLE:PB-10/S-10 DEPTH:41.0-43.5

CLAYEY SAND W/OCCASSIONAL GRAVEL

AT END OF CONSOLIDATION :
SAMPLE HEIGHT ..... = 5.983 INCHES
SAMPLE AREA ..... = 6.363 SQ. INCHES
EFFECTIVE CONFINING STRESS . = 3902. PSF
EFFECTIVE MAJOR PRIN. STRESS = 3902. PSF
PRINCIPAL STRESS RATIO ..... = 1.00

STRAIN PCT	SIGMA3E PSF	SIGMA1E PSF	RATIO SIG1E/SIG3E	PPRESS PSF	PBAR PSF	PTOT PSF	Q PSF
.0	3902.	3902.	1.0	0.	3902.	3902.	0.
.1	3038.	5209.	1.7	864.	4123.	4987.	1085.
.3	2405.	5610.	2.3	1498.	4007.	5505.	1602.
.4	2117.	5947.	2.8	1785.	4032.	5818.	1915.
.6	2002.	6411.	3.2	1901.	4206.	6107.	2204.
.8	1987.	6972.	3.5	1915.	4480.	6395.	2492.
.9	2045.	7671.	3.8	1858.	4858.	6716.	2813.
1.4	2419.	10359.	4.3	1483.	6389.	7872.	3970.
1.9	3096.	13991.	4.5	806.	8544.	9350.	5448.
2.4	3960.	18354.	4.6	-58.	11157.	11099.	7197.
3.0	5011.	23350.	4.7	-1109.	14181.	13072.	9170.
3.4	6206.	28735.	4.6	-2304.	17471.	15167.	11265.
3.9	7430.	34190.	4.6	-3528.	20810.	17282.	13380.
4.5	8669.	39525.	4.6	-4766.	24097.	19330.	15428.
5.1	9893.	44658.	4.5	-5990.	27275.	21285.	17383.
6.3	11981.	53189.	4.4	-8078.	32585.	24507.	20604.
7.6	13162.	57324.	4.4	-9259.	35243.	25984.	22081.
8.7	13680.	58397.	4.3	-9778.	36038.	26261.	22358.
10.0	14069.	58306.	4.1	-10166.	36187.	26021.	22119.
11.6	14342.	57471.	4.0	-10440.	35907.	25467.	21564.
13.5	14515.	55997.	3.9	-10613.	35256.	24643.	20741.
15.0	14587.	55310.	3.8	-10685.	34949.	24264.	20361.

STATIC TRIAXIAL TEST: S-3
WARNER DRAW DAM

CONSOLIDATED UNDRAINED TRIAXIAL TEST
WITH PORE PRESSURE MEASUREMENT

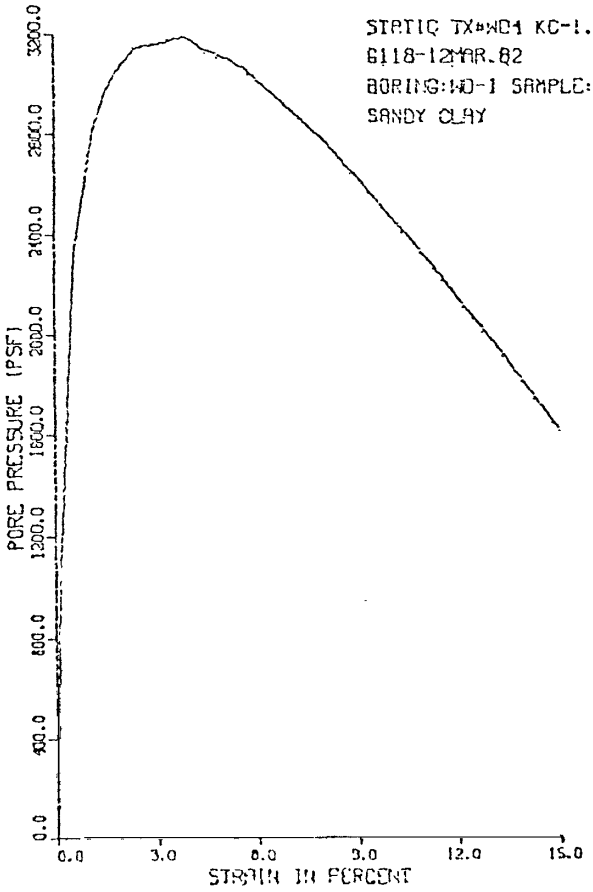

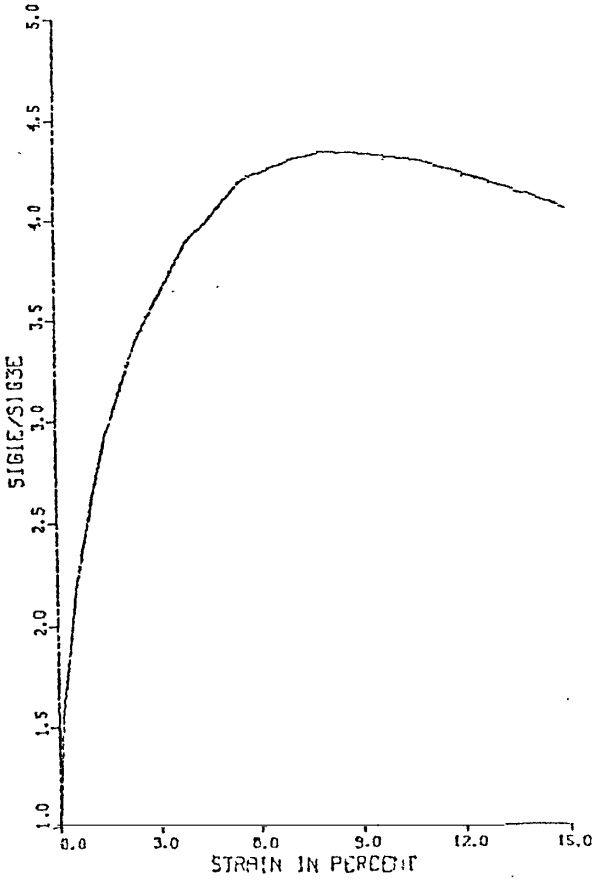

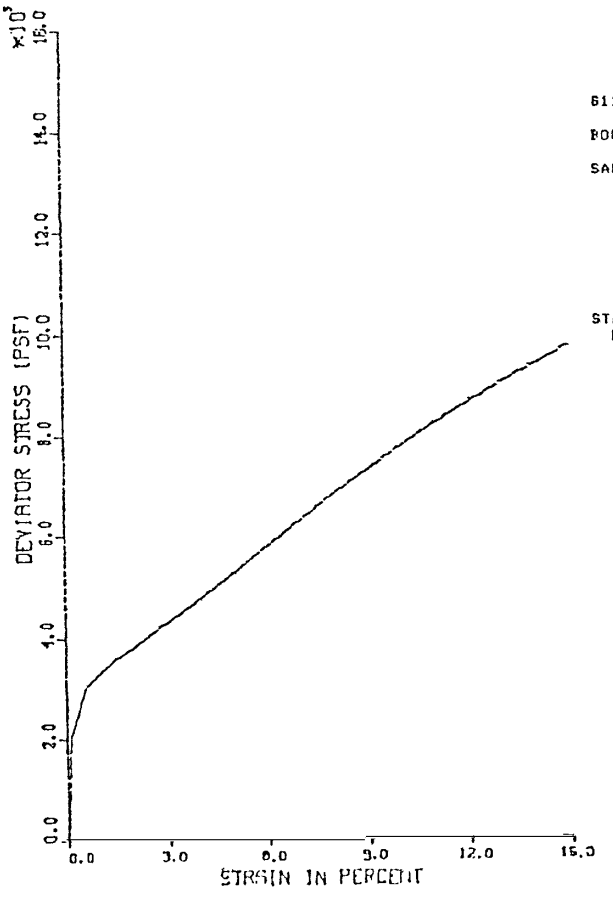

ISOTROPIC CONSOLIDATED UNDRAINED TRIAXIAL TEST
WITH PORE PRESSURE MEASUREMENTS
6118 UTAH DAMS WARNER DRAW DAM STATIC TX#WD4 3/12/82 REDUCED BY BW

BORING:WD-1 SAMPLE:PB-13/S-13 DEPTH:53.0-55.5

SANDY CLAY W/GRAVEL

AT END OF CONSOLIDATION :
SAMPLE HEIGHT ..... = 5.923 INCHES
SAMPLE AREA ..... = 6.409 SQ. INCHES
EFFECTIVE CONFINING STRESS . = 4810. PSF
EFFECTIVE MAJOR PRIN. STRESS = 4810. PSF
PRINCIPAL STRESS RATIO ..... = 1.00

STRAIN PCT	SIGMA3E PSF	SIGMA1E PSF	RATIO SIG1E/SIG3E	PPRESS PSF	PBAR PSF	PTOT PSF	Q PSF
.0	4810.	4810.	1.0	0.	4810.	4810.	0.
.1	3830.	5050.	1.5	979.	4840.	5819.	1010.
.6	2491.	5484.	2.2	2318.	3988.	6306.	1496.
1.1	2002.	5356.	2.7	2808.	3679.	6487.	1677.
1.5	1843.	5407.	2.9	2966.	3625.	6591.	1782.
1.8	1757.	5484.	3.1	3053.	3620.	6673.	1863.
2.4	1670.	5662.	3.4	3139.	3666.	6805.	1996.
2.8	1656.	5829.	3.5	3154.	3742.	6896.	2086.
3.9	1627.	6314.	3.9	3182.	3971.	7153.	2343.
4.1	1642.	6427.	3.9	3168.	4034.	7202.	2393.
4.4	1670.	6631.	4.0	3139.	4150.	7290.	2480.
5.0	1699.	6929.	4.1	3110.	4314.	7424.	2615.
5.6	1742.	7319.	4.2	3067.	4531.	7598.	2788.
7.0	1915.	8224.	4.3	2894.	5070.	7964.	3154.
8.0	2030.	8813.	4.3	2779.	5422.	8201.	3391.
8.9	2174.	9421.	4.3	2635.	5797.	8433.	3623.
10.0	2347.	10112.	4.3	2462.	6239.	8692.	3882.
10.8	2462.	10580.	4.3	2347.	6521.	8869.	4059.
11.6	2606.	11004.	4.3	2203.	6845.	9048.	4239.
13.2	2866.	11956.	4.2	1944.	7411.	9355.	4545.
15.0	3197.	12956.	4.1	1613.	8076.	9689.	4880.

STATIC TRIAXIAL TEST: S-4
WARNER DRAW DAM

CONSOLIDATED UNDRAINED TRIAXIAL TEST
WITH PORE PRESSURE MEASUREMENT

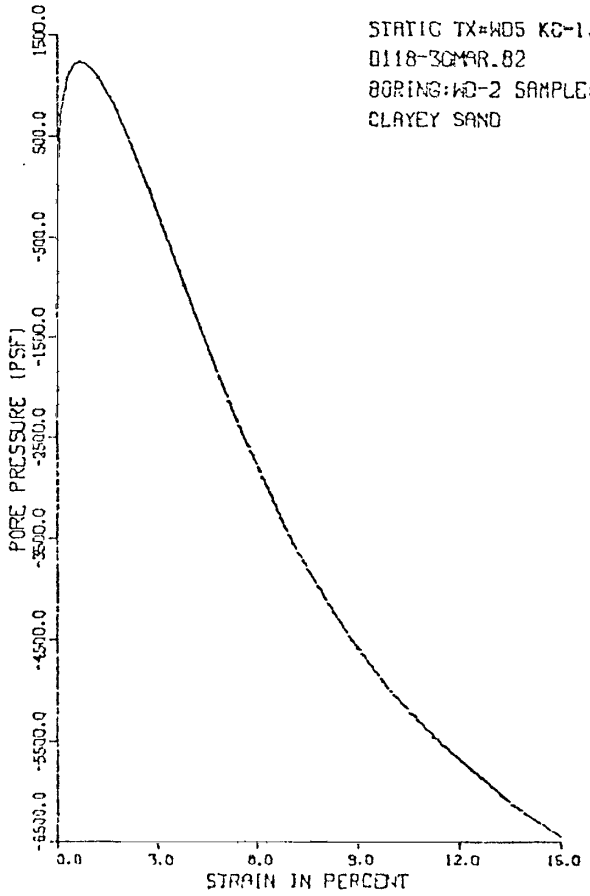

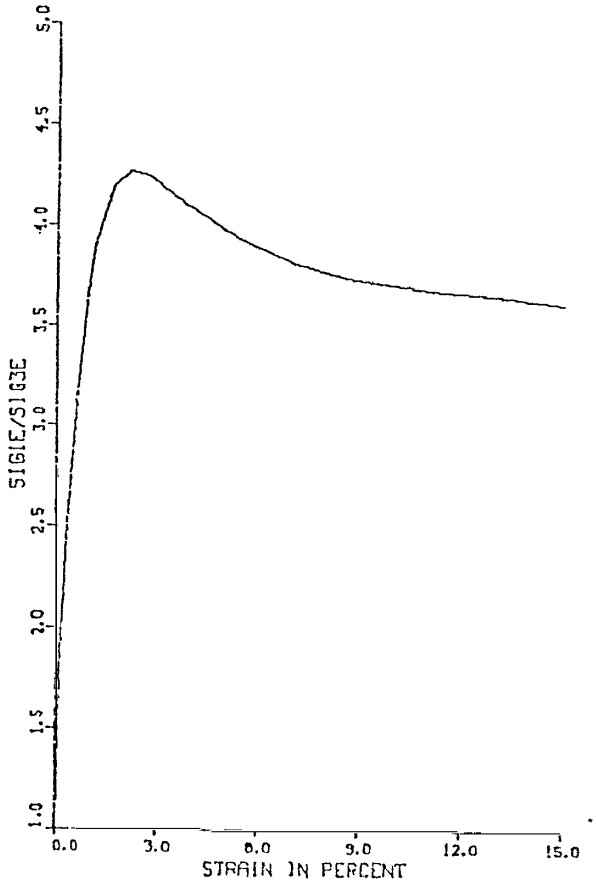

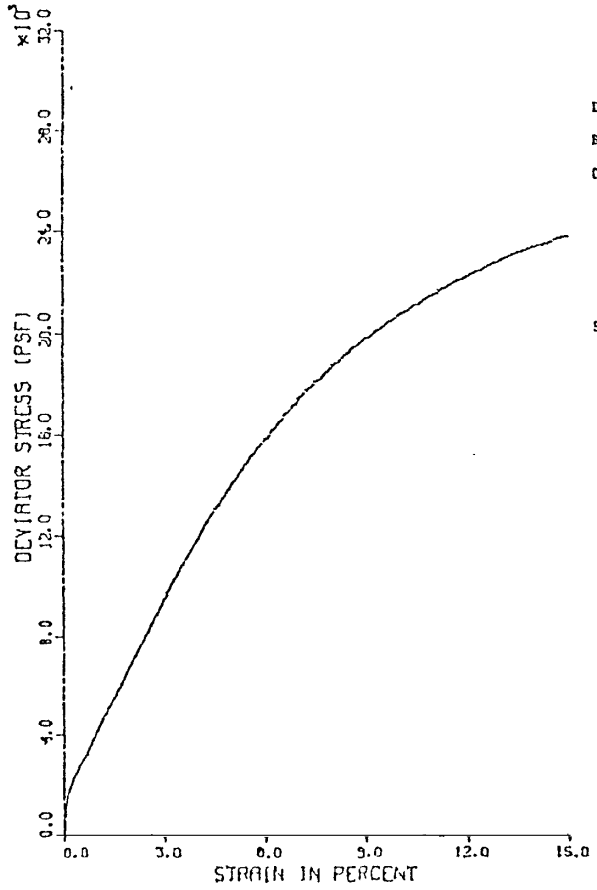

ISOTROPIC CONSOLIDATED UNDRAINED TRIAXIAL TEST
WITH PORE PRESSURE MEASUREMENTS
D118 UTAH DAMS-WARNER DRAW DAM STATIC TX#WD5 3/30/82 REDUCED BY BW

BORING:WD-2 SAMPLE:PB-6/S-6 DEPTH:24.5-27.0

CLAYEY SAND

AT END OF CONSOLIDATION :
SAMPLE HEIGHT ..... = 5.966 INCHES
SAMPLE AREA ..... = 6.376 SQ. INCHES
EFFECTIVE CONFINING STRESS . = 2678. PSF
EFFECTIVE MAJOR PRIN. STRESS = 2678. PSF
PRINCIPAL STRESS RATIO ..... = 1.00

STRAIN PCT	SIGMA3E PSF	SIGMA1E PSF	RATIO SIG1E/SIG3E	PPRESS PSF	PBAR PSF	PTOT PSF	Q PSF
.0	2678.	2678.	1.0	0.	2678.	2678.	0.
.1	1987.	3521.	1.8	691.	2754.	3445.	767.
.3	1627.	3834.	2.4	1051.	2731.	3782.	1103.
.5	1498.	4195.	2.8	1181.	2846.	4027.	1349.
.6	1440.	4582.	3.2	1238.	3011.	4249.	1571.
.8	1454.	5039.	3.5	1224.	3246.	4470.	1792.
1.0	1498.	5545.	3.7	1181.	3521.	4702.	2024.
1.2	1555.	6064.	3.9	1123.	3810.	4933.	2254.
1.7	1858.	7786.	4.2	821.	4822.	5643.	2964.
2.2	2261.	9637.	4.3	418.	5949.	6367.	3688.
2.7	2707.	11472.	4.2	-29.	7090.	7061.	4383.
3.2	3182.	13278.	4.2	-504.	8230.	7726.	5048.
3.8	3672.	15058.	4.1	-994.	9365.	8371.	5693.
4.3	4147.	16785.	4.0	-1469.	10466.	8997.	6319.
5.0	4709.	18697.	4.0	-2030.	11703.	9673.	6994.
5.6	5184.	20299.	3.9	-2506.	12741.	10236.	7557.
7.1	6250.	23785.	3.8	-3571.	15017.	11446.	8768.
8.6	7099.	26500.	3.7	-4421.	16799.	12379.	9700.
10.0	7704.	28478.	3.7	-5026.	18091.	13065.	10387.
11.5	8237.	30223.	3.7	-5558.	19230.	13672.	10993.
13.4	8784.	31973.	3.6	-6106.	20379.	14243.	11565.
15.0	9144.	33005.	3.6	-6466.	21075.	14609.	11931.

STATIC TRIAXIAL TEST: S-5
WARNER DRAW DAM

CONSOLIDATED UNDRAINED TRIAXIAL TEST
WITH PORE PRESSURE MEASUREMENT

STATIC TX#WD6A KC=1.0
D118-3GMAR.82
BORING:WD-2 SAMPLE:PB-2
CLAYEY SAND

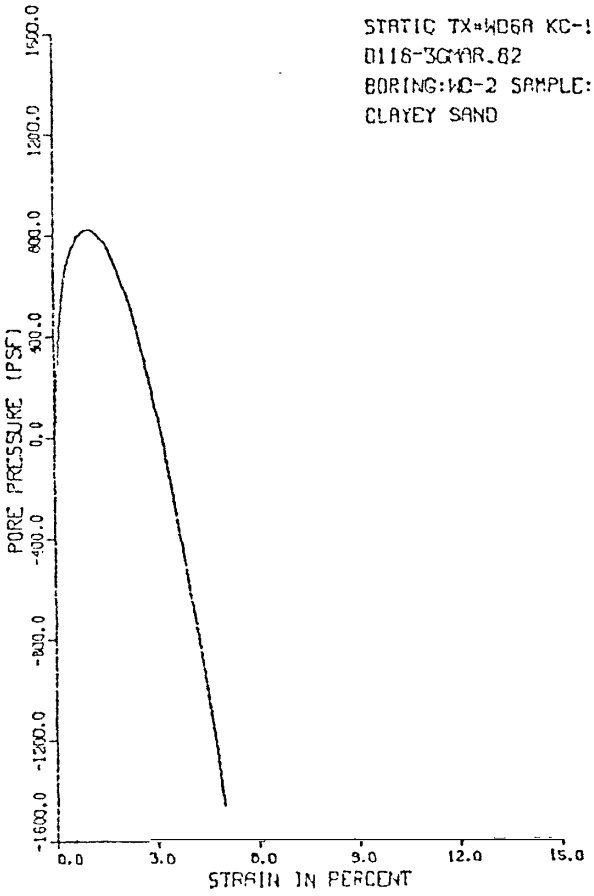

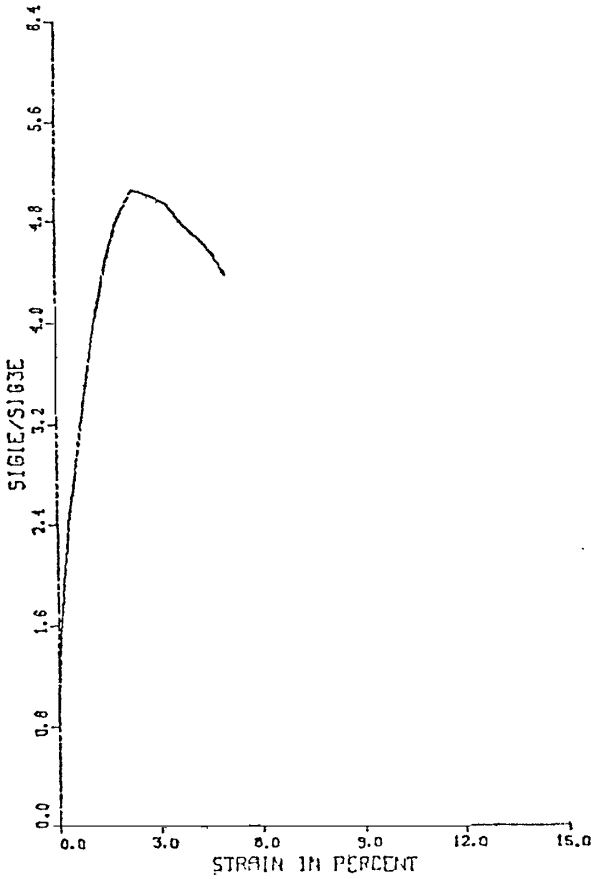

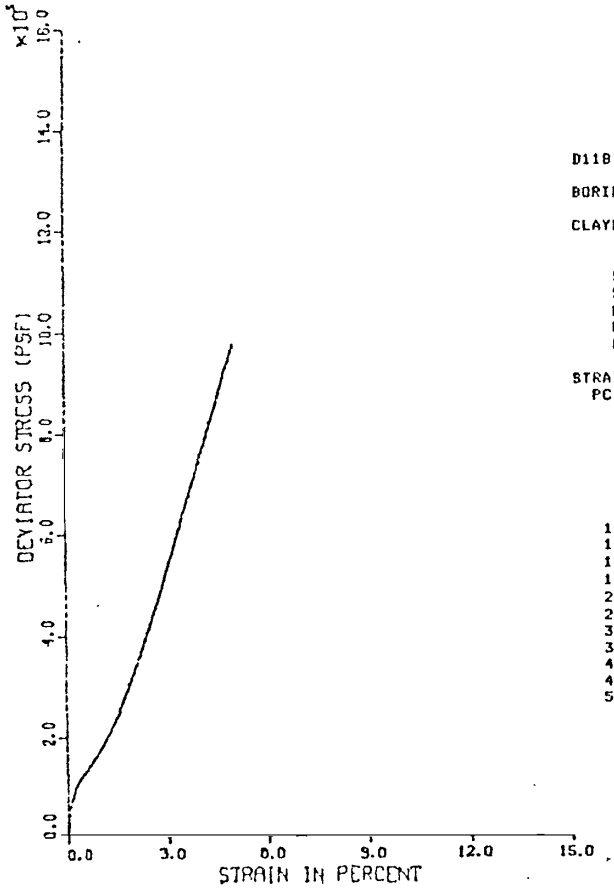

ISOTROPIC CONSOLIDATED UNDRAINED TRIAXIAL TEST
WITH PORE PRESSURE MEASUREMENTS
D11B UTAH DAMS-WARNER DRAW DAM STATIC TX#WD6A (STG 1) 3/30/82 RED.BY B

BORING:WD-2 SAMPLE:PB-2/S-2 DEPTH:8.5-11.0

CLAYEY SAND

AT END OF CONSOLIDATION :
SAMPLE HEIGHT ..... = 5.935 INCHES
SAMPLE AREA ..... = 6.385 SQ. INCHES
EFFECTIVE CONFINING STRESS . = 1440. PSF
EFFECTIVE MAJOR PRIN. STRESS = 1440. PSF
PRINCIPAL STRESS RATIO ..... = 1.00

STRAIN PCT	SIGMA3E PSF	SIGMA1E PSF	RATIO SIG1E/SIG3E	PPRESS PSF	PMAX PSF	PTOT PSF	Q PSF
.0	1440.	1440.	1.0	0.	1440.	1440.	0.
.1	1195.	1804.	1.5	245.	1499.	1744.	304.
.2	907.	1852.	2.0	533.	1390.	1913.	473.
.4	763.	1887.	2.5	677.	1325.	2002.	562.
.5	691.	1947.	2.8	749.	1319.	2068.	628.
.7	648.	2059.	3.2	792.	1353.	2145.	705.
.9	634.	2199.	3.5	806.	1416.	2223.	783.
1.0	619.	2360.	3.8	821.	1490.	2311.	871.
1.2	634.	2572.	4.1	806.	1603.	2409.	969.
1.5	677.	3054.	4.5	763.	1865.	2628.	1188.
1.8	763.	3664.	4.8	677.	2214.	2890.	1450.
2.3	936.	4726.	5.0	504.	2831.	3335.	1895.
2.8	1195.	5976.	5.0	245.	3596.	3830.	2390.
3.3	1483.	7330.	4.9	-43.	4407.	4364.	2924.
3.8	1858.	8846.	4.8	-418.	5352.	4934.	3494.
4.3	2261.	10462.	4.6	-821.	6361.	5541.	4101.
4.7	2563.	11572.	4.5	-1123.	7068.	5944.	4504.
5.0	2909.	12678.	4.4	-1469.	7794.	6325.	4885.

STATIC TRIAXIAL TEST: S-6A
WARNER DRAW DAM

CONSOLIDATED UNDRAINED TRIAXIAL TEST
WITH PORE PRESSURE MEASUREMENT

STATIC TX#WD6B KC-1.0
D118-3CMAR.82
BORING:WD-2 SAMPLE:PB-2
CLAYEY SAND

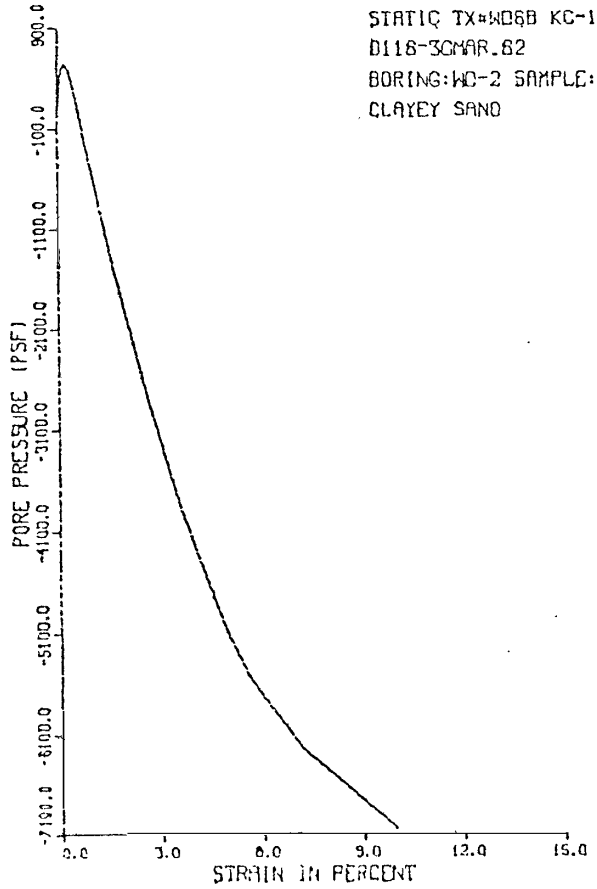

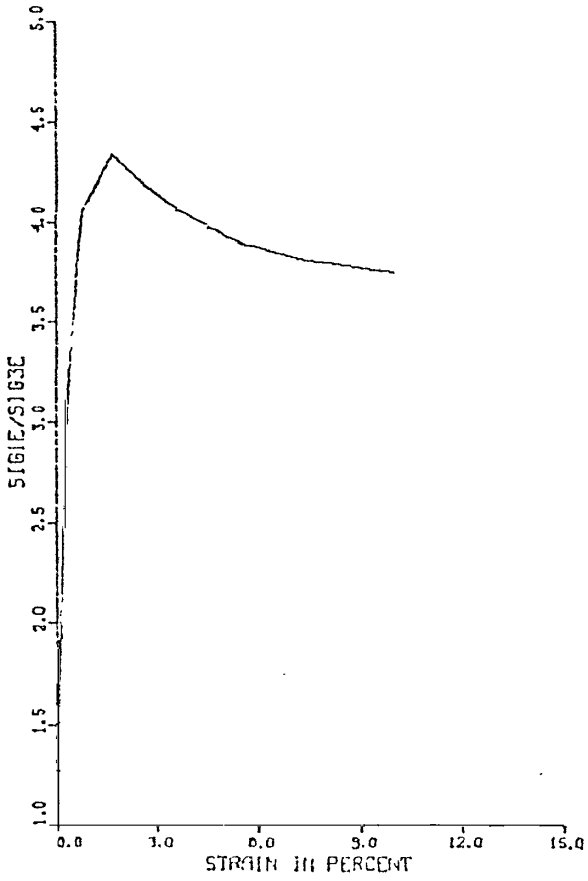

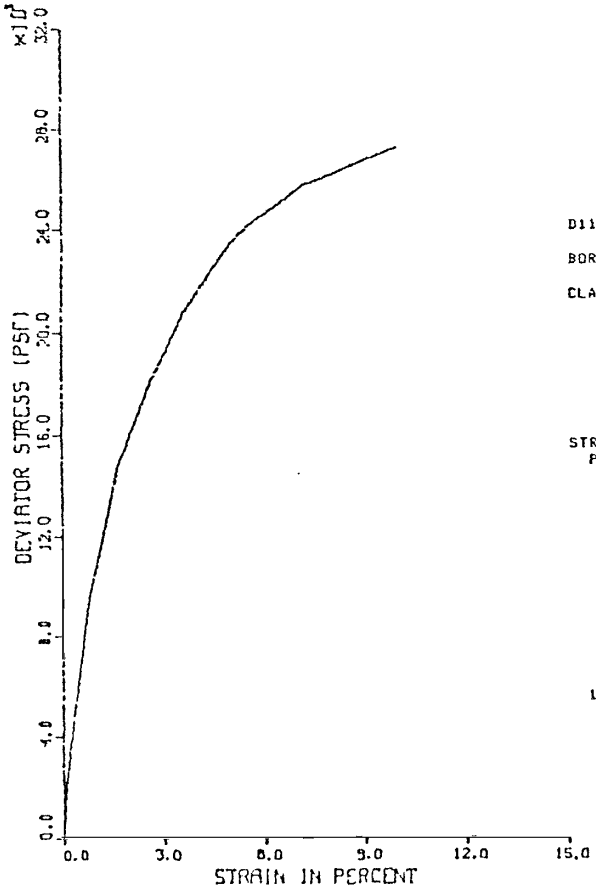

ISOTROPIC CONSOLIDATED UNDRAINED TRIAXIAL TEST
WITH PORE PRESSURE MEASUREMENTS
D11B UTAH DAMS-WARNER DRAW DAM STATIC TX#WD6B (STG 2) 3/30/82 REV. BY B

BORING:WD-2 SAMPLE:PB-2/S-2 DEPTH:8.5-11.0

CLAYEY SAND

AT END OF CONSOLIDATION :
SAMPLE HEIGHT ..... = 5.680 INCHES
SAMPLE AREA ..... = 6.586 SQ. INCHES
EFFECTIVE CONFINING STRESS . = 2880. PSF
EFFECTIVE MAJOR PRIN. STRESS = 2880. PSF
PRINCIPAL STRESS RATIO ..... = 1.00

STRAIN PCT	SIGMA3E PSF	SIGMA1E PSF	RATIO SIG1E/SIG3E	PPRESS PSF	PBAR PSF	PTOT PSF	Q PSF
.0	2880.	2880.	1.0	0.	2880.	2880.	0.
.0	2606.	3918.	1.5	274.	3262.	3536.	656.
.1	2405.	4807.	2.0	475.	3606.	4081.	1201.
.2	2333.	5976.	2.6	547.	4154.	4702.	1822.
.4	2419.	7387.	3.1	461.	4903.	5364.	2484.
.5	2592.	9010.	3.5	288.	5801.	6089.	3209.
.8	3110.	12634.	4.1	-230.	7872.	7642.	4762.
1.7	4435.	19251.	4.3	-1555.	11843.	10288.	7408.
2.6	5659.	23694.	4.2	-2779.	14677.	11898.	9018.
3.6	6739.	27420.	4.1	-3859.	17080.	13220.	10340.
5.0	7992.	31443.	3.9	-5112.	19717.	14605.	11725.
5.6	8395.	32604.	3.9	-5515.	20500.	14984.	12104.
7.2	9158.	34904.	3.8	-6278.	22031.	15753.	12873.
10.0	9950.	37224.	3.7	-7070.	23587.	16517.	13637.

STATIC TRIAXIAL TEST: S-6B
WARNER DRAW DAM

CONSOLIDATED UNDRAINED TRIAXIAL TEST
WITH PORE PRESSURE MEASUREMENT

STATIC TX#WD7A KC-1.0
D118-13MAY82
BORING:WD-2 SAMPLE:PB13
CLAYEY SAND

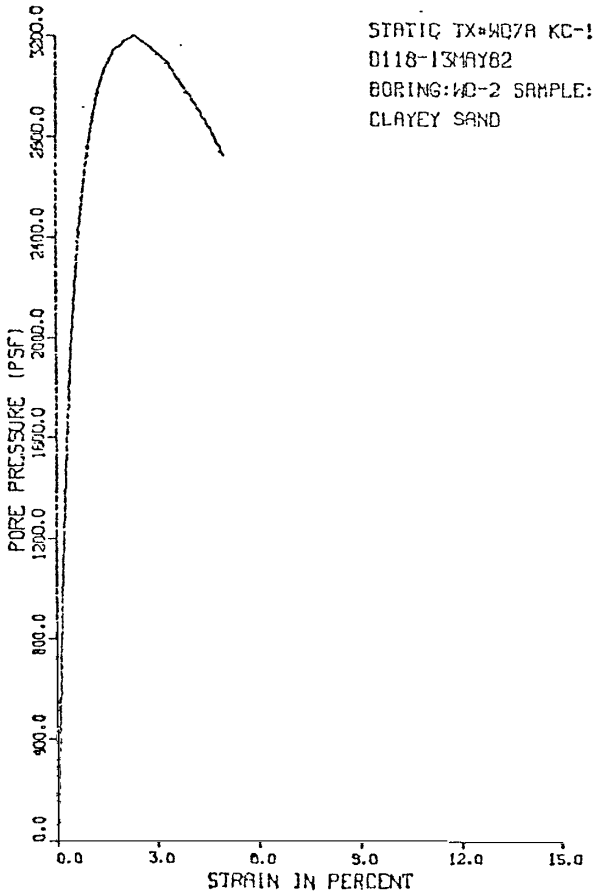

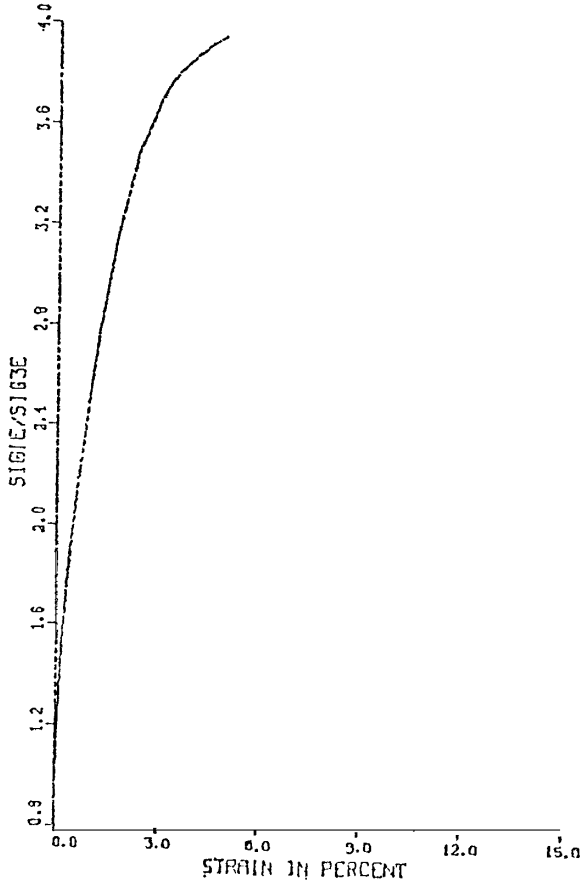

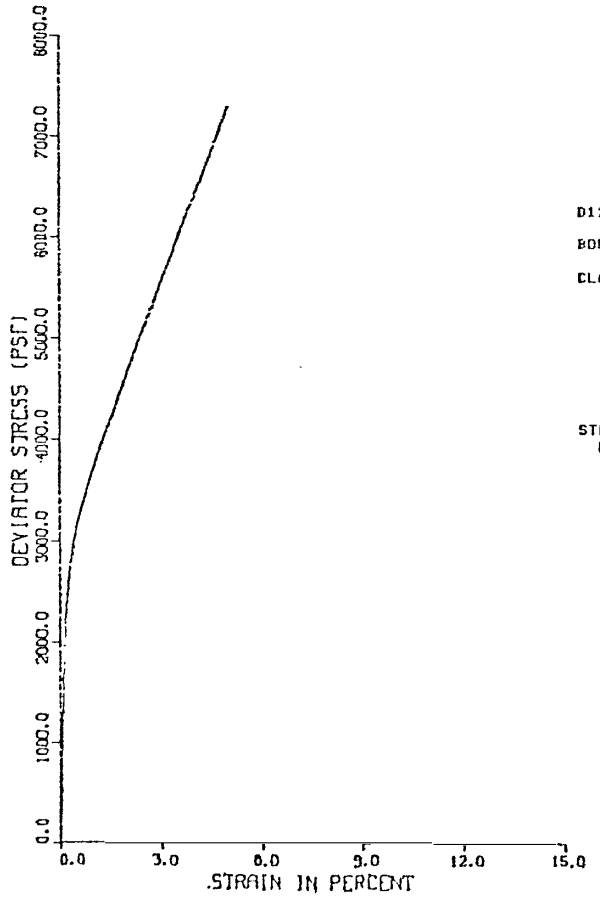

ISOTROPIC CONSOLIDATED UNDRAINED TRIAXIAL TEST
WITH PORE PRESSURE MEASUREMENTS
D118-UTAH DAMS-WARNER DRAW DAM STATIC TX#7A STAGE 1 5/13/82 RED. BY BW

BORING:WD-2 SAMPLE:PB-13/S-13 DEPTH:52.5-55.0

CLAYEY SAND

AT END OF CONSOLIDATION :
SAMPLE HEIGHT ..... = 5.977 INCHES
SAMPLE AREA ..... = 6.535 SQ. INCHES
EFFECTIVE CONFINING STRESS . = 5198. PSF
EFFECTIVE MAJOR PRIN. STRESS = 5198. PSF
PRINCIPAL STRESS RATIO ..... = 1.00

STRAIN PCT	SIGMA3E PSF	SIGMA1E PSF	RATIO SIG1E/SIG3E	PPRESS PSF	PBAR PSF	PTOT PSF	Q PSF
.0	5198.	5198.	1.0	0.	5198.	5198.	0.
.0	5069.	5730.	1.1	130.	5399.	5529.	330.
.1	4766.	6285.	1.3	432.	5526.	5958.	760.
.2	4248.	6448.	1.5	950.	5348.	6298.	1100.
.3	3744.	6402.	1.7	1454.	5073.	6528.	1329.
.4	3326.	6289.	1.9	1872.	4808.	6680.	1481.
.6	2995.	6195.	2.1	2203.	4595.	6798.	1600.
.7	2736.	6106.	2.2	2462.	4421.	6883.	1685.
.8	2549.	6088.	2.4	2650.	4319.	6968.	1770.
1.0	2405.	6113.	2.5	2794.	4259.	7053.	1854.
1.1	2290.	6145.	2.7	2909.	4217.	7126.	1928.
1.3	2218.	6198.	2.8	2981.	4208.	7189.	1990.
1.4	2146.	6272.	2.9	3053.	4209.	7261.	2063.
1.7	2059.	6476.	3.1	3139.	4267.	7407.	2208.
2.0	2030.	6714.	3.3	3168.	4372.	7540.	2342.
2.4	2002.	6972.	3.5	3197.	4487.	7683.	2485.
2.7	2030.	7285.	3.6	3168.	4657.	7825.	2627.
3.0	2059.	7595.	3.7	3139.	4827.	7966.	2768.
3.3	2102.	7918.	3.8	3096.	5010.	8106.	2908.
3.7	2174.	8289.	3.8	3024.	5231.	8255.	3057.
4.2	2275.	8822.	3.9	2923.	5549.	8472.	3273.
4.7	2390.	9386.	3.9	2808.	5888.	8696.	3498.
5.0	2477.	9782.	3.9	2722.	6130.	8851.	3653.

STATIC TRIAXIAL TEST: S-7A
WARNER DRAW DAM

CONSOLIDATED UNDRAINED TRIAXIAL TEST
WITH PORE PRESSURE MEASUREMENT

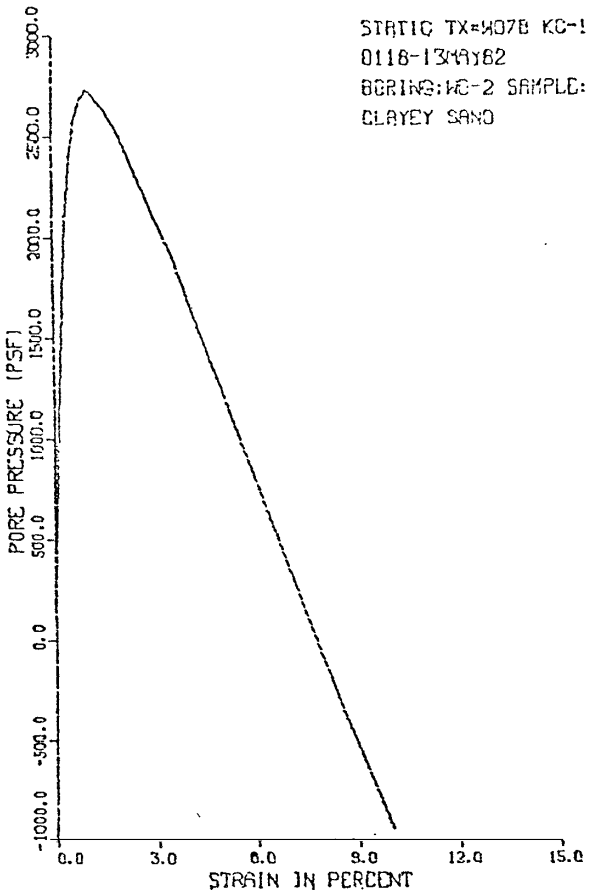

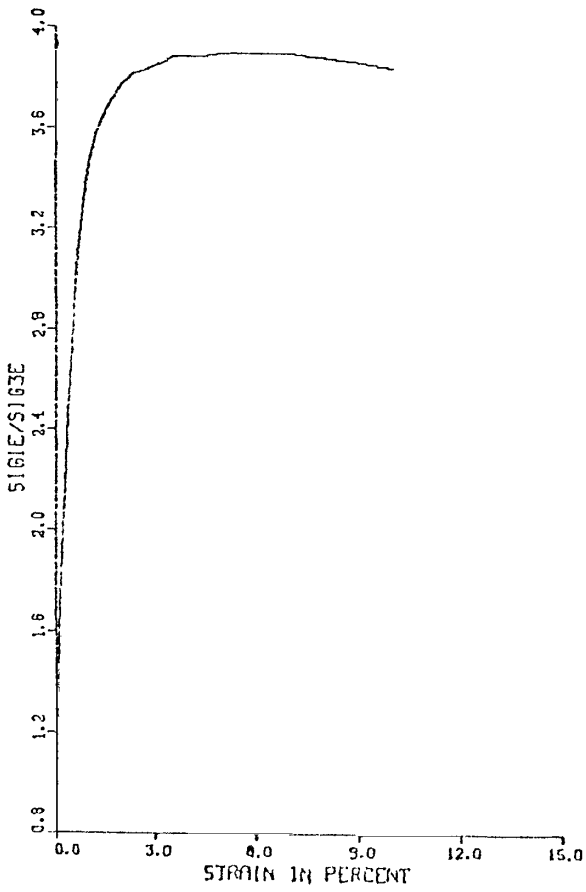

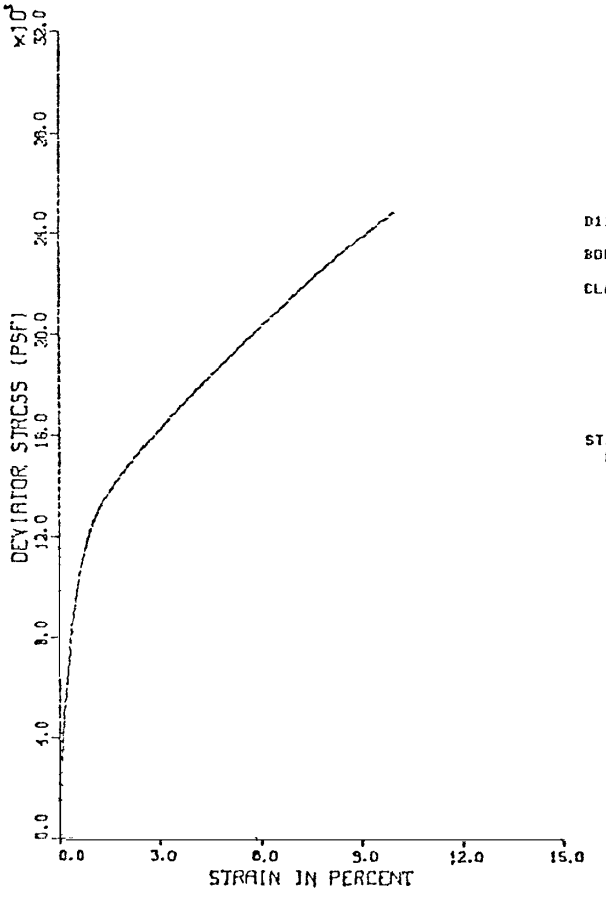

ISOTROPIC CONSOLIDATED UNDRAINED TRIAXIAL TEST
WITH PORE PRESSURE MEASUREMENTS
D118-UTAH DAMS-WARNER DRAW DAM STATIC TX#7B STAGE 2 5/13/82 PED. BY DW

BORING:WD-2 SAMPLE:PB-13/S-13 DEPTH:52.5-55.0

CLAYEY SAND

AT END OF CONSOLIDATION :
SAMPLE HEIGHT ..... = 5.697 INCHES
SAMPLE AREA ..... = 6.761 SQ. INCHES
EFFECTIVE CONFINING STRESS . = 7790. PSF
EFFECTIVE MAJOR PRIN. STRESS = 7790. PSF
PRINCIPAL STRESS RATIO ..... = 1.00

STRAIN PCT	SIGMA3E PSF	SIGMA1E PSF	RATIO SIG1E/SIG3E	PPRESS PSF	PBAR PSF	PTOT PSF	Q PSF
.0	7790.	7790.	1.0	0.	7790.	7790.	0.
.0	7574.	9022.	1.2	216.	8298.	8514.	724.
.1	7214.	10194.	1.4	576.	8704.	9280.	1490.
.1	6696.	11545.	1.7	1094.	9120.	10215.	2424.
.3	6163.	12834.	2.1	1627.	9499.	11126.	3335.
.4	5717.	14055.	2.5	2074.	9886.	11959.	4169.
.5	5400.	15167.	2.8	2390.	10283.	12674.	4883.
.7	5213.	16149.	3.1	2578.	10681.	13258.	5468.
.9	5112.	16958.	3.3	2678.	11035.	13713.	5923.
1.0	5069.	17609.	3.5	2722.	11339.	14061.	6270.
1.2	5083.	18169.	3.6	2707.	11626.	14333.	6543.
1.6	5170.	19107.	3.7	2621.	12138.	14759.	6969.
2.0	5285.	19940.	3.8	2506.	12612.	15118.	7328.
2.4	5429.	20712.	3.8	2362.	13071.	15432.	7642.
3.0	5674.	21814.	3.8	2117.	13744.	15861.	8070.
3.5	5904.	22914.	3.9	1886.	14409.	16295.	8505.
4.1	6178.	23982.	3.9	1613.	15080.	16693.	8902.
5.0	6552.	25531.	3.9	1238.	16041.	17280.	9489.
5.5	6797.	26492.	3.9	994.	16644.	17638.	9847.
7.0	7459.	29060.	3.9	331.	18260.	18591.	10801.
8.5	8122.	31426.	3.9	-331.	19774.	19443.	11652.
10.0	8741.	33604.	3.8	-950.	21172.	20222.	12431.

STATIC TRIAXIAL TEST: S-7B
WARNER DRAW DAM

FROG HOLLOW DAM

Earth Sciences Associates

CONSOLIDATED UNDRAINED TRIAXIAL TEST
WITH PORE PRESSURE MEASUREMENT

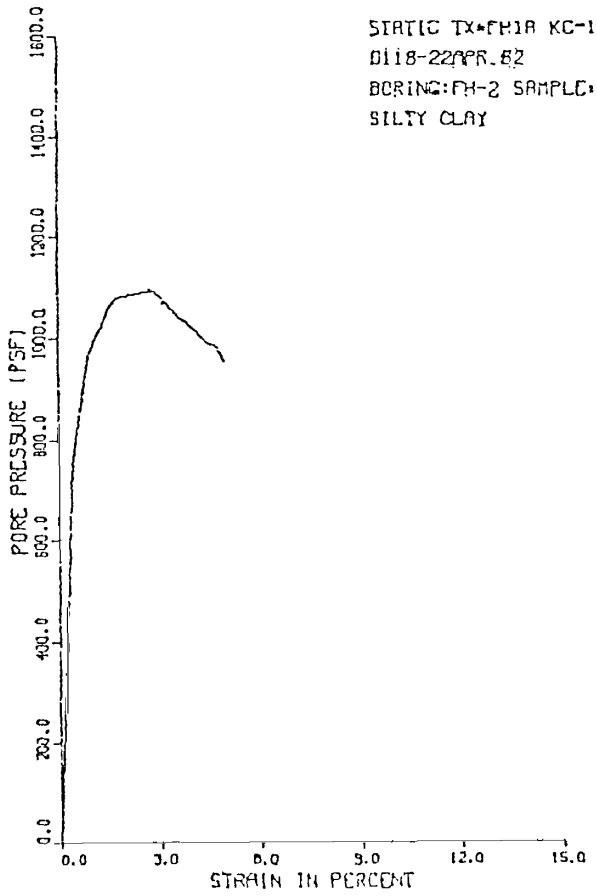

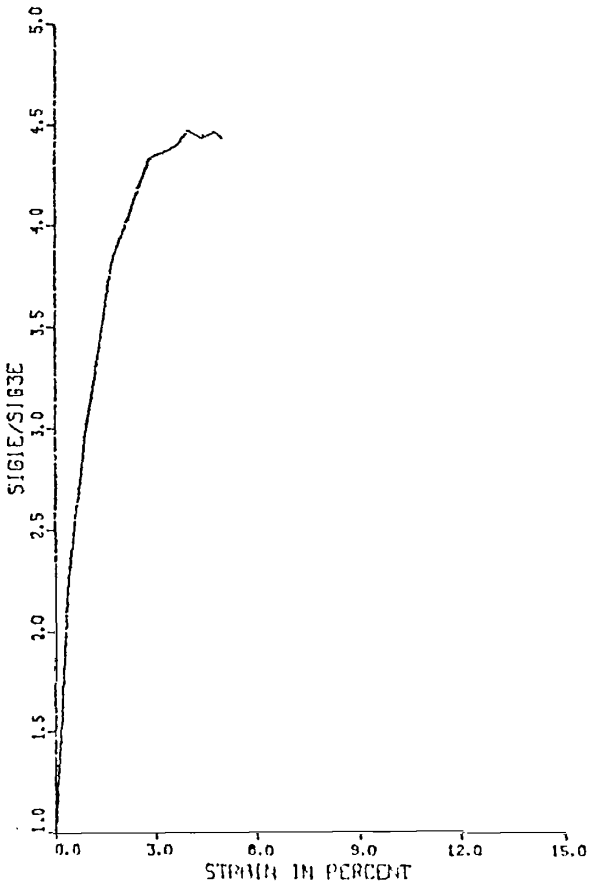

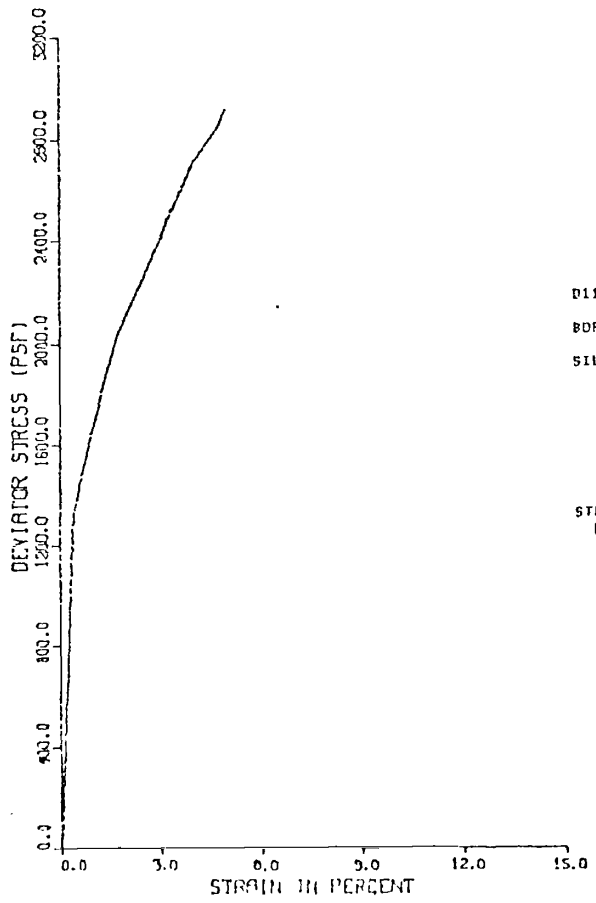

ISOTROPIC CONSOLIDATED UNDRAINED TRIAXIAL TEST
WITH PORE PRESSURE MEASUREMENTS
D118-UTAH DAMS-FROG HOLLOW STATIC TX*FH-1 STAGE1 4/22/82 RED BY BW

BORING:FH-2 SAMPLE:PB-6/S-4 DEPTH:23.0-25.5

SILTY CLAY

AT END OF CONSOLIDATION :

SAMPLE HEIGHT	=	5.829 INCHES
SAMPLE AREA	=	6.607 SQ. INCHES
EFFECTIVE CONFINING STRESS .	=	1800. PSF
EFFECTIVE MAJOR PRIN. STRESS	=	1800. PSF
PRINCIPAL STRESS RATIO	=	1.00

STRAIN PCT	SIGMA3E PSF	SIGMA1E PSF	RATIO SIG1E/SIG3E	PPRESS PSF	PBAR PSF	PTOT PSF	D PSF
.0	1800.	1800.	1.0	0.	1800.	1800.	0.
.4	1051.	2375.	2.3	749.	1713.	2462.	662.
.9	835.	2455.	2.9	965.	1645.	2610.	810.
1.4	763.	2634.	3.5	1037.	1698.	2735.	935.
1.5	734.	2687.	3.7	1066.	1711.	2776.	976.
1.7	720.	2755.	3.8	1080.	1737.	2817.	1017.
2.8	706.	3056.	4.3	1094.	1881.	2975.	1175.
3.0	720.	3129.	4.3	1080.	1925.	3005.	1205.
3.2	734.	3202.	4.4	1066.	1968.	3034.	1234.
3.6	763.	3347.	4.4	1037.	2055.	3092.	1292.
4.0	778.	3477.	4.5	1022.	2127.	3150.	1350.
4.4	806.	3579.	4.4	994.	2193.	3186.	1386.
4.7	821.	3665.	4.5	979.	2243.	3222.	1422.
5.0	850.	3769.	4.4	950.	2309.	3260.	1460.

STATIC TRIAXIAL TEST: S-1A
FROG HOLLOW DAM

CONSOLIDATED UNDRAINED TRIAXIAL TEST
WITH PORE PRESSURE MEASUREMENT

STATIC TX=FH1B KC=1.0
0118-22?FR.82
BORING:FH-2 SAMPLE:PB-6
SILTY CLAY

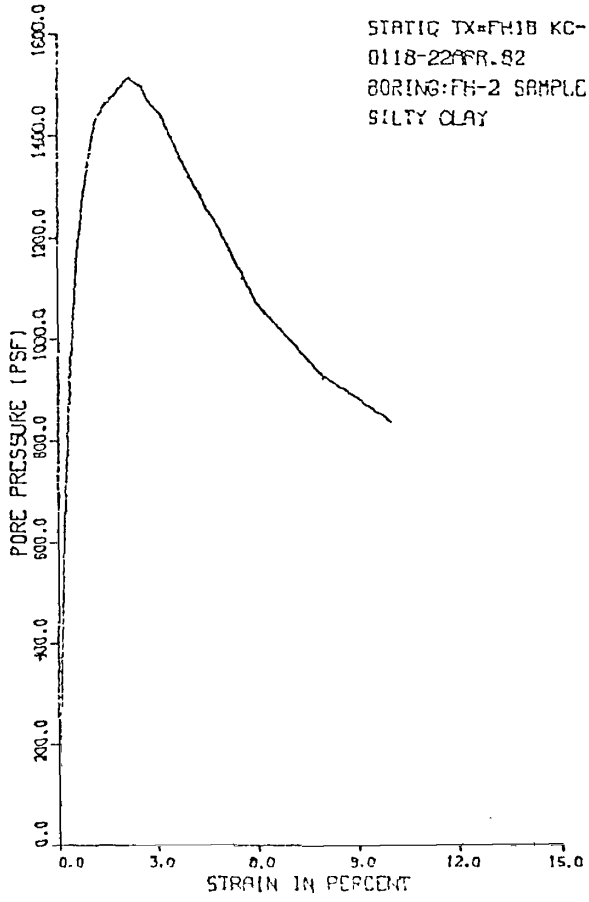

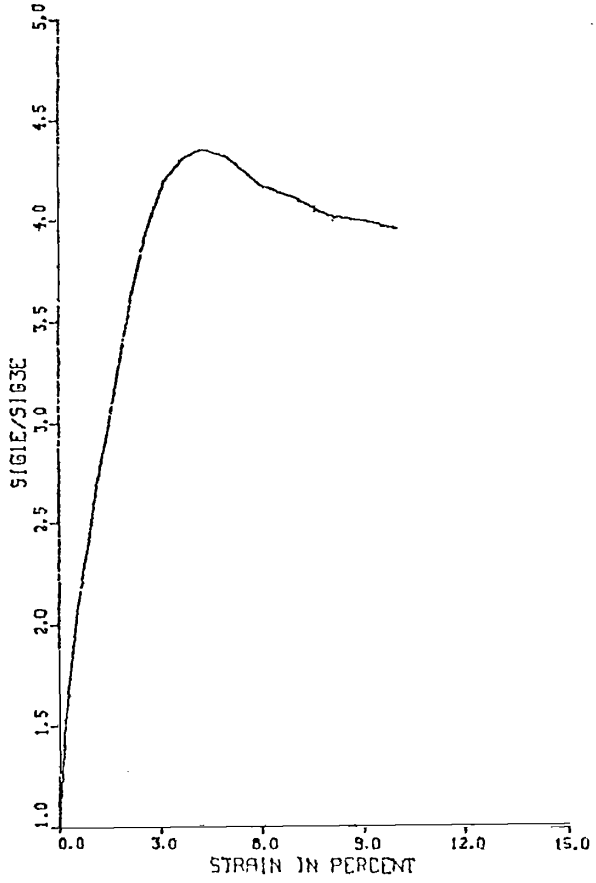

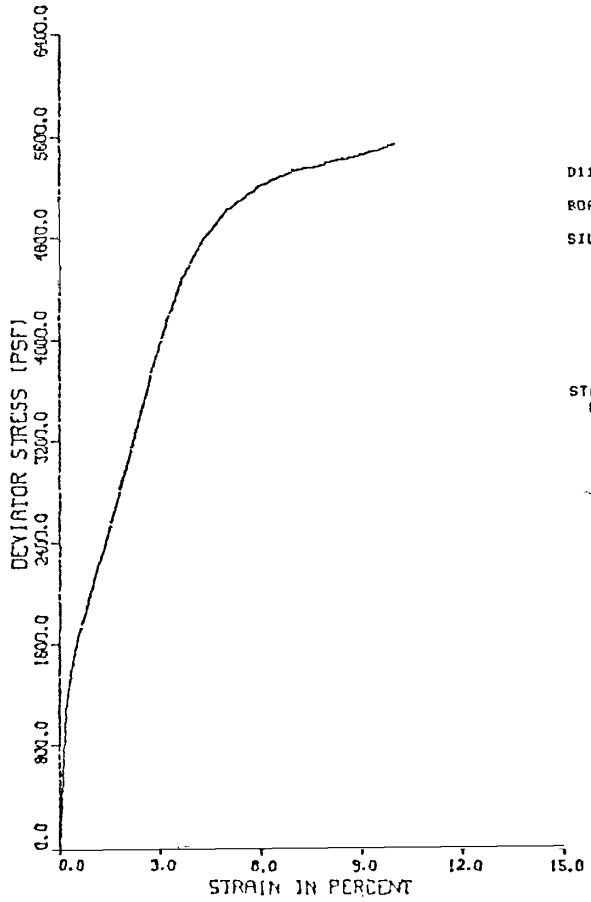

ISOTROPIC CONSOLIDATED UNDRAINED TRIAXIAL TEST
WITH PORE PRESSURE MEASUREMENTS
D118-UTAH DAMS-FROG HOLLOW STATIC TX#FH1B STAGE2 4/22/82 RED BY BW

BORING:FH-2 SAMPLE:PB-6/S-4 DEPTH:23.0-25.5

SILTY CLAY

AT END OF CONSOLIDATION :

SAMPLE HEIGHT	=	5.604 INCHES
SAMPLE AREA	=	6.793 SQ. INCHES
EFFECTIVE CONFINING STRESS .	=	2707. PSF
EFFECTIVE MAJOR PRIN. STRESS	=	2707. PSF
PRINCIPAL STRESS RATIO	=	1.00

STRAIN PCT	SIGMA3E PSF	SIGMA1E PSF	RATIO SIG1E/SIG3E	PPRESS PSF	RBAR PSF	RTOT PSF	R PSF
.0	2707.	2707.	1.0	0.	2707.	2707.	0.
.2	2074.	3132.	1.5	634.	2603.	3236.	529.
.4	1757.	3172.	1.8	950.	2464.	3415.	707.
.6	1555.	3199.	2.1	1152.	2377.	3529.	822.
.8	1426.	3256.	2.3	1282.	2341.	3622.	915.
1.0	1339.	3355.	2.5	1368.	2347.	3715.	1008.
1.2	1282.	3482.	2.7	1426.	2382.	3807.	1100.
1.4	1253.	3616.	2.9	1454.	2434.	3889.	1181.
1.7	1224.	3973.	3.2	1483.	2599.	4082.	1375.
2.1	1195.	4328.	3.6	1512.	2762.	4274.	1566.
2.5	1210.	4722.	3.9	1498.	2966.	4464.	1756.
2.7	1238.	4950.	4.0	1469.	3094.	4563.	1856.
3.1	1267.	5314.	4.2	1440.	3290.	4730.	2023.
3.7	1354.	5845.	4.3	1354.	3599.	4953.	2246.
4.3	1426.	6214.	4.4	1282.	3820.	5101.	2394.
5.0	1512.	6527.	4.3	1195.	4019.	5215.	2507.
6.0	1642.	6863.	4.2	1066.	4252.	5318.	2610.
7.0	1714.	7057.	4.1	994.	4385.	5379.	2672.
8.0	1786.	7188.	4.0	922.	4487.	5408.	2701.
9.0	1829.	7307.	4.0	878.	4568.	5446.	2739.
10.0	1872.	7424.	4.0	835.	4648.	5483.	2776.

STATIC TRIAXIAL TEST: S-1B
FROG HOLLOW DAM

CONSOLIDATED UNDRAINED TRIAXIAL TEST
WITH PORE PRESSURE MEASUREMENT

STATIC TX-FH2 KC-1.0
0118-SAFR.82
BORING:FH-1 SAMPLE:PB-6
CLAY

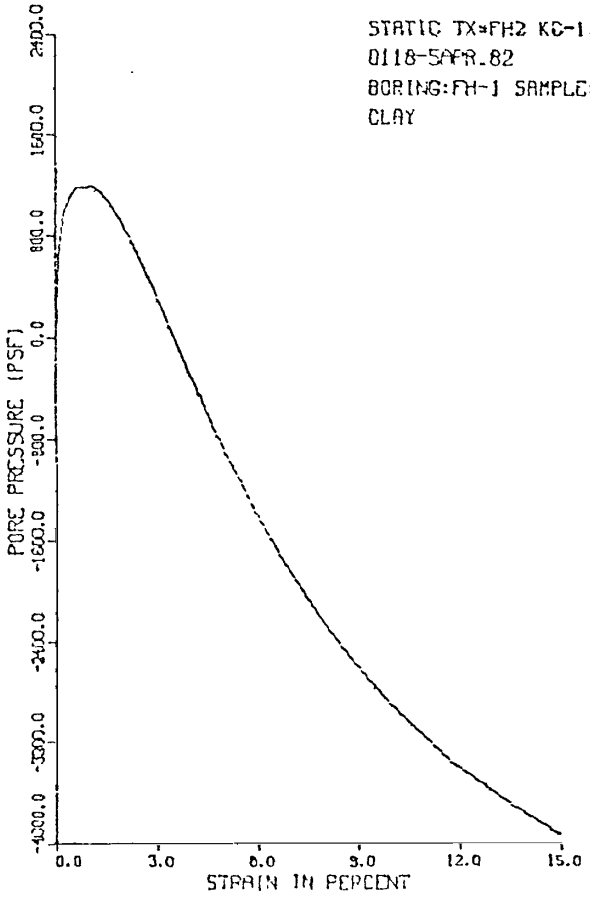

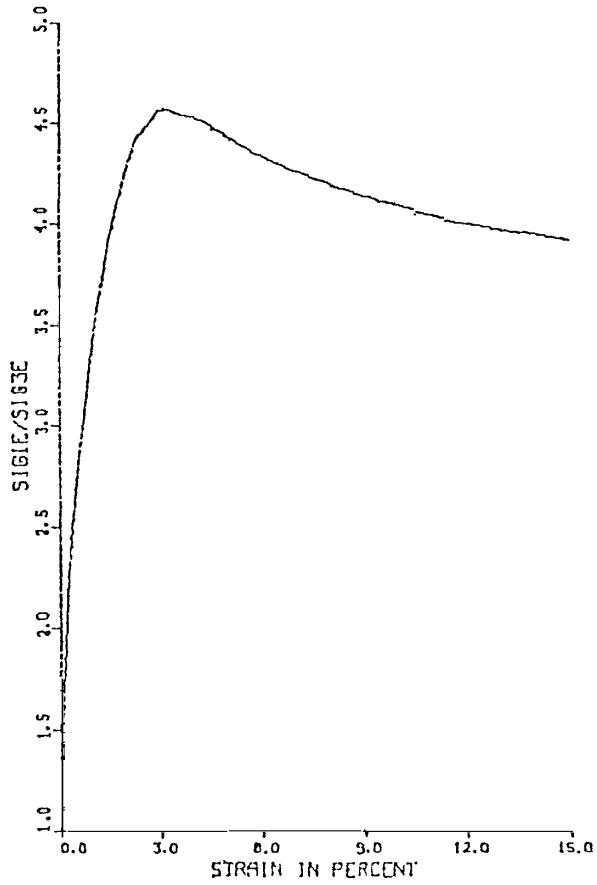

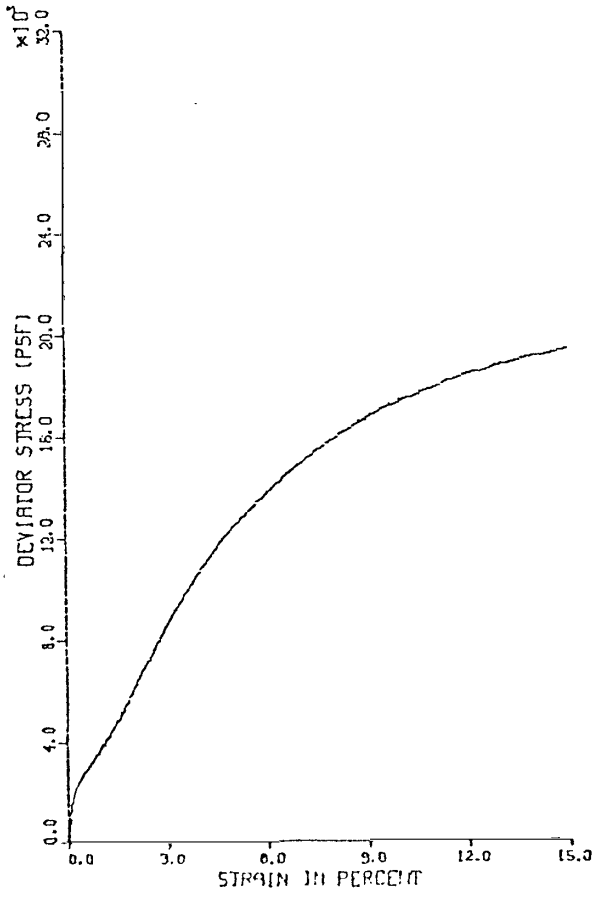

ISOTROPIC CONSOLIDATED UNDRAINED TRIAXIAL TEST
WITH PORE PRESSURE MEASUREMENTS
D118-UTAH DAMS-FROG HOLLOW STATIC TX-FH2 4/5/82 REDUCED BY RW

BORING:FH-1 SAMPLE:PB-6/S-5 DEPTH:22.5-25.0

CLAY W/GRAVEL

AT END OF CONSOLIDATION :
SAMPLE HEIGHT ..... = 5.965 INCHES
SAMPLE AREA ..... = 6.514 SQ. INCHES
EFFECTIVE CONFINING STRESS . = 2707. PSF
EFFECTIVE MAJOR PRIN. STRESS = 2707. PSF
PRINCIPAL STRESS RATIO ..... = 1.00

STRAIN PCT	SIGMA3E PSF	SIGMA1E PSF	RATIO SIG1E/SIG3E	PPRESS PSF	PBAR PSF	PDIF PSF	Q PSF
.0	2707.	2707.	1.0	0.	2707.	2707.	0.
.1	2088.	3523.	1.7	619.	2806.	3425.	718.
.3	1728.	3887.	2.3	979.	2808.	3787.	1080.
.4	1598.	4174.	2.6	1109.	2886.	3995.	1288.
.6	1541.	4463.	2.9	1166.	3002.	4168.	1461.
1.1	1526.	5462.	3.6	1181.	3494.	4675.	1968.
1.3	1570.	5848.	3.7	1138.	3709.	4846.	2139.
1.4	1613.	6276.	3.9	1094.	3944.	5039.	2331.
1.6	1670.	6717.	4.0	1037.	4194.	5230.	2523.
1.9	1814.	7689.	4.2	893.	4752.	5645.	2937.
2.3	1973.	8713.	4.4	734.	5343.	6077.	3370.
2.6	2174.	9752.	4.5	533.	5963.	6496.	3789.
3.0	2362.	10771.	4.6	346.	6566.	6912.	4205.
3.3	2578.	11770.	4.6	130.	7174.	7303.	4596.
3.6	2808.	12734.	4.5	-101.	7771.	7670.	4963.
4.0	3010.	13622.	4.5	-302.	8316.	8013.	5306.
4.3	3211.	14462.	4.5	-504.	8837.	8333.	5625.
4.7	3427.	15291.	4.5	-720.	9359.	8639.	5932.
5.0	3614.	16004.	4.4	-907.	9809.	8902.	6195.
5.8	4032.	17526.	4.3	-1325.	10779.	9454.	6747.
6.7	4450.	19032.	4.3	-1742.	11741.	9998.	7291.
7.6	4824.	20347.	4.2	-2117.	12586.	10469.	7762.
8.5	5170.	21509.	4.2	-2462.	13339.	10877.	8170.
9.4	5472.	22487.	4.1	-2765.	13980.	11215.	8508.
10.0	5630.	22999.	4.1	-2923.	14315.	11392.	8684.
11.8	6091.	24404.	4.0	-3384.	15248.	11864.	9157.
13.7	6437.	25483.	4.0	-3730.	15960.	12230.	9523.
15.0	6653.	26083.	3.9	-3946.	16368.	12422.	9715.

STATIC TRIAXIAL TEST: S-2
FROG HOLLOW DAM

CONSOLIDATED UNDRAINED TRIAXIAL TEST
WITH PORE PRESSURE MEASUREMENT

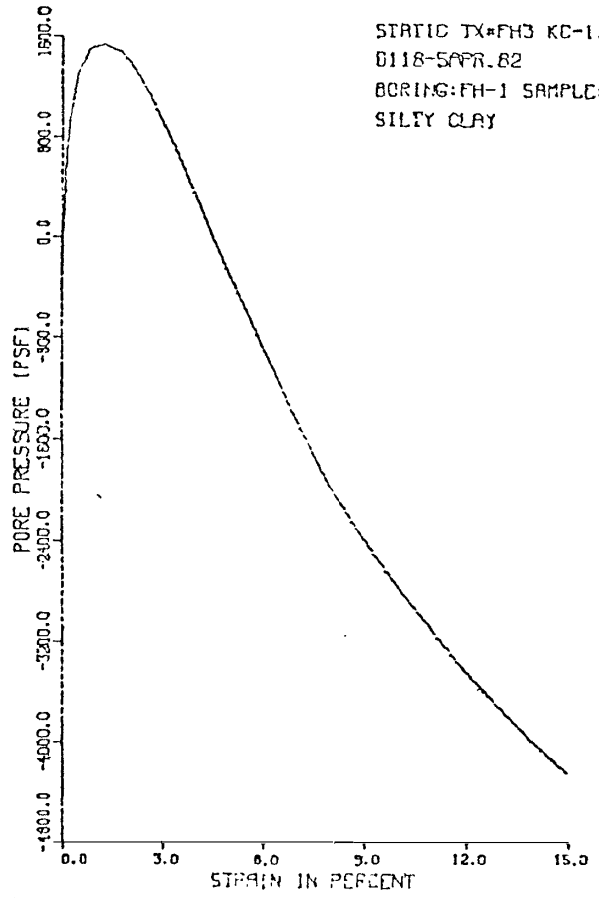

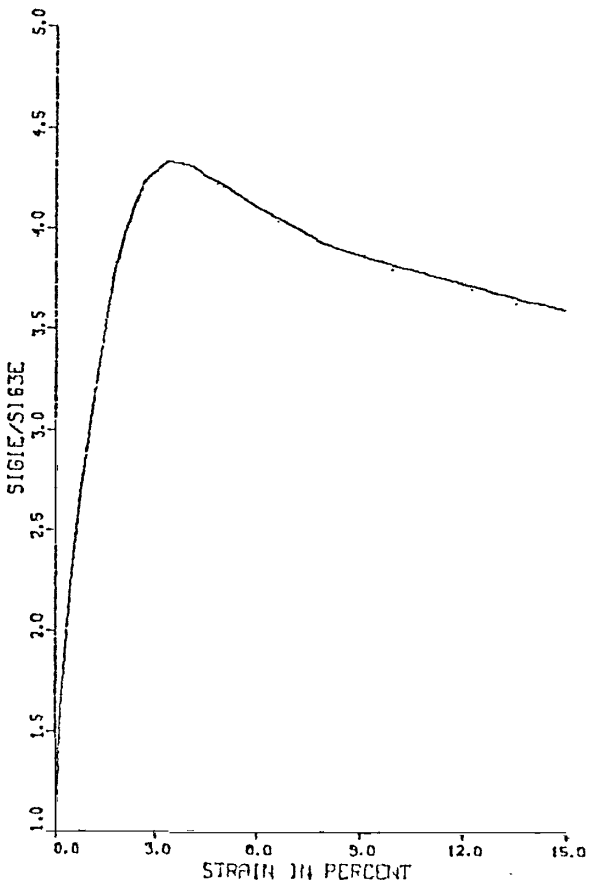

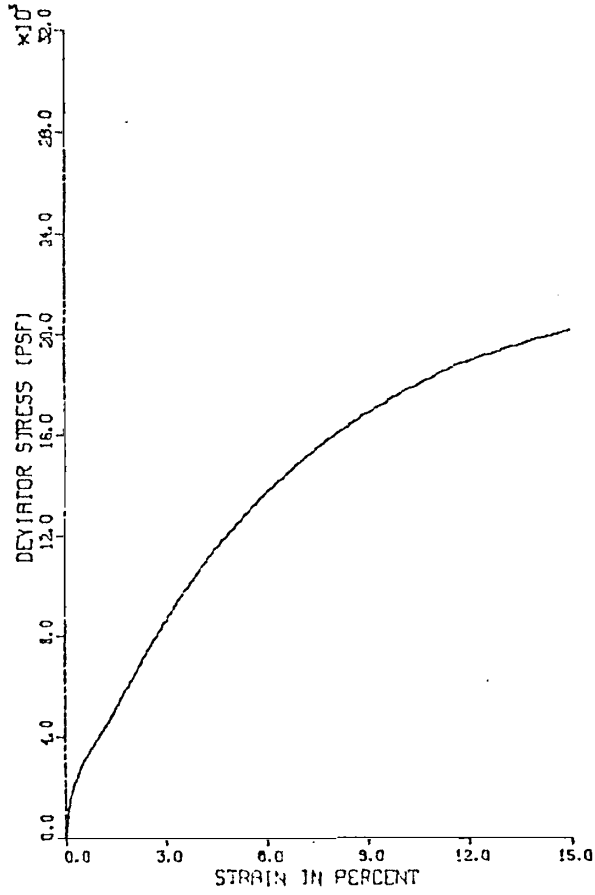

ISOTROPIC CONSOLIDATED UNDRAINED TRIAXIAL TEST
WITH PORE PRESSURE MEASUREMENTS
D118-UTAH DAMS-FROG HOLLOW STATIC TX#FH3 4/5/02 REDUCED BY BW

BORING:FH-1 SAMPLE:PB-10/S-9 DEPTH:38.0-40.5

SILTY CLAY

AT END OF CONSOLIDATION :

SAMPLE HEIGHT	=	5.931 INCHES
SAMPLE AREA	=	6.517 SQ. INCHES
EFFECTIVE CONFINING STRESS .	=	3499. PSF
EFFECTIVE MAJOR PRIN. STRESS	=	3499. PSF
PRINCIPAL STRESS RATIO	=	1.00

STRAIN PCT	SIGMA3E PSF	SIGMA1E PSF	RATIO SIG1E/SIG3E	PPRESS PSF	PRAR PSF	PTOT PSF	P PSF
.0	3499.	3499.	1.0	0.	3499.	3499.	0.
.1	3254.	3895.	1.2	245.	3575.	3819.	320.
.1	2837.	4337.	1.5	662.	3587.	4249.	750.
.2	2534.	4562.	1.8	965.	3548.	4513.	1014.
.4	2333.	4776.	2.0	1166.	3555.	4721.	1222.
.5	2189.	5003.	2.3	1310.	3596.	4906.	1407.
.7	2102.	5263.	2.5	1397.	3683.	5080.	1580.
.8	2016.	5501.	2.7	1483.	3759.	5242.	1742.
1.0	1987.	5795.	2.9	1512.	3891.	5403.	1904.
1.3	1973.	6467.	3.3	1526.	4220.	5746.	2247.
1.4	1987.	6823.	3.4	1512.	4405.	5917.	2418.
1.7	2030.	7610.	3.7	1469.	4820.	6289.	2790.
2.0	2131.	8451.	4.0	1368.	5291.	6659.	3160.
2.4	2275.	9351.	4.1	1224.	5813.	7037.	3538.
2.7	2419.	10246.	4.2	1080.	6333.	7413.	3913.
3.0	2606.	11157.	4.3	893.	6882.	7774.	4275.
3.4	2808.	12160.	4.3	691.	7484.	8175.	4676.
3.7	3024.	13084.	4.3	475.	8054.	8529.	5030.
4.1	3254.	14016.	4.3	245.	8635.	8880.	5391.
4.5	3499.	14916.	4.3	0.	9208.	9208.	5708.
5.0	3802.	16019.	4.2	-302.	9910.	9608.	6109.
6.0	4392.	18021.	4.1	-893.	11206.	10314.	6814.
6.9	4925.	19749.	4.0	-1426.	12337.	10911.	7412.
7.9	5429.	21279.	3.9	-1930.	13354.	11424.	7925.
8.9	5846.	22614.	3.9	-2347.	14230.	11883.	8384.
10.0	6278.	23918.	3.8	-2779.	15098.	12319.	8820.
11.9	6926.	25791.	3.7	-3427.	16359.	12931.	9432.
13.9	7502.	27250.	3.6	-4003.	17376.	13373.	9874.
15.0	7762.	27915.	3.6	-4262.	17838.	13576.	10077.

STATIC TRIAXIAL TEST: S-3
FROG HOLLOW DAM

CONSOLIDATED UNDRAINED TRIAXIAL TEST
WITH PORE PRESSURE MEASUREMENT

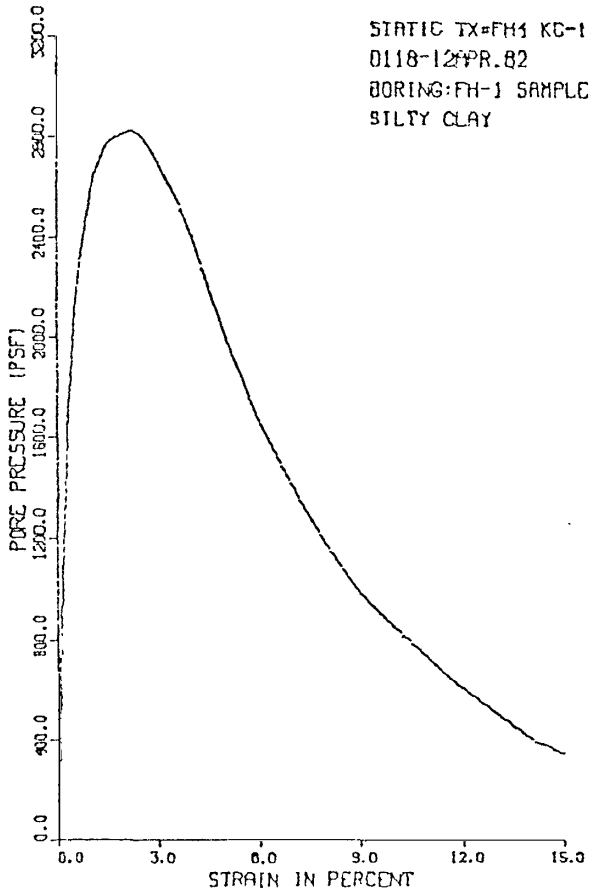

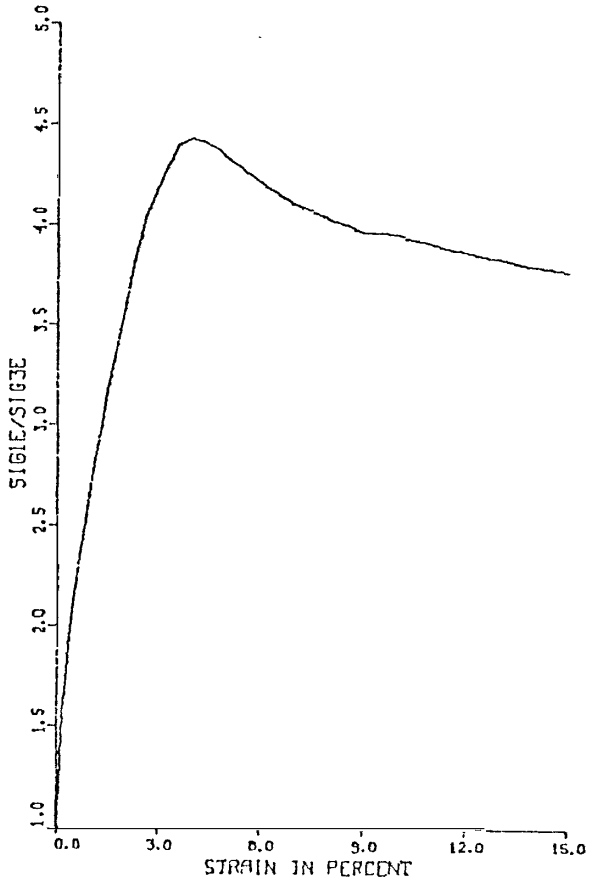

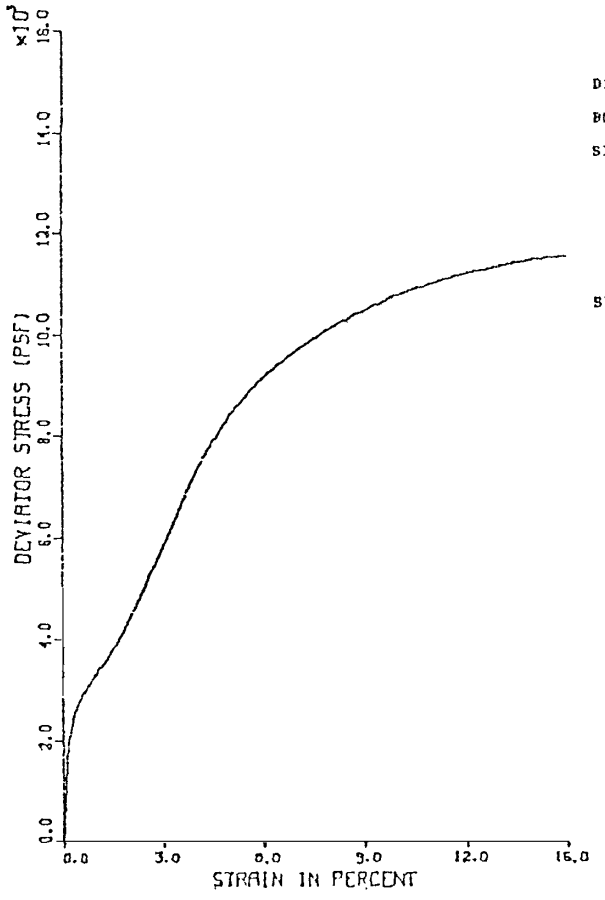

ISOTROPIC CONSOLIDATED UNDRAINED TRIAXIAL TEST
WITH PORE PRESSURE MEASUREMENTS
D118-UTAH DAMS-FROG HOLLOW STATIC TX#FH4 4/12/82 REDUCED BY BW

BORING:FH-1 SAMPLE:PB-14/S-12 DEPTH:55.0-56.8

SILTY CLAY W/SOME FINE SAND

AT END OF CONSOLIDATION :

SAMPLE HEIGHT	=	5.896 INCHES
SAMPLE AREA	=	6.290 SQ. INCHES
EFFECTIVE CONFINING STRESS .	=	4507. PSF
EFFECTIVE MAJOR PRIN. STRESS	=	4507. PSF
PRINCIPAL STRESS RATIO	=	1.00

STRAIN PCT	SIGMA3E PSF	SIGMA1E PSF	RATIO SIG1E/SIG3E	PPRESS PSF	PBAR PSF	PTOT PSF	Q PSF
.0	4507.	4507.	1.0	0.	4507.	4507.	0.
.2	3470.	5368.	1.5	1037.	4419.	5456.	949.
.3	2794.	5281.	1.9	1714.	4037.	5751.	1243.
.5	2405.	5183.	2.2	2102.	3794.	5896.	1389.
.7	2174.	5175.	2.4	2333.	3674.	6007.	1500.
.9	2016.	5192.	2.6	2491.	3604.	6095.	1588.
1.1	1872.	5246.	2.8	2635.	3559.	6194.	1687.
1.3	1800.	5348.	3.0	2707.	3574.	6281.	1774.
1.5	1742.	5509.	3.2	2765.	3626.	6390.	1883.
1.7	1714.	5675.	3.3	2794.	3694.	6488.	1981.
2.1	1699.	6138.	3.6	2808.	3919.	6727.	2220.
2.3	1685.	6384.	3.8	2822.	4034.	6857.	2350.
2.5	1699.	6657.	3.9	2808.	4178.	6986.	2479.
2.6	1728.	6766.	4.0	2779.	4347.	7126.	2619.
2.8	1771.	7288.	4.1	2736.	4530.	7266.	2758.
3.2	1872.	7987.	4.3	2635.	4929.	7565.	3057.
3.6	1973.	8682.	4.4	2534.	5327.	7862.	3354.
4.0	2117.	9370.	4.4	2390.	5743.	8134.	3627.
4.4	2275.	10024.	4.4	2232.	6150.	8382.	3874.
4.8	2419.	10573.	4.4	2088.	6496.	8584.	4077.
5.0	2520.	10914.	4.3	1987.	6717.	8704.	4197.
6.0	2837.	11944.	4.2	1670.	7391.	9061.	4554.
7.0	3110.	12759.	4.1	1397.	7935.	9332.	4824.
8.0	3326.	13417.	4.0	1181.	8372.	9553.	5045.
9.0	3528.	13985.	4.0	979.	8757.	9736.	5229.
10.0	3658.	14433.	3.9	850.	9045.	9895.	5388.
11.8	3888.	15058.	3.9	619.	9473.	10092.	5585.
14.1	4118.	15604.	3.8	389.	9861.	10250.	5743.
15.0	4176.	15735.	3.8	331.	9955.	10287.	5779.

STATIC TRIAXIAL TEST: S-4
FROG HOLLOW DAM

CONSOLIDATED UNDRAINED TRIAXIAL TEST
WITH PORE PRESSURE MEASUREMENT

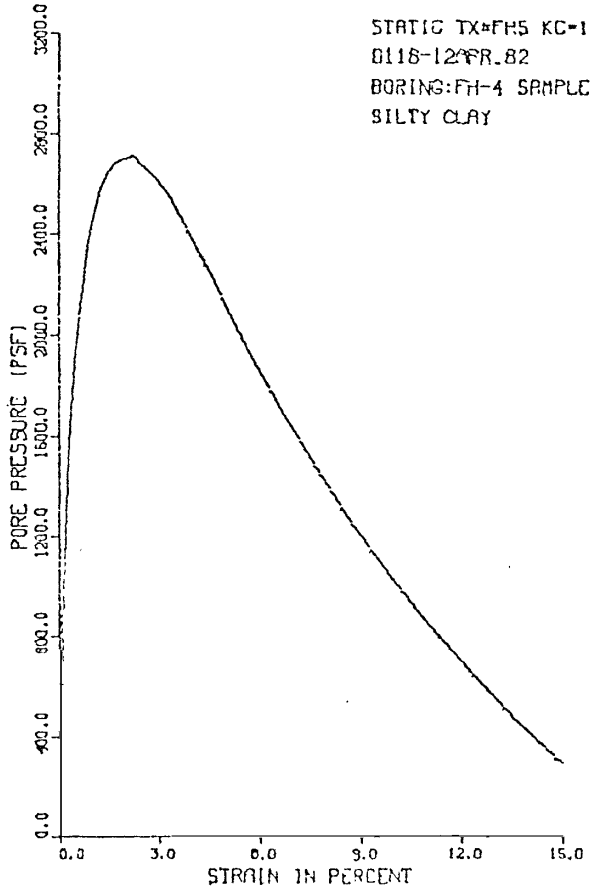

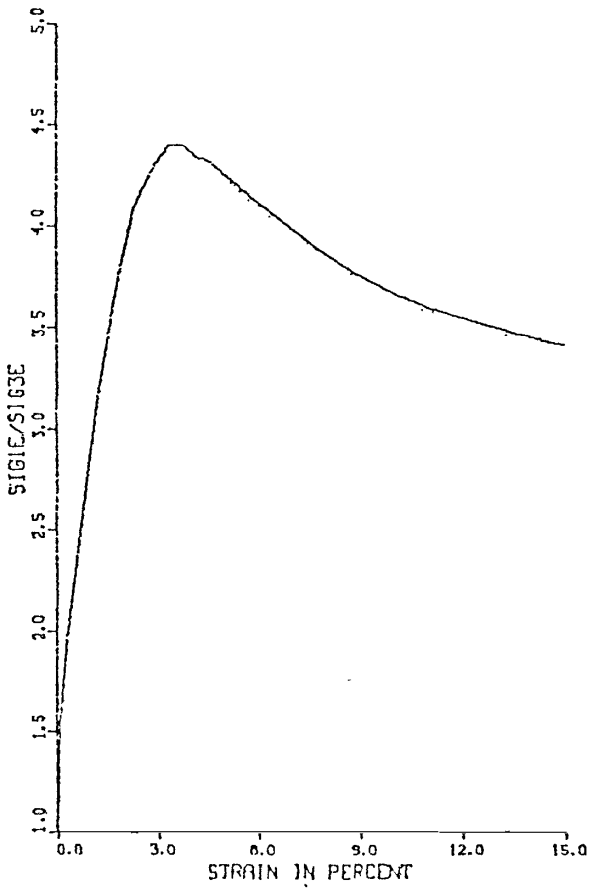

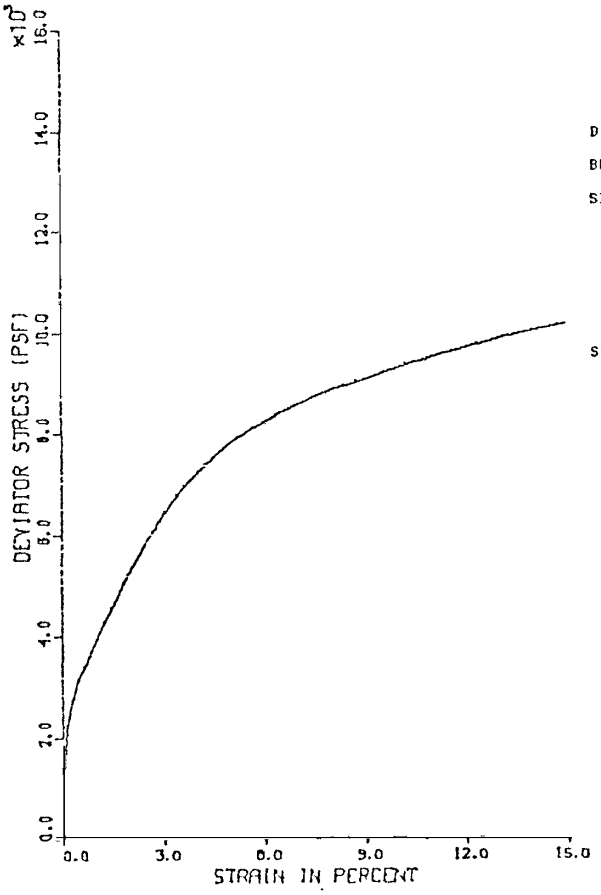

ISOTROPIC CONSOLIDATED UNDRAINED TRIAXIAL TEST
WITH PORE PRESSURE MEASUREMENTS
D118-UTAH DAMS-FROG HOLLOW STATIC TX#FH5 4/12/82 REDUCED BY BW

BORING:FH-4 SAMPLE:PB-3/S-3 DEPTH:53.0-55.0

SILTY CLAY W/SOME FINE SAND

AT END OF CONSOLIDATION :
SAMPLE HEIGHT ..... = 5.875 INCHES
SAMPLE AREA ..... = 6.623 SQ. INCHES
EFFECTIVE CONFINING STRESS . = 4507. PSF
EFFECTIVE MAJOR PRIN. STRESS = 4507. PSF
PRINCIPAL STRESS RATIO ..... = 1.00

STRAIN PCT	SIGMA3E PSF	SIGMA1E PSF	RATIO SIG1E/SIG3E	PPRESS PSF	PBAR PSF	PTOT PSF	Q PSF
.0	4507.	4507.	1.0	0.	4507.	4507.	0.
.0	4118.	5335.	1.3	389.	4727.	5116.	609.
.1	3514.	5685.	1.6	994.	4599.	5593.	1086.
.3	2995.	5705.	1.9	1512.	4350.	5862.	1355.
.5	2621.	5715.	2.2	1886.	4168.	6054.	1547.
.7	2362.	5752.	2.4	2146.	4057.	6203.	1695.
.9	2160.	5824.	2.7	2347.	3992.	6339.	1832.
1.3	1930.	6159.	3.2	2578.	4044.	6622.	2115.
1.5	1872.	6371.	3.4	2635.	4122.	6757.	2250.
1.7	1829.	6597.	3.6	2678.	4213.	6891.	2384.
1.9	1814.	6850.	3.8	2693.	4332.	7025.	2518.
2.3	1800.	7346.	4.1	2707.	4573.	7280.	2773.
2.5	1829.	7617.	4.2	2678.	4723.	7402.	2894.
2.7	1858.	7867.	4.2	2650.	4862.	7512.	3005.
2.9	1886.	8115.	4.3	2621.	5001.	7622.	3114.
3.3	1958.	8602.	4.4	2549.	5280.	7829.	3322.
3.7	2059.	9050.	4.4	2448.	5555.	8003.	3496.
4.1	2174.	9448.	4.3	2333.	5811.	8144.	3637.
4.6	2275.	9828.	4.3	2232.	6051.	8283.	3776.
5.0	2390.	10177.	4.3	2117.	6284.	8401.	3893.
5.5	2534.	10565.	4.2	1973.	6550.	8523.	4015.
6.6	2794.	11240.	4.0	1714.	7017.	8731.	4223.
7.7	3038.	11808.	3.9	1469.	7423.	8892.	4385.
8.8	3269.	12291.	3.8	1238.	7780.	9018.	4511.
10.0	3485.	12779.	3.7	1022.	8132.	9154.	4647.
11.1	3672.	13184.	3.6	835.	8428.	9263.	4756.
13.5	4032.	14002.	3.5	475.	9017.	9492.	4985.
15.0	4219.	14403.	3.4	288.	9311.	9599.	5092.

STATIC TRIAXIAL TEST: S-5
FROG HOLLOW DAM

CONSOLIDATED UNDRAINED TRIAXIAL TEST
WITH PORE PRESSURE MEASUREMENT

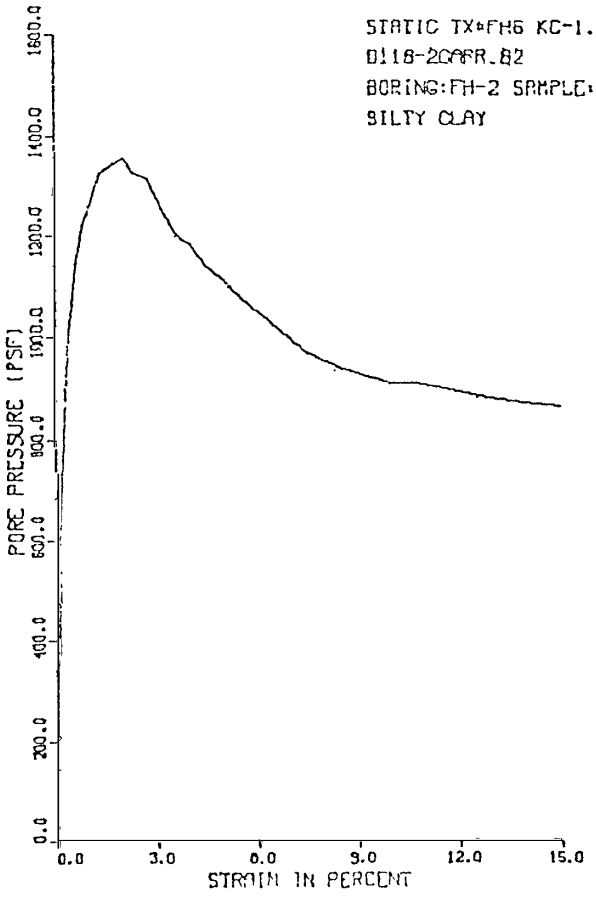

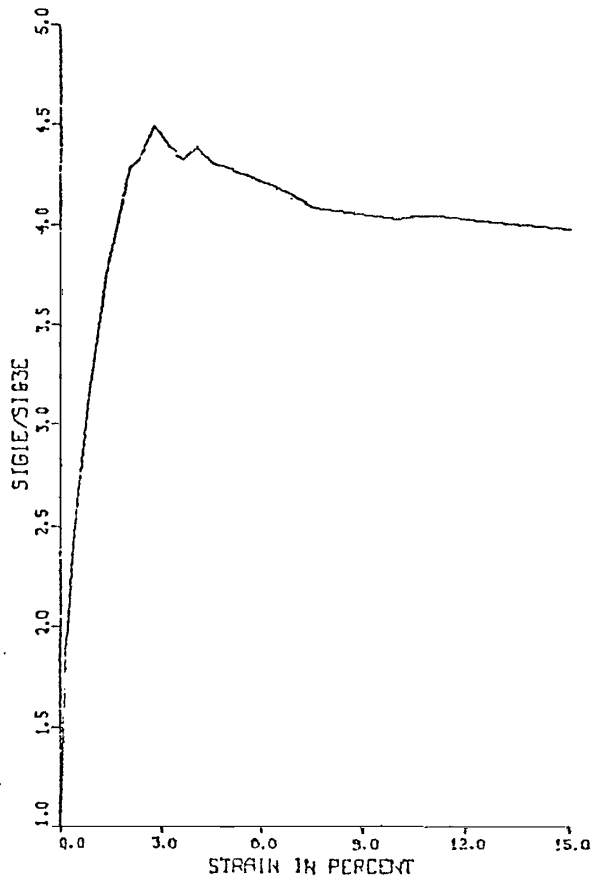

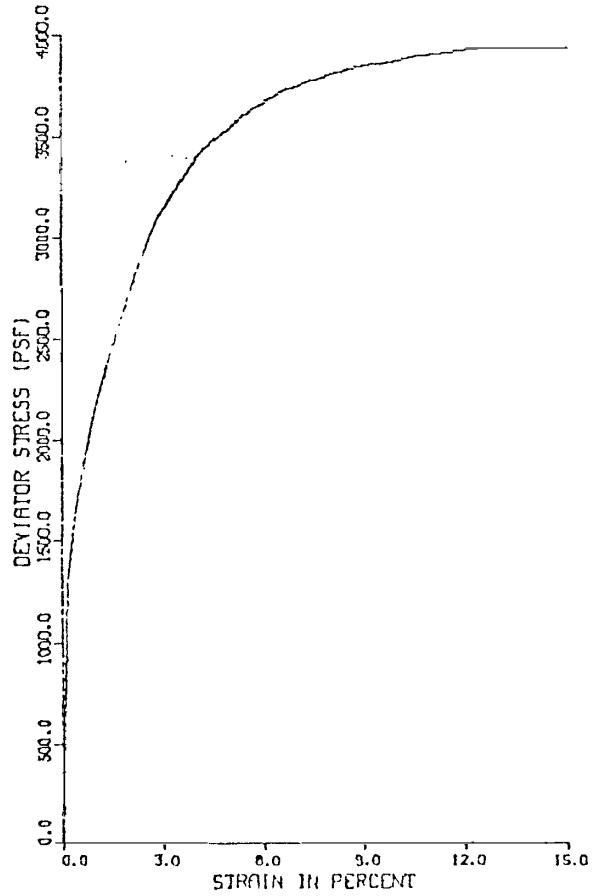

ISOTROPIC CONSOLIDATED UNDRAINED TRIAXIAL TEST
WITH PORE PRESSURE MEASUREMENTS
D118-UTAH DAMS-FROG HOLLOW STATIC TX*FH6 4/20/82 REDUCED BY BW

BORING:FH-2 SAMPLE:PB-7/S-5 DEPTH:27.0-29.5

SILTY CLAY

AT END OF CONSOLIDATION :

SAMPLE HEIGHT	=	5.920 INCHES
SAMPLE AREA	=	6.489 SQ. INCHES
EFFECTIVE CONFINING STRESS .	=	2189. PSF
EFFECTIVE MAJOR PRIN. STRESS	=	2189. PSF
PRINCIPAL STRESS RATIO	=	1.00

STRAIN PCT	SIGMA3E PSF	SIGMA1E PSF	RATIO SIG1E/SIG3E	PPRESS PSF	PBAR PSF	PTOT PSF	R PSF
.0	2189.	2189.	1.0	0.	2189.	2189.	0.
.2	1512.	2797.	1.8	677.	2154.	2831.	642.
.4	1181.	2838.	2.4	1008.	2010.	3018.	829.
.6	1037.	2911.	2.8	1152.	1974.	3126.	937.
.9	965.	3011.	3.1	1224.	1988.	3212.	1023.
1.1	922.	3138.	3.4	1267.	2030.	3297.	1108.
1.3	864.	3228.	3.7	1325.	2046.	3371.	1182.
2.1	835.	3574.	4.3	1354.	2205.	3558.	1369.
2.3	864.	3726.	4.3	1325.	2295.	3620.	1431.
2.8	878.	3942.	4.5	1310.	2410.	3721.	1532.
3.2	936.	4115.	4.4	1253.	2525.	3778.	1589.
3.6	994.	4287.	4.3	1195.	2640.	3835.	1647.
4.1	1008.	4414.	4.4	1181.	2711.	3892.	1703.
4.5	1051.	4527.	4.3	1138.	2789.	3927.	1738.
5.0	1080.	4622.	4.3	1109.	2851.	3960.	1771.
5.4	1109.	4718.	4.3	1080.	2913.	3993.	1805.
6.5	1166.	4881.	4.2	1022.	3024.	4046.	1857.
7.6	1224.	4999.	4.1	965.	3111.	4076.	1887.
8.6	1253.	5086.	4.1	936.	3169.	4105.	1917.
10.0	1282.	5156.	4.0	907.	3219.	4126.	1937.
10.7	1282.	5184.	4.0	907.	3233.	4140.	1951.
12.9	1310.	5254.	4.0	878.	3282.	4161.	1972.
15.0	1325.	5267.	4.0	864.	3296.	4160.	1971.

STATIC TRIAXIAL TEST: S-6
FROG HOLLOW DAM

CONSOLIDATED UNDRAINED TRIAXIAL TEST
WITH PORE PRESSURE MEASUREMENT

STATIC TX-7A KC-1.0
D118-20APR.82
BORING:FH-1 SAMPLE:PB-4
SILTY CLAY

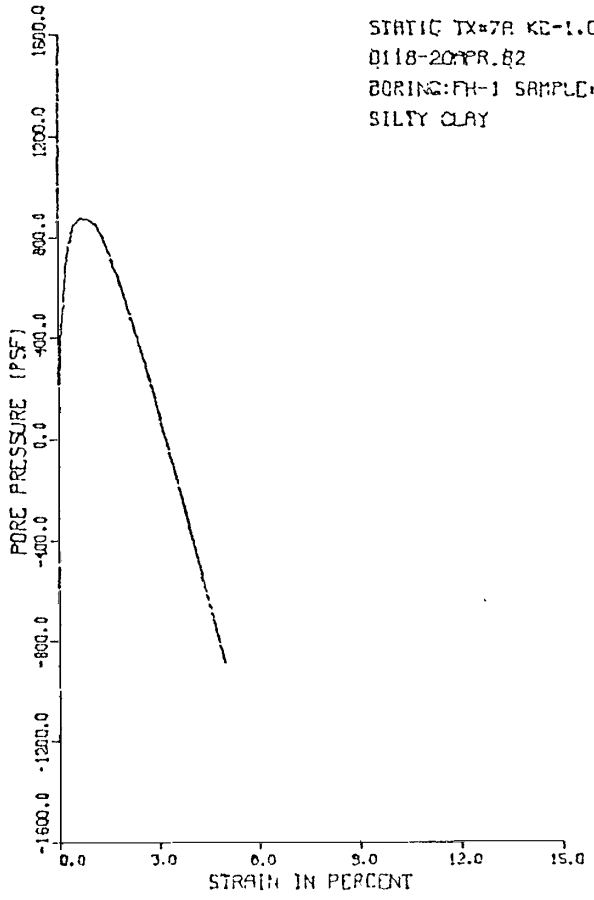

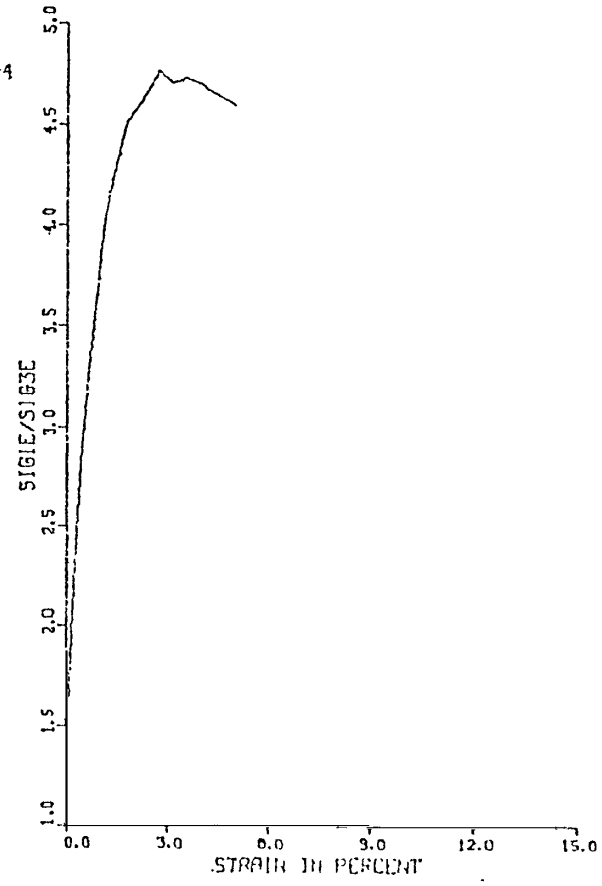

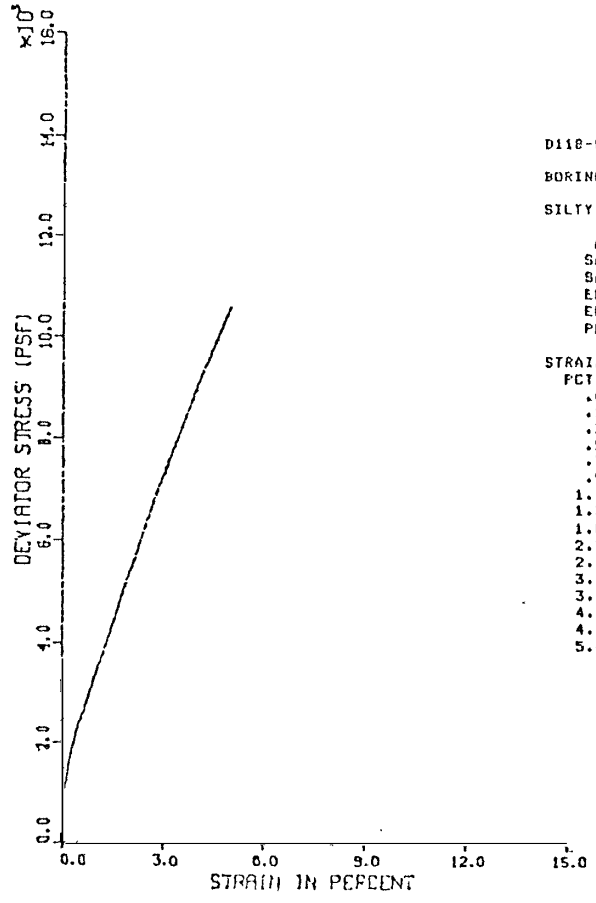

ISOTROPIC CONSOLIDATED UNDRAINED TRIAXIAL TEST
WITH PORE PRESSURE MEASUREMENTS
D118-UTAH DAMS-FROG HOLLOW STATIC TX#FH7A STAGE1 4/20/82 RED. BY BV

BORING:FH-1 SAMPLE:PB-4/S-3 DEPTH:14.5-17.5

SILTY CLAY

AT END OF CONSOLIDATION :

SAMPLE HEIGHT	=	5.957 INCHES
SAMPLE AREA	=	6.453 SQ. INCHES
EFFECTIVE CONFINING STRESS .	=	2045. PSF
EFFECTIVE MAJOR PRIN. STRESS	=	2045. PSF
PRINCIPAL STRESS RATIO	=	1.00

STRAIN PCT	SIGMA3E PSF	SIGMA1E PSF	RATIO SIG1E/SIG3E	PPRESS PSF	PBAR PSF	PTOT PSF	Q PSF
.0	2045.	2045.	1.0	0.	2045.	2045.	0.
.1	1670.	2652.	1.6	374.	2161.	2535.	491.
.3	1325.	3061.	2.3	720.	2193.	2913.	868.
.5	1195.	3461.	2.9	850.	2328.	3178.	1133.
.7	1166.	3849.	3.3	878.	2508.	3386.	1341.
.9	1181.	4300.	3.6	864.	2740.	3604.	1559.
1.1	1195.	4770.	4.0	850.	2983.	3832.	1788.
1.3	1253.	5282.	4.2	792.	3267.	4059.	2015.
1.8	1411.	6364.	4.5	634.	3888.	4521.	2476.
2.3	1613.	7458.	4.6	432.	4536.	4968.	2923.
2.7	1800.	8572.	4.8	245.	5186.	5431.	3386.
3.1	2016.	9495.	4.7	29.	5755.	5784.	3739.
3.6	2203.	10424.	4.7	-158.	6314.	6155.	4111.
4.0	2419.	11376.	4.7	-374.	6898.	6523.	4478.
4.4	2635.	12278.	4.7	-590.	7457.	6866.	4821.
5.0	2938.	13516.	4.6	-893.	8227.	7334.	5289.

STATIC TRIAXIAL TEST: S-7A
FROG HOLLOW DAM

CONSOLIDATED UNDRAINED TRIAXIAL TEST
WITH PORE PRESSURE MEASUREMENT

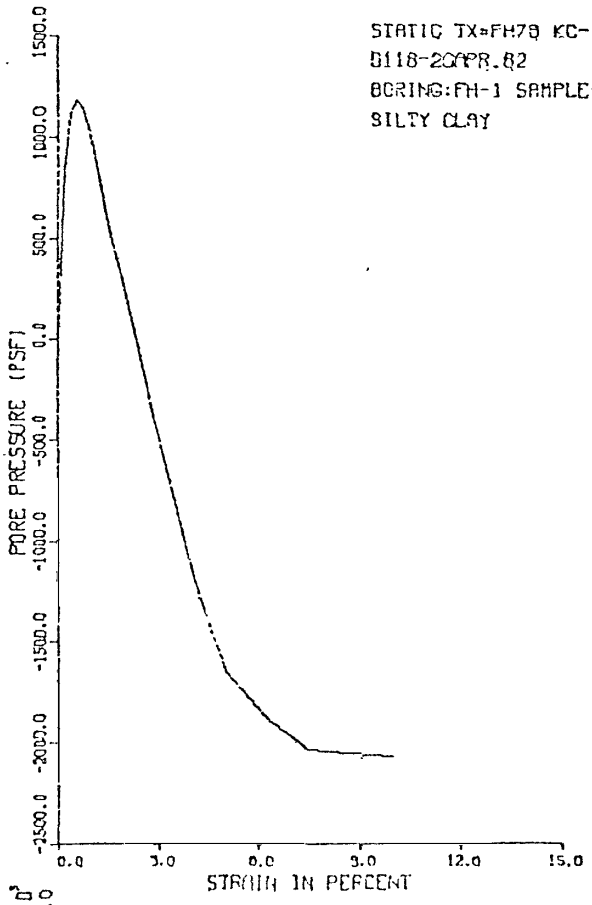

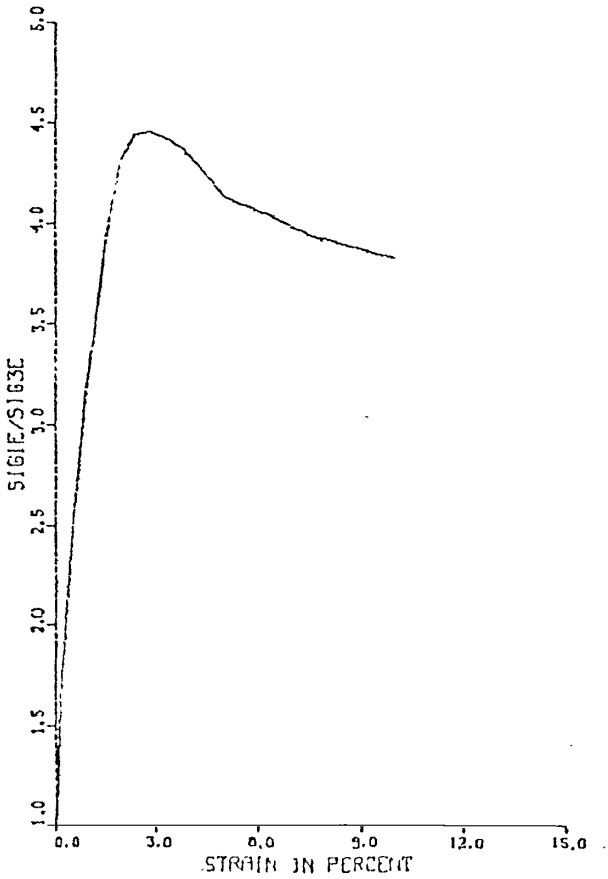

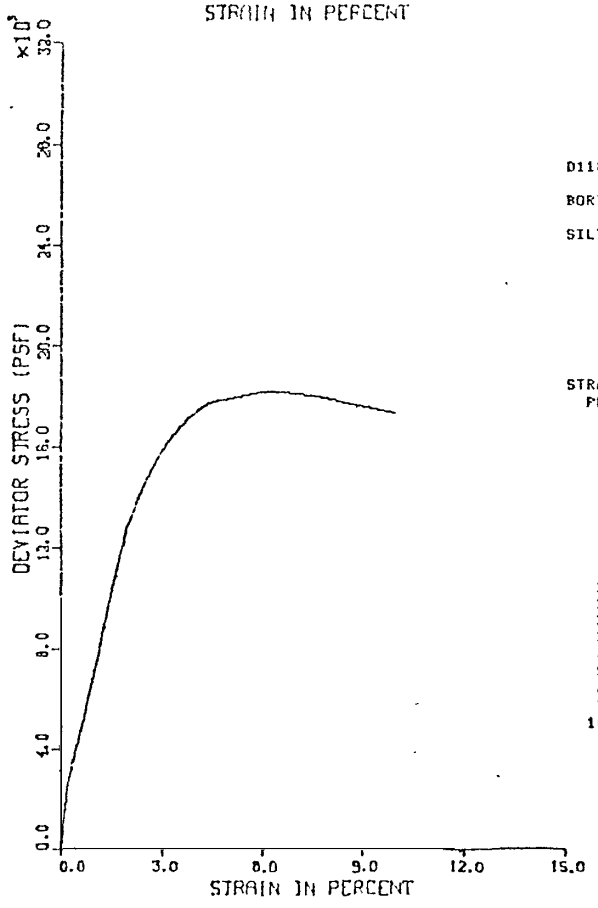

ISOTROPIC CONSOLIDATED UNDRAINED TRIAXIAL TEST
WITH PORE PRESSURE MEASUREMENTS
D118-UTAH DAMS-FROG HOLLOW STATIC TX#FH7B STAGE2 4/20/82 RED.BY BW

BORING:FH-1 SAMPLE:PB-4/S-3 DEPTH:14.5-17.5

SILTY CLAY

AT END OF CONSOLIDATION :
SAMPLE HEIGHT ..... = 5.756 INCHES
SAMPLE AREA ..... = 6.611 SQ. INCHES
EFFECTIVE CONFINING STRESS . = 4090. PSF
EFFECTIVE MAJOR PRIN. STRESS = 4090. PSF
PRINCIPAL STRESS RATIO ..... = 1.00

STRAIN PCT	SIGMA3E PSF	SIGMA1E PSF	RATIO SIG1E/SIG3E	PPRESS PSF	PBAR PSF	PTOT PSF	Q PSF
.0	4090.	4090.	1.0	0.	4090.	4090.	0.
.1	3730.	4926.	1.3	360.	4328.	4688.	598.
.2	3254.	5667.	1.7	835.	4461.	5296.	1206.
.4	2981.	6453.	2.2	1109.	4717.	5826.	1736.
.5	2909.	7393.	2.5	1181.	5151.	6332.	2242.
.7	2952.	8444.	2.9	1138.	5698.	6835.	2746.
.9	3053.	9635.	3.2	1037.	6344.	7381.	3291.
1.1	3211.	10965.	3.4	878.	7088.	7967.	3877.
1.5	3542.	13861.	3.9	547.	8702.	9249.	5159.
1.9	3830.	16454.	4.3	259.	10142.	10401.	6312.
2.4	4147.	18414.	4.4	-58.	11280.	11223.	7133.
2.8	4478.	19947.	4.5	-389.	12213.	11824.	7734.
3.3	4795.	21200.	4.4	-706.	12998.	12292.	8203.
3.8	5098.	22239.	4.4	-1008.	13668.	12660.	8571.
4.3	5386.	23024.	4.3	-1296.	14205.	12909.	8819.
5.0	5746.	23684.	4.1	-1656.	14715.	13059.	8969.
6.2	5976.	24151.	4.0	-1886.	15064.	13177.	9088.
7.5	6134.	24149.	3.9	-2045.	15142.	13097.	9007.
10.0	6163.	23534.	3.8	-2074.	14849.	12775.	8685.

STATIC TRIAXIAL TEST: S-7B
FROG HOLLOW DAM

CONSOLIDATED UNDRAINED TRIAXIAL TEST
WITH PORE PRESSURE MEASUREMENT

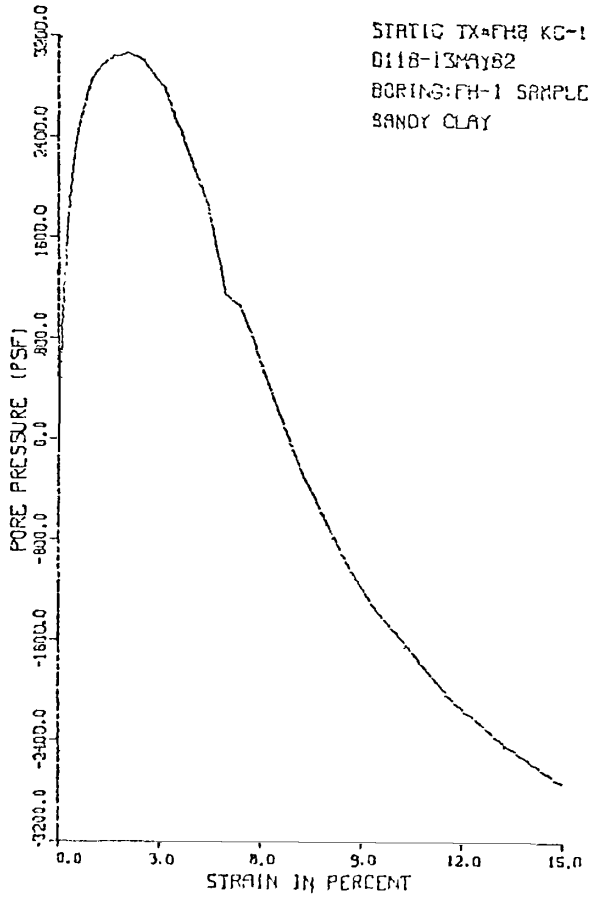

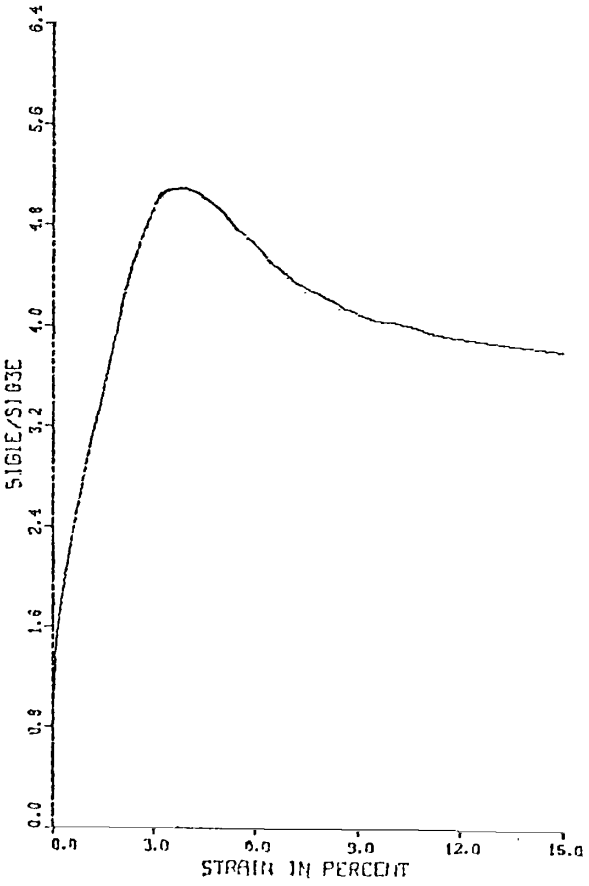

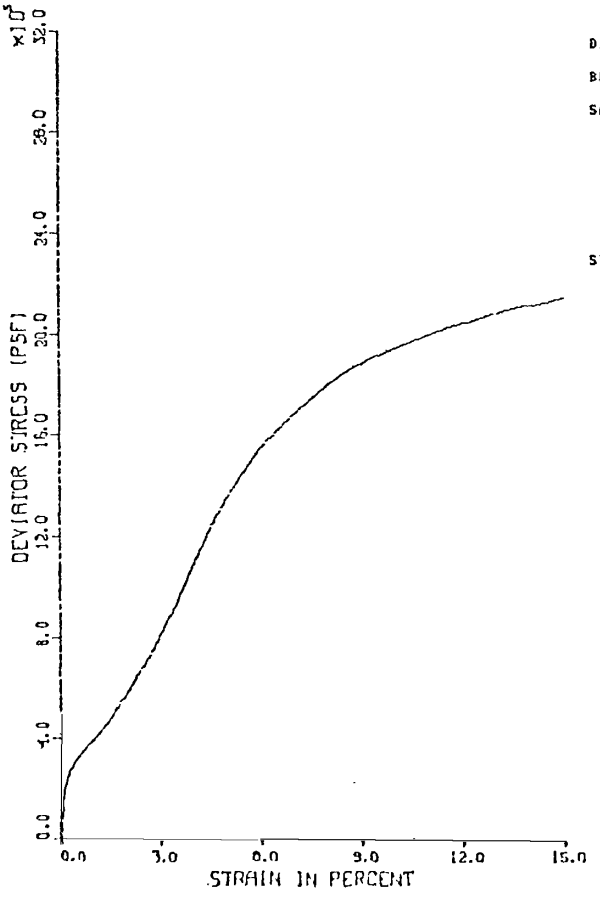

ISOTROPIC CONSOLIDATED UNDRAINED TRIAXIAL TEST
WITH PORE PRESSURE MEASUREMENTS
D118-UTAH DAMS-FROG HOLLOW STATIC TX#FH8 5/13/82 REDUCED BY BW

BORING:FH-1 SAMPLE:PB-12/S-11 DEPTH:46.0-48.5

SANDY CLAY

AT END OF CONSOLIDATION :
SAMPLE HEIGHT ..... = 5.897 INCHES
SAMPLE AREA ..... = 6.423 SQ. INCHES
EFFECTIVE CONFINING STRESS . = 4896. PSF
EFFECTIVE MAJOR PRIN. STRESS = 4896. PSF
PRINCIPAL STRESS RATIO ..... = 1.00

STRAIN PCT	SIGMA3E PSF	SIGMA1E PSF	RATIO SIG1E/SIG3E	PPRESS PSF	PBAR PSF	PTOT PSF	Q PSF
.0	4896.	4896.	1.0	0.	4896.	4896.	0.
.1	4061.	5920.	1.5	835.	4990.	5825.	929.
.3	3298.	5892.	1.8	1598.	4595.	6193.	1297.
.4	2822.	5815.	2.1	2074.	4319.	6392.	1496.
.6	2520.	5775.	2.3	2376.	4148.	6524.	1628.
.7	2318.	5813.	2.5	2578.	4066.	6644.	1748.
.9	2189.	5901.	2.7	2707.	4045.	6752.	1856.
1.0	2059.	5987.	2.9	2837.	4023.	6860.	1964.
1.2	1987.	6153.	3.1	2909.	4070.	6979.	2083.
1.3	1930.	6332.	3.3	2966.	4131.	7097.	2201.
1.5	1901.	6562.	3.5	2995.	4231.	7226.	2330.
1.7	1872.	6942.	3.7	3024.	4407.	7431.	2535.
2.1	1829.	7754.	4.2	3067.	4792.	7859.	2963.
2.3	1858.	8273.	4.5	3038.	5065.	8104.	3208.
2.6	1901.	8826.	4.6	2995.	5364.	8359.	3463.
2.8	1973.	9449.	4.8	2923.	5711.	8634.	3738.
3.2	2117.	10690.	5.1	2779.	6403.	9183.	4287.
3.5	2333.	11531.	4.9	2563.	6932.	9495.	4599.
3.7	2477.	12450.	5.0	2419.	7463.	9883.	4987.
4.1	2765.	13880.	5.0	2131.	8322.	10454.	5558.
4.5	3053.	15258.	5.0	1843.	9155.	10998.	6102.
5.0	3758.	17219.	4.6	1138.	10489.	11626.	6730.
5.4	3830.	18227.	4.8	1066.	11029.	12094.	7198.
5.9	4176.	19493.	4.7	720.	11835.	12555.	7659.
6.5	4608.	20694.	4.5	288.	12651.	12939.	8043.
7.2	5155.	22312.	4.3	-259.	13734.	13474.	8578.
8.0	5887.	23608.	4.2	-691.	14598.	13907.	9011.
8.7	5910.	24491.	4.1	-1022.	15205.	14182.	9286.
9.4	6221.	25284.	4.1	-1325.	15752.	14427.	9531.
10.0	6437.	25929.	4.0	-1541.	16183.	14642.	9746.
11.6	6955.	27264.	3.9	-2059.	17110.	15050.	10154.
13.3	7330.	28308.	3.9	-2434.	17819.	15385.	10489.
15.0	7646.	29123.	3.8	-2750.	18385.	15634.	10738.

STATIC TRIAXIAL TEST: S-8
FROG HOLLOW DAM

IVINS DIVERSION DAM NO. 5

CONSOLIDATED UNDRAINED TRIAXIAL TEST
WITH PORE PRESSURE MEASUREMENT

STATIC TX=IV1 KC=1.0
D118-1APR.82
BORING: IV-3 SAMPLE:PB-1
SILTY SAND

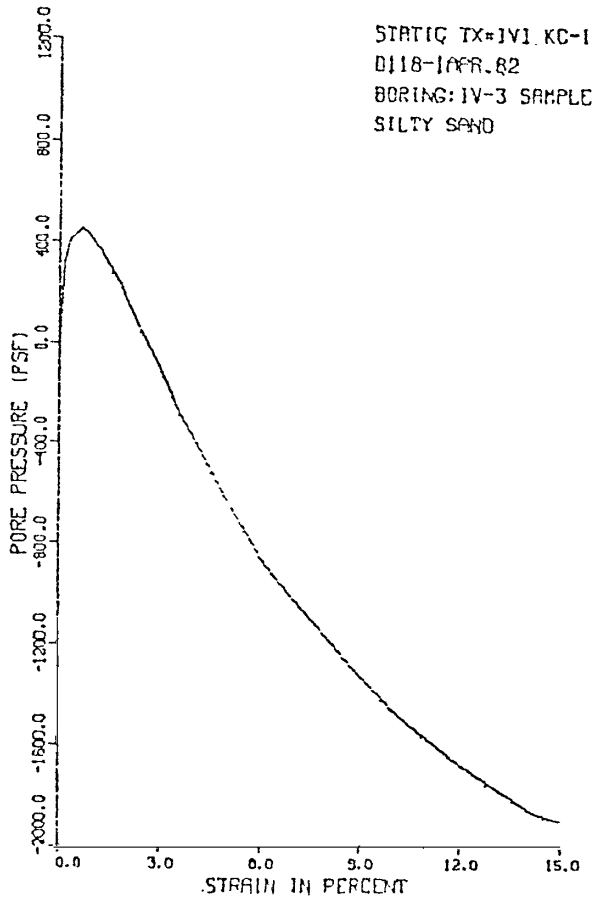

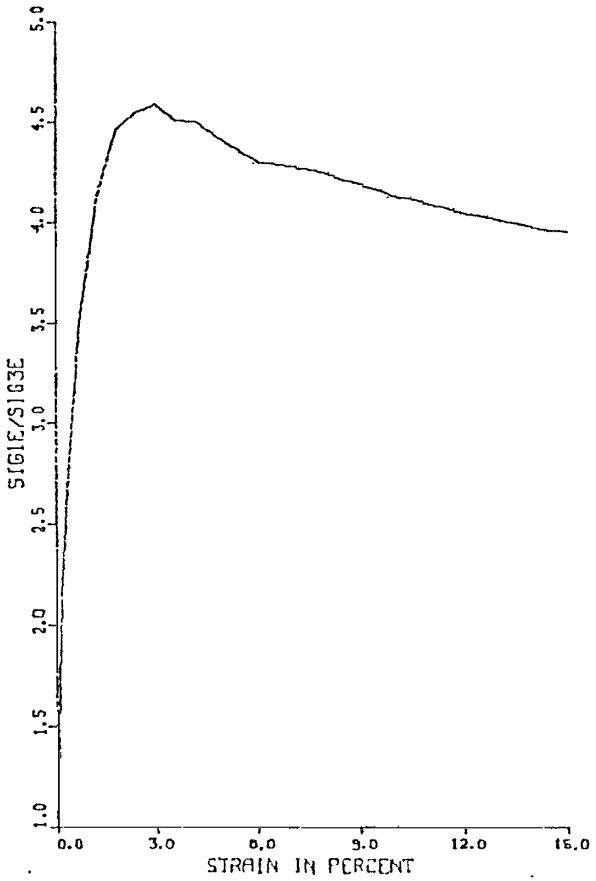

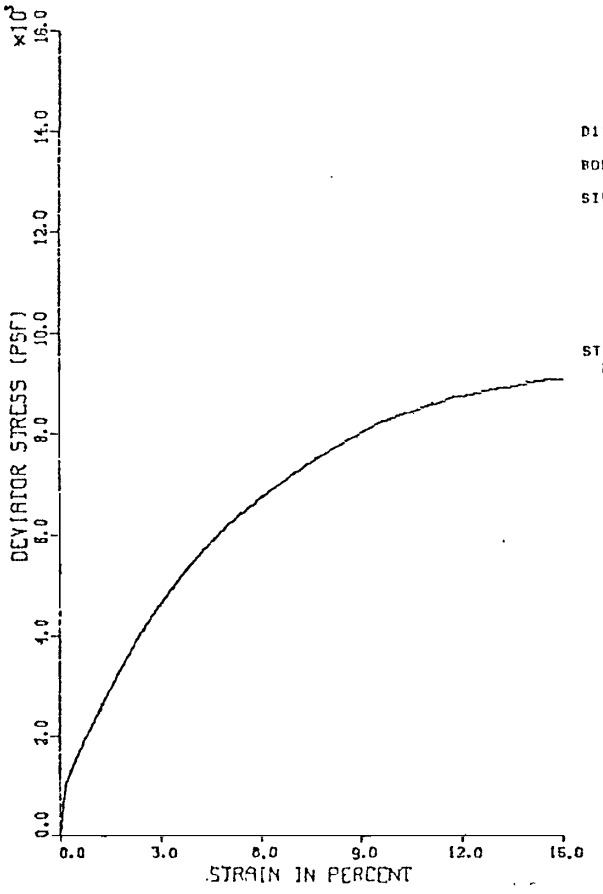

ISOTROPIC CONSOLIDATED UNDRAINED TRIAXIAL TEST
WITH PORE PRESSURE MEASUREMENTS
D118-UTAH DAMS-IVINS DIVERSION STATIC TX#IV1 4/1/82 REDUCED BY BW

BORING:IV-3 SAMPLE:PB-1/S-1 DEPTH:4.0-6.5

SILTY SAND

AT END OF CONSOLIDATION :

SAMPLE HEIGHT	=	5.979 INCHES
SAMPLE AREA	=	6.530 SQ. INCHES
EFFECTIVE CONFINING STRESS .	=	1181. PSF
EFFECTIVE MAJOR PRIN. STRESS	=	1181. PSF
PRINCIPAL STRESS RATIO	=	1.00

STRAIN PCT	SIGMA3E PSF	SIGMA1E PSF	RATIO SIG1E/SIG3E	PPRESS PSF	PBAR PSF	PTOT PSF	Q PSF
.0	1181.	1181.	1.0	0.	1181.	1181.	0.
.2	864.	1855.	2.1	317.	1359.	1676.	495.
.3	778.	2074.	2.7	403.	1426.	1829.	648.
.5	749.	2328.	3.1	432.	1539.	1971.	790.
.7	734.	2574.	3.5	446.	1654.	2101.	920.
.9	763.	2840.	3.7	418.	1801.	2219.	1038.
1.2	821.	3391.	4.1	360.	2106.	2466.	1285.
1.8	950.	4242.	4.5	230.	2596.	2826.	1646.
2.4	1123.	5106.	4.5	58.	3114.	3172.	1991.
3.0	1282.	5882.	4.6	-101.	3582.	3481.	2300.
3.6	1469.	6614.	4.5	-288.	4042.	3754.	2573.
4.2	1613.	7254.	4.5	-432.	4433.	4001.	2821.
5.0	1814.	7994.	4.4	-634.	4904.	4271.	3090.
6.1	2059.	8850.	4.3	-878.	5454.	4576.	3395.
7.0	2203.	9422.	4.3	-1022.	5812.	4790.	3609.
7.7	2304.	9816.	4.3	-1123.	6060.	4937.	3756.
8.6	2448.	10309.	4.2	-1267.	6378.	5111.	3930.
9.5	2578.	10759.	4.2	-1397.	6668.	5272.	4091.
10.0	2650.	10965.	4.1	-1469.	6807.	5339.	4158.
10.6	2722.	11195.	4.1	-1541.	6958.	5418.	4237.
11.8	2851.	11582.	4.1	-1670.	7216.	5546.	4365.
14.3	3053.	12109.	4.0	-1872.	7581.	5709.	4528.
15.0	3082.	12191.	4.0	-1901.	7636.	5736.	4555.

STATIC TRIAXIAL TEST: S-1
IVINS DIVERSION DAM NO. 5

CONSOLIDATED UNDRAINED TRIAXIAL TEST
WITH PORE PRESSURE MEASUREMENT

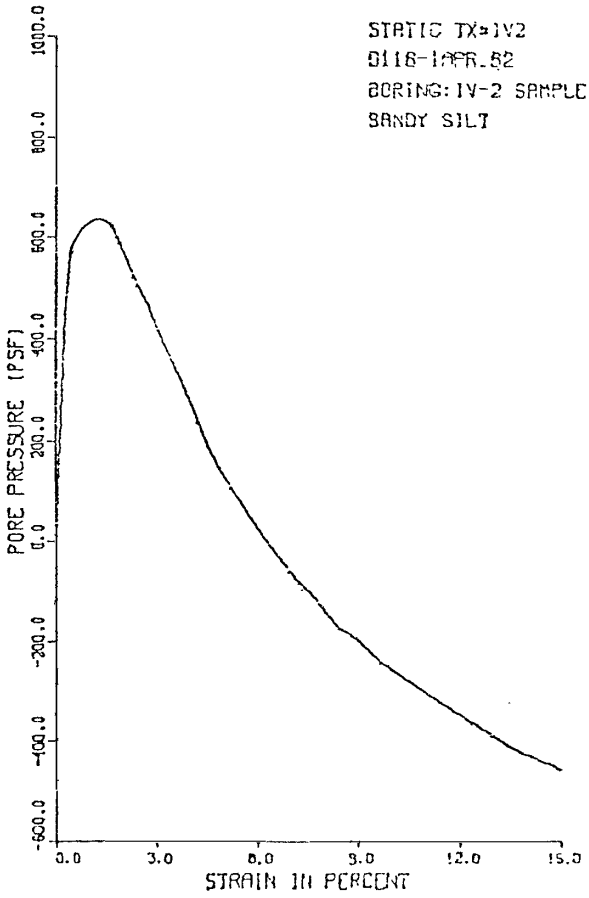

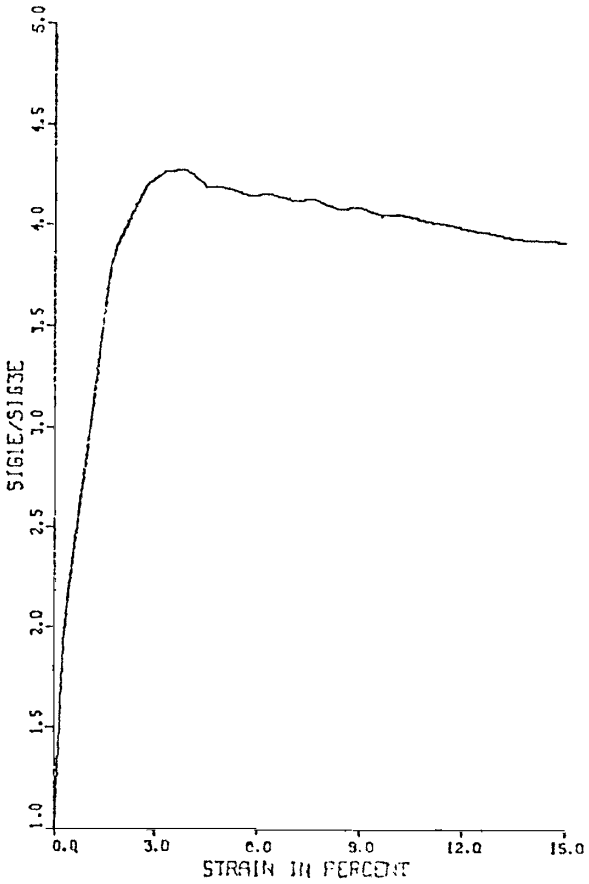

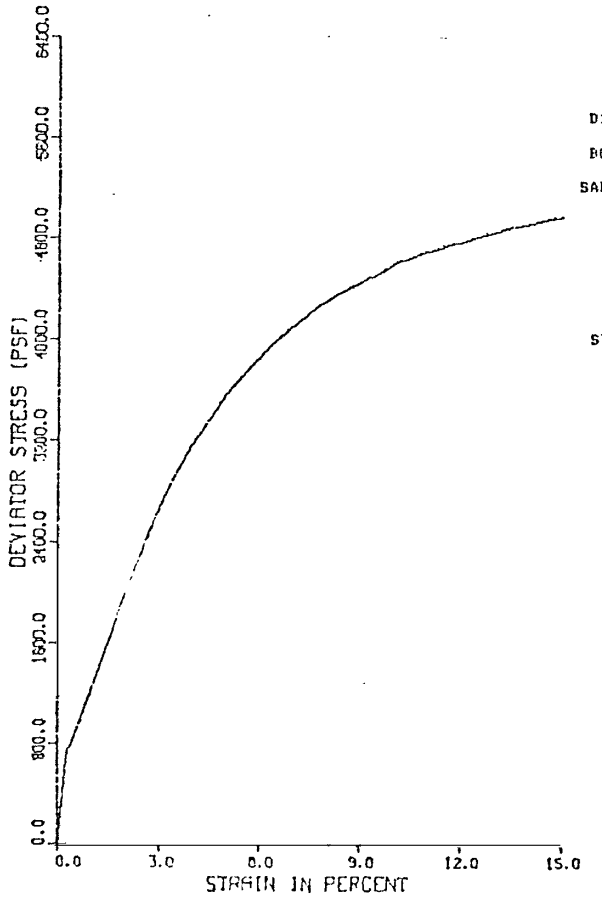

ISOTROPIC CONSOLIDATED UNDRAINED TRIAXIAL TEST
WITH PORE PRESSURE MEASUREMENTS
D118-UTAH DAMS-IVINS DIVERSION STATIC TX=IV2 4/1/82 REDUCED BY BW

BORING:IV-2 SAMPLE:PB-3/S-2 DEPTH:12.0-14.5

SANDY SILT

AT END OF CONSOLIDATION :

SAMPLE HEIGHT	=	5.919 INCHES
SAMPLE AREA	=	6.365 SQ. INCHES
EFFECTIVE CONFINING STRESS .	=	1253. PSF
EFFECTIVE MAJOR PRIN. STRESS	=	1253. PSF
PRINCIPAL STRESS RATIO	=	1.00

STRAIN PCT	SIGMA3E PSF	SIGMA1E PSF	RATIO SIG1E/SIG3E	PPRESS PSF	PBAR PSF	PTDT PSF	Q PSF
.0	1253.	1253.	1.0	0.	1253.	1253.	0.
.3	806.	1551.	1.9	446.	1179.	1625.	372.
.4	691.	1502.	2.2	562.	1097.	1658.	406.
1.7	634.	2391.	3.8	619.	1512.	2131.	879.
1.9	662.	2572.	3.9	590.	1617.	2207.	955.
2.2	720.	2888.	4.0	533.	1804.	2337.	1084.
2.8	792.	3321.	4.2	461.	2057.	2518.	1265.
3.4	878.	3743.	4.3	374.	2311.	2685.	1432.
3.9	965.	4116.	4.3	288.	2540.	2828.	1576.
4.6	1066.	4456.	4.2	187.	2761.	2948.	1695.
5.0	1123.	4691.	4.2	130.	2907.	3037.	1784.
5.8	1210.	5003.	4.1	43.	3106.	3149.	1896.
6.4	1267.	5246.	4.1	-14.	3257.	3242.	1990.
7.1	1325.	5445.	4.1	-72.	3385.	3313.	2060.
7.7	1368.	5627.	4.1	-115.	3497.	3382.	2129.
8.4	1426.	5799.	4.1	-173.	3612.	3440.	2187.
9.0	1454.	5920.	4.1	-202.	3687.	3486.	2233.
9.7	1498.	6053.	4.0	-245.	3776.	3531.	2278.
10.0	1512.	6114.	4.0	-259.	3813.	3554.	2301.
11.2	1570.	6289.	4.0	-317.	3929.	3612.	2360.
13.5	1670.	6561.	3.9	-418.	4116.	3698.	2446.
15.0	1714.	6694.	3.9	-461.	4204.	3743.	2490.

STATIC TRIAXIAL TEST: S-2
IVINS DIVERSION DAM NO. 5

CONSOLIDATED UNDRAINED TRIAXIAL TEST
WITH PORE PRESSURE MEASUREMENT

STATIC TX=IV3A KC=1.0
D118-28APR_82
BORING: IV-1 SAMPLE:PB-1
SILTY SAND

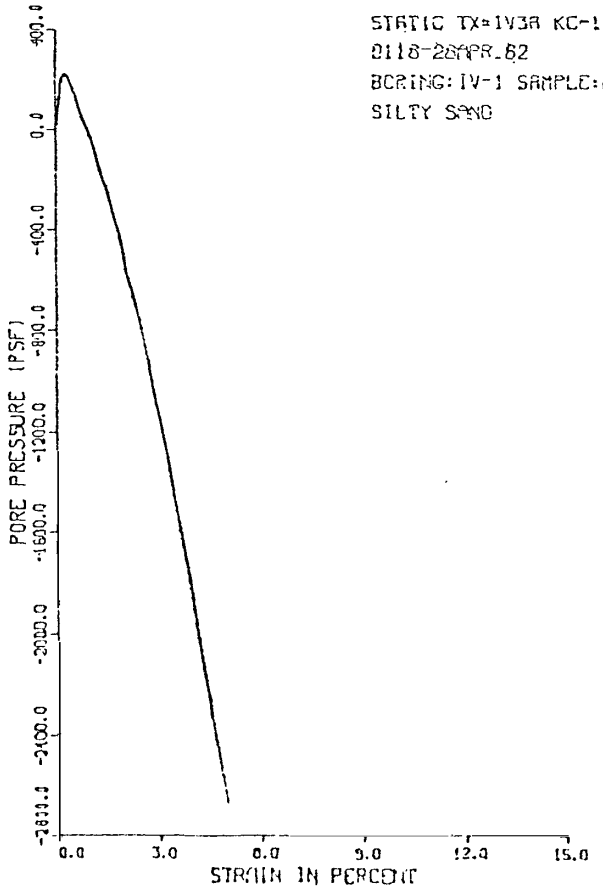

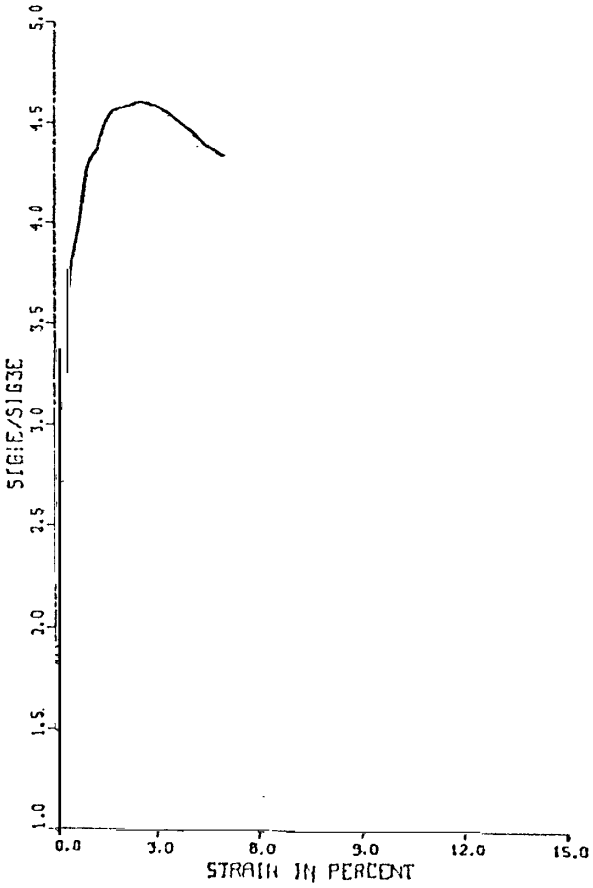

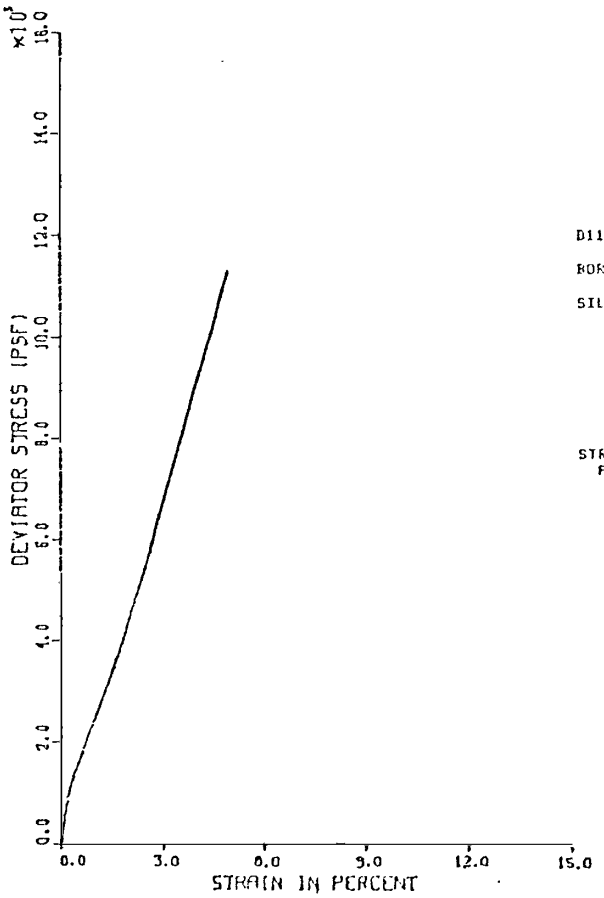

ISOTROPIC CONSOLIDATED UNDRAINED TRIAXIAL TEST
WITH PORE PRESSURE MEASUREMENTS
D118-UTAH DAMS-IVINS DIVERSION STATIC TX#IV3A STAGE1 4/28/82 RED. BY BW

BORING:IV-1 SAMPLE:PB-1/S-1 DEPTH:4.0-6.5

SILTY SAND

AT END OF CONSOLIDATION :
SAMPLE HEIGHT ..... = 6.059 INCHES
SAMPLE AREA ..... = 6.542 SQ. INCHES
EFFECTIVE CONFINING STRESS . = 720. PSF
EFFECTIVE MAJOR PRIN. STRESS = 720. PSF
PRINCIPAL STRESS RATIO ..... = 1.00

STRAIN PCT	SIGMA3E PSF	SIGMA1E PSF	RATIO SIG1E/SIG3E	PPRESS PSF	PBAR PSF	PTOT PSF	Q PSF
.0	720.	720.	1.0	0.	720.	720.	0.
.1	562.	1221.	2.2	158.	891.	1050.	330.
.3	490.	1521.	3.1	230.	1006.	1236.	516.
.4	518.	1834.	3.5	202.	1176.	1378.	658.
.5	562.	2138.	3.8	158.	1350.	1508.	788.
.8	677.	2708.	4.0	43.	1692.	1736.	1016.
1.0	749.	3232.	4.3	-29.	1991.	1962.	1242.
1.3	878.	3833.	4.4	-158.	2356.	2198.	1478.
1.5	979.	4425.	4.5	-259.	2702.	2443.	1723.
1.8	1109.	5064.	4.6	-389.	3086.	2698.	1978.
2.1	1282.	5787.	4.5	-562.	3534.	2973.	2253.
2.5	1512.	6964.	4.6	-792.	4238.	3446.	2726.
3.1	1944.	8894.	4.6	-1224.	5419.	4195.	3475.
3.8	2434.	10924.	4.5	-1714.	6679.	4965.	4245.
4.5	2966.	13018.	4.4	-2246.	7992.	5746.	5026.
5.0	3398.	14711.	4.3	-2678.	9055.	6376.	5656.

STATIC TRIAXIAL TEST: S-3A
IVINS DIVERSION DAM NO. 5

CONSOLIDATED UNDRAINED TRIAXIAL TEST
WITH PORE PRESSURE MEASUREMENT

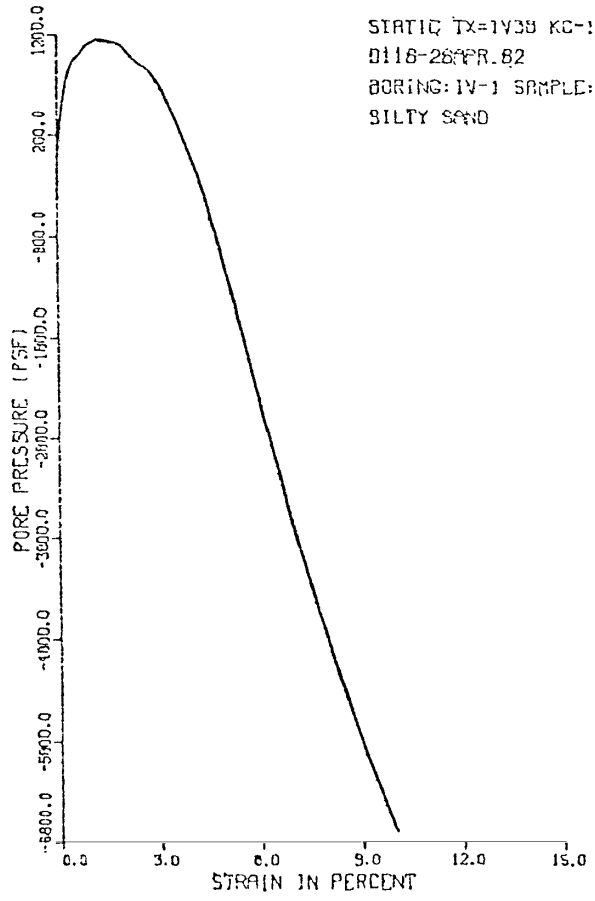

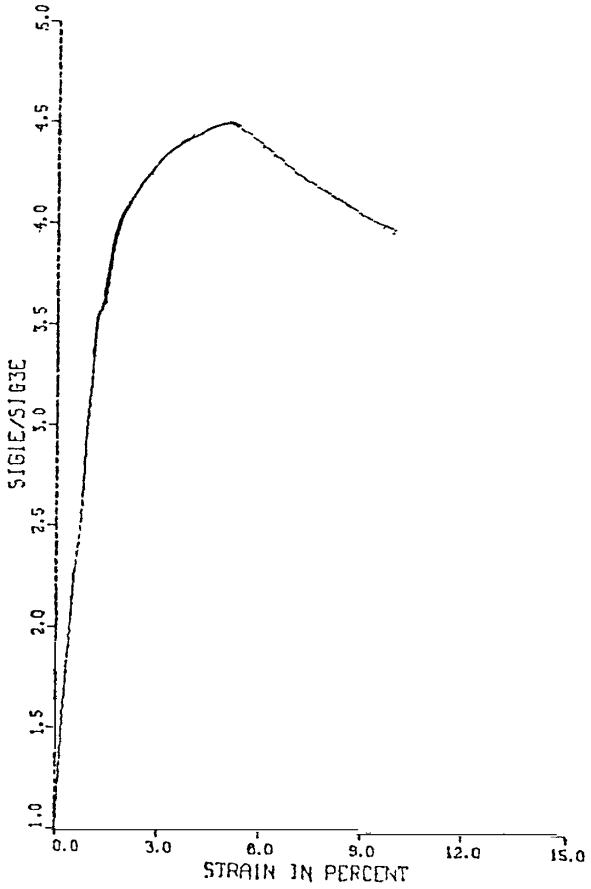

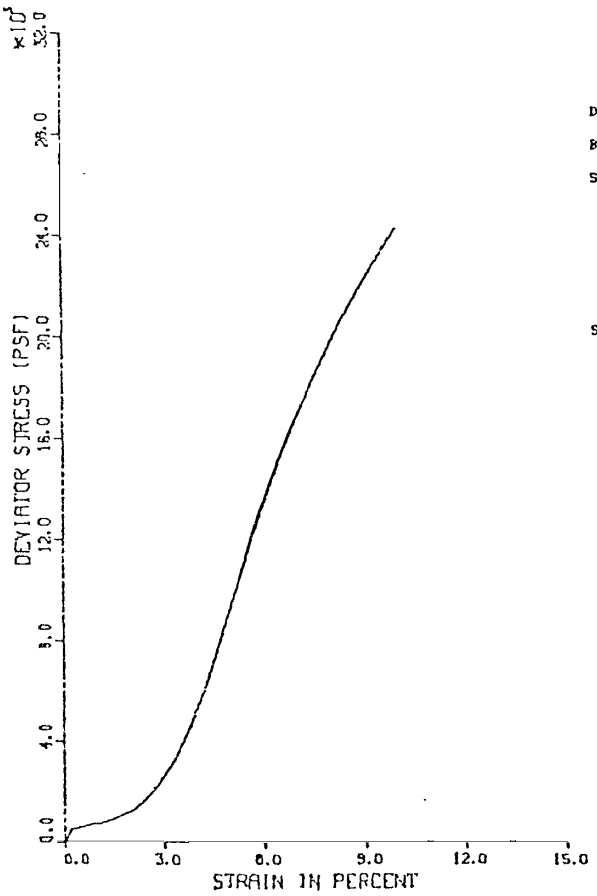

ISOTROPIC CONSOLIDATED UNDRAINED TRIAXIAL TEST
WITH PORE PRESSURE MEASUREMENTS
D118-UTAH DAMS-IVINS DIVERSION STATIC TX#IV3B STAGE2 4/28/82 RED BY BW

BORING:IV-1 SAMPLE:PB-1/S-1 DEPTH:4.0-6.5

SILTY SAND

AT END OF CONSOLIDATION :
SAMPLE HEIGHT ..... = 6.052 INCHES
SAMPLE AREA ..... = 6.547 SQ. INCHES
EFFECTIVE CONFINING STRESS . = 1440. PSF
EFFECTIVE MAJOR PRIN. STRESS = 1440. PSF
PRINCIPAL STRESS RATIO ..... = 1.00

STRAIN PCT	SIGMA3E PSF	SIGMA1E PSF	RATIO SIGIE/SIG3E	PPRESS PSF	PBAR PSF	PTOT PSF	R PSF
.0	1440.	1440.	1.0	0.	1440.	1440.	0.
.2	835.	1296.	1.6	605.	1066.	1671.	231.
.4	590.	1138.	1.9	850.	864.	1714.	274.
.5	475.	1066.	2.2	965.	771.	1735.	295.
.7	432.	1065.	2.5	1008.	749.	1757.	317.
.9	346.	1021.	3.0	1094.	684.	1778.	338.
1.1	317.	1035.	3.3	1123.	676.	1799.	359.
1.2	302.	1084.	3.6	1138.	693.	1831.	391.
1.4	331.	1177.	3.6	1109.	754.	1863.	423.
1.9	360.	1503.	4.2	1080.	932.	2012.	572.
2.3	490.	1908.	3.9	950.	1199.	2149.	709.
2.8	619.	2715.	4.4	821.	1667.	2488.	1048.
3.3	893.	3956.	4.4	547.	2424.	2971.	1531.
3.8	1310.	5754.	4.4	130.	3532.	3662.	2222.
4.3	1757.	7966.	4.5	-317.	4861.	4545.	3105.
4.8	2333.	10604.	4.5	-893.	6468.	5575.	4135.
5.0	2578.	11667.	4.5	-1138.	7122.	5985.	4545.
5.7	3528.	15679.	4.4	-2088.	9604.	7516.	6076.
6.6	4594.	19903.	4.3	-3154.	12249.	9095.	7655.
7.4	5630.	23731.	4.2	-4190.	14681.	10491.	9051.
8.3	6581.	27114.	4.1	-5141.	16848.	11707.	10267.
9.2	7459.	30072.	4.0	-6019.	18766.	12746.	11306.
10.0	8150.	32420.	4.0	-6710.	20285.	13575.	12135.

STATIC TRIAXIAL TEST: S-3B
IVINS DIVERSION DAM NO. 5

CONSOLIDATED UNDRAINED TRIAXIAL TEST
WITH PORE PRESSURE MEASUREMENT

STATIC TX-IV4A KC-1.0
D118-28?FR.82
BORING: IV-5 SAMPLE:PB-4
SILTY SAND

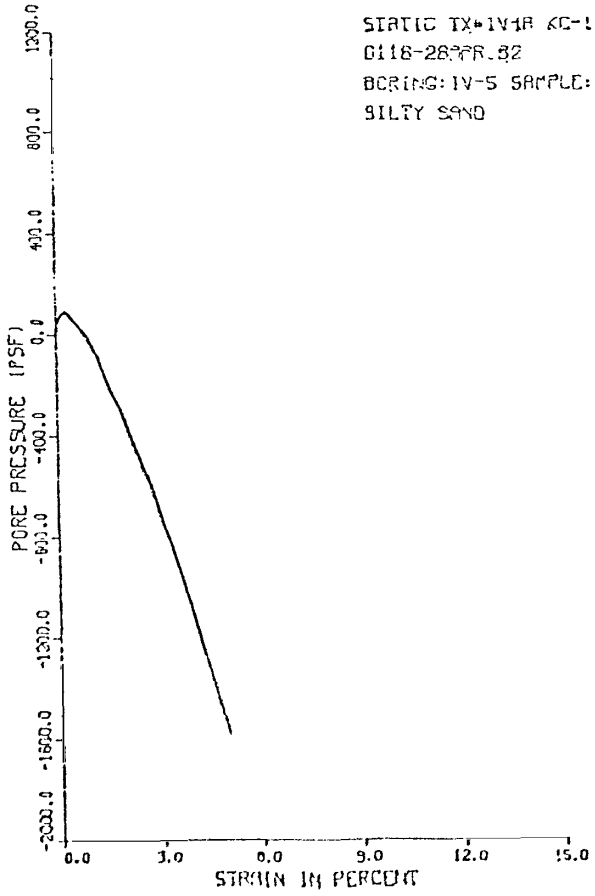

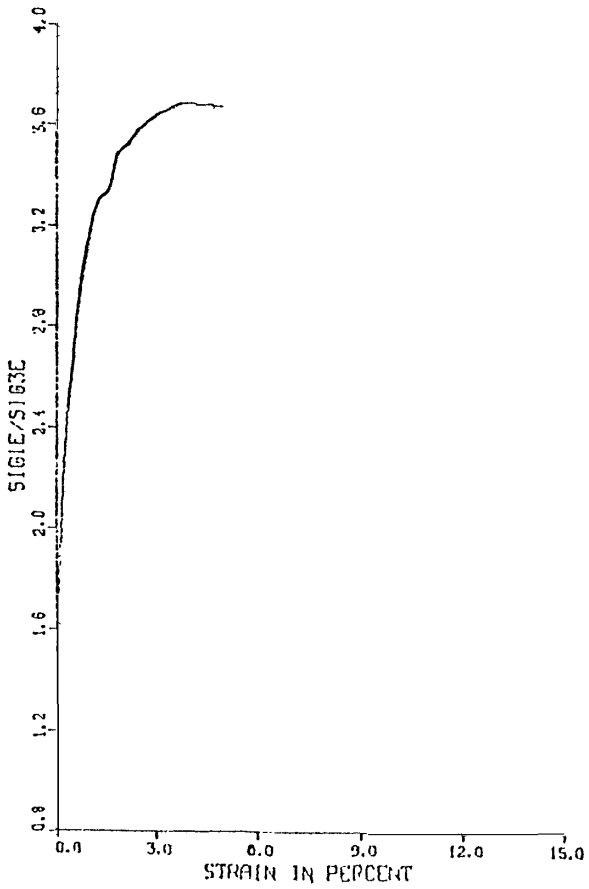

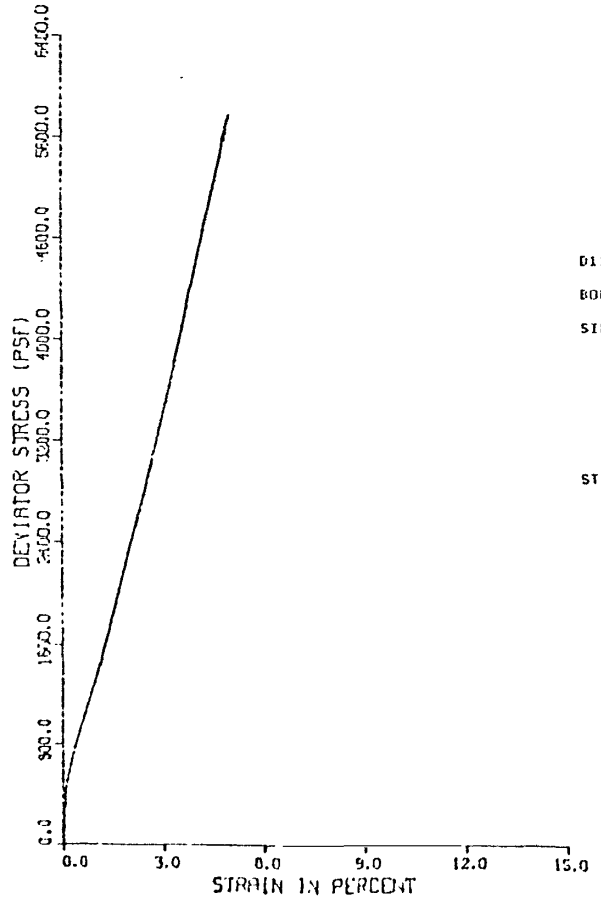

ISOTROPIC CONSOLIDATED UNDRAINED TRIAXIAL TEST
WITH PORE PRESSURE MEASUREMENTS
D118-UTAH DAMS-IVINS DIVERSION STATIC TX#IV4A STAGE1 4/28/82 RED. BY BW

BORING:IV-5 SAMPLE:PB-4/S-2 DEPTH:19.0-21.0

SILTY SAND

AT END OF CONSOLIDATION :
SAMPLE HEIGHT ..... = 5.929 INCHES
SAMPLE AREA ..... = 6.299 SQ. INCHES
EFFECTIVE CONFINING STRESS . = 576. PSF
EFFECTIVE MAJOR PRIN. STRESS = 576. PSF
PRINCIPAL STRESS RATIO ..... = 1.00

STRAIN PCT	SIGMA3E PSF	SIGMA1E PSF	RATIO SIG1E/SIG3E	PPRESS PSF	PBAR PSF	PTOT PSF	Q PSF
.0	576.	576.	1.0	0.	576.	576.	0.
.1	518.	930.	1.8	58.	724.	782.	206.
.2	490.	1105.	2.3	86.	798.	884.	308.
.4	504.	1256.	2.5	72.	880.	952.	376.
.6	547.	1569.	2.9	29.	1058.	1087.	511.
.9	605.	1896.	3.1	-29.	1250.	1221.	645.
1.2	677.	2235.	3.3	-101.	1456.	1355.	779.
1.5	792.	2638.	3.3	-216.	1715.	1499.	923.
1.8	864.	3018.	3.5	-288.	1941.	1653.	1077.
2.1	979.	3440.	3.5	-403.	2210.	1806.	1230.
2.4	1066.	3810.	3.6	-490.	2438.	1948.	1372.
3.2	1354.	4940.	3.6	-778.	3147.	2369.	1793.
3.9	1685.	6208.	3.7	-1109.	3947.	2838.	2262.
5.0	2160.	7937.	3.7	-1584.	5048.	3464.	2888.

STATIC TRIAXIAL TEST: S-4A
IVINS DIVERSION DAM NO. 5

CONSOLIDATED UNDRAINED TRIAXIAL TEST
WITH PORE PRESSURE MEASUREMENT

STATIC TX=IV43 KC-1.0
0118-28APR.82
BORING: IV-5 SAMPLE:PB-4
SILTY SAND

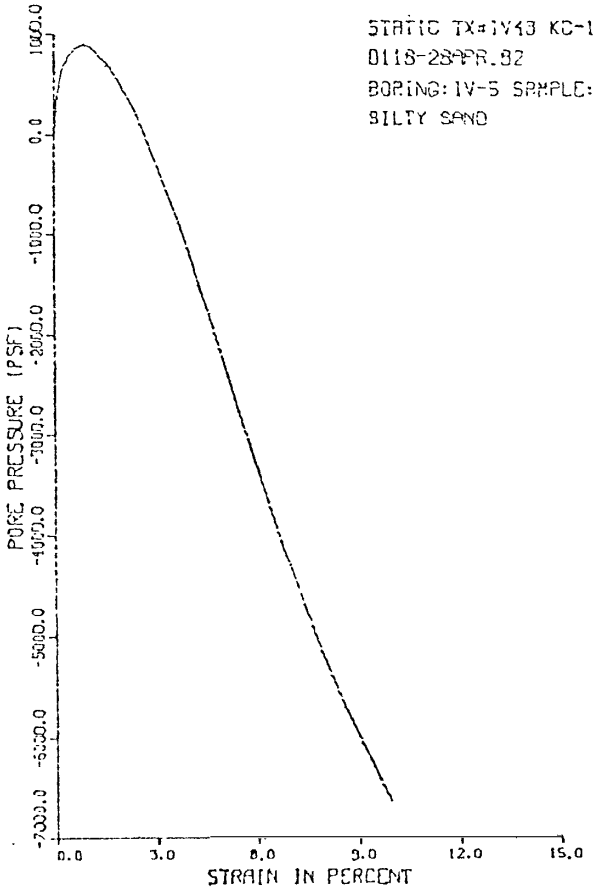

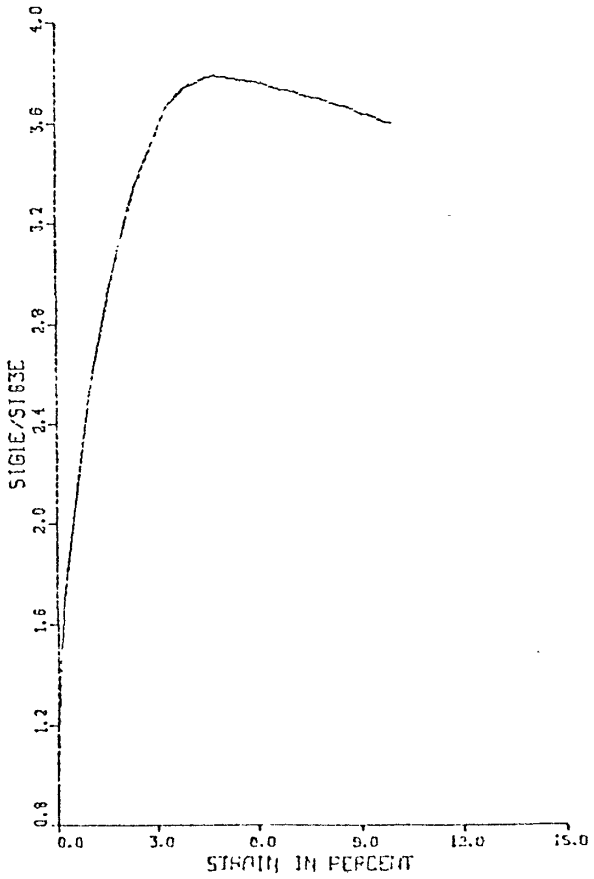

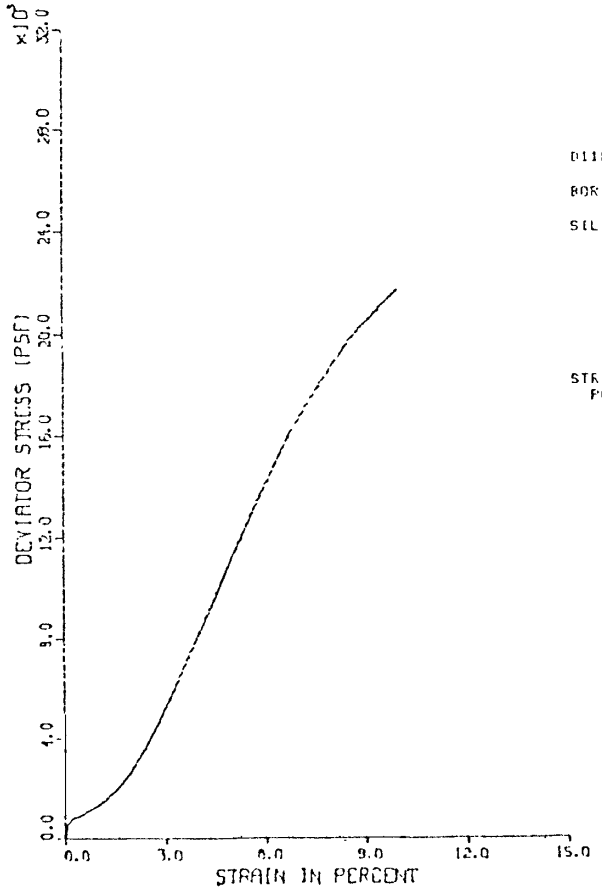

ISOTROPIC CONSOLIDATED UNDRAINED TRIAXIAL TEST
WITH PORE PRESSURE MEASUREMENTS
0118-UTAH DAMS-IVINS DIVERSION STATIC TXIIV4B STAGE2 4/28/82 REV. BY PI

BORING:IV-5 SAMPLE:PB-4/S-2 DEPTH:19.0-21.0

SILTY SAND

AT END OF CONSOLIDATION :
SAMPLE HEIGHT ..... = 5.831 INCHES
SAMPLE AREA ..... = 6.372 SQ. INCHES
EFFECTIVE CONFINING STRESS . = 1728. PSF
EFFECTIVE MAJOR PRIN. STRESS = 1728. PSF
PRINCIPAL STRESS RATIO ..... = 1.00

STRAIN PCT	SIGMA3E PSF	SIGMA1E PSF	RATIO SIG1E/SIG3E	PRESS PSF	PBAR PSF	PTOT PSF	Q PSF
.0	1728.	1728.	1.0	0.	1728.	1728.	0.
.1	1411.	1931.	1.4	317.	1671.	1988.	260.
.2	1109.	1875.	1.7	619.	1492.	2111.	383.
.4	965.	1843.	1.9	763.	1404.	2167.	439.
.6	893.	1801.	2.1	835.	1387.	2222.	474.
.9	835.	2067.	2.5	893.	1451.	2344.	616.
1.1	864.	2250.	2.6	864.	1557.	2421.	693.
1.3	907.	2469.	2.7	821.	1688.	2509.	781.
1.6	1022.	3002.	2.9	706.	2012.	2718.	990.
1.9	1181.	3664.	3.1	547.	2422.	2970.	1242.
2.4	1483.	4970.	3.4	245.	3226.	3471.	1743.
2.8	1872.	6571.	3.5	-144.	4221.	4077.	2349.
3.3	2290.	8385.	3.7	-562.	5337.	4776.	3048.
3.8	2765.	10379.	3.7	-1037.	6547.	5510.	3782.
4.3	3283.	12386.	3.8	-1555.	7835.	6279.	4551.
4.7	3658.	13868.	3.8	-1930.	8763.	6833.	5104.
5.0	3989.	15110.	3.8	-2261.	9549.	7287.	5561.
5.9	4910.	18525.	3.8	-3182.	11718.	8535.	6807.
6.7	5018.	21749.	3.7	-4090.	13783.	9694.	7966.
7.6	6667.	24699.	3.7	-4939.	15683.	10744.	9016.
8.6	7430.	27246.	3.7	-5702.	17338.	11636.	9908.
9.9	8366.	30101.	3.6	-6638.	19234.	12595.	10867.

STATIC TRIAXIAL TEST: S-4B
IVINS DIVERSION DAM NO. 5

CONSOLIDATED UNDRAINED TRIAXIAL TEST
WITH PORE PRESSURE MEASUREMENT

STATIC TX#IV5R KC-1.0
D118-30APR.82
BORING: IV-4 SAMPLE:PB-2
SILTY SAND

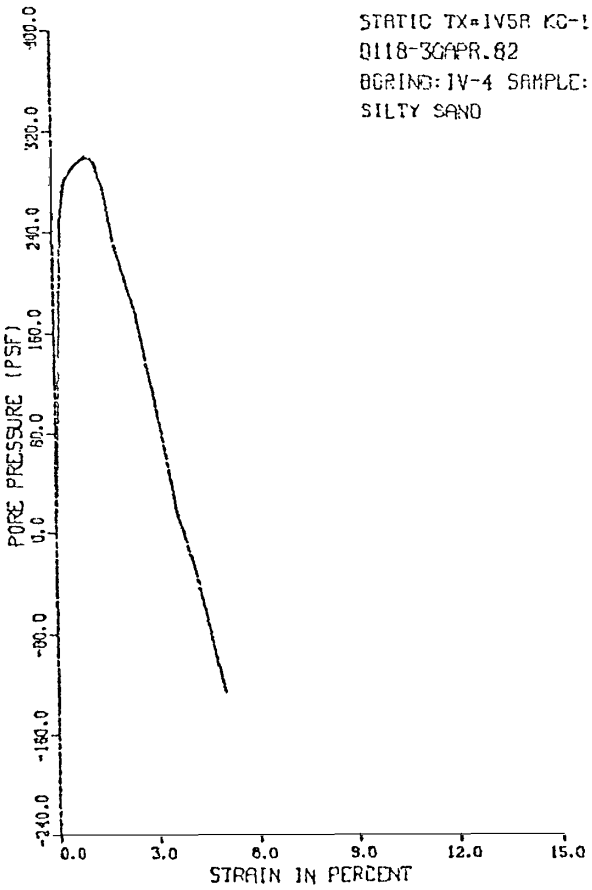

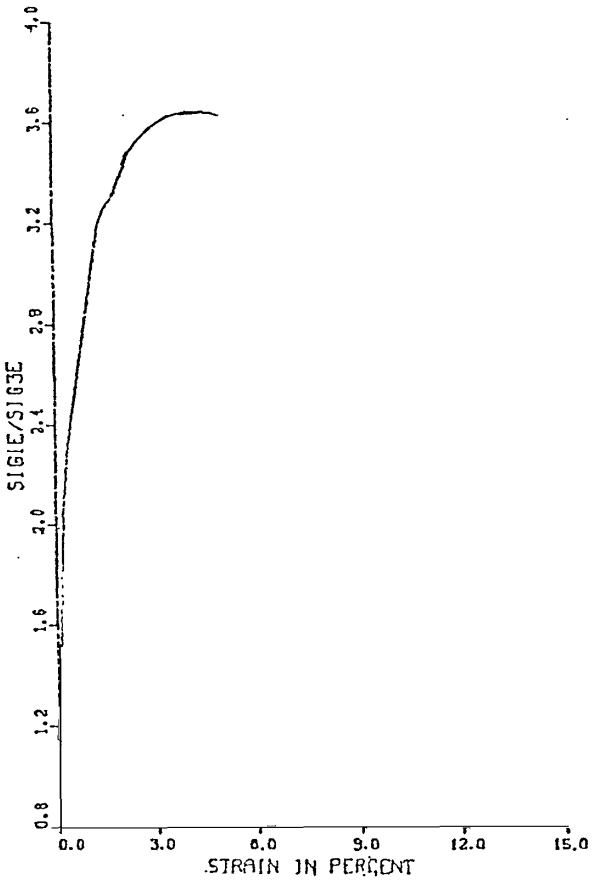

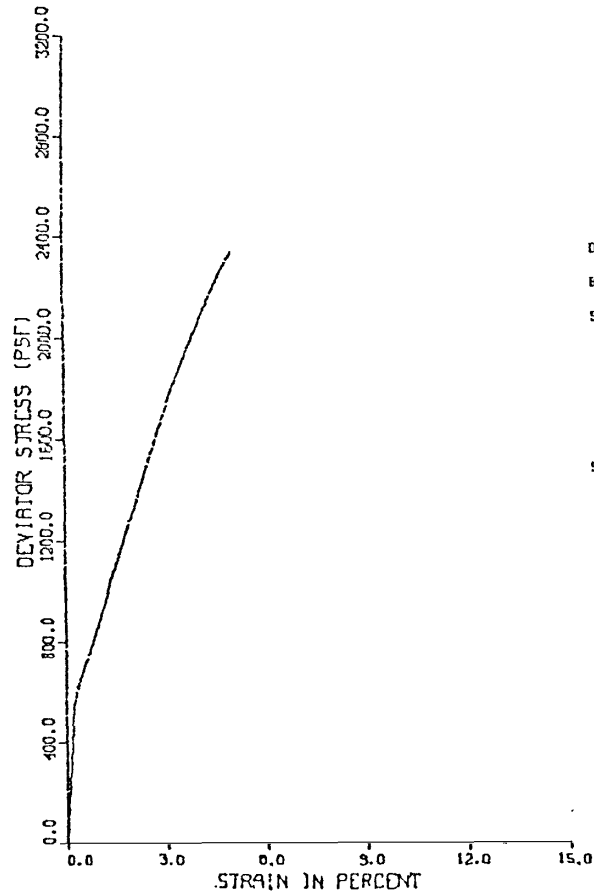

ISOTROPIC CONSOLIDATED UNDRAINED TRIAXIAL TEST
WITH PORE PRESSURE MEASUREMENTS
D118-UTAH DAMS-IVINS DIVERSION STATIC TX#IV5A STAGE1 4/30/82 RED. BY BW

BORING:IV-4 SAMPLE:PB-2/S-1 DEPTH:8.0-10.5

SILTY SAND

AT END OF CONSOLIDATION :

SAMPLE HEIGHT	=	5.965 INCHES
SAMPLE AREA	=	6.433 SQ. INCHES
EFFECTIVE CONFINING STRESS .	=	763. PSF
EFFECTIVE MAJOR PRIN. STRESS	=	763. PSF
PRINCIPAL STRESS RATIO	=	1.00

STRAIN PCT	SIGMA3E PSF	SIGMA1E PSF	RATIO SIG1E/SIG3E	PPRESS PSF	PBAR PSF	PTOT PSF	Q PSF
.0	763.	763.	1.0	0.	763.	763.	0.
.2	518.	1054.	2.0	245.	786.	1031.	268.
.4	475.	1100.	2.3	288.	787.	1075.	312.
1.2	461.	1412.	3.1	302.	936.	1239.	476.
1.3	475.	1513.	3.2	288.	994.	1282.	519.
1.5	490.	1592.	3.3	274.	1041.	1314.	551.
1.8	533.	1763.	3.3	230.	1148.	1379.	615.
2.2	562.	1920.	3.4	202.	1241.	1442.	679.
2.5	590.	2097.	3.6	173.	1344.	1516.	753.
2.8	634.	2265.	3.6	130.	1449.	1579.	816.
3.1	677.	2455.	3.6	86.	1566.	1652.	889.
3.6	749.	2690.	3.6	14.	1719.	1734.	971.
4.2	792.	2894.	3.7	-29.	1843.	1814.	1051.
4.6	850.	3091.	3.6	-86.	1970.	1884.	1121.
5.0	893.	3231.	3.6	-130.	2062.	1932.	1169.

STATIC TRIAXIAL TEST: S-5A
IVINS DIVERSION DAM NO. 5

CONSOLIDATED UNDRAINED TRIAXIAL TEST
WITH PORE PRESSURE MEASUREMENT

STATIC TX#1V5B KC-1.0
D118-3CAPR.82
BORING:IV-4 SAMPLE:FB-2
SILTY SAND

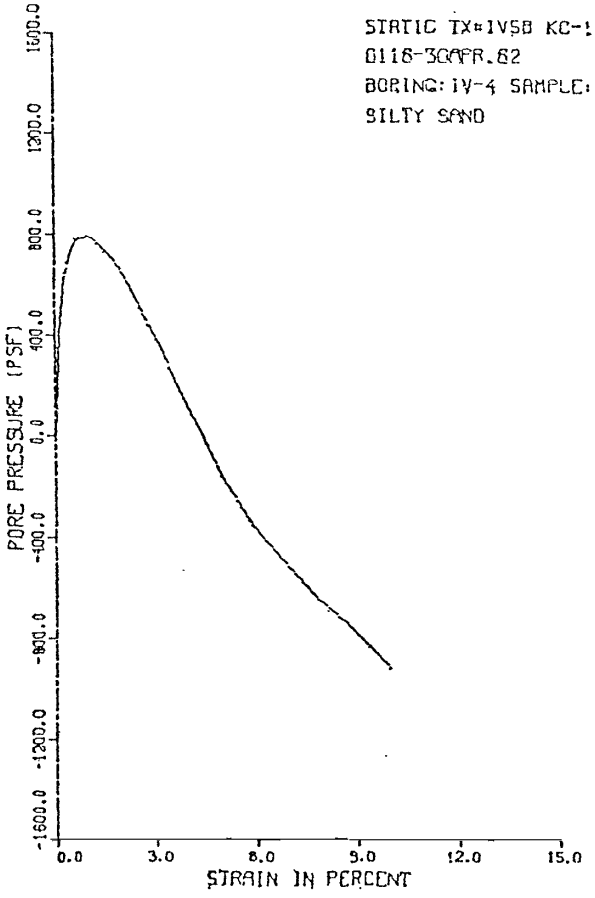

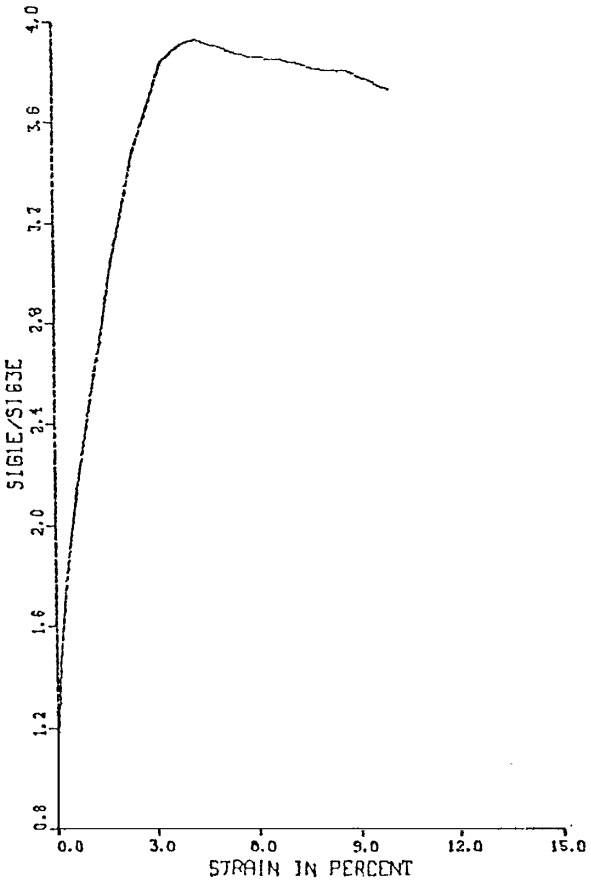

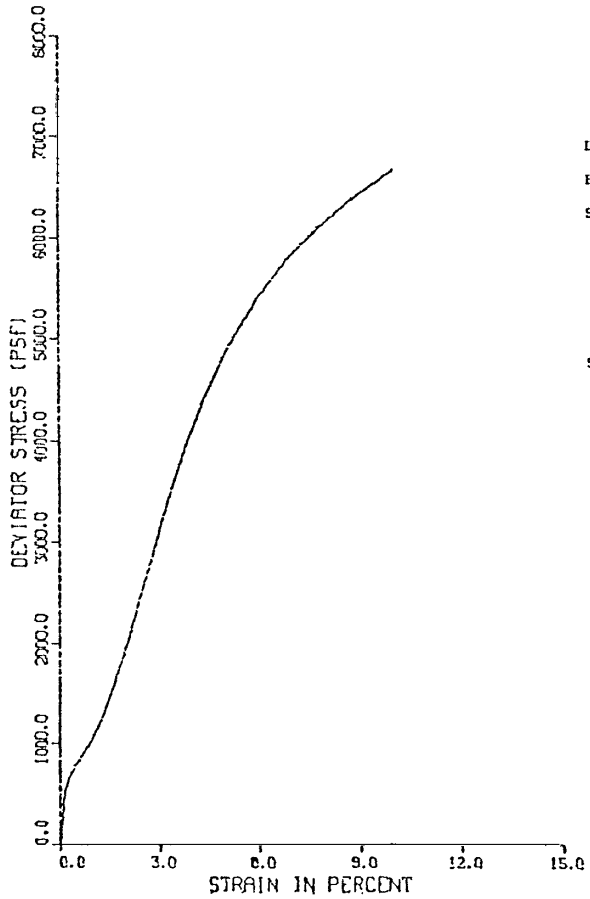

ISOTROPIC CONSOLIDATED UNDRAINED TRIAXIAL TEST
WITH PORE PRESSURE MEASUREMENTS
D118-UTAH DAMS-IVINS DIVERSION STATIC TX#5B STAGE2 4/30/82 RED. BY BW

BORING:IV-4 SAMPLE:FB-2/S-1 DEPTH:8.0-10.5

SILTY SAND

AT END OF CONSOLIDATION :
SAMPLE HEIGHT ..... = 5.825 INCHES
SAMPLE AREA ..... = 6.541 SQ. INCHES
EFFECTIVE CONFINING STRESS . = 1526. PSF
EFFECTIVE MAJOR PRIN. STRESS = 1526. PSF
PRINCIPAL STRESS RATIO ..... = 1.00

STRAIN PCT	SIGMA3E PSF	SIGMA1E PSF	RATIO SIG1E/SIG3E	PPRESS PSF	PBAR PSF	PTOT PSF	Q PSF
.0	1526.	1526.	1.0	0.	1526.	1526.	0.
.1	1123.	1629.	1.5	403.	1376.	1779.	253.
.3	907.	1566.	1.7	619.	1236.	1856.	329.
.5	806.	1573.	2.0	720.	1190.	1910.	383.
.7	749.	1602.	2.1	778.	1175.	1953.	426.
1.0	734.	1802.	2.5	792.	1268.	2060.	534.
1.2	749.	1945.	2.6	778.	1347.	2125.	598.
1.4	778.	2124.	2.7	749.	1451.	2200.	673.
1.7	821.	2487.	3.0	706.	1654.	2359.	833.
2.1	893.	2920.	3.3	634.	1906.	2540.	1013.
2.4	965.	3351.	3.5	562.	2158.	2719.	1193.
2.7	1066.	3850.	3.6	461.	2458.	2919.	1392.
3.2	1195.	4583.	3.8	331.	2889.	3220.	1694.
3.8	1354.	5273.	3.9	173.	3313.	3486.	1960.
4.3	1498.	5880.	3.9	29.	3689.	3717.	2191.
5.0	1685.	6558.	3.9	-158.	4121.	3963.	2437.
5.9	1886.	7272.	3.9	-360.	4579.	4219.	2693.
6.8	2030.	7814.	3.8	-504.	4922.	4418.	2892.
7.8	2174.	8286.	3.8	-648.	5230.	4582.	3056.
8.7	2275.	8647.	3.8	-749.	5461.	4712.	3186.
10.0	2448.	9125.	3.7	-922.	5787.	4865.	3339.

STATIC TRIAXIAL TEST: S-5B
IVINS DIVERSION DAM NO. 5

CONSOLIDATED UNDRAINED TRIAXIAL TEST
WITH PORE PRESSURE MEASUREMENT

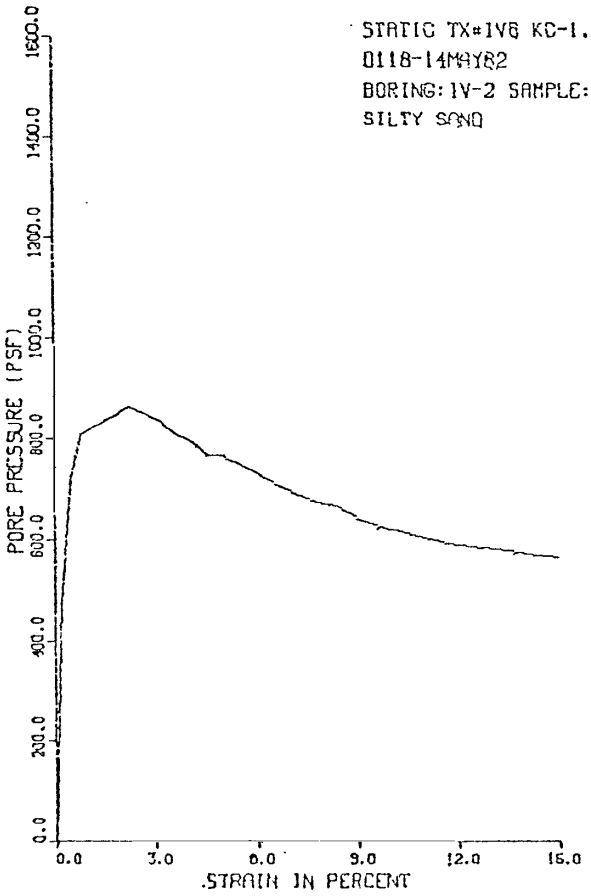

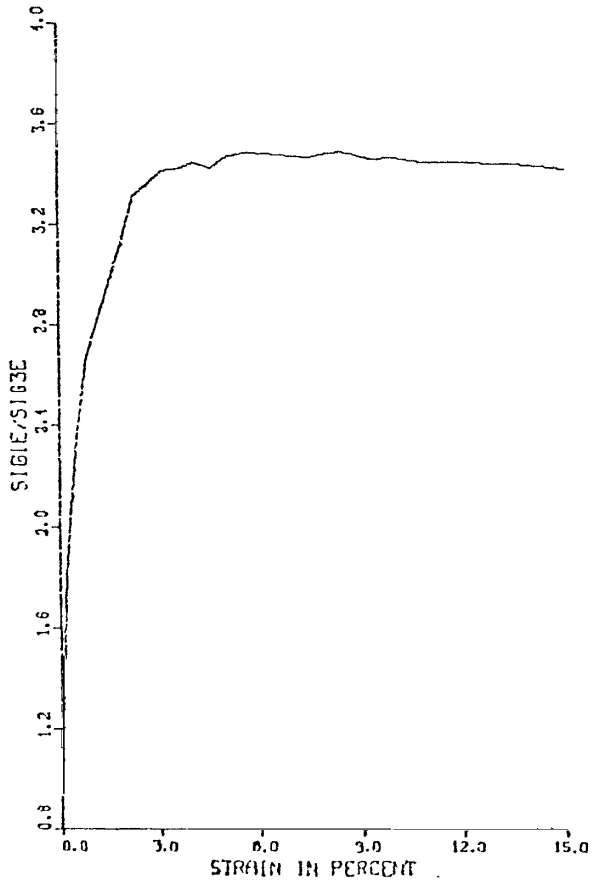

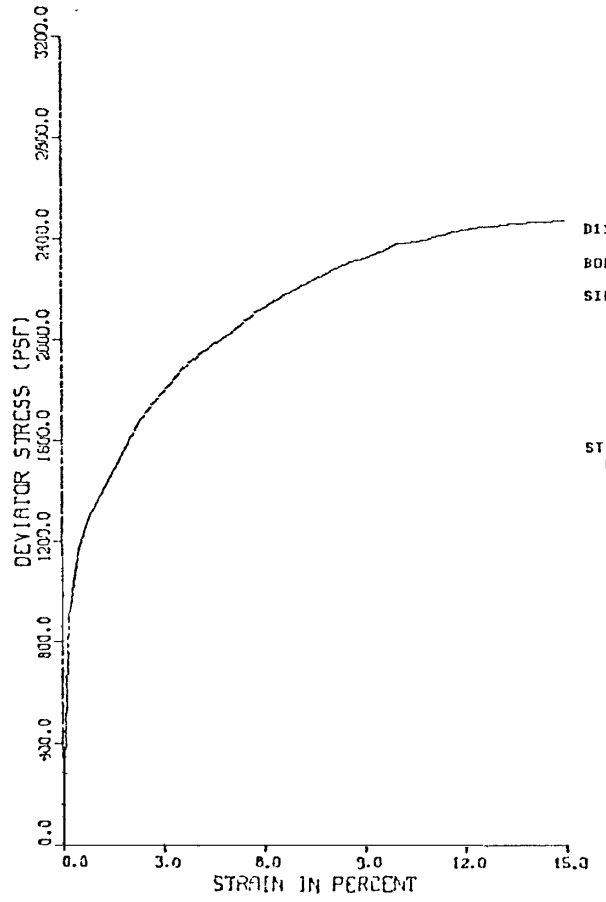

ISOTROPIC CONSOLIDATED UNDRAINED TRIAXIAL TEST
WITH PORE PRESSURE MEASUREMENTS
D118-UTAH DAMS-IVINS DIVERSION STATIC TX#IV6 5/14/82 REDUCED BY BW

BORING:IV-2 SAMPLE:PB-4/S-3 DEPTH:16.0-18.5

SILTY SAND

AT END OF CONSOLIDATION :
SAMPLE HEIGHT ..... = 5.773 INCHES
SAMPLE AREA ..... = 6.425 SQ. INCHES
EFFECTIVE CONFINING STRESS . = 1584. PSF
EFFECTIVE MAJOR PRIN. STRESS = 1584. PSF
PRINCIPAL STRESS RATIO ..... = 1.00

STRAIN PCT	SIGMA3E PSF	SIGMA1E PSF	RATIO SIG1E/SIG3E	PPRESS PSF	PBAR PSF	PTOT PSF	Q PSF
.0	1584.	1584.	1.0	0.	1584.	1584.	0.
.2	1109.	2004.	1.8	475.	1556.	2031.	447.
.5	864.	2024.	2.3	720.	1444.	2164.	580.
.8	778.	2067.	2.7	806.	1422.	2229.	645.
1.9	734.	2317.	3.2	850.	1526.	2375.	791.
2.3	720.	2385.	3.3	864.	1552.	2416.	832.
2.6	734.	2459.	3.3	850.	1597.	2446.	862.
3.1	749.	2552.	3.4	835.	1650.	2485.	901.
3.6	778.	2657.	3.4	806.	1717.	2524.	940.
4.1	792.	2726.	3.4	792.	1759.	2551.	967.
4.6	821.	2809.	3.4	763.	1815.	2578.	994.
5.0	821.	2844.	3.5	763.	1832.	2595.	1011.
5.8	850.	2961.	3.5	734.	1905.	2640.	1056.
6.7	878.	3054.	3.5	706.	1966.	2672.	1088.
7.5	907.	3146.	3.5	677.	2026.	2703.	1119.
8.4	922.	3221.	3.5	662.	2071.	2734.	1150.
9.3	950.	3289.	3.5	634.	2120.	2753.	1169.
10.0	965.	3345.	3.5	619.	2155.	2774.	1190.
10.8	979.	3377.	3.4	605.	2178.	2783.	1199.
11.7	994.	3427.	3.4	590.	2210.	2801.	1217.
13.5	1008.	3470.	3.4	576.	2239.	2815.	1231.
15.0	1022.	3499.	3.4	562.	2261.	2822.	1238.

STATIC TRIAXIAL TEST: S-6
IVINS DIVERSION DAM NO. 5

APPENDIX C

RESULTS OF CYCLIC TRIAXIAL TESTS

GREEN'S LAKE DAM NO. 3

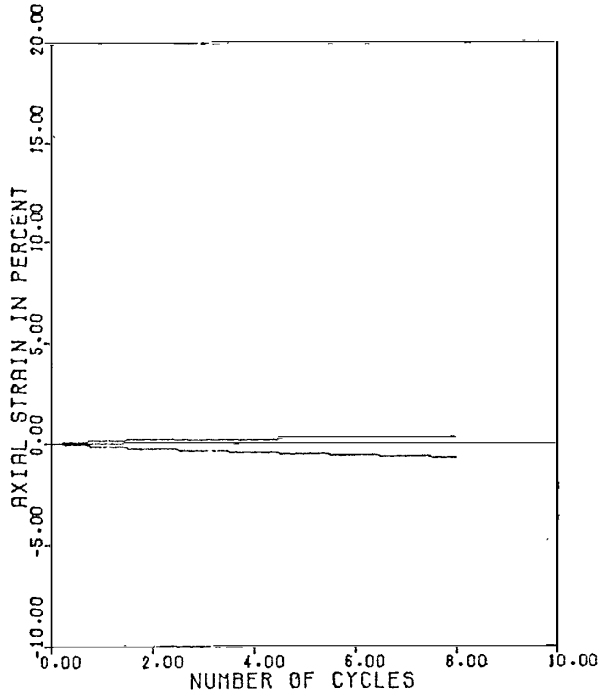

D118-UTAH DAMS-GREENS LAKE CYCLIC TX#GL1 TESTED 8/10/82 REDUCED BY BW
BORING:GL3-1 SAMPLE:PB-2/S-2 CLAYEY SAND

INITIAL DRY DENSITY = 116.2 PCF
MOISTURE CONTENT = 12.3 PERCENT
DRY DENSITY AFTER CONSOL = 116.4 PCF
MOISTURE CONT AFTER CONSOL = 15.2 PERCENT
SIG1 = 1108.8 PSF
SIG3 = 1108.8 PSF
KC = 1.0
SIGMEAN = 1108.8 PSF

CYC. NO.	PORE PRES. (PSF)	PWP/SIG3	CYCLIC SHEAR STRESS(PSF) COMP.	TENS.	CUMUL. AVE. CYCL. SHEAR STRESS	TAU/SIGMEAN	AXIAL STRN. PERCENT P.TO P.	MEAN
1	668.	.60	514.	-487.	501.	.45	.27	.00
2	783.	.71	526.	-503.	504.	.45	.47	-.03
3	852.	.77	535.	-512.	507.	.46	.60	-.03
4	910.	.82	544.	-521.	510.	.46	.67	-.07
5	956.	.86	544.	-521.	513.	.46	.80	-.07
6	979.	.88	544.	-521.	514.	.46	.87	-.10
7	1014.	.91	544.	-521.	515.	.46	.94	-.13
8	1037.	.94	544.	-521.	517.	.47	1.01	-.17

CYCLIC TRIAXIAL TEST: C-1
GREEN'S LAKE DAM NO. 3

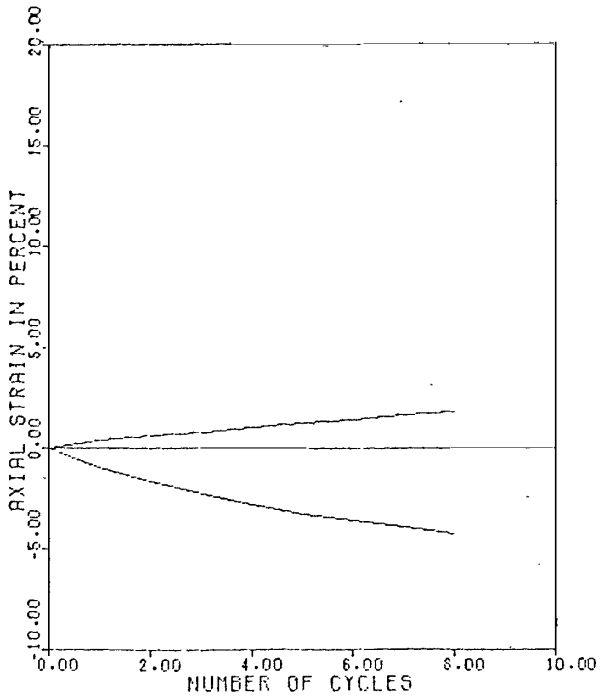

D118 UTAH DAMS GREENS LAKE CYCLIC TX#GL2 TESTED 8/19/82 REDUCED BY BU
BORING:GL3-2 SAMPLE:PB-6/S-4 DEPTH:25.5-28.0 SILTY SAND

INITIAL DRY DENSITY = 113.5 PCF
MOISTURE CONTENT = 13.3 PERCENT
DRY DENSITY AFTER CONSOL = 113.8 PCF
MOISTURE CONT AFTER CONSOL = 14.9 PERCENT
SIG1 = 2016.0 PSF
SIG3 = 2016.0 PSF
KC = 1.0
SIGMEAN = 2016.0 PSF

CYC. NO.	PORE PRES. (PSF)	PWP/SIG3	CYCLIC SHEAR STRESS(PSF) COMP.	TENS.	CUMUL. AVE. CYCL. SHEAR STRESS	TAU/SIGMEAN	AXIAL STRN. PERCENT P-TO P.	MEAN
1	720.	.36	1002.	-915.	958.	.48	1.36	-.27
2	1498.	.74	1032.	-932.	964.	.48	2.24	-.51
3	1786.	.89	1036.	-911.	966.	.48	3.06	-.71
4	1901.	.94	1032.	-889.	965.	.48	3.80	-.83
5	1958.	.97	1002.	-846.	961.	.48	4.48	-1.02
6	1958.	.97	989.	-824.	956.	.47	5.02	-1.09
7	1987.	.99	954.	-802.	951.	.47	5.57	-1.15
8	2016.	1.00	932.	-780.	945.	.47	6.04	-1.19

CYCLIC TRIAXIAL TEST: C-2
GREEN'S LAKE DAM NO. 3

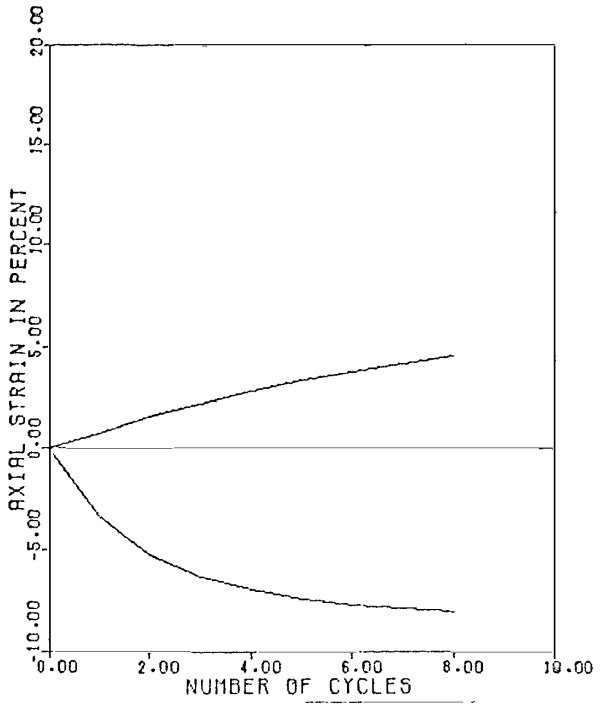

D118 UTAH DAMS GREENS LAKE CYCLIC TX:GL3 TESTED 23AUG.82 REDUCED BY BU
BORING:GL3-2 SAMPLE:PB-7/S-5 DEPTH:29.5-32.0 CLAYEY SAND

INITIAL DRY DENSITY = 108.6 PCF
MOISTURE CONTENT = 13.5 PERCENT
DRY DENSITY AFTER CONSOL = 108.8 PCF
MOISTURE CONT AFTER CONSOL = 21.8 PERCENT
SIG1 = 3024.0 PSF
SIG3 = 3024.0 PSF
KC = 1.0
SIGMEAN = 3024.0 PSF

CYC. NO.	PORE PRES. (PSF)	PWP/SIG3	CYCLIC SHEAR STRESS(PSF) COMP.	TENS.	CUMUL. AVE. CYCL. SHEAR STRESS	TAU/SIGMEAN	AXIAL STRN. PERCENT P.TO P.	MEAN
1	1440.	.48	1508.	-1330.	1419.	.47	4.02	-1.34
2	2880.	.95	1464.	-1264.	1405.	.46	6.77	-1.84
3	2966.	.98	1330.	-1142.	1277.	.46	8.51	-2.04
4	3053.	1.01	1209.	-1069.	1344.	.44	9.79	-2.08
5	3139.	1.04	1109.	-898.	1310.	.43	10.79	-2.04
6	3139.	1.04	998.	-820.	1276.	.42	11.46	-1.98
7	3110.	1.03	942.	-776.	1246.	.41	12.07	-1.88
8	3082.	1.02	887.	-721.	1219.	.40	12.60	-1.74

CYCLIC TRIAXIAL TEST: C-3
GREEN'S LAKE DAM NO. 3

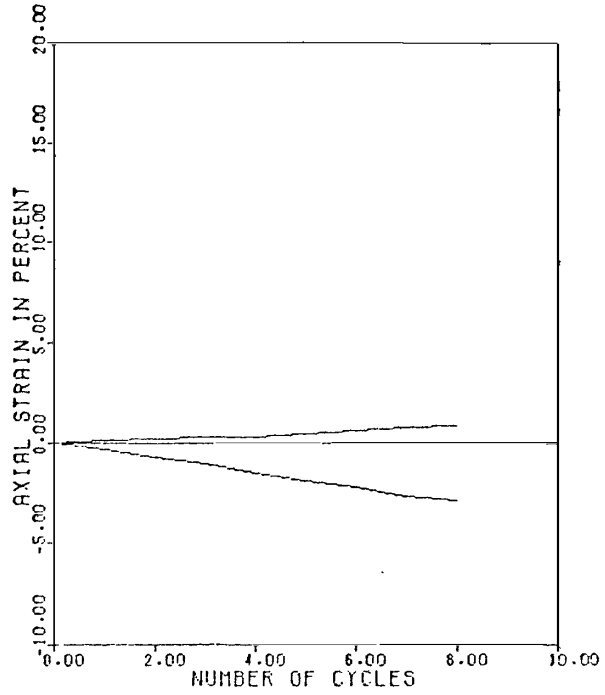

D118- UTAH DAMS-GREENS LAKE CYCLIC TX#GL4 TESTED 8/27/82 REDUCED BY PU
BORING:GL2-1 SAMPLE:PB-2/S-1 DEPTH;8.0-10.5

INITIAL DRY DENSITY = 114.7 PCF
MOISTURE CONTENT = 9.6 PERCENT
DRY DENSITY AFTER CONSOL = 114.5 PCF
MOISTURE CONT AFTER CONSOL = 23.5 PERCENT
SIG1 = 1353.6 PSF
SIG3 = 1353.6 PSF
KC = 1.0
SIGMEAN = 1353.6 PSF

CYC. NO.	PORE PRESS. (PSF)	PUP/SIG3	CYCLIC SHEAR STRESS(PSF) COMP.	TENS.	CUMUL. AVE. CYCL. SHEAR STRESS	TAU/SIGMEAN	AXIAL STRN. PERCENT P.TO P.	MEAN
1	720.	.53	642.	-583.	612.	.45	.48	-.10
2	950.	.70	651.	-610.	617.	.46	.90	-.24
3	1123.	.83	661.	-615.	620.	.46	1.31	-.38
4	1210.	.89	670.	-601.	622.	.46	1.79	-.55
5	1284.	.96	679.	-587.	623.	.46	2.35	-.69
6	1352.	1.02	674.	-564.	623.	.46	2.83	-.79
7	1411.	1.04	647.	-541.	621.	.46	3.38	-.93
8	1411.	1.04	628.	-509.	618.	.46	3.79	-1.00

CYCLIC TRIAXIAL TEST: C-4
GREEN'S LAKE DAM NO. 3

WARNER DRAW DAM

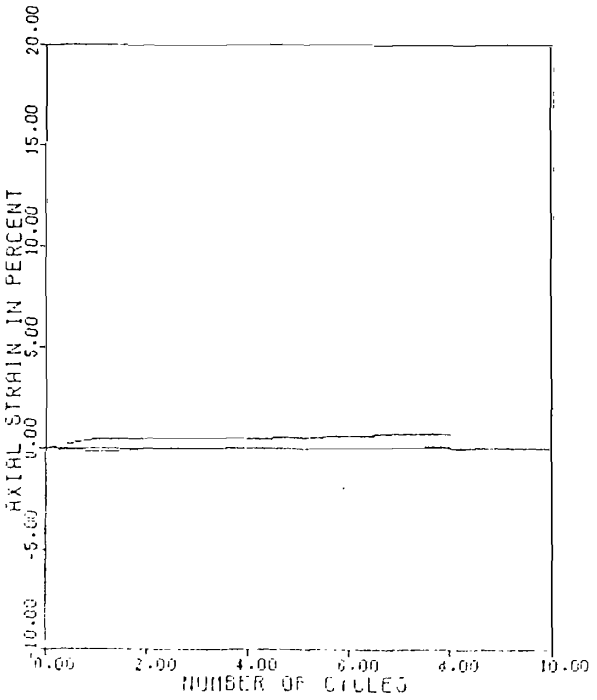

D118-UTAH DAMS-WARNER DRAW CYCLIC TX#UD1 TESTED 7/20/82 REDUCED BY BU
BORING:WD-1 SAMPLE:PB-2/3-2 CLAYEY SAND

INITIAL DRY DENSITY =	122.8 PCF
MOISTURE CONTENT =	9.2 PERCENT
DRY DENSITY AFTER CONSOL =	122.7 PCF
MOISTURE CONT AFTER CONSOL =	12.0 PERCENT
SIG1 =	1440.0 PSF
SIG3 =	1440.0 PSF
KC =	1.0
SIGMEAN =	1440.0 PSF

CYC. NO.	PORE PRES. (PSF)	PUP/SIG3	CYCLIC SHEAR STRESS(PSF) COMP.	TENS.	CUMUL. AVE. CYCL. SHEAR STRESS	TAU/SIGMEAN	AXIAL STRN. PERCENT P.TO P.	MEAN
1	979.	.68	416.	-432.	424.	.29	.60	.17
2	1083.	.75	421.	-432.	425.	.29	.53	.20
3	1129.	.78	432.	-432.	426.	.30	.53	.20
4	1164.	.81	432.	-432.	427.	.30	.47	.23
5	1187.	.82	432.	-432.	427.	.30	.53	.27
6	1221.	.85	432.	-432.	428.	.30	.60	.30
7	1267.	.88	432.	-432.	428.	.30	.67	.33
8	1279.	.89	432.	-432.	428.	.30	.60	.37

CYCLIC TRIAXIAL TEST: C-1
WARNER DRAW DAM

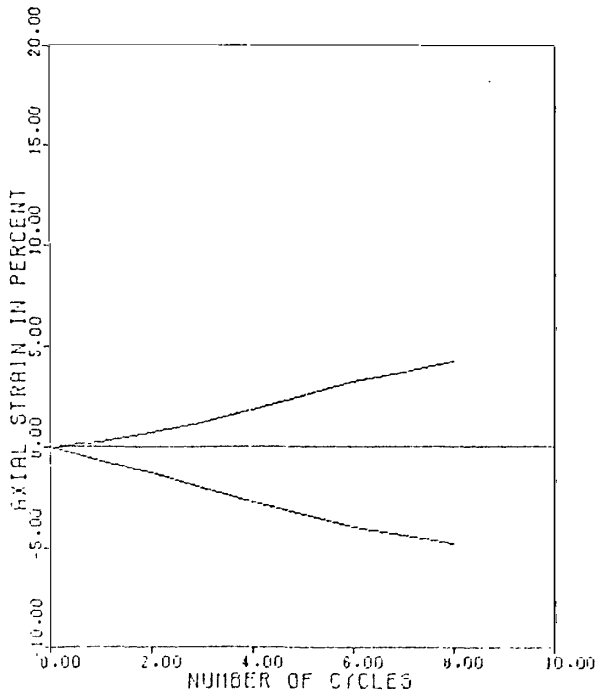

D118-UTAH DAMS-WARNER DRAW CYCLIC TX#WD2 TESTED 7/20/82 REDUCED BY BW
BORING:WD-2 SAMPLE:PB-6/S-6 CLAYEY SAND

INITIAL DRY DENSITY = 121.2 PCF
MOISTURE CONTENT = 11.1 PERCENT
DRY DENSITY AFTER CONSOL = 121.7 PCF
MOISTURE CONT AFTER CONSOL = 11.3 PERCENT
SIG1 = 2678.4 PSF
SIG3 = 2678.4 PSF
KC = 1.0
SIGMEAN = 2678.4 PSF

CYC. NO.	PORE PRES. (PSF)	PWP/SIG3	CYCLIC SHEAR STRESS(PSF) COMP.	TENS.	CUMUL. AVE. CYCL. SHEAR STRESS	TAU/SIGMEAN	AXIAL STRN. PERCENT P.TO P.	MEAN
1	300.	.11	1028.	-1050.	1039.	.39	.95	-.20
2	726.	.27	1028.	-1050.	1039.	.39	1.97	-.30
3	1164.	.43	1028.	-1028.	1037.	.39	3.19	-.44
4	1532.	.57	1028.	-1028.	1034.	.39	4.54	-.44
5	1878.	.70	1028.	-1028.	1035.	.39	5.90	-.44
6	2143.	.80	1028.	-1011.	1034.	.39	7.18	-.41
7	2339.	.87	1006.	-998.	1032.	.39	8.07	-.37
8	2488.	.93	998.	-985.	1029.	.38	8.95	-.27

CYCLIC TRIAXIAL TEST: C-2
WARNER DRAW DAM

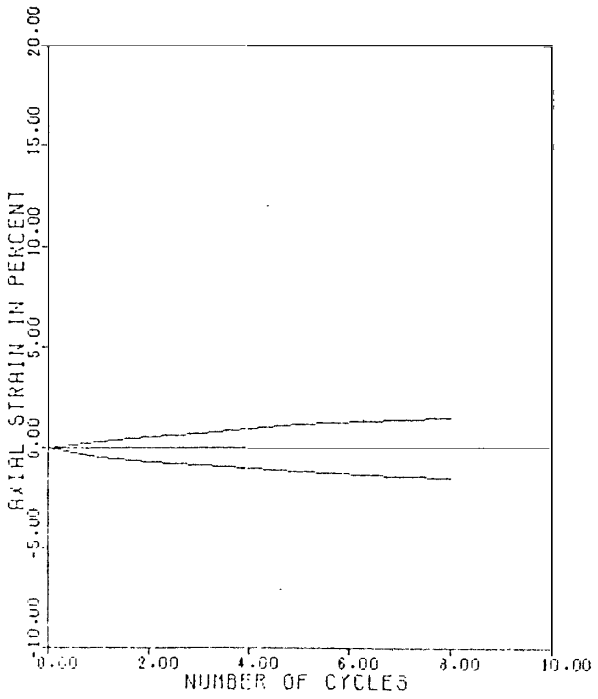

D118-UTAH DAMS-WARNER DRAW CYCLIC TX#WD3 TESTED 7/22/82 REDUCED BY BW
BORING:WD-1 SAMPLE:PBJ10/S-10 DEPTH:41.0-43.5 CLAYEY SAND

INITIAL DRY DENSITY	=	127.4 PCF
MOISTURE CONTENT	=	10.5 PERCENT
DRY DENSITY AFTER CONSOL	=	127.7 PCF
MOISTURE CONT AFTER CONSOL	=	9.8 PERCENT
SIG1	=	3902.4 PSF
SIG3	=	3902.4 PSF
NC	=	1.0
SIGMEAN	=	3902.4 PSF

CYC. NO.	PORE PRES. (PSF)	PUP/SIG3	CYCLIC SHEAR STRESS(PSF) COMP.	TENS.	CUMUL. AVE. CYCL. SHEAR STRESS	TAU/SIGMEAN	AXIAL STRN. PERCENT P.TO P.	MEAN
1	1440.	.37	1661.	-1661.	1661.	.43	.80	-.07
2	3254.	.83	1661.	-1661.	1661.	.43	1.27	-.10
3	3888.	1.00	1661.	-1661.	1661.	.43	1.60	-.07
4	4061.	1.04	1661.	-1661.	1661.	.43	1.94	-.03
5	4291.	1.10	1661.	-1649.	1660.	.43	2.27	.00
7	4106.	1.13	1661.	-1627.	1658.	.42	2.80	.00
8	4464.	1.14	1661.	-1616.	1656.	.42	2.94	.00

CYCLIC TRIAXIAL TEST: C-3
WARNER DRAW DAM

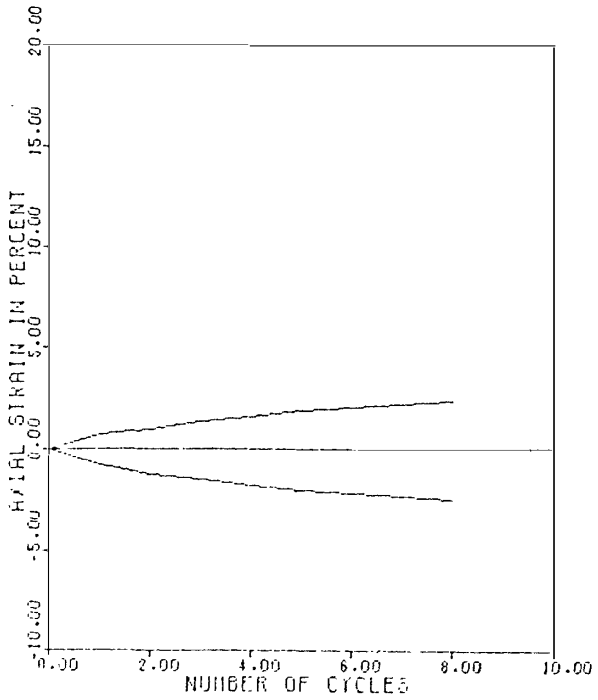

D118-UTAH DAMS-WARNER DRAW CYCLIC TX#WD4 TESTED 7/22/82 REDUCED BY BW
BORING:WD-1 SAMPLE:PB-13/S-13 CLAYEY SAND

INITIAL DRY DENSITY = 124.7 PCF
MOISTURE CONTENT = 11.3 PERCENT
DRY DENSITY AFTER CONSOL = 125.3 PCF
MOISTURE CONT AFTER CONSOL = 10.1 PERCENT
SIG1 = 4809.6 PSF
SIG3 = 4809.6 PSF
KC = 1.0
SIGMEAN = 4809.6 PSF

CYC. NO.	PORE PRES. (PSF)	PWP/SIG3	CYCLIC SHEAR STRESS(PSF) COMP.	TENS.	CUMUL. AVE. CYCL. SHEAR STRESS	TAU/SIGMEAN	AXIAL STRN. PERCENT P.TO P.	MEAN
1	1037.	.22	2044.	-2019.	2042.	.42	1.50	-.07
2	3168.	.66	2064.	-2019.	2042.	.42	2.18	-.14
3	4694.	.98	2053.	-1997.	2039.	.42	2.86	-.07
4	5616.	1.17	2012.	-1986.	2036.	.42	3.33	-.10
5	6134.	1.28	2031.	-1964.	2032.	.42	3.94	-.07
6	6394.	1.33	2008.	-1931.	2027.	.42	4.22	-.07
7	6422.	1.34	1997.	-1908.	2021.	.42	4.56	-.10
8	6624.	1.38	1986.	-1886.	2016.	.42	4.90	-.07

CYCLIC TRIAXIAL TEST: C-4
WARNER DRAW DAM

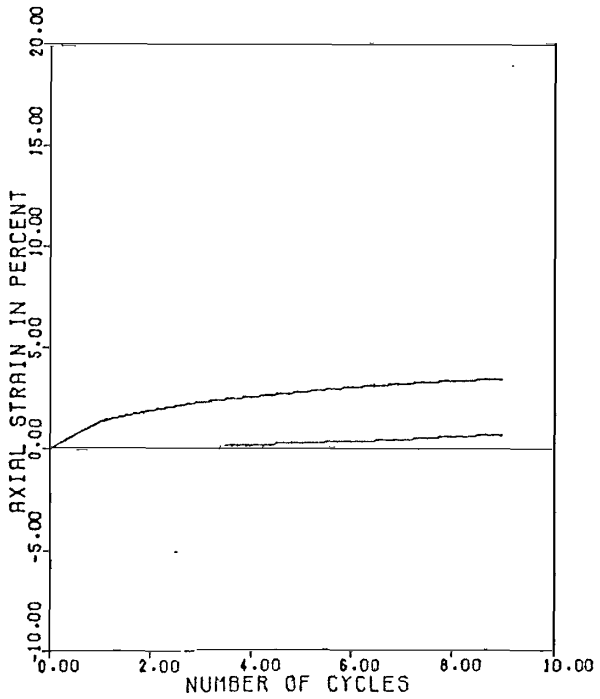

B118-UTAH DAMS-WARNER DRAW DAM CYCLIC#UD5 TESTED 8/16/82 REDUCED BY MLT
BORING:WD-1 SAMPLE:FB-6/S-6 SILTY SAND

INITIAL DRY DENSITY = 123.6 PCF
MOISTURE CONTENT = 10.4 PERCENT
DRY DENSITY AFTER CONSOL = .0 PCF
MOISTURE CONT AFTER CONSOL = .0 PERCENT
SIG1 = 3672.0 PSF
SIG3 = 2448.0 PSF
KC = 1.5
SIGMEAN = 2856.0 PSF

CYC. NO.	PORE PRES. (PSF)	PUP/SIG3	CYCLIC SHEAR STRESS(PSF) COMP.	TENS.	CUMUL. AVE. CYCL. SHEAR STRESS	TAU/SIGMEAN	AXIAL STRN. PERCENT P.TO P.	MEAN
1	1757.	.72	1543.	-1488.	1515.	.53	1.43	.64
2	2534.	1.04	1543.	-1488.	1515.	.53	1.90	.95
3	2909.	1.19	1554.	-1455.	1513.	.53	2.17	1.15
4	3168.	1.29	1554.	-1455.	1512.	.53	2.38	1.32
5	3398.	1.39	1565.	-1433.	1511.	.53	2.51	1.46
6	3456.	1.41	1565.	-1433.	1510.	.53	2.65	1.66
7	3485.	1.42	1565.	-1421.	1509.	.53	2.72	1.76
8	3456.	1.41	1565.	-1410.	1507.	.53	2.72	1.90
9	3456.	1.41	1565.	-1410.	1506.	.53	2.78	2.00

CYCLIC TRIAXIAL TEST: C-5
WARNER DRAW DAM

FROG HOLLOW DAM

Earth Sciences Associates

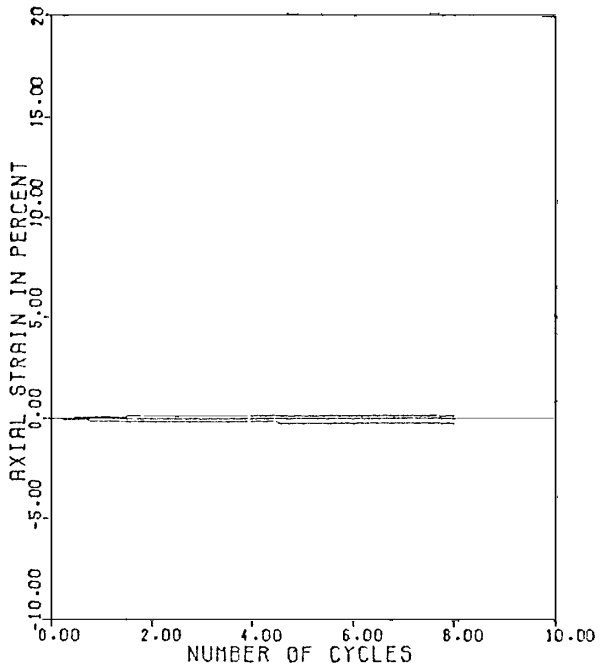

D118-UTAH DAMS-FROG HOLLOW CYCLIC TX:FH-1 TESTED 7/28/82 REDUCED BY BW
BORING:FH-1 SAMPLE:FB-4/S-3 DEPTH:14.5-17.5 SILTY CLAY

INITIAL DRY DENSITY = 108.8 PCF
MOISTURE CONTENT = 18.6 PERCENT
DRY DENSITY AFTER CONSOL = 108.9 PCF
MOISTURE CONT AFTER CONSOL = 18.9 PERCENT
SIG1 = 2044.8 PSF
SIG3 = 2044.8 PSF
KC = 1.0
SIGMEAN = 2044.8 PSF

CYC. NO.	PORE PRES. (PSF)	PUP/SIG3	CYCLIC SHEAR STRESS(PSF) COMP.	TENS.	CUMUL. AVE. CYCL. SHEAR STRESS	TAU/SIGMEAN	AXIAL STRN. PERCENT P.TO P.	MEAN
1	662.	.32	755.	-799.	777.	.38	.20	-.03
2	864.	.42	755.	-799.	777.	.38	.27	.00
3	922.	.45	755.	-799.	777.	.38	.27	.00
4	979.	.48	755.	-799.	777.	.38	.27	.00
5	1037.	.51	755.	-799.	777.	.38	.34	-.03
6	1094.	.54	755.	-799.	777.	.38	.34	-.03
7	1152.	.56	755.	-799.	777.	.38	.34	-.03
8	1181.	.58	755.	-799.	777.	.38	.34	-.03

CYCLIC TRIAXIAL TEST: C-1
FROG HOLLOW DAM

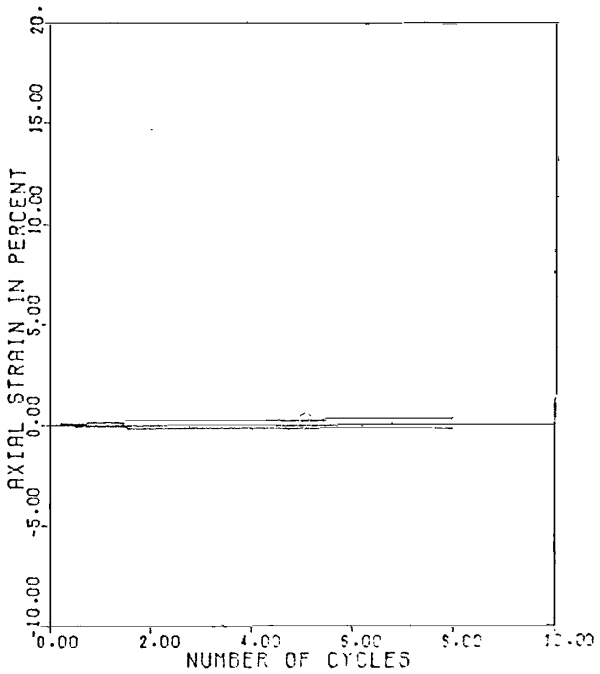

D118-UTAH DAMS-FROG HOLLOW CYCLIC TX#FH-2 TESTED 7/28/82 REDUCED BY BW
BORING:FH-1 SAMPLE:PB-6/S-5 DEPTH:22.5-25.0 SILTY CLAY

INITIAL DRY DENSITY = 111.7 PCF
MOISTURE CONTENT = 19.1 PERCENT
DRY DENSITY AFTER CONSOL = 112.1 PCF
MOISTURE CONT AFTER CONSOL = 19.0 PERCENT
SIG1 = 2707.2 PSF
SIG3 = 2707.2 PSF
KC = 1.0
SIGMEAN = 2707.2 PSF

CYC. NO.	PORE PRES. (PSF)	PWP/SIG3	CYCLIC SHEAR STRESS(PSF) COMP.	TENS.	CUMUL. AVE. CYCL. SHEAR STRESS	TAU/SIGMEAN	AXIAL STRN. PERCENT P.TO P.	MEAN
1	979.	.36	1082.	-1082.	1082.	.40	.20	.03
2	1296.	.48	1082.	-1082.	1082.	.40	.34	.03
3	1469.	.54	1082.	-1082.	1082.	.40	.34	.03
4	1613.	.60	1082.	-1082.	1082.	.40	.41	.07
5	1728.	.64	1082.	-1082.	1082.	.40	.41	.07
6	1786.	.66	1082.	-1082.	1082.	.40	.47	.10
7	1872.	.69	1082.	-1082.	1082.	.40	.47	.10
8	1901.	.70	1082.	-1082.	1082.	.40	.47	.10

CYCLIC TRIAXIAL TEST: C-2
FROG HOLLOW DAM

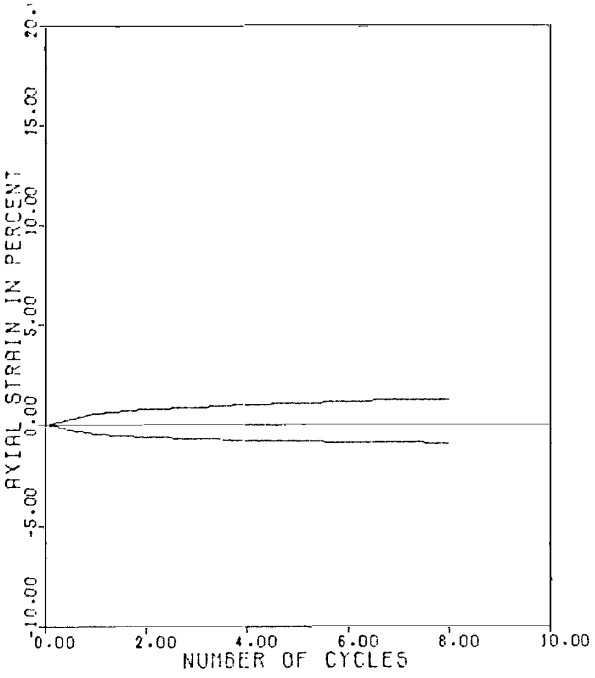

SILT-CLAY SAND-FROG HOLLOW CYCLIC TRIAX TESTED 7/26/82 REDUCED BY BW
ESPINOSA-1 SAMPLE:ES 13 3-9 DEPTH:33.0-40.5

INITIAL DRY DENSITY =	113.5 PCF
MOISTURE CONTENT =	15.0 PERCENT
DRY DENSITY AFTER CONSOL =	114.7 PCF
MOISTURE CONT AFTER CONSOL =	13.5 PERCENT
SIGC =	3499.2 PSF
SIGE =	3499.2 PSF
KC =	1.0
SIG-3AV =	3499.2 PSF

CYC NO	PORE PRES (PSF)	PWP/SIGC	CYCLIC SHEAR STRESS(PSF) COMP.	TENS.	CUMUL. AVE. CYCL. SHEAR STRESS	TAU/SIGMEAN	AXIAL STRN. PERCENT P.TO P.	MEAN
1	922.	.26	1458.	-1431.	1442.	.41	1.02	.03
2	1332.	.40	1458.	-1431.	1442.	.41	1.36	.07
3	1669.	.48	1458.	-1431.	1442.	.41	1.56	.10
4	1901.	.54	1458.	-1431.	1442.	.41	1.76	.14
5	2102.	.60	1458.	-1431.	1442.	.41	1.90	.14
6	2279.	.65	1458.	-1431.	1442.	.41	2.03	.14
7	2369.	.68	1458.	-1431.	1442.	.41	2.10	.17
8	2505.	.72	1458.	-1431.	1442.	.41	2.24	.17

CYCLIC TRIAXIAL TEST:C-3
FROG HOLLOW DAM

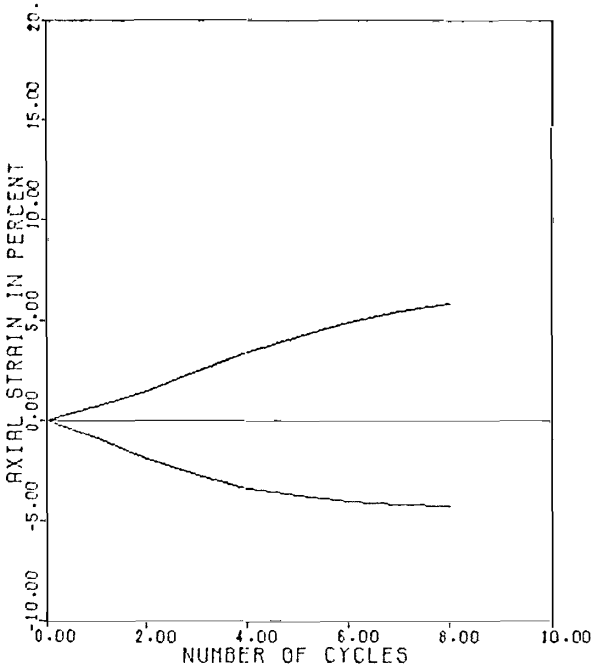

D118-UTAH DAMS-FROG HOLLOW CYCLIC TXIFH4 TESTED 7/26/82 REVISED BY EW
BORING:FH-1 SAMPLE:FB-14/S-12 DEPTH:55.0-56.8 SILTY CLAY

INITIAL DRY DENSITY = 110.1 PCF
MOISTURE CONTENT = 17.9 PERCENT
DRY DENSITY AFTER CONSOL = 110.7 PCF
MOISTURE CONT AFTER CONSOL = 15.6 PERCENT
SIG1 = 4507.2 PSF
SIG3 = 4507.2 PSF
K2 = 1.0
SIGMA0 = 4507.2 PSF

CYC. NO.	PORE PRES. (PSF)	PWP/SIG3	CYCLIC STRESS(PSF) COMP.	TENS.	CURVE, AVG. CYCL. SMEAN STRESS	TAN SIGMA	AXIAL STRN. PERCENT P-TO-P.	MEAN
1	2246.	.50	1964.	-1911.	1853.	.42	1.57	-.10
2	4090.	.91	1866.	-1734.	1866.	.41	3.34	-.17
3	4838.	1.07	1800.	-1624.	1840.	.41	5.18	-.07
4	5098.	1.13	1673.	-1503.	1810.	.40	6.81	.07
5	5184.	1.15	1602.	-1394.	1778.	.39	7.90	.27
6	5093.	1.13	1503.	-1317.	1748.	.39	8.93	.44
7	5069.	1.12	1427.	-1240.	1718.	.38	9.61	.65
8	5069.	1.12	1372.	-1185.	1491.	.38	10.03	.82

CYCLIC TRIAXIAL TEST:C-4
FROG HOLLOW DAM

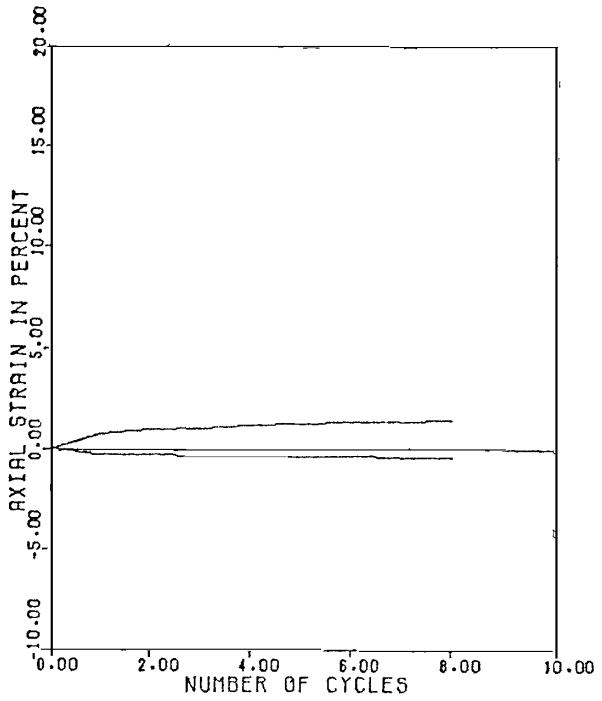

D11B-UTAH DAMS-FROG HOLLOW DAM CYCLIC#FH5 TESTED 8/16/82 REDUCED BY MLT
BORING:FH-1 SAMPLE:FB-10/S-9 SILTY CLAY

INITIAL DRY DENSITY = 111.9 PCF
MOISTURE CONTENT = 17.5 PERCENT
DRY DENSITY AFTER CONSOL = 112.7 PCF
MOISTURE CONT AFTER CONSOL = 17.5 PERCENT
SIG1 = 4795.2 PSF
SIG3 = 3196.8 PSF
KC = 1.5
SIGMEAN = 3729.6 PSF

CYC. NO.	PORE PRES. (PSF)	PWP/SIG3	CYCLIC SHEAR STRESS(PSF) COMP.	TENS.	CUMUL. AVE. CYCL. SHEAR STRESS	TAU/SIGMEAN	AXIAL STRN. PERCENT P.TO P.	MEAN
1	1325.	.41	2117.	-2051.	2084.	.56	1.08	.27
2	1872.	.59	2106.	-2073.	2085.	.56	1.29	.37
3	2304.	.72	2106.	-2073.	2086.	.56	1.42	.37
4	2592.	.81	2106.	-2073.	2087.	.56	1.63	.47
5	2880.	.90	2106.	-2073.	2087.	.56	1.69	.51
6	3024.	.95	2117.	-2062.	2087.	.56	1.76	.54
7	3197.	1.00	2128.	-2062.	2088.	.56	1.83	.51
8	3312.	1.04	2128.	-2062.	2088.	.56	1.90	.54

CYCLIC TRIAXIAL TEST: C-5
FROG HOLLOW DAM

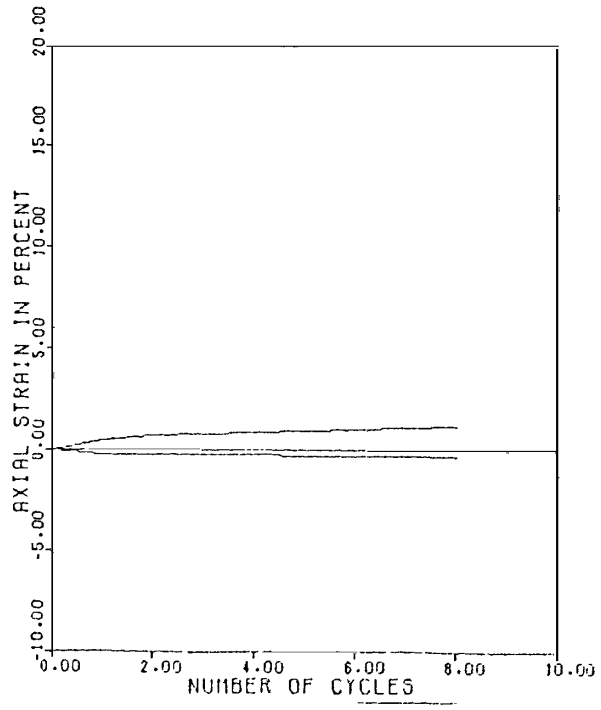

D118 UTAH DAMS FROG HOLLOW CYCLIC TX#FH6 TESTED 23AUG.82 REDUCED BY BU
BORING:FH-1 SAMPLE:FB-4/S-3 DEPTH:14.5-17.5 SILTY CLAY

INITIAL DRY DENSITY = 112.5 PCF
MOISTURE CONTENT = 17.0 PERCENT
DRY DENSITY AFTER CONSOL = 112.8 PCF
MOISTURE CONT AFTER CONSOL = 19.6 PERCENT
SIG1 = 2809.0 PSF
SIG3 = 1872.0 PSF
NC = 1.5
SIGMEAN = 2184.0 PSF

CYC. NO.	PORE PRES. (PSF)	PWP/SIG3	CYCLIC SHEAR STRESS(PSF) COMP.	TENS.	CUMUL. AVE. CYCL. SHEAR STRESS	TAU/SIGMEAN	AXIAL STRN. PERCENT P.TO P.	MEAN
1	1411.	.75	1137.	-1092.	1115.	.51	.68	.14
2	1584.	.85	1156.	-1110.	1119.	.51	.68	.24
3	1728.	.92	1174.	-1115.	1123.	.51	1.09	.27
4	1786.	.95	1178.	-1115.	1126.	.52	1.15	.31
5	1843.	.98	1183.	-1115.	1129.	.52	1.29	.31
6	1901.	1.02	1183.	-1115.	1130.	.52	1.36	.34
7	1930.	1.03	1183.	-1115.	1132.	.52	1.43	.37
8	1958.	1.05	1183.	-1115.	1133.	.52	1.49	.41

CYCLIC TRIAXIAL TEST: C-6
FROG HOLLOW DAM

IVINS DIVERSION DAM NO. 5

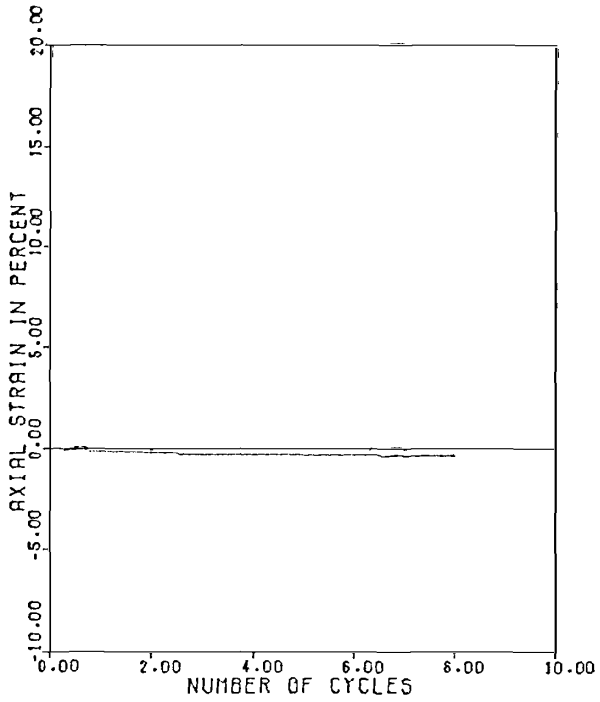

D118-UTAH DAMS-IVINS DIVERSION CYCLIC TX IV1 TESTED 7/30/82 RED. BY RW
BORING IV-1 SAMPLE PB-1/S-1 DEPTH 4.0-6.5 - SILTY SAND

INITIAL DRY DENSITY =	117.0 PCF
MOISTURE CONTENT =	11.5 PERCENT
DRY DENSITY AFTER CONSOL =	117.0 PCF
MOISTURE CONT AFTER CONSOL =	14.4 PERCENT
SIG1 =	720.0 PSF
SIG3 =	720.0 PSF
KC =	1.0
SIGMEAN =	720.0 PSF

CYC. NO.	PORE PRES. (PSF)	PUP/SIG3	CYCLIC SHEAR STRESS(PSF) COMP.	TENS.	CUMUL. AVE. CYCL. SHEAR STRESS	TAU/SIGMEAN	AXIAL STRN. PERCENT P.TO P.	MEAN
1	518.	.72	362.	-340.	351.	.49	.20	-.03
2	576.	.80	362.	-340.	351.	.49	.20	-.03
3	634.	.88	362.	-340.	351.	.49	.27	-.07
4	662.	.92	362.	-340.	351.	.49	.27	-.07
5	691.	.96	362.	-340.	351.	.49	.33	-.10
6	720.	1.00	362.	-340.	351.	.49	.33	-.10
7	749.	1.04	362.	-340.	351.	.49	.40	-.13
8	778.	1.08	362.	-340.	351.	.49	.40	-.13

CYCLIC TRIAXIAL TEST: C-1
IVINS DIVERSION DAM NO. 5

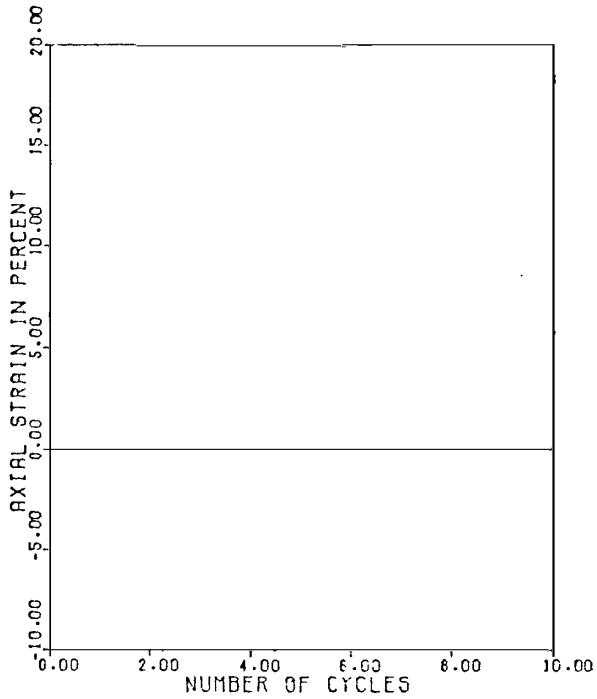

D118-UTAH DAMS-IVINS DIVERSION CYCLIC TX IV2 TESTED 7/30/82 RED. BY RU
BORING IV-3 SAMPLE PB-1/S-1 DEPTH 4.0-6.5 - SILTY SAND

INITIAL DRY DENSITY = 111.4 PCF
MOISTURE CONTENT = 13.2 PERCENT
DRY DENSITY AFTER CONSOL = 111.7 PCF
MOISTURE CONT AFTER CONSOL = 17.8 PERCENT
SIG1 = 1180.8 PSF
SIG3 = 1180.8 PSF
KC = 1.0
SIGMEAN = 1180.8 PSF

CYC. NO.	PORE PRES. (PSF)	PWP/SIG3	CYCLIC SHEAR STRESS(PSF) COMP.	CYCLIC SHEAR STRESS(PSF) TENS.	CUMUL. AVE. CYCL. SHEAR STRESS	TAU/SIGMEAN	AXIAL STRN. PERCENT P.TO P.	AXIAL STRN. PERCENT MEAN
1	346.	.29	443.	-376.	410.	.35	.00	.00
2	426.	.36	443.	-376.	410.	.35	.00	.00
3	484.	.41	443.	-376.	410.	.35	.00	.00
4	541.	.46	443.	-376.	410.	.35	.00	.00
5	576.	.49	443.	-376.	410.	.35	.00	.00
6	599.	.51	443.	-376.	410.	.35	.00	.00
7	645.	.55	443.	-376.	410.	.35	.00	.00
8	691.	.59	443.	-376.	410.	.35	.00	.00

CYCLIC TRIAXIAL TEST: C-2
IVINS DIVERSION DAM NO. 5

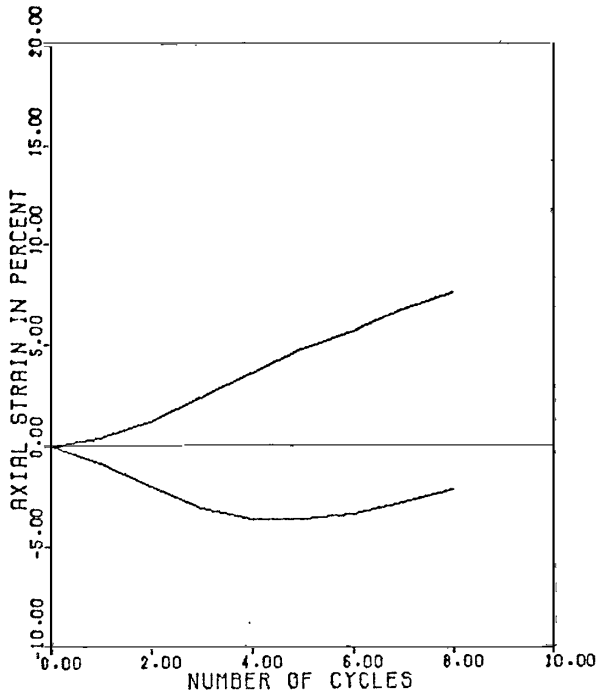

D118-UTAH DAMS-IVINS DIVERSION CYCLIC TRIAXIAL IV#3 8/4/82 BU
BORING IV-2 SAMPLE PB-4/S-3 DEPTH 16.0-18.5 SILTY SAND

INITIAL DRY DENSITY = 97.4 PCF
MOISTURE CONTENT = 14.3 PERCENT
DRY DENSITY AFTER CONSOL = 97.7 PCF
MOISTURE CONT AFTER CONSOL = 23.2 PERCENT
SIG1 = 1584.0 PSF
SIG3 = 1584.0 PSF
KC = 1.0
SIGMEAN = 1584.0 PSF

CYC. NO.	PORE PRES. (PSF)	PWP/SIG3	CYCLIC SHEAR STRESS(PSF) COMP.	TENS.	CUMUL. AVE. CYCL. SHEAR STRESS	TAU/SIGMEAN	AXIAL STRN. PERCENT P.TO P.	MEAN
1	576.	.36	749.	-697.	723.	.46	1.29	-.24
2	1198.	.76	754.	-635.	716.	.45	3.20	-.44
3	1590.	1.00	719.	-498.	698.	.44	5.45	-.41
4	1682.	1.06	586.	-353.	669.	.42	7.22	-.07
5	1705.	1.08	450.	-242.	637.	.40	8.38	.51
6	1716.	1.08	309.	-181.	604.	.38	8.99	1.09
7	1716.	1.08	291.	-176.	578.	.36	9.47	1.87
8	1716.	1.08	247.	-176.	555.	.35	9.67	2.59

CYCLIC TRIAXIAL TEST: C-3
IVINS DIVERSION DAM NO. 5

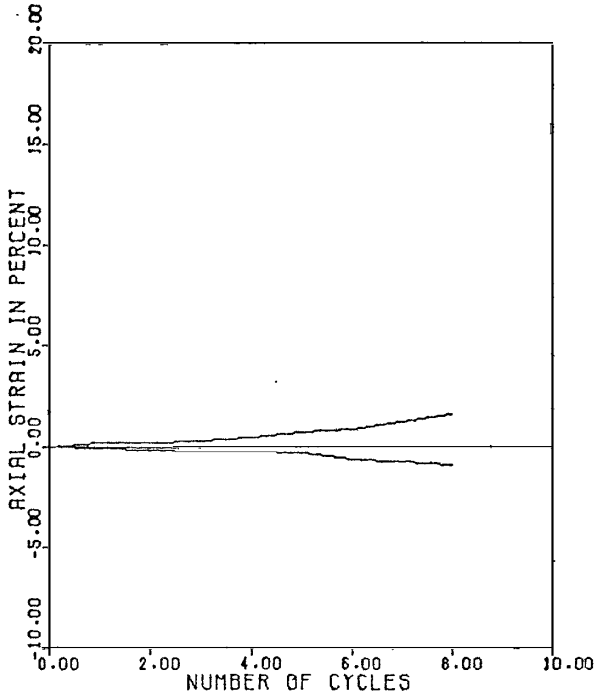

D118-UTAH DAMS-IVINS DIVERSION CYCLIC TRIAXIAL IV#4 8/4/82 BW
BORING IV-4 SAMPLE PB-2/S-1 DEPTH 8.0-10.5 SILTY SAND

INITIAL DRY DENSITY	=	106.1 PCF
MOISTURE CONTENT	=	16.6 PERCENT
DRY DENSITY AFTER CONSOL	=	106.3 PCF
MOISTURE CONT AFTER CONSOL	=	17.9 PERCENT
SIG1	=	763.2 PSF
SIG3	=	763.2 PSF
KC	=	1.0
SIGMEAN	=	763.2 PSF

CYC. NO.	PORE PRES. (PSF)	PWP/SIG3	CYCLIC SHEAR STRESS(PSF) COMP.	TENS.	CUMUL. AVE. CYCL. SHEAR STRESS	TAU/SIGMEAN	AXIAL STRN. PERCENT P.TO P.	MEAN
1	265.	.35	333.	-267.	300.	.39	.27	.07
2	415.	.54	340.	-280.	303.	.40	.40	.07
3	541.	.71	346.	-289.	305.	.40	.54	.07
4	634.	.83	355.	-294.	308.	.40	.74	.10
5	703.	.92	362.	-294.	310.	.41	1.01	.17
6	760.	1.00	368.	-294.	311.	.41	1.48	.13
7	795.	1.04	379.	-263.	312.	.41	1.95	.24
8	818.	1.07	372.	-263.	312.	.41	2.49	.37

CYCLIC TRIAXIAL TEST:C-4
IVINS DIVERSION DAM NO. 5

APPENDIX D

RESULTS OF POST-CYCLIC TRIAXIAL TESTS

GREEN'S LAKE DAM NO. 3

CONSOLIDATED UNDRAINED TRIAXIAL TEST
WITH PORE PRESSURE MEASUREMENT

PST.CYC.STAT.KC-1.0
D118-10AUG82
BORING:GL3-1 SAMPLE:PB-
CLAYEY SAND

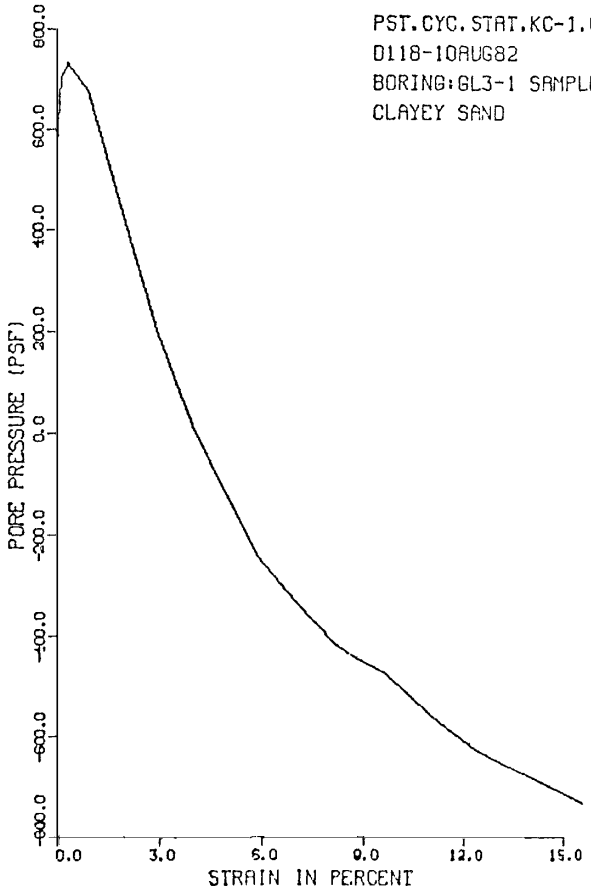

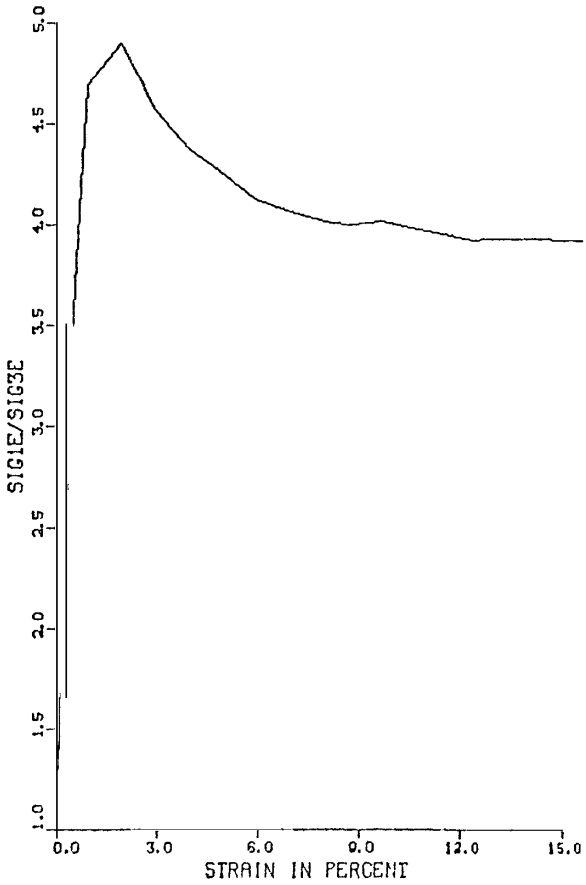

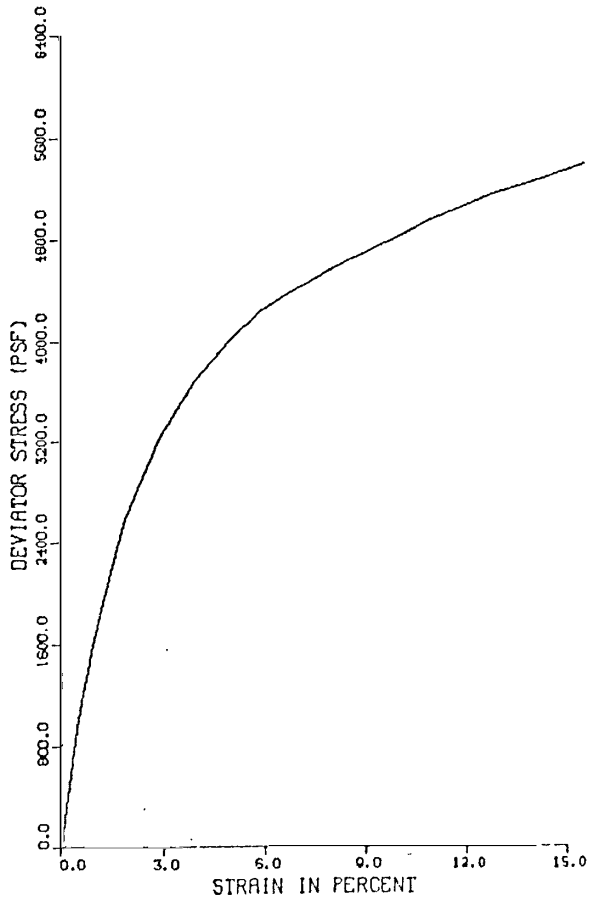

ISOTROPIC CONSOLIDATED UNDRAINED TRIAXIAL TEST
WITH PORE PRESSURE MEASUREMENTS
D118 UTAH DAMS-GREENS LAKE POST CYCLIC STATIC TX#GL1 TESTED 8/10/82 MLT

BORING:GL3-1 SAMPLE:PB-2/S-2 DEPTH:8.0-10.5

CLAYEY SAND

AT END OF CONSOLIDATION :
SAMPLE HEIGHT ..... = 5.983 INCHES
SAMPLE AREA ..... = 6.344 SQ. INCHES
EFFECTIVE CONFINING STRESS . = 1109. PSF
EFFECTIVE MAJOR PRIN. STRESS = 1109. PSF
PRINCIPAL STRESS RATIO ..... = 1.00

STRAIN PCT	SIGMA3E PSF	SIGMA1E PSF	RATIO SIG1E/SIG3E	PPRESS PSF	PBAR PSF	PTOT PSF	Q PSF
.0	547.	547.	1.0	562.	547.	1109.	0.
.2	403.	721.	1.8	706.	562.	1267.	159.
.3	389.	955.	2.5	720.	672.	1392.	283.
.4	374.	1076.	2.9	734.	725.	1459.	351.
.4	389.	1225.	3.2	720.	807.	1527.	418.
.5	389.	1337.	3.4	720.	863.	1583.	474.
1.0	432.	2028.	4.7	677.	1230.	1907.	798.
1.9	662.	3244.	4.9	446.	1953.	2400.	1291.
3.0	907.	4145.	4.6	202.	2526.	2728.	1619.
4.0	1094.	4777.	4.4	14.	2935.	2950.	1841.
5.1	1238.	5247.	4.2	-130.	3243.	3113.	2004.
6.0	1354.	5580.	4.1	-245.	3467.	3222.	2113.
7.0	1440.	5851.	4.1	-331.	3645.	3314.	2205.
8.2	1526.	6112.	4.0	-418.	3819.	3401.	2293.
8.8	1555.	6213.	4.0	-446.	3884.	3438.	2329.
9.7	1584.	6360.	4.0	-475.	3972.	3497.	2388.
11.0	1670.	6618.	4.0	-562.	4144.	3583.	2474.
12.4	1742.	6833.	3.9	-634.	4287.	3654.	2545.
12.9	1757.	6899.	3.9	-648.	4328.	3680.	2571.
13.8	1786.	7011.	3.9	-677.	4398.	3721.	2613.
15.6	1843.	7228.	3.9	-734.	4536.	3801.	2692.

POST CYCLIC STATIC TEST: PC-1
GREEN'S LAKE DAM NO. 3

CONSOLIDATED UNDRAINED TRIAXIAL TEST
WITH PORE PRESSURE MEASUREMENT

PST.CYC.STAT.TX.KG-1.0
D118-19AUG.82
BORING:GL3-2 SAMPLE:PB5
SILTY SAND

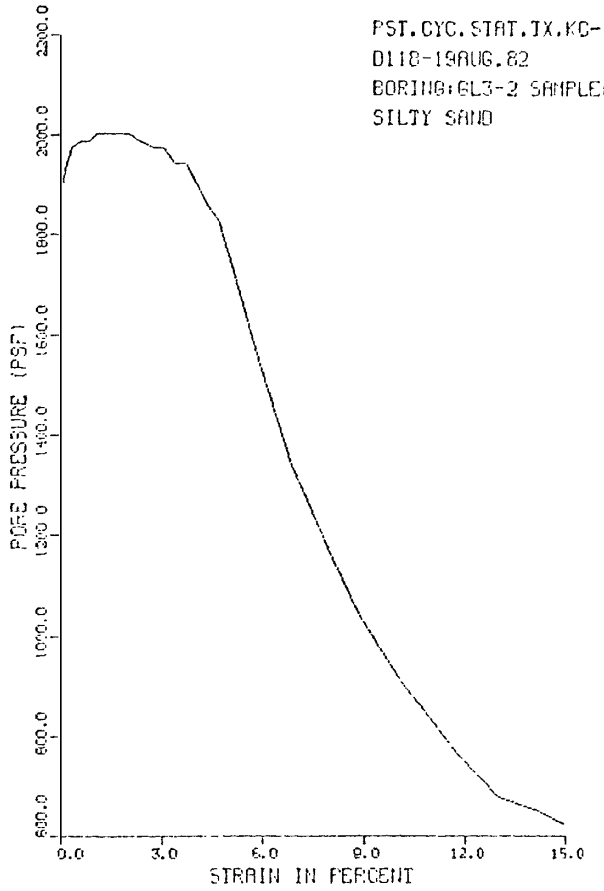

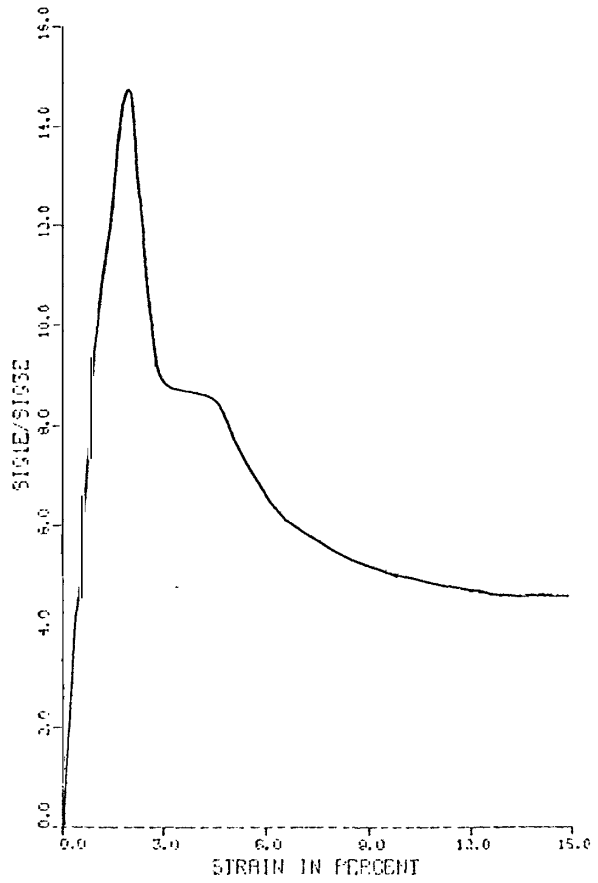

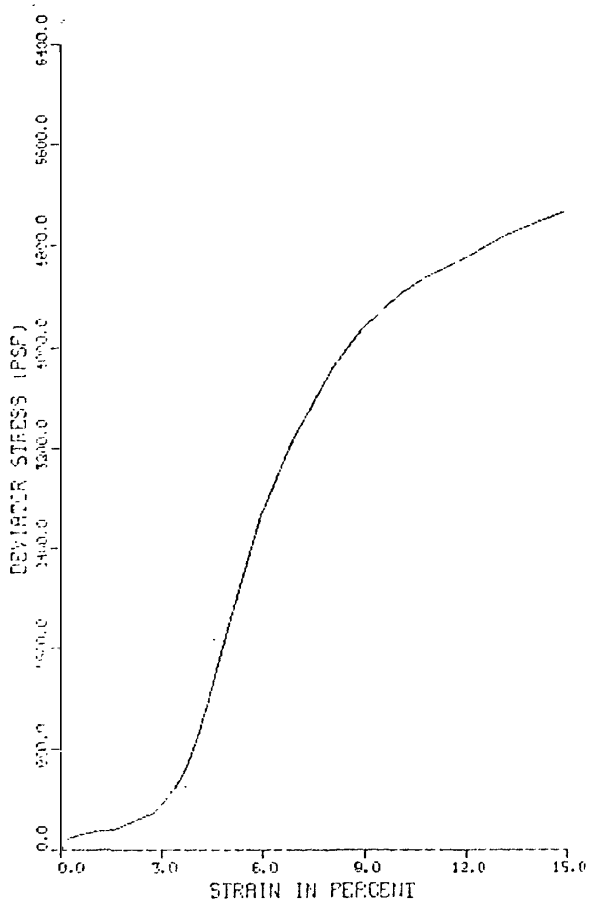

ISOTROPIC CONSOLIDATED UNDRAINED TRIAXIAL TEST
WITH PORE PRESSURE MEASUREMENTS
D119 UTAH DAMS GREENS LAKE POST CYCLIC STATIC TX&GL2 8/19/82 REV. BY PH

BORING:GL3-2 SAMPLE:PB-6/S-4 DEPTH=25.5-28.0

SILTY SAND

AT END OF CONSOLIDATION :
SAMPLE HEIGHT ..... = 5.851 INCHES
SAMPLE AREA ..... = 6.642 SQ. INCHES
EFFECTIVE CONFINING STRESS . = 2015. PSF
EFFECTIVE MAJOR PRIN. STRESS = 2016. PSF
PRINCIPAL STRESS RATIO ..... = 1.00

STRAIN PCT	SIGMA3E PSF	SIGMA1E PSF	RATIO SIG1E/SIG3E	PRESS PSF	PBAR PSF	PTOT PSF	Q PSF
.0	144.	144.	1.0	1872.	144.	2016.	0.
.2	96.	162.	1.7	1930.	124.	2054.	38.
.4	43.	140.	3.3	1973.	92.	2065.	49.
.6	29.	147.	5.1	1987.	88.	2075.	59.
.9	29.	158.	5.5	1987.	93.	2080.	64.
1.1	14.	154.	10.7	2002.	84.	2086.	70.
1.4	14.	164.	11.4	2002.	89.	2091.	75.
1.7	14.	185.	12.8	2002.	100.	2101.	85.
2.0	14.	216.	15.0	2002.	115.	2117.	101.
2.4	29.	272.	9.5	1987.	150.	2138.	122.
2.7	43.	328.	7.6	1973.	186.	2158.	142.
3.1	43.	411.	9.5	1973.	227.	2200.	184.
3.4	72.	554.	7.7	1944.	313.	2257.	241.
3.7	72.	708.	9.8	1944.	390.	2334.	318.
4.1	115.	968.	8.4	1901.	542.	2442.	426.
4.4	158.	1288.	8.1	1858.	723.	2581.	565.
4.7	187.	1644.	8.8	1829.	915.	2744.	728.
5.0	259.	2040.	7.9	1757.	1150.	2906.	890.
6.0	471.	3135.	6.6	1541.	1605.	3646.	1330.
6.9	677.	3937.	5.8	1333.	2307.	3640.	1630.
8.1	364.	4709.	5.4	1152.	2786.	3938.	1922.
8.9	979.	5106.	5.2	1037.	3043.	4079.	2063.
10.2	1109.	5540.	5.0	907.	3325.	4232.	2216.
11.0	1181.	5755.	4.9	835.	3463.	4303.	2287.
11.8	1251.	5929.	4.7	763.	3591.	4354.	2338.
13.0	1339.	6187.	4.6	677.	3763.	4440.	2424.
14.2	1348.	6253.	4.6	648.	3800.	4500.	2492.
15.0	1397.	6454.	4.6	619.	3926.	4545.	2529.

POST CYCLIC STATIC TEST: PC-2
GREEN'S LAKE DAM NO. 3

CONSOLIDATED UNDRAINED TRIAXIAL TEST
WITH PORE PRESSURE MEASUREMENT

PST.CYC.STAT.TX KC-1.0
D118-23AUG.82
BORING:GL3-2 SAMPLE:PB7
CLAYEY SAND

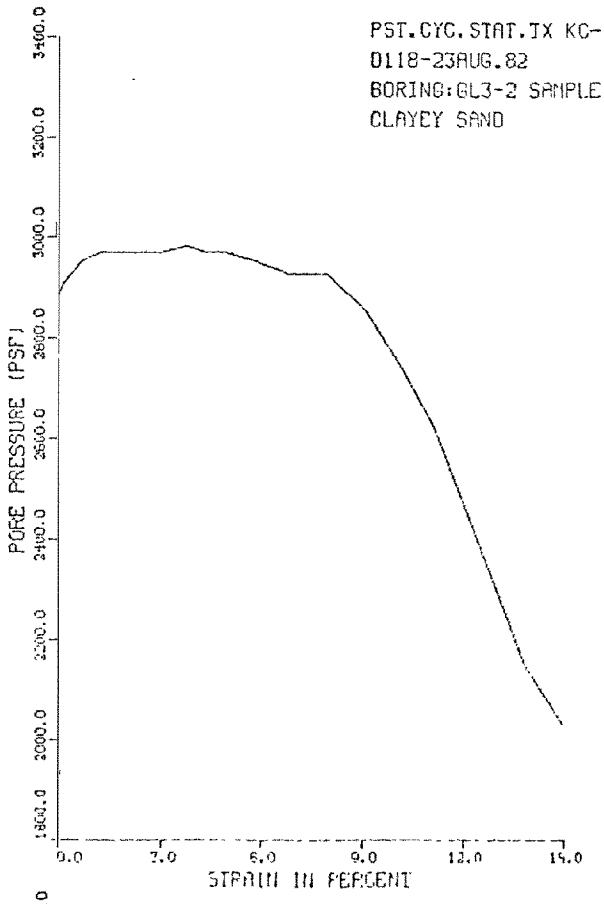

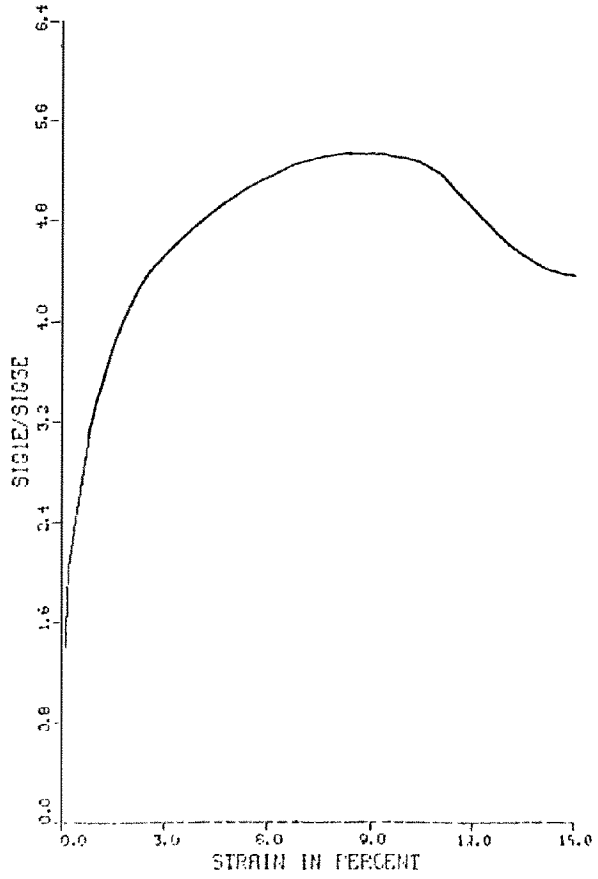

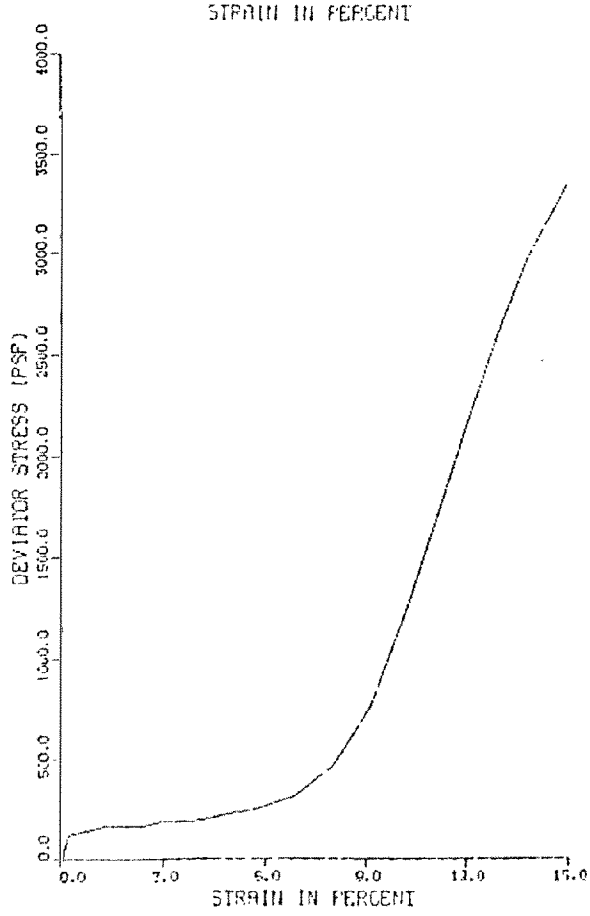

ISOTROPIC CONSOLIDATED UNDRAINED TRIAXIAL TEST
WITH PORE PRESSURE MEASUREMENTS
D118 UTAH DAMS GREENS LAKE POST CYCLIC STATIC TX#GL3 8/23/82 PED. BY EU

BORING:GL3-2 SAMPLE:PB-7/S-5 DEPTH:29.5-32.0

CLAYEY SAND

AT END OF CONSOLIDATION :
SAMPLE HEIGHT ..... = 6.358 INCHES
SAMPLE AREA ..... = 6.095 SQ. INCHES
EFFECTIVE CONFINING STRESS . = 3024. PSF
EFFECTIVE MAJOR PRIN. STRESS = 3024. PSF
PRINCIPAL STRESS RATIO ..... = 1.00

STRAIN PCT	SIGMA3E PSF	SIGMA1E PSF	RATIO SIG1E/SIG3E	PPRESS PSF	PBAR PSF	PIOT PSF	Q PSF
.0	144.	144.	1.0	2880.	144.	3024.	0.
.2	115.	233.	2.0	2909.	174.	3083.	59.
.8	72.	213.	3.0	2952.	142.	3094.	70.
1.3	58.	221.	3.8	2966.	139.	3105.	82.
1.9	58.	229.	3.8	2966.	139.	3105.	81.
2.5	58.	219.	3.8	2966.	133.	3105.	81.
3.0	58.	241.	4.2	2966.	149.	3116.	92.
3.9	43.	225.	5.2	2981.	134.	3115.	91.
4.4	58.	261.	4.5	2966.	159.	3126.	102.
5.0	58.	282.	4.9	2966.	170.	3136.	112.
5.8	72.	317.	4.4	2952.	194.	3146.	122.
6.9	101.	409.	4.1	2923.	255.	3178.	154.
8.0	101.	757.	5.5	2923.	329.	3252.	228.
9.1	173.	924.	5.3	2851.	548.	3400.	376.
10.2	288.	1518.	5.3	2736.	903.	3639.	615.
11.2	403.	2103.	5.2	2621.	1253.	3874.	850.
12.1	562.	2722.	4.8	2462.	1642.	4104.	1080.
13.0	720.	3311.	4.6	2304.	2016.	4320.	1296.
13.8	878.	3850.	4.4	2146.	2364.	4510.	1486.
15.0	994.	4327.	4.4	2030.	2660.	4691.	1667.

POST CYCLIC STATIC TEST: PC-3
GREEN'S LAKE DAM NO. 3

CONSOLIDATED UNDRAINED TRIAXIAL TEST
WITH PORE PRESSURE MEASUREMENT

PST.CYC.STAT.TX.KG-1.0
D118-27AUG.82
BORING:GL2-1 SAMPLE:PB2
SILTY SAND

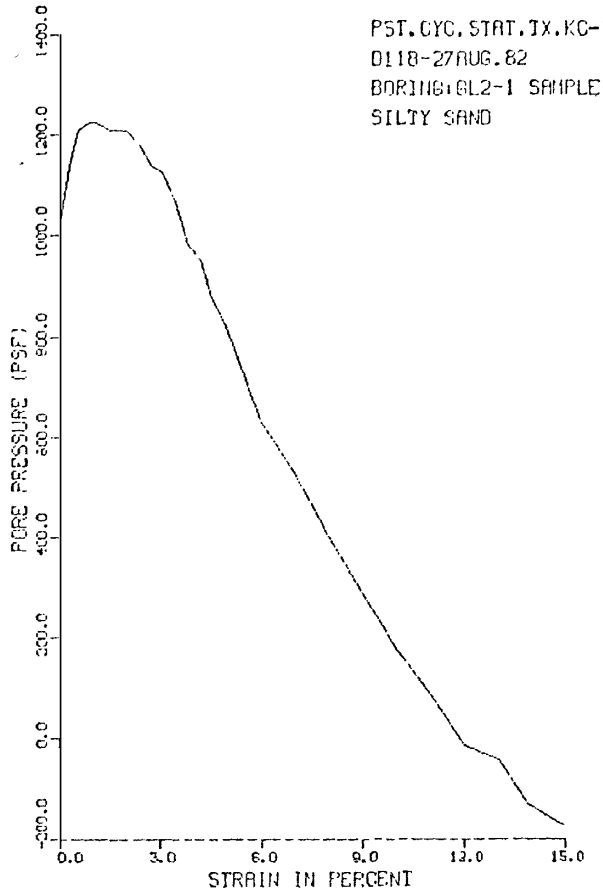

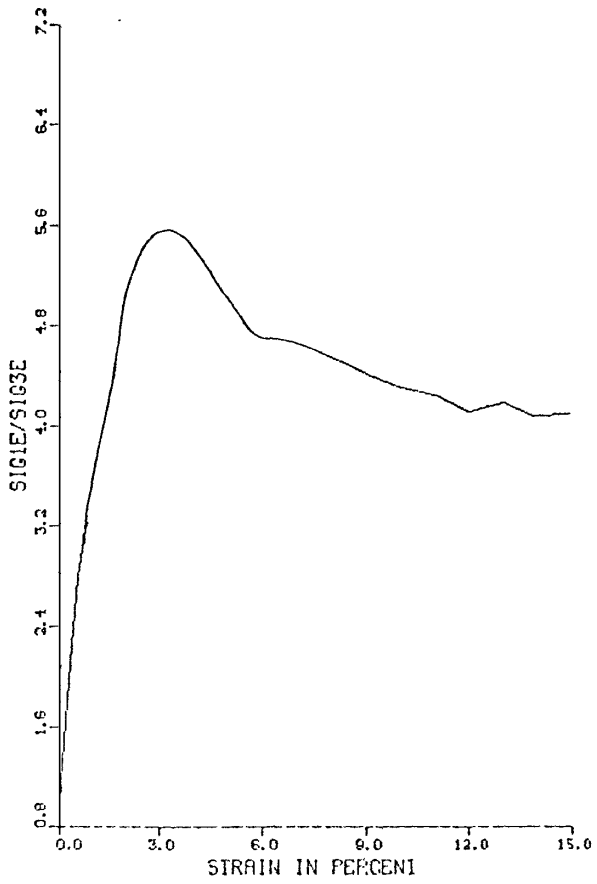

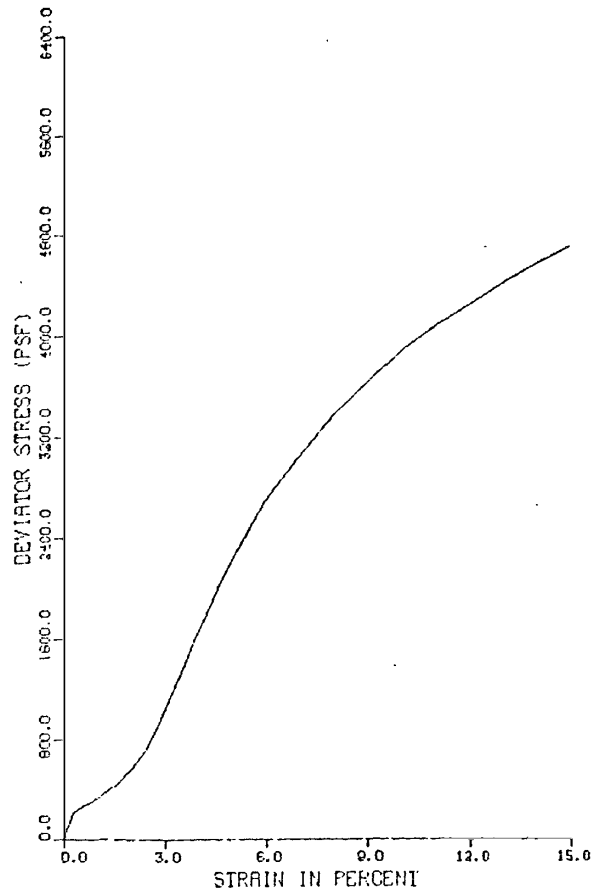

ISOTROPIC CONSOLIDATED UNDRAINED TRIAXIAL TEST
WITH PORE PRESSURE MEASUREMENTS
D118- ITAY DAMS-GREENS LAKE POST CYCLIC STATIC TRIAXIAL 8/27/82 REC. BY S

BORING:GL2-1 SAMPLE:PB2/S-1 DEPTH:8.0-10.5

SILTY SAND

AT END OF CONSOLIDATION :
SAMPLE HEIGHT ..... = 5.930 INCHES
SAMPLE AREA ..... = 6.139 SQ. INCHES
EFFECTIVE CONFINING STRESS . = 1354. PSF
EFFECTIVE MAJOR PRIN. STRESS = 1354. PSF
PRINCIPAL STRESS RATIO ..... = 1.00

STRAIN PCT	SIGMA3E PSF	SIGMA1E PSF	RATIO SIG1E/SIG3E	PRESS PSF	-PAR PSF	SQOT PSF	Q PSF
.0	731.	731.	1.0	1022.	331.	1354.	0.
.3	216.	427.	2.0	1138.	321.	1459.	105.
.6	144.	400.	2.8	1210.	272.	1482.	128.
.9	120.	432.	3.3	1224.	281.	1505.	151.
1.2	120.	477.	3.9	1224.	303.	1527.	174.
1.5	144.	560.	3.9	1210.	350.	1561.	208.
2.0	144.	718.	5.0	1210.	431.	1641.	287.
2.4	173.	882.	5.1	1181.	528.	1708.	355.
2.9	216.	1105.	5.1	1138.	661.	1798.	445.
3.3	259.	1344.	5.2	1103.	787.	1890.	537.
3.8	288.	1624.	5.6	1066.	956.	2021.	668.
3.9	331.	1933.	5.8	978.	1164.	2143.	789.
4.3	403.	2290.	5.7	950.	1402.	2352.	998.
4.4	475.	2467.	5.2	878.	1471.	2350.	996.
5.0	532.	2761.	5.2	821.	1647.	2468.	1114.
6.0	720.	3411.	4.7	634.	2063.	2698.	1345.
7.0	921.	7854.	4.7	703.	2537.	1370.	1517.
8.0	980.	4337.	4.4	444.	2644.	3047.	1693.
9.0	1044.	4714.	4.4	380.	2884.	3178.	1824.
10.0	1191.	5085.	4.3	163.	3173.	3396.	1752.
11.0	1247.	5378.	4.3	94.	3363.	3469.	2055.
12.0	1268.	5659.	4.5	-14.	3501.	3439.	2125.
13.0	1307.	5843.	4.5	-43	3620.	3577.	2223.
13.9	1423.	6049.	4.3	-130.	3766.	3636.	2283.
15.0	1526.	6252.	4.1	-173.	3898.	3726.	2364.

POST CYCLIC STATIC TEST: PC-4
GREEN'S LAKE DAM NO. 3

WARNER DRAW DAM

CONSOLIDATED UNDRAINED TRIAXIAL TEST
WITH PORE PRESSURE MEASUREMENT

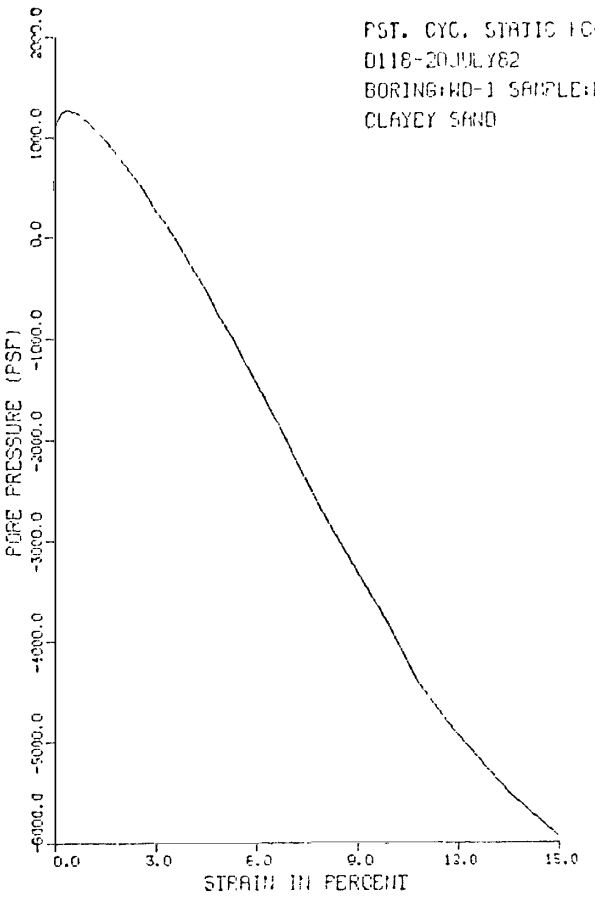

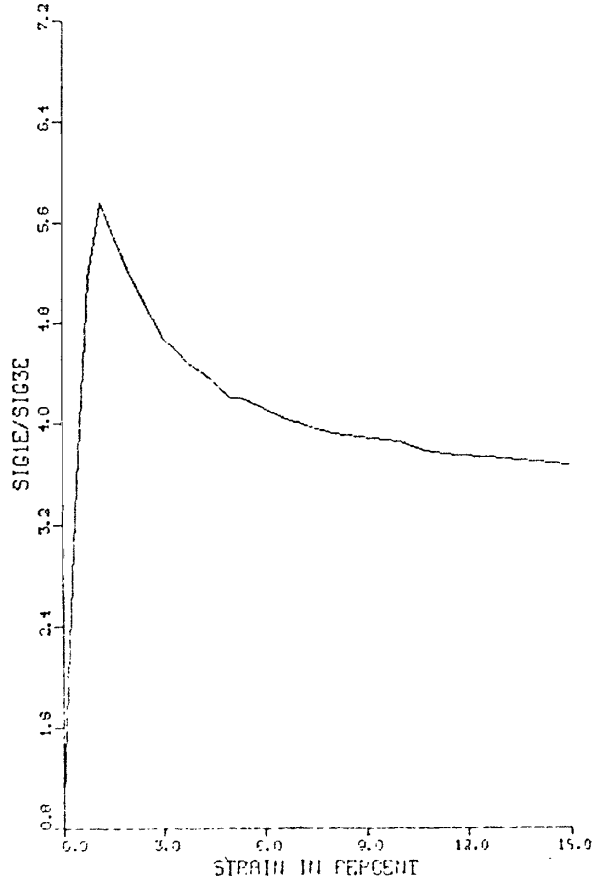

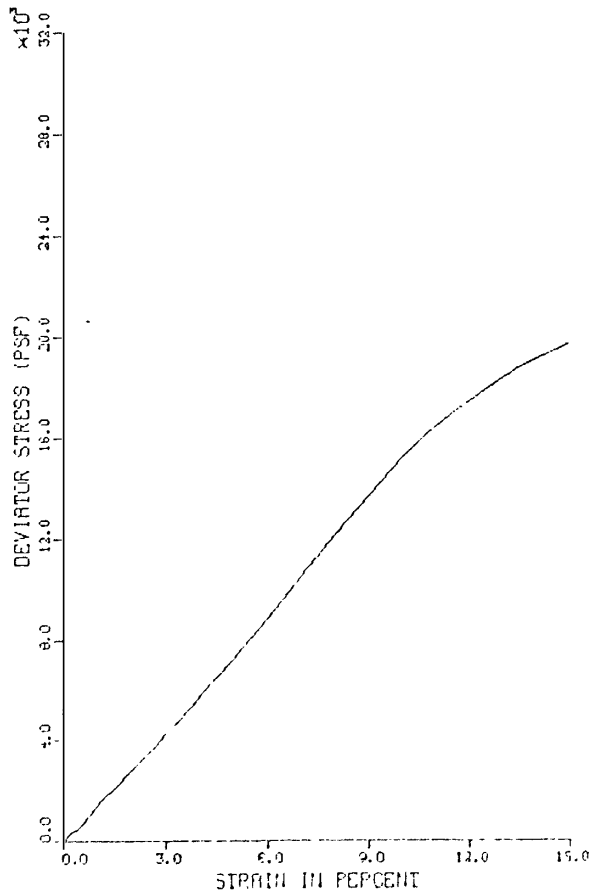

ISOTROPIC CONSOLIDATED UNDRAINED TRIAXIAL TEST
WITH PORE PRESSURE MEASUREMENTS
D118-UTAH DAMS-WARNER DRAW POST CYCLIC STATIC TX#1 7/20/82 RED. BY BW

BORING:WD-1 SAMPLE:PB-2/S-2 DEPTH:8.5-11.0

CLAYEY SAND

AT END OF CONSOLIDATION :
SAMPLE HEIGHT ..... = 6.054 INCHES
SAMPLE AREA ..... = 6.414 SQ. INCHES
EFFECTIVE CONFINING STRESS . = 1440. PSF
EFFECTIVE MAJOR PRIN. STRESS = 1440. PSF
PRINCIPAL STRESS RATIO ..... = 1.00

STRAIN PCT	SIGMA3E PSF	SIGMA1E PSF	RATIO SIG1E/SIG3E	PPRESS PSF	PBAR PSF	PTOT PSF	Q PSF
.0	331.	331.	1.0	1109.	331.	1440.	0.
.2	216.	435.	2.2	1224.	350.	1574.	134.
.4	197.	612.	3.3	1243.	400.	1652.	212.
.6	202.	849.	4.2	1238.	525.	1764.	324.
.8	230.	1188.	5.2	1210.	709.	1919.	479.
1.2	331.	1907.	5.8	1109.	1119.	2228.	788.
1.6	475.	2597.	5.5	965.	1536.	2501.	1061.
2.0	634.	3319.	5.2	806.	1976.	2783.	1343.
2.3	792.	3972.	5.0	648.	2382.	3030.	1590.
2.7	965.	4657.	4.8	475.	2811.	3286.	1846.
3.0	1152.	5375.	4.7	288.	3264.	3552.	2112.
3.4	1325.	6074.	4.6	115.	3700.	3815.	2375.
3.8	1526.	6820.	4.5	-86.	4173.	4087.	2647.
4.1	1714.	7547.	4.4	-274.	4630.	4357.	2917.
4.5	1915.	8306.	4.3	-475.	5110.	4635.	3195.
5.0	2246.	9434.	4.2	-806.	5840.	5034.	3594.
5.3	2419.	10157.	4.2	-979.	6288.	5309.	3869.
6.7	3269.	13199	4.0	-1829.	8234.	6405.	4965.
9.0	4162.	16302.	3.9	-2722.	10232.	7510.	6070.
10.0	5279.	20453.	3.9	-3839.	12876.	9017.	7577.
10.8	5818.	21983.	3.8	-4378.	13900.	9523.	8083.
11.7	6235.	23302.	3.8	-4795.	14809.	10014.	8574.
12.6	6610.	24676.	3.7	-5170.	15633.	10463.	9023.
13.6	6975.	25799.	3.7	-5515.	16377.	10862.	9422.
15.0	7387.	27139.	3.7	-5947.	17263.	11316.	9876.

POST CYCLIC STATIC TEST: PC-1
WARNER DRAW DAM

CONSOLIDATED UNDRAINED TRIAXIAL TEST
WITH PORE PRESSURE MEASUREMENT

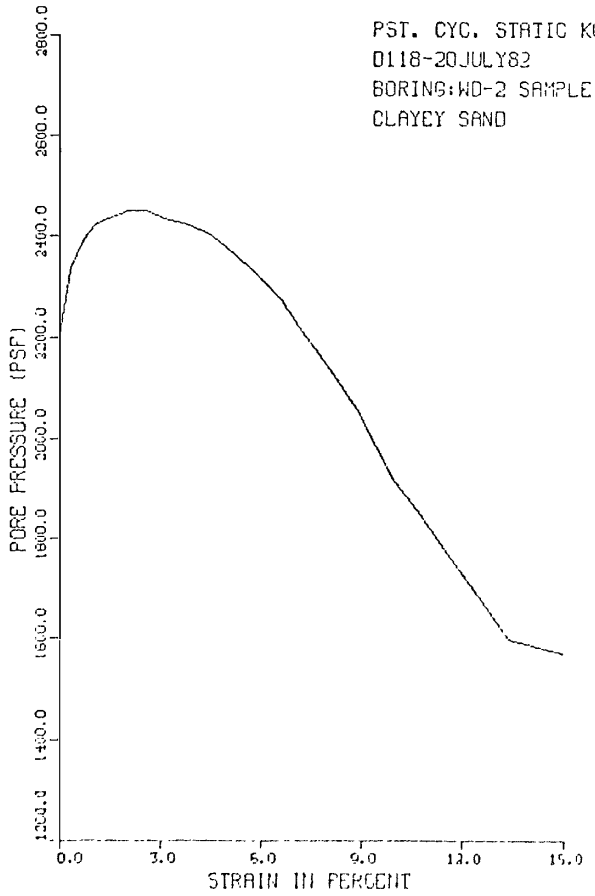

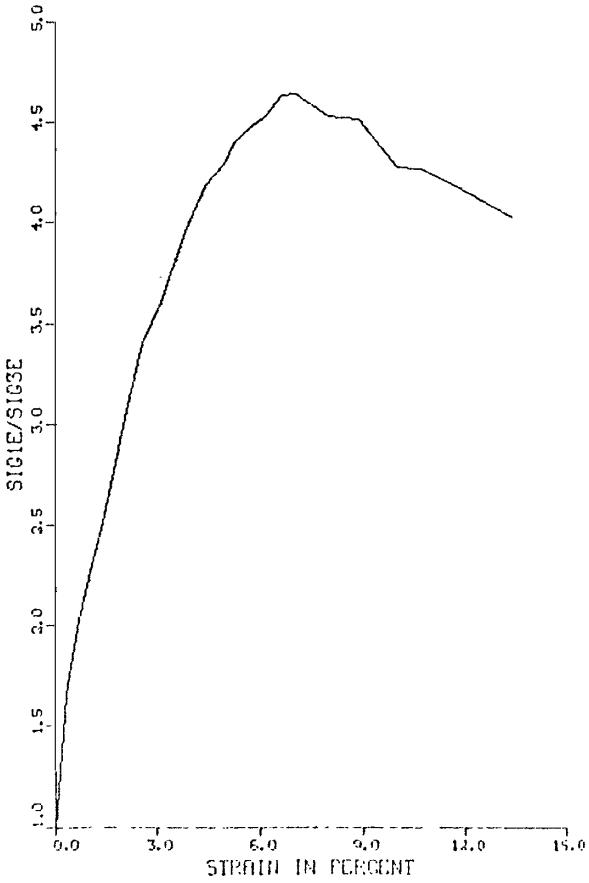

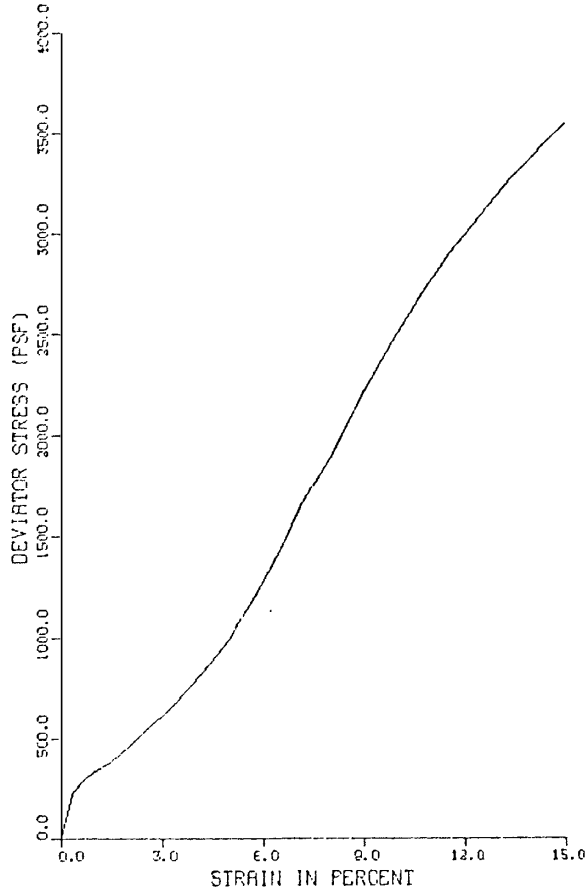

ISOTROPIC CONSOLIDATED UNDRAINED TRIAXIAL TEST
WITH PORE PRESSURE MEASUREMENTS
D118-UTAH DAMS-WARNER DRAW POST CYCLIC STATIC TX42 7/20/82 REV. BY BU

BORING:WD-2 SAMPLE:PS-6/S-6 DEPTH:24.5-27.0

CLAYEY SAND

AT END OF CONSOLIDATION :

SAMPLE HEIGHT	=	6.128 INCHES
SAMPLE AREA	=	6.339 SQ. INCHES
EFFECTIVE CONFINING STRESS .	=	2678. PSF
EFFECTIVE MAJOR PRIN. STRESS	=	2678. PSF
PRINCIPAL STRESS RATIO	=	1.00

STRAIN PCT	SIGMA3E PSF	SIGMA1E PSF	RATIO SIG1E/SIG3E	PRESS PSF	PBAR PSF	PTOT PSF	Q PSF
.0	475.	475.	1.0	2203.	475.	2678.	0.
.3	346.	572.	1.7	2333.	459.	2792.	113.
.7	288.	581.	2.0	2390.	435.	2825.	147.
1.1	259.	596.	2.3	2419.	428.	2847.	168.
1.5	245.	625.	2.6	2434.	435.	2869.	190.
2.1	230.	698.	3.0	2448.	464.	2912.	234.
2.6	230.	783.	3.4	2448.	507.	2955.	277.
3.2	245.	883.	3.6	2434.	564.	2997.	319.
3.9	259.	1023.	3.9	2419.	641.	3060.	382.
4.4	274.	1142.	4.2	2405.	708.	3113.	434.
5.0	302.	1295.	4.3	2376.	799.	3175.	496.
5.3	317.	1393.	4.4	2362.	855.	3216.	538.
5.7	346.	1545.	4.5	2333.	945.	3278.	600.
6.2	374.	1696.	4.5	2304.	1035.	3339.	661.
6.6	403.	1847.	4.6	2275.	1125.	3410.	732.
7.1	446.	2072.	4.6	2232.	1259.	3491.	813.
8.0	533.	2414.	4.5	2146.	1474.	3619.	941.
8.9	612.	2723.	4.5	2069.	1706.	3745.	1067.
10.0	763.	3257.	4.3	1915.	2010.	3935.	1247.
10.7	821.	3500.	4.3	1858.	2160.	4018.	1339.
11.6	907.	3800.	4.2	1771.	2354.	4125.	1446.
13.4	1080.	4346.	4.0	1598.	2713.	4311.	1633.
14.0	1109.	4642.	4.2	1570.	2876.	4445.	1767.

POST CYCLIC STATIC TEST: PC-2
WARNER DRAW DAM

CONSOLIDATED UNDRAINED TRIAXIAL TEST
WITH PORE PRESSURE MEASUREMENT

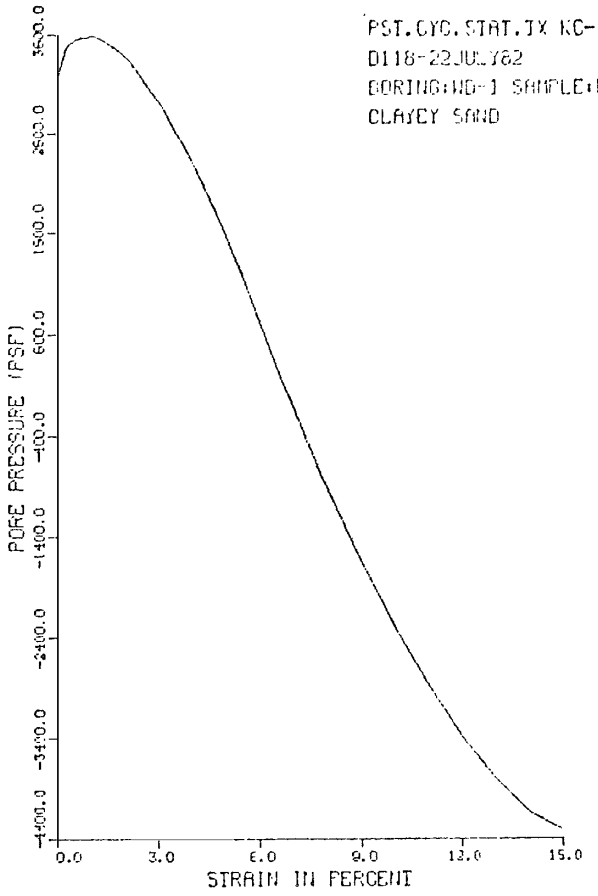

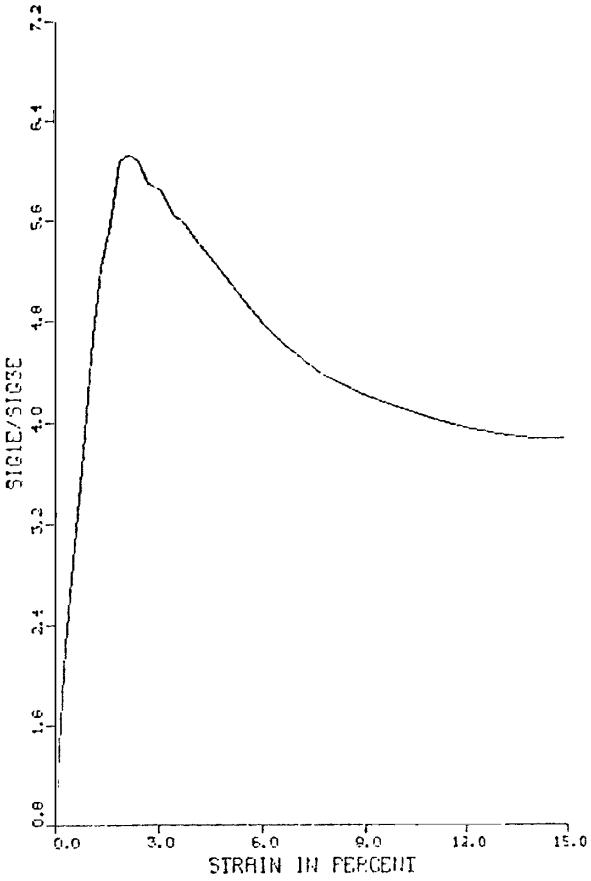

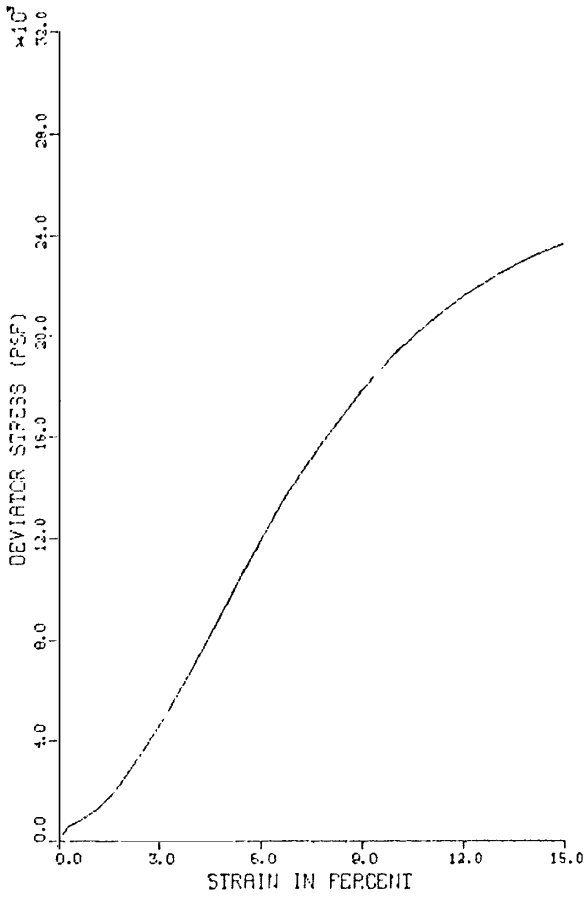

ISOTROPIC CONSOLIDATED UNDRAINED TRIAXIAL TEST
WITH PORE PRESSURE MEASUREMENTS
D118-UTAH DAMS-WARNER DRAW POST CYCLIC STATIC TX#3 7/22/82 REV. BY BW

BORING:WD-1 SAMPLE:PB-10/S-10 DEPTH:41.0-43.5

CLAYEY SAND

AT END OF CONSOLIDATION :
SAMPLE HEIGHT ..... = 5.985 INCHES
SAMPLE AREA ..... = 6.448 SQ. INCHES
EFFECTIVE CONFINING STRESS . = 3902. PSF
EFFECTIVE MAJOR PRIN. STRESS = 3902. PSF
PRINCIPAL STRESS RATIO ..... = 1.00

STRAIN PCT	SIGMA3E PSF	SIGMA1E PSF	RATIO SIG1E/SIG3E	PPRESS PSF	PRAR PSF	PTOT PSF	Q PSF
.0	763.	763.	1.0	3139.	763.	3902.	0.
.3	432.	966.	2.2	3470.	699.	4170.	267.
.6	360.	1093.	3.0	3542.	726.	4269.	366.
.9	346.	1298.	3.8	3557.	822.	4378.	476.
1.1	331.	1546.	4.7	3571.	938.	4510.	607.
1.4	360.	1879.	5.2	3542.	1120.	4662.	760.
1.7	418.	2328.	5.6	3485.	1373.	4858.	955.
2.0	475.	2884.	6.1	3427.	1679.	5107.	1204.
2.2	576.	3524.	6.1	3326.	2050.	5376.	1474.
2.5	691.	4197.	6.1	3211.	2444.	5655.	1753.
2.8	835.	4917.	5.9	3067.	2876.	5943.	2041.
3.1	1008.	5875.	5.8	2894.	3441.	6336.	2433.
3.5	1224.	6913.	5.6	2678.	4068.	6747.	2844.
3.9	1440.	8007.	5.6	2462.	4725.	7187.	3285.
4.2	1699.	9184.	5.4	2203.	5442.	7645.	3742.
5.0	2261.	11639.	5.1	1642.	6950.	8592.	4689.
5.6	2736.	13556.	5.0	1166.	8146.	9312.	5410.
6.1	3226.	15406.	4.8	677.	9316.	9993.	6090.
6.7	3730.	17212.	4.6	173.	10471.	10644.	6741.
7.3	4205.	18888.	4.5	-302.	11546.	11244.	7341.
7.9	4680.	20464.	4.4	-778.	12572.	11794.	7892.
9.0	5544.	23383.	4.2	-1642.	14463.	12822.	8919.
10.0	6192.	25506.	4.1	-2290.	15849.	13559.	9657.
11.0	6754.	27243.	4.0	-2851.	16998.	14147.	10245.
12.0	7286.	28842.	4.0	-3384.	18064.	14680.	10778.
13.0	7704.	30061.	3.9	-3802.	18882.	15081.	11178.
14.1	8050.	31138.	3.9	-4147.	19594.	15447.	11544.
15.0	8208.	31805.	3.9	-4306.	20006.	15701.	11798.

POST CYCLIC STATIC TEST: PC-3
WARNER DRAW DAM

CONSOLIDATED UNDRAINED TRIAXIAL TEST
WITH PORE PRESSURE MEASUREMENT

PST.CYC.STAT.TX. KC-1.0
D118-22JULY82
BORING:WD-1 SAMPLE:PB13
CLAYEY SAND

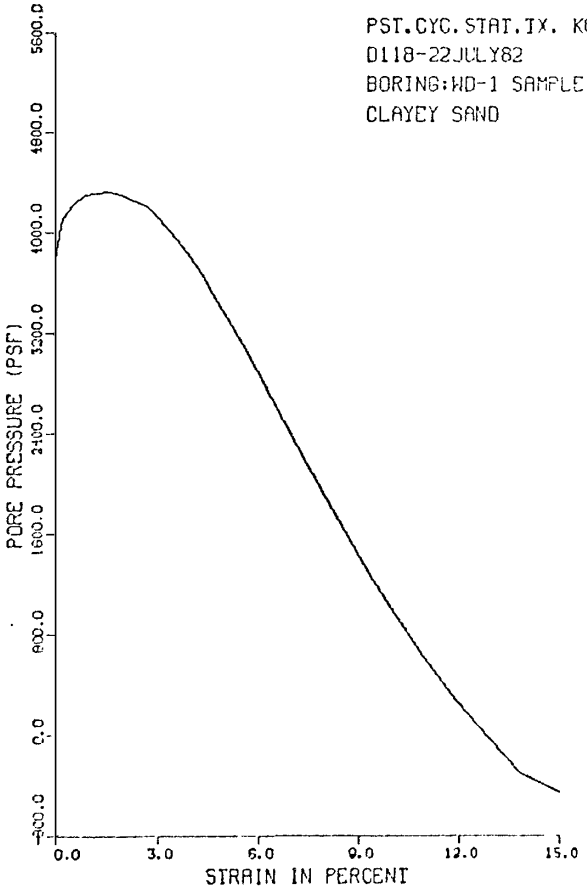

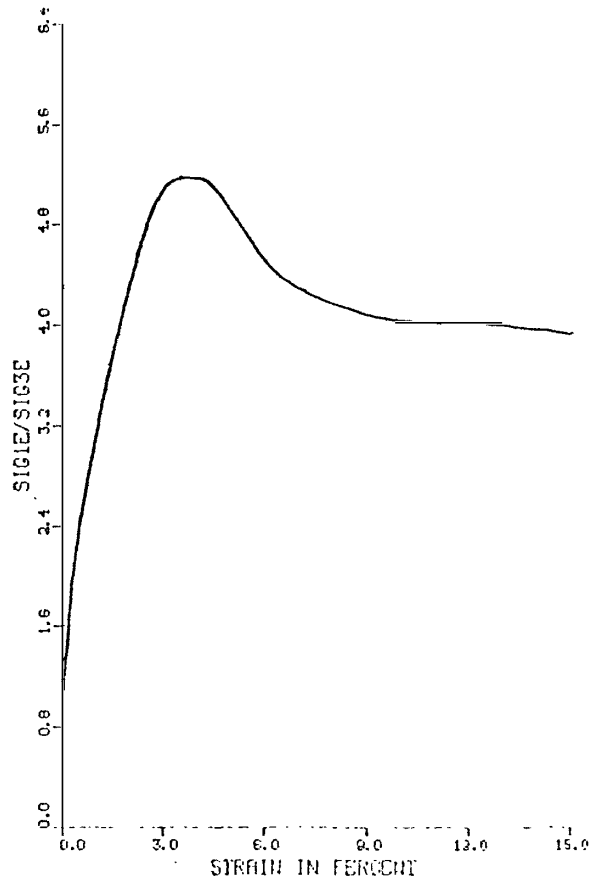

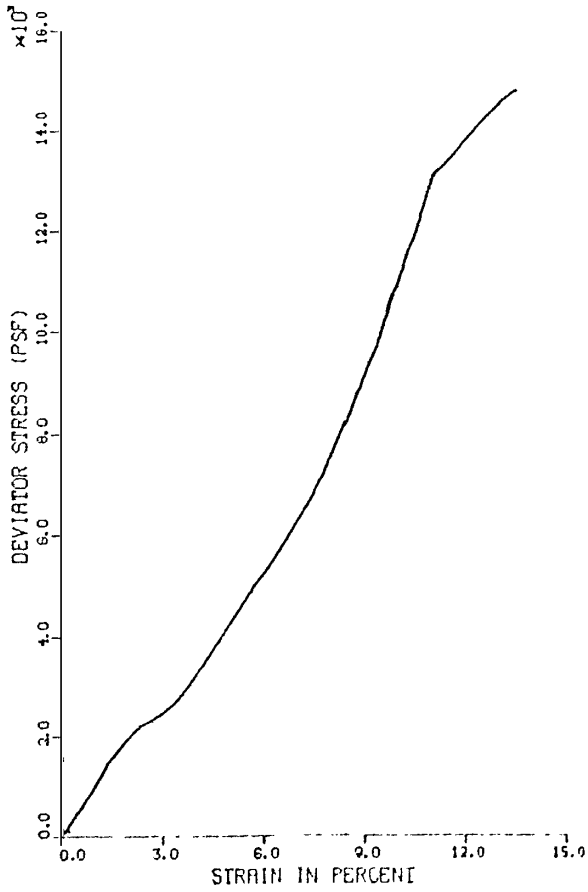

ISOTROPIC CONSOLIDATED UNDRAINED TRIAXIAL TEST
WITH PORE PRESSURE MEASUREMENTS
D118-UTAH DAMS-WARNER DRAW POST CYCLIC STATIC TX#4 7/22/82 RED. BY FU

BORING:WD-1 SAMPLE:PB-13/S-13 DEPTH:53.0-55.5

CLAYEY SAND

AT END OF CONSOLIDATION :
SAMPLE HEIGHT ..... = 5.963 INCHES
SAMPLE AREA ..... = 6.402 SQ. INCHES
EFFECTIVE CONFINING STRESS . = 4810. PSF
EFFECTIVE MAJOR PRIN. STRESS = 4810. PSF
PRINCIPAL STRESS RATIO ..... = 1.00

STRAIN PCT	SIGMA3E PSF	SIGMA1E PSF	RATIO SIG1E/SIG3E	PEFFSS PSF	PBAR PSF	PTOT PSF	Q PSF
.0	1022.	1022.	1.0	3787.	1022.	4810.	0.
.3	706.	1266.	1.8	4104.	986.	5090.	200.
.6	590.	1351.	2.3	4219.	971.	5190.	300.
.9	518.	1427.	2.8	4291.	998.	5289.	477.
1.2	504.	1659.	3.3	4306.	1082.	5387.	578.
1.7	490.	1927.	3.9	4320.	1208.	5528.	719.
2.0	518.	2038.	4.3	4291.	1378.	5669.	860.
2.4	562.	2318.	4.1	4248.	1440.	5688.	878.
2.7	605.	2902.	4.8	4205.	1754.	5958.	1149.
3.0	677.	3445.	5.1	4133.	2062.	6194.	1385.
3.4	778.	4016.	5.2	4032.	2397.	6429.	1619.
3.7	878.	4561.	5.2	3931.	2720.	6651.	1841.
4.0	1008.	5148.	5.1	3802.	3091.	6893.	2083.
4.4	1138.	5809.	5.1	3672.	3471.	7143.	2334.
4.7	1276.	6561.	5.0	3514.	3879.	7392.	2583.
5.0	1406.	6950.	4.9	3381.	4193.	7577.	2767.
5.6	1699.	7849.	4.6	3110.	4789.	7900.	3090.
7.7	2756.	9936.	3.6	2074.	6246.	8320.	3510.
9.1	3398.	12268.	3.6	1411.	8093.	9504.	4695.
10.0	3816.	14479.	3.8	994.	9385.	10387.	5577.
11.0	4159.	17049.	4.1	619.	10719.	11439.	6629.
11.9	4556.	18364.	4.0	274.	11450.	11723.	6914.
12.9	4878.	19756.	4.0	-9.	12097.	12069.	7259.
13.9	5112.	20167.	3.9	-302.	12639.	12337.	7527.
15.0	5279.	20568.	3.9	-461.	12089.	12478.	7619.

POST CYCLIC STATIC TEST:PC-4
WARNER DRAW DAM

CONSOLIDATED UNDRAINED TRIAXIAL TEST
WITH PORE PRESSURE MEASUREMENT

PST.CYC.STAT.KC-1.5
D118-16AUG82
BORING:WD-1 SAMPLE:PB-6
SILTY SAND

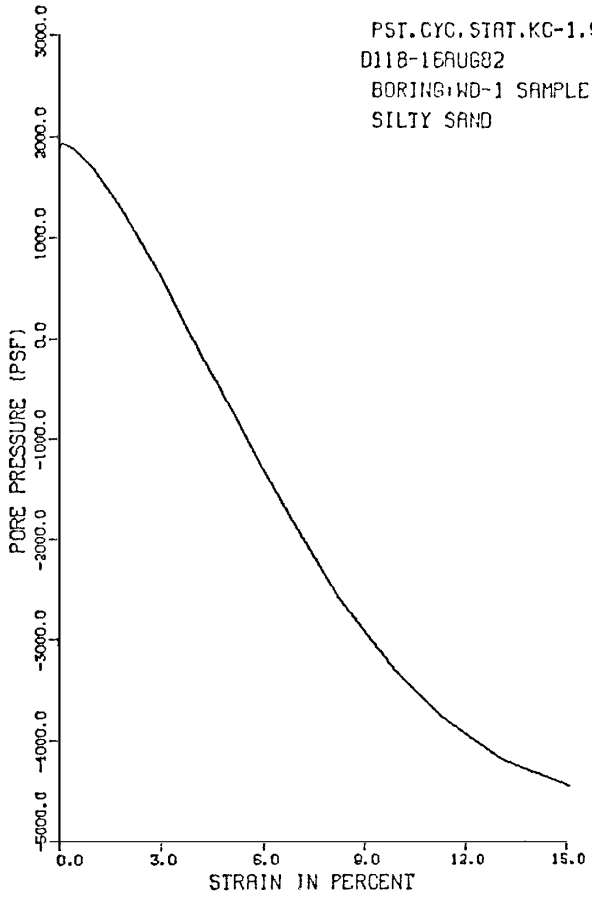

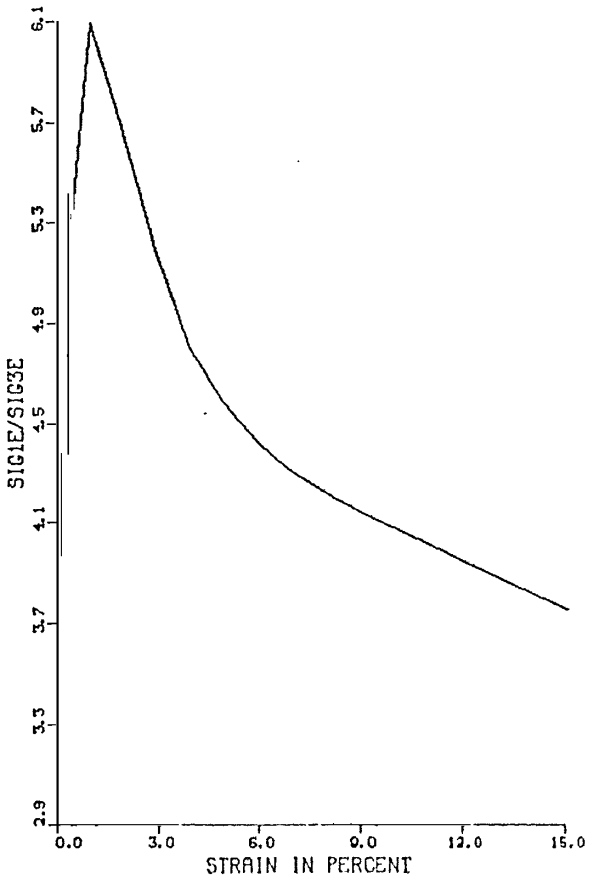

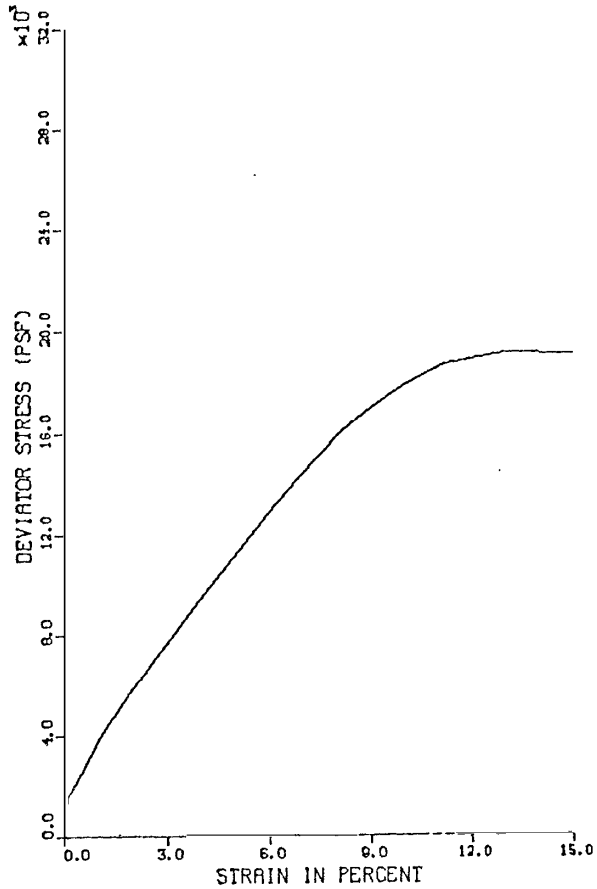

ANISOTROPIC CONSOLIDATED UNDRAINED TRIAXIAL TEST
WITH PORE PRESSURE MEASUREMENTS
D118-UTAH DAMS-WARNER DRAW DAM POST CYCLIC STATIC TX#WD5 TESTED 8/16/82

BORING:WD-1 SAMPLE:PB-6/S-6 DEPTH:24.5-27.0

SILTY SAND

AT END OF CONSOLIDATION :
SAMPLE HEIGHT ..... = 5.734 INCHES
SAMPLE AREA ..... = 6.715 SQ. INCHES
EFFECTIVE CONFINING STRESS . = 2448. PSF
EFFECTIVE MAJOR PRIN. STRESS = 3672. PSF
PRINCIPAL STRESS RATIO ..... = 1.50

STRAIN PCT	SIGMA3E PSF	SIGMA1E PSF	RATIO SIG1E/SIG3E	PPRESS PSF	PBAR PSF	PTOT PSF	Q PSF
.0	605.	1784.	3.0	1843.	1194.	3038.	590.
.1	533.	2054.	3.9	1915.	1293.	3209.	761.
.2	518.	2231.	4.3	1930.	1375.	3304.	856.
.5	576.	3062.	5.3	1872.	1819.	3691.	1243.
1.0	763.	4647.	6.1	1685.	2705.	4390.	1942.
2.0	1210.	6897.	5.7	1238.	4053.	5292.	2844.
3.0	1800.	9342.	5.2	648.	5571.	6219.	3771.
4.0	2462.	11817.	4.8	-14.	7140.	7125.	4677.
5.0	3082.	14136.	4.6	-634.	8609.	7975.	5527.
6.0	3744.	16560.	4.4	-1296.	10152.	8856.	6408.
6.9	4277.	18460.	4.3	-1829.	11369.	9540.	7092.
8.2	4997.	21005.	4.2	-2549.	13001.	10452.	8004.
9.1	5414.	22390.	4.1	-2966.	13902.	10936.	8488.
10.0	5774.	23549.	4.1	-3326.	14662.	11335.	8887.
11.3	6221.	24855.	4.0	-3773.	15538.	11765.	9317.
13.1	6638.	25749.	3.9	-4190.	16194.	12003.	9555.
15.1	6912.	25945.	3.8	-4464.	16429.	11965.	9517.

POST CYCLIC STATIC TEST:PC-5
WARNER DRAW DAM

FROG HOLLOW DAM

Earth Sciences Associates

CONSOLIDATED UNDRAINED TRIAXIAL TEST
WITH PORE PRESSURE MEASUREMENT

PST.CYC.STAT. KC-1.0
D118-28JULY82
BORING:FH1 SAMPLE:PB4
SILTY CLAY

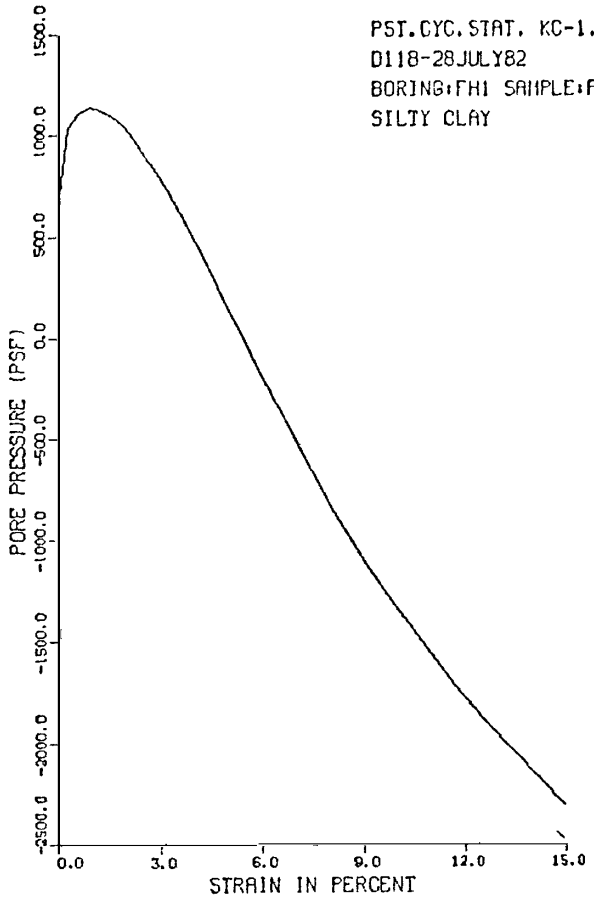

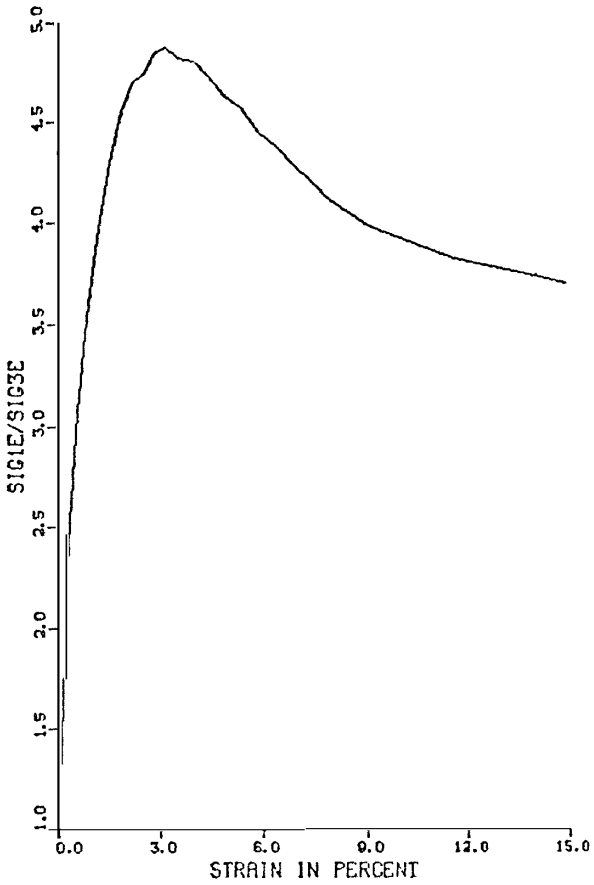

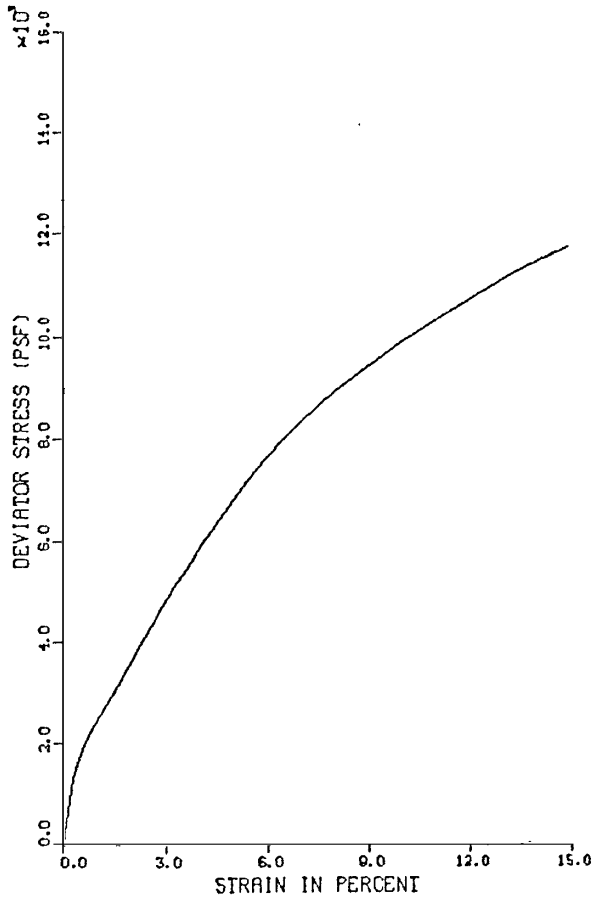

ISOTROPIC CONSOLIDATED UNDRAINED TRIAXIAL TEST
WITH PORE PRESSURE MEASUREMENTS
D118-UTAH DAMS-FROG HOLLOW POST CYCLIC STATIC TX#FH1 7/28/82 RED. BY PU

BORING:FH-1 SAMPLE:PB-4/S-3 DEPTH:14.5-17.5

SILTY CLAY

AT END OF CONSOLIDATION :
SAMPLE HEIGHT ..... = 5.967 INCHES
SAMPLE AREA ..... = 6.479 SQ. INCHES
EFFECTIVE CONFINING STRESS . = 2045. PSF
EFFECTIVE MAJOR PRIN. STRESS = 2045. PSF
PRINCIPAL STRESS RATIO ..... = 1.00

STRAIN PCT	SIGMA3E PSF	SIGMA1E PSF	RATIO SIG1E/SIG3E	PPRESS PSF	PBAR PSF	PTOT PSF	Q PSF
.0	1426.	1426.	1.0	619.	1426.	2045.	0.
.3	1008.	2315.	2.3	1037.	1662.	2698.	654.
.6	936.	2880.	3.1	1109.	1908.	3017.	972.
.9	907.	3263.	3.6	1138.	2085.	3223.	1178.
1.3	922.	3664.	4.0	1123.	2293.	3416.	1371.
1.6	950.	4078.	4.3	1094.	2514.	3608.	1564.
1.9	994.	4524.	4.6	1051.	2759.	3810.	1765.
2.3	1066.	4997.	4.7	979.	3031.	4010.	1966.
2.6	1152.	5459.	4.7	893.	3306.	4198.	2154.
2.9	1224.	5926.	4.8	821.	3575.	4396.	2351.
3.3	1310.	6384.	4.9	734.	3847.	4582.	2537.
3.6	1426.	6867.	4.8	619.	4146.	4766.	2721.
4.1	1570.	7537.	4.8	475.	4553.	5028.	2984.
4.5	1685.	7970.	4.7	360.	4828.	5188.	3143.
5.0	1872.	8650.	4.6	173.	5261.	5434.	3389.
5.5	2016.	9201.	4.6	29.	5609.	5637.	3593.
6.0	2203.	9789.	4.4	-158.	5996.	5838.	3793.
6.5	2362.	10322.	4.4	-317.	6342.	6025.	3980.
7.0	2534.	10843.	4.3	-490.	6689.	6199.	4154.
7.5	2693.	11305.	4.2	-648.	6999.	6351.	4306.
9.0	2866.	11776.	4.1	-821.	7321.	6500.	4455.
9.1	3168.	12623.	4.0	-1123.	7896.	6772.	4728.
10.0	3370.	13234.	3.9	-1325.	8302.	6977.	4932.
10.8	3571.	13816.	3.9	-1526.	8694.	7167.	5122.
11.7	3758.	14354.	3.8	-1714.	9056.	7343.	5298.
12.6	3931.	14869.	3.8	-1886.	9400.	7514.	5469.
13.5	4090.	15361.	3.8	-2045.	9725.	7681.	5636.
15.0	4349.	16043.	3.7	-2304.	10176.	7872.	5847.

POST CYCLIC STATIC TEST: PC-1
FROG HOLLOW DAM

CONSOLIDATED UNDRAINED TRIAXIAL TEST
WITH PORE PRESSURE MEASUREMENT

PST.CYC.STAT.KC-1.0
D118-28JULY82
BORING:FH-1 SAMPLE:PB-6
SILTY CLAY

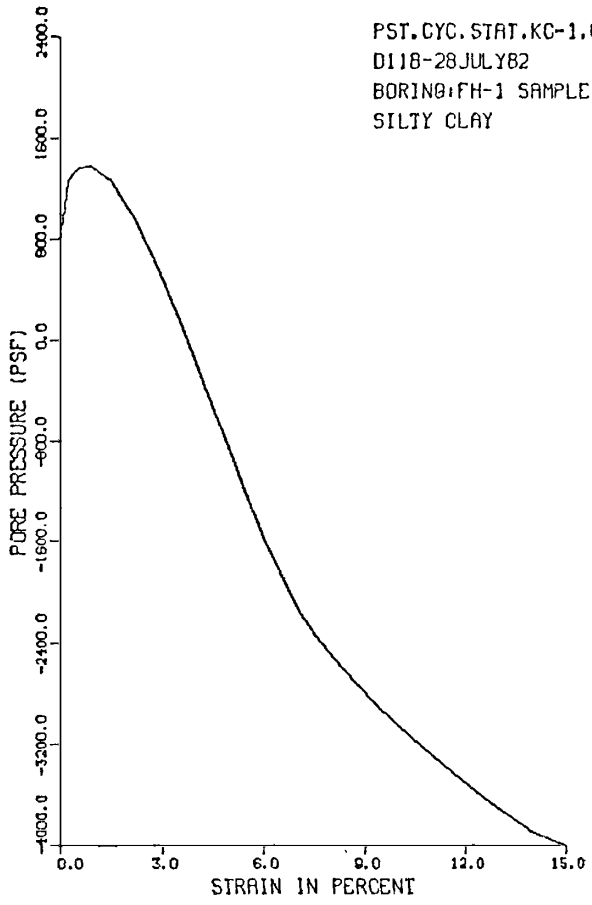

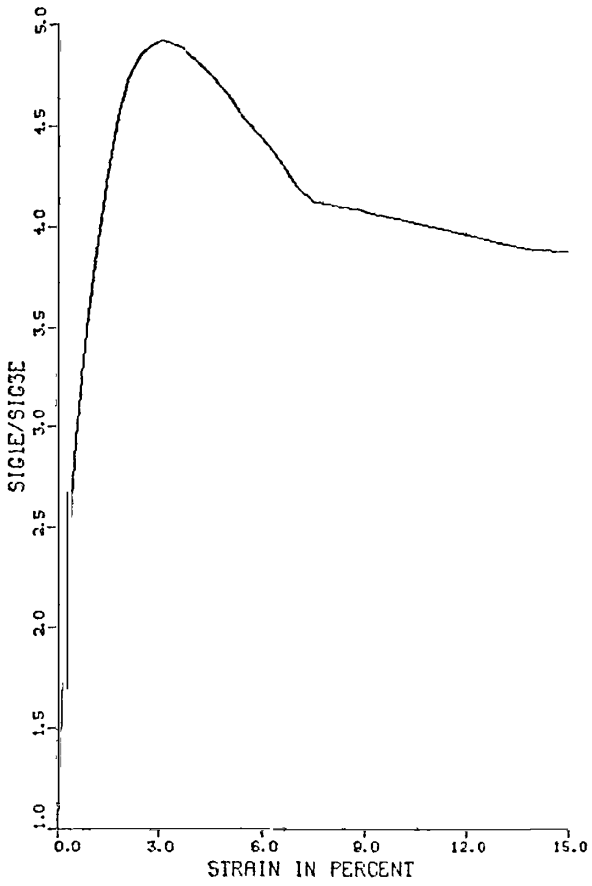

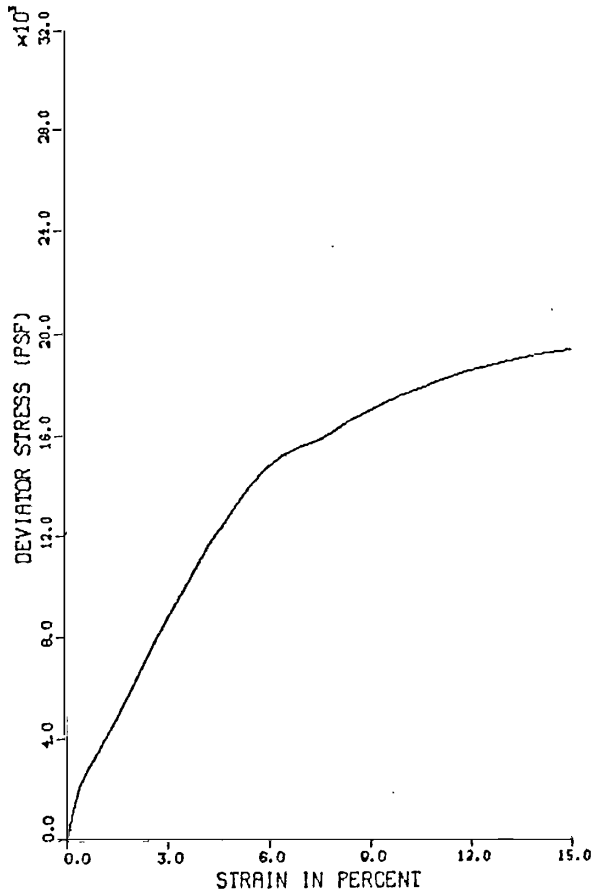

ISOTROPIC CONSOLIDATED UNDRAINED TRIAXIAL TEST
WITH PORE PRESSURE MEASUREMENTS
D118-UTAH DAMS-FROG HOLLOW POST CYCLIC STATIC TX#FH2 7/28/82 RED. BY BU

BORING:FH-1 SAMPLE:PB-6/S-5 DEPTH:22.5-25.0

SILTY CLAY

AT END OF CONSOLIDATION :

SAMPLE HEIGHT	=	5.916 INCHES
SAMPLE AREA	=	6.479 SQ. INCHES
EFFECTIVE CONFINING STRESS .	=	2707. PSF
EFFECTIVE MAJOR PRIN. STRESS	=	2707. PSF
PRINCIPAL STRESS RATIO	=	1.00

STRAIN PCT	SIGMA3E PSF	SIGMA1E PSF	RATIO SIG1E/SIG3E	PPRESS PSF	PBAR PSF	PTOT PSF	Q PSF
.0	1958.	1958.	1.0	749.	1958.	2707.	0.
.3	1454.	2895.	2.0	1253.	2175.	3428.	721.
.4	1382.	3639.	2.6	1325.	2511.	3836.	1128.
.6	1354.	3961.	2.9	1354.	2657.	4011.	1304.
1.0	1339.	4773.	3.6	1368.	3056.	4424.	1717.
1.2	1382.	5357.	3.9	1325.	3370.	4694.	1987.
1.5	1454.	6204.	4.3	1253.	3829.	5082.	2375.
1.8	1570.	7134.	4.5	1138.	4352.	5489.	2782.
2.1	1714.	8129.	4.7	994.	4922.	5915.	3208.
2.5	1886.	9148.	4.8	821.	5517.	6338.	3631.
2.8	2074.	10153.	4.9	634.	6114.	6747.	4040.
3.1	2275.	11190.	4.9	432.	6732.	7164.	4457.
3.6	2606.	12739.	4.9	101.	7673.	7773.	5066.
4.3	3082.	14739.	4.8	-374.	8910.	8536.	5829.
5.0	3557.	16567.	4.7	-850.	10062.	9213.	6505.
5.5	3917.	17803.	4.5	-1210.	10860.	9650.	6943.
6.0	4248.	18915.	4.5	-1541.	11582.	10041.	7334.
6.5	4565.	19795.	4.3	-1858.	12180.	10322.	7615.
7.0	4853.	20388.	4.2	-2146.	12621.	10475.	7768.
7.6	5054.	20850.	4.1	-2347.	12952.	10605.	7898.
7.9	5170.	21273.	4.1	-2462.	13221.	10759.	8052.
8.4	5314.	21787.	4.1	-2606.	13550.	10944.	8237.
8.8	5443.	22261.	4.1	-2736.	13852.	11116.	8409.
9.3	5573.	22671.	4.1	-2866.	14122.	11256.	8549.
10.0	5760.	23303.	4.0	-3053.	14532.	11479.	8772.
11.0	6005.	24060.	4.0	-3298.	15033.	11735.	9028.
11.9	6192.	24600.	4.0	-3485.	15396.	11911.	9204.
12.8	6379.	25072.	3.9	-3672.	15735.	12063.	9356.
14.0	6610.	25713.	3.9	-3902.	16161.	12259.	9552.
15.0	6710.	26017.	3.9	-4003.	16364.	12361.	9654.

POST CYCLIC STATIC TEST: PC-2
FROG HOLLOW DAM

CONSOLIDATED UNDRAINED TRIAXIAL TEST
WITH PORE PRESSURE MEASUREMENT

PST.CYC.STAT.TX KC-1.0
D118-26JULY82
BORING:FH-1 SAMPLE:PB10
SILTY CLAY

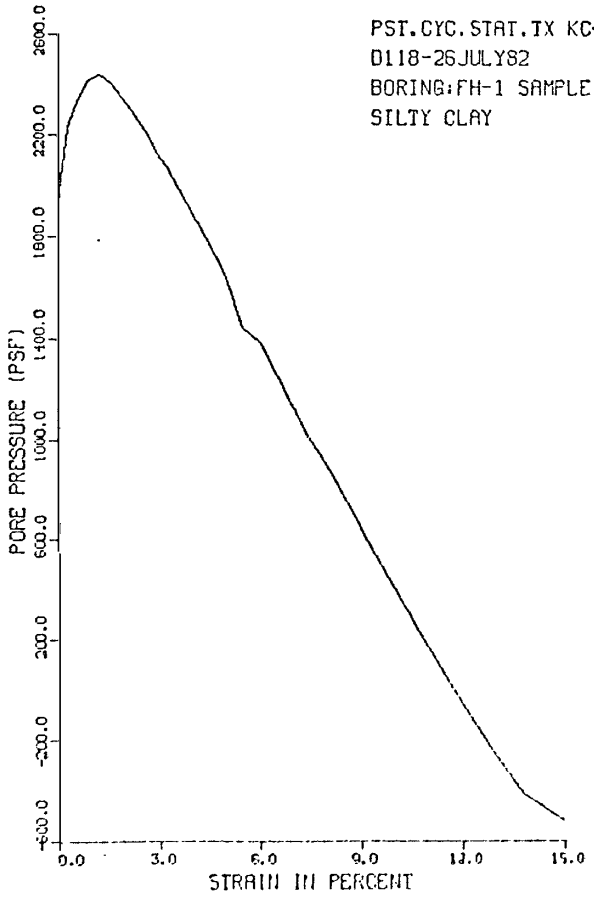

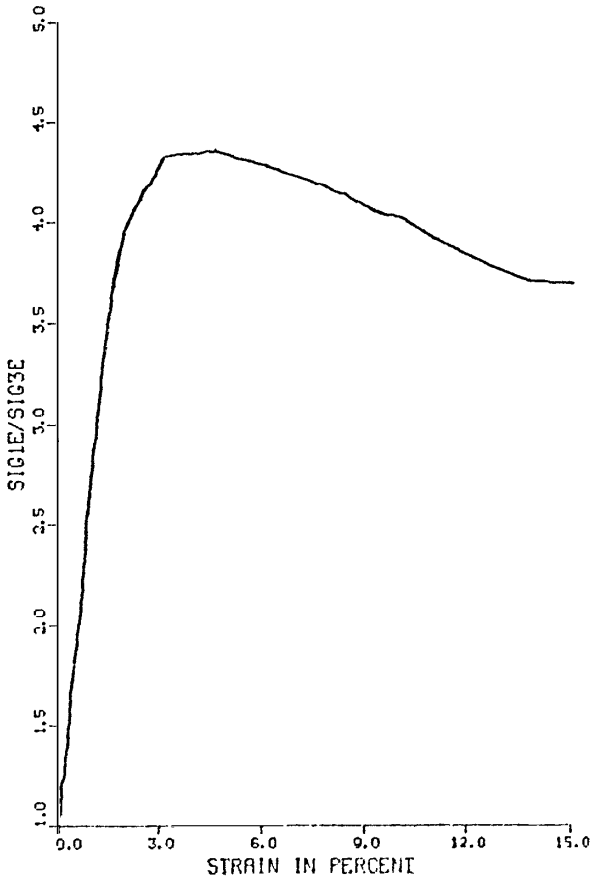

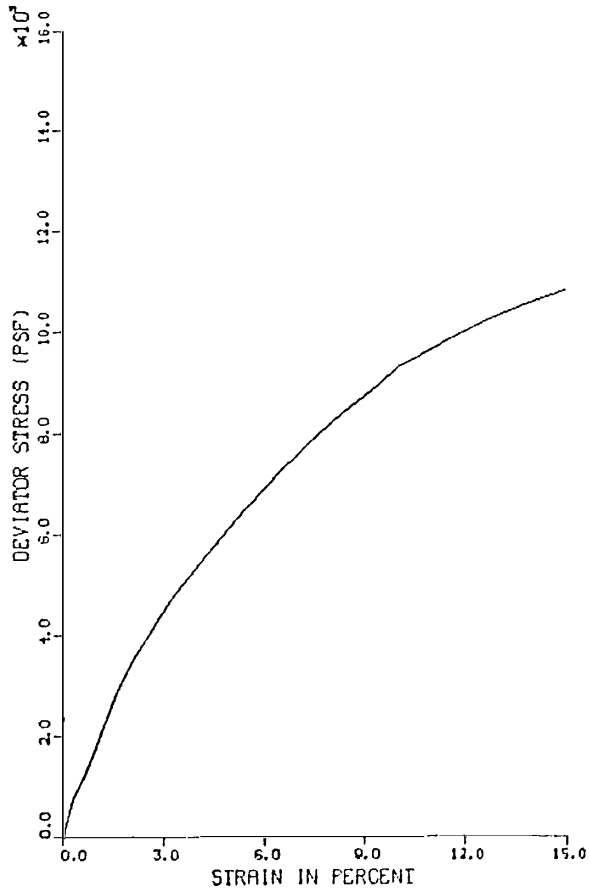

ISOTROPIC CONSOLIDATED UNDRAINED TRIAXIAL TEST
WITH PORE PRESSURE MEASUREMENTS
D118-UTAH DAMS-FROG HOLLOW POST CYCLIC STATIC TX#3 7/26/82 RED. BY EW

BORING:FH-1 SAMPLE:FB-10/S-9 DEPTH:38.0-40.5

SILTY CLAY

AT END OF CONSOLIDATION :
SAMPLE HEIGHT ..... = 5.932 INCHES
SAMPLE AREA ..... = 6.502 SQ. INCHES
EFFECTIVE CONFINING STRESS . = 3499. PSF
EFFECTIVE MAJOR PRIN. STRESS = 3199. PSF
PRINCIPAL STRESS RATIO ..... = 1.60

STRAIN PCT	SIGMA3E PSF	SIGMA1E PSF	RATIO SIG1E/SIG3E	PPRESS PSF	PEAK PSF	PLOT PSF	Q PSF
.0	1570.	1570.	1.0	1930.	1570.	3499.	0.
.3	1267.	2018.	1.6	2232.	1642.	3874.	375.
.6	1152.	2296.	2.0	2347.	1724.	4071.	572.
.9	1080.	2682.	2.5	2419.	1881.	4300.	801.
1.3	1066.	3231.	3.0	2434.	2148.	4582.	1083.
1.6	1094.	3841.	3.5	2405.	2468.	4873.	1373.
1.9	1152.	4367.	3.8	2347.	2760.	5107.	1608.
2.2	1210.	4835.	4.0	2290.	3017.	5307.	1808.
2.6	1282.	5273.	4.1	2218.	3277.	5495.	1996.
2.9	1368.	5711.	4.2	2131.	3539.	5671.	2171.
3.3	1426.	6117.	4.3	2074.	3771.	5845.	2346.
3.6	1512.	6507.	4.3	1987.	4009.	5996.	2497.
4.1	1642.	7076.	4.3	1858.	4359.	6216.	2717.
5.0	1843	7961.	4.3	1656.	4901.	6560.	3061.
5.4	2059.	8867.	4.3	1440.	5213.	6754.	3254.
6.0	2117.	9066.	4.3	1382.	5461.	6944.	3444.
6.4	2046.	9512.	4.6	1453.	5629.	7132.	3633.
7.1	2176.	9922.	4.6	1323.	5874.	7297.	3798.
7.4	2266.	10458.	4.6	994.	6167.	7461.	3961.
8.1	2431.	10846.	4.1	870.	6435.	7612.	4112.
8.4	2750.	11273.	4.1	749.	7012.	7759.	4261.
9.0	2866.	11611.	4.1	634.	7238.	7872.	4372.
9.4	2766.	11761.	4.0	533.	7449.	7981.	4482.
10.0	3026.	12401.	4.0	493.	7790.	8154.	4654.
10.7	3249.	12818.	3.9	236.	8041.	8274.	4775.
11.0	3557.	13492.	3.8	-58.	8373.	8419.	4920.
11.4	3741.	14044.	3.8	-242.	8623.	8543.	5045.
12.0	3917.	14420.	3.7	-418.	8791.	8627.	5129.
12.4	4018.	14713.	3.7	-519.	8949.	8712.	5213.

POST CYCLIC STATIC TEST: PC-3
FROG HOLLOW DAM

CONSOLIDATED UNDRAINED TRIAXIAL TEST
WITH PORE PRESSURE MEASUREMENT

PST.CYC.STAT.TX KC-1.0
D118-26JULY82
BORING:FH-1 SAMPLE:PB14
SILTY CLAY

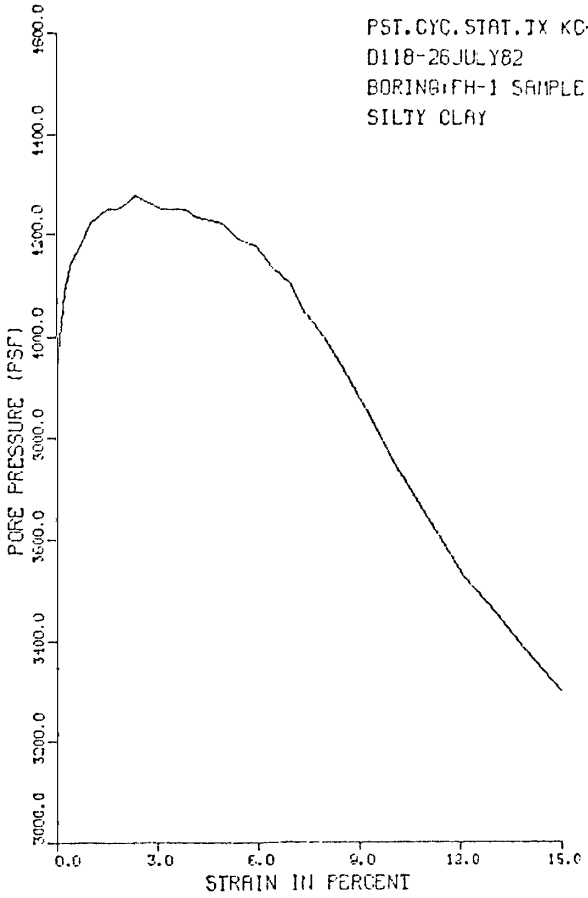

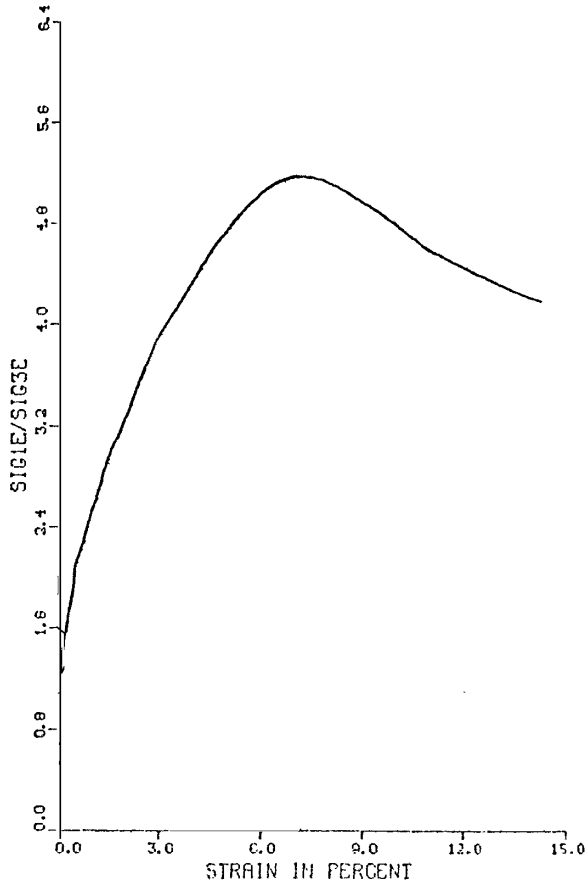

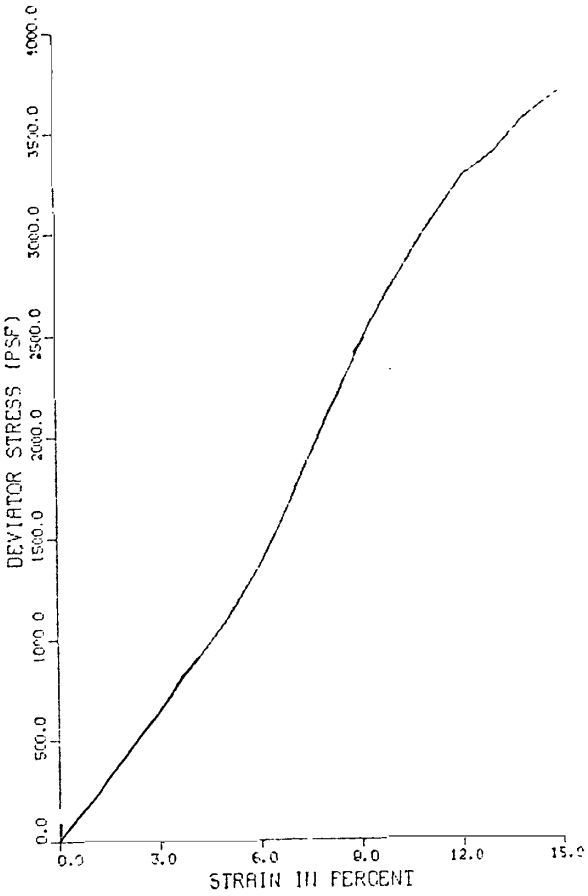

ISOTROPIC CONSOLIDATED UNDRAINED TRIAXIAL TEST
WITH PORE PRESSURE MEASUREMENTS
D118:UTAH DAMS-FROG HOLLOW POST CYCLIC STATIC TX#4 7/22/82 KED. BY EW

BORING :FH-1 SAMPLE:FB-1/S-12 DEPTH:55.0-56.8

SILTY CLAY

AT END OF CONSOLIDATION :
SAMPLE HEIGHT ..... = 6.059 INCHES
SAMPLE AREA ..... = 6.257 SQ. INCHES
EFFECTIVE CONFINING STRESS . = 1007. PSF
EFFECTIVE MAJOR PRIN. STRESS = 4507. PSF
PRINCIPAL STRESS RATIO ..... = 1.00

STRAIN PCT	SIGMA3F PSF	SIGMA1F PSF	RATIO SIG1E/SIG3E	FFRESS PSF	FPAR PSF	FTOT PSF	Q PSF
.0	576.	576.	1.0	3931.	576.	4507.	0.
.3	418.	734.	1.8	4090.	576.	4665.	159.
.5	360.	743.	2.1	4147.	552.	4699.	192.
.8	331.	758.	2.3	4176.	545.	4721.	214.
1.0	308.	736.	2.6	4219.	512.	4731.	224.
1.3	274.	765.	2.8	4234.	509.	4753.	246.
1.6	259.	777.	3.0	4248.	516.	4764.	256.
1.9	259.	815.	3.1	4248.	537.	4785.	278.
2.2	245.	843.	3.4	4262.	544.	4806.	299.
2.4	240.	849.	3.5	4267.	540.	4817.	309.
2.8	245.	905.	3.7	4262.	575.	4838.	330.
3.2	259.	935.	3.6	4248.	621.	4869.	362.
3.9	209.	1109.	4.3	4248.	691.	4939.	432.
4.3	274.	1161.	4.3	4234.	729.	4964.	457.
5.0	288.	1241.	4.3	4219.	826.	5045.	538.
5.5	317.	1514.	4.8	4190.	916.	5107.	600.
6.0	331.	1675.	5.1	4176.	1003.	5178.	671.
6.5	374.	1872.	5.0	4133.	1126.	5259.	752.
7.0	403.	2059.	5.1	4104.	1246.	5350.	843.
7.5	461.	2345.	5.0	4046.	1395.	5440.	933.
8.0	504.	2567.	5.1	4003.	1526.	5529.	1022.
8.5	562.	2800.	5.0	3945.	1681.	5626.	1119.
9.3	648.	3154.	4.9	3859.	1902.	5761.	1254.
10.0	749.	3481.	4.6	3758.	2115.	5873.	1366.
10.9	836.	3839.	4.5	3672.	2342.	6014.	1507.
12.1	979.	4365.	4.4	3528.	2671.	6199.	1692.
13.1	1091.	4854.	4.5	3416.	2954.	6370.	1863.
13.9	1152.	4969.	4.3	3354.	3067.	6421.	1913.
15.0	1210.	4966.	4.1	3296.	3068.	6364.	1856.

POST CYCLIC STATIC TEST:PC-4
FROG HOLLOW DAM

CONSOLIDATED UNDRAINED TRIAXIAL TEST
WITH PORE PRESSURE MEASUREMENT

PST.CYC.STAT.KC-1.5
D118-16AUG82
BORING:FH-1 SAMPLE:PB-1
SILTY CLAY

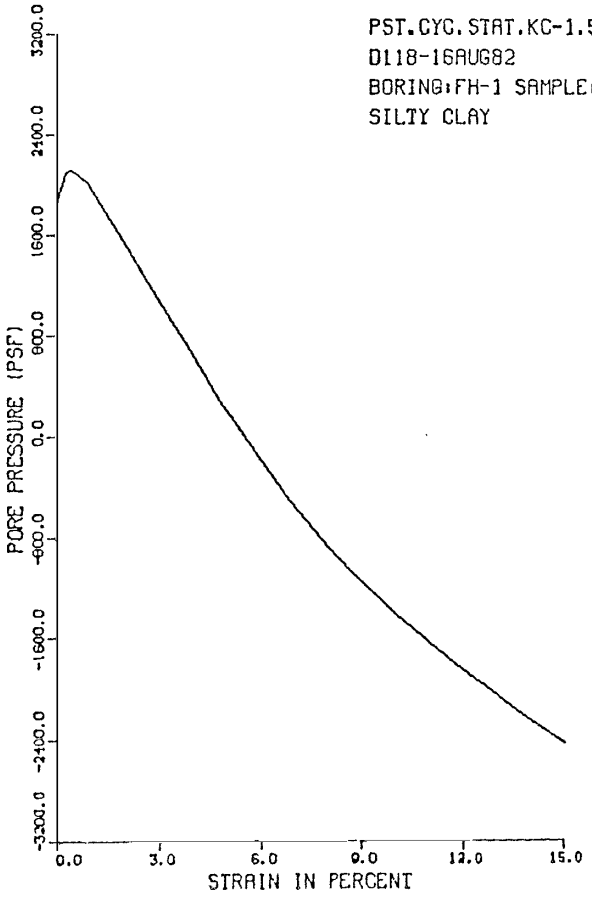

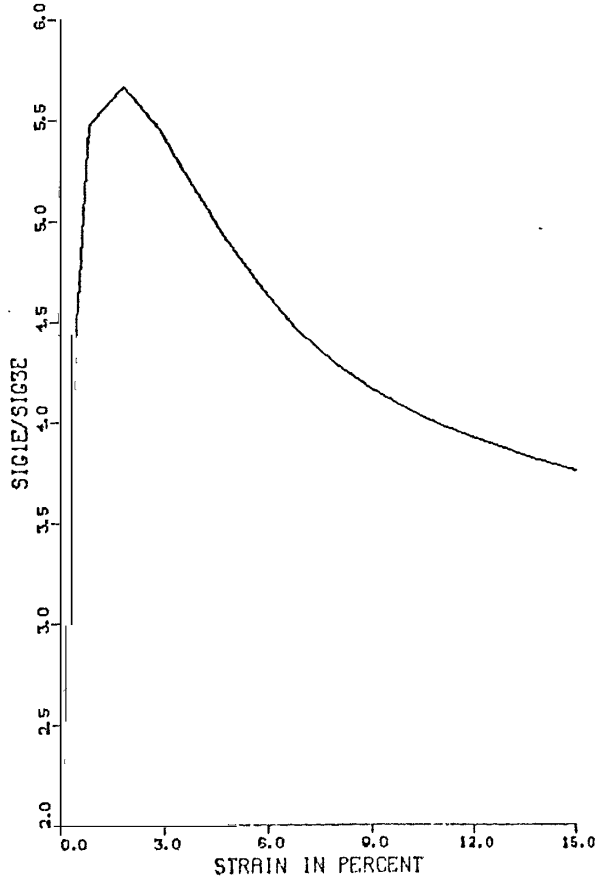

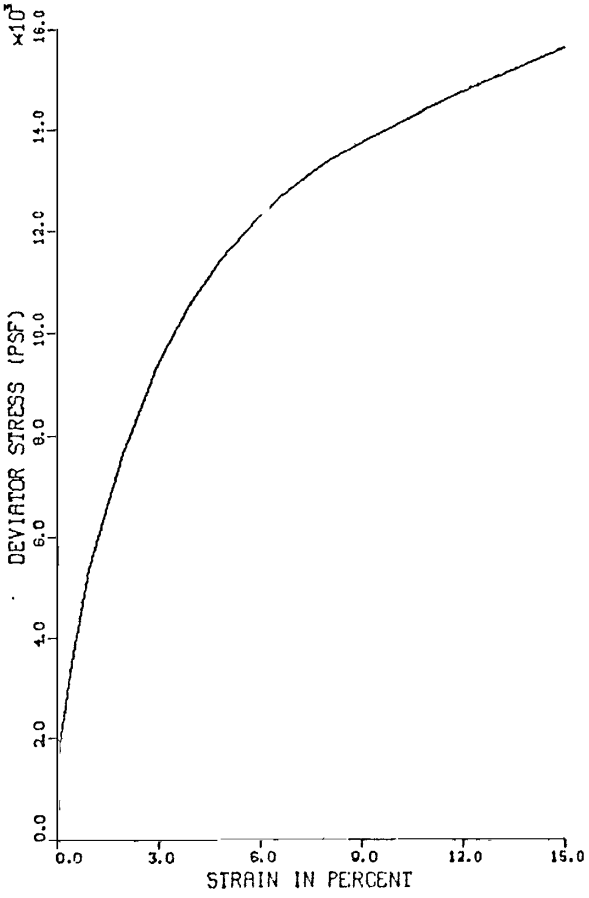

ANISOTROPIC CONSOLIDATED UNDRAINED TRIAXIAL TEST
WITH PORE PRESSURE MEASUREMENTS
D118-UTAH DAMS-FROG HOLLOW DAM POST CYCLIC STATIC TX#FH5 TESTED 8/16/82

BORING:FH-1 SAMPLE:PB-10/S-9 DEPTH:38.0-40.5

SILTY CLAY

AT END OF CONSOLIDATION :
SAMPLE HEIGHT ..... = 5.861 INCHES
SAMPLE AREA ..... = 6.544 SQ. INCHES
EFFECTIVE CONFINING STRESS . = 3197. PSF
EFFECTIVE MAJOR PRIN. STRESS = 4795. PSF
PRINCIPAL STRESS RATIO ..... = 1.50

STRAIN PCT	SIGMA3E PSF	SIGMA1E PSF	RATIO SIG1E/SIG3E	PPRESS PSF	PBAR PSF	PTOT PSF	Q PSF
.0	1368.	2952.	2.2	1829.	2160.	3989.	792.
.3	1107.	3983.	3.6	2088.	2546.	4634.	1437.
.5	1094.	4783.	4.4	2102.	2939.	5041.	1844.
1.0	1195.	6545.	5.5	2002.	3870.	5872.	2675.
2.0	1642.	9296.	5.7	1555.	5469.	7024.	3827.
3.0	2102.	11458.	5.4	1094.	6780.	7874.	4678.
3.9	2520.	13025.	5.2	677.	7773.	8449.	5253.
4.9	2909.	14318.	4.9	288.	8614.	8902.	5705.
6.0	3355.	15603.	4.7	-158.	9479.	9321.	6124.
6.9	3701.	16491.	4.5	-504.	10096.	9592.	6395.
8.1	4075.	17425.	4.3	-878.	10750.	9872.	6675.
9.1	4349.	18087.	4.2	-1152.	11218.	10066.	6869.
10.0	4608.	18701.	4.1	-1411.	11654.	10243.	7046.
10.8	4795.	19156.	4.0	-1598.	11976.	10377.	7181.
11.0	4838.	19266.	4.0	-1642.	12052.	10410.	7214.
12.0	5054.	19802.	3.9	-1858.	12428.	10571.	7374.
12.8	5213.	20191.	3.9	-2016.	12702.	10686.	7489.
13.7	5371.	20561.	3.8	-2174.	12966.	10792.	7595.
15.1	5630.	21152.	3.8	-2434.	13391.	10958.	7761.

POST CYCLIC STATIC TEST: PC-5
FROG HOLLOW DAM

CONSOLIDATED UNDRAINED TRIAXIAL TEST
WITH PORE PRESSURE MEASUREMENT

PST.CYC.STAT.TX.KC-1.5
D118-23AUG.82
BORING:FH-1 SAMPLE:PB4
SILTY CLAY

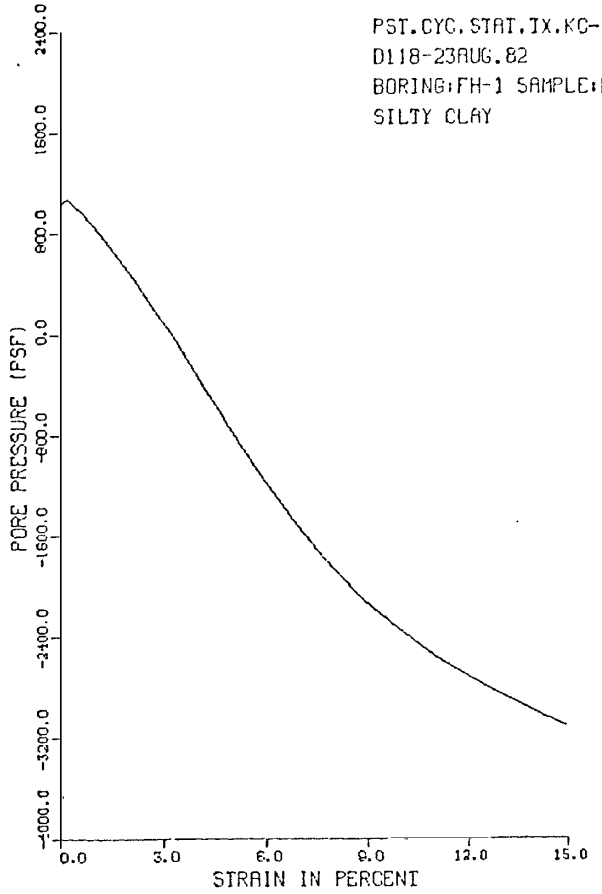

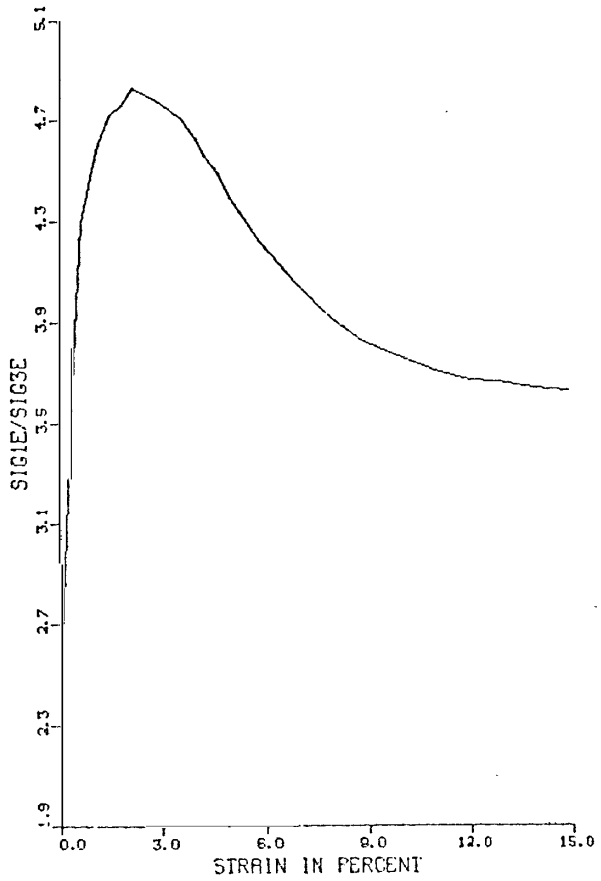

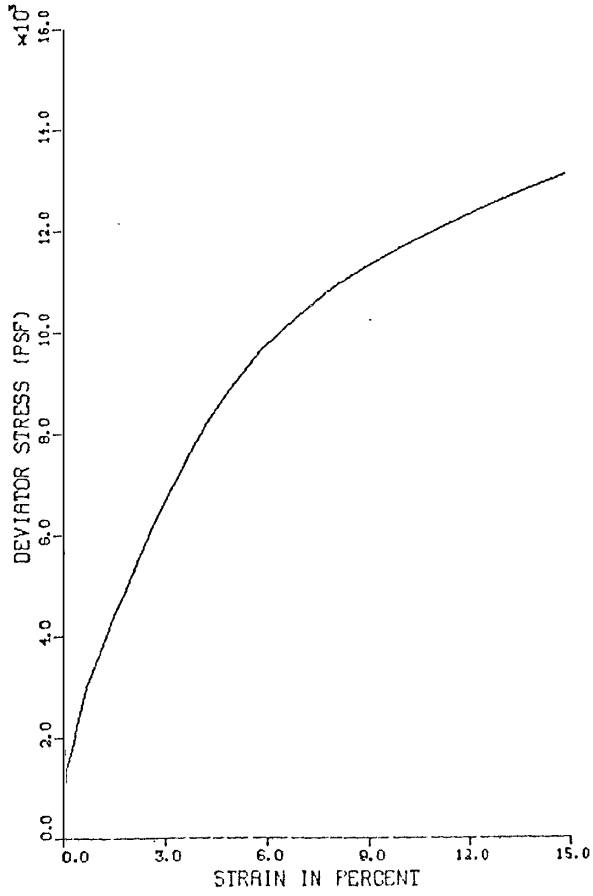

ANISOTROPIC CONSOLIDATED UNDRAINED TRIAXIAL TEST
WITH PORE PRESSURE MEASUREMENTS
D118 UTAH DAMS FROG HOLLOW POST CYCLIC STATIC TX:FH6 8/23/82 RED. BY BW

BORING:FH-1 SAMPLE:PB-4/S-3 DEPTH:14.5-17.5

SILTY CLAY

AT END OF CONSOLIDATION :
SAMPLE HEIGHT ..... = 5.858 INCHES
SAMPLE AREA ..... = 6.367 SQ. INCHES
EFFECTIVE CONFINING STRESS . = 1872. PSF
EFFECTIVE MAJOR PRIN. STRESS = 2808. PSF
PRINCIPAL STRESS RATIO ..... = 1.50

STRAIN PCT	SIGMA3E PSF	SIGMA1E PSF	RATIO SIG1E/SIG3E	PPRESS PSF	PBAR PSF	PTOT PSF	Q PSF
.0	936.	1863.	2.0	936.	1400.	2336.	464.
.1	835.	2191.	2.6	1037.	1513.	2550.	678.
.2	806.	2589.	3.2	1066.	1698.	2763.	891.
.4	835.	3043.	3.6	1037.	1939.	2976.	1104.
.7	907.	3894.	4.3	965.	2401.	3366.	1494.
.9	994.	4444.	4.5	878.	2719.	3597.	1725.
1.2	1066.	4909.	4.6	806.	2987.	3794.	1922.
1.5	1131.	5568.	4.7	691.	3374.	4066.	2194.
1.9	1310.	6237.	4.8	562.	3774.	4335.	2463.
2.2	1426.	6887.	4.8	446.	4157.	4603.	2731.
2.6	1570.	7541.	4.8	302.	4555.	4858.	2986.
2.9	1714.	8190.	4.8	159.	4952.	5110.	3238.
3.3	1858.	8813.	4.7	14.	5335.	5350.	3478.
3.6	2002.	9411.	4.7	-130.	5706.	5577.	3705.
4.0	2160.	9998.	4.6	-288.	6079.	5791.	3919.
4.4	2318.	10539.	4.5	-446.	6429.	5982.	4110.
4.7	2462.	11040.	4.5	-590.	6751.	6161.	4289.
5.0	2606.	11480.	4.4	-734.	7043.	6309.	4437.
5.9	2995.	12632.	4.2	-1123.	7814.	6690.	4818.
7.0	3384.	13690.	4.0	-1512.	8537.	7025.	5153.
8.1	3730.	14584.	3.9	-1858.	9157.	7299.	5427.
8.9	3974.	15200.	3.8	-2102.	9587.	7485.	5613.
10.0	4205.	15831.	3.8	-2333.	10018.	7685.	5813.
11.0	4421.	16394.	3.7	-2549.	10407.	7858.	5986.
12.1	4594.	16883.	3.7	-2722.	10718.	8016.	6144.
12.9	4709.	17253.	3.7	-2837.	10981.	8144.	6272.
14.0	4853.	17677.	3.6	-2981.	11265.	8284.	6412.
15.0	4982.	18075.	3.6	-3110.	11528.	8418.	6546.

POST CYCLIC STATIC TEST: PC-6
FROG HOLLOW DAM

IVINS DIVERSION DAM NO. 5

CONSOLIDATED UNDRAINED TRIAXIAL TEST
WITH PORE PRESSURE MEASUREMENT

PST.CYC.STAT.KC-1.0
D118-28JULY82
BORING IV-1 SAMPLE PB-1
SILTY SAND

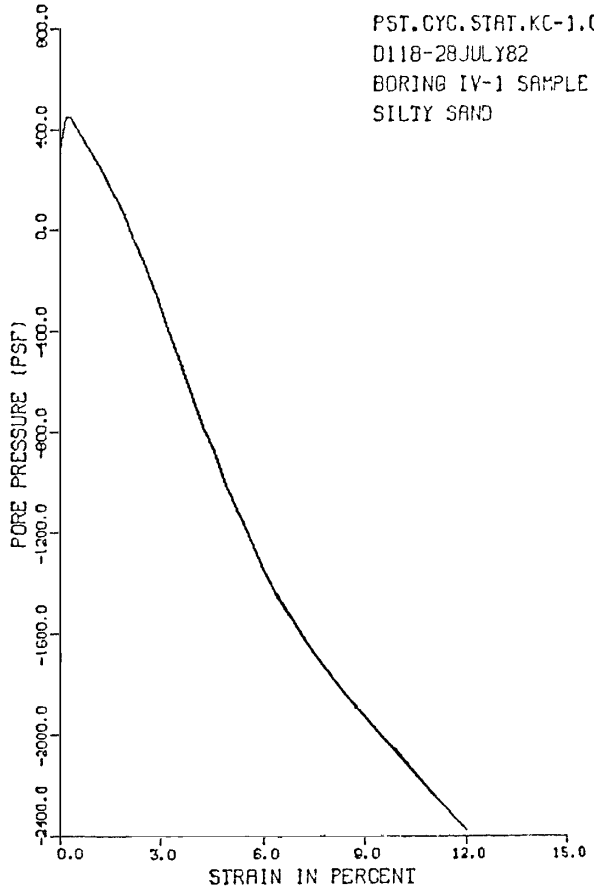

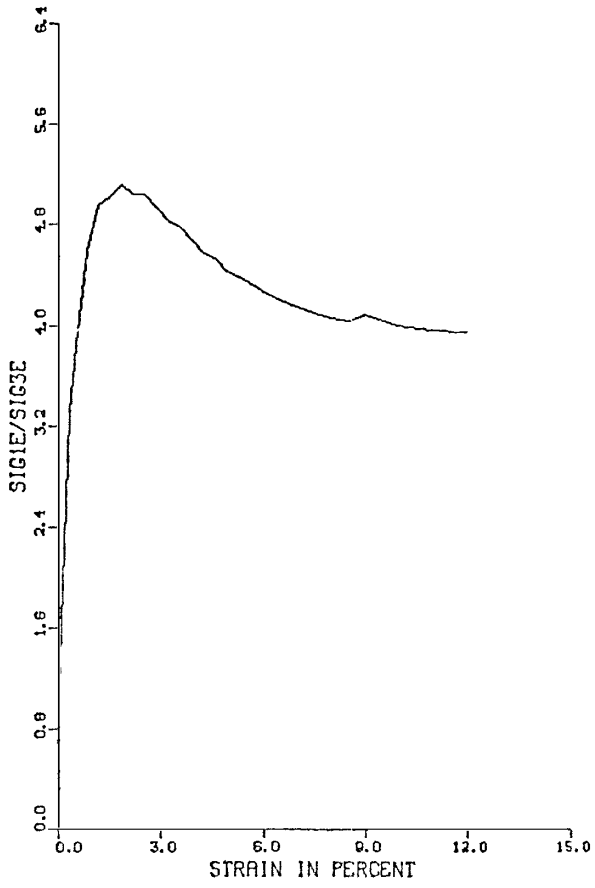

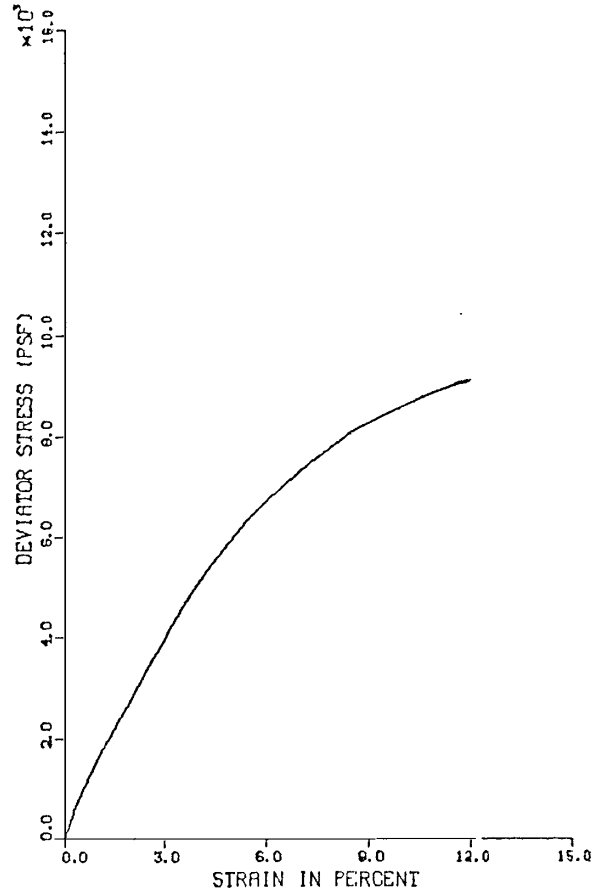

ISOTROPIC CONSOLIDATED UNDRAINED TRIAXIAL TEST
WITH PORE PRESSURE MEASUREMENTS
D118-UTAH DAMS-IVINS DIVERSION POST CYCLC STATIC TX IV-1 7/30/82 BU

BORING IV-1 SAMPLE PB-1/S-1 DEPTH 4.0-6.5

SILTY SAND

AT END OF CONSOLIDATION :
SAMPLE HEIGHT ..... = 6.000 INCHES
SAMPLE AREA ..... = 6.345 SQ. INCHES
EFFECTIVE CONFINING STRESS . = 720. PSF
EFFECTIVE MAJOR PRIN. STRESS = 720. PSF
PRINCIPAL STRESS RATIO ..... = 1.00

STRAIN PCT	SIGMA3E PSF	SIGMA1E PSF	RATIO SIG1E/SIG3E	PPRESS PSF	PBAR PSF	PTOT PSF	Q PSF
.0	403.	403.	1.0	317.	403.	720.	0.
.2	274.	613.	2.2	446.	443.	890.	170.
.4	274.	907.	3.3	446.	590.	1037.	317.
.5	317.	1220.	3.9	403.	768.	1171.	451.
.9	389.	1784.	4.6	331.	1086.	1417.	697.
1.2	461.	2277.	4.9	259.	1369.	1628.	908.
1.5	547.	2737.	5.0	173.	1642.	1815.	1095.
1.9	634.	3239.	5.1	86.	1936.	2023.	1303.
2.2	749.	3767.	5.0	-29.	2258.	2229.	1509.
2.6	850.	4277.	5.0	-130.	2563.	2434.	1714.
2.9	979.	4813.	4.9	-259.	2896.	2637.	1917.
3.2	1109.	5347.	4.8	-389.	3228.	2839.	2119.
3.6	1224.	5841.	4.8	-504.	3532.	3028.	2308.
3.9	1354.	6325.	4.7	-634.	3839.	3205.	2485.
4.3	1498.	6820.	4.6	-778.	4159.	3381.	2661.
4.6	1598.	7227.	4.5	-878.	4413.	3534.	2814.
5.0	1728.	7638.	4.4	-1008.	4683.	3675.	2955.
5.5	1886.	8215.	4.4	-1166.	5051.	3884.	3164.
6.0	2045.	8723.	4.3	-1325.	5384.	4059.	3339.
6.5	2189.	9191.	4.2	-1469.	5690.	4221.	3501.
7.0	2318.	9619.	4.1	-1598.	5969.	4370.	3650.
7.5	2448.	10024.	4.1	-1728.	6236.	4508.	3788.
8.0	2563.	10389.	4.1	-1843.	6476.	4633.	3913.
8.6	2664.	10736.	4.0	-1944.	6700.	4756.	4036.
9.0	2549.	10415.	4.1	-1829.	6482.	4653.	3933.
10.0	2794.	11148.	4.0	-2074.	6971.	4897.	4177.
11.0	2952.	11698.	4.0	-2232.	7325.	5093.	4373.
12.0	3096.	12199.	3.9	-2376.	7647.	5271.	4551.

POST CYCLIC STATIC TEST: PC-1
IVINS DIVERSION DAM NO. 5

CONSOLIDATED UNDRAINED TRIAXIAL TEST
WITH PORE PRESSURE MEASUREMENT

PST.CYC.STAT.KC-1.0
D118-30JULY82
BORING IV-3 SAMPLE PB-1
SILTY SAND

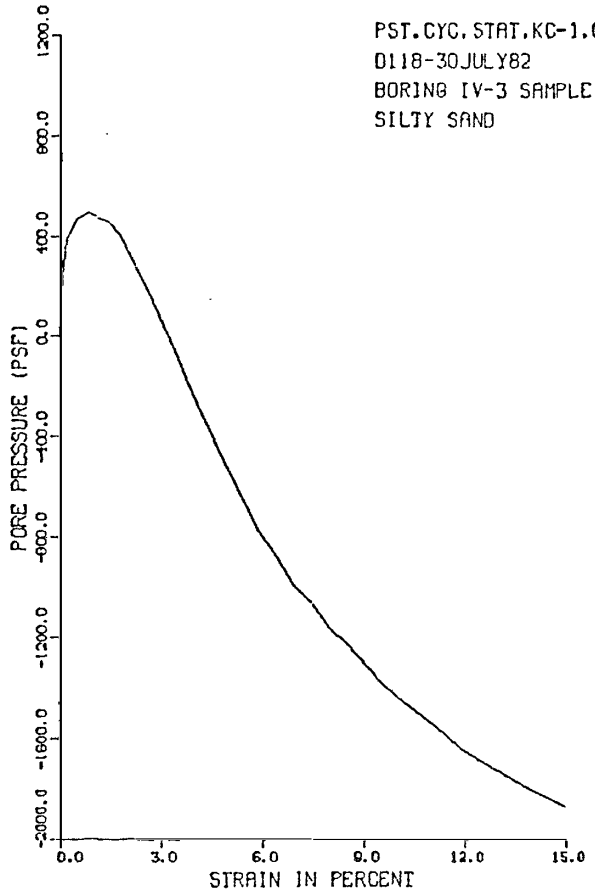

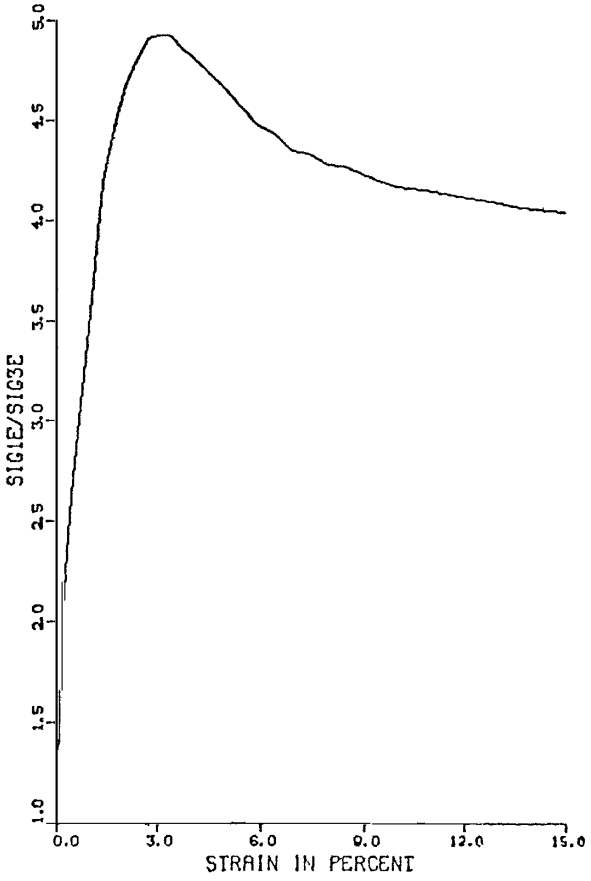

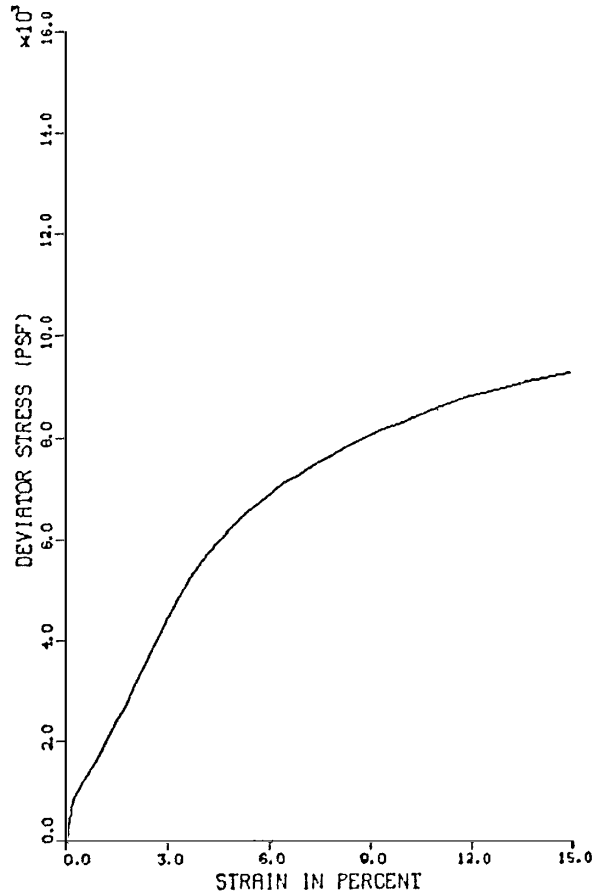

ISOTROPIC CONSOLIDATED UNDRAINED TRIAXIAL TEST
WITH PORE PRESSURE MEASUREMENTS
D118-UTAH DAMS-IVINS DIVERSION POST CYCILC STATIC TX IV-2 7/30/82 BV

BORING IV-3 SAMPLE PB-1/S-1 DEPTH 4.0-6.5

SILTY SAND

AT END OF CONSOLIDATION :
SAMPLE HEIGHT ..... = 6.004 INCHES
SAMPLE AREA ..... = 6.499 SQ. INCHES
EFFECTIVE CONFINING STRESS . = 1181. PSF
EFFECTIVE MAJOR PRIN. STRESS = 1181. PSF
PRINCIPAL STRESS RATIO ..... = 1.00

STRAIN PCT	SIGMA3E PSF	SIGMA1E PSF	RATIO SIG1E/SIG3E	PPRESS PSF	PPAR PSF	P1OI PSF	Q PSF
.0	1008.	1008.	1.0	173.	1008.	1181.	0.
.2	792.	1632.	2.1	389.	1212.	1601.	420.
.5	706.	1918.	2.7	475.	1312.	1787.	606.
.8	691.	2229.	3.2	490.	1460.	1950.	769.
1.2	706.	2611.	3.7	475.	1658.	2133.	953.
1.4	720.	3013.	4.2	461.	1866.	2327.	1146.
1.8	778.	3498.	4.5	403.	2138.	2541.	1360.
2.1	864.	4031.	4.7	317.	2448.	2764.	1584.
2.4	950.	4561.	4.8	230.	2756.	2986.	1805.
2.7	1037.	5088.	4.9	144.	3062.	3206.	2026.
3.1	1138.	5605.	4.9	43.	3371.	3414.	2234.
3.4	1238.	6097.	4.9	-58.	3668.	3610.	2429.
3.7	1354.	6579.	4.9	-173.	3966.	3794.	2613.
4.1	1454.	7002.	4.8	-274.	4228.	3955.	2774.
4.6	1598.	7561.	4.7	-418.	4579.	4162.	2981.
5.0	1714.	7937.	4.7	-533.	4850.	4317.	3136.
5.4	1829.	8368.	4.6	-648.	5098.	4150.	3269.
5.9	1958.	8774.	4.5	-778.	5366.	4589.	3403.
6.4	2059.	9128.	4.4	-878.	5594.	4715.	3535.
6.9	2174.	9453.	4.3	-994.	5814.	4820.	3637.
7.5	2246.	9731.	4.3	-1066.	5989.	4923.	3742.
8.0	2347.	10035.	4.3	-1166.	6191.	5025.	3844.
8.5	2405.	10273.	4.3	-1224.	6339.	5115.	3934.
9.4	2549.	10715.	4.2	-1368.	6632.	5264.	4083.
10.0	2621.	10936.	4.2	-1440.	6779.	5339.	4158.
11.1	2736.	11340.	4.1	-1555.	7038.	5483.	4302.
11.9	2822.	11630.	4.1	-1642.	7226.	5584.	4404.
12.8	2894.	11855.	4.1	-1714.	7375.	5661.	4480.
13.7	2966.	12069.	4.1	-1786.	7518.	5732.	4551.
15.0	3053.	12338.	4.0	-1872.	7695.	5823.	4643.

POST CYCLIC STATIC TEST:PC-2
IVINS DIVERSION DAM NO. 5

CONSOLIDATED UNDRAINED TRIAXIAL TEST
WITH PORE PRESSURE MEASUREMENT

PST.CYC.STAT.KC-1.0
D118-4AUG.82
BORING IV-4 SAMPLE PB-2
SILTY SAND

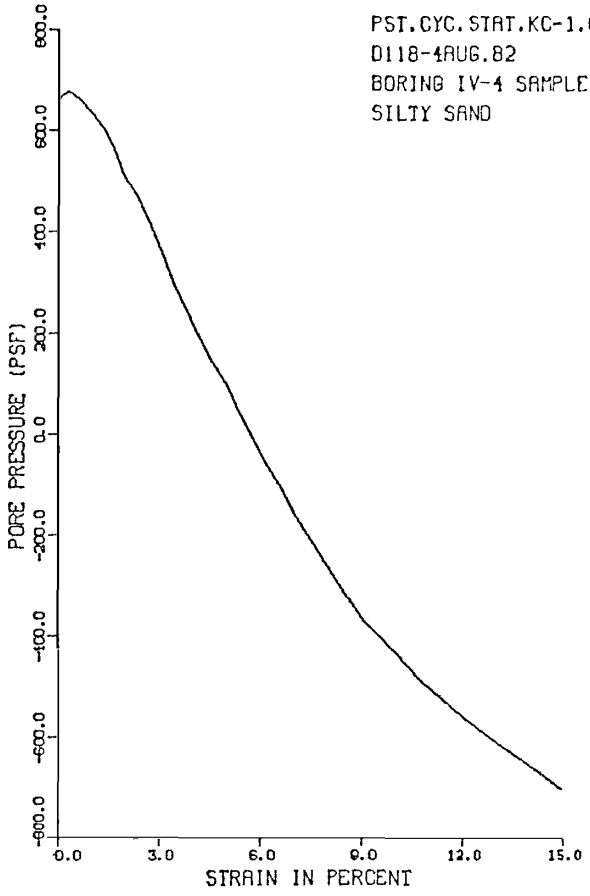

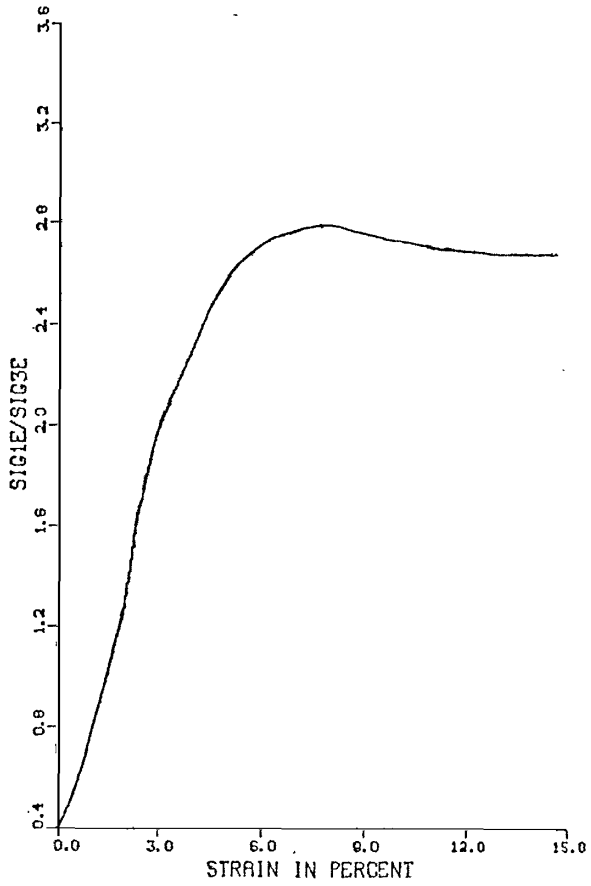

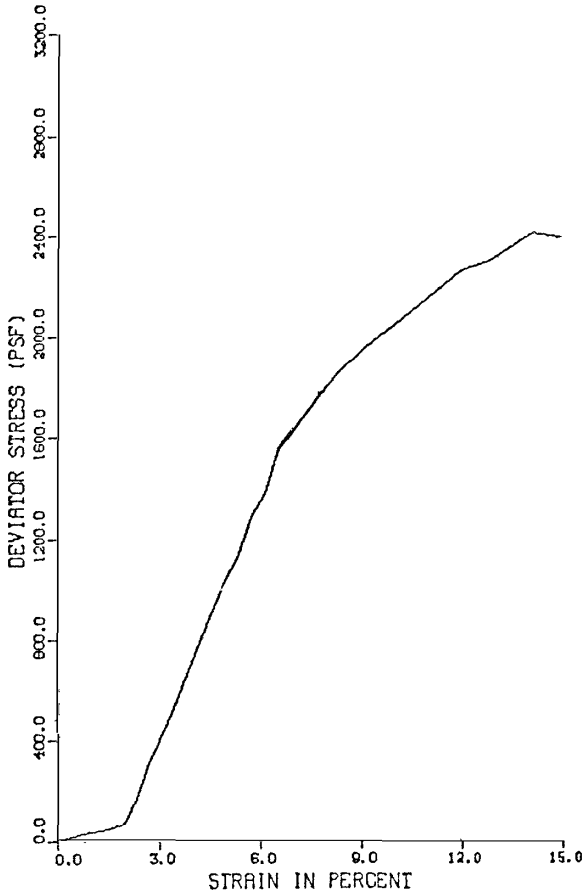

ISOTROPIC CONSOLIDATED UNDRAINED TRIAXIAL TEST
WITH PORE PRESSURE MEASUREMENTS
D118-UTAH DAMS-IVINS DIVERSION POST CYCILC STATIC TX IV-4 7/30/82 BW

BORING IV-4 SAMPLE PB-2/S-1 DEPTH 4.0-6.5

SILTY SAND

AT END OF CONSOLIDATION :
SAMPLE HEIGHT ..... = 5.884 INCHES
SAMPLE AREA ..... = 6.663 SQ. INCHES
EFFECTIVE CONFINING STRESS . = 763. PSF
EFFECTIVE MAJOR PRIN. STRESS = 763. PSF
PRINCIPAL STRESS RATIO ..... = 1.00

STRAIN PCT	SIGMA3E PSF	SIGMA1E PSF	RATIO SIG1E/SIG3E	PPRESS PSF	PBAR PSF	PTOT PSF	Q PSF
.0	101.	101.	1.0	662.	101.	763.	0.
.3	86.	97.	1.1	677.	92.	769.	5.
.7	101.	122.	1.2	662.	112.	774.	11.
1.0	130.	162.	1.2	634.	146.	779.	16.
1.3	158.	201.	1.3	605.	180.	785.	21.
1.6	202.	255.	1.3	562.	228.	790.	27.
2.0	259.	323.	1.2	504.	291.	795.	32.
2.3	288.	457.	1.6	475.	372.	848.	84.
2.7	331.	626.	1.9	432.	478.	910.	147.
3.0	389.	787.	2.0	374.	588.	962.	199.
3.4	461.	983.	2.1	302.	722.	1024.	261.
4.5	605.	1493.	2.5	158.	1049.	1207.	444.
5.0	662.	1710.	2.6	101.	1186.	1287.	524.
5.3	706.	1831.	2.6	58.	1268.	1326.	563.
5.7	763.	2047.	2.7	0.	1405.	1405.	642.
6.2	821.	2200.	2.7	-58.	1510.	1453.	690.
6.6	864.	2419.	2.8	-101.	1641.	1540.	777.
7.0	922.	2570.	2.8	-158.	1746.	1587.	824.
7.4	965.	2745.	2.8	-202.	1855.	1654.	890.
7.8	1008.	2781.	2.8	-245.	1894.	1649.	886.
8.3	1051.	2895.	2.8	-288.	1973.	1685.	922.
9.1	1138.	3082.	2.7	-374.	2110.	1736.	972.
10.0	1195.	3237.	2.7	-432.	2216.	1784.	1021.
10.8	1253.	3374.	2.7	-490.	2313.	1824.	1061.
12.0	1325.	3587.	2.7	-562.	2456.	1894.	1131.
12.9	1368.	3665.	2.7	-605.	2517.	1912.	1149.
14.1	1426.	3838.	2.7	-662.	2632.	1970.	1206.
15.0	1469.	3858.	2.6	-706.	2663.	1958.	1195.

POST CYCLIC STATIC TEST: PC-4
IVINS DIVERSION DAM NO. 5

APPENDIX E

POSTULATED EARTHQUAKE GROUND MOTIONS FOR MAGNITUDE 6.0 NEAR-FIELD EARTHQUAKE

Appendix E

POSTULATED EARTHQUAKE GROUND MOTIONS FOR MAGNITUDE 6.0 NEAR-FIELD EARTHQUAKE

An accelerogram representative of a near-field Magnitude 6.0 earthquake is developed in this appendix. This event could occur on either the Hurricane or Washington fault zones in the vicinity of the dam sites. The accelerogram described herein was used in analyses to evaluate the dynamic response of several representative cross sections of the following dams:

1. Green's Lake Dam No. 3
2. Warner Draw Dam
3. Frog Hollow Dam
4. Ivins Diversion Dam No. 5

Although various procedures may be used for developing an accelerogram corresponding to a particular earthquake level for a given site, the most direct procedure would be to use an actual earthquake record which is similar to the design earthquake in all of the following aspects:

1. Earthquake magnitude.

2. Fault rupture mechanism (type of faulting, focal depth, amount of displacement, etc.).

3. Distance from source to site.

4. Transmission path.

5. Regional and local geologic conditions.

Because of the limited number of existing strong motion accelerograms, it is generally not possible to find an accelerogram which satisfies all of the above criteria. Therefore, it is usually necessary to modify existing accelerograms or to develop synthetic records which meet most of the criteria specified for the design earthquake.

The mean peak horizontal accelerations listed in Table V-1 for each of the four dam sites were selected as representative values which could be expected to occur in the foundation rock during a Magnitude 6.0 earthquake on the nearby faults. These values were established on the basis of attenuation relationships proposed by Seed (1980) and Campbell (1981). The following criteria were also established for the postulated Magnitude 6.0 earthquake:

1. Total duration of about 20 to 25 seconds.

2. Bracketed duration of acceleration above 0.05 g of about 10 to 12 seconds (Bolt, 1973).

3. An interval between P- and S-wave onsets of about 2 to 3 seconds.

4. A pulse following the S-wave arrival that models the "fling" of the fault rebound as the rupture goes by the site. This should appear at about 3 seconds from the beginning of the record.

5. A pseudo-relative velocity spectrum that resembles in shape and level various spectra obtained from earthquake ground motions of a number of past events of similar magnitudes.

In developing a representative accelerogram to be used in the dynamic response analyses, one of the major criterion was to establish the response spectrum shape appropriate for rock sites for a Magnitude 6.0 near-field earthquake. An appropriate earthquake response spectrum was chosen from a compilation of response spectra that have been presented in the literature or recommended by various regulatory agencies. A brief review of the findings and recommendations made by previous investigators is provided in the following text.

The spectral response of earthquake ground motions has been the topic of many investigations (Newmark and Hall, 1969, 1973; Newmark et al., 1973; Mohraz, 1976; Hall et al., 1976; Guzman and Jennings, 1976; Johnson and Traubenik, 1978; Johnson, 1980). Results of these investigations, in the form of generalized response spectral shapes, have been recommended for use in design of various types

of important facilities, such as nuclear power plants (Newmark and Hall, 1969; NRC, 1973; Guzman and Jennings, 1976), pipeline facilities (Newmark, 1975) and offshore drilling platforms (API, 1978). Previous investigations have analyzed numerous response spectra generated from available strong motion records that have been compiled over the years.

The importance of local site geologic conditions on spectral shape has been widely demonstrated (Seed et al., 1974; Mohraz, 1976) and has been generally accepted as a criterion for the selection of appropriate design response spectra (Guzman and Jennings, 1976; Johnson and Traubenik, 1978; Johnson, 1980). Seed et al. (1974) statistically analyzed spectral shapes of over 100 ground motion records and showed that clear differences in spectral shapes exist for different local geologic conditions. Mohraz (1976) arrived at similar conclusions. Because of the lack of strong motion records prior to the 1971 San Fernando earthquake, a disproportionate number of accelerograms from that event was included in both studies. Seed et al. (1974) recognized this limitation in the data set used in their investigation and developed anticipated mean site-dependent response spectra only for a Magnitude 6.5 earthquake at a distance of 8 and 32 kilometers. Results presented by Mohraz, although not explicitly stated in his investigation, are also only applicable to spectral shapes corresponding to a Magnitude 6.5 event.

Johnson (1980) and Johnson and Traubenik (1978) in their investigations of magnitude-dependent near-source ground motion response spectra concluded that spectral shape is a function of earthquake magnitude, geologic site conditions, and source to site distance. McGuire (1977) arrived at basically the same conclusions in his investigation of Fourier amplitude spectra. Thus, the results of these investigations suggest that the amplitude and shape of the response (or Fourier) spectrum should change to reflect distance and geologic effects and increased long period motions associated with increasing earthquake magnitude.

From our review of available SCS geologic reports and information obtained during the Phase I investigation, the local geologic site conditions present at the four dam sites was established. Warner Draw and Frog Hollow dams have been constructed on bedrock near their maximum cross sections. Green's Lake Dam No. 3 and Ivins Diversion Dam No. 5 dams have been constructed on relatively shallow

alluvial/colluvial deposits. As is described in Appendix F, the one-dimensional soil column models of the two dams that are founded on the alluvial/colluvial sites (namely, Green's Lake Dam No. 3 and Ivins Diversion Dam No. 5) include the foundation soils to an assumed average bedrock depth. Since these models include the foundation soils, the ground motions used as input to the models should be representative of the type of motions expected to occur on bedrock during the design earthquake. The one dimensional soil column models of the remaining two dams (i.e., Warner Draw and Frog Hollow Dams) include only the embankment soils to bedrock. Therefore, the ground motions used as the input to these models should also be representative of bedrock ground motions. It is for these reasons that only one representative accelerogram, appropriate for a rock site, had to be developed for the purposes of this investigation.

The earthquake response spectrum shown in Figure E-1 was selected for use in the development of the accelerogram used in this investigation. This spectrum was chosen from a compilation of spectra that have been recommended in the literature. In our judgment, the broad-banded spectrum shown in this figure is a conservative estimate of the spectrum that would be computed from ground motions recorded on bedrock during a Magnitude 6.0 earthquake.

Having established the shape of the response spectrum for the Magnitude 6.0 design earthquake, it was then necessary to produce an accelerogram which satisfied, as closely as possible, all of the other various requirements previously specified. A number of strong motion accelerograms from past earthquakes with magnitudes of about 6.0 are available. Unfortunately, these records do not satisfy all the criteria (such as source-to-site distance, fault rupture mechanism, site conditions, etc.) that were previously mentioned. It is for these reasons that we chose not to modify an existing accelerogram. Instead, a synthetic accelerogram was developed.

A number of synthetic accelerograms are currently available. These include accelerograms developed by investigators at the California Institute of Technology (Jennings et al., 1968, 1969), and the University of California at Berkeley (Seed and Idriss, 1969; Bolt, 1979). Portions of the Cal-Tech A-1 synthetic accelerogram were modified and used in combination with a synthetic accelerogram developed by

Professor Bruce Bolt to construct the accelerogram used in this investigation. The frequency content of the constructed accelerogram was modified so that its response spectrum closely matched the 5 percent damped spectrum shown in Figure E-1. The resulting accelerogram was then baseline corrected to ensure that the velocity and displacement were approximately zero at the end of the record.

The final accelerogram used in the analyses of the four embankments has the characteristics listed in Table E-1. These correspond closely to the values previously specified. It should be noted that the bracketed duration (Bolt, 1973) of the accelerogram is nearly 18 seconds when scaled to 0.66 g, and 12 seconds when scaled to 0.38 g. Originally, a bracketed duration of 10 to 12 seconds was specified; however, it was extremely difficult to obtain this value and at the same time satisfy the response spectral shape requirement.

Plots of the baseline corrected acceleration, velocity, and displacement time histories for the Magnitude 6.0 design earthquake scaled to 1 g are presented in Figure E-2. It can be noted from the velocity time history that this motion has a "fling" component which occurs at about 3 seconds after the beginning of the earthquake. A comparison of the 5 percent damped "target" spectrum with the spectrum obtained from the synthetic accelerogram (scaled to 1 g) is shown in Figure E-3. As can be seen from this figure, the two spectra match very closely over most periods. Acceleration and velocity spectra computed from the synthetic accelerogram (scaled to 1 g) are plotted in Figure E-4 for 2, 5 and 10 percent damping.

Table E-1

Characteristics of Synthetic Accelerogram Developed to Represent a Magnitude 6 Earthquake on a Nearby Fault

Total Duration	= 20.7 seconds	
Significant Duration	= 8.9 seconds (based on Arias Intensity)	
Scaled Peak Acceleration	0.66 g	0.38 g
Peak Velocity	34 cm/sec	19.6 cm/sec
Peak Displacement	22.5 cm	13.0 cm
Bracketed Duration	17.8 seconds	12.0 seconds
Response Spectrum	See Figure E-3	

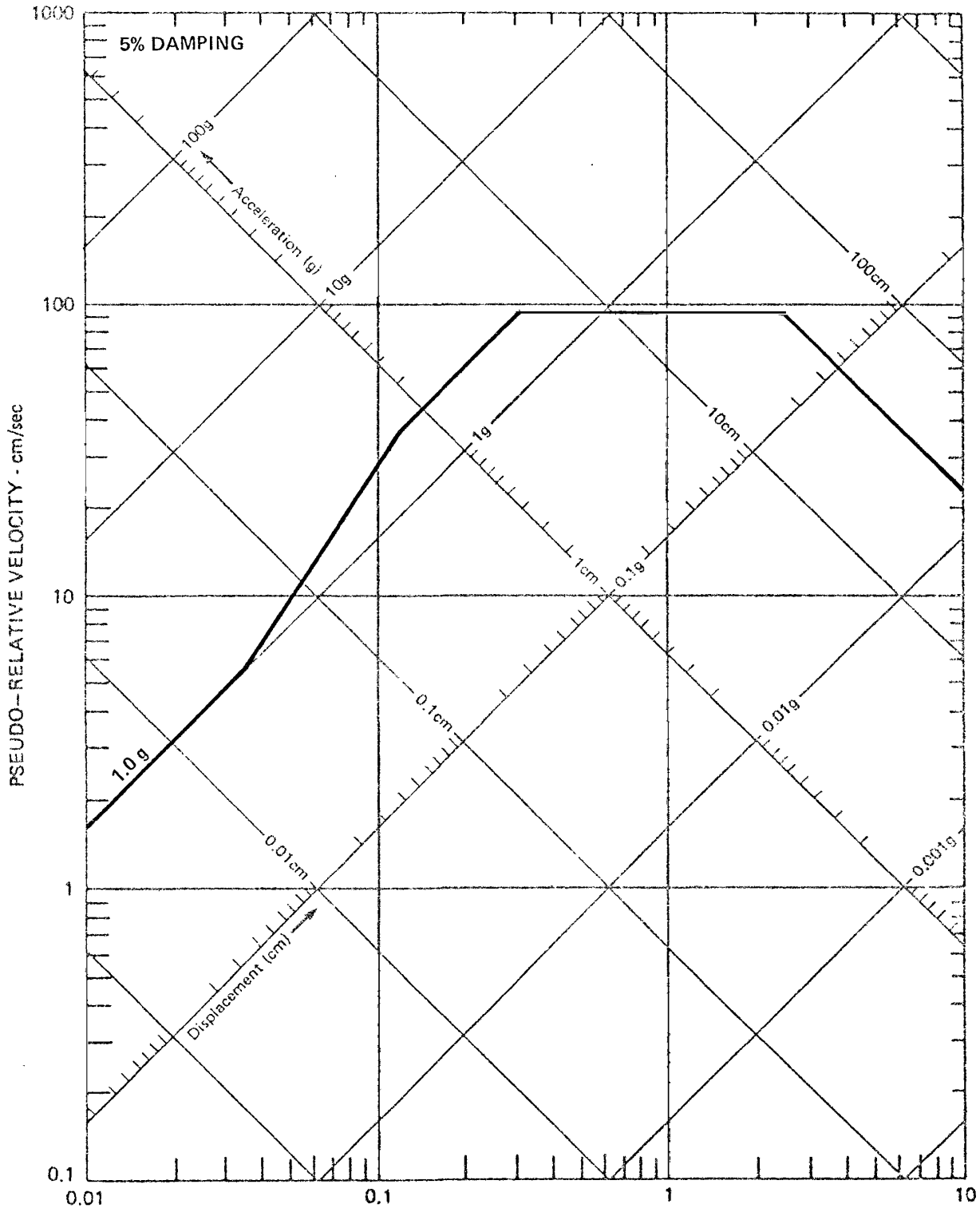

Note: Spectrum Normalized to 1.0 g.

Earth Sciences Associates Palo Alto, California			
SEISMIC SAFETY INVESTIGATION OF EIGHT SCS DAMS **TARGET SPECTRUM FOR MAGNITUDE 6.0 EARTHQUAKE**			
Checked by MLT Date 9/20/82 Approved by J.E. Valera Date 9/22/82	Project No. D118	Figure No. E-1	

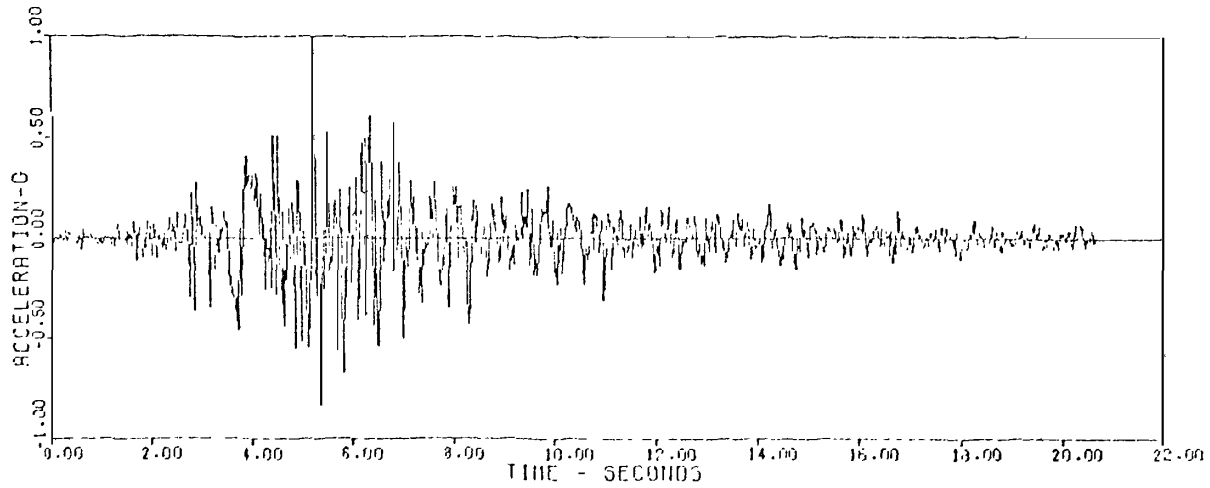

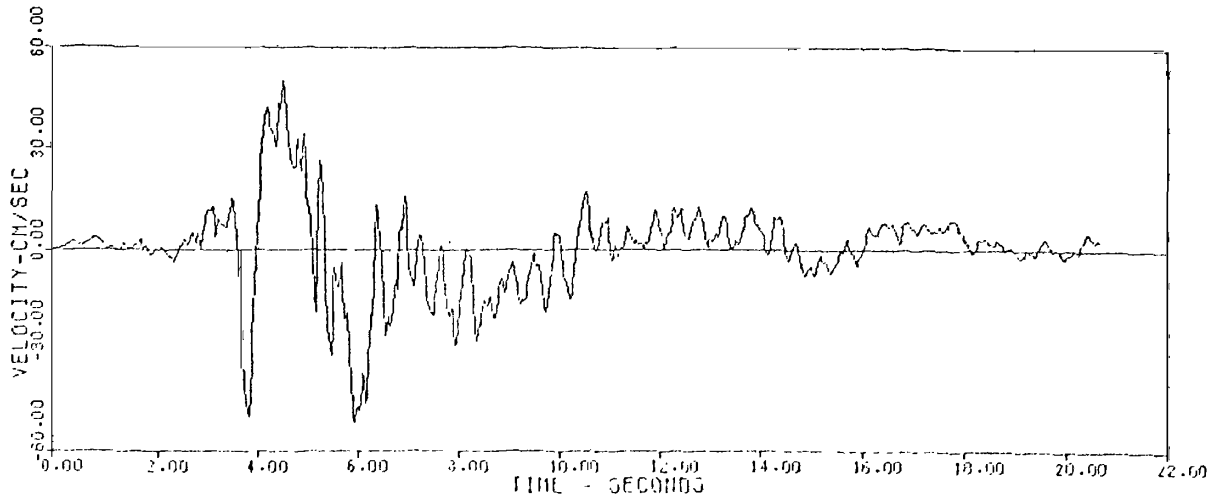

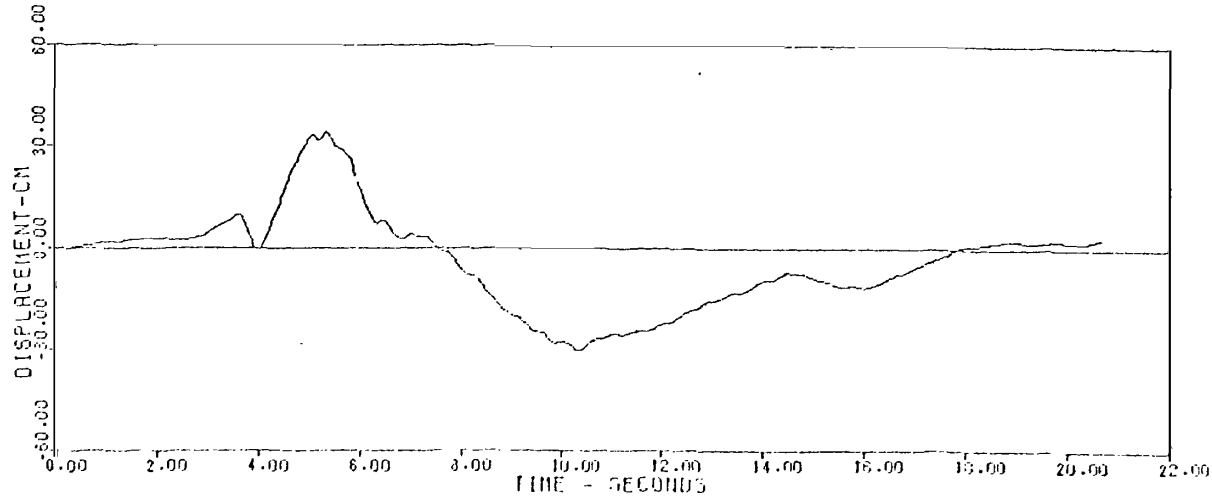

Note : Time-Histories Normalized To 1.0g.

Earth Sciences Associates
Palo Alto, California

SEISMIC SAFETY INVESTIGATION OF EIGHT SCS DAMS
ACCELERATION, VELOCITY AND DISPLACEMENT TIME HISTORIES FOR MAGNITUDE 6.0 EARTHQUAKE

Checked by MLT Date 9/20/82	Project No.	Figure No.
Approved by J.E. Valera Date 9/22/82	D118	E-2

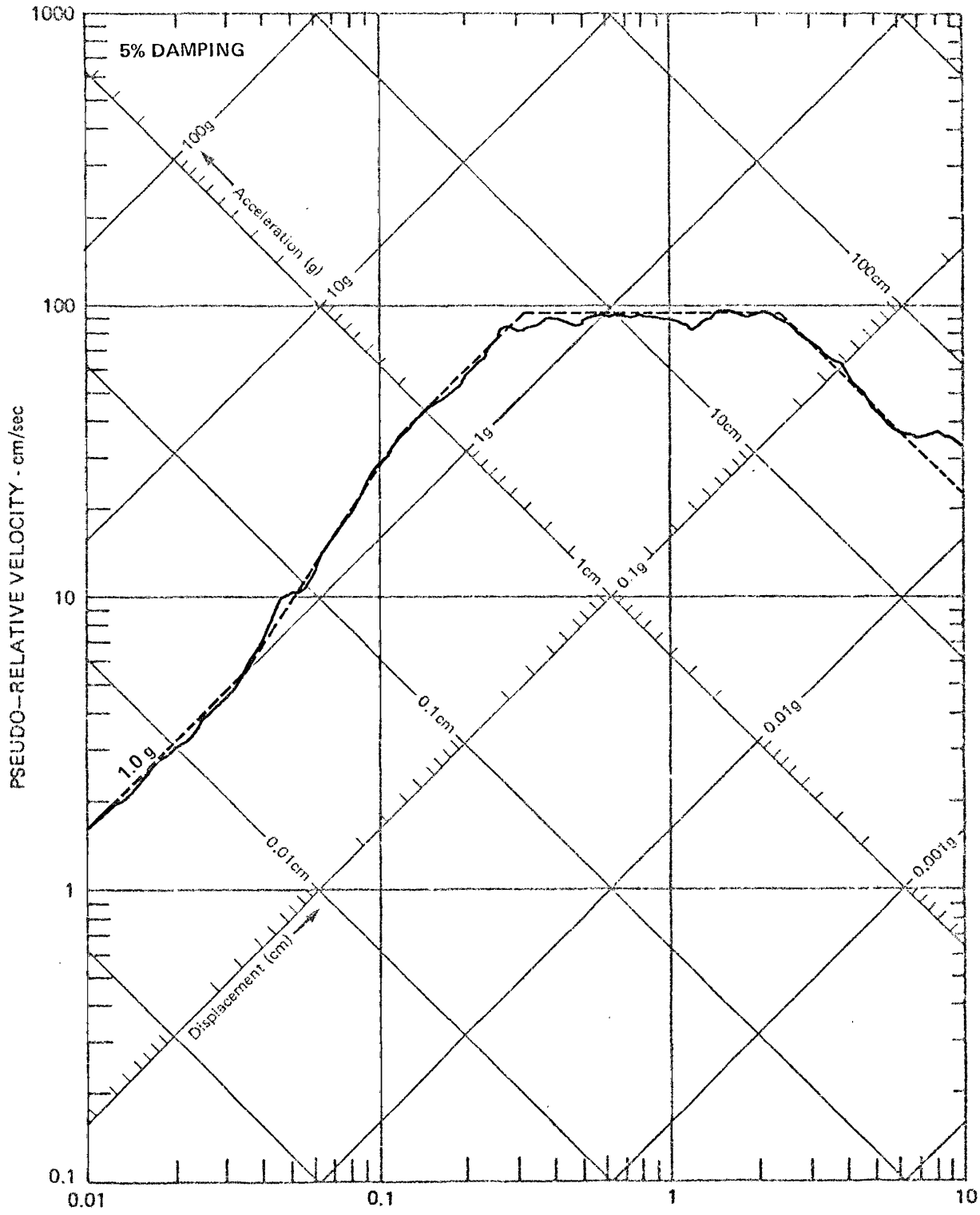

Note : Spectra Normalized to 1.0g.

Earth Sciences Associates
Palo Alto, California

SEISMIC SAFETY INVESTIGATION OF EIGHT SCS DAMS
COMPARISON OF MAGNITUDE 6.0 EARTHQUAKE
TARGET SPECTRUM WITH ACCELEROGRAM SPECTRUM

Checked by MLT Date 9/20/82	Project No.	Figure No.
Approved by J. E. Valera Date 9/22/82	D118	E-3

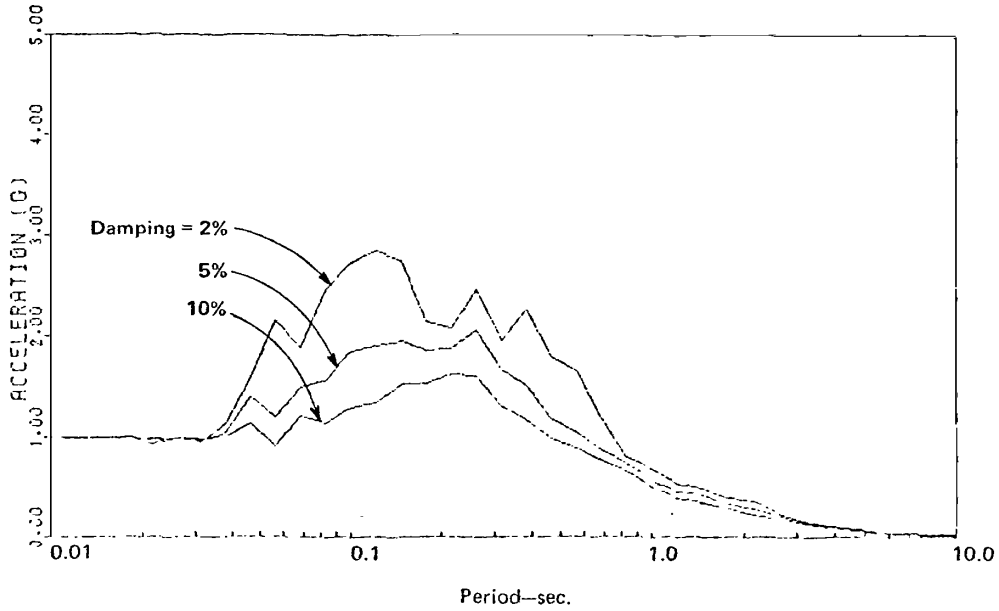

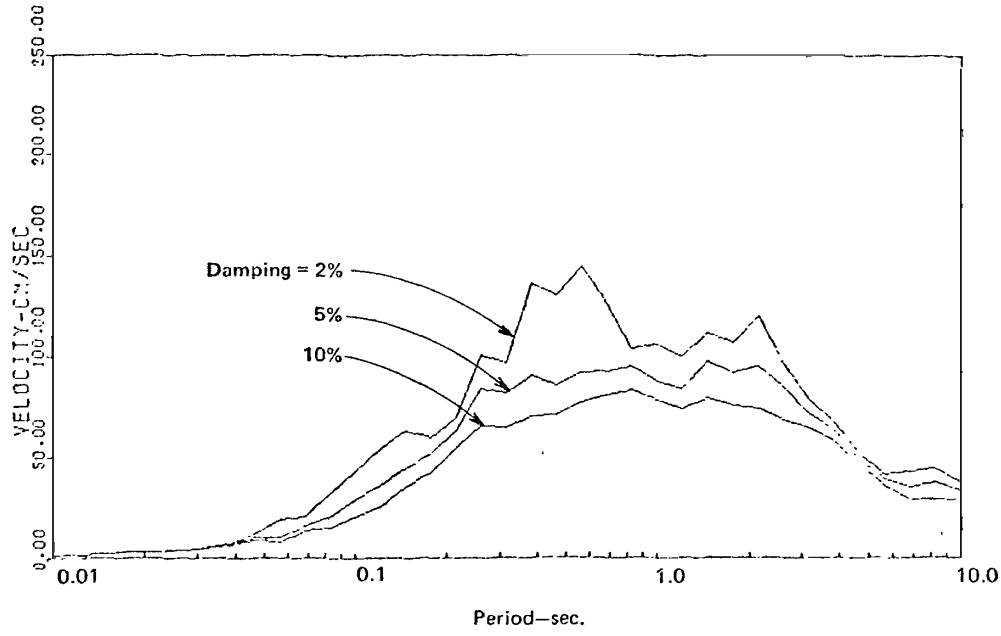

Note : Spectra Normalized to 1.0g.

Earth Sciences Associates Palo Alto, California			
SAFETY INVESTIGATION OF EIGHT SCS DAMS ACCELERATION AND VELOCITY SPECTRA MAGNITUDE 6.0 EARTHQUAKE			
Checked by MLT Date 9/20/82 Approved by J.E. Valera Date 9/22/82		Project No. D118	Figure No. E-4

APPENDIX F

DYNAMIC RESPONSE ANALYSES

Appendix F

DYNAMIC RESPONSE ANALYSES

Introduction

A series of one-dimensional wave propagation analyses were performed to establish the dynamic response of four selected dams during a Magnitude 6.0 earthquake. The four dams for which one-dimensional dynamic response analyses were performed are:

1) Green's Lake Dam No. 3
2) Warner Draw Dam
3) Frog Hollow Dam, and
4) Ivins Diversion Dam No. 5

Since each of the dams listed above are located close (generally less than 8 km) to potentially active earthquake-producing faults, analyses were performed using a synthetic accelerogram which was developed utilizing earthquake ground motion criteria considered appropriate for a nearby Magnitude 6.0 earthquake (see Appendix E for details on the postulated earthquake ground motion accelerogram). Results of these analyses were used to estimate: 1) the distribution of induced dynamic shear stresses, 2) the peak acceleration at the crest of each embankment, and 3) the fundamental period of the embankments during the earthquake ground motions postulated for each site. In addition, results of the analyses were used as a guide in establishing the induced dynamic shear stresses of the four other dam embankments (and foundations) for which dynamic response analyses were not performed.

Analyses were carried out using the computer program SHAKE (Schnabel et al., 1972). Results of these types of analyses have been shown to compare favorably with those evaluated using more sophisticated finite element techniques (Vrymoed et al., 1978). This appendix describes the models and analyses that have been carried out to evaluate the dynamic response of the four dam embankments. In addition to the one-dimensional dynamic response analyses, simplified analyses were performed on representative cross-sections of Gypsum Wash and Stucki dams. These analyses were used to estimate the levels of stresses induced by

the earthquake ground motions postulated for these sites and were used to evaluate the liquefaction potential of the embankment and foundation soils. These simplified analyses are described in the last section of this appendix.

The results and conclusions derived from the analyses described in this appendix are discussed in Appendix G and are also summarized in the main text of this report (see Chapters VI and VII).

One-Dimensional Soil Column Models

A total of six one-dimensional soil column models were developed and analyzed as part of this investigation. Four of the soil column models were used to represent profiles through each dam crest at its maximum cross section. Since the Warner Draw and Frog Hollow Dam embankments are founded on bedrock at their maximum cross sections, the soil column models used in the analyses of these dams included only embankment materials as shown in Figure F-1A. Green's Lake Dam No. 3 and Ivins Diversion Dam No. 5, on the other hand, are both founded on shallow soil foundations. Therefore, the soil column models of these dams included both the embankment and foundation soils to bedrock, as shown in Figure F-1B. In addition to the four soil column models described above, two soil column models representing the foundation soils near the upstream toes of Green's Lake Dam No. 3 and Ivins Diversion Dam No. 5 were also developed and analyzed (see Figure F-1B). Information pertaining to all the soil column models is summarized in Table F-1.

Dynamic Soil Properties

Dynamic soil properties consisting of dynamic shear modulus and hysteretic soil damping, and their variation with the level of cyclic shear strain are required for the dynamic response analyses described above. These properties are usually established on the basis of field downhole or crosshole geophysical surveys and laboratory testing programs. Field geophysical surveys and laboratory testing programs of this type can be quite expensive even when the dynamic properties for only one dam embankment need to be established. The cost of performing these investigations on the dams considered in this study prohibited their application.

Table F-1

Summary of Soil Column Models Analyzed

Dam	Profile Represented[1]	Approximate Station of Profile	Total Depth of Profile (ft)	Height of Embankment (ft)/ Number of Soil Layers Representing Embankment	Thickness of Foundation Soils (ft)/ Number of Soil Layers Representing Foundation	Range of Layer Thickness (ft)	Depth[2] to Phreatic Surface (ft)
Green's Lake No. 3	Embankment and foundation to bedrock	11+00	68	20/3	48/5	6-10	6
	Foundation near upstream toe	--	50	--/--	50/5	10	0
Warner Draw	Embankment to bedrock	16+00	68	68/9	--/--	5-10	16
Frog Hollow	Embankment to bedrock	11+77	58	58/8	--/--	5-10	10
Ivins Diversion No. 5	Embankment and foundation to bedrock	20+00	60	20/4	40/4	4-12	4
	Foundation near upstream toe	--	40	--/--	40/4	10	0

Notes:

(1) The profiles are located near maximum cross section of embankment. For profiles through embankments, top of profile is at the dam crest.

(2) The depth to the phreatic surface for the profiles representing the dam embankments was established by assuming the impounded reservoir elevation at either the principal spillway crest, R/C chute or inlet riser crest elevation.

Therefore, the dynamic soil properties for each of the dams for which dynamic response analyses were performed were established on the basis of published and unpublished data, as well as engineering judgment.

Results of a number of studies performed by various investigators have shown that for materials similar to those comprising the dam embankments considered in this investigation, the dynamic shear modulus is a function of the mean effective confining pressure (Hardin and Black, 1968, 1969; Hardin and Drnevich, 1972; Seed and Idriss, 1970; Anderson et al., 1978; Stokoe and Lodde, 1978; Stokoe et al., 1978). A comprehensive survey of the factors affecting the shear moduli and damping characteristics of soils and expressions for determining these properties have been presented by Hardin and Drnevich (1972). Relationships were presented to establish the maximum shear modulus, G_{max}, corresponding to essentially zero shear strain. The expression used for evaluating the maximum shear modulus is:

$$G_{max} = 14760 \frac{(2.973-e)^2}{1+e} (OCR)^a (\sigma_m')^{\frac{1}{2}} \qquad (1)$$

where

G_{max} = maximum shear modulus (psf)

e = void ratio

OCR = overconsolidation ratio

a = a parameter that depends on the plasticity index of the soil, and

σ_m' = mean effective confining stress (psf).

Equation (1) may be rewritten to have the form:

$$G_{max} = 1000 K_{2max} (\sigma_m')^{\frac{1}{2}} \qquad (2)$$

where

$$K_{2max} = 14.76 \frac{(2.973-e)^2}{1+e} (OCR)^a \qquad (3)$$

When moderate to high levels of cyclic strain are anticipated, the values of G_{max} evaluated using Equations (1) or (2) need to be modified to account for the reduction of G_{max} with increasing cyclic strain.

For those dams for which dynamic response analyses were performed, values of K_{2max} were estimated for the various soils comprising the dam embankments (and their foundation soils, if present) using Equation (3). The void ratios of the various materials were estimated using the equation:

$$e = G_s \frac{\gamma_w}{\gamma_d} - 1 \qquad (4)$$

where

G_s = specific gravity

γ_w = unit weight of water (equal to 62.4 pcf)

γ_d = dry unit weight of the soil (psf).

Average values of the dry unit weight of the soils were established from compilations of data obtained from 1) in situ density tests performed during construction of the embankments available in SCS files, 2) in situ density tests performed during the Phase I field investigation, and 3) laboratory tests performed during Phase II. Average specific gravities of the soils were either determined from results of laboratory tests available in the SCS files, or estimated from published data for similar soil types. Since most of the embankment and foundation soils are probably normally consolidated, the term $(OCR)^a$ in Equation (3) is equal to one, and values of K_{2max} may be easily evaluated. Values of γ_d, G_s, e and K_{2max} estimated for the various soils comprising the dams and their foundations are summarized in Table F-2. The values of K_{2max} listed in Table F-2 are within the range of values reported by Seed and Idriss (1970) for similar types of site conditions. The values of K_{2max} reported by Seed and Idriss (1970) are based on results of both laboratory test and in situ shear wave velocity measurements. Therefore, the values of K_{2max} listed in Table F-2 are probably within the range of values which would be obtained from field geophysical surveys performed on the dam embankments and their foundations.

Table F-2

Summary of Average Soil Properties of Selected Embankments

Dam	Zone	Soil Type	Dry Unit Weight γ_d (pcf)	Specific Gravity G_s	Void Rate e	Average K_{2max}
Green's Lake Dam No. 3	Zone II (core)	Silty sand-clayey sand	117	2.70	0.44	66
	Zone I (shells)	Silty sand, sandy silt with gravel & cobbles	114	2.70	0.48	62
	Foundation	Alluvium/ colluvium	112	2.70	0.50	60
Warner Draw	Zone I (core)	Silty sand clayey sand w/gravel	127	2.75	0.35	75
Frog Hollow	Zone I (core)	Silty clay sandy clay	115	2.80	0.52	58
Ivins Diversion Dam No. 5	Zone I (core & most of the embankment)	Silty sand, sandy silt	114	2.75	0.50	60
	Foundation	Silty sand, sandy silt some clay & gravel	105	2.75	0.63	50

Having established values of K_{2max} appropriate for low levels of strain, values of the corresponding dynamic shear modulus, G_{max}, at any depth in the profile may be computed from Equation (2). Values of dynamic shear modulus and soil hysteretic damping at other cyclic strain levels can be evaluated from the relationships shown in Figure F-2. The relationships shown in this figure were selected from a review of published and unpublished data and are based on both field and laboratory test data for sands and clays. Similar relationships have been used by other investigators to evaluate the dynamic response of other dam embankments similar to those considered in this investigation.

Discussion of Results

Results of the one-dimensional wave propagation analyses carried out on the six soil profiles are presented in Figures F-3 through F-14. Results are in the form of plots showing 1) acceleration time histories obtained at the surface of the profile, 2) response spectrum of the surface motions, and 3) shear stress time-histories for various depths within the profiles analyzed.

The peak accelerations obtained at the surfaces of the various soil column models are summarized in Table F-3. These values are compared with the peak bedrock accelerations used as the input motion at the base of each profile. From the results presented in Table F-3, it can be seen that, with the exception of the profile representing the foundation at the upstream toe of Ivins Diversion Dam No. 5, the peak accelerations at the top of the soil profiles are, on an average, about 28 percent lower than the peak bedrock accelerations. This reduction of peak acceleration at the surface of the profile was used as a guide in establishing the peak ground accelerations for the remaining four dams for which detailed dynamic response analyses were not performed.

Shear stress time histories at three depths within each of the soil column models are shown in Figures F-9 through F-14. All shear stress histories show an increase in magnitude with increasing depth.

In addition to the results of the dynamic response analyses presented in Figures F-3 through F-14, induced cyclic shear stress ratios were computed and plotted versus depth for each of the profiles analyzed. For those embankments

Table F-3

Comparison of Peak Bedrock Accelerations with Peak Accelerations at Top of Profile

Dam	Profile	Peak Bedrock Acceleration (g)	Peak Acceleration at Surface of Profile (g)	Remarks
Green's Lake No. 3	Embankment and Foundation to Bedrock	0.66	0.42	36% Reduction
"	Foundation Near Upstream Toe	0.66	0.50	24% Reduction
Warner Draw	Embankment to Bedrock	0.66	0.48	27% Reduction
Frog Hollow	Embankment to Bedrock	0.65	0.45	31% Reduction
Ivins Diversion No. 5	Embankment and Foundation to Bedrock	0.38	0.29	24% Reduction
"	Foundation Near Upstream Toe	0.38	0.42	11% Increase

and foundations consisting primarily of sandy (cohesionless) soils, the induced cyclic shear stress ratio was computed by dividing the "average" dynamic shear stress, $(\tau_{cy})_{avg}$, by the effective overburden pressure, σ_o, corresponding to the depth considered. The average dynamic shear stress was computed as 65 percent of the maximum dynamic shear stress induced within a soil layer by the earthquake ground motions (Seed, 1979). The cyclic stress ratio $(\tau_{cy}/\sigma_o)_{avg}$ was computed in this manner for the following dams:

1. Green's Lake No. 3,
2. Warner Draw and
3. Ivins Diversion No. 5.

A large portion of Frog Hollow Dam consists primarily of clayey soils. The average cyclic shear stress ratio for this dam was computed as $(\tau_{cy}/S_u)_{avg}$, where S_u is the average undrained shear strength of the soil at the depth of interest. The cyclic stress ratio $(\tau_{cy}/S_u)_{avg}$, computed in this manner is a more useful parameter by which to judge the severity of earthquake loading for clayey soils.

Cyclic stress ratios computed from the results of the dynamic response analyses described above were used to establish the testing conditions for laboratory cyclic triaxial tests. Comparisons of the results of the dynamic response analyses with the results of the laboratory tests are presented in Appendix G of this report. For those embankments and foundations consisting of primarily sandy soils, the cyclic shear stress ratios computed from the results of the dynamic response analyses are also compared with the cyclic stress ratios required to cause initial liquefaction computed from results of Standard Penetration Tests. Comparisons of this type are useful in evaluating liquefaction potential of the various soils comprising the embankments and foundations. These comparisons are presented in Appendix G of this report.

Fundamental Periods of Embankments

The fundamental period, T_o, of an embankment is one of the parameters used in methods to estimate the amount of permanent deformation that the embankment might undergo as a result of earthquake ground shaking. Values of T_o may

be estimated using the relationship (Makdisi and Seed, 1979):

$$T_o = \frac{2\pi}{2.4} \frac{h}{v_s} \qquad (5)$$

where

h = height of the embankment (ft), and

v_s = average shear wave velocity of the embankment soils during earthquake ground shaking (fps).

Average shear wave velocities, v_s, of the embankment soils obtained from the results of dynamic response analyses are summarized in Table F-4. The fundamental periods, computed for each embankment using these values of v_s and Equation (5) are also listed in Table F-4.

Simplified Procedures to Determine Cyclic Shear Stress Ratios for Gypsum Wash and Stucki Dams

In addition to the one-dimensional dynamic response analyses described above, analyses were performed on representative cross-sections of Gypsum Wash and Stucki Dams. These analyses were used to estimate the cyclic shear stress ratio, $(\tau_{cy}/\sigma'_o)_{avg}$, versus depth profiles induced by the earthquake ground motions postulated for these sites. Results of these analyses were used along with results of Standard Penetration Tests (SPT) to help evaluate the liquefaction potential of the soils comprising the embankments and foundations of these dams (see Appendix G).

The cyclic stress ratio versus depth profiles for Gypsum Wash and Stucki Dams were estimated using the simplified procedure described by Seed (1979a). In this method, the cyclic stress ratio at any depth of a soil profile may be estimated using the relationship:

$$(\tau_{cy}/\sigma'_o)_{avg} = 0.65 \times a_{max} \times \frac{\sigma_o}{\sigma'_o} \times r_d \qquad (6)$$

where, a_{max} = peak acceleration at the surface of the profile, σ_o = total overburden pressure at a given depth; σ_o' = effective overburden pressure; and r_d = a stress reduction factor varying from a value of 1.0 at the ground surface to an average value of approximately 0.6 at a depth of 100 feet.

Table F-4

Average Shear Wave Velocity and Fundamental Periods of Embankments

Dam	Average Shear Wave Velocity- v_s (fps)	Computed Fundamental Period - T_o (sec)
Green's Lake No. 3	419	0.13
Warner Draw	450	0.40
Frog Hollow	367	0.41
Ivins Diversion No. 5	438	0.12

The peak horizontal bedrock accelerations expected to occur at each dam site during the postulated Magnitude 6.0 earthquake have been discussed in Chapter V of the main text of this report. The results of the one-dimensional dynamic response analyses summarized in Table F-3 indicate that the peak acceleration expected to occur at the surface of the soil column profiles are, on the average, 28 percent less than the input peak bedrock accelerations. Based on these results, the value of a_{max} used in equation 6 for Gypsum Wash and Stucki Dams was assumed to be approximately equal to 72 percent of the peak bedrock acceleration values listed in Table V-1. The total and effective overburden pressures in equation (6) were calculated for various depths within representative profiles of these two dams using estimated average total and buoyant until weights of the embankment and foundation soils.

Profiles showing the variation of the cyclic stress ratio with depth for the profiles representing Gypsum Wash and Stucki Dams are presented in Appendix G.

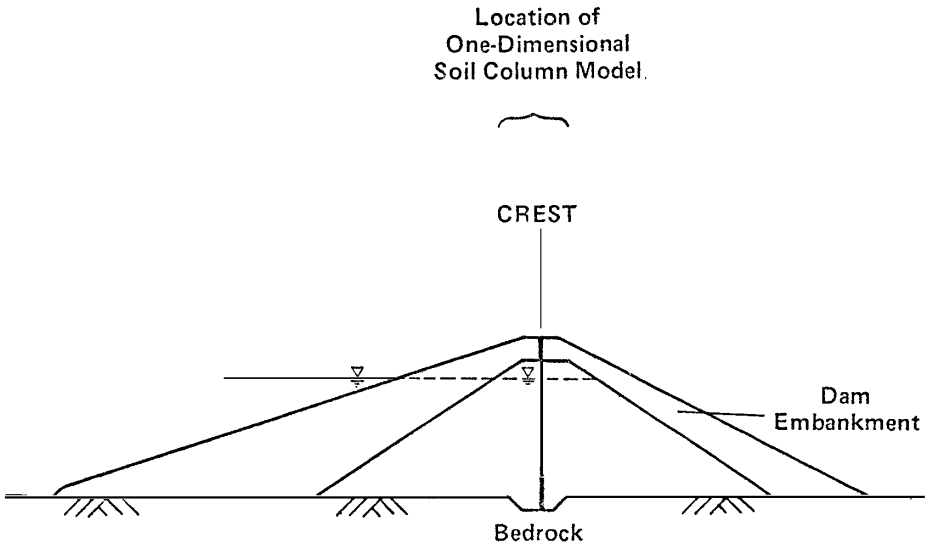

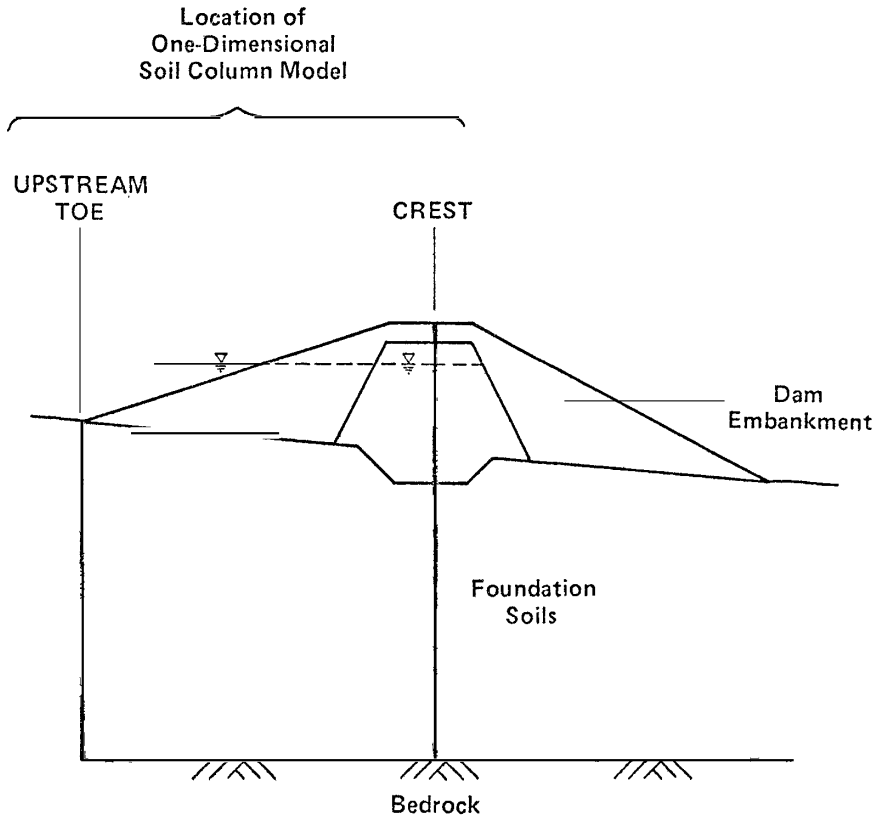

- WARNER DRAW
- FROG HOLLOW

- GREEN'S LAKE DAM NO. 3
- IVINS DIVERSION DAM NO. 5

Earth Sciences Associates
Palo Alto, California

SEISMIC SAFETY INVESTIGATION OF EIGHT SCS DAMS
LOCATION OF ONE-DIMENSIONAL
SOIL COLUMN MODELS

Checked by MLT Date 9/20/82	Project No.	Figure No.
Approved by J. E. Valera Date 9/22/82	D118	F-1

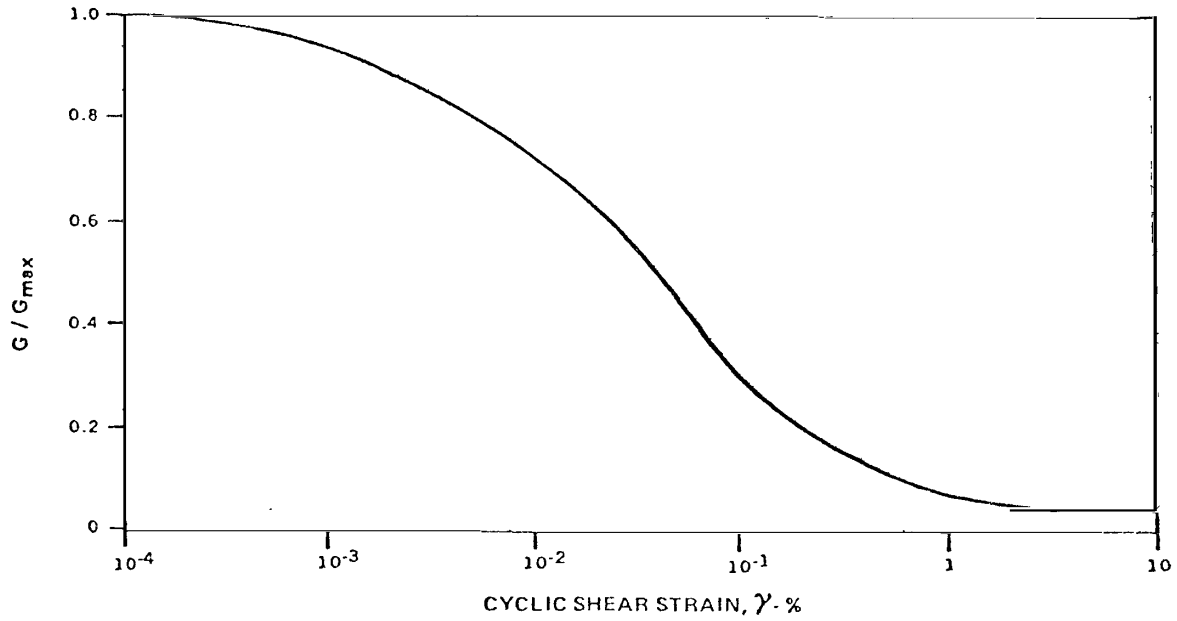

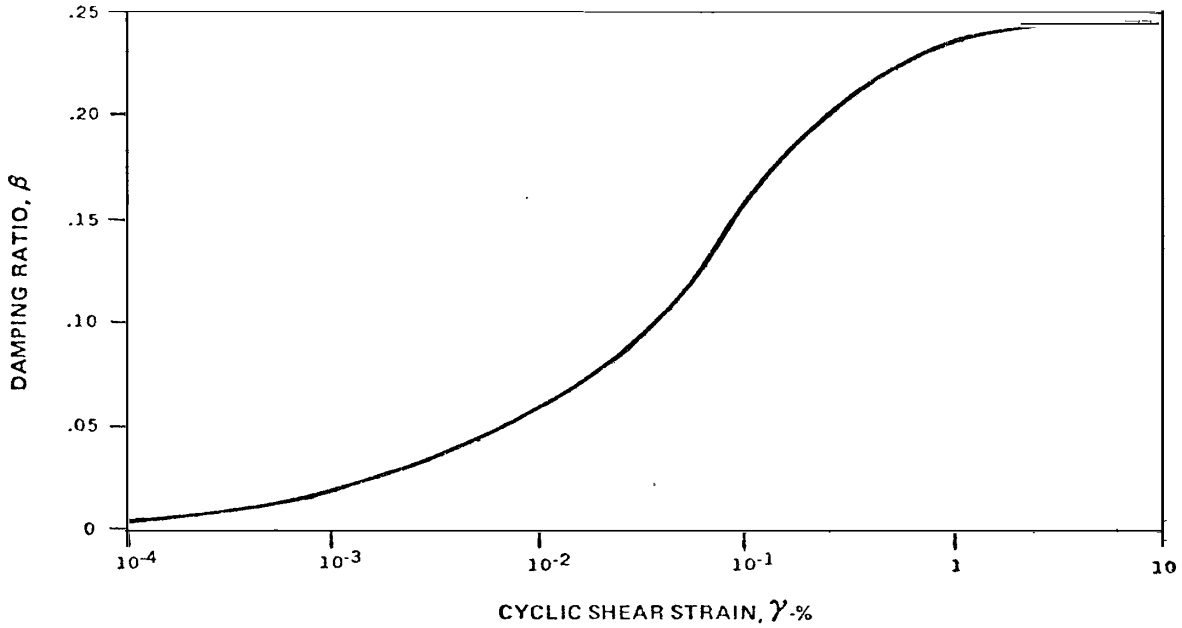

Earth Sciences Associates
Palo Alto, California

SEISMIC SAFETY INVESTIGATION OF EIGHT SCS DAMS
VARIATION OF SHEAR MODULUS AND
HYSTERIC DAMPING WITH CYCLIC SHEAR STRAIN

Checked by MLT Date 9/20/82	Project No.	Figure No.
Approved by J. E. Valera Date 9/22/82	D118	F-2

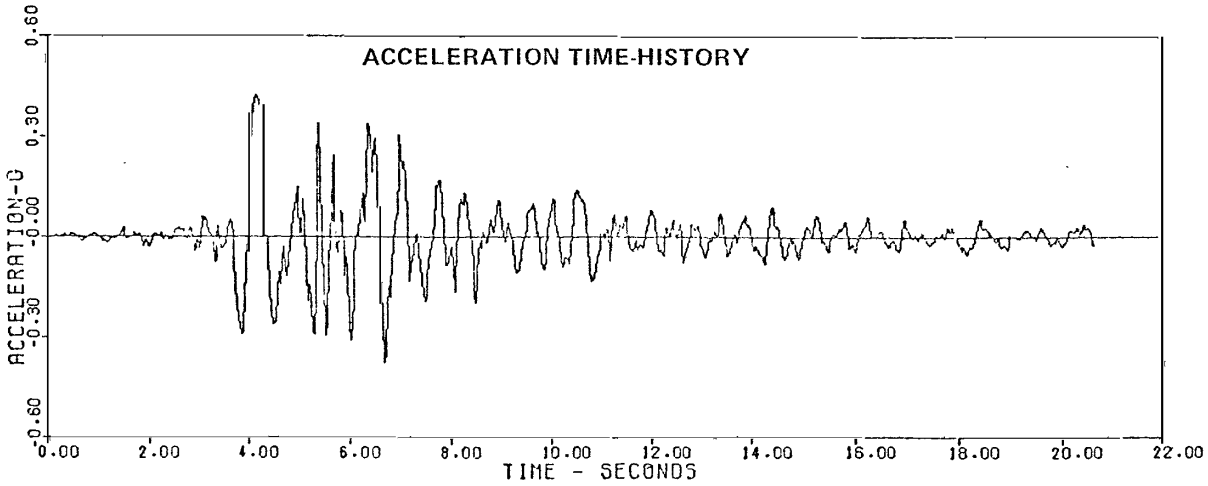

RESPONSE SPECTRUM

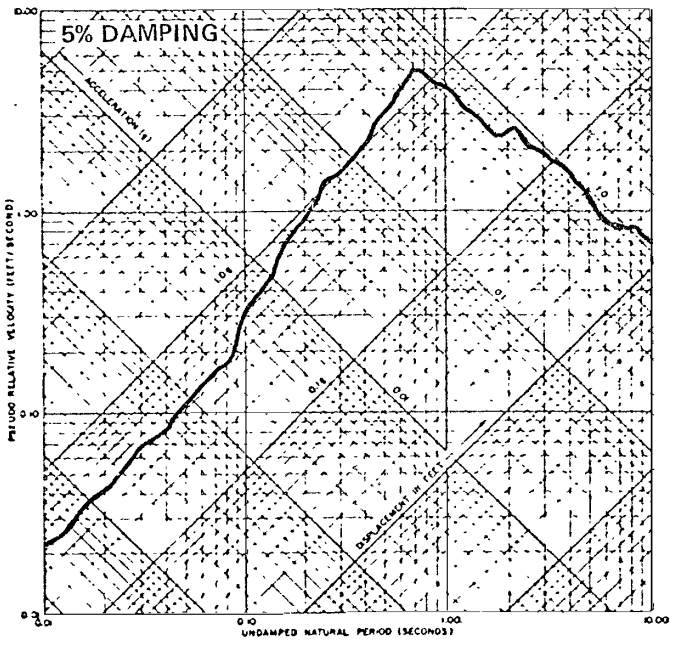

Earth Sciences Associates Palo Alto, California			
SEISMIC SAFETY INVESTIGATION OF EIGHT SCS DAMS **DYNAMIC RESPONSE AT DAM CREST – MAXIMUM CROSS-SECTION** **GREEN'S LAKE DAM NO. 3**			
Checked by MLT Date 9/20/82 Approved by J.E. Valera Date 9/22/82	Project No. D118	Figure No. F-3	

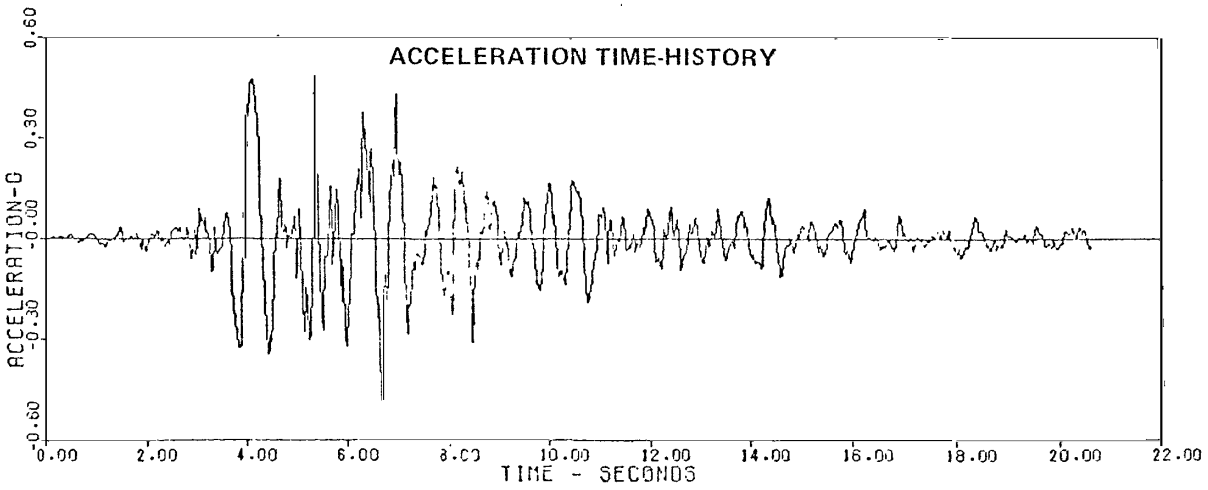

RESPONSE SPECTRUM

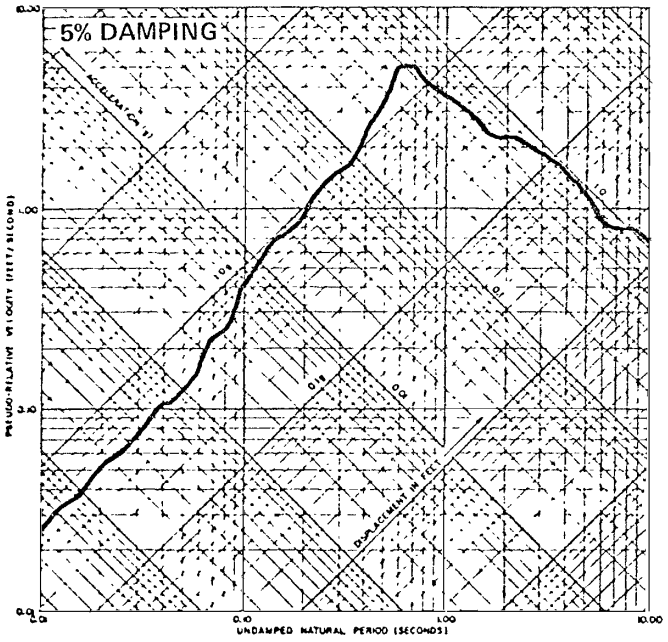

Earth Sciences Associates Palo Alto, California			
SEISMIC SAFETY INVESTIGATION OF EIGHT SCS DAMS DYNAMIC RESPONSE AT UPSTREAM TOE OF EMBANKMENT GREEN'S LAKE DAM NO. 3			
Checked by MLT Date 9/20/82 Approved by J.E. Valera Date 9/22/82		Project No. D118	Figure No. F-4

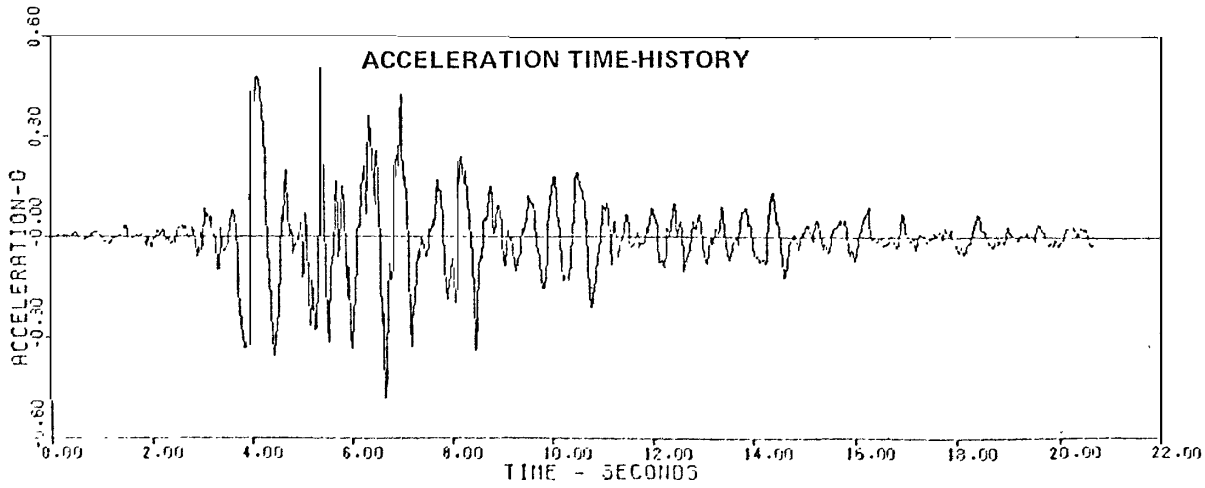

RESPONSE SPECTRUM

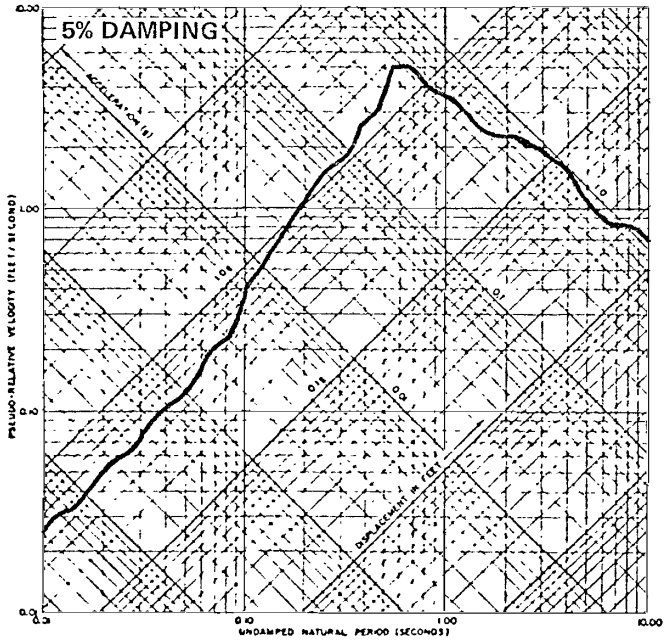

Earth Sciences Associates
Palo Alto, California

SEISMIC SAFETY INVESTIGATION OF EIGHT SCS DAMS
DYNAMIC RESPONSE AT DAM CREST – MAXIMUM CROSS-SECTION
WARNER DRAW DAM

Checked by MCT	Date 9/20/82	Project No.	Figure No.
Approved by J.E. Valera	Date 9/22/82	D118	F-5

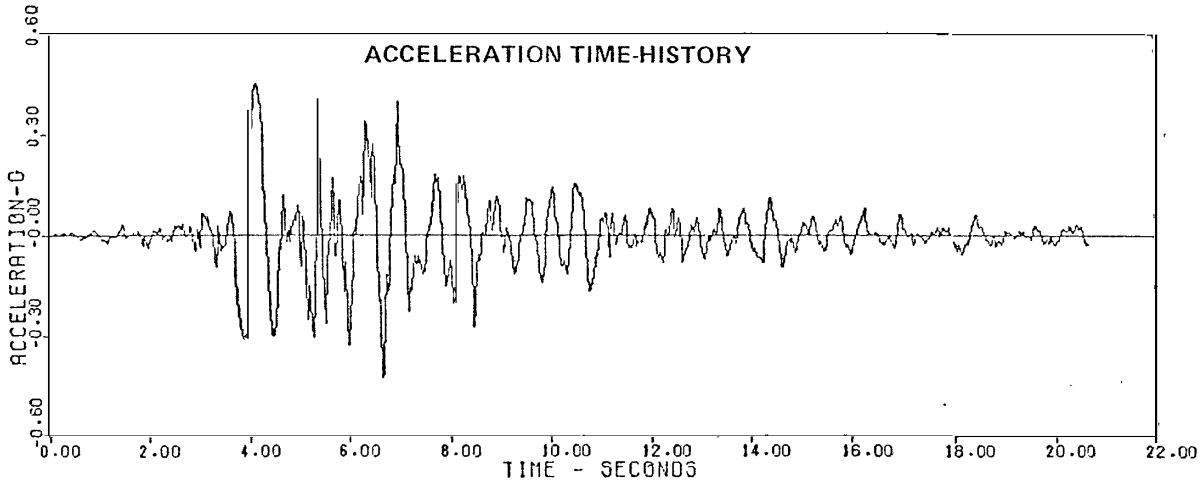

RESPONSE SPECTRUM

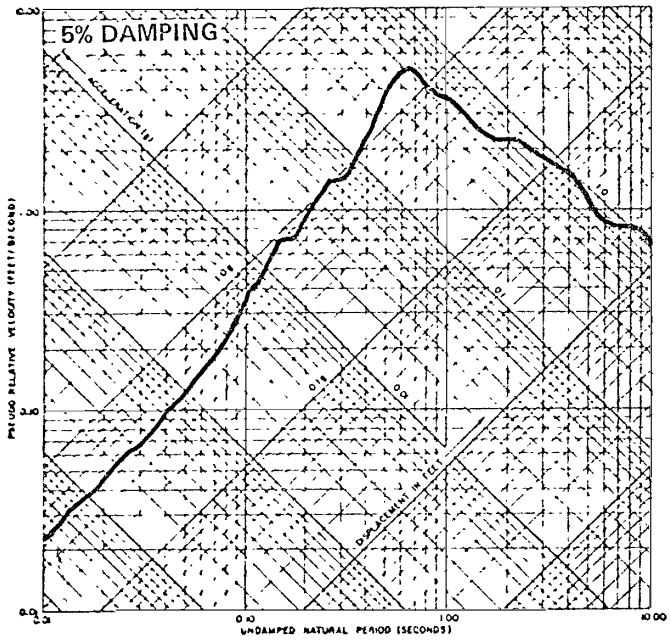

Earth Sciences Associates Palo Alto, California		
SEISMIC SAFETY INVESTIGATION OF EIGHT SCS DAMS **DYNAMIC RESPONSE AT DAM CREST – MAXIMUM CROSS-SECTION** **FROG HOLLOW DAM**		
Checked by MLT Date 9/20/82 Approved by J. E. Valera Date 9/22/82	Project No. D118	Figure No. F-6

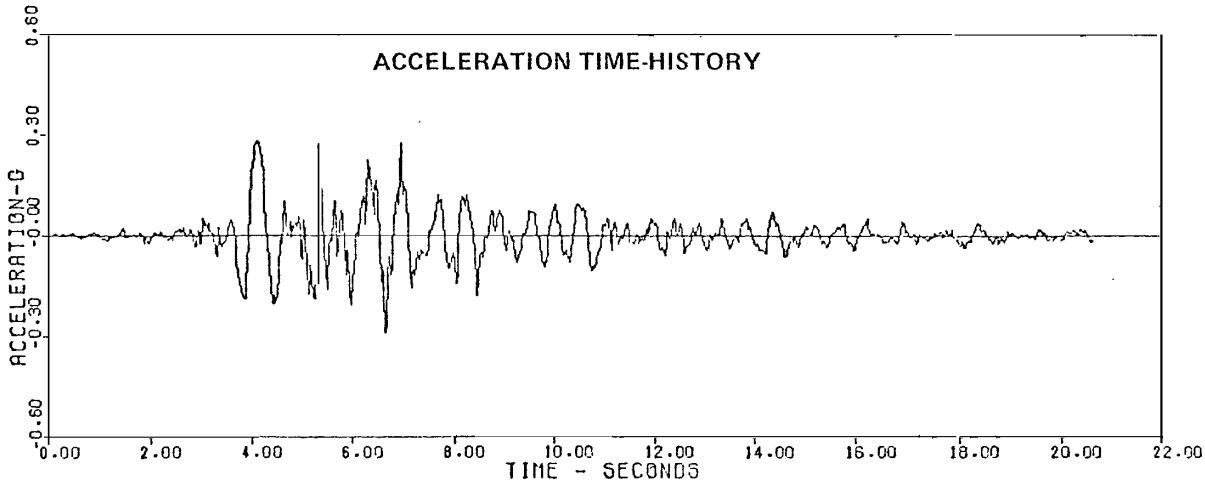

RESPONSE SPECTRUM

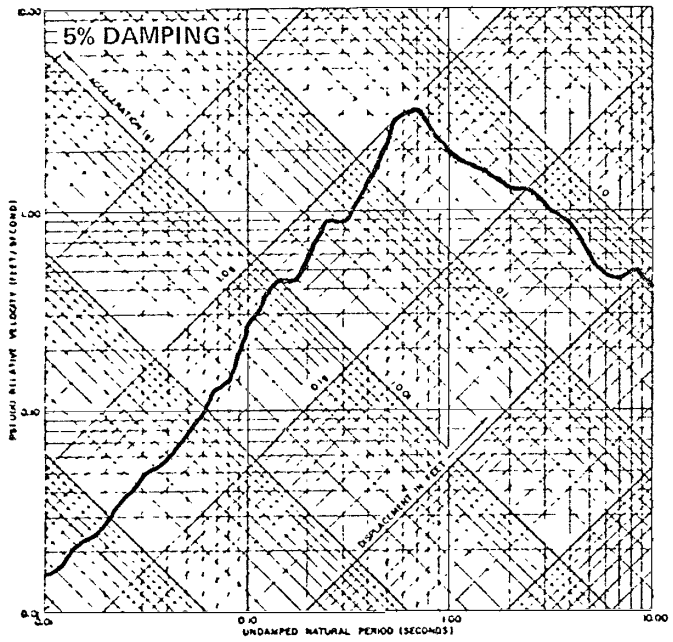

Earth Sciences Associates
Palo Alto, California

SEISMIC SAFETY INVESTIGATION OF EIGHT SCS DAMS
DYNAMIC RESPONSE AT DAM CREST –
MAXIMUM CROSS-SECTION
IVINS DIVERSION DAM NO. 5

Checked by MLT Date 9/20/82	Project No.	Figure No.
Approved by J.E. Valera Date 9/22/82	D118	F-7

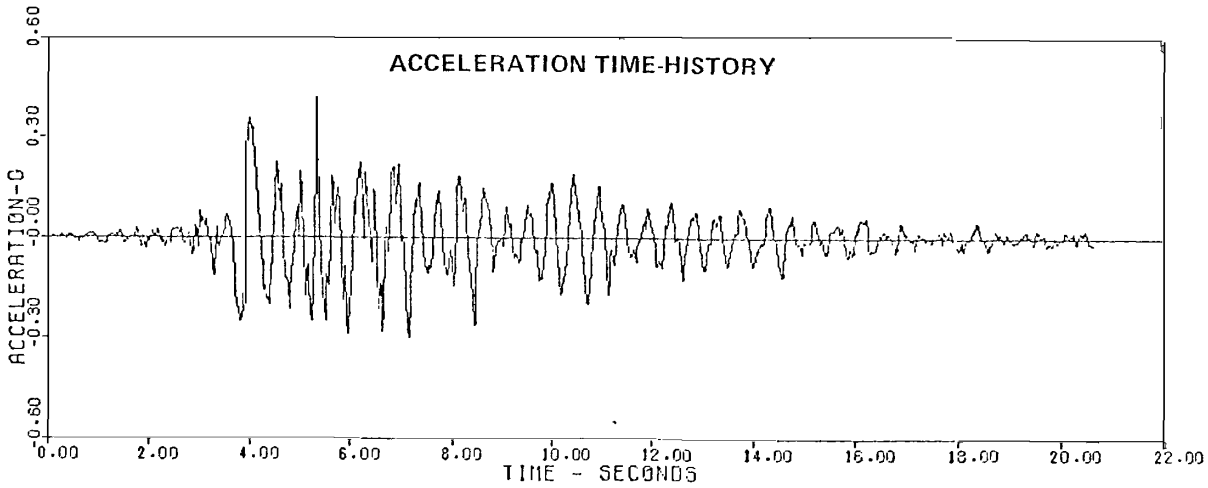

RESPONSE SPECTRUM

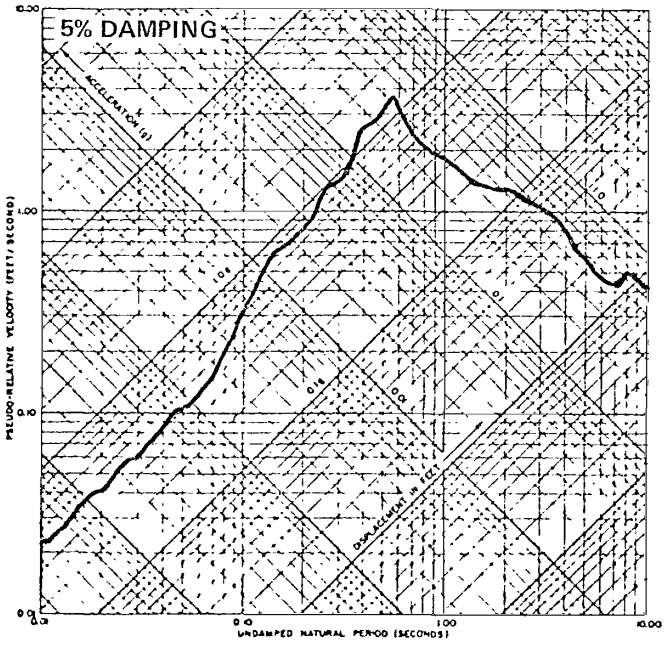

Earth Sciences Associates Palo Alto, California	
SEISMIC SAFETY INVESTIGATION OF EIGHT SCS DAMS DYNAMIC RESPONSE AT UPSTREAM TOE OF EMBANKMENT IVINS DIVERSION DAM NO. 5	
Checked by MJT Date 9/20/82 Approved by J.E. Valera Date 9/22/82	Project No. D118 / Figure No. F-8

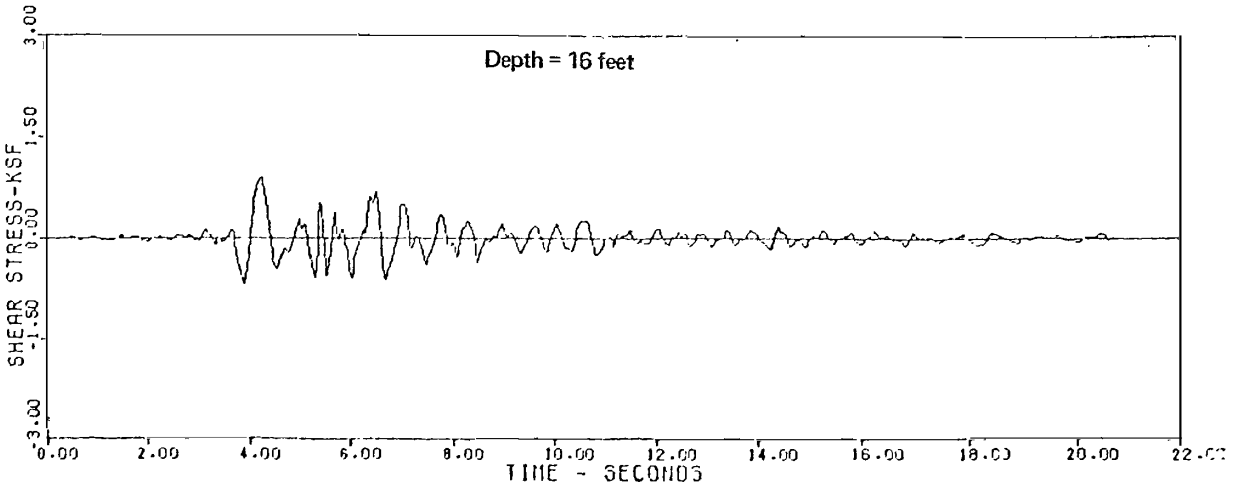

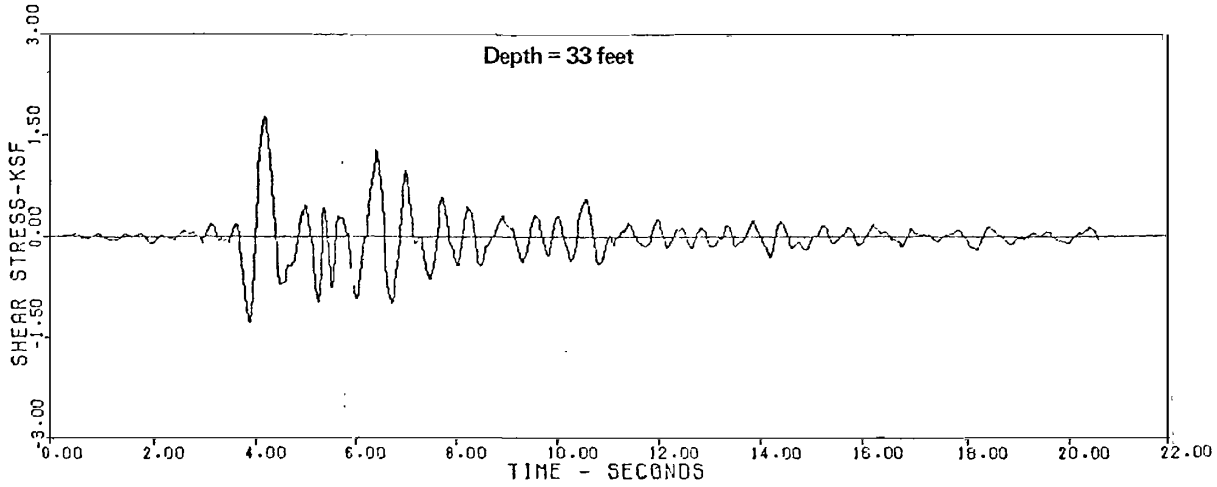

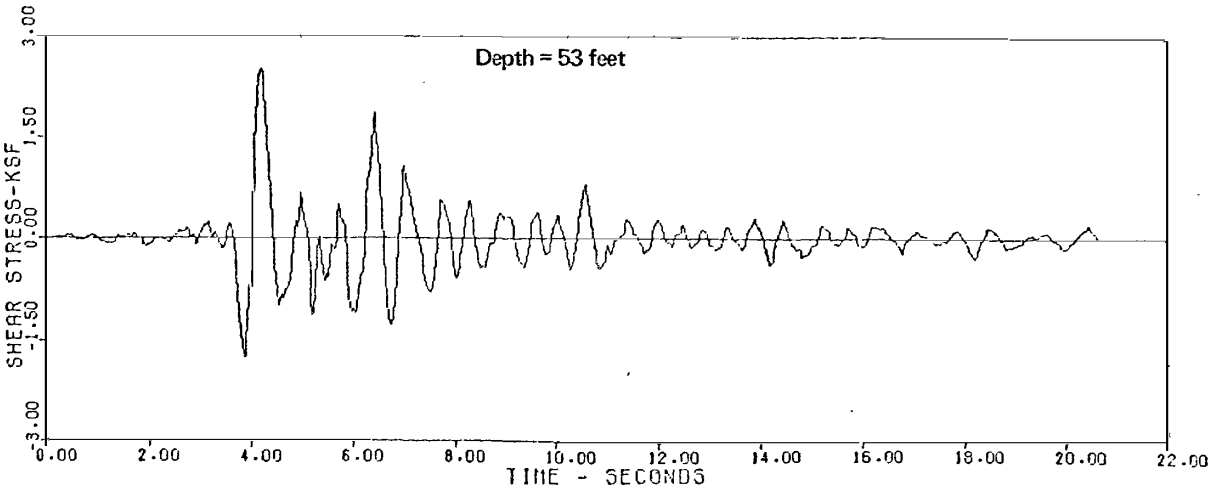

Earth Sciences Associates
Palo Alto, California

SEISMIC SAFETY INVESTIGATION OF EIGHT SCS DAMS
SHEAR STRESS TIME HISTORIES BELOW DAM CREST
MAXIMUM CROSS SECTION
GREEN'S LAKE DAM NO. 3

Checked by MLT	Date 9/20/82	Project No.	Figure No.
Approved by J.E. Valera	Date 9/22/82	D118	F-9

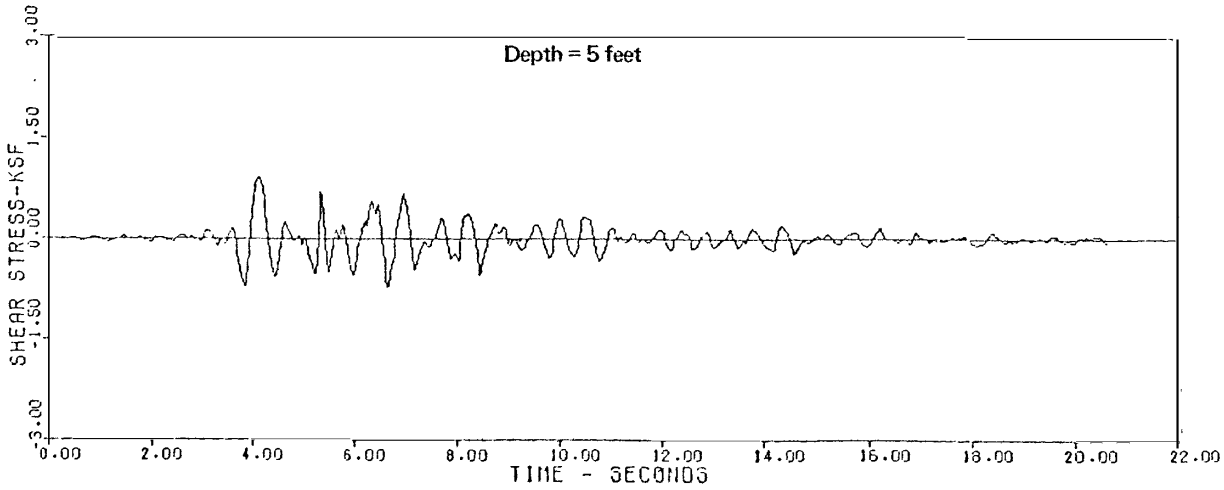

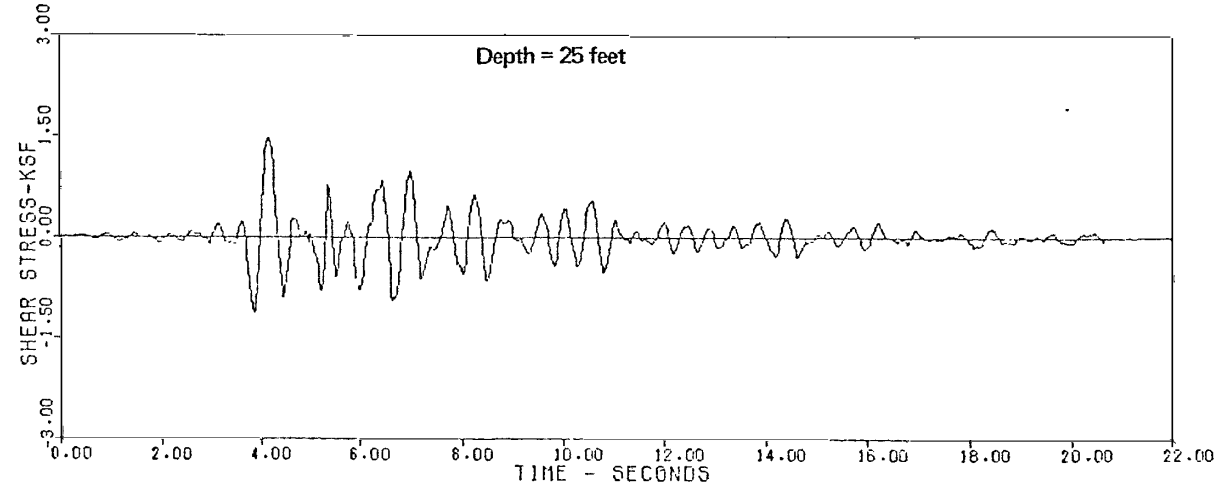

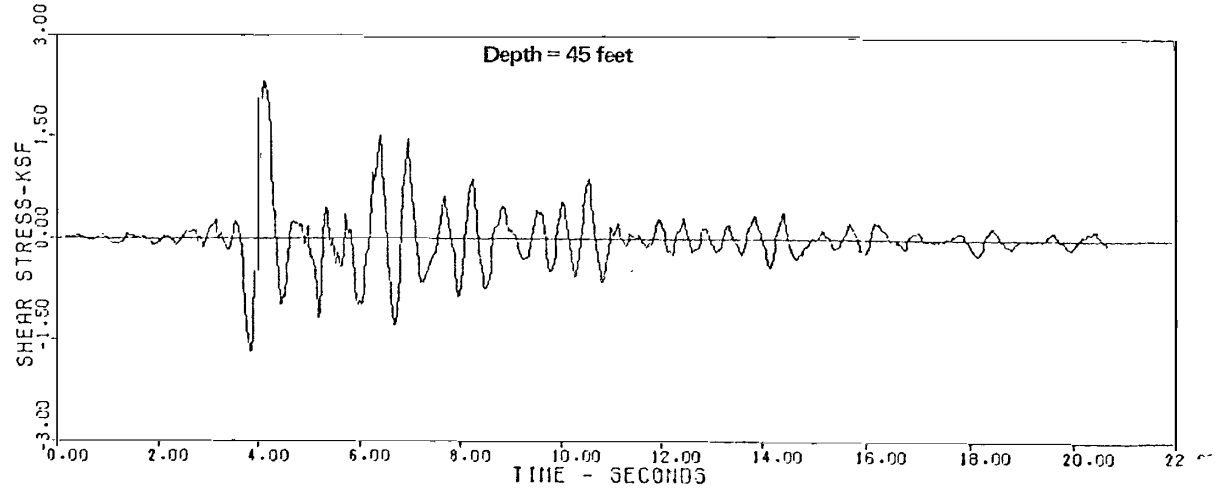

Earth Sciences Associates
Palo Alto, California

SEISMIC SAFETY INVESTIGATION OF EIGHT SCS DAMS
SHEAR STRESS TIME HISTORIES BELOW UPSTREAM TOE
GREEN'S LAKE DAM NO. 3

Checked by MLT	Date 9/20/82	Project No.	Figure No.
Approved by J. E. Valera	Date 9/22/82	D118	F-10

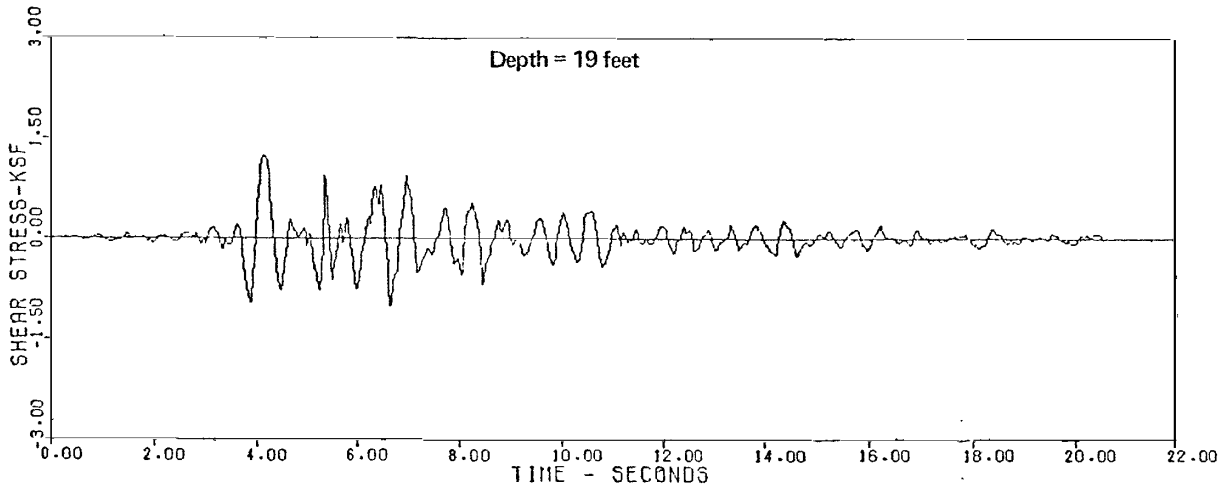

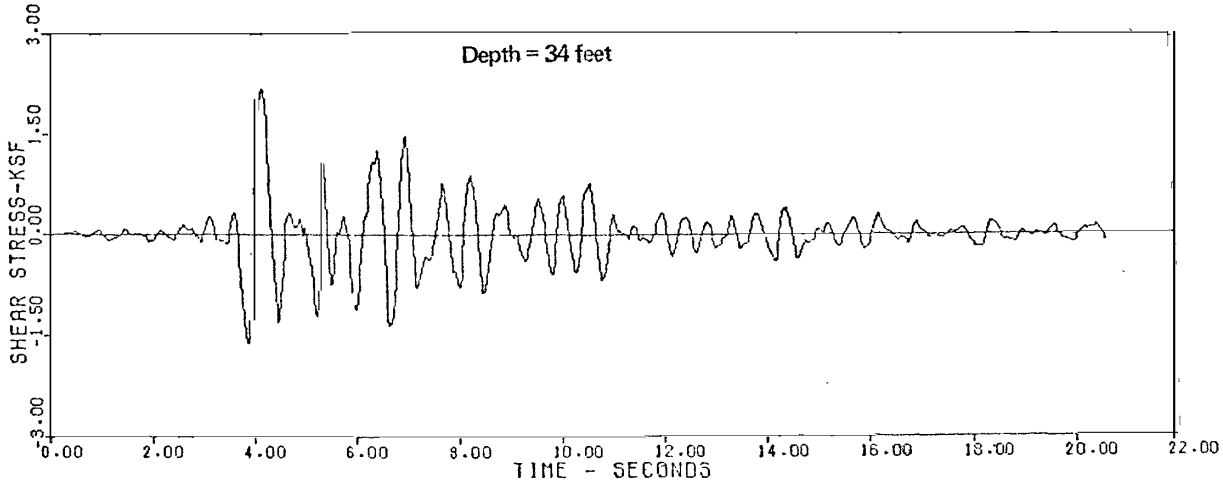

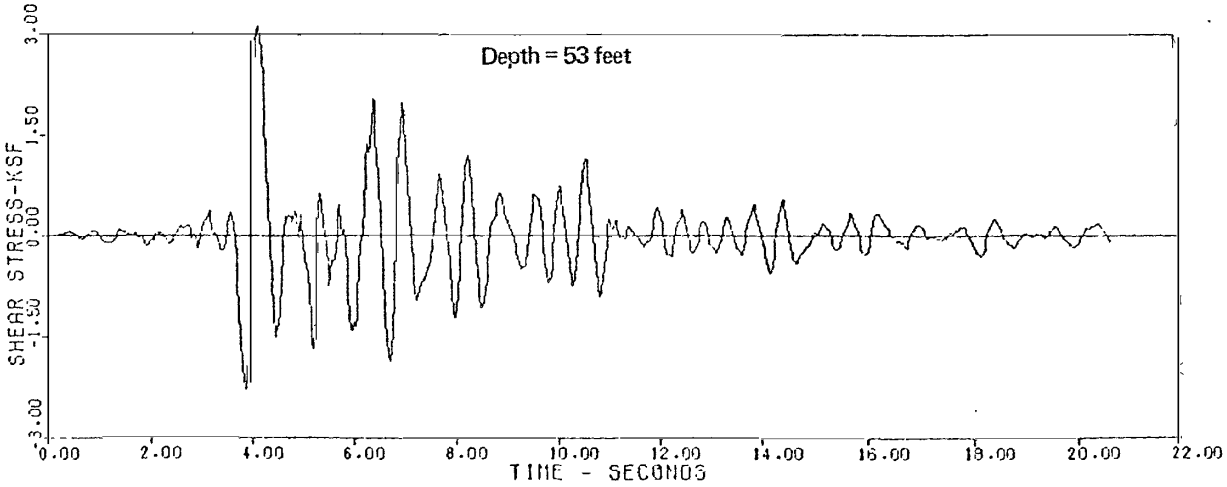

Earth Sciences Associates
Palo Alto, California

SEISMIC SAFETY INVESTIGATION OF EIGHT SCS DAMS
SHEAR STRESS TIME HISTORIES BELOW DAM CREST
MAXIMUM CROSS SECTION
WARNER DRAW DAM

Checked by MLT	Date 9/20/82	Project No.	Figure No.
Approved by J. E. Valera	Date 9/22/82	D118	F-11

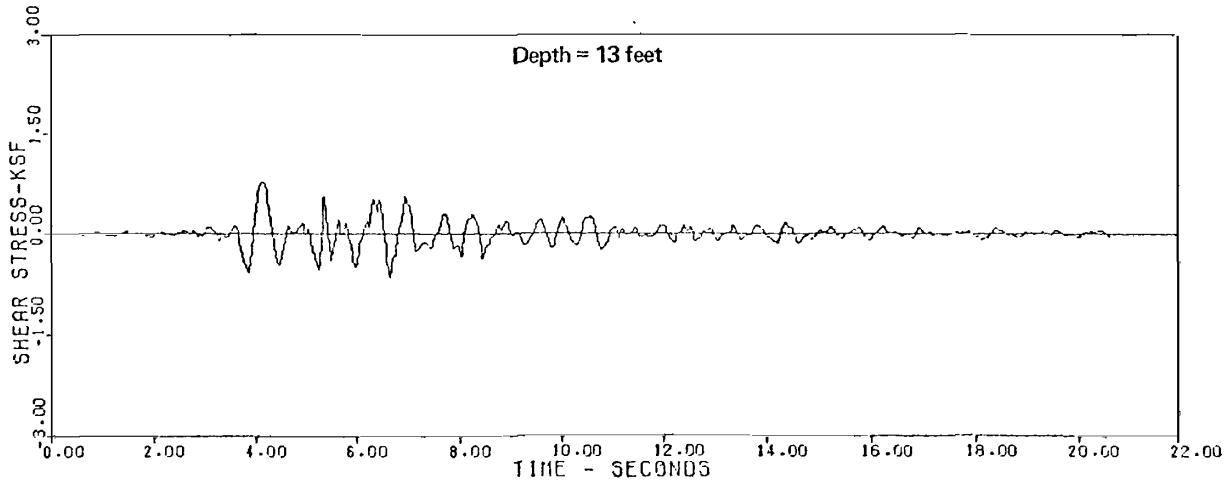

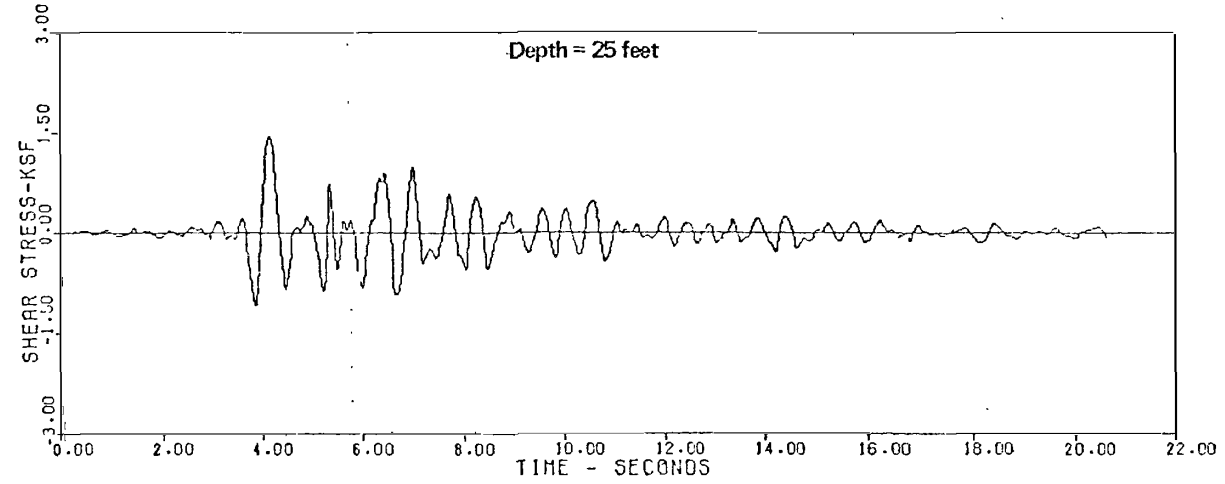

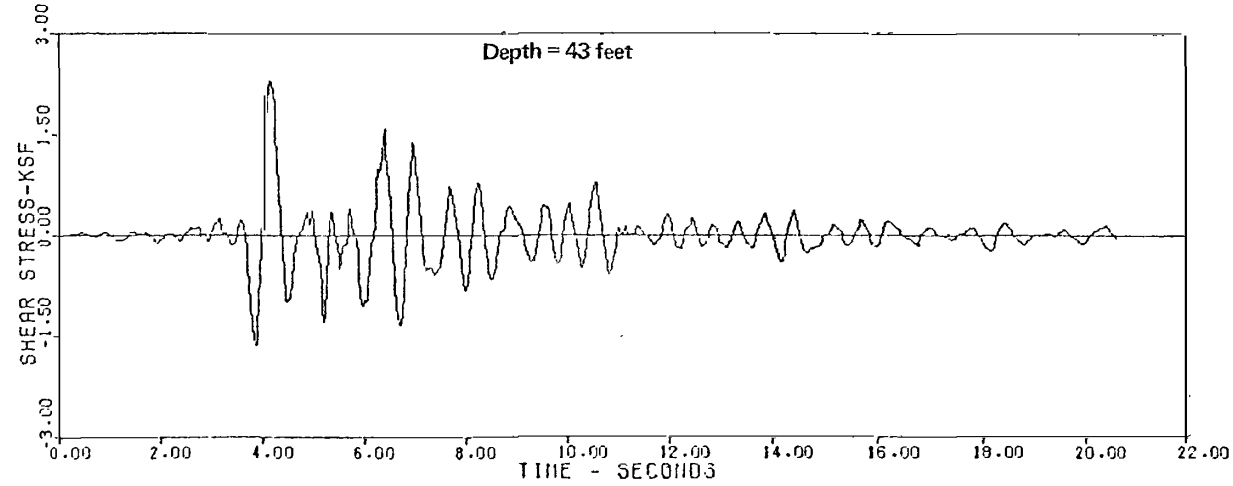

Earth Sciences Associates
Palo Alto, California

SEISMIC SAFETY INVESTIGATION OF EIGHT SCS DAMS
SHEAR STRESS TIME HISTORIES BELOW DAM CREST
MAXIMUM CROSS SECTION
FROG HOLLOW DAM

Checked by MLT	Date 9/20/82	Project No.	Figure No.
Approved by J.E. Valera	Date 9/22/82	D118	F-12

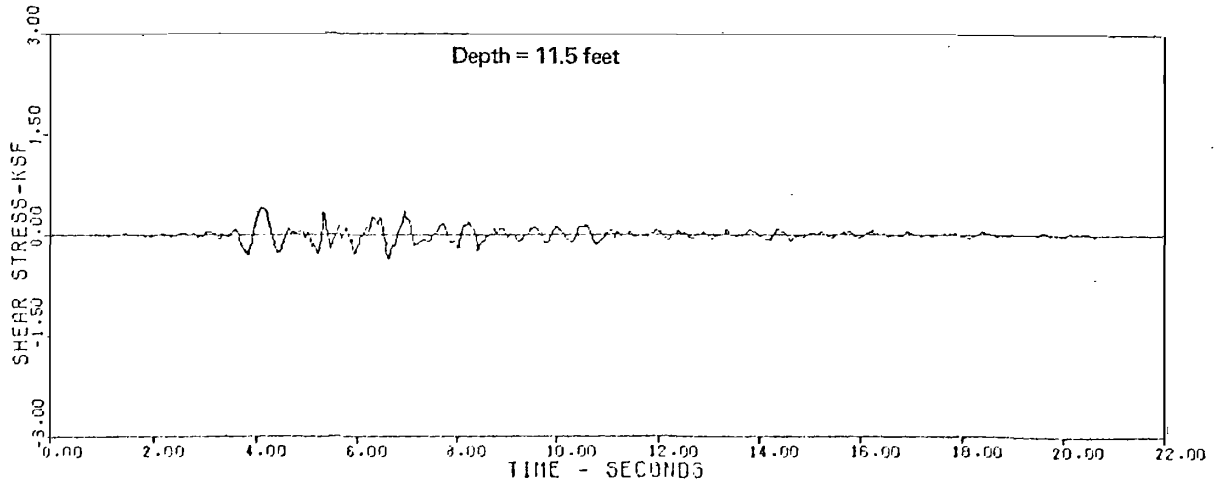

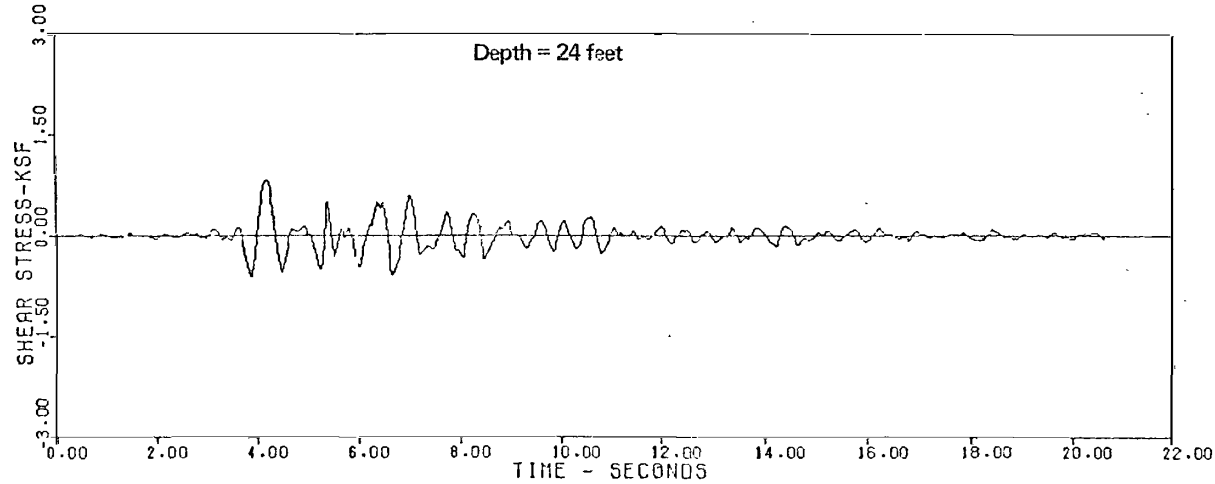

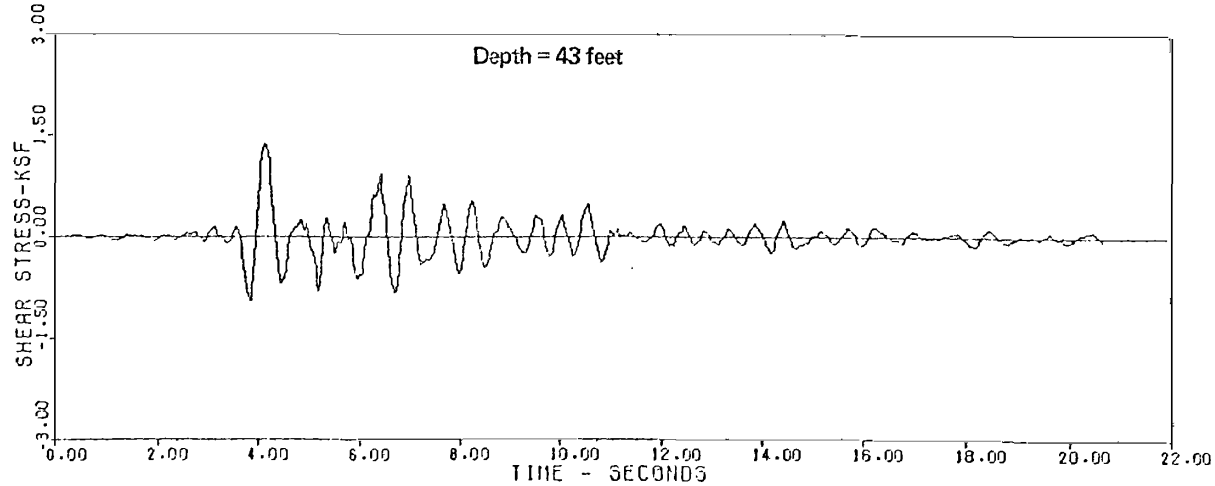

Earth Sciences Associates
Palo Alto, California

SEISMIC SAFETY INVESTIGATION OF EIGHT SCS DAMS
SHEAR STRESS TIME HISTORIES BELOW DAM CREST
MAXIMUM CROSS SECTION
IVINS DIVERSION DAM NO. 5

Checked by MJ Date 9/20/82	Project No.	Figure No.
Approved by J.E. Valera Date 9/22/82	D118	F-13

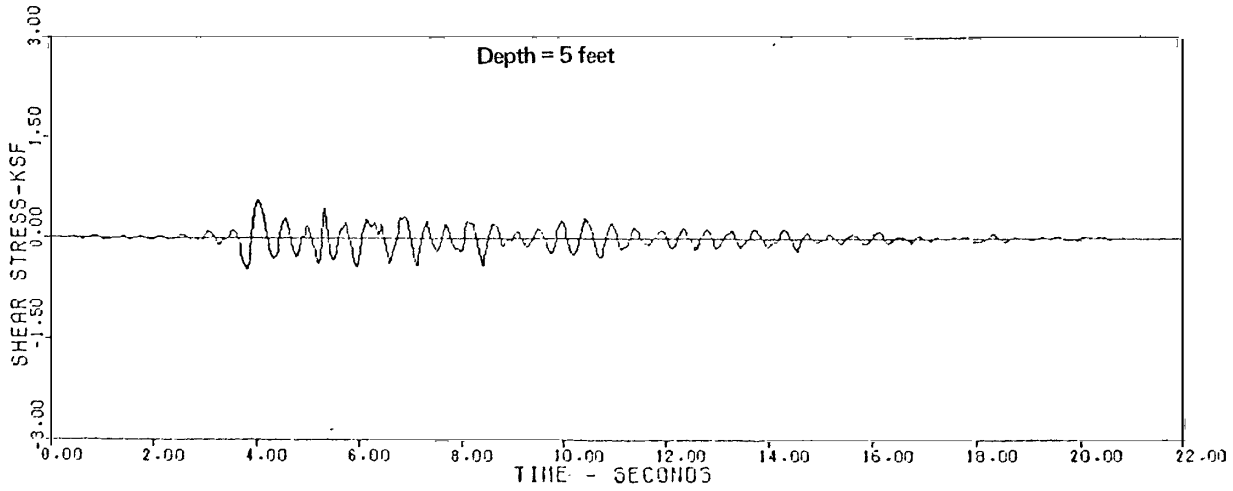

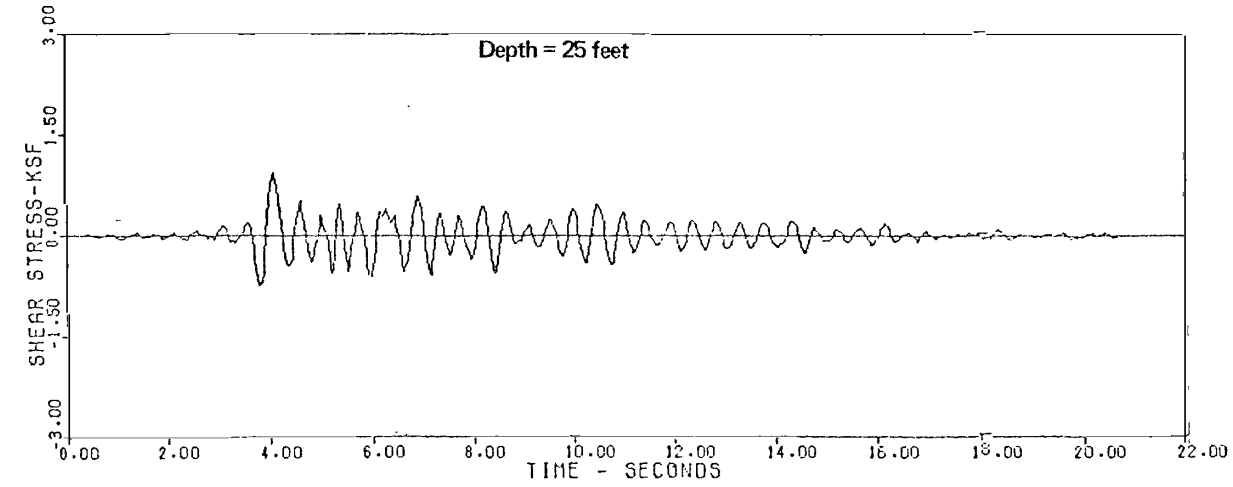

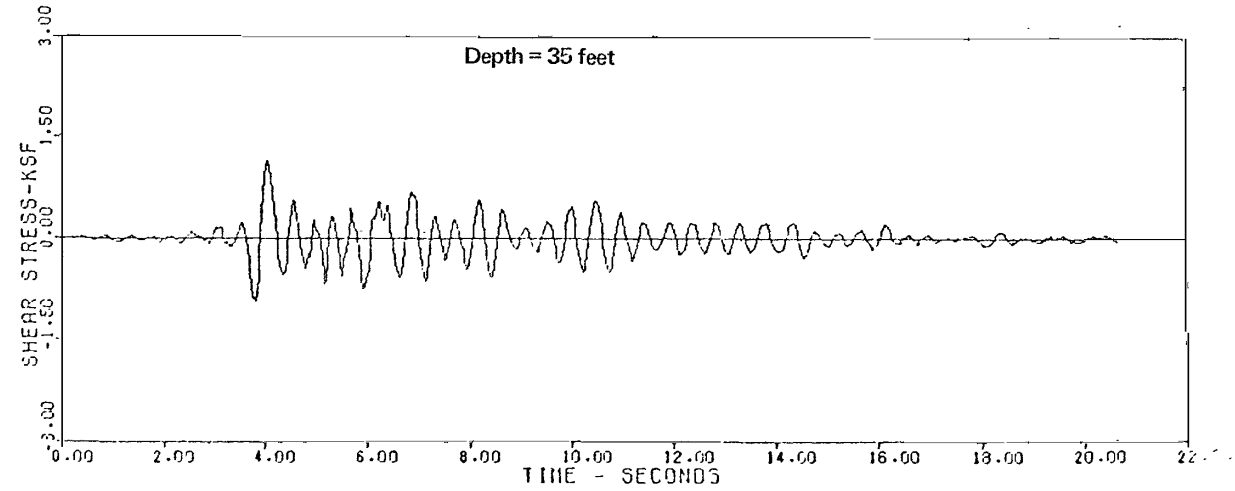

Earth Sciences Associates
Palo Alto, California

SEISMIC SAFETY INVESTIGATION OF EIGHT SCS DAMS
SHEAR STRESS TIME HISTORIES BELOW UPSTREAM TOE
IVINS DIVERSION DAM NO. 5

Checked by MLT	Date 9/20/82	Project No.	Figure No.
Approved by J.E. Valera	Date 9/22/82	D118	F-14

APPENDIX G

LIQUEFACTION POTENTIAL EVALUATION OF EMBANKMENT AND FOUNDATION SOILS

Appendix G

LIQUEFACTION POTENTIAL EVALUATION OF EMBANKMENT AND FOUNDATION SOILS

Introduction

The procedure which was used to estimate the magnitude of the earthquake-induced deformations of the four selected dam embankments is described in Chapter VII of this report. The procedure used is strictly valid for embankments which are constructed of soils that maintain most of their original shear strength after earthquake shaking. That is, the procedure is valid for embankments constructed of soils which do not liquefy. The four dams that were selected for detailed stability and deformation analyses include:

1) Green's Lake Dam No. 3
2) Warner Draw Dam
3) Frog Hollow Dam
4) Ivins Diversion Dam No. 5

In addition to the analyses performed on these four selected dams, simplified analyses were carried out on the remaining embankments to help in evaluating the performance of these embankments during the postulated earthquake ground motions. The dams for which simplified analyses were performed are:

1) Green's Lake Dam No. 2
2) Green's Lake Dam No. 5
3) Gypsum Wash Dam
4) Stucki Dam

This appendix describes the various analyses that were performed to evaluate the liquefaction potential of the embankment and foundation soils. Results of each analysis procedure are discussed within the text and are summarized in the last section of this appendix.

Review of Procedures Used to Evaluate Liquefaction and Cyclic Mobility

The basic cause of liquefaction or cyclic mobility in a saturated cohesionless soil during an earthquake is the result of a build up of excess hydrostatic pressure due to the application of cyclic shear stresses induced by earthquake ground motions. "Liquefaction" denotes the condition where the porewater pressure equals the effective confining stress. In this state, a soil will undergo continued deformation at a low residual resistance. The occurrence of liquefaction will depend on the void ratio or relative density of the soil as well as other factors. It may also be caused by a hydraulic gradient during an upward flow of water in a deposit. The "Cyclic Mobility" of a soil denotes the condition in which a number of cyclic stress applications develop peak cyclic pore pressures equal to the applied effective confining pressure and subsequent applied cyclic stresses cause limited strains to develop.

There are basically three methods available for evaluating the liquefaction or cyclic mobility potential of a saturated cohesionless soil subjected to earthquake ground shaking (Seed, 1979a, SW-AJA, 1972). They are:

1. Methods based on observations of cohesionless soil deposits in previous earthquakes,

2. Methods based on evaluation of stress conditions in the field and determinations of stress conditions causing liquefaction or cyclic mobility of soils in the laboratory, and

3. Comparisons of the gradations of soils with the gradations of materials which have liquefied during past earthquakes and which are considered most susceptible to liquefaction in laboratory tests.

The first method is based primarily on results of Standard Penetration Tests (SPT) performed in saturated cohesionless soil deposits. In this method, corrected SPT blow counts obtained from a comprehensive collection of site conditions, where evidence of liquefaction or no liquefaction was known to have taken place during past earthquakes, were used to develop empirical relationships which correlate the values of cyclic stress ratio (τ/σ_o') required to cause liquefaction or

liquefaction with limited shear strain potential. Relationships of this type have been developed for earthquakes of various intensity levels. The relationships shown in Figure G-1 were proposed by Professor H. B. Seed (1979a) and can be used for any given site (subjected to a given earthquake ground surface acceleration) to evaluate the possibility of liquefaction or the cyclic mobility potential. While this method is intended for use in the evaluation of soil liquefaction and cyclic mobility for level ground conditions, results of this method provides a useful guide in the evaluation of the liquefaction potential for other ground conditions.

The second method requires two independent determinations consisting of: 1) an evaluation of the cyclic stresses induced at different levels in the deposit by the earthquake shaking, along with 2) a laboratory investigation to determine the cyclic stresses which will cause the soil to liquefy or undergo various degrees of cyclic strain. The evaluation of liquefaction or cyclic mobility of the soil is then based on a comparison of the cyclic stresses induced in the field with the stresses required to cause liquefaction or limited straining in representative laboratory test samples.

The third method simply requires a comparison of gradations of the soils for which the liquefaction characteristics are being assessed with a compilation of gradations of soils which have liquefied during past earthquakes and/or considered most susceptible to liquefaction in laboratory tests. Comparisons of this type should only be used as a preliminary guide for establishing the liquefaction potential of a soil. The empirical relationships are based on observations which suggest that fine sands and silty sands (i.e., generally cohesionless soils) are most susceptible to liquefaction. Cohesive soils do not undergo liquefaction and the liquefaction potential of gravelly soils is considered as being low, due to their generally high permeability which prevents the build up of high excess pore water pressures.

For those embankments for which detailed dynamic response analyses were not performed, the liquefaction potential of the embankments and foundation soils was evaluated using Methods 1 and/or 3. Methods 1 and 3 were used in the liquefaction evaluation of Green's Lake Dam No. 2, Gypsum Wash Dam and Stucki Dam. Method 3 was used in the evaluation of Green's Lake Dam No. 5. Method 1 was not used in the case of this dam since the embankment and foundation soils are generally clayey (cohesive) in nature and since this method is only applicable

to generally cohesionless soils. Since cohesive soils do not undergo liquefaction, comparisons of the gradations of the embankment and foundation soils with the gradations of soils susceptible to liquefaction are presented for completeness only. Method 2 was not used in the liquefaction evaluation of the four dams mentioned above since this method requires results of a relatively detailed laboratory testing investigation which was not included in the scope of work of this study.

All three methods were used to evaluate the liquefaction potential of the embankment and foundation soils in the cases of Green's Lake Dam No. 3, Warner Draw Dam and Ivins Diversion Dam No. 5. Method 2 was employed in the evaluation of all the above-mentioned dams for the following reasons: 1) laboratory tests were performed on representative samples of the embankment and foundation soils, and 2) the comparisons of the cyclic stress ratios induced by the postulated earthquake ground motions with those used in the laboratory tests provides an indication of the behavior of the various soils during the postulated earthquake ground motions. Method 3 was used in the case of Frog Hollow Dam. Methods 1 and 2 were not employed in this case since the embankment and foundation soils are generally clayey in nature and, therefore, the soils can be considered as having a low liquefaction potential.

Table G-1 summarizes the analysis procedures that were performed on each dam considered in this investigation.

The following sections of this appendix describe the analyses procedures outlined above. Results of these analyses (where appropriate) are also discussed. A summary of the conclusions reached is given in the last section of this appendix.

METHOD 1 - Method Based on Observations of Performance in Previous Earthquakes

This approach was used to evaluate the liquefaction potential of the embankment and foundation soils of the following dams:

1) Green's Lake Dam No. 2
2) Green's Lake Dam No. 3
3) Gypsum Wash

Table G-1

Summary of Analysis Procedures Used
in Liquefaction Potential Evaluation

Dam	Analysis Procedure		
	Method 1	Method 2	Method 3
Green's Lake No. 2	Yes	No	Yes
Green's Lake No. 3	Yes	Yes	Yes
Green's Lake No. 5	N. A.*	No	Yes
Gypsum Wash	Yes	No	Yes
Warner Draw	Yes	Yes	Yes
Stucki	Yes	No	Yes
Frog Hollow	N. A.*	Yes	Yes
Ivins Diversion No. 5	Yes	Yes	Yes

*Note:

This method not used since it is not applicable to soils which are generally clayey (cohesive) in nature.

4) Warner Draw

5) Stucki

6) Ivins Diversion Dam No. 5

As was previously noted, the soils found at Green's Lake Dam No. 5 and Frog Hollow Dam are generally clayey in nature. Therefore, this procedure was not used in the analyses of these dams since these types of materials have not been known to undergo liquefaction during previous earthquakes.

The approach used in this method consisted of the following steps:

1) Measured SPT blow count data available for each dam were corrected to account for the effects of effective overburden pressure present at the time of drilling. Blow count data obtained during the Phase I field exploration program and data obtained from SCS files were utilized.

2) Profiles representing the subsurface conditions beneath the centerline of each dam and, if appropriate, the foundation conditions along the upstream toe of each embankment were developed. Conservative estimates of the phreatic surfaces existing in the embankments and foundations during flood stage were assumed.

3) Corrected SPT blow count data along with empirical relationships were used to estimate the cyclic stress ratios required to cause liquefaction with limited shear strain potential for the postulated earthquake.

4) Cyclic stress ratios induced by the postulated earthquake ground motions at various depths within the representative dam and foundation profiles were calculated.

5) The stress ratios computed in Step 3 were compared with those obtained in Step 4 to identify those soils most susceptible to liquefaction and/or which may exhibit limited shear strain potential during cyclic loading during the postulated earthquakes.

Step 1 - Correction of SPT Blow Count Data

Use of SPT blow count data for evaluating the liquefaction potential of a saturated cohesionless soil deposit requires that measured blow counts be corrected for the effects of effective overburden pressure. The "corrected" blow count of a soil can be determined using the relationship:

$$N_1 = C_N N$$

where N_1 is the corrected blow count in blows/foot, C_N is the correction factor and N is the measured blow count. The values of C_N have been routinely determined in the past using relationships developed by Gibbs and Holtz (1957), Marcuson and Bieganousky (1977a,b), Seed (1979a), Peck et al. (1973), among others. For this investigation, the value of C_N was calculated from the relationship:

$$C_N = 0.77 \log \frac{20}{\sigma_o'}$$

where σ_o' is the effective overburden pressure in tons per square foot (tsf) (Peck et al., 1973).

SPT blow count data obtained from the boreholes drilled during the Phase I field program and from borehole logs available in the SCS files were corrected for the effective overburden pressure. Effective stresses were evaluated for the conditions present at the time of the drilling operations. Since, in all cases, no groundwater was noted in any of the logs of boreholes, the effective overburden pressures were evaluated using the average moist unit weights.

Step 2 - Development of Representative Subsurface Profiles

Subsurface profiles representing the soil conditions beneath the centerline of each dam near the maximum cross section were developed. For those embankments resting on soil foundations, profiles representing the subsurface conditions either along the upstream toe of the embankment or beneath the dam abutments were also developed. Water levels were assumed for each of the profiles analyzed. For the profiles representing the dam centerlines, water levels were based on

estimates of the steady-state phreatic surface within each dam embankment assuming that the water level within the impounded reservoir was at the principal (or primary) spillway crest elevation. The profiles that were analyzed and other pertinent information are summarized in Table G-2. For the profiles representing the dam foundations along the upstream toe of the embankment, the water level was assumed to be present at the ground surface. It should be noted that the water levels listed in Table G-2 are probably conservative since it is unlikely that the embankments and foundations would become completely saturated during the brief periods of time the dams impound water.

Step 3 - Estimation of Cyclic Stress Ratios Required to Cause Liquefaction

The empirical relationships showing the correlations of the field liquefaction behavior of saturated sands for level ground conditions and penetration resistance are shown in Figure G-1 (Seed, 1979a). The corrected blow count data were used along with the relationship shown for a Magnitude 6.0 earthquake to evaluate the liquefaction potential of the various soils. The cyclic stress ratios obtained from this relationship and the corrected SPT blow counts are shown in Figures G-2 through G-7 as individual data points for each of the dams considered in this analysis. In these figures, SPT blow count data yielding a cyclic stress ratio (τ / σ_o') greater than 0.60 are shown with arrows pointing to the right. Those blow counts which may be affected by the presence of gravel (i.e., the blow count value may be too high), are indicated by an asterisk (*) next to the data point. Blow count measurements taken in generally cohesive soils are shown by a darkened symbol. As previously discussed it is highly unlikely that these soils would be subject to liquefaction. However, these data points are shown for completeness only.

Step 4 - Calculation of Cyclic Stress Ratios Induced by Earthquake Ground Motions

Cyclic stress ratios (τ / σ_o') induced by the postulated earthquake ground motions at various depths within the representative dam and foundation profiles were calculated. Cyclic stress ratios were computed from the results of one-dimensional dynamic response analyses using embankment and foundation soil column models (see Appendix F) of the following dams:

1) Green's Lake Dam No. 3
2) Warner Draw Dam
3) Ivins Diversion Dam No. 5

Table G-2

Method 1 - Summary of Profiles Analyzed

Dam	Profile [1] Represented	Approximate Station of Profile	Depth[2] of Profile (ft)	Depth[3] to Phreatic Surface
Green's Lake No. 2	Embankment and foundation	8 + 00	63	6
	Foundation near upstream toe	———	46	0
Green's Lake No. 3	Embankment foundation to bedrock	11 + 00	68	6
	Foundation near upstream toe	———	50	0
Gypsum Wash	Embankment to bedrock	28 + 00	37	7
Warner Draw	Embankment to bedrock	16 + 00	68	16
	Foundation below crest at left abutment	12 + 00	63	16
Stucki	Embankment and foundation	14 + 00	79	10
	Foundation near upstream toe	———	49	0

Table G-2 (continued)

Method 1 - Summary of Profiles Analyzed

Dam	Profile [1] Represented	Approximate Station of Profile	Depth[2] of Profile (ft)	Depth[3] to Phreatic Surface
Ivins Diversion No. 5	Embankment and foundation to bedrock	20 + 00	60	4
	Foundation near upstream toe	———	40	0

Notes:

(1) For profiles through embankments, the profiles are located near maximum cross section and top of profile is at dam crest.

(2) The depth of the profile determined by either the known (or assumed) depth to bedrock, or is the deepest depth of available SPT blow count measurement.

(3) The depth to the phreatic surface for the profiles representing the dam embankments was established by assuming the impounded reservoir elevation at either the principal spillway crest, R/C chute, or inlet riser crest elevation.

Since the embankment and foundation conditions at Green's Lake Dam No. 2 are similar to those at Green's Lake Dam No. 3, the cyclic stress ratios computed from the one-dimensional dynamic response analyses of Green's Lake Dam No. 3 were also used for Green's Lake Dam No. 2. For the remaining two dams that were analyzed using this method (i.e., Gypsum Wash and Stucki Dams), the cyclic stress ratios were computed using a simplified procedure outlined by Seed (1979a). This procedure is also discussed in Appendix F.

The cyclic stress ratios induced in each profile by the postulated earthquake ground motions are shown as lines in Figures G-2 through G-7. The cyclic stress ratios are shown only for those depths which are below the assumed water level depth and for which SPT blow count data are available.

Step 5 - Comparison of Induced and SPT Cyclic Stress Ratios

Comparisons of the stress ratios computed from the SPT blow count data in Step 3 with those estimated in Step 4 (as shown in Figures G-2 through G-7) help identify those soils that might be susceptible to liquefaction and/or which may exhibit limited shear strain potential during the postulated earthquake ground shaking. When the cyclic stress ratio evaluated from a SPT blow count measurement is less than (i.e., falls to the left of) the induced cyclic stress ratio at a particular depth, liquefaction of the soil may occur during the earthquake. If the cyclic stress ratio computed from the SPT blow count exceeds the induced stress level, liquefaction of the soil is unlikely.

From the comparisons shown in Figures G-2 through G-7, the liquefaction potential of the soils comprising the dams and their foundations has been evaluated and is summarized in Table G-3. In this table the liquefaction potential of the soils has been described as either low, limited or high. The term "high" is used to describe those cases where most of the SPT blow count measurements indicates liquefaction or where excessive cyclic straining may occur. "Limited" describes cases where some data suggests liquefaction or limited cyclic straining may occur, or where the stress ratios from the SPT blow count data are nearly equal to the cyclic stress ratios induced by earthquake ground motions. Finally, the term "low" is used in the cases where most of the SPT blow count data suggests liquefaction will not occur.

Table G-3

Evaluation Summary of Liquefaction Potential
Method 1

Dam	Profile	Liquefaction Potential	
		Embankment	Foundation
Green's Lake No. 2	Embankment and foundation	Low	Limited
	Foundation near upstream toe	---	High
Green's Lake No. 3	Embankment and foundation to bedrock	Low	High
	Foundation near upstream toe	---	High
Gypsum Wash	Embankment to bedrock	Low	----
Warner Draw	Embankment to bedrock	Limited to high	----
	Foundation below crest at left abutment	---	Low
Stucki	Embankment and foundation	Low	Low
	Foundation near upstream toe	---	Low
Ivins Diversion No. 5	Embankment and foundation to bedrock	Low	Limited to high
	Foundation near upstream toe	---	Limited to high

Explanation

Low - Most data suggest liquefaction and/or excessive cyclic straining will not occur.

Limited - Some data suggest liquefaction and/or excessive cyclic straining will occur.

High - Most data suggest liquefaction and/or excessive cyclic straining will occur.

From the summary provided in Table G-3, the liquefaction potential of the soils comprising most of the embankments, as evaluated from the available SPT blow count data, appears to be low or limited. This seems to be a reasonable conclusion in light of the fact that all the embankments were built using modern compaction techniques which were (generally) carefully monitored during construction. The only exception to this appears to be Warner Draw Dam. In this case, some of the SPT blow counts below a depth of 30 feet yield cyclic stress ratios which are less than the induced stress levels. The foundation soils of some of the dams, however, may liquefy (or may devclop significant cyclic shear straining) during the postulated earthquake. This appears to be the case for Green's Lake Dams No. 2 and 3 and Ivins Diversion Dam No. 5.

METHOD 2 - Comparison of Induced Cyclic Stresses with Laboratory Test Behavior

As was previously described, this method requires two independent determinations consisting of: 1) an evaluation of the cyclic stresses induced at different levels in the deposit by earthquake shaking, along with 2) a laboratory investigation to establish the cyclic stresses which will cause the soil to liquefy or undergo limited cyclic straining. The liquefaction potential of the soil is based on a comparison of the cyclic stresses induced in the field with the stresses required to cause liquefaction in representative laboratory test samples. This method of analyses was used to evaluate the liquefaction potential and/or shear strain potential of the soils comprising the following dams and foundations:

1) Green's Lake Dam No. 3
2) Warner Draw Dam
3) Ivins Diversion Dam No. 5

A series of stress-controlled cyclic triaxial tests were performed in the laboratory on representative, relatively undisturbed Pitcher tube samples obtained from the field. A detailed description of the tests performed and the test results are presented in Appendices A, B, C, and D for each of the dams listed above.

Cyclic triaxial tests were performed mainly on samples consolidated isotropically (K_c = 1.0) to represent the expected range of stress conditions in the

embankment and foundation profiles. A limited number of tests were also conducted on samples consolidated anisotropically (K_c = 1.5). Samples were subjected to a maximum of 8 cycles of loading. This number of equivalent uniform stress cycles was selected as a conservative estimate of the number of cycles expected to develop in the field for the postulated Magnitude 6.0 earthquake (Seed et al., 1975). A correction factor ranging from 0.60 to 0.70 is normally applied to cyclic triaxial tests performed on isotropically-consolidated cohesionless soils to account for differences between the laboratory conditions and those believed to exist in the field during an earthquake. However, for the purpose of this investigation no correction factor was applied to the laboratory test results when presenting laboratory test data.

Results of the laboratory tests are shown in Figures G-3, G-5 and G-7 as individual data points for the cyclic tests performed for Green's Lake No. 3, Warner Draw and Ivins Diversion No. 5 Dams, respectively. The laboratory test data points shown in these figures are plotted at depths corresponding to the major principal stresses to which the samples were consolidated to in the laboratory. In some cases, the data are plotted on both soil column profiles (i.e., the profile at the maximum cross section and the profile near the upstream toe) although the samples may not have been obtained at the locations of the profile represented. Even so, the consolidation stresses used in the laboratory tests were equivalent to stress conditions representative of the location at which the data were plotted. The percent of axial strain developed at the end of 8 cycles of loading are also indicated next to each test data point.

From the comparisons of the cyclic stress ratios induced in the field with those used to test the laboratory samples as shown in Figures G-3, G-5 and G-7, the following conclusions regarding the possible behavior of the various soils during earthquake loading were developed:

1. Cyclic triaxial tests on the embankments soils developed low to moderate cyclic strains (less than 10 percent) during the levels of cyclic loading expected to occur in the field. In some cases, high levels of pore water pressures developed during cyclic loading, however, all test samples of these materials were capable of sustaining static loads after cyclic loading (see Appendix A, C, and D).

2. Cyclic triaxial tests performed on the soil samples obtained from the foundations of Green's Lake Dam No. 3 and Ivins Diversion Dam No. 5 developed moderate to large axial strains during cyclic loading. High levels of pore water pressures developed in these test samples. Some of these samples were unable to maintain static loads after cyclic loading indicating that liquefaction and significant strength loss of these samples had occurred.

These conclusions are generally supportive of those reached from the results of the Method 1 analyses, that is, the embankment soils will probably not liquefy during the postulated earthquake ground motions, however, they may develop small to moderate levels of cyclic straining. Results of the cyclic triaxial tests of the foundation soil of Green's Lake No. 3 and Ivins Diversion Dam No. 5, on the other hand, suggest that liquefaction and/or excessive cyclic straining may occur during the earthquake ground motions postulated for these sites.

While it has been previously mentioned that the clayey soils which comprise a major portion of the embankment and foundation soils at Frog Hollow Dam are not subject to liquefaction, it is, nevertheless, interesting to examine the laboratory behavior of the cyclic triaxial test samples in comparison with the field loading conditions. The field loading conditions expressed in terms of the cyclic stress ratio $(\tau_{cy}/S_u)_{avg}$, were calculated using results of the dynamic response analyses and average undrained strength parameters obtained from static triaxial tests (see Appendix F). The cyclic stress ratios computed in this way for the Frog Hollow Dam maximum cross-section are shown in Figure G-8. Also plotted in this figure are the results of the cyclic triaxial tests performed in the laboratory on the representative undisturbed samples obtained from the field. These results are shown as individual data points. The cyclic stress ratio for these tests were calculated from results of paired static and cyclic triaxial tests. The undrained shear strength was established from a static test on a test sample, whereas the cyclic shear stress corresponds to that used in the accompanying cyclic test (see Appendix A). The laboratory test data points are plotted at depths corresponding to the major principal stresses to which the samples were consolidated in the laboratory. Values of percent axial strain developed at the end of 8 cycles of loading are indicated next to each test data point.

The data plotted in Figure G-8 show that the soils do not exhibit excessive amounts of straining during levels of cyclic loading similar to that expected to occur in the field during the postulated earthquake. With the exception of only one test sample, axial strains were less than 3 percent. The one test that developed an axial strain of about 11 percent was performed on the material obtained from the "weak" embankment zone found during the field drilling investigation (see Appendix B of Phase I report).

From the results plotted in Figure G-8, it appears reasonable to conclude that the soils comprising a major portion of the Frog Hollow Dam (i.e., Zone I) will not develop excessive amounts of strain during the levels of cyclic loading considered in this investigation. Some of the test samples did experience moderate amounts of shear strength reduction as a result of cyclic loading (see Appendix A). These reductions were considered in subsequent slope stability analyses and are discussed in Chapter VIII of the main text of this report.

METHOD 3 - Comparison of Gradational Characteristics

Another factor which may be considered in evaluating the liquefaction potential of a soil is the gradation characteristics of the material. A compilation of the ranges of gradational characteristics of soils which have liquefied during past earthquakes and/or are considered most susceptible to liquefaction in the laboratory is shown in Figure G-9.

The ranges shown in Figure G-9 have been compiled by Lee and Fitton (1968), Seed and Idriss (1967), Kishida (1969), and Youd (1982) and appear to indicate that the soils types most susceptible to liquefaction consist of primarily poorly graded silty sands and sandy silts. It is important to note that all the gradational ranges shown in Figure G-9 have less than 10 percent by weight clay size particles (i.e., particles less than 0.002 mm) suggesting that clayey (cohesive) soils have a low liquefaction potential. Gradational characteristics typical of gravels and gravelly soils are also absent from Figure G-9 suggesting, in part, that these types of soils may not be capable of developing high excess pore pressures either because they are capable of draining rapidly during the cyclic loading or because these types of materials are usually more efficiently packed (i.e., denser) in situ than soils that consist of uniformly sized particles.

While the liquefaction potential of a soil is dependent on many factors other than gradation (such as the relative density of the soil, the intensity and duration of cyclic loading, among others), comparisons of the gradational characteristics of a soil with those ranges shown in Figure G-9 provides a useful guide in establishing the liquefaction potential of a soil.

The gradational characteristics of the various soils which comprise the embankments and foundations of the eight dams considered in this investigation were compiled from laboratory test data available in the SCS files and from laboratory tests performed during this investigation. In the cases of the zoned earthfill embankments, the gradational characteristics of the various fill materials were grouped together by zone (if the data permitted) and were compared separately. The comparisons of the gradations of the embankment and foundation soils for each dam with the ranges of gradations of the sandy soils shown in Figure G-9, are presented in Figures G-10 through G-20. Conclusions on the liquefaction potential of various material groups which are based on the comparisons shown on these figures are summarized on Table G-4. The material groups have been identified as having low or high liquefaction potential. "High" liquefaction potential has been assigned to those material groups which, in our judgment, have gradational characteristics which are reasonably close to the gradational characteristics of liquefiable soils (Figure G-9) and generally have less than 15 percent clay-size particles. A "low" liquefaction potential designation has been assigned to those material groups which, in general, have more than 15 percent of clay-size particles and/or are well graded.

Other Considerations Related to Liquefaction Potential

Observations made during field exploration and laboratory testing may also provide information which may be useful in determining whether or not a saturated cohesionless soil is susceptible to liquefaction. Observations which answer the following questions help identify those soils which may be loose and, therefore, liquefiable:

1. During drilling and sampling of the exploratory boreholes, were there any materials that drilled or sampled quickly indicating a loose deposit or fill? Were there any soils that were difficult to sample, that is, did the samples have a tendency to fall out of the Pitcher tube or was sample recovery poor?

Table G-4

Summary of Liquefaction Potential Evaluation
Method 3

Dam	Material	Liquefaction Potential	Remarks
Green's Lake No. 2	Embankment (Zone I and II)	Low	Limited data
	Foundation	Low	—
Green's Lake No. 3	Core (Zone III)	High	Limited data - however, consistent
	Shell (Zone I)	Low	Limited data - however, consistent
	Foundation	High	—
Green's Lake No. 5	Embankment and foundation	Low	Limited data - however, consistent
Gypsum Wash	Core (Zone I)	High	—
	Shell (Zone (III)	Low	—
Warner Draw	Core (Zone I)	Low	—
	Shell (Zone III)	High	Limited data
	Foundation (Left abutment)	Low	—
Stucki	Embankment (Zone I and III)	Low	—
	Foundation	High	—
Frog Hollow	Core (Zone I)	Low	—
	Shell (Zone III)	Low	Limited data
	Old embankment	Probably Low	No data, however, probably similar to Zone III
	Foundation	Low	Limited data

Table G-4 (Continued)

Summary of Liquefaction Potential Evaluation
Method 3

Dam	Material	Liquefaction Potential	Remarks
Ivins Diversion No. 5	Embankment	High	Limited data - however, consistent
	Foundation	High	---

Explanation

Low - In general, material groups has more than 15 percent clay size particles and/or are uniformly graded.

High - Material group has gradational characteristics which are reasonably close to those shown in Figure G-9 and have less than 15 percent clay size particles.

2. During laboratory testing, were there materials that were extremely difficult to extrude and set up in the triaxial chamber? Did the samples slump or tilt under their own weight after being extruded?

In general, the drilling of most of the exploratory boreholes during the Phase I field investigation proceeded well. Some soils were difficult to sample because of their high gravel content, however, an adequate number of testable Pitcher tube samples of the finer-grained soils (and probably those materials more subject to liquefaction) were obtained. Some difficulty was experienced, however, in obtaining Pitcher tube samples of the foundation soils at Green's Lake Dam No. 3 (see Appendix B of Phase I report, log of borehole GL3-2 at a depth interval of 4.0 to 16.0 feet). Some of the soils encountered in this borehole were difficult to sample, had relatively low SPT blow count measurements, and tended to fall or wash out during sampling. Similar sampling difficulties were encountered at Frog Hollow Dam in the boreholes drilled along the dam crest and at the upstream toe of the embankment (see Appendix G of Phase I report and Appendix B, log of borehole FH-2) and at Ivins Diversion Dam No. 5 (see logs of boreholes IV-1, IV-2, IV-4, and IV-5). While the materials that were difficult to sample at Frog Hollow Dam were cohesive in nature and, therefore, probably not subject to liquefaction during earthquake loading, the materials at Green's Lake Dam No. 3 and Ivins Diversion Dam No. 5 were generally silty sands. As was described in the previous section of this appendix, these materials can be susceptible to liquefaction.

Few drilling and sampling difficulties were encountered and noted at the remaining dam sites and recovery of attempted soil samples was quite good (see Appendix B of Phase I report).

During the laboratory testing program, the samples of the foundation soils that were recovered from Green's Lake Dam No. 3 and Ivins Diversion Dam No. 5 were extremely fragile and difficult to extrude. The samples were wet and tended to slump or tilt under their own weight during extrusion. Since many of the sampling attempts during drilling yielded little or no sample, it is our judgment that the "best" samples of the foundation soils present at these two dams were tested in the laboratory. These considerations suggest that foundation conditions at Green's Lake Dam No. 3 and Ivins Diversion Dam No. 5 are unsatisfactory.

Conclusions on Liquefaction Potential

The results of the various analyses and the discussion of the other considerations presented in this appendix provide a basis upon which to judge the liquefaction potential and/or cyclic mobility of the various soils comprising the embankments and foundations of the dams during the postulated earthquake ground motions. Our conclusions, which are also based on our engineering judgment, are summarized in Table G-5 for each of the dams considered in this investigation.

It is our judgment that, with the exception of the foundation soils at Green's Lake Dam No. 3 and Ivins Diversion Dam No. 5, the embankment materials and foundation soils, where present, should behave satisfactorily during the postulated Magnitude 6.0 earthquake. During the cyclic loading produced by an event of this magnitude and under certain in situ conditions, the various field and laboratory test data suggest that some excess pore water pressures may develop in the embankment and foundation soils that could produce a moderate reduction in shear strength of the soils. It is likely that only limited cyclic straining would occur which would not impair the performance and operation of the dams. Some of the foundation soils at Green's Lake Dam No. 3 and at Ivins Diversion Dam No. 5, on the other hand, may be subject to liquefaction and/or excessive cyclic straining. After the earthquake, excessive levels of pore water pressure could be built up which would cause rather significant reductions in shear strength in these soils.

While the analyses and data presented in this appendix tend to support the conclusions summarized in Table G-4 and those discussed above, it should be noted that they are based on a number of conservative simplifying assumptions. These include:

1. The earthquake ground motions that have been postulated for each of the dam sites are based on the closest source-to-site distances. Based on published data, this assumption is probably conservative because it results in ground motions which possess high levels of ground acceleration (and velocity) at frequencies which are in the range of those of the dam embankments. The stresses induced in the soils by these motions are, in our judgment, conservative.

2. Significant portions of the embankments and the entire foundations were assumed to be saturated at the time of the earthquake. As was previously mentioned, this is conservative since the intended use of the dams is to impound rainfall runoff water for only brief periods of time. While saturated soil conditions may be a conservative assumption, it is not an "impossible" condition. Successive rainstorms coupled with the rather pervious soils which comprise most of the embankments and foundations could produce saturated conditions, however, as long as the impounded water is discharged rapidly, this condition would probably exist for only brief periods of time.

Since liquefaction can only occur if saturated conditions exist, the analyses and discussions presented herein emphasize the need for careful maintenance of systems used to discharge rainfall runoff. Conditions similar to those which existed during 1967 at Green's Lake Dam No. 3 (see Appendix G of Phase I report - water was allowed to remain in the reservoir for up to 3 months) should not be allowed to develop. As long as the dams are operated as temporary flood control structures, liquefaction (accompanied by a severe loss of strength) of the soils comprising the embankments and foundations should, in our judgment, be considered unlikely.

Table G-5

Summary of Liquefaction Evaluation Conclusions

Dam	Liquefaction Potential Embankment	Liquefaction Potential Foundation	Remarks
Green's Lake No. 2	Low	Low	
Green's Lake No. 3	Low	High	High pore pressures may develop in foundation soils during cyclic loading which may cause liquefaction, excessive cyclic straining or severe reduction in shear strength.
Green's Lake No. 5	Low	Low	
Gypsum Wash	Low	—	
Warner Dam	Low	Low	
Stucki	Low	Low to Limited	Excess pore water pressure may develop in some of the foundation soils at depth, having little or no affect on the embankment's performance.
Frog Hollow	Low	Low	
Ivins Diversion No. 5	Low	High	High pore pressures may develop in foundation soils during cyclic loading which may cause liquefaction, excessive cyclic straining or severe reduction in shear strength.

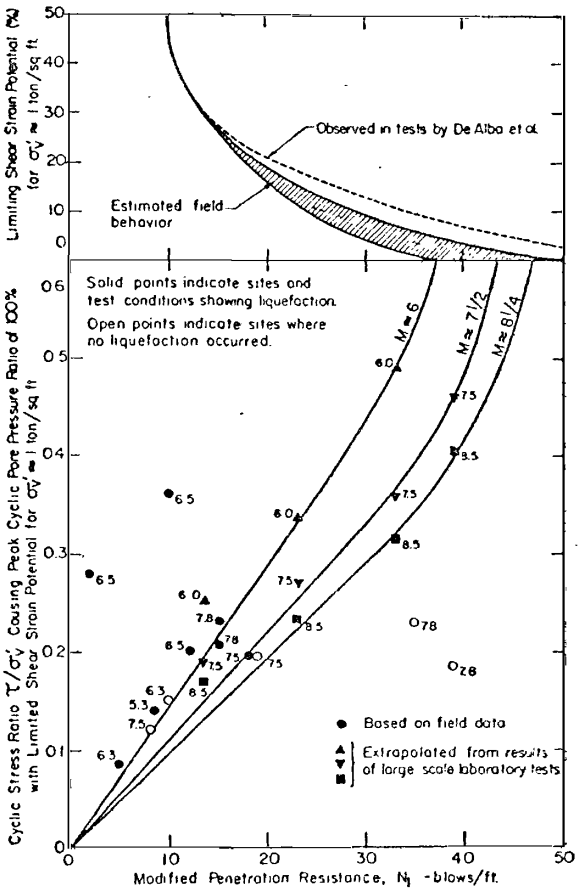

(after Seed 1979a)

Earth Sciences Associates Palo Alto, California		
SEISMIC SAFETY INVESTIGATION OF EIGHT SCS DAMS CORRELATION BETWEEN FIELD LIQUEFACTION AND BEHAVIOR OF SANDS FOR LEVEL GROUND CONDITIONS AND PENETRATION RESISTANCE		
Checked by MLT Date 9/20/82 Approved by J.E. Valera Date 9/22/82	Project No. D118	Figure No. G-1

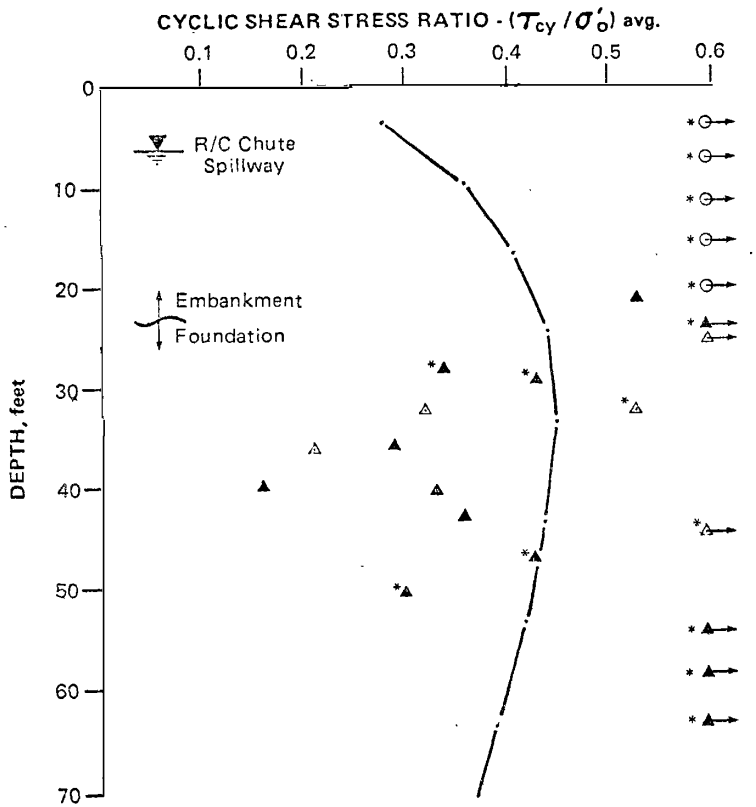

PROFILE: DAM AT MAXIMUM CROSS-SECTION

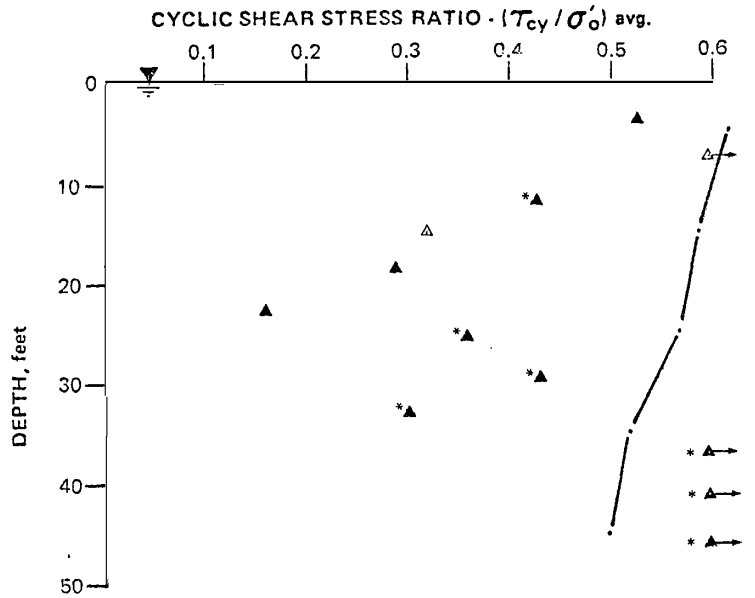

PROFILE: FOUNDATION NEAR UPSTREAM TOE

KEY:

1) ——·—— Average cyclic shear stress ratio induced by Magnitude 6.0 earthquake.

2) ⊙ Cyclic shear stress ratio computed from SPT blow count obtained from embankment soils.

△ Cyclic shear stress ratio computed from SPT blow count obtained from foundation soils.

Open symbol indicates generally cohesionless soil
Darkened symbol indicates generally cohesive soil.

* Indicates presence of gravel.

Earth Sciences Associates
Palo Alto, California

SEISMIC SAFETY INVESTIGATION OF EIGHT SCS DAMS
EVALUATION OF LIQUEFACTION POTENTIAL
GREEN'S LAKE DAM NO.2

Checked by MLT	Date 9/20/82	Project No.	Figure No.
Approved by J.E. Valera	Date 9/22/82	D118	G-2

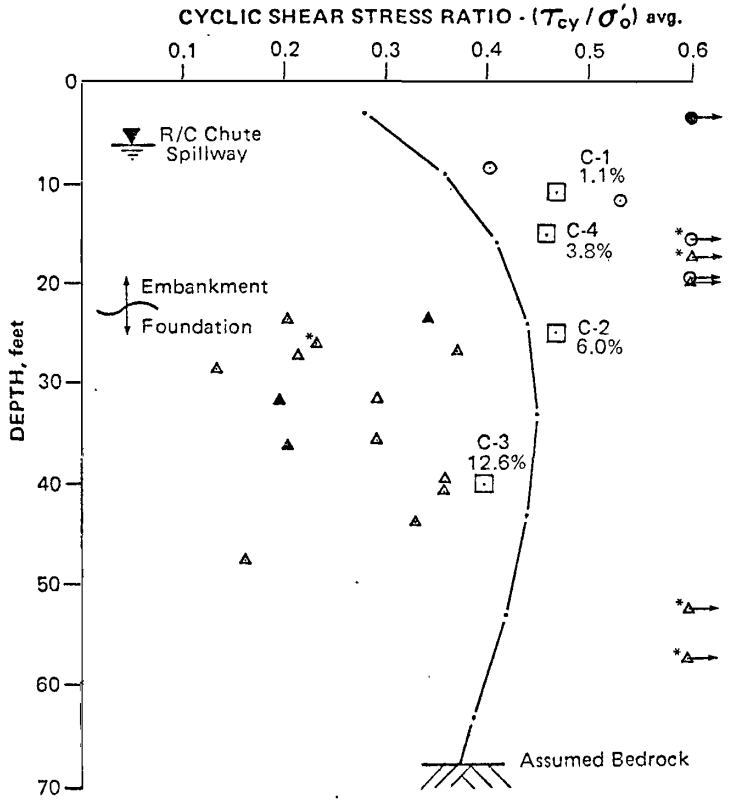

PROFILE: DAM AT MAXIMUM CROSS-SECTION

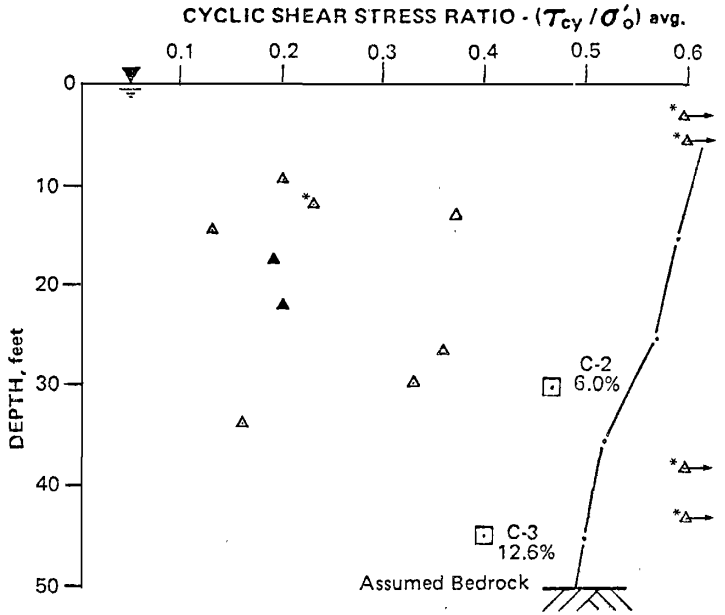

PROFILE: FOUNDATION NEAR UPSTREAM TOE

KEY:

1) Average cyclic shear stress ratio induced by Magnitude 6.0 earthquake.

2) Cyclic shear stress ratio computed from SPT blow count obtained from embankment soils.

Cyclic shear stress ratio computed from SPT blow count obtained from foundation soils.

Open symbol indicates generally cohesionless soil. Darkened symbol indicates generally cohesive soil,

* Indicates presence of gravel.

3) C-1 1.0% Cyclic triaxial test with K_c=1.0. Peak-to-peak strain value indicated next to symbol.

Earth Sciences Associates
Palo Alto, California

SEISMIC SAFETY INVESTIGATION OF EIGHT SCS DAMS
EVALUATION OF LIQUEFACTION POTENTIAL
GREEN'S LAKE DAM NO. 3

Checked by MCT	Date 9/20/82	Project No.	Figure No.
Approved by J. E. Valera	Date 9/22/82	D118	G-3

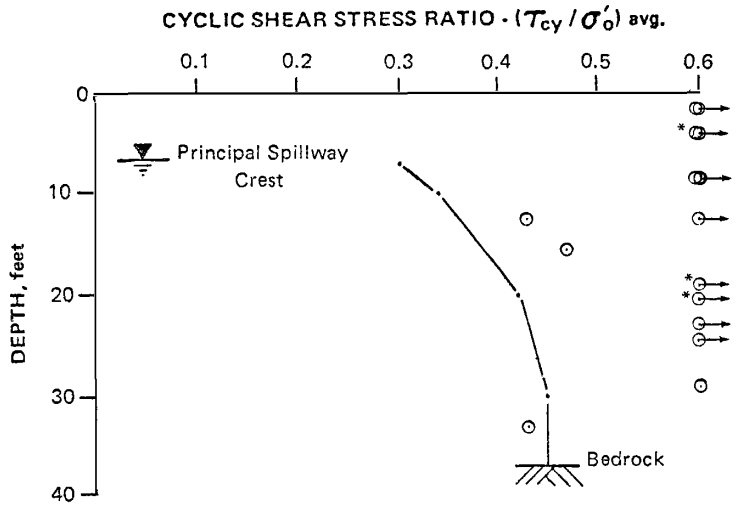

PROFILE: DAM AT MAXIMUM CROSS-SECTION

KEY:

1) ——·—— Average cyclic shear stress ratio induced by Magnitude 6.0 earthquake.

2) ⊙ Cyclic shear stress ratio computed from SPT blow count obtained from embankment soils.

* Indicates presence of gravel.

Earth Sciences Associates
Palo Alto, California

SEISMIC SAFETY INVESTIGATION OF EIGHT SCS DAMS
EVALUATION OF LIQUEFACTION POTENTIAL
GYPSUM WASH DAM

Checked by MLT	Date 9/20/82	Project No.	Figure No.
Approved by J. E. Valera	Date 9/22/82	D118	G-4

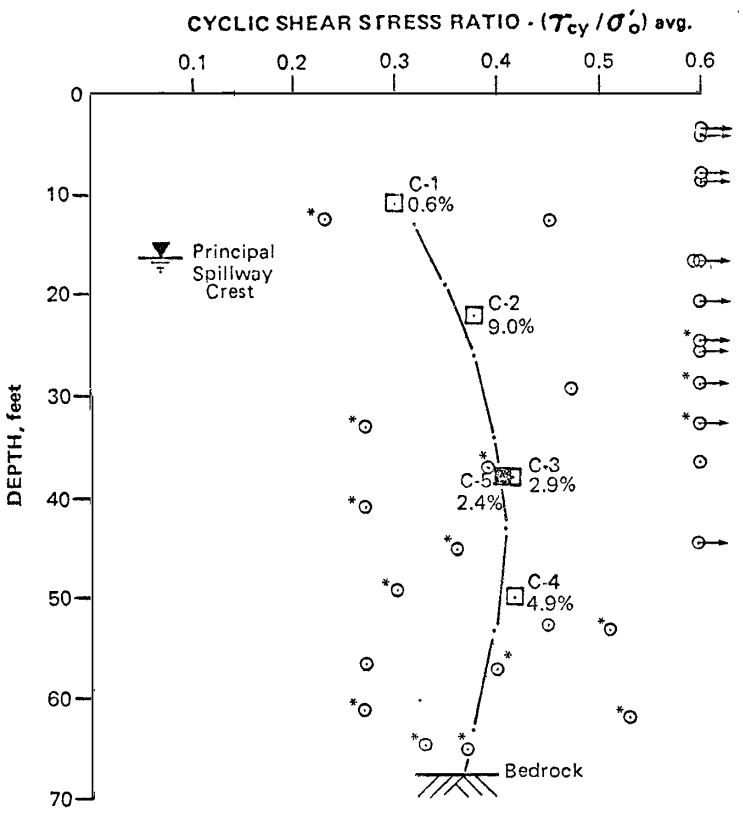

PROFILE: DAM AT MAXIMUM CROSS-SECTION

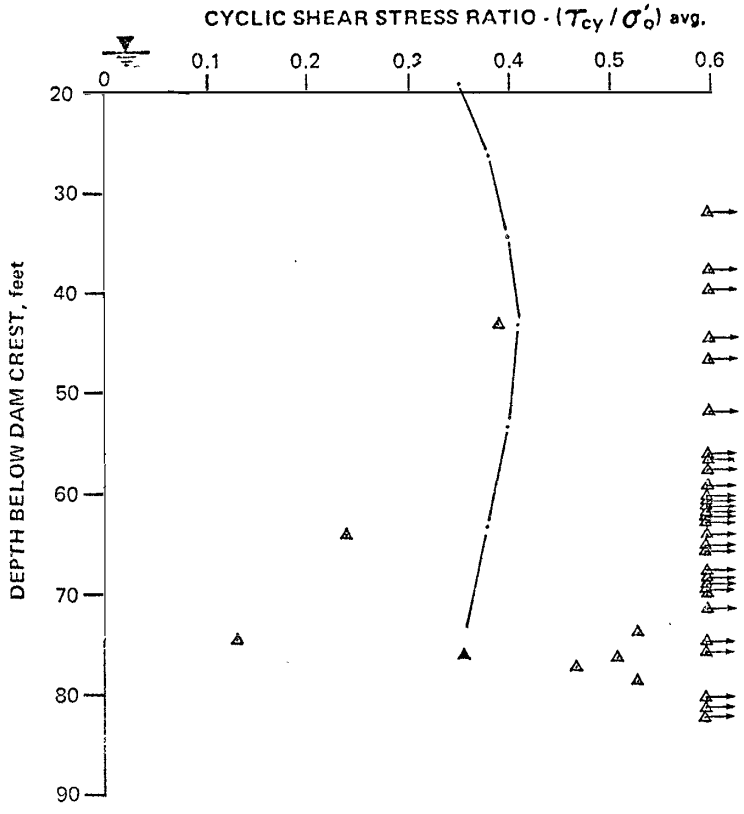

PROFILE: FOUNDATION LEFT ABUTMENT

KEY:

1) Average cyclic shear stress ratio induced by Magnitude 6.0 earthquake.

2) Cyclic shear stress ratio computed from SPT blow count obtained from embankment soils.

Cyclic shear stress ratio computed from SPT blow count obtained from foundation soils.

Open symbol indicates generally cohesionless soil. Darkened symbol indicates generally cohesive soil.

* Indicates presence of gravel.

3) C-1 0.6% — Cyclic triaxial test with K_c=1.0. Peak-to-peak strain value indicated next to symbol.

C-5 2.4% — Cyclic triaxial test with K_c=1.5. Peak permanent strain value indicated next to symbol.

Earth Sciences Associates
Palo Alto, California

SEISMIC SAFETY INVESTIGATION OF EIGHT SCS DAMS
EVALUATION OF LIQUEFACTION POTENTIAL
WARNER DRAW DAM

Checked by MLT	Date 9/20/82	Project No.	Figure No
Approved by J.C. Valera	Date 9/22/82	D118	G-5

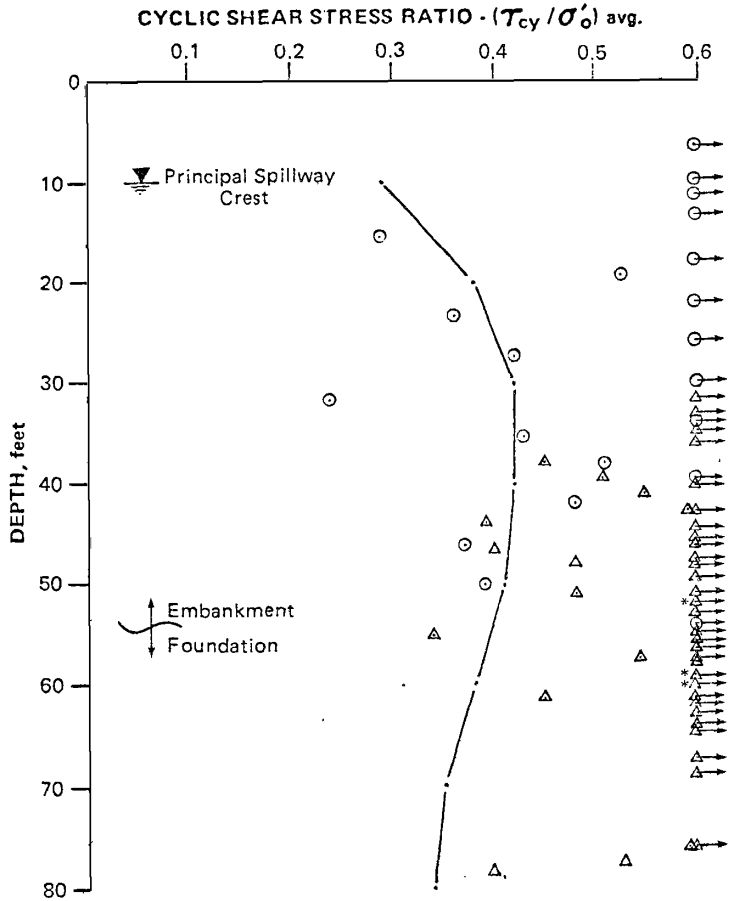

PROFILE: DAM AT MAXIMUM CROSS-SECTION

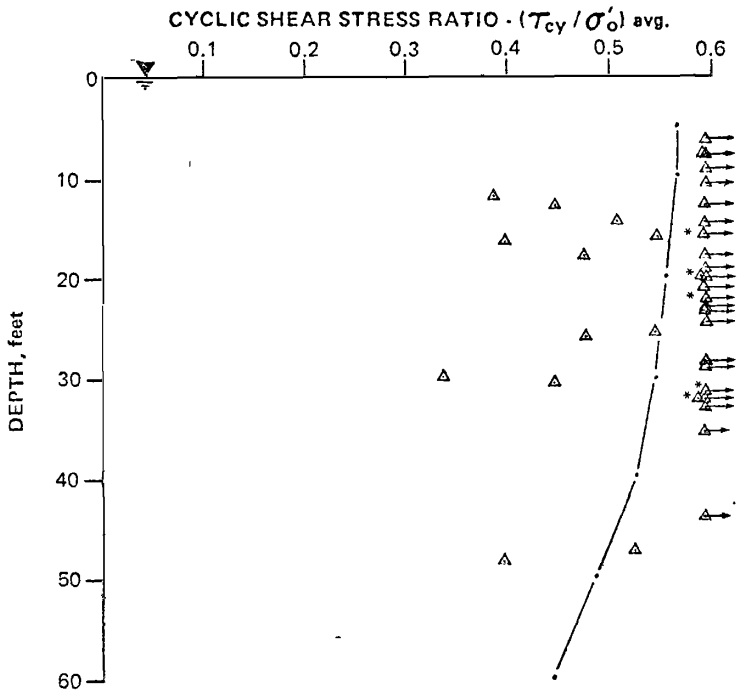

PROFILE: FOUNDATION NEAR UPSTREAM TOE

KEY:

1) ——·—— Average cyclic shear stress ratio induced by Magnitude 6.0 earthquake.

2) ⊙ Cyclic shear stress ratio computed from SPT blow count obtained from embankment soils.

△ Cyclic shear stress ratio computed from SPT blow count obtained from foundation soils.

* Indicates presence of gravel.

Earth Sciences Associates
Palo Alto, California

SEISMIC SAFETY INVESTIGATION OF EIGHT SCS DAMS
EVALUATION OF LIQUEFACTION POTENTIAL
STUCKI DAM

Checked by MLT	Date 9/20/82	Project No.	Figure No
Approved by J.E. Valera	Date 9/22/82	D118	G-6

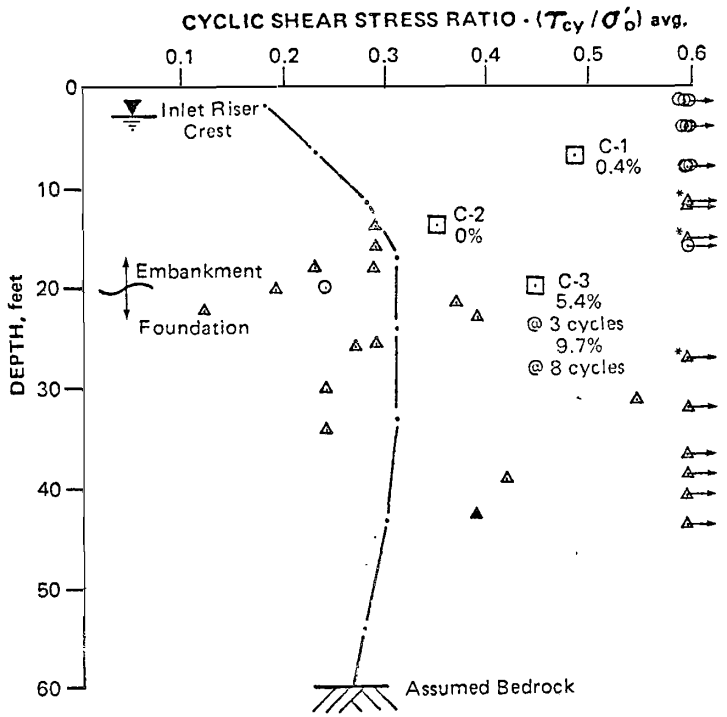

PROFILE: DAM AT MAXIMUM CROSS-SECTION

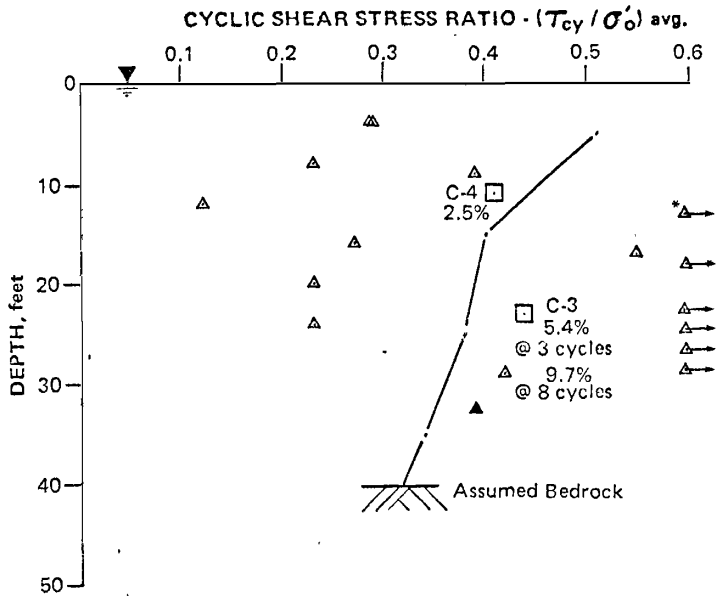

PROFILE: FOUNDATION NEAR UPSTREAM TOE

KEY:

1) Average cyclic shear stress ratio induced by Magnitude 6.0 earthquake.

2) ⊙ Cyclic shear stress ratio computed from SPT blow count obtained from embankment soils.

△ Cyclic shear stress ratio computed from SPT blow count obtained from foundation soils.

Open symbol indicates generally cohesionless soil, Darkened symbol indicates generally cohesive soil,

* Indicates presence of gravel.

3) ⊡ C-1 0.4% Cyclic triaxial test with K_c=1.0. Peak-to-peak strain value indicated next to symbol.

Earth Sciences Associates
Palo Alto, California

SEISMIC SAFETY INVESTIGATION OF EIGHT SCS DAMS
EVALUATION OF LIQUEFACTION POTENTIAL
IVINS DIVERSION DAM NO. 5

Checked by MLT Date 9/20/82	Project No.	Figure No.
Approved by J.C. Valera Date 9/22/82	D118	G-7

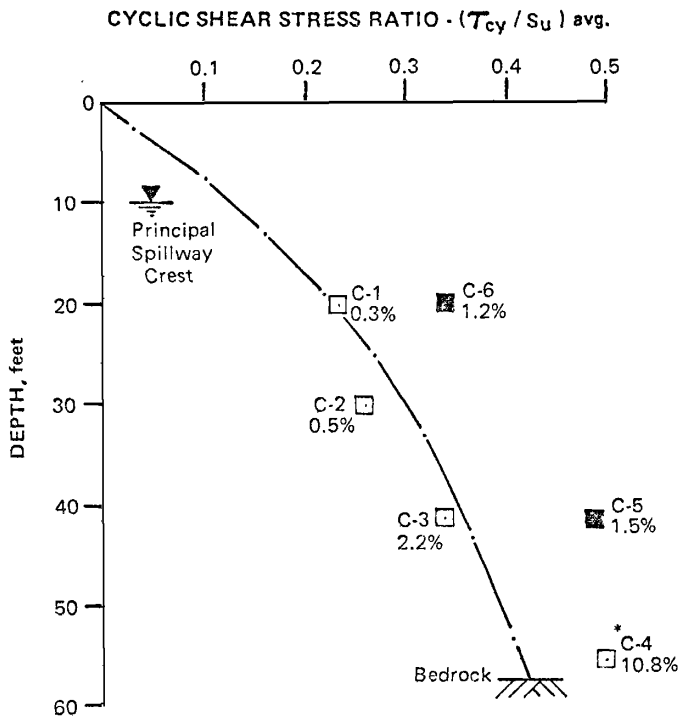

PROFILE: DAM AT MAXIMUM CROSS-SECTION

KEY:

1) Average cyclic shear stress ratio induced by Magnitude 6.0 earthquake.

2) C-1 0.3% — Cyclic triaxial test with K_c=1.0. Peak-to-peak strain value indicated next to symbol.

C-6 1.2% — Cyclic triaxial test with K_c=1.5. Peak permanent strain value indicated next to symbol.

* Material from weak embankment zone.

Earth Sciences Associates
Palo Alto, California

SEISMIC SAFETY INVESTIGATION OF EIGHT SCS DAMS
EVALUATION OF LIQUEFACTION POTENTIAL
FROG HOLLOW DAM

Checked by MCT	Date 9/20/82	Project No.	Figure No.
Approved by J. L. Valera	Date 9/22/82	D118	G-8

Appendix H

BIBLIOGRAPHY

Appendix H

BIBLIOGRAPHY

American Petroleum Institute, 1978, API recommended practice for planning, design and constructing fixed offshore platforms, API RP 2A, Eighth Edition, April 1977 revision.

Anderson, D. G., Espana, C., and McLamore, V. R., 1978, Estimating in situ shear moduli at competent sites: Proceedings of Conference on Earthquake Engineering and Soil Dynamics, Geotechnical Engineering Division (ASCE), Specialty Conference, v. I, Pasadena, California, June, p. 181-197.

Arabasz, W. J., 1982, University of Utah, Salt Lake City, personal communication.

Bolt, B. A., 1973, Duration of strong ground motion: Proceedings, 5th World Conference on Earthquake Engineering, Rome, v. 1, 6-D, Paper No. 292.

Bolt, B. A., 1979, Strong seismic ground motion for design purposes at the Lawrence Berkeley Laboratory, July 10.

Boutrup, E., 1977, Computerized slope stability analysis for Indiana highways: Joint Highway Research Project, C-36-36L, Engineering Experiment Station, Purdue University, Indiana, June.

Bucknam, R. C., Algermissen, S. T., and Anderson, R. E., 1980, Patterns of late Quaternary faulting in western Utah and an application in earthquake hazard evaluation: U.S. Geol. Survey Spec. Conf. on Earthquake Hazards Along the Wasatch-Sierra Nevada Frontal Fault Zones, Open-File Report 80-801, p. 299-314.

Campbell, K. W., 1981, Near-source attenuation of peak horizontal acceleration, Bulletin of the Seismological Society of America, v. 71, no. 6, December, p. 2039-2070.

Casagrande, A., 1971, On liquefaction phenomena: Report of a Lecture Prepared by Green, P. A. and Ferguson, P. A. S., Geotechnique, v. XXI, November, p. 197-202.

Casagrande, A., 1975, Liquefaction and cyclic deformation of sands--a critical review: Paper presented at Fifth Pan American Conference on Soil Mechanics and Foundation Engineering, Buenos Aires, Argentina, November, 1975.

Castro, G., 1969, Liquefaction of sands: Harvard Soil Mechanics Series No. 81, Harvard University, Cambridge, Massachusetts.

Chang, F. K., and Krinitzsky, E. L., 1977, State-of-the-art for assessing earthquake hazards in the United States; duration, spectral content, and predominant period of strong motion earthquake records from western U.S.: U.S. Army Corps of Engineers, Waterways Experimental Station, Vicksburg, Mississippi, Report 8.

Committee on Soil Dynamics of the Geotechnical Engineering Division, 1978, Definition of terms related to liquefaction: Journal of the Geotechnical Engineering Division, ASCE, v. 104, no. GT9, September, p. 1197-1200.

Franklin, A. G., and Chang, F. K., 1977, Earthquake resistance of earth and rockfill dams; Report 5, Permanent displacements of earth embankments by Newmark sliding block analysis: Waterways Experiment Station, Vicksburg, Mississippi.

Earth Sciences Associates, 1982, Phase I Report, Seismic safety investigation of eight SCS dams in southwestern Utah, June.

Gibbs, H. J., and Holtz, W. G., 1957, Research on determining the density of sands by spoon penetration testing: Proceedings, Fourth International Conference on Soil Mechanics and Foundation Engineering, London, England, v. 1.

Guzman, R. A., and Jennings, P. C., 1976, Design spectra for nuclear power plants: Journal of the Power Division ASCE, November, p. 165-178.

Hall, W. J., Mohraz, B., and Newmark, N. W., 1976, Statistical studies of vertical and horizontal earthquake spectra: prepared for Division Safety, U.S. NRC, Contract AT (4905)-2667, Urbana, Illinois.

Hardin, B. O., and Black, W. L., 1968, Vibration modulus of normally consolidated clay: JSMFD, ASCE, v. 94, no. SM2, March, p. 353-369.

Hardin, B. O., and Black, W. L., 1969, Closure to vibration modulus of normally consolidated clays, JSMFD, ASCE, v. 95, no. SM6, November, p. 1531-1537.

Hardin, B. O., and Drnevich, V. P., 1972, Shear modulus and damping of soils; design equations and curves: Journal of the Soil Mechanics and Foundation Division, ASCE, v. 98, no. SM7, July, p. 667-692.

Harr, M. E., 1962, Groundwater and seepage, McGraw-Hill, 307 p.

Jennings, P. C., and others, 1968, Simulated earthquake motions: Earthquake Engineering Research Laboratory, California Institute of Technology, Pasadena, California.

Jennings, P. C., Housner, G. W., and Tsai, N. C., 1969, Simulated earthquake motions for design purposes: Proceedings Fourth World Conference Earthquake Engineering, Session A1, Santiago, Chile, No. 145.

Johnson, J. A., 1980, Spectral characteristics of near source strong ground motion: Proceedings of the Seventh World Conference on Earthquake Engineering, September 8-13, Istanbul, Turkey, v. II, p. 131-134.

Johnson, J. A., and Traubenik, M. L., 1978, Magnitude-dependent near source - ground motion spectra: Proceedings of the ASCE Geotechnical Engineering Division Specialty Conference on Earthquake Engineering and Soil Dynamics, June 19-21, Pasadena, California, v. I., p. 530-539.

Kishida, H., 1969, Characteristics of liquefied sands during Mino-Owari, Tohnakai and Fukui earthquakes, Soils and Foundations (Japan), v. 9, no. 1, March, p. 75-92.

Lee, K. L., and Fitton, J. A., 1968, Factors affecting the cyclic loading strength of soil, vibration effects of earthquakes on soils and foundations, American Society for Testing and Materials, Special Technical Publication 450.

Lowe, III, J., 1967, Stability analysis of embankments: Journal of the Soil Mechanics and Foundations, Division ASCE, no. SM4, July, p. 1-33.

Marcuson, W. F., and Bieganousky, W. A., 1977a, Laboratory standard penetration tests on fine sands: Journal of the Geotechnical Engineering Division, ASCE, v. 103, no. GT6, June, p. 565-588.

Marcuson, W. F., and Bieganousky, W. A., 1977b, SPT and relative density in coarse sands: Journal of the Geotechnical Engineering Division, ASCE, v. 103, no. GT11, November, p. 1295-1309.

Makdisi, F. I., and Seed, H. B., 1978, Simplified procedures for estimating dam and embankment earthquake-induced deformations: Journal of the Geotechnical Engineering Division, ASCE, v. 104, no. GT7, July, p. 849-867.

Makdisi, F. I., and Seed, H. B., 1979, Simplified procedure for evaluating embankment response: Journal of Geotechnical Engineering Division, ASCE, v. 105, no. GT12, December, p. 1427-1434.

McGuire, R. K., 1977, A simple model for estimating Fourier amplitude spectra of horizontal ground acceleration: U.S. Geological Survey, unumbered Open-File Report.

Mohraz, B., 1976, A study of earthquake response spectra for different geologic conditions: Bulletin of the Seismological Society of America, v. 66, no. 3, p. 915-935.

Newmark, N. M., 1965, Effects of earthquakes on dams and embankments, Geotechnique, v. 5, no. 2, June, p. 139-160.

Newmark, N. M., 1975, Seismic design spectra for Trans-Alaska Pipeline: U.S. National Conference on Earthquake Engineering, Ann Arbor, Michigan, June, p. 94-103.

Newmark, N. M., and Hall, W. J., 1969, Seismic design criteria for nuclear reactor facilities: Proceedings Fourth World Conference Earthquake Engineering, Santiago, Chile, B-4, 37-50.

Newmark, N. M., and Hall, W. J., 1975, Pipeline design to resist large fault displacement: Proceedings of the U.S. National Conference on Earthquake Engineering, June, 1975, Oakland, California, Earthquake Engineering Research Institute, p. 416-425.

Newmark, N. M., and Hall, W. H., 1973, Seismic design spectra for Trans-Alaska pipeline: Proceedings Fifth World Conference on Earthquake Engineering, Session 2B, Rome, Italy, Proc. No. 60.

Nuclear Regulatory Commission, 1973 (ACE), Design response spectra for seismic design of nuclear power plants: Reg. Guide 1.60, Directorate of Regulatory Standards, Washington, D.C.

Peck, R. B., Hanson, W. E., and Thornburn, T. H., 1973, Foundation engineering: Second Edition, John Wiley and Sons, Inc., New York, N.Y.

Richart, F. E., Jr., Hall, J. R., Jr., and Woods, R. D., 1970, Vibrations of soils and foundations: Prentice-Hall, Inc., Englewood Cliffs, N.J.

Richter, C. F., 1958, Elementary seismology: W. H. Freeman and Company, 768 p.

Sarma, S. K., 1975, Seismic stability of earth dams and embankments, Geotechnique, v. 25, no. 4, December, p. 743-761.

Slemmons, D. B., 1977, State-of-the-art for assessing earthquake hazards in the United States, faults and earthquake magnitude: U.S. Army Engineer Waterways Expt. Station Soils and Pavements Lab., Misc. Paper 5-73-1, Report 6.

Slemmons, D. B., 1980, Design earthquake magnitudes for the Western Great Basin, Proceeding of Conference X, Earthquake Hazards along the Wasatch-Sierra-Nevada Frontal Fault Zones, National Earthquake Hazards Reduction Program 29, July 1979-1 August 1979, USGS Open-File Report 80-801.

Schnabel, P. B., Lysmer, J., and Seed, H. B., 1972, SHAKE--A computer program for earthquake response analysis of horizontally layered sites: Report No. EERC 72-12, Earthquake Engineering Research Center, University of California, Berkeley, California, December.

Seed, H. B., 1979a, Soil liquefaction and cyclic mobility evaluation for level ground during earthquakes: Journal of the Geotechnical Engineering Division, ASCE, v. 105, no. GT2, February, p. 201-255.

_____, 1979b, Consideration in the earthquake resistance design of earth and rockfill dams: Rankine Lecture published in Geotechnique, September.

Seed, H. B., 1980, University of California, Berkeley, personal communication.

Seed, H. B., and Idriss, I. M., 1969, Rock motion accelerograms for high magnitude earthquakes: EERC 69-7, University of California, Berkeley, California.

Seed, H. B., and Idriss, I. M., 1967, Analysis of soil liquefaction: Niigata earthquake: Journal of the Soil Mechanics and Foundations Division, ASCE, v. 93, no. SM3, Proc. Paper 5233, May, p. 83-108.

Seed, H. B., and Idriss, I. M., 1970, Soil moduli and damping factors for dynamic response analysis: Earthquake Engineering Research Center, Report No. EERC 70-10, University of California, Berkeley, California, December.

Seed, H. B., Idriss, I. M., Makdisi, F., and Banerjee, N., 1975, Representation of irregular stress time histories by equivalent uniform stress series in liquefaction analyses: Report No. EERC 75-29, University of California, Earthquake Engineering Center, Berkeley, California, October.

Seed, H. B., Makdisi, F. I., and De Alba, P., 1978, Performance of earth dams during earthquakes, Journal of the Geotechnical Engineering Division, ASCE, v. 104, no. GT7, July, p. 967-994.

Seed, H. B., Murarka, R., Lysmer, J., Idriss, I. M., 1975, Relationships between maximum acceleration, maximum velocity, distance from source and local site conditions for moderately strong earthquakes: Earthquake Engineering Research Center Report No. EERC 75-17, College of Engineering, University of California, Berkeley, California.

Seed, H. B., Murarka, R., Lysmer, J., and Idriss, I. M., 1976, Relationships of maximum acceleration, maximum velocity, distance from source, and local site conditions for moderately strong earthquakes: Bull. Seis. Soc. Am., v. 66, p. 1323-1342.

Seed, H. B., Ugas, C., Lysmer, J., 1974, Site-dependent spectra for earthquake-resistant design: Earthquake Engineering Research Center Report No. EERC 74-12, College of Engineering, University of California, Berkeley, California.

Shannon and Wilson, Inc. and Agbabian-Jacobsen Associates (SW-AJA), 1972, Soil behavior under earthquake loading conditions, state-of-the-art evaluation of soil characteristics for seismic response analyses: Report prepared under subcontract no. 3354, Union Carbide Corporation, Nuclear Division, Oak Ridge National Laboratory, Oak Ridge, Tennessee for U.S. Atomic Energy Commission, Contract No. W-7405-eng-26, January.

Sherard, J. L., et al., 1976, Pinhole test for identifying dispersive soils, Journal of the Geotechnical Division, v. 102, no. GT1, January, p. 69-86.

Siegel, R. A., 1975, Computer analysis of general slope stability problems, Joint Highway Research Project, JHRP-75-8, Engineering Experiment Station, Purdue University, Indiana, June.

Stokoe, K. H., II et al., 1978, In situ and laboratory shear velocity and modulus: Specialty Conference on Earthquake Engineering and Soil Dynamics, v. III, Pasadena, California, June, p. 1498-1502.

Stokoe, K. H., II, and Lodde, P. F., 1978, Dynamic response of San Francisco Bay Mud: Proceedings, Specialty Conference on Earthquake Engineering and Soil Dynamics, v. II, Pasadena, California, June, p. 940-959.

Valera, J. E., and Donovan, N. C., 1977, Soil liquefaction procedures--a review: Journal of the Geotechnical Engineering Division, ASCE, v. 103, no. GT6, June, p. 607-625.

Vrymoed, J. L., and Calzascia, E. R., 1978, Simplified determination of dynamic stresses on earth dams: Proceedings of the ASCE Geotechnical Engineering Division Specialty Conference, Earthquake Engineering and Soil Dynamics, v. II, June, p. 991-1006.

Wiegel, R. L., 1970, Earthquake engineering, Prentice-Hall, Inc., Englewood Cliffs, N. J.

Youd, L. T., 1982, U.S. Geological Survey, Menlo Park, personal communication.